

EVALUATION OF PERSONAL COOLING SYSTEMS AND SIMULATION OF THEIR  
EFFECTS ON HUMAN SUBJECTS USING BASIC AND ADVANCED VIRTUAL  
ENVIRONMENTS

by

JOHN CRAIG ELSON

B.S., Kansas State University, 2005

AN ABSTRACT OF A DISSERTATION

submitted in partial fulfillment of the requirements for the degree

DOCTOR OF PHILOSOPHY

Department of Mechanical Engineering  
College of Engineering

KANSAS STATE UNIVERSITY  
Manhattan, Kansas

2016

## Abstract

The research presents the investigation of personal cooling systems (PCS) and their effects on humans from a thermodynamic perspective. The original focus of this study was to determine the most appropriate PCS for dismounted U.S. Army soldiers in a desert environment. Soldiers were experiencing heat stress due to a combination of interrelated factors including: environmental variables, activity levels, and clothing/personal protective equipment (PPE), which contributed to the buildup of thermal energy in the body, resulting in heat stress. This is also a common problem in industry, recreation, and sports. A PCS can serve as a technological solution to mitigate the effects of heat stress when other solutions are not possible.

Viable PCS were selected from the KSU PCS database, expanded to over 300 PCS in the course of this study. A cooling effectiveness score was developed incorporating the logistical burdens of a PCS. Fourteen different PCS configurations were tested according to ASTM F2370 on a sweating thermal manikin. Four top systems were chosen for ASTM F2300 human subject testing on 22 male and 2 female soldiers in simulated desert conditions: dry air temperature = 42.2 °C, mean radiant temperature = 54.4 °C, air velocity = 2.0 m/s, relative humidity = 20%. Subjects wore military body armor, helmets and battle dress uniforms walking on treadmills at a metabolic rate of approximately 375-400W. All the PCS conditions showed significant reductions in core temperature rise, heart rate, and total sweat produced compared to the baseline ( $p < 0.05$ ).

The expected mean body temperature was higher in the human subjects than expected based on the cooling obtained from the sweating manikin test. Lowered sweat production was determined to be the likely cause, reducing the body's natural heat dissipation. The ASHRAE two-node model and TAItherm commercial human thermal models were used to investigate this

theory. A method to account for fabric saturation from dripping sweat was developed and is presented as part of a new model. This study highlights that the response of the human body is highly complex in high-activity, high-temperature environments. The modeling efforts show the PCS moved the body from uncompensable to compensable heat stress and the body also reduced sweating rates when the PCS was used. Most models assume constant sweating (or natural heat loss) thus the PCS sweat reduction is the likely cause of the higher than expected core temperatures, and is an important aspect when determining the purpose of a PCS.

EVALUATION OF PERSONAL COOLING SYSTEMS AND SIMULATION OF THEIR  
EFFECTS ON HUMAN SUBJECTS USING BASIC AND ADVANCED VIRTUAL  
ENVIRONMENTS

by

JOHN CRAIG ELSON

B.S., Kansas State University, 2005

A DISSERTATION

submitted in partial fulfillment of the requirements for the degree

DOCTOR OF PHILOSOPHY

Department of Mechanical Engineering  
College of Engineering

KANSAS STATE UNIVERSITY  
Manhattan, Kansas

2016

Approved by:

Major Professor  
Steven Eckels

# **Copyright**

JOHN CRAIG ELSON

2016

## Abstract

The research presents the investigation of personal cooling systems (PCS) and their effects on humans from a thermodynamic perspective. The original focus of this study was to determine the most appropriate PCS for dismounted U.S. Army soldiers in a desert environment. Soldiers were experiencing heat stress due to a combination of interrelated factors including: environmental variables, activity levels, and clothing/personal protective equipment (PPE), which contributed to the buildup of thermal energy in the body, resulting in heat stress. This is also a common problem in industry, recreation, and sports. A PCS can serve as a technological solution to mitigate the effects of heat stress when other solutions are not possible.

Viable PCS were selected from the KSU PCS database, expanded to over 300 PCS in the course of this study. A cooling effectiveness score was developed incorporating the logistical burdens of a PCS. Fourteen different PCS configurations were tested according to ASTM F2370 on a sweating thermal manikin. Four top systems were chosen for ASTM F2300 human subject testing on 22 male and 2 female soldiers in simulated desert conditions: dry air temperature = 42.2 °C, mean radiant temperature = 54.4 °C, air velocity = 2.0 m/s, relative humidity = 20%. Subjects wore military body armor, helmets and battle dress uniforms walking on treadmills at a metabolic rate of approximately 375-400W. All the PCS conditions showed significant reductions in core temperature rise, heart rate, and total sweat produced compared to the baseline ( $p < 0.05$ ).

The expected mean body temperature was higher in the human subjects than expected based on the cooling obtained from the sweating manikin test. Lowered sweat production was determined to be the likely cause, reducing the body's natural heat dissipation. The ASHRAE two-node model and TAItherm commercial human thermal models were used to investigate this

theory. A method to account for fabric saturation from dripping sweat was developed and is presented as part of a new model. This study highlights that the response of the human body is highly complex in high-activity, high-temperature environments. The modeling efforts show the PCS moved the body from uncompensable to compensable heat stress and the body also reduced sweating rates when the PCS was used. Most models assume constant sweating (or natural heat loss) thus the PCS sweat reduction is the likely cause of the higher than expected core temperatures, and is an important aspect when determining the purpose of a PCS.

# Table of Contents

List of Figures .....	xiii
List of Nomenclature .....	xx
List of Tables .....	xxv
Acknowledgements.....	xxix
Dedication .....	xxx
Chapter 1 - Introduction.....	1
1.1 Background.....	1
1.2 The significance of the research .....	2
1.3 Objective.....	2
1.4 Document Organization .....	3
1.5 Scope of work .....	4
Chapter 2 - Literature Review.....	5
2.1 Introduction.....	5
2.2 Heat Stress .....	7
2.2.1 Measurement on humans .....	11
2.2.2 Natural heat transfer modes from the body.....	12
2.2.2.1 Conduction.....	13
2.2.2.2 Convection .....	13
2.2.2.3 Radiation.....	16
2.2.2.4 Evaporation .....	21
2.2.3 Human factor effects.....	24
2.2.3.1 Clothing/PPE.....	24
2.2.3.2 Activity Level .....	25
2.3 Human Thermal Models .....	26
2.3.1 Single node.....	26
2.3.2 Two Node Models.....	27
2.3.3 Multiple node Models .....	28
2.3.4 PCS Human Thermal Modeling.....	30
2.4 Personal Cooling System Types .....	32



2.4.1 Cold Boundary Technologies .....	32
2.4.1.1 Phase Change Materials .....	32
2.4.1.2 Vapor Compression Refrigeration Cycle .....	34
2.4.1.3 Thermoelectric Cooling .....	36
2.4.2 Mass transfer energy removal .....	39
2.4.2.1 Forced Evaporation/Air Motion .....	39
2.4.2.2 Free Evaporation/Saturated Material .....	40
2.4.3 PCS Application Methods .....	41
2.4.3.1 Liquid Cooling Garment .....	41
2.4.3.2 Direct Expansion Vapor Cooling Garment .....	43
2.4.3.3 Encapsulated materials .....	44
2.4.3.4 Air Vests .....	45
2.4.3.5 Passive Garments .....	46
2.5 Other Cooling Methods .....	47
2.6 Previous Studies .....	47
Chapter 3 - PCS Selection and Testing .....	81
3.1 PCS Selection .....	81
3.1.1 KSU PCS Database .....	81
3.1.2 PCS Selection Criteria .....	84
3.1.2.1 Factors .....	85
3.1.2.2 Supply Portability Factor .....	85
3.1.2.3 Ergonomic Factor .....	86
3.1.2.4 Mobility Factor .....	87
3.1.2.5 User Maintenance Factor .....	87
3.1.2.6 Cooling Effectiveness Factor .....	88
Metabolic Rate .....	90
Natural Heat Loss .....	92
Storage .....	92
Cooling Rate .....	94
3.1.3 Scoring of Systems .....	98
3.2 Thermal Manikin Testing .....	100

3.2.1 Apparatus .....	100
3.2.2 Base Ensemble Testing .....	102
3.2.3 PCS Manikin Testing.....	108
3.3 Human Subject Testing.....	117
3.3.1 Test methods .....	117
3.3.1.1 Data Collection .....	120
3.3.1.2 Test Schedule .....	121
3.3.2 PCS Results.....	125
3.4 Human subject to thermal manikin PCS discussion .....	136
3.4.1 Heat Storage.....	136
3.4.2 Discussion .....	139
Chapter 4 - Modeling human subjects with and without PCS .....	145
4.1 Two Node Model .....	146
4.1.1 Human conditions .....	147
4.1.2 Boundary conditions .....	148
4.1.2.1 Temperature and humidity .....	148
4.1.2.2 Heat and mass transfer .....	148
4.1.2.3 Clothing.....	149
4.1.3 Modeling Environment .....	150
4.2 Multi-Node Model .....	150
4.2.1 Chamber Setup.....	153
4.2.2 Solar lamps.....	155
4.2.3 Human boundary conditions .....	164
4.2.4 Initial conditions .....	167
Chapter 5 - Comparison of baseline results to models .....	169
5.1 Two node model comparison.....	169
5.1.1 Comparison of ASHRAE two node model to human subject results .....	170
5.1.2 Modification of ASHRAE two node model.....	173
5.1.2.1 Spot Creation .....	174
5.1.2.2 Spot Energy Balance.....	180
5.1.2.3 Sweat Rate Modification.....	183

5.1.3 Comparison of modified ASHRAE two node model to human subject results.....	185
5.2 Multi-node Model .....	192
5.2.1 Comparison of the standard multi-node model to human subject results .....	193
5.2.2 Comparison of the modified multi-node model to human subjects results.....	199
5.2.2.1 Sweat Rate Modification of the multi-node model.....	200
5.2.2.2 Sweat Rate and Evaporative Resistance Modification of the Multi-Node Model .....	204
5.3 Conclusions.....	211
Chapter 6 - Comparison of PCS results to models .....	213
6.1 Two-node model PCS comparison .....	215
6.1.1 PCS #1 Entrak Ventilation Vest .....	215
6.1.2 PCS #9 PCVZ-KM Zipper Front Vest by Polar Products .....	220
6.1.3 PCS #12 Cool UnderVest by Steele.....	225
6.1.4 PCS #20 Hummingbird II by Creative Thermal Solutions (CTS).....	230
6.2 Multi-Node Model PCS Comparison .....	235
6.2.1 PCS #1 Entrak Ventilation Vest .....	236
6.2.2 PCS #9 PCVZ-KM Zipper Front Vest by Polar Products .....	249
6.2.3 PCS #12 Cool UnderVest by Steele.....	257
6.2.4 PCS #20 Hummingbird II by Creative Thermal Solutions.....	265
6.3 Conclusions.....	273
Chapter 7 - Discussion .....	275
7.1 Introduction.....	275
7.2 PCS Effects .....	275
7.2.1 Core Temperature .....	276
7.2.2 Sweat Rate .....	277
7.2.3 Heart Rate .....	280
7.2.4 Tradeoff.....	280
7.3 Testing Methodology.....	281
7.3.1 Losses to the environment .....	281
7.3.2 Maximum thermal manikin heat flux.....	283
7.3.3 Manikin sweat rate .....	283

7.4 Wetted Clothing Model .....	284
7.4.1 Spot Size .....	284
7.4.2 Sweat Rate .....	290
7.5 Conclusions.....	291
Chapter 8 - Conclusions.....	294
Appendix A - Testing Images .....	319
Appendix B - Modeling Initial Values.....	352
Appendix C - Thermal Models .....	369
Appendix D - Testing Results.....	452
Appendix E Permissions .....	504

## List of Figures

Figure 3.1 KSU PCS Database product report form page .....	83
Figure 3.2 KSU PCS Database company report form page.....	84
Figure 3.3 STAN, Newton-type sweating thermal manikin showing location of 20 zones .....	101
Figure 3.4 PCS 1 cooling by thermal manikin segment .....	112
Figure 3.5 PCS 9 cooling by thermal manikin segment .....	113
Figure 3.6 PCS 12 cooling by thermal manikin segment .....	114
Figure 3.7 PCS 20 cooling by thermal manikin segment .....	115
Figure 3.8 Average core temperatures of session 1 subjects while wearing different PCS.....	127
Figure 3.9 Mean skin temperatures of session 1 subjects while wearing different PCS .....	128
Figure 3.10 Average torso (back and chest) skin temperatures of session 1 subjects while wearing different PCS.....	129
Figure 3.11 Average heart rates of session 1 subjects while wearing different PCS.....	130
Figure 3.12 Average core temperatures of session 2 subjects while wearing different PCS.....	131
Figure 3.13 Mean skin temperatures of session 2 subjects while wearing different PCS. ....	132
Figure 3.14 Average torso (back and chest) skin temperatures while wearing different PCS. .	133
Figure 3.15 Average heart rates of session 2 subjects while wearing different PCS.....	134
Figure 4.1 TAItherm body part map file assigning virtual manikin segments to human simulation body parts .....	152
Figure 4.2 Isometric view of human model in chamber with two walls, light reflectors, and ceiling hidden.....	154
Figure 4.3 Reversed isometric view of human model in chamber with two walls, light reflectors, and ceiling hidden .....	155
Figure 4.4 Two axis of four-direction light intensity study with 1-inch movement of pyranometer .....	156
Figure 4.5 Hemispherical intensity by degrees of one light plotted radially from center .....	157
Figure 4.6 Isometric view of light study with can reflector and light.....	158
Figure 4.7 Top view of light study with light shape and view of floor elements .....	159
Figure 4.8 Solar intensity at distances on floor for different reflective can lengths in TAItherm compared to the experimental floor average.....	160

Figure 4.9 Model of black globe in chamber under convection to determine solar component of load.....	162
Figure 4.10 Mean Radiant Temperature black globe test recreation .....	163
Figure 4.11 TAItherm convection coefficients on manikin using built in Human Comfort Convection Module, velocity 2.0 m/s .....	167
Figure 5.1 Baseline core temperature comparison graph average subject Two-Node Model (TN) and Human Subject (HS) Results with two data sets for human subject results to show impact of ending time on average core temperature .....	172
Figure 5.2 Spot size measurement on fabric using wetted discoloration.....	178
Figure 5.3 Depiction of area calculation in spot size per area calculations. Area was calculated by two semi circles tangent to a central rectangle. ....	178
Figure 5.4 Graph of plotted absorbed mass and resulting spot area showing linear approximation overlay.....	179
Figure 5.5 Energy balance on the wetted fabric .....	183
Figure 5.6 Baseline core temperature comparison graph average subject Two-Node Model (TN), Modified Two-Node Model (TNM) and Human Subject (HS) Results with two data sets for human subject results to show impact of ending time on average core temperature.....	187
Figure 5.7 Subject 16 local skin temperatures as example of human subject baseline data.....	190
Figure 5.8 Skin wettedness on left axis for unmodified and modified two-node models. Percent of body surface covered by wetted spot in the modified two-node model is on right axis	191
Figure 5.9 Baseline core temperature comparison graph average subject Standard Multi-Node Model and average Human Subject (HS) mean skin temperature and core temperatures..	194
Figure 5.10 Baseline local skin temperature graph of average of subject Human Subject (HS) to show trends in external skin temperatures. ....	194
Figure 5.11 Baseline local skin temperature graph of average of subject Standard Multi-Node Model to show trends in external skin temperatures.....	195
Figure 5.12 Baseline core temperature comparison graph average subject Sweat Rate Modified Multi-Node Model and average Human Subject mean skin temperature and core temperatures. Results with two data sets for human subject results to show impact of ending time on average core temperature .....	201

Figure 5.13 Baseline core temperature comparison graph average subject ReCl and Sweat Rate Modified Multi-Node Model and average Human Subject (HS) mean skin temperature and core temperatures. Results with two data sets for human subject results to show impact of ending time on average core temperature ..... 205

Figure 5.14 Baseline core temperature comparison graph average subject Whole Body Average ReCl Sweat Rate Modified Multi-Node Model and average Human Subject (HS) mean skin temperature and core temperatures. Results with two data sets for human subject results to show impact of ending time on average core temperature..... 208

Figure 6.1 PCS #1 Ventilation Vest by Entrak core and mean skin temperature results of the Unmodified (TN) and Modified Two-Node Model (TNM) compared to the average Human Subject (HS) results, not including subjects 5 and 6..... 216

Figure 6.2 PCS #1 skin wettedness on left axis for unmodified and modified two-node models including potential and actual skin wettedness for unmodified two-node model. Percent of body surface covered by wetted spot in the modified two-node model is on right axis..... 219

Figure 6.3 PCS #9 PCVZ-KM Zipper Front Vest by Polar Products core and mean skin temperature results of the Unmodified (TN) and Modified (TNM) Two-Node Model compared to the average Human Subject (HS) results, not including subjects 5 and 6..... 221

Figure 6.4 PCS #9 skin wettedness on left axis for unmodified and modified two-node models including potential and actual skin wettedness for unmodified two-node model. Percent of body surface covered by wetted spot in the modified two-node model is on right axis..... 224

Figure 6.5 PCS #12 Cool UnderVest by Steele core and mean skin temperature results of the Unmodified (TN) and Modified \*(TNM) Two-Node Model compared to the average Human Subject (HS) results, not including subjects 5 and 6..... 226

Figure 6.6 PCS #12 skin wettedness on left axis for unmodified and modified two-node models including potential and actual skin wettedness for unmodified two-node model. Percent of body surface covered by wetted spot in the modified two-node model is on right axis..... 229

Figure 6.7 PCS #20 Hummingbird II by Creative Thermal Solutions (CTS) core and mean skin temperature results of the Unmodified (TN) and Modified (TNM) Two-Node Model compared to the average Human Subject (HS) results, not including subject 15..... 231

Figure 6.8 PCS# 20 skin wettedness on left axis for unmodified and modified two-node models including potential and actual skin wettedness for unmodified two-node model. Percent of body surface covered by wetted spot in the modified two-node model is on right axis.....	234
Figure 6.9 PCS 1 Ventilation Vest by Entrak core temperature and mean skin temperature comparison graphs between average subject Standard Multi-Node Model and average Human Subject (HS) results.....	238
Figure 6.10 PCS #1 Ventilation Vest by Entrak torso skin temperatures graphs of subject Human Subject (HS) to show trends in skin temperatures contacting PCS. ....	239
Figure 6.11 PCS #1 Ventilation Vest by Entrak local skin temperature graph of average of Human Subject (HS) to show trends in external skin temperatures. ....	240
Figure 6.12 PCS #1 Ventilation Vest by Entrak Standard Multi-Node Model predicted local skin temperature graph showing trends in external skin temperatures.....	241
Figure 6.13 Skin wettedness of the Standard Multi-Node Model with PCS 1 .....	243
Figure 6.14 PCS 1 Ventilation Vest by Entrak core temperature and mean skin temperature comparison graphs between average subject Standard Multi-Node Model and average Human Subject (HS). ....	244
Figure 6.15 PCS #1 Ventilation Vest by Entrak Sweat Rate Modified Multi-Node Model predicted local skin temperature graph showing trends in external skin temperatures. ....	245
Figure 6.16 Skin wettedness of the Sweat Rate Modified Multi-node Model with PCS 1 .....	245
Figure 6.17 Predicted cooling power of PCS1 based on predicted body external energy balance. ....	248
Figure 6.18 PCS #9 PCVZ-KM Zipper Front Vest by Polar Products core and mean skin temperature comparison graphs between average subject Standard Multi-Node Model and average Human Subject (HS).....	250
Figure 6.19 PCS #9 PCVZ-KM Zipper Front Vest by Polar Products torso skin temperatures graphs of subject Human Subject (HS) to show trends in skin temperatures contacting PCS. ....	251
Figure 6.20 PCS #9 PCVZ-KM Zipper Front Vest by Polar Products local skin temperature graph of average of subject Human Subject (HS) to show trends in external skin temperatures.....	252



Figure 6.21 PCS #9 PCVZ-KM Zipper Front Vest by Polar Products Standard Multi-Node Model predicted local skin temperature graph showing trends in external skin temperatures. .....	253
Figure 6.22 Skin wettedness of the Standard Multi-Node Model with PCS 9 .....	256
Figure 6.23 PCS #12 Cool UnderVest by Steele core and mean skin temperature comparison graphs between average subject Standard Multi-Node Model and average Human Subject (HS).....	258
Figure 6.24 PCS #12 Cool UnderVest by Steele torso skin temperatures graphs of subject Human Subject (HS) to show trends in skin temperatures contacting PCS. ....	259
Figure 6.25 PCS #12 Cool UnderVest by Steele local skin temperature graph of average of subject Human Subject (HS) to show trends in external skin temperatures. ....	260
Figure 6.26 PCS #12 Cool UnderVest by Steele Standard Multi-Node Model predicted local skin temperature graph showing trends in external skin temperatures. ....	261
Figure 6.27 Skin wettedness of the Standard Multi-Node Model with PCS 12 .....	264
Figure 6.28 PCS #20 Hummingbird II by Creative Thermal Solutions core and mean skin temperature comparison graphs between average subject Standard Multi-Node Model and average Human Subject (HS). Included are the mean skin and core temperature averages with and without the subjects who did not finish the test. ....	266
Figure 6.29 PCS #20 Hummingbird II by Creative Thermal Solutions torso skin temperatures graphs of subject Human Subject (HS) to show trends in skin temperatures contacting PCS. .....	267
Figure 6.30 PCS #20 Hummingbird II by Creative Thermal Solutions local skin temperature graph of average of subject Human Subject (HS) to show trends in external skin temperatures. ....	268
Figure 6.31 PCS #20 Hummingbird II by Creative Thermal Solutions Standard Multi-Node Model predicted local skin temperature graph showing trends in external skin temperatures. .....	269
Figure 6.32 Skin wettedness of the Standard Multi-node Model with PCS 20 .....	272
Figure 7.1 Depiction of area calculation in spot size per area calculations. Area was calculated by two-semi circles tangent to a central rectangle. ....	287
Figure 7.2 Energy balance on the wetted fabric .....	290

Figure 8.1 Base ensemble #1 top, front .....	319
Figure 8.2 Base ensemble #1 back.....	320
Figure 8.3 Base ensemble #2 top, front .....	321
Figure 8.4 Base ensemble #2 back.....	322
Figure 8.5 Base ensemble #2 front bottom .....	323
Figure 8.6 Base ensemble #3 front .....	324
Figure 8.7 Base ensemble #3 front, bottom .....	325
Figure 8.8 Base ensemble #4 front, top .....	326
Figure 8.9 Base ensemble front, bottom .....	327
Figure 8.10 Fans, air temperature sensors, humidity sensors, and TV .....	328
Figure 8.11 Subject ingestible pillbox labeled by days .....	329
Figure 8.12 Ingestible core temperature pill .....	329
Figure 8.13 Subject changing and instrumentation room. ....	330
Figure 8.14 Heart Rate chest strap.....	331
Figure 8.15 Skin temperature thermocouple under transpore hospital tape .....	332
Figure 8.16 No MRI wrist band worn by subjects throughout the test week to ensure safety when not at the test center .....	333
Figure 8.17 Subject weighing procedure .....	334
Figure 8.18 Subject hydration.....	335
Figure 8.19 Metabolic cart measurement.....	336
Figure 8.20 Metabolic cart procedure .....	337
Figure 8.21 Baseline ensemble front .....	338
Figure 8.22 Baseline ensemble rear .....	339
Figure 8.23 PCS #1 Entrak VentilationVest, no armor, front.....	340
Figure 8.24 PCS #1 Entrak VentilationVest, no armor, rear .....	341
Figure 8.25 PCS #1 Entrak VentilationVest, armor, front.....	342
Figure 8.26 PCS #1 Entrak VentilationVest, armor, rear .....	343
Figure 8.27 PCS #9 PCVZ-KM Zipper Front Vest by Polar Products, no armor, front.....	344
Figure 8.28 PCS #9 PCVZ-KM Zipper Front Vest by Polar Products, armor, front.....	345
Figure 8.29 PCS #12 Cool UnderVest by Steele, no armor, front.....	346
Figure 8.30 PCS #12 Cool UnderVest by Steele, no armor, back.....	347

Figure 8.31 PCS #20 Hummingbird II by Creative Thermal Solutions, armor, front .....	348
Figure 8.32 PCS #20 Hummingbird II by Creative Thermal Solutions, armor, side .....	349
Figure 8.33 PCS #20 Hummingbird II by Creative Thermal Solutions, armor, back .....	350
Figure 8.34 Human subject testing .....	351
Figure 8.35 Initial temperature, chamber outside, front isometric .....	443
Figure 8.36 Initial temperature, chamber inside with light cans, front isometric .....	443
Figure 8.37 Initial temperature, chamber inside without light cans, front isometric .....	444
Figure 8.38 Initial temperature, chamber inside zoomed on human.....	445
Figure 8.39 Initial temperature, chamber outside, back isometric.....	446
Figure 8.40 Initial temperature, chamber inside with light cans, back isometric .....	447
Figure 8.41 Initial temperature, chamber inside without light cans, back isometric .....	448
Figure 8.42 Initial temperature, chamber inside zoomed on human, back .....	449
Figure 8.43 Initial temperature, chamber inside, bottom view of roof subject and belt .....	450
Figure 8.44 Final temperatures, human subject, treadmill, lights.....	451

## List of Nomenclature

Symbol	Description
$A$	Surface area
$A_D$	Dubois Area
$A_w$	Area of skin wetted
$C$	Cylinder in cross flow Nusselt number constant
$C_b$	Body convection heat transfer
$CE$	Cooling effectiveness
$Cl$	Cooling provided by the PCS
$C_p$	Specific heat of the phase-change material
$C_{p_b}$	Average specific heat of tissue
$C_{p_{b,i}}$	Body segment specific heat
$C_{p_{bl}}$	Specific heat of blood
$C_{p_L}$	Specific heat for the liquid phase of the phase change material
$C_{p_S}$	Specific heat for the solid phase of the phase change material
$C_{res}$	Convection respiratory heat transfer
$C_{sk}$	Specific heat of the skin node
$c_{sw}$	Sweat rate coefficient
$D$	Characteristic length: the diameter
$dA$	Differential area of emitting source
$E_b$	Body evaporative heat transfer
$EG$	Ergonomic factors
$E_{max}$	Maximum possible evaporation from body surface for specified conditions
$E_{PCS,i}$	Energy removed from the body by the PCS at iteration step, i
$E_{res}$	Latent respiratory heat transfer
$E_{rsw}$	Evaporation energy from the regulatory sweat rate
$E_{sk}$	Energy removed from the body by evaporation
$E_{spot}$	Evaporation energy from the spot
$E_\lambda$	Hemispherical emissive power
$f_{cl}$	Clothing area factor
$g$	Acceleration of gravity
$G$	Slope or grade
$Gr$	Grashof number
$G_\lambda$	Spectral irradiation
$H$	Horizontal component of energy expenditure
$h$	Average heat transfer coefficient
$h_c$	Convective heat transfer coefficient

$h_D$	Mass transfer coefficient
$h_e$	Evaporative heat transfer coefficient
$h_{fg}$	Latent heat of vaporization of sweat
$h_r$	Linearized radiation heat transfer coefficient
$HS$	Human subject
$Ht$	Sum of the natural heat transfer to/from the body
$h_t$	Total dry heat transfer coefficient
$Ht_{PCS}$	Sum of the natural heat transfer to/from the body with a PCS
$h_x$	Heat transfer coefficient
$i_m$	Clothing permeability index
$J_\lambda$	Spectral radiosity
$k$	Thermal conductivity
$LHF$	Latent heat of fusion of the phase-change material
$Lo$	Mass of load carried
$LR$	Lewis ratio
$L_{th}$	Characteristic length
$\dot{m}$	Mass flow rate of evaporating sweat
$m_b$	Mass of the body
$m_c$	Cylinder in cross flow Nusselt number constant
$MO$	Mobility
$m_{PCM}$	Mass of PCM
$Mr$	Metabolic rate
$\dot{m}_{rsw}$	Regulatory sweat mass flow rate
$Mr_w$	Weight-adjusted metabolic rate
$m_{spot}$	Mass of wetted spot
$\dot{m}_{spot,i}$	Mass in wetted spot at time step
$\dot{m}_{spot,i+1}$	Mass in wetted spot at next time step
$\dot{m}_{spot,in}$	Mass entering the spot from excess sweat
$\dot{m}_{spot,net}$	Net exchange of the spot at any instant
$\dot{m}_{spot,out}$	Mass exiting the spot from excess sweat
$Nu$	Nusselt number
$\overline{Nu}$	Average Nusselt number
$\phi$	Relative humidity
$PCM$	Phase change material
$PCS$	Personal cooling system
$Pr$	Prandtl number
$P_{sat}(T)$	Saturated pressure of water at temperature, T
$P_{sat,air}$	Saturated pressure of the air

$P_{sat,spot}$	Partial pressure at the surface of the saturated spot
$P_{sk}$	Partial pressure of 100% wetted skin surface
$q$	Radiant energy emitted
$q''$	Heat flux
$Q_{bl}$	Blood volumetric flow rate
$Q_{body}$	Heat transfer from the body to the wetted spot
$Q_{C+R}$	Energy gained in the spot due to convection and radiation
$Q_{evap}$	Latent energy losses from the spot
$R$	Resting component of energy expenditure
$r$	Radius
$R_a$	Boundary layer resistance of the clothing
$R_b$	Body radiation heat transfer
$R_{cl}$	Intrinsic dry clothing resistance
$R_{cl,w}$	Thermal resistance of the saturated clothing
$Re_a$	Boundary layer evaporative resistance of the clothing
$Re_{cl}$	Thermal resistance value for the clothing without the air layer
$Re_D$	Reynolds number
$Re_t$	Thermal evaporative resistance value for the clothing with the air layer
$R_t$	Total thermal resistance value for the clothing with the air layer
$R_w$	Gas constant for water vapor
$S$	Seebeck coefficient
$SP$	Supply portability factors
$St$	Heat storage by the body
$\dot{S}t$	Heat storage rate by the body
$SW_{mod}$	Sweat rate proportional gain term
$T$	Terrain coefficient
$t$	Time
$T_{\infty}$	Ambient temperature of the surroundings
$T_a$	Ambient air temperature
$T_{abs}$	Absolute temperature distribution between the junctions
$T_{avg}$	Average temperatures of $T_{skin}$ and $T_{\infty}$
$T_b$	Mean body temperature
$T_{bset}$	Mean body set point temperature
$T_c$	Core body temperature
$T_{cr,i}$	Core temperature at iteration step, i
$T_{final}$	Final equilibrium temperature
$T_{initial}$	Sub cooled starting temperature of the PCM
$T_{MP}$	PCM melting temperature

$T_o$	Operative temperature
$T_{PC}$	Phase change temperature
$T_{sk}$	Temperature of the skin
$T_{sl,i}$	Skin temperature at iteration step, i
$T_{spot}$	Temperature of the spot
$UM$	User maintenance
$V$	Velocity of the fluid
$V$	Velocity or walk rate
$Vert$	Vertical component of energy expenditure
$VO_2$	Volumetric rate of oxygen consumption
$v_{wind}$	Wind velocity
$w$	Skin wettedness coefficient
$w_c$	Spot wettedness coefficient
$Wr$	Work rate performed on the environment
$Wt$	Body mass
$Wt_i$	Body segment mass
$ZT$	Figure of merit
$\alpha$	Thermal diffusivity of air
$\alpha_{sk}$	Core to skin body mass fraction term
$\beta$	Thermal expansion coefficient
$\Delta t$	Time period
$\Delta T_b$	Bulk temperature change
$\Delta T_{b,i}$	Change in body segment temperature
$\Delta T_c$	Measured core temperature change
$\Delta T_c$	Core temperature change
$\Delta t_{PCS}$	PCS cooling time
$\Delta T_{sk}$	Measured skin temperature change
$\Delta T_{sk}$	Mean skin temperature change
$\Delta t_{tmax}$	Maximum mission time
$\Delta t_{TT}$	Task time
$\Delta t_{TTMAX}$	Maximum task time
$\epsilon_1$	Emissivity of object
$\epsilon_s$	Efficiency value of wetted spot
$\theta$	Angle from the normal of emitting surface from 0 to $\pi$ radians
$\theta_{CE}$	Cooling effectiveness factor modification term
$\theta_{EG}$	Ergonomics factor modification term
$\theta_{MO}$	Mobility factor modification term
$\theta_{SP}$	Supply portability factor modification term
$\theta_{UM}$	User maintenance factor modification term

$\kappa$	Thermal conductivity
$K$	Thermal conductivity between skin and core
$\kappa_E$	Thermal conductivity due to electronic factors
$\kappa_L$	Thermal conductivity due to the lattice structure
$\lambda$	Wavelength of the emitted radiation
$\nu$	Kinematic viscosity of the air
$\Pi$	Peltier coefficient
$\varpi$	Solid angle
$\rho_{bl}$	Blood density
$\sigma_{sb}$	Stefan-Boltzmann constant
$\sigma_t$	Electrical conductivity value
$\phi$	Angle in plane with the emitting surface in from 0 to $2\pi$ radians
$\varphi_w$	Fraction of sweat rate available for spot
$\omega$	Solid angle dependent on the distance $r$ from the source



## List of Tables

Table 3.1- Selected work-rate levels for the dismounted soldier from Sawka et al. (2003).....	90
Table 3.2 STAN, Newton-type sweating thermal manikin zone segment information.....	102
Table 3.3 U.S. Army dismounted soldier base ensembles tested .....	103
Table 3.4 Thermal insulation values for base ensembles .....	107
Table 3.5 Evaporative resistance data for base ensembles .....	108
Table 3.6 Results of sweating heated manikin testing on PCS.....	110
Table 3.7 Results for the Personal Cooling System human subject tests .....	135
Table 3.8 Percent difference between initial cooling power estimate and thermal manikin( <i>Table 3 from Applied Ergonomics, Vol. 48, pg. 38 J. Elson and Eckels (2015) used with permission from Elsevier Ltd.</i> ).....	136
Table 3.9 Updated Cooling Effectiveness rating score using thermal manikin results ( <i>Table 4 from Applied Ergonomics, Vol. 48, pg. 38 J. Elson and Eckels (2015) used with permission from Elsevier Ltd.</i> ) .....	137
Table 3.10 – Estimated and human subject heat storage results ( <i>Table 5 from Applied Ergonomics, Vol. 48, pg. 38 J. Elson and Eckels (2015) used with permission from Elsevier Ltd.</i> ).....	137
Table 4.1 Army Ensemble 3 clothing resistances by manikin/model segment in TAItherm...	165
Table 4.2 Body convection coefficients Danielsson (1993) pg82 table 3.4, velocity 2.0 m/s...	166
Table 5.1 Baseline data comparison: Two-Node Model (TN) vs. Human Subject (HS) .....	171
Table 5.2 Baseline data comparison: Modified Two-Node Model (TNM) vs. Human Subject (HS).....	186
Table 5.3 Baseline data comparison: Standard Multi-Node Model vs. Human Subject core, mean skin, and local skin temperatures. ....	197
Table 5.4 Baseline sweat total comparison: Standard Multi-Node Model vs. Human Subject (HS) sweat rates with human subject results as the comparator.....	199
Table 5.5 Baseline data comparison: Sweat Rate Modified Multi-Node Model vs. Human Subject (HS) core, mean skin, and local skin temperatures.....	202
Table 5.6 Baseline sweat total comparison: Sweat Rate Modified Multi-Node model vs. Human Subject (HS) sweat rates with human subject results as the comparator.....	203

Table 5.7 Improvement in core temperature change between Sweat Rate Modified Multi-Node Model vs. Human Subjects (HS) results. ....	203
Table 5.8 Baseline data comparison: ReCl and Sweat Rate Modified Multi-Node Model vs. Human Subject core, mean skin, and local skin temperatures. ....	206
Table 5.9 Baseline sweat total comparison: ReCl Sweat Rate Modified Multi-Node Model vs. Human Subject sweat rates with human subject results as the comparator. ....	207
Table 5.10 Improvement in core temperature change between ReCl Sweat Rate Modified Multi-Node Model vs. Standard multi-node model. ....	207
Table 5.11 Baseline data comparison: Whole Body Average ReCl Sweat Rate Modified Multi-Node Model vs. Human Subject core, mean skin, and local skin temperatures. ....	209
Table 5.12 Baseline sweat total comparison: Whole Body Average ReCl Sweat Rate Modified Multi-Node Model vs. Human Subject sweat rates with human subject results as the comparator. ....	210
Table 5.13 Improvement in core temperature change between Whole Body Average ReCl Sweat Rate Modified Multi-Node Model vs. Standard multi-node model. ....	210
Table 6.1 Personal cooling systems (PCS) tested on human subject and to be compared to human thermal models. ....	214
Table 6.2 PCS #1 Ventilation Vest by Entrak results of Unmodified Two-Node Model (TN) .	217
Table 6.3 PCS #1 Ventilation Vest by Entrak results of Modified Two-Node Model (TNM) .	218
Table 6.4 PCS #9 PCVZ-KM Zipper Front Vest by Polar Products results of Unmodified Two-Node Model (TN) .....	222
Table 6.5 PCS #9 PCVZ-KM Zipper Front Vest by Polar Products results of Modified Two-Node Model (TNM) .....	223
Table 6.6 PCS #12 Cool UnderVest by Steele results of Unmodified Two-Node Model (TN).	227
Table 6.7 PCS #12 Cool UnderVest by Steele results of Modified Two-Node Model (TNM) .	228
Table 6.8 PCS #20 Hummingbird II by Creative Thermal Solutions (CTS) results of Unmodified Two-Node Model (TN).....	232
Table 6.9 PCS #20 Hummingbird II by Creative Thermal Solutions (CTS) results of Modified Two-Node Model (TNM) .....	233
Table 6.10 Convection coefficients under the body armor including fabric resistance.....	237

Table 6.11 PCS #1 Ventilation Vest by Entrak Standard Multi-Node Model vs. Human Subject (HS) core, mean skin, and local skin temperatures including initial and final conditions..	242
Table 6.12 PCS #1 Ventilation Vest by Entrak Standard Multi-Node Model vs. Human Subject (HS) sweat rates with human subject results as the comparator. ....	243
Table 6.13 PCS #1 Ventilation Vest by Entrak Sweat Rate Modified Multi-Node Model vs. Human Subject (HS) core, mean skin, and local skin temperatures including initial and final conditions. ....	246
Table 6.14 PCS #1 Ventilation Vest by Entrak Sweat Rate Modified Multi-Node Model vs. Human Subject (HS) sweat rates with human subject results as the comparator. ....	247
Table 6.15 PCS #9 PCVZ-KM Zipper Front Vest by Polar Products Standard Multi-Node Model vs. Human Subject (HS) core, mean skin, and local skin temperatures including initial and final conditions. ....	255
Table 6.16 PCS #9 PCVZ-KM Zipper Front Vest by Polar Products Standard Multi-Node Model vs. Human Subject (HS) sweat rates with human subject results as the comparator. ....	256
Table 6.17 PCS #12 Cool UnderVest by Steele Standard Multi-Node Model vs. Human Subject (HS) core, mean skin, and local skin temperatures including initial and final conditions..	263
Table 6.18 PCS #12 Cool UnderVest by Steele Standard Multi-Node Model vs. Human Subject (HS) sweat rates with human subject results as the comparator. ....	264
Table 6.19 PCS #20 Hummingbird II by Creative Thermal Solutions Standard Multi-Node Model vs. Human Subject core, mean skin, and local skin temperatures including initial and final conditions. ....	271
Table 6.20 PCS #20 Hummingbird II by Creative Thermal Solutions Standard Multi-Node Model vs. Human Subject (HS) sweat rates with human subject results as the comparator. ....	272
Table 8.1 Human subject initial and final values for baseline two-node modeling (PCS# 0)...	352
Table 8.2 Human subject weight, speed, and vertical distance values for baseline two-node modeling work calculations (PCS# 0) .....	353
Table 8.3 Human subject initial and final values for PCS two-node modeling (PCS# 1 and PCS #9) .....	354
Table 8.4 Human subject weight, speed, and vertical distance values for PCS two-node modeling work calculations (PCS# 1 and PCS# 9) .....	355

Table 8.5 Human subject initial and final values for PCS two-node modeling (PCS# 12 and PCS #20) .....	356
Table 8.6 Human subject weight, speed, and vertical distance values for PCS two-node modeling work calculations (PCS# 12 and PCS# 20) .....	357
Table 8.7 Thermal manikin average cooling for PCS used in two-node modeling .....	358
Table 8.8 Multi-Node Model (TAITherm) initial body temperatures for 50% height 75% weight simulated subject.....	361
Table 8.9 Multi-Node Model Modified ReCl values based on two-node model results .....	365
Table 8.10 Multi-Node Model physiology.txt values .....	367
Table 8.11 Session 1 Human subject baseline results average (Subjects 1-12).....	462
Table 8.12 Session 1 Human subject PCS #1 results average (Subjects 1-12).....	466
Table 8.13 Session 1 Human subject PCS #12 results average (Subjects 1-12).....	470
Table 8.14 Session 1 Human subject baseline results average (Subjects 1-3, 7-8,10-12).....	474
Table 8.15 Session 1 Human subject PCS #1 results average (Subjects 1-3, 7-8,10-12).....	478
Table 8.16 Session 1 Human subject PCS #12 results average (Subjects 1-3, 7-8,10-12).....	482
Table 8.17 Session 2 Human subject baseline results average (Subjects 13-24) .....	492
Table 8.18 Session 1 Human subject PCS #9 results average (Subjects 1-12).....	496
Table 8.19 Session 2 Human subject PCS #20 results average (Subjects 1-12).....	500

## Acknowledgements

First, I would like to thank Dr. Steve Eckels for providing an excellent example as my major professor and advisor. He has taught me much about research, teaching, professional involvement, patience, and life. I could not ask for a better mentor and guide throughout my PhD. I am very blessed to have had this opportunity and cannot thank him enough.

I would next like to thank Dr. Elizabeth McCullough for imparting her knowledge and experience concerning testing procedures and methods as well as for serving as lead project investigator for the Army tests. The opportunity to work for someone with an intense depth of knowledge and as focused, organized, and precise as Dr. McCullough was a unique and exceptional opportunity for which I am incredibly grateful. This would not have been possible without her guidance and support.

Third, I would like to convey my gratitude to my committed members, Dr. Byron Jones, Dr. Donald Fenton, and Dr. Brad Behnke. This multi-disciplinary project benefited greatly from their expert guidance and advice. In addition, I appreciate their comments and thoughts on this work, including those of Dr. Ruth Welti who graciously served as the outside chairperson for my defense.

I am indebted to the miracle workers of IER: Eric Waters, Luke Schooler, Garret Mann, Jacob Wagner, and Andrew Featherstone for keeping the human subject and thermal manikin testing running and ensuring high fidelity data collection. I would be remiss if I also did not thank Kristin Umscheid for her amazing work with the thermal manikin and human subjects, coordinating, planning, setting up, and instrumenting for each test allowing all of this data to be collected.

I would like to finish this acknowledgment by thanking all of the people who made this possible including my family and friends. I would especially like to thank my wife Anna for her love and support. I would also like to thank my parents, Craig and Kathy and my Grandfather Robert for instilling in me a love of science and engineering. Many more people deserve acknowledgement for their assistance with this work that cannot fit on this page. I would like to express my deepest gratitude to them for all of their help and support.

## **Dedication**

*To my wife Anna.*

# Chapter 1 - Introduction

## 1.1 Background

Military operations, by their nature, are not always conducted in the most ideal environments. This also holds true for many businesses, recreational activities, and sports where physical activity must be performed in conditions not compatible with human thermoregulation, with equipment that impairs thermoregulations, or a combination of these factors. With the conflicts in the Middle East, the military is operating in desert environments with high air temperatures and radiant loads. Although, the United States has been fighting in conflicts in the Middle East for more than a century, in the most recent conflict dismounted soldiers were in some cases wearing and carrying over 100 pounds of clothing and equipment. Also included in this load were ballistic armor, and in some cases nuclear, radiological, chemical, biological protective clothing to protect against weapons of mass destructions, WMDs. The armor alone was shown to inhibit the body's natural means of thermoregulation resulting in warfighters succumbing to heat stress, or ceasing operations due to the onset of heat stress (Buller et al., 2008). Due to the important protection provided by the advanced ballistic armor worn by the warfighter in areas that included close quarters, city fighting, and improvised explosive devices (IEDs) there was need to mitigate heat stress using technological means. U.S. Army was interested in possibly selecting a personal cooling system for use with dismounted soldiers along with their body armor. The Institute for Environmental Research (IER) at Kansas State University was awarded a research project to review the available personal cooling systems on the market and in literature, assemble the data based on the parameters of the PCS, perform thermal manikin testing on the first group of PCSs selected, and then test the best four PCSs on human subjects. After the completion of the testing portion, IER has analyzed the resultant data

to add to the literature and understanding on the effects of PCS on humans and to strengthen the predictive power of the thermal manikin in evaluating PCS. This effort included basic and advanced human thermal modeling of the base case (battle dress as outlined above) and PCS tests (base case plus PCS), including the development of a new model for use with high sweat rates, PCS, and humans clad in encapsulating, semi-permeable garments.

## **1.2 The significance of the research**

This research expands the knowledge on the effects of personal cooling systems (PCS) on the human body as well as the effectiveness of measurement and modeling techniques to determine the effect of a cooling system on a human. This information is useful for situations where high temperature and/or restrictive clothing and personal protective equipment are present where people work, fight, and recreate. These results can be used to inform the engineering developing the next generation PCS and help with the proper selection of systems to meet the needs of the end user.

## **1.3 Objective**

The objective of this work is to add to the knowledge concerning personal cooling systems and thermoregulation. This includes testing using a sweating thermal manikin according to ASTM standard F2371-10 (ASTM, 2010b). Also, human subject data of 24 subjects, 22 male and 2 female, that are tested within ASTM standard 2300-10 (ASTM, 2010a).

The research investigates the heat transfer effects on a human with and without the cooling provided by the personal cooling system. The heat transfer research is accomplished by using the experimental data with basic and advanced models of human thermal regulation, environmental characteristics, and thermodynamic principles. In addition, the research seeks to determine the effectiveness of the basic and advanced human thermal models for evaluating



armored subjects performing moderate intensity exercise in a hot, dry environment and the applicability of standards to properly test PCS for specific and general conditions.

## **1.4 Document Organization**

The document is divided into eight chapters and four appendices. The first chapter is the introduction to the research containing background, significance, objective, scope of work, and document organization. Chapter 2 is comprised of the literature review, which includes background on heat stress, PCS technology, testing standards, thermal models, and the literature review of previous PCS studies, previous Army PCS studies, and use of thermal models. Chapter 3 covers the selection of PCSs using the KSU PCS evaluation tool and the methodology and results of testing of PCSs on the thermal manikin and human subjects with a basic analysis of the results.

The remaining chapters explore using human thermal modeling in an attempt to predict the effects of high temperature, dry conditions on human subjects with and without PCS. Chapter 4 covers the setup procedures for both the ASHRAE two-node model (ASHRAE, 2013) and Dusan Fiala, Lomas, and Stohrer (1999) derived TAItherm/RadTherm human thermal model. Chapter 5 includes the comparison of the different human thermal models with the baseline data from the human subject tests. In Chapter 6, the results of modeling PCS in the human thermal models are compared to the human subject data.

The primary purpose of Chapter 7 is the discussion of standards, the applicability of the different models, sources of error, challenges, and recommendations. Chapter 8 comprises the conclusion of the research followed by the appendices including visuals of the TAItherm simulation environment, MathCad worksheets of mean radiant temperature calculation and the two-node model, and images of testing.

## **1.5 Scope of work**

The research explores the effects of personal cooling systems (PCS) on humans. This includes raw data and analysis taken from testing performed as part of U.S. Army contract #W91CRB-10-C-0005. This project includes testing clothing and equipment ensembles with and without a personal cooling system (PCS). This work covers the selection, testing, and evaluation of PCSs and explores testing pitfalls and PCS effects on humans.

A database of commercially available, and some research, personal cooling systems is developed to aid Army officials in evaluating commercial off the shelf (COTS) systems for testing. Due to the large number of systems on the market and the many situations you could find the dismounted soldier, a set of selection criteria is formulated based on the cooling power, runtime, weight, and portable rechargeable supplies to inform selection. A unique methodology was developed to address the impact of the logistical factors of PCS weight, PCS operation time, and mission time and is presented.

A sweating thermal manikin of the Newton type (MTNW/Thermetrics) is used to evaluate dry and evaporative resistances of clothing and equipment worn on the manikin. The manikin is composed of 20 independent sweating zones. The manikin can also be used to measure the cooling power provided by a PCS using an isothermal skin temperature per ASTM standard F2371-10 (ASTM, 2010b).

PCS that were estimated to provide adequate cooling power were identified and the top four were chosen to be tested on human subjects. This testing was performed in a large climatic thermal chamber at the Institute for Environmental Research in Kansas State University. Chamber conditions cover 42.2°C air temperature, 54.4°C mean radiant temperature, 20% relative humidity, with a 2.2 m/s air velocity. Subjects walked at a velocity designed to create a 375W metabolic load.

Exploration of the human subject and manikin results involve using an energy balance, a two node model and a commercially available advanced model of human thermoregulation based on the work by Dusan Fiala et al. (1999) and integrated into the RadTherm/TAITherm program (A. Curran, Hepokoski, Curlee, Nelson, & Biswas, 2006). A new two-node model is developed as a modification to the existing two-node model used in this analysis to improve the prediction capabilities in the studied conditions.

The effects of PCS on humans is explored scientifically and critiques of the testing methods and evaluation tools are given. This includes the discussion of the multiple effects of PCS and tradeoffs in actual use. Recommendations are made for best practices when performing future PCS design, selection, and testing.

## **Chapter 2 - Literature Review**

### **2.1 Introduction**

There is a need for technology that can mitigate the effects of heat stress on people in environments where the human body cannot compensate naturally for the conditions, i.e. uncompensable environments. This is especially true in desert and jungle conditions, deep mines, firefighting or other locations where high radiant loads, high air temperatures, high humidity, personal protective equipment or a combination of these elements, can lead to heat stress incidents (Bennett, Hagan, Huey, Minson, & Cain, 1995; Buller et al., 2008; Chou, Tochiara, & Kim, 2008). Intense ambient conditions coupled with the high work rates make heat stress a major concern in the operational capability of humans. In high temperature applications, where the ambient temperature is greater than body temperature, the body's only defense against heat stress is the ability to evaporate sweat. Unfortunately, personal protective equipment (PPE) and clothing limit the body's ability to evaporate sweat, and therefore also can

limit the ability to expel energy via mass evaporation to the environment (Cadarette, Matthew, & Sawka, 2005). This leads to the buildup of energy in the body, raising the body's core temperature and eventually leading to heat stress. Therefore, a personal cooling system (PCS) could potentially mitigate the heat stress imposed by the environment and compounded by personal protective equipment (PPE) without compromising the ensemble's protective effects.

The use of personal cooling systems (PCSs) has been investigated for over four decades by all branches of the United States military, foreign governments, private and public organizations, and universities. (J. C. Elson, McCullough, & Eckels, 2013; E.A.; McCullough & Eckels, 2008; E.A.; McCullough & Eckels, 2009; Kent B.; Pandolf et al., 1995; Xu & Gonzalez, 2011). A more detailed list of publications is found in the table at the end of this chapter. The analysis of PCSs can be a difficult due to the inherent variability in human subject physiology and ergonomics, the range of environmental conditions, clothing and equipment, and the many possible applications. Baseline information on PCS is often confusing because test protocols vary between laboratory including desired measurements, available equipment, desired use, and other factors. The reviewed literature shows most systems are tested on human subjects, but some use thermal manikins to measure the heat removal. The heat removed can be applied to estimate the effect on humans with a reasonable amount of success (Hepokoski, Packard, Curran, & Rothschild, 2012) however, as noted later in this work this is dependent on a number of factors. The thermal manikin provides an indication of the effectiveness of the PCS on humans while wearing clothing and equipment without the expense and complications of human subject testing. There are over 300 different systems available on the market which makes manikin testing of all systems cost prohibitive and human subject testing of all those systems essentially impossible.

There are different standards relating to testing PCS using humans and manikins. In this study standards from ASTM International, formerly the American Society for Testing and Materials, were used for both testing types, however many different manikin test protocols are used in literature. A brief overview of these standards and instances of PCS tests using standards are covered.

Also of importance is the modeling of human thermal physiology. Many models have been developed for the prediction of human physiological responses to different metabolic rates in various environments. Significant models are generally those that are often cited in literature and modified by other researchers. Models can range in complexity from simple one- and two-node models representing the human as a lumped capacitance system through segmented models to complex, million node voxelized human forms (Nelson et al., 2009). For the purpose of this literature review, lumped capacitance models and segmented models will be the primary focus as versions of these are used in this research. However, it is recognized in literature, and in this work, that time and money could be saved if PCS could be pre-screened for a specific application. A brief discussion of the limited PCS modeling efforts in literature will provide a backdrop for the modeling efforts discussed in this work.

Finally, methods and results of different studies of PCS tests in literature are presented. This information provides a solid groundwork for the current research and much of it is used as a basis when completing the current research. The works of multiple researchers are presented to highlight types of PCS, testing methods, environments, PPE, and physiologies.

## **2.2 Heat Stress**

In researching PCS literature, the primary intended use of PCS was mitigation of heat stress. Heat stress is affected by many factors specific to each individual, but it is generally

accepted that the core body temperature, and temperature where cells begin to die, is approximately 41°C rectal temperature. At this point, hypothalamic proteins may be damaged and heat stroke can occur. Once heat stroke is reached recovery is frequently irreversible (K. Parsons, 2002).

The rise in core body temperature is comprised of a number of different and sometimes interrelated factors. First, it has been shown that there is an exercise-related rise in the core body temperature. This is part of the body's natural thermoregulation system that sends heat towards the extremities as the temperature increases (Livingstone, Grayson, Frim, Allen, & Limmer, 1983). However, the dangerous rise in core body temperature comes from additional storage of energy as extremity temperature rise and core temperature continues to rise.

The first law of thermodynamics governs the energy exchange of the body. All the energy produced by the body's metabolism becomes heat and mechanical work which can lead to stored energy (ASHRAE, 2013) and heat stress if not transferred to the environment. Unfortunately, the amount of physical work performed is generally a small fraction of the metabolic energy generated.

The rise in core temperature does lead to higher skin temperature for increased heat transfer to, or decreased absorption from the environment. However as heat loss become uncompensable, as in hot conditions with limited evaporation potential (Buller et al., 2008), the body temperature raise. This storage depends on the specific heat, mass of the body. The approximate total heat storage before heat stress occurs for an average sized person is 670 kJ (ASHRAE, 2013).

A first-order energy balance example is a simple approach and was also used in research done for the Air Force (Kent B.; Pandolf et al., 1995) and in the research of James R. House et

al. (2013) and many other sources. Derived from the first law of thermodynamics, the balance of energy being generated, entering and leaving the body is conserved. In many models the mass balance portion is ignored and assumed small or replenished by consumption as is done here (ASHRAE, 2013; Gagge & Gonzalez, 1996; Gagge & Nishi, 1977). The result is an energy balance where evaporated sweat given as a latent heat loss value:

$$0 = Mr - Wr - Cres - Eres - Cb - Rb - Eb - \dot{St} \quad (2.1)$$

where  $Mr$  is metabolic rate (W),  $Wr$  is work rate performed on the environment (W),  $Cres$  is convection respiratory heat transfer (W),  $Eres$  is latent respiratory heat transfer (W),  $Cb$  is body convection heat transfer (W),  $Rb$  is body radiation heat transfer (W),  $Eb$  is body evaporative heat transfer (W),  $\dot{St}$  is heat storage rate by the body (W). Conduction for a standing person is considered negligible (ASHRAE, 2013).

The heat transfer values to the environment can be simplified to the sum of the natural heat transfer to/from the body,  $Ht$ , in Watts and the equation can be rearranged to solve for the energy storage rate term,  $\dot{St}$ , in Watts.

$$\dot{St} = Mr - Wr - Ht \quad (2.2)$$

The human body's mostly liquid and solid composition allows for the use of specific heat  $Cp_b$  to estimate the amount of energy stored in the body per unit mass, time, and temperature change. This term would be represented by the

$$\dot{St} = Wt * Cp_b * \Delta T_b / \Delta t \quad (2.3)$$

$Wt_i$  is body segment mass (kg),  $Cp_{b,i}$  is body segment specific heat (kJ/kg\*°C),  $\Delta T_{bi}$  is the change in body segment temperature (°C) over the  $\Delta t$ .

In Equation ( 2.1 ), the rearranging the time parameter, task time in seconds; by multiplying it by both sides results in a total energy storage value in kJ for the defined time period.

$$St = \sum_1^i [Wt_i * Cp_{b,i} * \Delta T_{b,i}] = (Mr - Wr - Ht) * \Delta t \quad ( 2.4 )$$

where, St, is energy storage for the defined task time (kJ),  $Wt_i$  is body segment mass (kg),  $Cp_{b,i}$  is body segment specific heat (kJ/kg\*°C),  $\Delta T_{b,i}$  is the change in body segment temperature (°C) over the  $\Delta t$ , Ht is natural heat transfer to/from the body (W), and  $\Delta t$  is task time (sec). The work rate performed on the environment (Wr) is the physical effect of expending metabolic energy such as moving the body by walking, biking, climbing, cranking, etc. Metabolic rate (Mr) and heat loss to the environment (Ht) will be discussed later. In the most simplistic model, the body is represented by one compartment. Other models will use two or more compartments to model the body. The storage term summation highlights the effects of different specific heats, temperatures and masses of different body segments and layers if applied. In a simplistic analysis,  $i=1$ , yielding  $St=Wt*Cpb*\Delta Tb$ , where all values are the average body values. The goal of employing a heat stress management plan is to minimize or eliminate the storage term to a tolerable level over the task time. Currently, the standard recommendation to control storage is to use work-rest cycles. This creates an average work rate that meets the needs of the end user, whether safety or survivability is the primary concern (ISO, 2003; Sawka et al., 2003).

As presented in Equation ( 2.4 ), the body can be split up into multiple segments or compartments with different temperatures, specific heats, and masses. In human body models, these can be linked by a common blood pool and sometimes conduction (ASHRAE, 2013; Dusan Fiala, Havenith, Bröde, Kampmann, & Jendritzky, 2012; Dusan Fiala & Lomas, 2001; Dusan Fiala et al., 1999; D. Fiala, Lomas, & Stohrer, 2001; J. A. J. Stolwijk & Hardy, 1966).



### 2.2.1 Measurement on humans

The energy storage concept is also employed when measuring values on human subjects. Energy storage is represented by one compartment, two-compartments, or three and more compartments. The most commonly used in the literature of PCS applications is the two-compartment model. A notable example of the two-compartment method is the work of M. J. Barwood, Newton, and Tipton (2009). It has been shown by Jay et al. (2006), Jay and Kenny (2007), and Jay et al. (2007) that more compartments will lead to better accuracy, but will require subcutaneous measurement, which is costly, painful, and more dangerous. The more common two-compartment model is as follows (André L Vallerand, Savourey, Hanniquet, & Bittel, 1992):

$$St = Wt * Cp_b * (0.8 * \Delta Tc + 0.2 * \Delta Tsk) \quad (2.5)$$

The storage term is calculated from the weight of the subject  $Wt$  (kg), specific heat of the body  $Cp_b$  (J/(kg\*K)) (ASHRAE, 2013), and the measured core temperature change  $\Delta Tc$  (K), and the measured skin temperature change  $\Delta Tsk$  (K). These are the two common measurements taken according to the ASTM human subject PCS testing standard F2300-10 (ASTM, 2010a), other works in literature change the weighting coefficients. An example of this is in the work by Siegel et al. (2010) where 0.66 was used as the core weighting coefficient and 0.34 as the skin weighting coefficient.

The effect of PCS is very simple, theoretically speaking. There is an additional energy transfer mechanism being added to the body. This could be through additional convection, conduction, radiation, or evaporation induced by the PCS. In an ideal world, the quantity of heat removed from the body in terms of energy, (Watts) or energy across time (Joules), would be added to the energy losses by the other paths, as defined in Equation ( 2.4 ) as the natural heat transfer, or baseline heat transfer. This equation would look identical to Equation ( 2.4 ), if

cooling could be maintained through the entire time at a constant rate, with only the addition of an extra term,  $Cl$  in Watts, which is the cooling provided by the PCS.

$$St = \sum_{i=1} [Wt_i * Cp_{b,i} * \Delta T_{b_i}] = (Mr - Wr - Ht - Cl) * \Delta t \quad (2.6)$$

This method was used by in the literature and in this paper. It has been noted both here and elsewhere that this balance is not necessarily correct, and is a major topic of the current work (M. J. Barwood et al., 2009; James R. House et al., 2013).

### ***2.2.2 Natural heat transfer modes from the body***

In this research, we have termed the natural heat transfer from the body,  $Ht$ , as the baseline heat transfer from the body at a set of steady state conditions without PCS cooling. In compensable thermal exchanges from the body, this value equals the metabolic heat production, less work, and provides for no heat storage. In uncompensable conditions, the natural heat loss becomes the net maximum amount of energy the person can transfer to the environment.

Situations where the body is not expelling heat are rare but possible, and generally occur in water immersion (Leyva & Goehring, 2004) where the fluid temperature is higher than body temperature or encapsulated PPE (Kamon, Kenney, Deno, Soto, & Carpenter, 1986). The natural heat transfer is the sum of the different heat transfer regimes: conduction, convection, radiation, and evaporation. For each mode of heat transfer other than conduction, it is generally beneficial to describe it using Newton's law of cooling as shown in Equation ( 2.7 ).

$$Q = h_x \cdot A \cdot (T_{sk} - T_{\infty}) \quad (2.7)$$

The variables represent the energy transferred over time (Watts), heat transfer coefficient,  $h_x$  (W/(m<sup>2</sup>K)); surface area,  $A$  (m<sup>2</sup>); temperature of the surroundings,  $T_{\infty}$  (K); and temperature of the skin,  $T_{sk}$  (K). The heat transfer coefficient  $h_x$ , will have appropriate subscript assigned to

radiation ( $h_r$ ) or convection ( $h_c$ ). An equation of similar form can be used for evaporation with the coefficient  $h_e$ . Evaporation is actually driven by the mass concentration difference between the body and the environment and is covered more in depth in Section 2.2.2.4. The following sections provide a fundamental view of the conduction, convection, radiation, and evaporation mechanisms that makeup the natural heat loss.

### **2.2.2.1 Conduction**

Conduction is one of the fundamental heat transfer modes. In conduction heat is transferred between direct contact, on a molecular scale (Incropera, DeWitt, Bergman, & Lavine, 2007). The application in human thermal studies largely depends on the position of the human and what they are touching, as well as clothing and equipment. Conduction is primarily in the clothing, which can create a temporary barrier during transients. Conduction occurs during contact with a different temperature object such as in sitting on a hot car seat, sleeping on cold ground, etc. The transient nature obviously depends on the energy capacity of the energy sink or source before steady state. The fundamental energy equation is Fourier's law given below where  $\Delta T$  is the difference between the two objects with the energy flowing into the first temperature, if this value is positive. The value,  $k$ , is the conduction coefficient  $W/(m \cdot K)$ , the reciprocal of this value,  $R_{cond}$ , is the conduction resistance in units, and  $(m \cdot K)/W$ .  $A$ , is the surface area in conduction.

$$Q_{cond} = -k \cdot A \cdot \Delta T \quad (2.8)$$

### **2.2.2.2 Convection**

Convection tends to dominate human comfort and heat exchange in the cold and in everyday thermal comfort. One of the two types of convection free (natural) or forced are found in some way or in combination whenever there is a temperature difference involving at least one

fluid and gravity. The Nusselt number, Equation ( 2.7 ), is often correlated because it represents a dimensionless heat transfer coefficient.

$$Nu = \frac{h_c \cdot L_{th}}{k} \quad (2.9)$$

In forced convection, the Nusselt number can be calculated based on the shape and surface properties of the object, the properties of the fluid, and the velocity of the flow. Free or natural convection is driven by the temperature difference and the difference in density, and therefore buoyancy, it creates in the fluid. The driving force is represented by the unitless Rayleigh number, and for a vertical surface is given by (Danielsson, 1993):

$$Ra = Gr \cdot Pr = \frac{g \cdot \beta \cdot (T_{sk} - T_{\infty}) \cdot L_{th}^3}{\nu \cdot \alpha} \quad (2.10)$$

where  $g$  = Acceleration of gravity  $9.81 \text{ (m/s}^2\text{)}$ ;  $L_{th}$  = Characteristic length (m);  $T_{\infty}$  = Temperature of the surroundings (K);  $T_{sk}$  = Temperature of the skin (K);  $\nu$  = Kinematic viscosity of the air ( $\text{m}^2/\text{s}$ );  $\beta$  = Thermal expansion coefficient ( $\text{K}^{-1}$ );  $\alpha$  = Thermal diffusivity of air ( $\text{m}^2/\text{s}$ );  $Gr$  = Grashof number;  $Pr$  = Prandtl Number.

The Grashof number represents the ratio of viscous forces to buoyancy forces in the flow:

$$Gr = \frac{g \cdot L_{th}^3 \cdot (T_{sk} - T_{\infty})}{\nu^2 \cdot T_{\infty}} \quad (2.11)$$

where:  $g$  = Acceleration of gravity  $9.81 \text{ (m/s}^2\text{)}$ ;  $L$  = Vertical height of the body (m);  $T_{\infty}$  = Temperature of the surroundings (K);  $T_{sk}$  = Temperature of the skin (K);  $\nu$  = Kinematic viscosity of the air ( $\text{m}^2/\text{s}$ ). The flow is fully turbulent if  $Gr > 10^{10}$  and laminar when  $Gr < 10^9$ . In human heat transfer, the an example of the appropriate Nusselt number for the whole body,  $Nu$ , is given in Equation ( 2.11 ) in still air as (Clark, McArthur, Monteith, & Wheldon, 1981):

$$Nu = 0.63 \cdot Gr^{0.25} \cdot Pr^{0.25} \quad (2.12)$$

For the human in air, the range of temperatures is limited based on survivability and Equation ( 2.12 ) can be simplified by defining  $Pr=0.71$  .

$$Nu = 0.58 \cdot Gr^{0.25} \quad (2.13)$$

Forced convection is created by the relative, externally driven, movement of the fluid over a more stationary object. The faster the movement of the fluid, the more energy is transmitted. In human thermal applications related to PCS use this is the common heat transfer mechanism. The increased metabolic activity is also driving movement which creates or takes place in fluid flow such as running or swimming. If the fluid temperature is higher than the body temperature, the energy is transferred into the body. Different fluids affect the heat transfer coefficient, with liquids being higher than gasses. The convection is characterized Nusselt Number using the characteristic length, L for specific shapes (Incropera et al., 2007). An example of a forced convection correlation is a cylinder in cross flow. The boundary layer is dependent on the dimensionless Reynolds number for a cylinder is given (Incropera et al., 2007):

$$Re_D = \frac{VD}{\nu} \quad (2.14)$$

Where V is the Velocity, D is the characteristic length: the diameter (m), and  $\nu$  is the kinematic viscosity ( $m^2/s$ ). The Reynolds number is used to determine an average Nusselt number for a cylinder in cross flow with different constants, “C” and “m” corresponding to different Reynold Number,  $Re_D$ , ranges. The corresponding tables can be found in Table 7.2 on page 426 of Incropera et al. (2007).

$$\overline{Nu}_D = C Re_D^m Pr^{1/3} \quad (2.15)$$

The bar over the Nusselt number, denotes the average value for the surface. The Nusselt number from Equation ( 2.15 ) can be used in Equation ( 2.9 ) and the heat transfer coefficient becomes the average  $h$  for the surface and the characteristic length is  $D$ . The average length can be redefined as  $h_c$ .

$$Nu = \frac{\bar{h} \cdot D}{k} = \frac{h_c \cdot D}{k} \quad (2.16)$$

The convective heat transfer coefficient can be approximated as spheres and cylinders (J.A.J. Stolwijk, 1971) or may be taken from measured data taken on thermal manikins or humans (Danielsson, 1993). The form of Equation ( 2.7 ) for convective heat transfer is shown below.

$$Q = h_c \cdot A \cdot (T_{sk} - T_{\infty}) \quad (2.17)$$

### **2.2.2.3 Radiation**

Unlike the previous methods of heat transfer discussed, radiation does not require contact with a medium to transfer energy. In this application, the radiation referred to is thermal radiation, as opposed to higher energy particle radiation found in nuclear applications. Thermal radiation is the transfer of energy from one point to another through light energy. Thermal radiation is dependent on the surface temperature of a substance, the surface properties, and the medium through which the radiation is transmitting. The net rate of transmission will depend on the temperature difference between the two objects.

In human thermal applications, radiation is important when studying thermal comfort in automobiles with sun shining through the window (A. Curran et al., 2006), workers in high radiant environments (Choi, Kim, & Lee, 2008) metal work reference, and in the military in desert conditions (Buller et al., 2008). The complexity of the interaction of radiation with

different surfaces can lead to radiation being generalized or specifically modeled. In indoor applications radiation can sometimes be easily generalized if there are no significant, non-uniform temperature differences.

The radiation leaving a surface by emission or reflection is a point source that leaves a differential area  $dA_i$  and is transmitted over a solid angle subtended by  $dA_j$  which views  $dA_i$  at some angle  $\theta$ . Radiative heat transfer occurs from one surface to another conceptually as a small differential element emitting radiation throughout the arc of a semicircle. This is given as a differential solid angle  $d\omega$  and is applied at the surface of the hypothetical hemisphere as a differential area  $dA$ .

$$d\omega = \sin(\theta) d\theta d\Phi \quad (2.18)$$

Where:

$\theta$  = Angle from the normal of emitting surface from 0 to  $\pi$  radians

$\Phi$  = Angle in plane with the emitting surface in from 0 to  $2\pi$  radians

Spectral radiation intensity will allow application to a surface that is not directly tangent to the hypothetical surface. The radiation incident on the surface is then the component of  $dA$  perpendicular to the direction of radiation per unit wavelength interval  $d\lambda$ . Redefining the viewing surface as at some angle  $\theta$ , which is 0 normal to the surface, the outer hemisphere views the differential emitting area  $dA$  as:

$$dA = dA \cdot \cos(\theta) \quad (2.19)$$

Because the intensity is dependent on the wavelength, this allows the spectral intensity of emitted radiation to be defined as:

$$I_{\lambda,e} = \frac{dq}{dA \cdot \cos(\theta) \cdot d\omega \cdot d\lambda} \quad (2.20)$$

Where:

$\theta$  = Angle from the normal of emitting surface from 0 to  $\pi$  radians

q = Radiant energy emitted (W)

dA = Differential area of emitting source

$\lambda$  = Wavelength of the emitted radiation ( $\mu\text{m}$ )

$\omega$  = Solid angle dependent on the distance r from the source

Rearranging Equation for dq, and integrating over the total hemisphere, the total hemispherical emissive power per unit area and unit wavelength,  $E_\lambda$ , can be calculated and has units  $\text{W}/(\text{m}^2 \cdot \mu\text{m})$ . Similar concepts can be therefore applied to irradiation radiation that is incident on a surface. Irradiation can come from emission and reflection coming from other surfaces and will have the same directional and spectral distributions defined by spectral intensity from Equation ( 2.20 ). The spectral irradiation,  $G_\lambda$ , is the rate of radiation at wavelength  $\lambda$  is incident on surface per unit area and unit wavelength. By employing the concept of a diffuse emitter at a surface, the intensity of the emitted and incident radiation is independent of the direction. This means that  $I_\lambda$  is independent of  $\omega$  and  $\theta$  and can be removed from the integrand as a constant making equations for the  $E_\lambda(\lambda)$  and  $G_\lambda(\lambda)$ :

$$E_\lambda(\lambda) = I_{\lambda,e}(\lambda)\pi \quad (2.21)$$

$$G_\lambda(\lambda) = I_{\lambda,i}(\lambda)\pi \quad (2.22)$$

The last term of the radiative heat flux is radiosity, which accounts for all of the radiant energy leaving a surface. The radiosity, J, includes the reflected portion of the irradiated energy



as well as the emitted energy. The spectral radiosity  $J_\lambda$ , is similar to the incident spectral radiation intensity, except that it includes the reflected portion of irradiation. It has units of  $W/(m^2 \cdot \mu m)$  and is expressed by the term:

$$J_\lambda(\lambda) = \int_0^{2\pi} \int_0^{\pi/2} I_{\lambda,e+r}(\lambda, \theta, \Phi) \cdot \cos(\theta) \cdot \sin(\theta) d\theta d\Phi \quad (2.23)$$

Similarly, if the surface is both a diffuse reflector and diffuse emitter then,  $I_{\lambda,e+r}$  is independent of  $\theta$  and  $\Phi$ , and the spectral radiosity can be defined as:

$$J_\lambda(\lambda) = I_{\lambda,e+r}(\lambda)\pi \quad (2.24)$$

Introducing the concept of a blackbody in radiation heat transfer allows the evaluation of emissive power, irradiation and radiosity of real surfaces. Blackbody's absorb all incident radiation regardless of direction, wavelength; no surface at the same temperature and wavelength can emit more energy. The black body is a diffuse emitter, compared to a specular emitter that is dependent on incident and emission direction.

In order to simplify calculations a view factor can be calculated for an object's relation to another object. This is defined as  $F_{i-j}$ , where the view factor is the fraction of radiation leaving surface  $i$  that is intercepted by surface  $j$ . In an enclosure, the sum of all view factors is equal to 1. View factors are important because they allow the use of basic heat transfer functions for complex surfaces and allow for the reduction of the radiation to the basic form from Equation (2.7) through the calculation of a linearized heat transfer coefficient. Without this, a complex FEA or Monte Carlo simulation can be run using the fundamental equations.

If the view factor summation in an enclosure is applied to a small convex object in a large cavity, an equation can be formulated for a blackbody

$$q_{12} = \sigma_{sb} \cdot A_1 \cdot \epsilon_1 \cdot (T_{sk}^4 - T_{\infty}^4) \quad (2.25)$$

and then reorganized into the form of Equation (2.7)

$$h_r \cdot (T_{skin} - T_{\infty}) \cdot A = \sigma \cdot A_1 \cdot \epsilon_1 \cdot (T_{sk}^4 - T_{\infty}^4) \quad (2.26)$$

where:

- $T_{skin}$  = Temperature of the skin (K)
- $T_{\infty}$  = Wall temperature of the enclosure (K)
- $\sigma_{sb}$  = Stefan-Boltzmann constant  $5.670 \cdot 10^{-8}$  (W/(m<sup>2</sup>·K<sup>4</sup>))
- $A = A_1$  = Area of object 1 (m<sup>2</sup>)
- $\epsilon_1$  = Emissivity of object 1
- $h_r$  = Linearized heat transfer coefficient (W/(m<sup>2</sup>·K))

The purpose of this abbreviated derivation is to define the linearized heat transfer coefficient, which is achieved when solving for  $h_r$  and yields two equations, the equation for the linearized heat transfer coefficient and the Newton's Law of Cooling equation.

$$h_r = \sigma_{sb} \cdot \epsilon_1 \cdot (T_{skin} + T_{\infty})(T_{sk}^2 + T_{\infty}^2) \quad (2.27)$$

$$Q = h_r \cdot (T_{sk} - T_s) \cdot A \quad (2.28)$$

In the model the view factor is accounted for by using the mean radiant temperature of assumed temperatures. Empirical values are used to define values for a standing person or a seated person in a rectangular room using the temperatures at each wall. Using these values, the linearized heat transfer value can be defined. This can be found in Chapter 9 of the ASHRAE Fundamentals Handbook 2013 for use in human thermal modeling (ASHRAE, 2013).

In many cases, convection will play a larger part in energy transfer to and from the body than radiation. However, in this application convection will likely have a smaller energy transfer to or from the body due to the skin temperature being within about 5 °C of the air temperature.

Although the convective coefficient is approximately 3 times larger than the radiation coefficient used for the simple model, the difference between skin temperature and the mean radiant temperature is also three times larger than the convective coefficient. In this case convection and radiation may share a more equal role in fundamental heat transfer. However, this does not incorporate the clothing effects discussed below in Section 2.2.3.1. The results from the human thermal models presented in Chapter 5 include some discussion on this issue.

#### ***2.2.2.4 Evaporation***

The last heat transfer method utilized by the human body to expel energy is through evaporation of sweat. Technically, evaporation is not a heat transfer mechanism and is actually a mass transfer application. Evaporation removes energy from the body when the air causes liquid water on the skin, or absorbed in the clothing, to change phase and become a gas. The process of changing phase requires energy, which is supplied by the body or clothing. This energy goes into the liquid increasing its energy level in accordance with the first law of thermodynamics. The vapor becomes part of the air and increases the mass fraction of water in the air. The mixture has a limit at which it can hold water at any given temperature, represented by the relative humidity, and listed as a percentage. The relative humidity can also be related to the concept of partial pressures. The partial pressure is the actual pressure of the water vapor that occurs in the air mixture at a given temperature. If the partial pressure reaches the water's saturation pressure the liquid condenses, and the relative humidity is 100%. The higher the relative humidity, the less ability water has to evaporate. The local concentration next to the body is affected by the speed of movement of the air, changing the available concentration gradient. In the current application of a dismounted soldier in the desert of the middle east, the higher air temperature and low relative humidity causes evaporation to dominate the heat loss from the human. The energy lost

to evaporation is the evaporated mass transfer rate multiplied by the latent heat of evaporation:  
heat loss is as follows.

$$Q = \dot{m} \cdot h_{fg} \quad ( 2.29 )$$

where:

$\dot{m}$  = Mass flow rate of evaporating sweat (kg/s)

$h_{fg}$  = Latent heat of vaporization of sweat (J/kg)

This mass transfer,  $\dot{m}$ , is driven by the diffusivity and mass concentrations differences. The mass concentrations or densities can be converted to partial pressures. It is common in human comfort research to cast this energy transfer into an equivalent Newton's law using an evaporative heat transfer coefficient. Known psychrometric principles can be applied based on both the skin surface and the ambient air temperatures. The air is assumed to have a relative humidity  $\phi$ , the relative humidity is defined as the partial pressure of a percentage of water vapor with air over the partial pressure of the water vapor fully saturated and air both at a specific temperature. The mass transfer equation can then be written in terms of the relative humidity of the surface of the skin and the air. The surface of the skin is assumed to be completely saturated, defined as having liquid water present.

$$Q = h_e \cdot (P_{sat}(T_{skin}) - P_{sat}(T_{\infty}) \cdot \phi) \cdot A_w \quad ( 2.30 )$$

And

$$h_e = \frac{h_D \cdot h_{fg}}{R_w \cdot T_{avg}} \quad ( 2.31 )$$

where:

$h_e$  = Evaporative heat transfer coefficient (W/(Pa·m<sup>2</sup>))

$P_{sat}(T_{skin})$  = Saturated pressure of water at skin temperature (Pa)

$P_{sat}(T_{\infty})$  = Saturated pressure of water at surrounding air temperature (Pa)

$\phi$  = Relative humidity

$R_w$  = Gas constant for water vapor 461.37625 (J/(kg·K)) (Moran and Shapiro 2004)

$T_{avg}$  = Average temperatures of  $T_{skin}$  and  $T_{\infty}$  (K)  
 $h_D$  = Mass transfer coefficient ((kg/(s·m<sup>2</sup>))/(kg/m<sup>3</sup>))  
 $A_w$  = Area of skin wetted (m<sup>2</sup>)

The mass transfer coefficient, and mass density of the water are also not values commonly measured. Using the Lewis Ratio,  $LR$ , from the properties of ideal gas and tabulated values for air, the heat and mass transfer analogy can be applied to relate convection to evaporation. The Lewis Ratio is the ratio of the evaporative heat transfer coefficient to the convective heat transfer coefficient. The derivation is well documented and will not be repeated here. The structure for the derivation can be found in Incropera et al. (2007)

The heat and mass transfer analogy includes a large number of assumptions. The Lewis Ratio does vary with respect to pressure, as pressure decreases the ratio increases. This can create errors when comparing to data formulated by others which was normalized to sea level Gage and Nishi (1977). Similarly, the value evaporative transfer coefficient can be inverted to form an evaporative resistance, which can then be used as clothing resistances.

To address the sweat rate of the body when the skin is not completely saturated with sweat, a skin wettedness factor,  $w$ , is used in some models. In the popular two-node model adapted in ASHRAE (2013). This is a function, which relates the extent to which the skin is saturated in the defined conditions, and is multiplied by the Dubois Area, the body surface area, to supply the term for the wetted area  $A_w$ , in Equation ( 2.30 ). This model is limited, because it does not account for the effects of excess sweat and wetting of clothing fabric. This is a major limitation in the model in hot, uncompensable environment possibly not modeling all the heat loss to the environment and is a fundamental topic of Chapter 5.

### ***2.2.3 Human factor effects***

Some causes of heat stress can be mitigated by the human's actions. It is assumed that the human experiencing energy storage would change indoor ambient conditions, or wait for the weather to change outdoors, if possible. This leaves things immediately under the control of the human, generally clothing including personal protective equipment and activity level. Even with individual control over clothing, equipment, and activity level, is not always possible in the extreme conditions in which military operations take place to maintain the function of PPE and address heat stress concerns by removing equipment. This ultimately creates an interrelation between both clothing/PPE and activity level where the warfighter can't stop and rest because mission success and survivability rely on continuing, and can't change clothing and PPE due to rule and regulations as well as meeting the existing threats (Buller et al., 2008; Cadarette, Blanchard, Staab, Kolka, & Sawka, 2001; Potter, Karis, & Gonzalez, 2013).

#### ***2.2.3.1 Clothing/PPE***

Clothing and personal protective equipment (PPE) are two major causes of decreased natural heat transfer and lead to heat storage in the body. Clothing provides a barrier to thermal heat transfer including radiation, convection, and conduction as well as to latent heat transfer by evaporation. This resistance makes it more difficult to transfer energy to the environment. The modern idea of thermal clothing resistance goes back to Gagge, Burton, and Bazett (1941) with the introduction of the clo unit. One clo is approximately equal to the thermal resistance of a man's wool business suit. In SI units one clo is  $0.155 \text{ (m}^2\text{K)/W}$ . The evaporative resistance is given in terms as the inverse of the evaporative heat transfer coefficient as the partial pressure gradient  $\text{(m}^2\text{Pa)/W}$  (ASHRAE, 2013).

In some cases, clothing and equipment is required as personal protective equipment. In military applications, clothing provides some protection against the sun, plants, and other parts of

the natural environment. Other equipment, such as body armor and CBRN MOPP (Mission Oriented Protective Posture) gear may be required to protect against ballistic and fragmentation threats or WMD's respectively.

In a field study by Buller et al. (2008), a marine who overheated had to remove his ballistic vest once inside the vehicle in order to increase the ability to expel heat to the environment and prevent deadly heat stroke. The link between heat stress and PPE is basic and well established by the amount of literature related to heat stress management in PPE. This is evidenced by the majority of the articles concerning PCS found in the review table at the end of this section are related to restrictive PPE such as HAZMAT, firefighting, body armor, or CBRN.

#### ***2.2.3.2 Activity Level***

The metabolic rate is the final piece of the heat storage equation that the human can exert control on through activity level. A main component of the metabolic rate is the weight being carried. A warfighter marching 20 km in 3 hours would require more energy expenditure if they were carrying 50 kg rather than 10 kg. The classic equation by K. B. Pandolf, Givoni, and Goldman (1977) allows for the estimation of the metabolic rate and thus human thermal effects.

In cases where the activity level is too high, efforts have to be made to bring the average activity level down, allowing the body to dissipate stored energy to the environment to prevent heat stress. This became an important issue in training camps in the United States during World War Two, where death from heat stroke was becoming a serious issue. Researchers developed the now standard Wet Bulb Globe Temperature (WBGT) to determine the ability of the trainees to dissipate metabolic energy to the environment. Ultimately, a set of WBGT temperature ranges were created, which corresponded to the color of flag that was flown over the base, which

determined the maximum activity level, by type, that could be performed in those conditions (Budd, 2008).

The WBGT is still used in both military and civilian applications, and the average activity level is primarily managed through the use of tabulated work rest cycles. Depending on the task that is to be completed, a work rest cycle is selected which specifies a time period where the warfighter can work, and then must rest as shown on page 13 in “Heat Stress Control and Heat Casualty Management” (Sawka et al., 2003) This same approach is used in civilian applications, however the amount of heat storage is more conservative to protect the safety of the worker (ISO, 2004).

## **2.3 Human Thermal Models**

Thermal modeling of the human body in some form has been around for over 100 years. The first representations used heated objects to represent human temperature going as far back as Faraday (K. Parsons, 2002). Although thermal modeling as it is incorporated today is a relatively new field. Early notable studies by Adolph (1947) on heat stress examined the effects of different temperatures on humans. Beginning in the early 20<sup>th</sup> century the first “modern” model was designed by Machle and Hatch (1947). Human thermal models vary in complexity by layers used, number of body segments, number of elements, heat transfer equations, clothing effects, and physiological control mechanisms among other effects. For simplicity, the models will be split up by one, two, and multiple node models.

### **2.3.1 Single node**

Single node models are the most basic models, using one compartment to represent the entire body. Many of these models, if they can be described as such, use one measurement to predict the state of the body. They are usually based strictly on empirical data or are a lumped



capacitance body model. These can be found in specialized applications such as Fanger's PMV prediction model (Fanger, 1973). These are also in common use for temperature rating of clothing and sleeping bags according to ASTM and EN standards (ASTM, 2011; EN, 2012) With only one compartment variations between core and skin are ignored, which can lead to a loss of resolution.

### ***2.3.2 Two Node Models***

A two node model, Machle and Hatch (1947), was the first of the modern, advanced human thermal model. This was a core and shell model and the precursor of the current two node models. This class of node models represented a core node surrounded by a skin node. The skin blood flow determined the percentage of the body's mass allocated to each compartment. The skin and core were each assumed to be at uniform temperatures. The respiratory exchange takes place between the core and the outside while the rest of the exchange is with the skin surface. The next, and arguably most significant two node model, was developed by Gagge, along with Stolwijk and Hardy (Gagge, Stolwijk, & Hardy, 1967), and was a simplification of the multimode model created by J. A. J. Stolwijk and Hardy (1966), discussed in the next section. This model, also known as the Pierce Model, was continually updated and was improved by Gagge and Nishi (1977). This model would go on to be modified and incorporated into the Fundamentals Handbook for the American Society of Heating, Ventilating, and Air Conditioning Engineers, now ASHRAE (ASHRAE, 2013). X. Wang (1994) would publish a correction to the Gagge model to add a proportional adjustment based on the net rate of body energy storage to improve the reaction to ramp transients. The KSU Model was intended to improve the prediction of thermal sensation and separates the thermal sensation votes (TSV) for warm and cold environments (Azer & Hsu, 1977).

A number of different models took advantage of the simple nature of the two-node approach and used it as a basis for improved modeling of clothing effects. A number of clothing models were developed at Kansas State University as part of models containing two or more segments. The Tranmod model, is a modification of the Gagge model except that the moisture transport through the clothing is modeled and the skin node is split up into multiple segments, each with the area and thermal and evaporative resistances of the clothing covering that area (Jones & Ogawa, 1992; Jones & Ogawa, 1993). The Clo-Man model, by Lotens (1993) is another simple two node model with an improved clothing model incorporating moisture transport. This research uses the current formulation of the ASHRAE model, while exploring improvements on the sweat model.

### ***2.3.3 Multiple node Models***

The next step in model complexity involved the division of the body into multiple segments with different segments modeled with an energy balance and layers linked by basic heat transfer (Eugene H. Wissler, 1961, 1964). The Wissler model used six cylinders representing the legs, arms, trunk, and head linked to heart and lung representations. This model was used as the basis of the first model by J. A. J. Stolwijk and Hardy (1966) with a head, trunk, and one extremities node, four layers, and a common blood pool. This was followed by the popular model by J.A.J. Stolwijk (1971) which was developed for NASA and expanded to 25 nodes, using symmetry to cut down on calculations, but removing the ability to handle asymmetric effects. Wissler also expanded on his model to simulate the thermoregulation process of the body and interface with an automatic thermal control system for astronauts (K.L. Nyberg, Diller, & Wissler, 2000; Karen L. Nyberg, Diller, & Wissler, 2001). The body was

represented by 15-elements, each with 15 nodes for a total of 225 nodes. Each element contains muscle, bone, fat, and a blood exchange system (E. Wissler, 1985; E. H. Wissler, 1971).

Gordon, Roemer, and Horvath (1976) expanded Stolwijk's model to 14 compartments with 11 layers. Arkin's model (Arkin, Xu, & Holmes, 1994) used 14 concentric cylinders with 4 layers and handles small blood vessels with blood at different velocities along with a counter-current heat exchanger for large vessels. The Smith-Fu models also developed at K-State by Dr. Jones and has 15 cylindrical nodes, divided into concentric layers (Fu, 1995; C. E. Smith, 1991). Each layer is divided and assigned properties according to the type of tissue: brain, bone, fat, lung, muscle, etc. Smith used measured blood flows to get correct blood to each layer. This model was later expanded by Fu adding heat exchange between the blood and body tissue, separating the fat layers, and introducing the Jones and Ogawa clothing model.

Further expansions of the Stolwijk model include the model by Tanabe, Kobayashi, Nakano, Ozeki, and Konishi (2002), Li's Model (Yi, Fengzhi, Yingxi, & Zhongxuan, 2004), Salloum's Model (Salloum, Ghaddar, & Ghali, 2007), and the 33 Node comfort model (33 NCM) based on the work by Tanabe (Streblow, 2010).

The model developed by Fiala (Dusan Fiala et al., 2012; Dusan Fiala & Lomas, 2001; Dusan Fiala et al., 1999; D. Fiala et al., 2001; Lomas, Fiala, & Stohrer, 2003; Nelson et al., 2009) is a multi-node, multi-layer model and is based on Wissler, Stolwijk and Hardy, and Gagge, among others. Using the data from 26 experiments, a set of empirical equations were developed to represent the body's control of shivering, sweating, vasodilation, and vasoconstriction that arrived at good agreement with core and skin temperatures. This model uses over 3000 elements and can interact with non-uniform boundary conditions.

Fiala's model was incorporated by Curran into the commercial radiation thermal solving program TAItherm/RadTherm (A. Curran et al., 2006). The TAItherm/RadTherm program allows the simulated human to interact with the environment through radiation, convection, conduction and evaporation. In this formulation, a number of changes were made to the base version of Fiala's model to better match experimental data. This model is covered in more detail in Section 5.1.2.

#### ***2.3.4 PCS Human Thermal Modeling***

The modeling of PCS on humans is seen in literature to generally try to predict change in core or mean body temperature or cooling effect on the body. Some attempts use existing models, such as the current work, and others develop new models to be able to predict the effects. Biermann (2005) modeled soft body armor and a wicking material around the armor using a version of the Wissler model. Similarly, Eugene H. Wissler (1986) did an evaluation of a PCS type known as a Liquid Cooling Garment (LCG) using his model for more terrestrial endeavors. This thermal model has also been used to develop and evaluate cooling systems for astronauts in protective space suits (K.L. Nyberg et al., 2000; Karen L. Nyberg et al., 2001; Pisacane, Kuznetz, Logan, Clark, & Wissler, 2006). These systems must remove body heat and expel it outside the protective and insulated space suit. The goal of the physical system is to dissipate the metabolic energy and keep the sweat rate down to avoid the complications of moisture in microgravity. Bogerd, Psikuta, Daanen, and Rossi (2010) and Hepokoski et al. (2012) both used physiologically controlled manikins to evaluate PCS. The U.S. military has used a human thermal model to evaluate personal cooling systems in work by T. L. Endrusick, Berglund, Gonzalez, Gallimore, and Zheng (2006), Yokota, Endrusick, Gonzalez, and MacLeod (2010), and T. Endrusick, Gonzalez, and Berglund (2007) among the other examples listed in

this section. Kuznetz (1980) used the 6-cylinder Stolwijk and Hardy model to evaluate PCS for NASA. Perez, Tooker, and Nunez (1994) used the ASHRAE model to predict values for a combination spacer vest and personal cooling system. Xu's six-cylinder model was used in a variety of ensembles including seminude, BDU/ACU with body armor, and CBRN/MOPP equipment. A number evaluations and predictions of PCS using LCGs (Xu, 1999; Xu, Berglund, Chevront, Endrusick, & Kolka, 2004; Xu et al., 2005; Xu, Endrusick, Laprise, Santee, & Kolka, 2006) and an evaluation and prediction of an Air Circulation system (Xu & Gonzalez, 2011).

## **2.4 Personal Cooling System Types**

Conventionally, the goal of the PCS is to reduce or eliminate the stored heat in the body. Removing energy from the body allows for longer working times before heat stress becomes an issue. However, some PCS systems may be detrimental because they may create vasoconstriction in the wearer, prevent some of the body's natural cooling abilities, or due to weight, size or logistical difficulties may not be applicable to the final intended use. The different types of PCS available and their advantages and disadvantages are discussed. This section will cover the two aspects of PCS function: energy removal mechanisms and their application methods. The previous section provided the background on the mechanism of energy transfer and this section will discuss the mechanisms of providing either or both the temperature difference or mass concentration difference necessary to achieve energy removal from the body in a PCS. The final part of this section is the table compiled reviewing previous PCS studies, their test methods, and applications.

### ***2.4.1 Cold Boundary Technologies***

The energy removal section is focused on the technology required to create the transfer of energy away from the body. This can be only done by the creation of either or both a temperature gradient or a mass concentration gradient. The cooling methods described in this section provide a cold boundary temperature to the body through the application method by either storing energy in a material or rejecting energy to the environment. The three major types are phase change materials (PCM), vapor compression refrigeration cycles, and thermoelectric cooling.

#### ***2.4.1.1 Phase Change Materials***

One of the most common technology used in PCS on the market are materials that absorb heat during their phase change process. This could technically describe almost all of the PCS, in

this application. For this application the Phase Change Materials (PCM) are designed to absorb heat during their transition between one phase to another, specifically PCM that absorb heat to change phase from solid to liquid and solid to vapor and are not considered part of a refrigeration cycle. This includes subliming solids such as frozen CO<sub>2</sub> (Dry-Ice) transitioning to vapor. Most of the phase change materials that are in the KSU PCS database consist of solid to liquid phase change with the exception of the aforementioned CO<sub>2</sub> systems. These materials encompass three different types of phase change products; Ice, Paraffin, and Gels. There are multiple formulations of each of these and there are also different packing methods.

All solid to liquid phase change materials do share similarities. As these materials change phase, the temperature of the material stays constant until the phase change process is complete. In addition, as the materials change phase their heat transfer properties change. This can delay or speed up the phase change. This can be especially problematic for recharging phase change materials by converting them back to their solid state. The issue occurs when the outside of the PCM freezes and insulates the inside of the material from freezing. This requires more time and power to freeze the material (Zalba, Marín, Cabeza, & Mehling, 2003).

The fundamental thermodynamics behind the phase change process is the same from material to material. Each material has latent heat of fusion (LHF), which is the amount of energy that must be added or removed during the phase change per unit mass. This quantity is specific to each material. In addition, the amount of energy to be dissipated or absorbed to change temperature before and after the phase change is dependent on the specific heat and the temperature differences. In this case, the temperature differences will be from the cold temperature to the phase change temperature, and from the phase change temperature to the final body or environment temperature for melting. The equation for the total energy absorbed by the

PCM can be found in Equation ( 2.32 ) below.  $Cp_S$  is the specific heat for the solid phase of the material,  $Cp_L$  is the specific heat for the liquid phase of the material, and  $LHF$  is the latent heat of fusion and  $m_{pcm}$  is mass of the PCM.  $T_{initial}$  is the sub cooled starting temperature of the PCM,  $T_{PC}$  is the phase change temperature, and  $T_{final}$  is the final equilibrium temperature.

$$\text{Energy} = (Cp_S \cdot m_{PCM})(T_{PC} - T_{initial}) + LHF * m_{PCM} + (Cp_L * M)(T_{final} - T_{PC}) \quad ( 2.32 )$$

A large portion of the energy absorption during this process takes place during the phase change process. Therefore, the LHF is the value that will be compared from material to material with weight as a constant. The higher the LHF, the more energy the material can absorb and therefore the longer it can function or less mass is required for energy removal over a set time period.

The materials are incorporated into many different forms to allow heat to be transferred from the body. The different materials and their advantages and disadvantages have advantages and disadvantages from a perspective of personal cooling for the dismounted Soldier. The information provided in Pasupathy, Velraj, and Seeniraj (2008) and Zalba et al. (2003) provide the best references covering different types of phase change materials and their properties in their respective review articles.

#### **2.4.1.2 Vapor Compression Refrigeration Cycle**

The vapor compression refrigeration cycle is a relatively common cooling mechanism responsible for air conditioning and refrigeration. This process uses a liquid to gas transition (evaporator) to provide the cooling. It also contains a nozzle, a compressor, and a condenser to create a cooling cycle. This is done by using the change in enthalpy in the phase change from liquid to gas, and then to a lesser extent the energy absorbed by the expanding gas to absorb heat



from the object being cooled. The evaporated vapor is compressed, requiring an energy input into the compressor from a power source to run the motor, The phase change process back to liquid requires the rejection of the energy gained and brings the vapor back to the liquid state. After flashing through the nozzle the liquid/vapor mixture is at the starting point to begin the cycle again. This cycle has the advantage of removing large amounts of energy. Smaller, portable forms of these systems have been created that can be carried as a cooling source, other PCS applications can also be tethered to a larger, stationary system. The rejection of energy to the environment requires a power source that either must be carried or tethered. It would also be feasible to use a passive device where the potential energy sink would have to be carried, as in an absorption system.

Unfortunately, this technology requires relatively complex machinery compared to the other PCS devices. Conceivably, these systems could require more maintenance over the life of the device compared with some of the other systems. Some compressors make noise as it is compressing the gas into a liquid, which we have noted in our studies, and may not be ideal if noise discipline is an issue in the end use application. This type of system will also have a hot spot that is rejecting the heat from the body at high heat flux. This high heat flux creates high temperatures that show up very easily on thermal imaging. A portable power source is also required, if tethering is not an option, and likely be a battery of some kind that would have to be replaced to extend the life of the device. This would create extra weight and bulk for the dismounted soldier to carry. Other power sources could include liquid fuel generators, engines, or fuel cells. In addition, the system will also need to have a compressed vapor canister. These contain the vapor under high pressures and can cause frostbite or impact wounds from a punctured or damaged canister. The mechanical and thermodynamic efficiencies of these

systems are limited by the design and construction of the device, which requires more power available than the cooling provided. If sufficient power is available, this type of system can theoretically provide a high amount of cooling.

#### **2.4.1.3 Thermoelectric Cooling**

Thermoelectric cooling is the most obscure of the methods of personal cooling and unlike vapor compression refrigeration cycles, the fundamental information can be found in some of the standard undergraduate thermodynamics texts. The principles of thermoelectrics have been around since the 1800's when Seebeck and Peltier made two separate, but related discoveries. First Seebeck discovered when two dissimilar metals were joined at each end to form a loop and if each end were exposed to a different temperature, a voltage and current were created. Using this application, thermal energy could be harvested and applied to produce electrical energy. A few years later Peltier made a similar discovery; if a voltage potential and current were applied to two dissimilar metals arranged in a loop with the junction ends as the two different potentials, then these junctions would be different temperatures. This discovery, termed the Peltier Effect, is when a voltage flux is applied across two dissimilar materials from junction to junction, a heat flux will travel in the same direction as the electrons.

With this principle, a hot or cold effect can be applied to either terminal by changing the voltage input. This gives the user flexibility in using the device both for heating and cooling depending on the conditions. The efficiency of the thermoelectric cooler is dependent on the Peltier coefficient. The Peltier coefficient is directly related to the more commonly discussed Seebeck coefficient by Equation ( 2.33 )

$$\Pi = S \cdot T_{abs} \quad ( 2.33 )$$

where  $\Pi$  is the Peltier coefficient,  $S$  is Seebeck coefficient and  $T_{abs}$  represents the absolute temperature distribution between the junctions.

The Seebeck coefficient is a property of the materials being used for each side of the junction. The nature of the thermoelectric system is such that the efficiency of the heat transfer or energy generation is dependent on the material properties. For both energy generation and cooling the efficiency is dependent on the Seebeck coefficient, which compares the efficiency between the two materials. In addition, these materials are in a voltage and thermal potential. This must mean that the thermal and electrical conductivity must be taken into account. In order to achieve the most efficient system possible the electrical conductivity must be as high as possible to limit the heat generation by resistance,  $Q_{res}=IR$ , where  $I$  is the current and  $R$  is the resistance (inverse of conductance) of the material (R. Yang & Chen, 2005). Heat production will negate the cooling effect being produced by rejecting energy through the system. The thermal conductivity of the material is also a concern in the efficiency. As the objective is to maintain the largest temperature difference possible, either in cooling or energy generation, any heat moving to the cooler side of the junction will negate this difference and decrease the efficiency of the device. The ideal thermoelectric material will have a high Seebeck coefficient: a high electrical conductivity and a low thermal conductivity (insulated). Unfortunately, in most materials the electrical and thermal conductivities of materials are affected by the same atomic structures. In many cases, increasing one will increase the other property essentially negating whatever beneficial properties the other factor achieved. The electrical conductivity value in this case will be defined as  $\sigma$ . However, the thermal conductivity  $\kappa$  is composed of two different components  $\kappa_L$  and  $\kappa_E$ . The thermal conductivity due to the lattice structure  $\kappa_L$  is dependent on the free path and efficiency of the lattice structure characterized by phonons. The factor  $\kappa_E$  is

thermal conductivity due to electronic factors. The thermal conductivity  $\kappa$  is the sum of these two functions. In order to quantify all of these effects on a material in a figure of merit,  $ZT$ , was developed. This figure of merit as defined in Equation ( 2.34 ) allows a comparison of effectiveness from material to material at similar temperatures. The figure of merit in most, if not all materials is temperature dependent.

$$ZT = \frac{\sigma \cdot S^2 \cdot T}{\kappa} \quad ( 2.34 )$$

Metals have high thermal conductivities and generally low Seebeck coefficients making them poor thermoelectric materials. Semiconducting materials such as silicon have proven to be mediocre thermoelectric materials with a maximum  $ZT$  value of approximately 1. This has been the cap of the thermoelectric device since its development in the 1800's and has limited these devices to specialized markets such as optoelectronics and thermal imaging and small coolers. With a better understanding of the structure of atoms and the use of quantum physics in the past decade, problems associated with thermoelectric materials could be explored. This understanding, coupled with the development of nanotechnology, allows for the ability to manipulate the atomic structure of the crystalline materials to achieve the desired properties.

Much of the research on thermoelectric is being concentrated on the thermoelectric materials used for high temperature energy collection and generation, such as waste heat. Although there are laboratory materials achieving a figure of merit as high as 2.4 at 300K these are still in the laboratory test phases and are not close to viable for mass production and implementation. The most efficient, near to commercial thermoelectric module at this point has a figure of merit of approximately 1.5. This translates to a refrigeration efficiency of about 15% in terms of electrical energy supplied.

Thermoelectric devices are extremely lightweight requiring only the battery and the module. They do not have any moving parts and are very rugged. Radioisotope Thermoelectric Generators (RTGs) have been used since the 1970's in space probes and are still functioning today. In thermoelectric cooling applications there are some disadvantages. The heat dissipation side of the junction requires a heat sink that will be expelling not only the heat drawn from the cold side, but also the heat from the electrical energy required to create the heat transfer effect. This can create an extremely hot heat sink that could be dangerous to the touch. If nothing else, this high heat flux will create a thermal heat bloom that could be easily seen in a thermal camera, sight, or scope and reveal the soldier's position. Finally, the low efficiency will mean that the amount of heat that can be drawn from the body will be small (Tritt, 2007; Tritt & Subramanian, 2006).

#### ***2.4.2 Mass transfer energy removal***

All of the mass transfer systems covered in this subsection are supplemental evaporation systems. The differences are how the evaporation is accomplished to aid the body in cooling. The subsections represent the treatments of providing more or faster dry airflow, providing more water to be evaporated, and providing space for the sweat to evaporate (lowering effective evaporative resistance).

##### ***2.4.2.1 Forced Evaporation/Air Motion***

The motion systems generally circulate ambient, conditioned, or pressurized air inside and under the high resistance clothing to aid in evaporation of sweat from the body. The conditioning can come from any of the energy removal systems listed (P. A. Bishop, Nunneley, & Constable, 1991; Hepokoski et al., 2012). The goal of these systems can be any combination

of three components: increase convection coefficient, increased driving potential for evaporation by provide dry air exchange, or increase evaporative coefficient.

As seen in formulations for Equation ( 2.17 ) and ( 2.29 ) both convection and evaporation are linked through the Lewis Ratio, LR, and changing one coefficient will change the other. When cooling with ambient air higher than skin temperature, the convection heat transfer can negatively affect heat storage. This type of PCS can still be desirable because the air circulation system may overcome the limitations of encapsulating or impermeable materials that prevent the evaporation of sweat because of lack of a vapor pressure gradient driving the evaporation. The air circulation system can address both of these issues, which increase the heat loss, if sufficient air can be exchanged with the outside.

#### ***2.4.2.2 Free Evaporation/Saturated Material***

Free evaporation systems are the most basic and one of the easiest to maintain personal cooling systems on the commercial market today and make up a significant portion of the market as well. The term free evaporation is used here to denote unpowered cooling systems relying on evaporation alone, and without externally supplemented airflow. These are phase change and mass transfer systems. They operate by saturating a material with water and by allowing the evaporation of this water to cool the wearer. This can theoretically be used to provide evaporative cooling in places where the body cannot. The low humidity of the surrounding air in desert conditions creates a large potential for cooling through evaporation. Some systems are a laminated bag of liquid waterproof, but vapor permeable material that is filled with water. However, in a high humidity environment this system will be much less effective and possibly a detriment. In order for the evaporation to take place, the material must be exposed to the ambient air with a lower water vapor pressure and may not be covered by impermeable PPE

### ***2.4.3 PCS Application Methods***

PCS application methods are how the cooling device interacts with the body to provide cooling. Some cooling methods are applied to the body in many different ways. This provides both benefits and detriments to the cooling technology. Some cooling technology will only be feasible in certain application methods depending on the end user application, therefore it is useful to separate the concepts.

#### ***2.4.3.1 Liquid Cooling Garment***

The liquid cooling garment (LCG) has become a popular form of PCS application and has been used by the military for aircraft and ground vehicle crews as well as for astronauts. It can provide significant amounts of cooling to anyone who is stationary, can be tethered to a central cooling system, or carries a liquid cooling technology. In addition to the military and astronauts, racecar drivers, professional athletes and surgeons are among the other markets. The self-contained nature of the LCG is beneficial in applications where encapsulating clothing and equipment must be worn and a pass through of PPE needs to maintain the integrity of the PPE against the environment. A liquid cooling garment can cover the torso, the arms, legs head or any combination. The garment consists of a number of small capillary tubes that are sewn into or onto the garment. Cooled water or another fluid is circulated around the suit through the tubes and removes heat from the body through conduction and by convection inside the tubes. The liquid is returned to the cooling unit where the energy is removed and then the liquid restarts the cycle. The cooling system is attached to the wearer by supply and return tubes. The liquid cooling garment system can be attached to a stationary system with a tether and would limit the distance the user could be away from the system. There are also liquid cooling garments that have portable cooling systems that the soldier could carry when dismounted. The cooling system

for LCG systems primarily consists of three different types: phase change materials, vapor compression refrigeration systems, and thermoelectric systems although adsorption and heat pump systems have been tested but operate the much the same as vapor compression refrigeration cycle systems.

Phase change materials are used in some LCG systems to cool the circulated liquid. The PCM used varies among the different manufacturers. Many of these systems use water as the phase change material and the working fluid. A number of PCS mentioned in the literature used solid CO<sub>2</sub> to absorb heat from body and provide potential dry air for evaporation. As mentioned in the section on phase change materials, the weight of the material is directly proportional to the amount of energy that can be absorbed. This means that for a LCG that is cooled by PCM would require a liquid cooling garment full of circulating liquid, a device to circulate the liquid, and a power source for this process. This can create extra weight for the soldier to carry with the same energy absorption as a smaller weight of a PCM vest. However, the main advantage of the PCM LCG is that the placement of the PCM is external to the vest, not underneath like that of a PCM vest. This can facilitate faster cooling material changes and replacements without compromising the soldier's protective posture by removing PPE.

The LCG garment could be used with vehicle mounted liquid cooling systems or electrical power sources so the soldier on a vehicular patrol would have a fresh charge of power when he or she dismounts. The garment can fit comfortably under body armor in many cases. In addition, because the LCG composes a closed system it could be possible to use it when attired in mission oriented protective posture (MOPP) protective gear for CBRN threats. The main disadvantages include the weight of the vest and liquid, when the capillary tubes can also be bent, kinked, and punctured. This compromises the usefulness of the device. In addition, the



fluid inside the PCS must be fungus and bacteria resistant as growth of organic material will grow inside the garment. This can create unpleasant odors and cause clogs that can compromise the flow inside the device, reducing the effectiveness of the liquid cooling garment.

#### ***2.4.3.2 Direct Expansion Vapor Cooling Garment***

Direct expansion vapor cooling garments are some of the oldest systems. Direct vapor cooling garments are composed much the same way as liquid cooling garments with a tube suit or vest. This system releases the gas, liquid, or two-phase mixture directly into the garment to change phase and expand taking the place of the evaporator in a vapor compression cycle. The phase change from liquid to vapor and the expanding gas draws energy from the body to expanding gas. In some cases, the gas is circulated through a tube suit back to the compressor or it is expelled to the environment. In other examples, air is used and is released into an encapsulated garment to provide oxygen for breathing and dry air for evaporation potential as well as cold boundary cooling.

The first type of vapor cooling garments is composed of any of a combination of trousers, shirts, or headwear that consists of capillary tubing. In this case, the capillary tubing is connected to a canister of compressed gas, sometimes a two-phase mixture. In some commercial applications, the gas is a refrigerant gas such as that is used in the vapor compression refrigeration applications. There are two types of PCS that use this technology.

In the first, this gas then exits through ports in the suit. This system is very lightweight as it uses a liquid phase changing to gas as the working fluid in the tubes instead of a circulating liquid when in operation, and the tubes are empty when not in operation. The system also produces a very refreshing cooling sensation for the wearer. The capillaries can suffer some of the same problems as those found in the liquid cooling garment. The tubes can become plugged,

clogged, kinked, and punctured. In addition, the gas that is exiting the canister into atmospheric conditions is under high pressure and very cold when changing phase and expanding. This could cause a danger to the user either from frostbite, or moderate fragmentary risks from an exploding or punctured canister. Furthermore, there are concerns with some of these refrigerants being released into the atmosphere as they may contribute to the depletion of the ozone layer and climate change. From a logistics standpoint, the canisters of gas have to be continually supplied to the user and the cooling effect is in a burst and is temporary.

Comparatively, the vapor compression cycle direct expansion system suits have the advantages of requiring less gas, which decreases the risks of the other type of direct expansion system. In this case, the cooling garment becomes the evaporator of a vapor compression refrigeration cycle invoking the drawbacks of: weight, noise, maintenance. They require a power source that could be a battery, liquid fuel generator, or engine. However, there are potential weight savings compared to an LCG based system with a separate cooling unit.

Direct expansion systems using cryogenic air were tested for use by rocket propellant handlers. One main advantage of this type of system is the breathing apparatus and cooling system were the same. The worker would be in an encapsulated suit to be protected from the chemicals used in the rocket fuel preventing evaporation (Doerr, 2001).

#### ***2.4.3.3 Encapsulated materials***

The most common type of application of phase change materials is encapsulated in garments or packs. This is a container, usually a pouch, which is filled with the phase change material and sealed. Garments are worn that have these packets sewn into the material or pockets are sewn for the packets to be placed and removed for recharging. Garments can consist of head cooling pads in helmets, neckbands, vests, whole body suits, palm straps, arm garments, etc.

Some PCM garments are insulated on the outside of the garment to protect from gaining too much heat from the environment.

#### ***2.4.3.4 Air Vests***

Air vests have a distribution system such as a rigid or flexible spacer, expandable tubes or bladders. These vests are generally very lightweight, as they only require a plastic or fabric vest, a fan or compressor, and a power source for circulation device. In conditions with a low relative humidity such as desert or mountain climates, these vests can be very effective (Bomalaski, Chen, & Constable, 1995; Chen, Constable, & Bomalaski, 1997; Chinevere et al., 2008; Xu & Gonzalez, 2011). The air that is introduced into the vest evaporates the body's sweat. The sweat evaporation and the convection from the fluid remove heat and the circulation rejects the now humid air and replaces it with the dry air.

There are multiple blown air systems on the market today. Many are battery powered but some are tethered to compressed air supplies like those used for pneumatic tools. There are also examples of chilled and ambient air systems used in military aviation and crew as well as spaceflight applications that are tethered to a refrigeration system (Uglene, Iaconis, & Ciammaichella, 2002). These would be examples of combination systems employing both air circulation and vapor compression refrigeration technology, usually through the use of an air vest or garment. Other tethered systems use a "vortex tube" that takes advantage of fluid and thermodynamic principles to separate the hot and cold parts of the air and only feed the cold component to the wearer. However, any kind of tethered vest would not be useful for the dismounted soldier, as the cooling would be removed when exiting a vehicle or other stationary position. As a result, air circulation systems will refer to ambient air garments keeping with the convention of describing the cooling mechanism.

Blown air vests in this application will need to be fitted underneath an armored vest weighing 40lb or more with water, ammunition and other supplies. This weight could compress the air channels underneath the vest and make it impossible to circulate air. In addition, the effect of the vest is directly proportional to the relative humidity of the outside air and quantity of sweat available for evaporation. The higher the humidity, the lower the capacity for the sweat to be absorbed and the cooling ability is negatively impacted. Also, the vest must be able to introduce fresh air and not allow the higher humidity air under the vest to stagnate as this would eliminate the cooling effect. The battery powered portable systems have the advantage of long runtimes and low weight, which will have less of an impact on the user.

#### ***2.4.3.5 Passive Garments***

Free evaporation and saturated garment PCS are generally worn tight against the body. This will immediately limit any PCS that operates by free evaporation and is covered by impermeable clothing and armor, with encapsulating PPE providing even more limitations unless feasible to be built into the PPE. This could also apply to spacer vests where they may not be practical because they don't provide enough standoff while maintaining PPE protection or the PPE still restricts the airflow. This will restrict many of the commercial free evaporation cooling systems in the application studied in this work, which would be covered by the PPE armor and helmet. The heat removal will also depend on the amount of exposed area for evaporation to take place. With a fully armored and uniformed soldier there are not many places such a garment would be able to remove heat. The available body locations would also be experiencing convection and evaporation from the sweating from the body's natural thermoregulation system. This would make the system something new the soldiers would have to carry and maintain. At 100% skin wettedness the uniform would be wetted as well and would allow for evaporation.

## **2.5 Other Cooling Methods**

In reviewing the literature, PCS were often compared to other forms of body cooling to increase performance and safety to prevent heat stress. Common methods were compared that were used for first responders, military, industry, and sport. Some of the more common were water immersion of a part or all of the body, spray with water, misting with water, stationary in front of a fan, or being placed in an air-conditioned vehicle. Although, in the literature, where these methods are studied are sometimes not portable, or necessarily personal, they do provide a comparison to heat removal by PCS.

## **2.6 Previous Studies**

This section would be incomplete without a review of personal cooling systems in literature. There have been many reviews of PCS in literature. For the sake of this review, PCS literature published in journals, conferences, and government reports will be included, especially considering the military application targeted in this work. A selection of PCS literature relevant to this work will be covered in more detail. Appended in this section will be a table including a near complete list of PCS studies available in literature included with relevant information to assist other researchers in their work. The table is split up under the following titles: Authors, Date), PCS technology, PCS implementation, Type of PCS Evaluation and Measurement techniques. The Authors (Date) field is hyperlinked to the Bibliography for ease of use. The fields are designed to follow the structure of the description of PCS in literature, a brief summary of each topic follows.

The PCS energy removal field denotes the type of system removing heat from the body. The PCS technology either stores the energy as in the case of PCM, or rejects it to the environment in a vapor compression cycle. Many of the systems reviewed are in research tests,

especially in designing PCS systems and PCS implementation systems. In many research situations, a temperature-controlled water supply is used, or the source for cool water or air is not specified, in these cases the term “external cooling source” is used as a placeholder. In many cases, this could be a vapor compression refrigeration, PCM, or thermoelectric cooling source for portable cooling. This field does not describe how the energy is removed from the body, which is covered in the PCS application field.

The PCS application field covers the heat and or mass exchange from body to the PCS. Examples of this field include liquid cooling garments (LCG) in their various coverage areas, air vest, saturated garments, and PCM vests. Types of PCS describe how the PCS is being evaluated in the paper including thermal manikin and human subject testing. This could also include the development of a PCS. The intended use field includes the application of the PCS to a specific garment or end use. In many articles and reports, the use of personal protective equipment (PPE) is very common, usually involving military ensembles, body armor, HAZMAT, chemical biological radiological and nuclear (CBRN), firefighting, first responders. The dominant civilian applications are sport and industry. Finally, the measurement technique field includes details of how the tests were performed, design goals, research objectives, PCS types, and measurements taken. The goal of the table of review articles is to provide a reference for future research on PCS.

Authors (Date)	PCS Technology	PCS Implementation	Type of PCS Evaluation	Intended End Use	Measurement Technique
(Aitken et al., 2002)	PCM, Cryogenic, Compressed Air, Air Circulation	Garment, Dewar	Thermal manikin, Human subject	HAZMAT	Underpants, shorts, t-shirt, socks, trainers, hazmat, Rectal temperature, skin temperature 10 sites, heart rate
(ALGERA, 1985)	PCM	LCG, Backpack	Human Subject, System Design	Military, Ground crew, PPE	Single subject, work rest cycle until cutoff, core temperature limited design, rectal temperature, MOPP gear, CRBN, treadmill
(Amorim, Yamada, Robergs, & Schneider, 2007)	PCM	LCG, Palm, Immersion	Human subjects	Military, sport, first responders, PPE	10 subjects, treadmill, counterbalanced heat stress tests, 50% VO <sub>2</sub> max, separated by 41 min cooling and rehydration, summer fatigues, backpack, body armor
(Arens et al., 1998)	Air Circulation	Tethered, Stationary	Human subject	Office, Industrial	Evaluate comfort in office setting using subject controlled fans at different temperatures and fill out comfort questionnaires
(Bansevicius, Račkienė, & Virbalis, 2007)	Thermoelectric	Clothing	Theoretical	Military, industrial, First responders, sport	Discussion on possible PCS cooling technologies, Carnot cycle, thermoelectric, magnetocaloric cooling
(Barbosa, Ribeiro, & de Oliveira, 2011)	Vapor Compression Refrigeration	LCG,	Technology literature review	First responders, Military, Medical	Battery, fuel cell, internal combustion engine, direct expansion vapor compression refrigeration, indirect expansion vapor compression refrigeration, survey of mechanical vapor compression systems for personal cooling, cooling capacity, COP, efficiencies
(Bartkowiak, Dabrowska, & Marszalek, 2014)	External cooling supply	LCG	Human subject	Industrial, PPE	Thermal chamber, t-shirt base with LCG vest, aluminized heat protective clothing, heart rate, core temperature, skin temperature, temperature and %RH of undergarment, 6 subjects, baseline, coolant 22.5±0.5°C, and coolant 19±0.5°C, EN ISO 9886 (2004)

(M. Barwood, Davey, House, & Tipton, 2009)	Air Circulation, PCM Immersion	Immersion, tethered, LCG, Vest, External Fan	Human subjects	Sport, Post exercise cooling	Test until rectal temperature cutoff 38.5°C. Five PCS treatments, thermal comfort, thermal sensation (H. Zhang, 2003), VO <sub>2</sub> , heart rate, skin blood flow, blood pressure, skin temperature four sites.
(M. J. Barwood et al., 2009)	Air Circulation	Air vest, tethered	Human subjects	Military, PPE	Body armor, 10-d acclimation, 6-hour test exposure, 45°C, 10% RH, treadmill, 5km/hr, 2% grade, Ventilated vest, control condition, 8 men, body armor, helmet, BDU, rectal temperature, 5 skin temperatures, heart rate, thermal comfort, RPE, work rest cycle
(Bennett et al., 1995)	PCM	Vest	Human subject	Firefighting, Military, Navy	Navy firefighting ensemble, dungarees, 12 men, control, four-pack PCM vest, six-pack PCM vest, rectal temperature, 4 skin temperatures, three ECG heart rate blood pressure, met, 30-min rest, 30 min work, work rest cycle, treadmill 1.12m/s, 0% grade,
(Biermann, 2005)	Free Evaporation	Wicking material	Human subject, Thermal modeling, Hot plate	Police, Military, First responder	Soft body armor, Berkeley comfort, Wissler model, cool, warm, hot/humid, hot/dry, with and without vest, 3 men, stationary cycle, 34 min, 4 min warm-up, 30 min test, constant pedal and heart rate, no body armor, body armor, moisture wicking, canal temperature, microclimate temperature and RH%.
(P. A. Bishop et al., 1991)	Air Circulation, PCM, A/C, Vapor Compression Refrigeration	LCG Vest, Air Vest, tethered	Human Subject	Military, Industrial, PPE, MOPP	12 males, 2 females, environmental chamber, WBGT 26°C, treadmill 1.34 m/s 40% VO <sub>2</sub> Max, work rest cycle to physiological cut-off, 45 min walk, 15 min rest, LCG worn at rest, Air cooling at rest, conditioned air vest, US Army tank A/C system, rectal temperature, 4 skin temperatures, heart rate, water drinking ad libitum during rest, nude pre and post weights for sweat
(P. Bishop, Ray, & Reneau, 1995)	PCM, Air circulation, Vapor compression,	Tethered, ambient air, conditioned air, LCG	Review Article, Human subjects, Thermal manikin	Military, industry, PPE, CRBN	Review of prominent heat stress and PCS articles before 1995
(Bogerd et al., 2010)	PCM, Free Evaporation	Saturated water shirt, PCM vest	Thermal manikin, Human Subjects, Thermal modeling, Testing methodology	Sport	8 men, 24.6 °C air temperature, 24% RH. Cooling while sitting 45 min, rectal temperature, 8 skin temperatures ISO9886, mean body temperature $\alpha=0.75$ , body heat capacity, 22 segment manikin, constant manikin temperature 34 °C, thermal model is physiologically controlled manikin



(Bolster et al., 1999)	PCM, vapor compression, etc.	Body immersion, Precooling	Human subjects	Sport	6 men, swimming, precooling lower Tre -0.5 °C before swimming. Simulated triathlon, isokinetic cycle ergometer, VO <sub>2</sub> , heart rate, rectal temperature, 4 skin temperatures, thermal sensation, RPE, swim 15 min, cycle 45 min at 70% VO <sub>2</sub> max, body heat storage, sweat rate
(Bomalaski et al., 1995)	Air circulation, Vapor compression refrigeration	Air Vest, Conditioned Air, Tethered	Human subjects	Military, CBRN, MOPP	40% Vo <sub>2</sub> max, warm or hot environment, three trials, four hour trial, work rest cycle, Intermittent conditioned air cooling applied during rest only, no cooling, ambient air cooling during work period, conditioned during rest. 45-30min work, 15-30 min rest (warm-hot), thermal comfort, RPE, 15 men, rectal temperature, 4 skin temperatures mean skin temperature, sweat production, sweat evaporation, heart rate
(Bouskill & Parsons, 1996)	PCM	LCG, neck cooling	Human subjects	Military, air crew	8 men, specifically non-acclimated to heat, air temperature 39.9°C, RH 27%, 60 min tests, first 10 min rest, 50 min exercising, stepping exercise, 1 step/sec, no cooling, neck cooling during exercise, 4 skin temperatures, sublingual temperature, heart rate, aural temperature, VO <sub>2</sub> , ASHRAE comfort and sensation
(Branson, Farr, Peksoz, Nam, & Cao, 2005)	PCM	LCG, PCM vest	Focus group, system design, subjective response	HAZMAT A&B, First responder, PPE, NFPA	Material selection, HAZMAT, 30-60 min air bottle HAZMAT A, industry remote airline. 60 min bottle lasts 30-40 min, PCS design for HAZMAT, expert recommendation, prototype feedback, feedback on existing cooling solutions, 2.27kg or less
(B. S. Cadarette et al., 2001)	Vapor compression, PCM, Air circulation	Tethered, LCG, full body,	Human subject	HAZMAT, Military, STEPO, TAP	6 men 2 women, different suits, VO <sub>2</sub> , 4-h test, work rest cycle, 20 min work 10 min rest, treadmill 5-d acclimation, rectal temperature, heart rate, 4 skin temperatures, mean body weight, heat storage, mean body temperature, sweat rate
(Cadarette et al., 2002)	PCM, Vapor compression refrigeration,	LCG shirt, LCG total body,	Human Subject	HAZMAT, Military, STEPO	MCC, PIC, 6 men, 2 women, work rest cycle, 20 min work 10 min rest, 4 hr test, treadmill, two different vests, two different PCS, rectal temperature, 4 skin temperatures, heart rate, heat storage, sweat rate,
(Cadarette et al., 2003)	PCM	LCG	Human subject	HAZMAT, Military, TAP, ITAP	6 men, 2 women, 2 hour test, treadmill, heat strain limited, 2 cooling treatments, one baseline, work rest cycle 20 min work, 10 min rest, rectal temperature, 4 skin temperatures, heart rate, heat storage, sweat rate, PSI,
(Cadarette, Santee, Robinson, & Sawka, 2007)	Reflective Inserts, RTI	Vest inserts	Human subject, Thermal manikin	Military	4 men, 10 min rest, 100 min walking, 1.56 m/s, ASTM, IBA, acclimation, rectal temperature, heart rate, five 5 skin temperatures, mean skin temperature, 3 armor temperatures, solar radiation

(Caldwell, Patterson, & Taylor, 2012)	External cooling supply	LCG	Human subject, Cognitive function	Military, aircrew, MOPP,	8 men, cycle ergometer, temperate, hot, control temperate, hot-dry water off, hot-dry water on, solar radiation, liquid cooling 15°C, core temperature, auditory canal and rectal temperature, 8 skin temperatures, heart rate, sweat rate, MiniCog Rapid Assessment Battery, cognitive function, work rest cycle, 13 min work, 2 min rest, 2 hr test, helicopter
(Cao, Branson, Nam, Peksoz, & Farr, 2005)	External cooling supply	LCG	Hotplate, System design	Industry, Military, Sport	ASTM F 1868, Hot plate, liquid cooling garment test method, LCG T&E, Predict cold liquid temperature for cooling effect
(Cao, Branson, Peksoz, Nam, & Farr, 2006)	External cooling supply	LCG	Hotplate, System design	Industry, Military, Sport	ASTM F 1868, ASTM D1777-64, ISO 11092 Hot plate, liquid cooling garment test method, LCG T&E, Predict cold liquid temperature for cooling effect, inner fabric layer suitability study, thermal resistance, vapor permeability
(Chen et al., 1997)	Air circulation, Vapor compression	Air vest, tethered, conditioned air, ambient air	Human subject	HAZMAT, Military,	Portable ambient air cooling, conditioned air cooling at rest, work rest cycle, 40 min work, 20 min rest, 7 men, MOPP, treadmill, 4.8 km/hr, 40% VO <sub>2</sub> max, rectal temperature, heart rate, no cooling, intermittent cooling, continuous cooling, mean skin temperature, 4 skin temperatures, sweat loss and evaporation, thermal comfort
(Cheuvront, Kolka, Cadarette, Montain, & Sawka, 2003)	External cooling supply	LCG	Human subject	Military, HAZMAT, MOPP,	Intermittent regional cooling (IRC), Constant cooling (CC), 5 men, 5-d acclimation, treadmill 1.36 m/s, 2% grade, 100 min test, two 50 min tests with 10 min rest in between, rectal temperature, 8 skin temperatures, heart rate, VO <sub>2</sub> , sweat rate, full body LCG, MOPP-3, 6 W per %AD, warm, dry, CC to four body regions, , IRC to two body regions, IRC to two body regions, no cooling, mean skin temperature, mean body temperature, 220 W met rate
(Cheuvront, Goodman, Kenefick, Montain, & Sawka, 2008)	Free Evaporation, Spacer Vest	Spacer Vest	Human subject	Military, First responder, Sport	Body Armor, Spacer vest, passive cooling, 11 men, 3 trials, hot dry, 4 hours, work rest cycles, 50 min work, 10 min rest, BDU, BDU + armor, BDU + armor + spacer vest, treadmill, load carriage adjusted speed, heart rate, VO <sub>2</sub> , sweat rate, intestinal core temperature, 4 skin temperatures, mean skin temperature, mean body temperature, normalized metabolic rate

(Cheuvront, Montain, Stephenson, & Sawka, 2009)	External cooling supply	LCG	Human subject	Military, PPE,	Two studies, intermittent cooling, intermittent regional cooling, constant cooling, whole body cooling, heart rate, core temperature, mean skin temperature Study 1: 5 men, Met 500W, warm, PPE, 4 body cooling regions, constant perfusion, no cooling, 4 intermittent and regional cooling. Study 2: same conditions as 1, 8 men, three trials, constant perfusion, two min cycle intermittent cooling, skin temperature feedback
(Chinevere et al., 2008)	Air Circulation	Air vest, Ambient air	Human subject	Military, Body armor, First responders	1 men, 1 women, 3 environments: hot dry, hot wet, warm wet, body ventilation system, BVS, IBA, helmet, BDU, ACU, SAPI, rectal temperature, heart rate, 5 skin temperatures, mean skin temperature, heat storage, calorimetry, thermal comfort, thermal sensation, RPE, PSI, 12-d acclimation, BVS worn but off, BVS worn but on, no BVS, treadmill 1.34 m/s for 2 hours, ~200W met, sweat production, no sweat evaporation
(Choi et al., 2008)	Free Evaporation, PCM	Neck scarf, Head PCM, PCM Vest	Human subject	Industry, Farming	12 men, Eight conditions, climatic chamber, work rest cycle, 50 min work, 10 min rest, 120 min total time, control, PCM neck cooling scarf A (area 69 cm <sup>2</sup> ), PCM neck cooling scarf B (area 154 cm <sup>2</sup> ), brimmed hat with frozen gel pack, PCM cooling vest (area 606cm <sup>2</sup> ), Hat+ Neck Scarf B, Hat + Vest, Hat + neck scarf B+ vest, saturated fabric water based crystals gel, solar radiation, rectal temperature, 7 skin temperatures, microclimate temperature and humidity, heart rate, PSI, ISO thermal sensation, ISO thermal comfort, sweat rate
(Chou et al., 2008)	PCM	PCM vest, Ice, PCM 5°C, PCM 20°C	Human subject		8 subjects, VO <sub>2</sub> max, cycle ergometer, rectal temperature, mean skin temperature, heart rate, sweat rate, sweat evaporated, BWL, 20 min rest, 50 min work, 55% VO <sub>2</sub> max, 10 min recovery, mean body temperature, thermal sensation, control, PCM Ice, PCM 5°C, PCM 20°C
(Cilen, Ultman, & Kamon, 1983)	PCM	PCM Pack, Lithium Nitrate, Ice	PCM model, Thermal model, Human subject	Industry,	Mathematical model, numerical model, heat flux sensor, skin temperature, pack placed against left side of the abdomen, lithium nitrite, comparison of ice to LiNO <sub>3</sub> , subject at rest
(Colburn et al., 2011)	PCM, Tap water,	PCM, LCG, Immersion, air conditioned	Human subject	Firefighting, NFPA, SCBA,	23 men, 2 women, VO <sub>2</sub> max, heart rate, blood pressure, intestinal core temperature pill, oral temperature NFPA 1403 live-fire evolution, test ~20 min, firefighter ensemble, SCBA, rehabilitation cooling three types. Forearm and hand immersion in cool water, liquid-perfused cooling vest (PCM based LCG), cooling in air conditioned medical trailer, cooling time 30 min,

(Coleman, 1989)	PCM	PCM Vest	Calorimetry, Thermal model	Industry	Gelled coolants, Ice, heated water bath, coolant pack heat storage,
(Colvin, Hayes, Bryant, & Myers, 1993)	PCM	PCM Vest	Human subject, Thermal model, PCS design	Military, CBRN, NBC, MOPP	1 man, warm day, high met level, treadmill, 3.5 m/s run, winter parka, differential scanning calorimetry, DSC, cornstarch/water gel-type material, melting temperature (-5°C to 8°C), absorbed rate 57 cal/g, freezing temperature -20°C, Current test: melt 18°C to 31°C, absorbed rate 54 cal/g, 1-D average, infrared tympanic membrane thermometer
(Colvin & Lokody, 2003)	PCM	PCM neck collar	Computer model, Human subject	Military, CBRN, NBC, MOPP, PPE, Firefighting, Sport, Industry	1 man, triathlon athlete, environmental chamber, 50% RH, 40.5°C, phase change temperature 18°C, skin temperature, IR scan, heart rate, blood pressure, sweat rate.
(Stefan H Constable, 1993)	External cooling supply, PCM	LCG, tethered	Human subject	Military, CBRN, NBC, MOPP, PPE	5 men, 3 women, treadmill, work rest, 30 min work, 30 min of rest, VO <sub>2</sub> max, 40% VO <sub>2</sub> max, rectal temperature, skin temperature, control (light clothing), chemical protective ensemble, chemical protective ensemble + intermittent microclimate cooling,
(S. H. Constable, Bishop, Nunneley, & Chen, 1994)	External cooling supply, PCM	LCG, tethered	Human subject	Military, CBRN, NBC, MOPP, PPE	5 men, 3 women, treadmill, work rest, 30 min work, 30 min of rest, VO <sub>2</sub> max, 40% VO <sub>2</sub> max, rectal temperature, skin temperature, control (light clothing), chemical protective ensemble, chemical protective ensemble + intermittent microclimate cooling,
(Corcoran, 2002)			Feedback and recommendation article	Industrial	User feedback
(Cotter, Sleivert, Roberts, & Febbraio, 2001)	PCM	PCM, LCG	Human subject	Sport	9 men, three trials, precooling: control, cold air 3 °C, leg cooling, VO <sub>2</sub> peak, 65% VO <sub>2</sub> peak, 35 min cycle exercise, 20 min at 65% VO <sub>2</sub> peak, then a 15min work performance trial, oeseophagus temperature, rectal temperature, forearm blood flow, heart rate, 9 skin temperatures, heart rate, body temperature
(D'Angelo, 2009)	Air circulation,	Air vest	Thermal manikin, Thermal modeling,	Military	Air vest, 10cfm, design replica torso, thermoelectric, body temperature simulation, torso as alumina cylinder, skin replicated by silicon sheets

(Delkumbur ewatte & Dias, 2011)	Thermoelectric	Mini refrigerant channels	PCS design, PCS development	Military, CBRN, PPE	High pressure liquid refrigerant cylinder, Peltier, spacer, sweat, sealed environment,
(Dionne, Makris, Semeniuk, Teal, & Laprise, 2003)	External cooling supply	LCG	Thermal manikin	Military, CBRN, PPE, Body armor	Sweating thermal manikin, two flow rates,
(Doerr, 2001)	Air Circulation	Air Vest, LCG	PCS design	PPE, Rocket propellant handler's suit	Supercritical air, 2 hour duration, 7 kg of air, environmental control unit
(Drost & Friedrich, 1997)	Vapor compression, heat pump	LCG	PCS Design	Military, NBC, CBRN	Power from combustion of liquid fuel, desorber, condenser, evaporator, regenerative heat exchanger, combustor, solution pump, coefficient of performance COP
(Duffield & Marino, 2007)	Water, PCM	Immersion, Ice vest, precooling	Human subject	Sport	Precooling,, 9 men, rugby players, determine if precooling procedures improve both maximal sprint and sub-maximal work during intermittent-sprint, 2x30min intermittent sprint. 15 m sprint every minute, mean skin temperature, warm, hot, sweat rate, sweat loss, heart rate, intestinal core pill, 4 skin temperatures, mean skin temperature, thermal comfort, blood lactate, potassium, sodium, plasma, hematocrit (Het), Control, Ice vest, Ice bath
(Duffield, Green, Castle, & Maxwell, 2010)	Water, PCM	Precooling, Immersion	Human subject	Sport	Effects of precooling on pacing in self-paced exercise, 8 men , cycling, cyclists, 20 min lower body cold water immersion, no cooling, maximal voluntary contraction, MVC, superimposed force (SIF), evoked twitch force, PF, muscle temperature, blood metabolites, sweat rate, sweat loss, 4 skin temperatures, heart rate, mean skin temperature, hydration state, muscle temperature
(Duncan & Konz, 1975)	PCM	Dry ice jacket	PCS Design, Human subject	Industry	2 men, bicycle ergometer, two cooling surface areas 800 cm <sup>2</sup> , and 1600 cm <sup>2</sup> , work 55 kcal/hr, heart rate, body weight, rectal temperature, 9 skin temperatures, VO <sub>2</sub> , sweat loss, mean skin temperature, heat flow rate, 60 min test,
(J. C. Elson et al., 2013)	PCM, Air circulation, Vapor compression refrigeration	Air Vest, PCM Vest, LCG	Thermal manikin, Human subject	Military	24 subjects, intestinal core temperature, heart rate, 8 skin temperatures, mean skin temperature, body armor, SPC

(J. Elson & Eckels, 2015)	PCM, Air circulation, Vapor compression refrigeration	Air Vest, PCM Vest, LCG	Thermal model, PCS selection, Thermal manikin, Human subject	Military, Industry, Sport,	24 subjects, intestinal core temperature, heart rate, 8 skin temperatures, mean skin temperature, body armor, SPC, PCS effects, mean body temperature, thermal modeling, PPE, body heat storage, task time, PCS selection process
(T. Endrusick et al., 2007)	Free evaporation, spacer vest	Spacer Vest	Thermal manikin, Thermal model	Military	Spacer vest, sweating thermal manikin, body armor, 3 configurations, temperate battle dress uniform (TBDU) baseline, with IBA, with IBA and spacer vest, used to predict human results, predict core temperature, skin temperature, heart rate, sweat rate, skin wettedness, total body water loss, standard soldier 70 kg, 1.7m, desert environments, work rest cycle, intermittent exercise, 10 min rest, 30 min work,
(T. L. Endrusick et al., 2006)	Air circulation, Free evaporation, Spacer vest	Air vest, Spacer vest	Thermal manikin, Thermal model	Military	Interceptor Ventilation Vest (IVV), Body Ventilation System (BVS), sweating thermal manikin, ASTM F1291-99, ASTM F2370-05, ASTM F2371-05, used to predict human results, predict core temperature, skin temperature, heart rate, sweat rate, skin wettedness, total body water loss, standard soldier 70 kg, 1.7m, desert environments, work rest cycle, intermittent exercise, 10 min rest, 30 min work,
(Ernst & Garimella, 2013)	Vapor compression refrigeration	LCG, Direct vapor expansion vest	PCS Design	Military, Industry, First responders	R-134a, vapor compression system, backpack configuration, cooling garment, refrigeration lines, liquid fuel combustion engine power, heat removal, energy density, prototype testing, RPM
(Farid, Khudhair, Razack, & Al-Hallaj, 2004)	PCM	Materials	Review Article	PCS design	PCS types and applications, paraffin waxes, hydrated salts, PCM encapsulation, heat transfer area, phase change volume control, phase change method of heat storage, PCM problems
(Flouris & Cheung, 2006)	External cooling supply	LCG	Review Article, PCS Design	Military,	Tubing network properties, tubing distribution, cooling distribution, temperature control, flow control, optimization, automatic control, manual control, skin temperature feedback, skin temperature control
(J. Frim, 1989)	PCM, External cooling supply	LCG	Human subject		6 men, control, no fluid circulating, only torso cooling, torso and head cooling, cooling fluid 10°C, thermal comfort, solar load, cooling vest and cap, flight suit, pilot, 12 skin temperatures, heart rate, rectal temperature, heat storage, sweat rate, sweat evaporation, VO <sub>2</sub> , RER, physical performance, mental performance,

(John Frim & Glass, 1991)	PCM, External cooling supply	LCG, ICE vest	Human subject	Military, Navy	Navy, engine room, boiler, 12 men, work clothing, work clothing with cooling, chemical defense clothing, chemical defense clothing with cooling, EXOTEMP, 90 min, rectal temperature, skin temperature, heart rate, heat flux
(John Frim & Morris, 1992)	External cooling supply	LCG	Thermal manikin, PCS deign	Military, Navy	Three tubing lengths for LCG. 20 cm, 37cm, 50cm, threw flow rates 200 ML/min, 500 mL/min, 1000 mL/min, three fluid inlet temperatures 5°C, 15°C, 25°C, constant ambient, constant manikin surface temp, helicopter pilot ensemble,
(John Frim, Michas, & Cain, 1996)	Air circulation, Free Evaporation, PCM	LCG, Air Vest, Spacer Vest	Human subject	Military, EOD, PPE, First responders	7 young men, 4 old men, Three environmental conditions, treadmill, 10 min, unstacking/carrying/stacking boxes 10 min, rest period, 15 min, repeat sequence, work rest cycle, 90 min test, rectal temperature, skin temperature, heart rate, sweat rate, sweat evaporation, VO <sub>2</sub> , thermal comfort, RPE, PCM based LCG, VO <sub>2</sub> max, blood analyses, Na <sup>+</sup> , K <sup>+</sup> , Cl <sup>-</sup> , Hematocrit
(Fujii, Horie, Tsutsui, & Nagano, 2008)	Ambient liquid, Immersion	Liquid water	Human subject	Industrial	11 subjects, non-refrigerated water, 2 L of 23.0°C water on head and hands for one min, every 20 min, environmental chamber, heart rate, rectal temperature, esophageal temperature, skin temperatures, ear canal temperature, work rest cycle, 10 min rest, 3 intervals of 20 min cycling, 15 min of rest, stabilometry, visual reaction time, questionnaire evaluating equilibrium, concentration, alertness, tiredness at beginning and end
(Furtado, Craig, Chard, Zaloom, & Chu, 2007)	PCM	LCG Vest, Tethered	Human subject	Industry	12 men, students from India, cooling shirt 15 m of tube, Chilled water 15 L ice chest re-circulated in closed loop, submaximal arm ergometer, Heart rate, VO <sub>2</sub> , tympanic temperature, subjective responses, productivity, error rates, PCM based LCG
(Chuansi Gao, Kuklane, & Holmér, 2010)	PCM	PCM Vest	Thermal manikin, PCS selection, PCS design	Firefighter, PPE, First responder, Military, Sport	Thermal manikin, climatic chamber, three PCM melting temperatures 24°C, 28°C, 32°C, different mass, different covering areas, two manikin temperatures 34°, 38°C, firefighting ensemble, latent heat of fusion, cooling rate, temperature gradient
(Chuansi Gao, Kuklane, & Holmér, 2011)	PCM	PCM Vest	Human subjects	Firefighter, PPE, First responder	Six men, objective investigate cooling effects of the two melting temperatures on human subjects, PCM melting temperature 24°C, 28°C, control no vest, treadmill, 55°C=Ta, 30% RH, sodium sulphate decahydrate, Glauber's salt, firefighting ensemble, VO <sub>2</sub> max, thermal sensation, cycling, heart rate, 6 skin temperatures, body temperature, rectal temperature, RPE

(C. Gao, Kuklane, Wang, & Holmér, 2012)	PCM	PCM Vest	Thermal manikin, Human subjects	Industry, Office	Thermal comfort, office work, 34°C, sodium sulfate, 17 zone thermal manikin, constant manikin temperature, constant heat flux, human subjects, 8 men, rectal temperature, 10 skin temperatures, subject weight, no air conditioning, thermal sensation, VO <sub>2</sub> ,
(Gentile, 2006)	Thermoelectric	Heat pipe in vest, Tethered	PCS design	Military	IBA, thermoelectric, heat pipe, battery, COP=0.3 maximum thermoelectric, COP heat pipes =4, Thermoelectrics, CPI.4-127-045L, at 117 Watts for 2.2 A and 19.4 V and 150Watts for 2.5 A and 22 V, heat sink box,
(Glitz et al., 2011)	Air circulation	Air Vest, Tethered	Human subject	Military, Industry	1 man, isolated protective overall, treadmill, three air temperatures, 18°C, 25°C, 32°, all at 50% RH, vair 0.2m/s, time 2 hr, 10 min, treadmill, work rest cycle, 10 min rest, 30 min work, 18° without dry ventilation 25°C with and without dry ventilation, 32° with dry ventilation. External generated dehumidified air %5 RH Heart rate, VO <sub>2</sub> , intestinal pill temperature, mean skin temperature, sweat rate
(Gonzalez, Berglund, Endrusick, & Kolka, 2006)	Air circulation	Air Vest	Thermal manikin	Military	Battery powered ventilation system (BVS) IBA, body armor, BDU, ASFM F2371, thermal resistance, evaporative resistance, inlet flow 9 L/s, Fan off power, fan on power, ASTM F1291, ASTM F2370
(Goodman, Diaz, Cadarette, & Sawka, 2008)	Air circulation, PCM	LCG, Air Vest, Ambient	Human subject, Field study	Military	Core body temperature effect, effect on ability to fight, soldier protection effect, ability to wear in an operational environment, is it compatible with current weapons and equipment, effect on mobility, intestinal pill temperature, 4-5 member teams, different random PCS each day, 5 events per day, individual movement technique IMT obstacle course, road march vehicle patrol live fire exercise, soldier battle lab, MCCA, microclimate cooling systems, army combat uniform ACU, Army combat shirt, Improved Outer Tactical Vest (IOTV), Baseline, Ambient air ventilation system, PCM based LCG, heart rate
(Dennis A. Grahn, Cao, & Heller, 2005)	External cooling supply	LCG, hand cooling, sub atmospheric pressure	Human subject	Sport	26 subjects,6 men 2 women esophageal thermocouple, 10 men and 8 women short term study, 7 men 2 women long term study, treadmill, VO <sub>2</sub> max, heart rate, sweat rate, heat extraction device, chilled grip, vacuum pressure cuff
(D. A. Grahn, Dillon, & Heller, 2009)	External cooling supply	LCG, hand cooling, sub atmospheric pressure	Human subject	Military, MOPP, CBRN	17 men, treadmill, 5.6km/hr, esophageal temperature, sweat rate, heart rate, hot, insulated recovery in hot environment, post exercise cooling, control, 10°C water to hands, feet, or multiple glabrous skin regions, or sub atmospheric pressure to the face, feet, multiple glabrous skin regions



(Grzyll & Balderson, 1997)	Adsorption	LCG Vest	PCS design	Military	Renewable adsorbent evaluation, non-regenerable adsorbent evaluation, benchtop testing, evaporator, chiller, prototype, pump, battery, desiccant,
(Grzyll & McLaughlin, 1997)	Vapor compression refrigeration	LCG Vest	PCS design, PCS review	Military, MOPP,	NBC compatible, STEPO Microclimate, Thermoelectric, Phase Change, Adsorption, Bryton Cycle, Compressed Air, Vapor compression, chilled water for LCG, vehicle crew, earthmover, field testing
(Guo, Zhang, & Yuan, 2014)	Air circulation	Air vest, Tethered	PCS design	Industry	Unsealed, well-ventilated, jacket, ventilation pipe, ergonomics, testing
(Hadid, Yanovich, Erlich, Khomenok, & Moran, 2008)	Air circulation	Air vest	Human subject	Military	12 men, 40C 40% RH, 35C 60% RH, 115 min exercise routine, 70 min resting recovery, BDU, body armor, cooling, no cooling, 6-d acclimatization, hot, 2 hr test protocol, treadmill, speed 5 km/hr, 2% incline, two cycles of 50 min followed by 10 min of rest, work rest cycle, rectal temperature, 3 skin temperatures, mean skin temperatures, heart rate, RPE, heat storage rate, sweat rate, PSI,
(Hagan, Huey, & Bennett, 1994)	PCM	PCM Vest	Human subject	Firefighting, Military	Two PCM cooling vests, Navy firefighting protective ensemble, small 4 pack cooling vest, large 4 pack cooling vest, oxygen breathing apparatus, work rest cycle, 8 men, hot, humid, trials: no vest, small 4-pack, large 4 pack, temperature 48C dry bulb, RH=50%, dungarees, cotton t-shirt, US Navy firefighting ensemble, 30 min work, 30 minutes rest, treadmill 1.56 km/hr, work to max cycles, rectal temperature, mean skin temperature, heart rate, mean body temperature, four skin temperatures CO2 production, VCO2, RPE
(Harrison & Belyavin, 1978)	External cooling supply	LCG	Review article	Military, Air crew	Review of 12 years of LCG studies at the RAF institute of Aviation Medicine. Heat exchange proportional to inlet temperature, resting subjects, environmental temperature, length of exchange tubing, insulation of clothing, mean skin temperature, core temperature
(Heled, Epstein, & Moran, 2004)	PCM, Water spray	LCG,	Human subject	Military, CBRN, MOPP	6 men, 125 min test, 40C, 40% RH, active cooling vest sublimation of dry ice, tap water spraying, rectal temperature, 3 skin temperatures, mean skin temperature, heart rate, heat storage, AD, mean body temperature, PSI, sweat rate, thermal comfort

(Hepokoski et al., 2012)	Air circulation, Thermoelectric	Air vest	Thermal manikin, Human subject, Thermal model, PCS design	Military, PPE	ASTM F2371, physiological controlled manikin, core temperature, closed loop air circulation, cooling power, sweating thermal manikin, human subjects 45°C 40%RH, air vel 2 m/s, open loop air cooling, open loop air cooling with thermoelectric cooled air, control,
(Martin Hexamer & Werner, 1995)	External cooling supply	LCG	Human subject		10 subjects, AD, VO <sub>2</sub> max, 10 skin temperatures, mean skin temperature, rectal temperature, cycle ergometer, blood pressure, heat storage, manual control of PCS cooling, oscillating PCS cooling, thermal sensation, heart rate, sweat rate, local sweat rate ventilated capsule, thermal comfort controlled LCG inlet temperature
(Martin Hexamer, Xu, & Werner, 1996)	External cooling supply	LCG	Human subject		4 subjects, 75W, 125 W, controlled LCG inlet temperature, three exercise rates: rest, 75W, 125W, fixed T <sub>skin</sub> at 32°C, controller, heart rate, heart rate and skin temperature controlled inlet temperature, multi-loop LCG local controllers, arms, trunk legs LCG
(M. Hexamer & Werner, 1998)	External cooling supply	LCG	Human subjects		Human subjects from testing. Developing control algorithms for controlling liquid cooling garments, developing classes to describe cooling control mechanism. ILC-Dover LCG with constant flow (1.8L/min). rectal temperature, mean skin temperature, metabolic rate, mean body temperature
(J.R. House, 1996)	PCM	PCM Vest, Immersion	Human subject	Military	10 men, 40°C50% RH, 5 tests, stepping 22.5 cm box, 12 steps per min, 30 min test, 30 min of seated rest, control, ice vest Steele, Ice Vest Dover, Ice Vest LSSI, hand immersion 20°C, ice vest worn throughout both work and rest periods, hand immersion was only during rest periods, aural temperature, rectal temperature, mean skin temperature, heart rate, sweat rate, sweat evaporation, ANOVA, work rest cycle,
(J.R. House, Groom, Hodgdon, Heaney, & Buono, 1998)	External cooling supply	LCG, Forearm	Human subject	Military, Navy, Firefighting	10 men, VO <sub>2</sub> , Royal Navy firefighting clothing, 40°C DB, 28.8°C WBT, 5 tests, stepping 22.5cm box, 12 steps per min, 12 per min, 40 min of seated rest, control, hand immersion during rest, large cuff during exercise, large cuff worn during rest, small cuff worn during rest, water perfused cuff, heart rate, aural temperature, rectal temperature, mean skin temperature, heart rate, sweat rate, sweat evaporation, ANOVA, work rest cycle,

(J.R. House et al., 2005)	PCM, External cooling supply	LCG, Forearm	Human subject	Military, Navy, CBRN, PPE, MOPP	10 men, 36.3°DB, 55%, Royal Navy CBRN PPE, box stepping, 22.5 cm box, 12 steps per min, 10 min work, 5 min rest, work rest cycle, maximum of 3 hours, control no cooling, hand immersion 10°C, hand immersion 0°C, during rest periods, combined hand immersion, rectal temperature, mean skin temperature, 4 skin temperatures, body heat storage, heart rate,
(James R. House et al., 2013)	PCM	PCM Vest	Human subject	Military, Firefighting	Four melting temperature 0, 10, 20 30 °C, during exercise and recovery 10 men, firefighting, no-cool control, 40°C DB, 46% RH, stepping exercise for 45 min, seated recovery 45 min, 22.5 cm box, 12 steps per minute, mean skin temperature, 4 skin temperatures, extra skin temperature abdomen under PCS, heart rate, VO <sub>2</sub> , skin blood flow, Doppler flowmetry LDF, user preference, sweat rate
(Hu & Chao, 2008)	Absorption heat pump	LCG	PCS design	PPE, Industry, Firefighters, HAZMAT	Electroosmotic pump-driven micro LiBr Absorption heat pump system, performance of heat pump, evaporator, condenser, review of existing heat pumps, fabrication, performance, temperature effects, ethanol,
(Jette, Dionne, Semeniuk, & Makris, 2003)	External cooling supply	LCG, tethered	Thermal manikin	HAZMAT, PPE, Armor, firefighting, CBRN	Hazmat Level B, firefighting turnout jacket, crowd management PPE torso protector, 100% wool sweater, baseline no LCG, effective cooling rate, dry thermal manikin, sweating thermal manikin, 100% wet, Selectively permeable membrane, Joint service lightweight integrated suit technology, JLIST, CBRN, body armor, cooling power, tightness of fit
(Jetté, Dionne, Rose, & Makris, 2004)	External cooling supply	LCG, tethered	Thermal manikin	HAZMAT, PPE, Armor, firefighting, CBRN	Dry thermal manikin torso, LCG single flow rate of 300 mL/min, two inlet temperatures 7°C and 14°C, inlet temperature, outlet temperature, three manikin temperatures 30°C, 34°C, 38°C, ambient temp 23.5°C, baseline with PCS on but turned off, insulating garments, PCS efficiency
(Jovanović, Karkalić, Tomić, Veličković, & Bajić, 2012)	PCM	LCG	Human subject	Military	10 men, exertional heat stress test EHST, treadmill, 5km/hr, 40°C DB, camouflage uniform, no cooling, and waist pack personal cooling system, mean skin temperature, tympanic temperature, heart rate, sweat rate, PCM based LCG, 45 min test, 5 skin temperatures
(Jovanović, Karkalić, Zeba, Pavlović, & Radaković, 2014)	PCM	PCM Vest, PCM Underwear	Human subject	Military, NBC, CBRN,	10 men, exertional heat stress test EHST, treadmill, 5.5km/hr, 40°C DB, camouflage uniform, no cooling, three PCS vests, one underwear PCS, mean skin temperature, tympanic temperature, heart rate, sweat rate, PCM based LCG, 45 min test, 5 skin temperatures, CBRN contamination clothing,

(Kamon et al., 1986)	PCM	PCM Jacket	Human subject	Industrial, HAZMAT,	Two groups, 5 men acclimated, 6 men non acclimated, treadmill, 2.5 mph, work rest cycle, 5 min sitting on stool, 5 min walking, second level of work alternating 5 min of walking 3 mph and 5 min of arm cranking 150 kilo-pound-meter/meter ice, long vest covering trunk buttocks and upper thigh, short jacket covering trunk, different weight PCM using different number of packs, VO <sub>2</sub> , radiation coverall, heart rate, rectal temperature, 10 skin temperatures, mean skin temperature, sweat rate, respirator, field studies, 2 men, bulk, partial calorimetry
(Katica et al., 2011)	External cooling supply	Forearm immersion, Leg immersion	Human subject	Firefighting, NFPA	10 men, non-acclimatized, VO <sub>2</sub> max, control, heart rate, leg cooling, arm cooling, sweat rate, rectal temperature, 5 skin temperatures, cooling during rest, precooling, NFPA fire fighting clothing, SCBA, treadmill, 3.5 mph, exercise to exhaustion or core temp cutoff, post cooling, thermal comfort, RPE
(Jonathan W Kaufman & Fatkin, 2001)	Air circulation	Ambient air cooling	PCS design, Thermal model, PCS literature review	Military, CBRN, MOPP, Aircraft, Helicopter	Airflow rates, evaporation, ventilation, enthalpy, convection, radiation, VO <sub>2</sub> max, MOPP, CBRN, encapsulating garment, body heat storage, mean skin temperature, core temperature, heat extraction criteria, air circulation literature review, integrating metabolic heat production
(J. W. Kaufman, 2001)	PCM, Free evaporation, supercritical air	LCG, PCM Vest, Air Vest, Saturated Vest	Human subject	Military, CBRN, MOPP, HAZMAT	HAZMAT level A, work rest cycle, 25 min walking alternating walking 4.8 km/hr at 5% and walking 0% with 22.7kg load, up to 2hours, 5 min rest, Air 37°C 75% RH, liquid cooled vest with hood PCM based, PCM vest, Wetted vest, LCG supercritical air, HAILSS air conditioning garment system, no cooling, JLIST, MOPP, NASA-TLX, MAACL-R, rebreather
(Jonathan W Kaufman, 2002)	PCM, Free evaporation, supercritical air	LCG, PCM Vest, Air Vest, Saturated Vest	Human subject	Military, CBRN, MOPP, HAZMAT	4 men, HAZMAT level A, hot humid, rebreather, work rest cycle, 25 min walking alternating walking 4.8 km/hr at 5% and walking 0% with 22.7kg load, up to 2hours, 5 min rest, Air 37°C 75% RH, up to 2 hours,
(Kenny et al., 2011)	PCM	PCM Vest	Human subject	CBRN	10 men, hot humid 35°C DB, 65% RH, 3mph, 2% incline, seminude, NBC suit with ice vest, NBC suit without cooling, 120 min work or volitional fatigue/cutoff. Esophageal temperature, heart rate, thermal sensation RPE, Borg scale,
(Khomenok et al., 2008)	External cooling supply	Hand immersion, cold water	Human subject	CBRN, MOPP,	17 men, bulletproof vest, armor, 35°C DB 50% RH, work rest cycle, 125 min total, 50 min work, 10 min rest, treadmill 5km/hr 5% grade, random cross-over design, one rest with hands in one rest without, rectal temperature, 3 skin temperatures, heart rate, heat storage, mean body temperature, sweat rate, physiological strain index PSI, RPE, Borg,

(J. Kim & Cho, 2002)	PCM	PCM microcapsule fabric	PCS design, Human subject	Industry	Thermostatic fabric, 100% polyester coated with octadecane microcapsules, heat content of fabric increased 56-94%, 10 launderings, stiffer less smooth fabric, hand, subjective performance, chest temperature
(J.-H. Kim, Coca, Williams, & Roberge, 2011)	External cooling supply	LCG, tethered	Human subject, LCG study	PPE, Industry, Firefighting, CBRN	6 men, VO <sub>2</sub> max, treadmill, firefighting ensemble, SCBA, two LCGs, one top cooling garment and shortened cooling garment, different surface areas covered, CBRN, 35°C DB, 50% RH, discomfort, rectal temperature mean skin temperature, 4 skin temperatures, heart rate, PSI, 18°C LCG inlet, visual analogue scale VAS, thermal comfort, fatigue, work rest cycle, 15 min work, 10 min rest, treadmill 75% VO <sub>2</sub> max,
(S. Konz, Hwang, Perkins, & Borell, 1974)	PCM	PCM vest	Human subject	Industry	1 man, dry ice PCM sweat rate, sweat evaporation, PCM weight, PCM evaporation, 15 to 31 skin temperatures, rectal temperature, heart rate, blood pressure, air 43.3°C DB, MRT 42.8°C 45-55%RH, 18 experiments, dry ice shape, insulation, seminude, heat balance, body heat storage, jacket, sweating efficiency, mean body temperature
(SA Konz, 1984)	Air circulation, vapor compression refrigeration, saturated garment, PCM	Air vest, Saturated vest, LCG, PCM vest	PCS review of literature, Thermal model	Industry, HAZMAT	Heat balance equation, evaporative cooling, convective cooling, ambient air cooling, conditioned air cooling, saturated garment, mean body temperature, mean skin temperature, radiant heat transfer, convection, evaporation, conduction, clo, OSHA,
(Kuennen, Gillum, Amorim, Kwon, & Schneider, 2010)	External cooling supply	LCG hand	Human subject	HAZMAT, PPE,	10 men, hot, dry, 42.2 °C DB, mean skin temperature, mean body temperature, simulated armored vehicle transport, no cooling, palm cooling, palm cooling with vacuum, sub-atmospheric, cooling during rest, treadmill 6.1 km/hr, 2-4% grade, VO <sub>2</sub> max, chemical protective clothing, heart rate, 4 skin temperatures, oesophageal temperature, PSI, skin blood flow, laser Doppler, exercise to 38.8 °C core, inlet temperature 10 °C

(Kuznetz, 1980)	External cooling supply	LCG	PCS Design, Thermal model, Human subject	Astronaut, EVA	Automatic controller LCG inlet, 41-Node Metabolic man computer program, Stolwijk-Hardy, space suit, respiratory heat loss, convective transfer, radiation heat transfer, evaporation, 3 subjects, 21 experiments, Skylab-2 EVA, 1 to 2 hr test, all tests with LCG, coveralls, arctic thermal garment, flow 109 L/hr or 52 L/hr, 3 skin temperatures, rectal temperature 5 other skin temperatures, measured LCG, body heat storage, subjective ratings, thermal comfort, sweat rate
(Kwon et al., 2010)	External cooling supply	Palm cooling, negative pressure	Human subject	Sport	16 male subjects, regular weight trainers, one- repetition maximum (IRM) supine bench press, 5 min rest, three endurance set to fatigue at 85% of IRM, 2seconds up 2 seconds down, during rests between sets 2 and 4 hand was exposed to either negative cooling, local palm cooling with negative pressure, or local palm heating negative pressure, water temperature 10C cooling, 45C heating, RPE EMG, esophageal temperature, palm skin temperatures, heart rate
(Laprise, Teal, Zuckerman, & Cardinal, 2005)	PCM, Free evaporation, Vapor compression, Compressed air, Thermoelectric		Thermal manikin, Human subject	Military, First responder,	COTS, MCS, PPE, body armor, thermal manikin, ASTM, Cooling, Sweat evaporation, Cooling products, PCS database, ASTM F2371-05
(Laprise, 2012)	General	General	PCS selection method	Military, First Responders	Microclimate cooling system proposal standard, moving parts, fuel, PPE, ASTM F2371-05, weight, consumable, bulk, volume, noise, controls, support equipment, PPE Integration, MCS Safety and Health Hazards, Human factors engineering, launder-ability, environmental performance, High/Low Temperature Storage,
(LeDuc, Reardon, Persson, Gallagher, & Dunkin, 2002)	Vapor compression refrigeration	LCG Vest	Human subject	Military, Aircrew, MOPP	8 UH-60 qualified pilots, CS= cool standard 70° F & MOPPO; CM=cool MOPP 70 °F MOPP4 vest worn but off, HM=hot MOPP 100 °F MOPP4 cooling vest turned on, 20 min precondition treadmill walk at 3 mph, 0% grade, walk to simulators with 50% RH and 90 °F WBGT, 2 two-hour simulated sorties, UH-60 simulator, flight performance data, rectal temperature, mean body temperature, four skin temperatures: chest, arm, thigh, calf; heart rate; dehydration, mood evaluation, 5 hours total time, NASA TLX questionnaire, 180 W cooling

(Lee & Haymes, 1995)	Air	Ambient air	Human subject	Sport	14 men, runners, high-intensity running tests, rest 24 °C, precooling 30 min by resting in 24 °C or 5 °C, then rest at 24 °C, then exercise at 82% VO <sub>2</sub> max, rectal temperature, VO <sub>2</sub> max, heart rate, fingertip blood, glucose, L-lactate, 4 skin temperatures, body heat storage, mean body temperature
(Levine, Cadarette, & Kolka, 2003)	PCM	LCG shirt	Human subject	Military, HAZMAT, MOPP, PPE	STEPO, PICS, rebreather, work rest cycle, 10 min rest, 20 min work, treadmill, 300-350W, three environments, hot 32.2 °C 30%, moderate 23.9 °C 40%, cool 15.6 °C 50% RH, Rectal temperature, skin temperatures, heart rate, body weight, dehydration, PSI,
(Leyva & Goehring, 2004)	PCM	LCG, Tethered	Human subject	Diver, Military, PPE	Military, diver, contaminated water, no systematic testing, feedback survey, thermal stress, ambient temp > 100 °C, 10 dives, 2 days, NEDU,
(Lim, Song, Law, Sng, & Soh, 2002)	PCM, Water spray, Air circulation	Immersion, Spray, Ambient air, fan, PCM vest	Human subject,	Military	101 men, 5 cooling methods, body cooling unit, BCU, chilled gas spray, cold pack, combination, pressured water spray, core temperature, intestinal core temperature, air 35 °C dB 70% RH, treadmill 5.5 l/hr 5% grade, military uniform, work until core 39.5°C for 1 min, post cooling, cooling stopped when core 38 °C,
(Luechtefeld et al., 2003)	Vapor compression refrigeration	LCG Vest, tethered	Human subject, Thermal model, Thermal manikin	Military, Air crew, Helicopter, MOPP, HAZMAT, CBRN	324 watts, at least 180 W of cooling, PCS design, details, MOPP, mean core temperature, thermal modeling, MCS, Microclimate Cooling System, MIL-STD-704 aircraft power, bench test, field test, thermal manikin,
(Luomala et al., 2012)	PCM	PCM Vest	Human subjects	Sport	7 subjects, 10 min cycles, of nine min at 60% of VO <sub>2</sub> max and the 1 min sprint at 80% VO <sub>2</sub> max, ice vest, 30 min cycling, ventilator and thermal responses, EMG, 4 muscle dominate leg, warm humid, bicycle ergometer, no cool, cool, 30 °C DB 40% RH, rectal temperature, 11 skin temperatures, mean body temperature, neuromuscular response,
(Maier-Laxhuber, Schmidt, & Grupp, 2002)	Air Circulation	Air Vest, desiccant,	PCS design, Bench test	Military, Industry	Zeolite, Air circulation, desiccant, regenerative desiccant, heating, cooling, air vest, MiCS, heat exchanger, AIRSAVE Vest, refrigeration unit,
(Martini, 2011)	PCM, Air cooling	LCG suit, Air vest, PCM Vest	Human subject	Military, MOPP, CBRN,	PCM based LCG, 10 min rest, 40 min activity, 20 min rest 3.6 km/hr, 13% grade, sweat rate, core temperature, Chemical protection, NORMANS, Air vest, two fans, Ai vest 1 fan, PCM vest, Glauber salt,

(McClure, McClure, & Melton, 1991)	Air cooling, PCM, Compressed gas	PCM Vest, Vortex tube,	Industry publication	Industry, PPE,	Industry journal, PCM Vest, Vortex tube cooling, compressed vest cooling, NASA
(E. McCullough, 2001)	PCM	PCM	Hot plate, Thermal manikin	Industry, PPE,	PCS technology article, PCM description, testing methods, ASTM D1518, ASTM F 1868, ASTM F 1291, PCM fabric,
(E.A.; McCullough & Eckels, 2008)	PCM Air Circulation, Vapor compression refrigeration	P PCM , LCG, PCM Vest, Air circulation	Thermal Manikin, Human subjects	Military	ASTM F2371, 9 PCS, Military DCU, Interceptor Body Armor, Human subject tests, ASTM F2300, 12 test subjects in 3 week session, 36 subjects in all, male soldiers, Air temperature 40C, RH 20%, air velocity 2.0 m/s, MRT 54.4 C, Metabolic rate 350-360W, two hour test, VO2, rectal temperature, whole body sweat rate, heart rate, personal opinions on PCS,
(E.A.; McCullough & Eckels, 2009)	PCM Air Circulation, Vapor compression refrigeration	PCM , LCG, PCM Vest, Air circulation	Thermal Manikin, Human subjects,	Military	ASTM F2371, 9 PCS, Military DCU, Interceptor Body Armor, Human subject tests, ASTM F2300, 12 test subjects in 3 week session, 36 subjects in all, male soldiers, Air temperature 40C, RH 20%, air velocity 2.0 m/s, MRT 54.4 C, Metabolic rate 350-360W, two hour test, VO2, rectal temperature, whole body sweat rate, heart rate, personal opinions on PCS,
(E.A.; McCullough, Eckels, & Elson, 2013)	PCM Air Circulation, Vapor compression refrigeration	PCM , LCG, PCM Vest, Air circulation	PCM , LCG, PCM Vest, Air circulation	Military	ASTM F2371, 12 PCS tested on thermal manikin, Military BDU w/ combat shirt, Soldier Plate Carrier (SPC), Human subject tests, ASTM F2300, 4 PCS evaluated, 4 test subjects in 3 week session, 24 subjects in all, 22 male and 2 female soldiers, Air temperature 42.2C, RH 20%, air velocity 2.0 m/s, MRT 54.4 C, Metabolic rate 375-400W, two hour test, VO2, rectal temperature, whole body sweat rate, heart rate, personal opinions on PCS,
(McDermott et al., 2009)	PCM, immersion, cooling aggregate,	Immersion, PCM VEST, Ice pack, Ambient air, Fanning	PCS review article	Industry, PPE,	Cooling rate, 37 cooling methods, cooling rates, recommendations, precooling, post cooling, water immersion, PCM pack, ice pack, ambient air fanning, cool air fanning, control, limitations
(T. M. McLellan & Daanen, 2012)	PCM, Air circulation,	LCG, Air circulation, PCM Vest,	Thermal manikin, Human subject	CBRN, PPE, HAZMAT, Military,	Microclimate cooling, vertical, horizontal PCM vest, no cooling, treadmill 3.5 km/hr, 7 men, no acclimatization, VO2max, heart rate, NBC overgarment, rectal temperature, thermal manikin sweating thermal manikin, sweat rate, mean skin temperature, 4 torso skin temperatures, 7 other skin temperatures, RPE, blood, hematocrit, plasma osmolality, ANOVA, sweat efficiency
(McLeilan, 2002)	PCM, Air circulation, Liquid	PCM Vest, Air Vest, LCG, Immersion	PCS Review article	Military, Navy, CBRN	Air cooling, liquid cooling, PCM based LCG, PCM Vest, Navy, engine room, tethered,



(T. M. McLellan, Frim, & Bell, 1999)	Air circulation, External cooling supply	Air vest, LCG	Thermal manikin, Human subject	Military, CBRN, PPE	8 men, no acclimatization, VO <sub>2</sub> max, treadmill, heart rate, NBC, light work, heavy work, , no cooling, liquid cooling, air cooling, rectal temperature, 3 hr max, 39.3 °C max, heart rate, 95% heart rate, volitional, RPE, blood, hematocrit, plasma osmolality, ANOVA, sweat rate, treadmill 4.8 km/hr 5% grade,
(Thomas M. McLellan & Frim, 1994)	Air circulation, PCM, External cooling supply	Air vest, PCM vest, LCG	PCS review	Military, CBRN, PPE	Chemical defense clothing, insulation, liquid, LCG, flight ensemble, working fluid, heat sink, PCM based LCG, PCM Vest, Air vest, vapor compression refrigeration,, compressed gas, pilot, aircrew,
(Mokhtari Yazdi & Sheikhzadeh , 2014)	Air circulation, PCM, Vapor compression refrigeration	Air vest, PCM vest, LCG,	PCS review	Military, CBRN, Industry, Medical	PCS review 2014, hot environments, protective clothing, thermoregulation, heat storage, multiple sclerosis, air cooled garments ACG, liquid cooled garments LCG, phase change garments PCG,
(Moore, Lakeman, & Mepsted, 2002)	Vapor compression refrigeration	LCG, PEM fuel cell	PCS design	Military, CBRN, Industry	PEM fuel cell, hydrogenation, batteries, vapor compression, power density
(Ian H. Muir, Bishop, & Ray, 1999)	PCM	PCM vest	Human subject	Military, Industry, PPE, HAZMAT	Ice system, recharge without PPE removal, 3 air temperatures, 28°C, 23°C, 18°C, PPE, PCM outside PPE, rectal temperature, 3 skin temperatures, heart rate, treadmill, 4.83 km/hr 3% grade, 15 min walk, 10 arm curls 14.6 kg 5 minutes, work rest cycle, 30 min recovery, max length 2.5 hours, rectal temp cutoff 38.7 °C, HR max 10 bpm age max, ice
(I. H. Muir & Myhre, 2005)	PCM	PCM vest	Human subject	Sport, Industry, PPE	8 men, acclimated, VO <sub>2</sub> max, precooling, upper body cooling, increase skin surface area coverage, 18 packs, PCS fit, reflective fabric, radiant load, cooling 30 min of rest than 30 min of light warm up, test no cooling 70% VO <sub>2</sub> max , control same protocol no cooling, exercise until core 39.5 °C or volitional exhaustion, rectal temperature 5 skin temperatures, heart rate, sweat loss, thermal comfort
(Muza, Pimental, Cosimini, & Sawka, 1987)	Air circulation	Air vest	Human subject	Military, HAZMAT, PPE, CBRN, MOPP	6 men, acclimation, four 250 min exposures, Microclimate conditioning vest MCV, backpack system, crew uniforms, body armor, MOPP, three conditions 35.1 °C DB, 19.7 °C DB, 40.6 °C DB, 1.0 °C DB, 1.1 m/s, 0% grade, work rest cycle 420 W met, 150 W rest, treadmill exercise, seated rest, 50 min work, 50 min rest, 10-18 CFM flow, hot dry, warm wet. MCV backpack, PCS weight 5kg,

(Myhre & Muir, 2005)	PCM	PCM Vest	Human subject	Sport	8 men, shorts, rest 30 min, don short sleeve T, intermittent rest and light exercise in hot 35 °C DB, 50% RH. Treadmill, control, ice vest with T-shirt during rest and exercise, heart rate, 6 skin temperatures, rectal temperature,
(Nag, Pradhan, Nag, Ashtekar, & Desai, 1998)	External cooling supply	LCG Vest	Human subjects	Industrial, HAZMAT, Military	LCG Vest, 20% body area covered, areas between latex tubes free for evaporation, chilled water supply 10-12 °C, three water flow rates, vest = 0.75 kg, pump plus reservoir 1 kg, 4 men, three dry bulb temperatures 30 °C, 35 °, and 40 °C; air velocities of 0.3, 0.6, and 0.9 m/s, RH 50-60%, core temperature, skin temperature, sweat rate, ET, Ereq, Esk
(Nagavarapu & Garimella, 2011)	Vapor compression, heat pump	LCG Vest	PCS design		Absorption heat pump, microscale heat and mass exchanger, even distribution, compact, modular, versatile, can be mass produced,
(Nam et al., 2005)	External cooling supply	LCG	PCS design, Human thermal	HAZMAT, PPE, military, First responder	Two LCG's, 3D body scanner, PCS fit, 13 subjects, 8 men met criteria, 1 women, first responder, firefighter, test ratings,
(S. A. Nunneley, 1970)	External cooling supply	LCG	PCS Review	Military, HAZMAT, PPE, CBRN, MOPP, Sport	Liquid cooling garment LCG review, Gas cooling, limitations, development of water cooling, NASA, space suit, current designs and application, RAF, whole body suit, diamond pattern suit, design variables, cooling control, regional cooling,
(S. Nunneley, Diesel, Byrne, & Chen, 1998)	Air circulation, Vapor compression refrigeration	LCG, Air vest, tethered	Human subject	Military, Aircraft, Pilot	8 men, f-16 flight ensemble, control, air cooling, APECS cooling, five subjects wear F22 ensemble, rectal temperature, 2 skin temperatures, g-suit, pilot, preflight conditions, treadmill 2.5 mph 20 min, ejection seat, oxygen max, air cooling 425 L/min, 13 °C, APECS LCG torso and arms, 0.6 L/min of water-antifreeze mix at 17 °C. Flight phase 30 min of period of gradual decline in ambient temperature, 60 min of maintenance at the level representing cockpit conditions during cruise
(Karen L. Nyberg et al., 2001)	External cooling supply	LCG	Thermal model	Astronaut, space suit	Space suit, automatic controller, thermal control system, liquid cooling garment LCG, ventilation gas flow, test efficacy of specific physiological state measurements to provide temp feedback data for input to automatic control, transient physiological parameters, metabolic rate, skin temperatures, core temperature, EVA, human simulation, Wissler model, prediction of LCG controller efficacy

(Odom & Phelan, 2012)	Vapor compression refrigeration	LCG	PCS Design	Military, HAZMAT, Firefighting, First responder, Industry	Spray cooling Air-Cooled Condenser, Microclimate vapor compression refrigeration cooling device, portable refrigeration, battery life, battery weight, cooling efficiency, liquid weight, spray cooling condenser,
(O'Hara, Eveland, Fortuna, Reilly, & Pohlman, 2008)	PCM, Free evaporation, saturated garments,	LCG, saturated garment,	PCS review article	Military,	Literature review 1990-2007, heat stress, neck cooling, head cooling, torso cooling, ice vest, RPE, rectal temperature, drinking cool water, cooling hood, LCG, arterial blood cooling, artery-cooling patch, CACP
(Kent B.; Pandolf et al., 1995)	PCM, Air circulation, Vapor compression refrigeration, External cooling supply	Air Vest, LCG, PCM Vest	PCS review article, Human subject, Thermal modeling	Military, Aircrew, Ground crew, CBRN, MOPP, PPE	PCS review article pre 1995, U.S. Army: chemical protective clothing, thermal manikin, field liquid-cooled undergarments, air cooled vests, desert, tropic, eight studies using LCU, one study PCM Vest, eight studies ACV, U.S. Navy: microclimate cooling systems (MCS), commercial systems, modification, passive cooling, used in fleet, general utility clothing, engine room, encapsulating garments, chemical protective garment, firefighter ensemble, U.S. Air Force: protective clothing, warm, hot, environments, air circulation, LCG, commercial systems, in-house prototypes, backpack system, partial system, ground crew
(Parrish & Scaringe, 1993)	Adsorption	Adsorption backpack, LCG	PCS design, Bench test	Military	LCG vacuum, Adsorbent bed backpack, pressure valve, prototype, chemical protective gear, 6 hr runtime, 300W= 6,480 kJ, proof of concept, desiccant, laboratory scaled measurements
(Paul, Gim, & Westerfeld, 2014)	Thermoelectric	Thermoelectric suit	PCS design	Industry	Peltier effect, temperature sensor, thermal comfort, control software, LCD, heating, cooling, controller
(Peksoz et al., 2009)	External cooling supply	LCG suit	Human subject	HAZMAT, PPE, First responder	HAZMAT A, HAZMAT B, OSHA, chemical protective clothing, two cooling units tested, core temperature, 2 skin temperatures, sweat rate, heart rate, perceived comfort levels, garment satisfaction, 35°C DB, 25%RH, 5 men, 50 min test max, 38.5°C core cutoff, 90% of max HR, volitional fatigue, 5 tests: Level B no cooling, Level B with cooling unit 1, Level B with cooling unit 2, Level A no cooling, Level A cooling unit 3, treadmill 2 mph

(Perez et al., 1994)	PCM	PCM Vest	PCS design, Thermal modeling, Bench test		Ice, PCM Vest, assumed adiabatic, ice pack evaporator, PCM in spacer vest, 2cm air gap, natural convection, rates of evaporation and condensation assumed equal, assumed steady state, heat and mass transfer analogy, Lewis number, ASHRAE model*
(Nancy A Pimental & Avellini, 1989)	PCM	LCG Vest, PCM Vest	Human subject	Military, Navy	8 men, no cooling, PCM vest 1, PCM vest 2, PCM based LCG vest/backpack, Air 43°C DB, 45% RH, WBGT, Navy utility uniform, 3 hour max test, treadmill 1.6 m/s, rectal cutoff 39.5°C, HR over 180 bpm, volitional exhaustion, rectal temperature, 3 skin temperatures, heart rate, sweat rate, thermal sensation, logistical concerns, freezer space
(Nancy A Pimental & Avellini, 1992)	PCM	PCM Vest	Human subject	Military, Navy	8 men, hot humid, hot dry, heat acclimation, Air 38-49°C DB 20-80% RH, WBGT 36-39°C, wind 1 m/s, 272W exercise, PCM vest, 4 hour maximum tests, cutoff for time, core, heart rate, volitional exhaustion, rectal temperature, heart rate, 3skin temperatures, mean skin temperatures, thermal sensation, 5.1 kg
(N.A. Pimental, Avellini, & Heaney, 1992)	PCM	PCM Vest	Human subject	Military, Navy	14 men, acclimation, six heat stress tests, 3 environments, 44°C DB 46°BG 49% RH, 51°C DB, 53°C BG 33% RH, 57°C DB 59°BG 25% RH, no cooling, PCM Vest cooling, treadmill 1.1 m/s 3% grade, 6 hour exposure, work rest cycle, 20 min work, 40 min of rest, average metabolic rate 208 W, U.S. Navy work uniform, PCS on T-shirt and work shirt, rectal temperature, 4 skin temperatures, heart rate, sweat rate, rectal cutoff 39.5°C, HR over 160-180 bpm 5 min during rest-work, volitional exhaustion,
(Pozos, Wittmers, Hoffinan, Ingersoll, & Israe12)	Thermoelectric	LCG suit	Human subject	CBRN, PPE, Military,	Two studies, two cycles of treadmill walking CBR suit, MOPP, 50 min work 10 min rest, 3 mph 2% grade, 10 min rest work rest cycle, Air 100°F DB 40% RH, 7 test conditions, Fatigues only, CBR only, Vest, Vest plus cap, vest plus legs, legs vest plus cap plus legs, location of cooling panels, ethylene glycol-water, inlet 14°C, 450 mL/min, ice bath backup, rectal temperature, heat flux transducers 6 sites, mean heat flow, heat rate, blood pressure, RPE, temperature perception, sweat rate
(RAČKIEN Ė)	Thermoelectric	Thermoelectric module	PCS design, Theoretical	Military, Industry	Finite element analysis, thermoelectric, thermal resistance, assumed linear resistance, assumed constant skin flux,

(M. M. Rahman, 1993)	Air circulation	Air Vest	PCS design, Theoretical	Military,	Heat engine and heat pump, Brayton cycle, provides temperature controlled air, generates electrical energy to power other equipment, produces drinking water, centrifugal compressor, two turbines/expanders/combustion chamber, three heat exchangers, water separator, electric generator, working fluid atmospheric air, diesel fuel, combustion, thermodynamic analysis, system efficiency, air-fuel ratio, system design
(M. Rahman, 1996)	Air circulation	Air vest	PCS design, Theoretical	Military	Heat engine and heat pump, Brayton cycle, centrifugal compressor, provides temperature controlled air, generates electrical energy to power other equipment, produces drinking water, two turbines/expanders/combustion chamber, three heat exchangers, water separator, electric generator, working fluid atmospheric air, diesel fuel, combustion, thermodynamic analysis, system efficiency, air-fuel ratio, system design, further analysis of previous paper
(Reffeltrath, Daanen, & den Hartog, 2002)	Air circulation	Air vest	Human subject	Military, Airforce, pilot, PPE	Royal Netherland Airforce RNA, survival suit, PPE, prototype, air cooling, integrate with current PPE, flight simulator, pilot error, flight performance, 5 men, 1 women, rectal temperature, 4 skin temperatures, sweat loss, heart rate, oxygen consumption, flight performance, cognitive performance, thermal comfort, thermal sensation, three tests conditions, one at 15°C WBGT 15°C DB, 29°C BG, 50% RH, other at 32°C WBGT 32°C DB, 49°C BG, 50% RH with and without cooling, pilot survival suit, sweat rate, sweat evaporation
(Reinertsen et al., 2008)	PCM	PCM Vest	Human subject	Industry, Surgeon	PCM, Glauber's salt, microcapsules, surgery in operating theater, well-insulated PPE, 6 subjects, VO <sub>2</sub> , heart rate, rectal temperature, mean skin temperature, 13 skin temperatures, sweat rate, thermal sensation, thermal comfort, skin wetness, Surgery: 1 man 23° DB, 50% RH wind 0.3 m/s, 20 min treadmill, 20 min of surgery tasks, 20 min of treadmill, Well-insulated PPE, 6 men, air 27°C 50% RH wind 1.5 m/s, effective cooling, freedom of movement, sufficient moisture transport,
(Rosen, Magill, & Legner, 2007)	External cooling supply, thermoelectric	LCG, Hand cooling	PCS Design, Thermal model, PCS Review article	Military, PPE	Military, Body armor, sub-atmospheric palm cooling, cooling glove, vacuum, calorimeter, heat sink shape, vasoconstriction, see other work by Heller et al., arterio-venous anastomoses, AVA, combat vehicles,

(Rothmaier, Weder, Meyer-Heim, & Kesselring, 2008)	Free evaporation	Three-layer laminate evaporative cooling	Human subjects, PCS Design	No PPE	Three layer laminate, waterproof/vapor permeable membrane, hydrophilic fabric, waterproof/vapor permeable membrane, dependent on environmental conditions, mini cylinder test device, MICY, saturated fabric, heat flux through membrane, 2 skin temperatures, 12 men, 23°C DB, 50% RH, no wind, treadmill, 4km/hr, 40 ml of water to right leg fabric, mean skin temperature
(Ryan et al., 2013)	Air circulation	Air vest	Human subjects	Military, Law Enforcement, Soft Body Armor	9 men, Soft body armor, chimney effect, 100L/min airflow, under buttoned shirt, rectal temperature VO <sub>2</sub> , walking, treadmill, 1.1 m/s with grade for 350 kcal/hr, Arm curls with 14.3 kg bar to 180 Kcal/hr, work rest cycle, WBGT 30C, Dry Bulb 35C, RH 57%, thermal sensation scale, rectal temperature, heart rate, RPE, sweat loss
(Sahta, Baltina, & Blums, 2011)	Thermoelectric	Thermoelectric vest	PCS Design, Human subjects	Industry	Solar cells, batteries Peltier elements, vest, skin temperature, Air temperature 26.3C, RH 59.9%, 1 minute long physical exercises on upper body, 3.5 minutes rest, PCS cooling cycled
(Sawka et al., 2003)	PCM, vapor compression refrigeration, Air circulation	LCG, Air vest, PCM Vest	Review Article, Standards	Military	LCG, Air cooling, Ice vest, heat stress control, technical bulletin
(Scheidler, Saunders, Hanson, & Devor, 2013)	PCM	PCM Palm pack	Human subjects	Sport	12 subjects, control, PCM palm cooling device, time to exhaustion runs, treadmill, 75% VO <sub>2</sub> max, air 30°C DB 50% RH, core initial 37.5°C, heart rate, RPE, feeling scale, core temperature, intestinal core temperature pill
(Semeniuk et al., 2005)	PCM,	LCG	Human subjects	HAZMAT, CBRN, NBC	5 men, heat acclimated, three trials, standard work clothing, HAZMAT suit, HAZMAT suit with torso LCG cooling, Dry bulb temperature 35C, RH 50%, air velocity 0.5 m/s, Treadmill, 300W, 90 min work or core temperature cutoff (38.5C) or heart rate (95% age max), or fatigue, disorientation, discomfort, subject to discontinue, PCM frozen 2L ice bottle, chilled water, flow rate 350 ml/min, battery life 4.5 hr Med-Eng Cardio COOL™ and PortaCOOL™, heart rate, rectal temperature, VO <sub>2</sub> , Douglas air bag,

(Shapiro et al., 1982)	Air circulation, vapor compression refrigeration,	LCG, Air Vest	Human subjects, Thermal manikin	Military, CBRN, PPE, MOPP	12 men, acclimated, simulated tank crews, 120 min max, 100 min rest, 20 min work, 4 min exercise period every 17 minutes, bench stepping, cycling, arm cranking, weight lifting, VO <sub>2</sub> , heart rate, rectal temperature, 3 skin temperatures, mean skin temperature, mean body temperature, body heat storage, sweat rate, sweat evaporation, hot wet 35°C 75% RH, hot dry 49°C DB 20% RH 68°C BG, air inlet 21°C hot dry, 19°C hot wet,
(Shim, McCullough, & Jones, 2001)	PCM	PCM Fabric	PCS Design, Thermal manikin	Industry	One and two layer body suits, with and without PCM, microcapsules, 60% PCM microcapsules, octadecane, 28.3° melting point, hexadecane, 18.3°C, fit, outside of garment, ASTM D1776, ASTM D 1388, ASTM D 3776, ASTM D2863, ASTM F1868, ASTM F 1291, thermal transients,
(Shitzer, Chato, & Hertig, 1973)	External cooling supply, thermoelectric	LCG, tethered	Human subject, PCS Design	Astronaut	5 men, VO <sub>2</sub> , treadmill 3.2 km/hr -6.4 km/hr, inlet water temperature 16°C, outlet temperature, regional cooling, heart rate,
(Shitzer, 1997)	External cooling supply, thermoelectric	LCG, tethered	Human subject, PCS Design	Astronaut, EVA	5 men, work rest cycle, standing, level treadmill, 6 regions of cooling, EVA, VO <sub>2</sub> , aural temperature, thermal comfort, step activity level, treadmill 6.4 km/hr, duration of each work/rest 15 min, 23°C and 60% RH, sweat rate
(Shvartz, 1972)	External cooling supply, thermoelectric	LCG, tethered	PCS review	Military, Astronaut, PPE	10 reviewed papers, water cooled LCG, different cooling suits, neck head, entire body, hands, feet, face, torso, upper arms, arms, thighs, heat strain reduction, surface area cooled, body area covered, experimental conditions, PPE, isolated, moderate, hot, mild work
(Siegel et al., 2010)	PCM	PCM ingestion	Human subject	Sport	10 men, 7.5 g/kg ice slurry (-1°C) or cold water (4°C) ingestion precooling, run to exhaustion, hot, air 34°C DB 54.9% RH, rectal temperature, 4 skin temperatures, heart rate, sweat rate, thermal sensation, RPE, mean skin temperature, mean body temperature, body heat storage, VO <sub>2</sub> max, skinfold thickness,
(Sleivert, Cotter, Roberts, & Febbraio, 2001)	PCM, External cooling supply, thermoelectric	PCM Vest, LCG cuff	Human subject	Sport	9 men, pre cooling, no cooling control, precooling torso only thighs warm, precooling torso and thighs, high intensity exercise 45 sec, influence of post cooling warmup, rectal temperature oesophageal temperature, forearm blood flow, mean skin temperature, VO <sub>2</sub> max, 45 min precooling, 6 min warmup 45-50% VO <sub>2</sub> max, 6 min rest, 45 second power test cycle ergometer, air 33°C 60% RH, 9 skin temperatures, strain gauge plethysmograph, LCG, power output, mean body temperature, mean skin temperature,

(Speckman et al., 1988)	PCM, External cooling supply, thermoelectric, Air circulation	PCM Vest, LCG vest, LCG suit, Air vest	PCS Review, Human subject, Thermal manikin,	Military, PPE, CBRN, MOPP,	Air cooling, conditioned air cooling, ambient air cooling, liquid cooling garment, liquid cooling undergarments LCU, PCM based LCG, desert, tropic, armored vehicles, seven studies LCG/LCU, six studies ACV, cooling surface area, temperature, humidity, air flow rates, liquid flow rates, sweat rate, core body temperature, rectal temperature, skin temperatures, USARIEM,
(Stephenson, Vernieuw, Leammukda, & Kolka, 2007)	External cooling supply, thermoelectric	LCG	Human subject, PCS Design	PPE, CBRN, MOPP	8 men, warm dry, 30°C DB, 11°C DP, treadmill, met 225W, 80 min, LCG 72% BSA, inlet temperature, outlet temperature, electrical power, skin temperature feedback control, regional body LCG, CBRN, MOPP, three tests, control, constant cooling all regions, pulsed cooling to all regions bases on mean skin temperature, 34.5°C pump on, 33.5°C pump off, treadmill 1.36 m/s 2% grade, heart rate, intestine pill core temperature, 8 skin temperatures,
(Sun, Cheong, & Melikov, 2012)	Air circulation	Fan	Human subject	Industry, Office	Office chair, 4 fans, displacement ventilation supplementation, thermal comfort, thermal sensation, three air temperature 20°C, 22°C, 24°C, tropically acclimatized, 32 subjects, local thermal sensation, LTS, IAQ,
(Tan & Fok, 2006)	PCM	PCM helmet	PCS design	Sport, Motorcycle	PCM, motorcycle helmet, thermal comfort, 2 hour cooling, energy balance, one directional heat transfer, thermal modeling
(Tayyari, Burford, & Ramsey, 1989)	PCM	PCM Vest	Human subject, PCS Design	Industry	4 men, acclimation, Air 40 °C DB, 35 °C WB, 75% RH 37 °C WBGT, heart rate, rectal temperature, sweat rate, 95 min, treadmill,
(WB Teal, 1994)	PCM	PCM Vest	Thermal manikin	Military, PPE, CBRN, TAP	Thermal manikin, CPO, TAP suit, US Navy CBRN, PCM vest, control, PCM over ensemble, PCM under ensemble, ensemble with exterior pockets for the cooling packs, 29 cooling packs, air 35 °C 60% RH 0.9 m/s wind, 35 °C thermal manikin temperature,
(W Teal, 1996)	External cooling supply, PCM	LCG tethered	Thermal manikin	Military, PPE, CBRN, TAP	Thermal manikin, TAP suit, military, LCG, flow rates 4.5, 7.0, 9.7 gallons per hour, inlet temperatures 50°F and 70°F, prediction 95°F environment, flow rate to cooling equation, thermal manikin LCG test method
(Terzi, Marcaletti, & Catenacci, 1989)	External cooling supply,	LCG	Human subject, PCS design	Sport, Industry	10 men, 6 women, no cooling control, upper body cooling with leg heating, thermal control sensation location, LCG inlet temp, LCG outlet temp, VO <sub>2</sub> peak, rectal temperature, 9 skin temperatures, mean skin temperature, 10 heat flux transducers, LCG skin contact, four 30s cycle ergometer 90 rpm power output 120% VO <sub>2</sub> peak, work rest cycle,



(Teunissen et al., 2014)	Free evaporation, PCM	LCG, water saturated fabric	Human subject	Firefighter, PPE	9 men, work rest cycle, 30 min walking 6 km/hr, 10 min rest, hot, heart rate, rectal temperature, sweat rate, thermal sensation, thermal comfort, RPE, firefighting garment, air 30°C 50% RH, 4 skin temperatures, mean skin temperatures, sweat evaporation,
(Torii, Adachi, Miyabayashi, Arima, & Iwashita, 2005)	PCM	PCM packs	Human subject		7 men, bicycle ergometer, 40 min, PCM, ice pack, hot 30°C DB, 40%RH, wind 0.3 m/s partial body cooling, 60-70% VO <sub>2</sub> max, tympanic temperature, rectal temperature, 6 skin temperatures, skin blood flow, local sweat rate, ventilated capsule, one location, heart rate, thermal sensation, ice pack provided 20 min into test during cooling, 50 RPM, bilateral carotid cooling,
(Tuck, 1999)	PCM, vapor compression refrigeration,	LCG, tethered, PCM Vest, Air vest	PCS review, PCS design	Industry, Mining	Requirements for PCS use in mining, compressed air movers, fans, ice jacket, air conditioning, sedentary work pattern, dry ice, tethered PCS, compressed gas cooling, vapor expansion vest, vent to atmosphere
(Uglene et al., 2002)	Vapor compression refrigeration, free evaporation	LCG, tethered, Air vest, conditioned, free evaporation	Human subjects	Military, Aircrew	7 men, seated, aircrew simulation, environmental chamber, ejection seat, no wind, aircrew survival equipment, G-suit, air cooling, conditioned air, two tests, with air vest with conditioned air, air vest with conditioned air and enhanced cooling vest, enhanced cooling vest waterproof vapor permeable vest bladder containing liquid water at static pressure, vest inlet air temperature, sweat rate, heart rate, rectal temperature, mean skin temperature, heat flux, air flow rate, thermal comfort max test length 3 hr, rectal temperature max 39°C, 2°C above initial, heat stress symptoms, volitional exhaustion, cooling part of test
(A L Vallerand, Schmegner, & Michas, 1993)	Air circulation, Vapor compression refrigeration	Air Vest conditioned	Human subjects	Military, CBRN, PPE, Aircrew	7 men, three Canadian chemical defense individual protection ensembles, hot cockpit conditions, control no cooling, air-cooling vest, 37°C DB 50% RH, max time 150 min unless stopped, helicopter, G-suit, rectal temperature, 12 skin temperatures, heart rate, treadmill 10 min walk 4km/hr 0% grade, 20 min rest, work rest cycle, 10 min of work at 50@ ergocycle, 10 min rest, for 150 min unless stopped, sweat rate, sweat evaporation rate, thermal comfort, VO <sub>2</sub> , conditioned air vest, heat storage, heat balance
(Van Rensburg, Mitchell, Walt, & Strydom, 1972)	PCM, External cooling supply,	LCG, ICE Vest	Human subject	Industry, mining	2 men, acclimated, LCG inlet temperature, LCG outlet temperature, LCG cooling aggregate, 48 to 54 L/hr, rectal temperature, heart rate, sweat rate, working nude in neutral environment, nude in hot humid environment, hot humid environment but protected by a cooling system, worked at 35 W box stepping 12 times per minute,

(Vernieuw, Stephenson, & Kolka, 2007)	External cooling supply,	LCV suit	Human subject	Military, CBRN, MOPP, PPE	8 men, moderate work 425W, 3 cooling tests, LCG, circulating fluid head, torso, thighs, constant cooling, pulsed cooling, pulsed cooling controlled by skin temperature, thermal comfort, thermal sensation, intestinal core temperature pill, heart rate, sweat rate, chemical protective suit, inlet temp 21..5°C flow 1.2L/min, warm dry 30°C DB, 30% RH, treadmill 80 min, walk 1.36 m/s, 2% grade, ~225 W/m <sup>2</sup> , 425W, wind 0.939 m/s, 8 skin temperatures,
(von Restorff, Dybala, & Glitz)	Air circulation	Air	Human subject	Military, CBRN, MOPP, PPE	8 men, VO <sub>2</sub> max, treadmill, German NBC PS, CBRN, control no cooling, with filtered air cooling, ambient air through filter canisters at back by kidney, 1/3 guided to face mask to provide breathing air, heart rate, 2 skin temperature, two microclimate humidity, rectal temperature,
(J. Wang, Dionne, & Makris, 2005)	External cooling supply,	LCG	Thermal manikin	HAZMAT, PPE, Firefighting	Thermal manikin, LCG inlet water temperatures 8-24°C, LCG flow rate 0.35 to 0.65 L/min, HAZMAT level B, firefighting gear, sweating test with SPM CBRN suit, 35°C air, 35°C manikin temperature,
(J. Wang & Makris, 2005)	External cooling supply, Vapor compression refrigeration	LCG	Thermal manikin	HAZMAT, EOD, Military, Industry, Firefighting,	Thermal manikin, influence of fit on LCG performance, use of thermal manikin to determine average heat transfer coefficient for LCG, LCG worn under HAZMAT Level B suit, natural test (on top of T-shirt) and snug (tape rewrapping around torso to provide a closer fit
(Warme-Janville & Anelli, 2002)	Air circulation, PCM,	LCG, PCM Vest, Compressed air, Zeolite	Thermal manikin, Human subjects	Military	Suit insulation ASTM 1291, cooling power, human subjects Air 35 °C, RH 40%, wind 1m/s, 20 min seated rest, 30 min walk 4 km/hr 0% grade, 10 min seated rest, 30 min walk 4 km/hr 0% grade, 30 min seated recovery, 10 types of different types, rectal temperature, skin temperature, heart rate, sweat loss, sweat evaporation, questionnaire about PCS, compression. Blowers ice packs, zeolite-air, cooling, body heat storage,
(Warpeha et al., 2011)	External cooling supply,	LCG	Human subject	Astronaut	4 men, 2 women, VO <sub>2</sub> , core temperature, skin temperature, heart rate, local sweat rate, skin wettedness data,
(Webster, Holland, Sleivert, Laing, & Niven, 2005)	PCM	PCM Vest	Human subject	Sport	8 men, 8 women, precooling, VO <sub>2</sub> max, control, three cooling vests, cooling vests A, B, C, Vests were worn during rest stretch, warm-up 50% VO <sub>2</sub> max, not during 30 min run 70%, rectal temperature, skin temperatures, treadmill, 7 skin temperatures, heart rate, sweat rate, thermal sensation, skin wetness, cooling strategy,

(Weller, Greenwood, Redman, & Lee, 2008)	PCM	LCG Vest	Human subject	Military, aircrew	6 men, hot flight scenario, three test conditions, High LCG flow rate, Low LCG flow rate, LCG worn over combat shirt with a “high” flow rate, treadmill walking, 400W met, 20 min, leg press exercise 200W met 80 min, WBGT 34°C, summer aircrew equipment assembly, heat strain, rectal temperature, torso temperature, heart rate, rate of water loss, sweat rate, PCM based LCG
(White, Glenn, Hudnall, Rice, & Clark, 1991)	PCM, Compressed gas	LCG, vapor expansion suit FREON	Human subject	Military, CBRN, PPE	9 men 30% VO <sub>2</sub> max, four conditions, control w/ shirts shirt helmet shoes SCBA, CRS w/ control ensemble, CRS w/ control ensemble PCM based LCG, CRS w/ control ensemble Freon cooling system, work rest cycle 5 min work, 10 min rest, max work time 45 min or until cutoff, heart rate, skin temperature, rectal temperature axillary temperatures, treadmill 4 km/hr,
(Wickwire et al., 2009)	Free evaporation saturated garment	Saturated fabric head pad	Human subject	Military, PPE, Body Armor	10 men, Rectal temperature, heart rate, 1 skin temperature forehead, PASGT helmet, blood sample, hemoglobin hematocrit, air 33.79 °C WB, 38.47 °C DB, 38.43 °C Globe, treadmill, 4.8 km/hr, 0% grade, 2 hour test, rest every 12-15 min, body armor, flipping cooling pack, RPE, 10 bicep curls 14.3 kg, sweat rate,
(Williams, Mcewen Jr, Montgomery, & Elkins, 1975)	External cooling supply, PCM,	LCG	PCS Review	Military, Industry, Medical, Mining	Head cooling, liquid cooling, liquid cooling brassiere, breast cancer screening, infant LCG, head-neck cooling, partitioned cooling, chemotherapy, hair loss, thermographic breast scan,
(Williamson, Carbo, Luna, & Webbon, 1999)	Air circulation, Compressed gas	Air Suit, vapor expansion suit	Human subject	HAZMAT	NASA, 12 men, HAZMAT Level A, two suits, two life support systems, prototype HAZMAT suit, liquid air breathing system, convection from compressed gas, VO <sub>2</sub> max, 5 minute standing, 3 min walking 2.5km/hr, 45 min walk 3.2 km/hr., 3 min cool down 2.6 km/hr, standing 5 min, treadmill 0% grade, Control with T-shirts, HAZMAT suits with SCBA, HAZMAT suits with cryogenic liquid air backpack replacing SCBA, Air 24.4°C DB, 40-45% RH, NFPA, heart rate, rectal temperature, 5 skin temperatures, mean skin temperatures, ear canal temperature, RPE, oxygen cost of exercise, mean body temperature
(Eugene H. Wissler, 1986)	External cooling supply,	LCG	Thermal model	HAZMAT, Military	Wissler model, advanced human modeling, thermal modeling personal cooling system, fluid conditioned garment, heat exchanger elements, validation against (Shapiro et al., 1982)

(Wittmers, Hodgdon, Canine, & Hodgdon, 1998)	PCM, External cooling supply,	LCG vest, Encapsulated PCM in LCG vest, tethered	Human subjects	CBRN, MOPP, Military	10 subjects, three conditions, control, LCG, LCG with Encapsulated Phase Change Material EPCM, EPCM slurry, treadmill 3 mph 2% grade, 120 walking, Air 98-100°F, liquid water 5.15cc/min inlet temperature 14°C, rectal temperature, 4 skin temperatures, blood pressure heart rate, MOPP III, Fluid w/ EPCM 20% EPCM 1% Triton X-100, core regression, mean skin temperature, thermal sensation]
(Wu, Ma, & Zhong, 2009)	Vapor compression refrigeration,	None	Bench test	None	Testing 2 miniature Wankel compressors, 300W cooling capacity, developed for MCS, weight <0.26 kg, system prototype <2.85 kg, compressor ratio, coefficient of performance, efficiency
(Xu, 1999)	External cooling supply,	LCG	Human subject, Thermal model		8 men, Three loop LCG, torso, arms legs, separate control, two conditions, first water inlet temp adjusted according to local thermal sensation, second inlet for torso and arms and inlet for legs were regulated by skin temperature for each, theoretical analysis mathematical models, rectal temperature, 10 skin temperatures, VO <sub>2</sub> , Air 35 °C 40% RH, thermal sensation, water inlet, thermal sensation control, automatic cooling control, six cylinder human thermal model,
(Xu et al., 2004)	External cooling supply,	LCG	Thermal model	CBRN, MOPP, PPE, Military	Human thermal model, six cylinder human thermal model, model of thermoregulation, LCG, MOPP, intermittent regional cooling IRC, constant cooling, energy savings
(Xu et al., 2005)	External cooling supply,	LCG	Thermal manikin	Military, PPE	Dry thermal manikin, Sweating thermal manikin, three ensembles, cooling vest only, cooling vest plus BDU, Cooling vest plus BDU overgarment, 18 zone, thermal manikin surface 33 °C during all tests, air 30 °C 50% RH, inlet temperatures 15, 20, 25 °C respectively, flow rate 0.5 L/min, LCG, thermal resistance, evaporative resistance, cooling efficiency wet, cooling efficiency dry,
(Xu et al., 2006)	External cooling supply,	LCG	Thermal model, Thermal manikin	Military, PPE,	Dry thermal manikin, Sweating thermal manikin, three ensembles, cooling efficiency of LCG, development of equation to estimate LCG cooling efficiency, energy balance, cooling vest only, cooling vest plus BDU, Cooling vest plus BDU overgarment, 18 zone, thermal manikin surface 33 °C during all tests, air 30 °C 50% RH, inlet temperatures 15, 20, 25 °C respectively, flow rate 0.5 L/min, LCG, thermal resistance, evaporative resistance, cooling

(Xu & Gonzalez, 2011)	Air circulation	Air vest	Thermal manikin	Military, PPE	Body armor, EOD, body ventilation system BVS, heat stress, thermal modeling, cooling capacity, inlet humidity, outlet humidity, efficiency is ratio, sweating thermal manikin, dry thermal manikin, turned on flow rate 4.7 L/s, turned off, 11 ambient conditions,
(Y. Yang, 2011)	Vacuum desiccant cooling	Desiccant pads	PCS design, Human subject	Military, CBRN, PPE	Adsorption vacuum membrane evaporative cooling, man-portable, water temperature 12.5 °C, human subject test, NWBC nuclear warfare biological chemical suit, 12 cooling pads, treadmill 2 mph, Air 40 °C 50% RH, core temperature
(Y. Yang, Stapleton, Diagne, Kenny, & Lan, 2012)	Vacuum desiccant cooling	Desiccant pads	PCS design, Human subject	Military, CBRN	Vacuum desiccant cooling VDC, cooling pads, core temperature, weight 3.4 kg, 12 cooling pads, 0.4 m <sup>2</sup> surface area, treadmill 3 mph 2% grade 60 min, air 40 °C 50% RH, NBC suit, evaporative cooling
(Yazdi & Sheikhzadeh , 2013)	PCM	PCM vest	PCS design		Performance of cooling garment measure, thermal comfort, thermal stress, simulation about real use, proposed parameter, represent success of cooling vest, body heat exchange with environment, cooling power of cooling garment, dimensionless, smaller the PCG lower ability of cooling garment in reaching thermal comfort, calculation for a cooling vest, body heat storage
(Yermakova, Candas, & Tadejeva, 2005)	Air Circulation	Air vest	PCS model	Military	PCS model, MCS impermeable clothing, computer simulation, microclimate cooling system, cooling system on, cooling system off, blood temperature, mean skin temperature, convection, evaporation
(Yokota et al., 2010)	Air circulation	Air flow in wrap	Thermal model	Military, medical, CBRN, MOPP	U. S. Army protective patient wrap PPW, desert, jungle, temperate conditions with and without sun, with and without fan ventilation, patient protection in CBRN environment
(Yoshida, Shin-ya, Nakai, Ishii, & Tsuneoka, 2005)	Cooling aggregate	LCG	Human subject	Sport	6 men, three sessions 20 min cycling, light intensity 250 W/m <sup>2</sup> , Air 28 °C WBGT, 7 conditions, 3 sets of clothing, suits at 14 °C, 20 °C, 26 °C, and fencing uniforms without cooling by water perfusion, thermal sensation, heart rate, total sweat loss, esophageal temperature, LCG inlet temperature, LCG outlet temperature,
(Young, Sawka, Epstein, Decristofano , & Pandolf, 1987)	Cooling aggregate	LCG	Human subject	Military	6 men, 6 exercise, hot, air 38 °C, 30% RH, low moisture permeability clothing, VO <sub>2</sub> , arm crank exercise, with torso cooling, with torso and arm cooling, inlet temp 20 °C, four lower body exercises, torso cooled 20 °C, 26 °C, and torso arm cooled 20 °C, 26 °C, thermal sensation, rectal temperature,

(Zalba et al., 2003)	PCM		PCS Review Article, PCS information		Review of phase change materials and heat transfer analysis, properties, applications, material types and compositions, classification, stability, moving boundary, numerical solutions, convection, conduction, heat exchanger geometry
(Y. Zhang, Bishop, Casaru, & Davis, 2009)	PCM	LCG hand	Human subject	Firefighting, PPE	8 men, VO <sub>2</sub> peak, sweat rate, heart rate, rectal temperature, firefighter turnout gear, ensemble mass 19.1 kg, air 33.7°C WBGT 36°C DB 33°C WB 36°C globe 44% RH, 40 min of combined arm and leg activities, sub-atmospheric, vacuum, palm cooling, PCM based LCG palm cooling,
(Y. Zhang, Bishop, Green, Richardson, & Schumacker, 2010)	Compressed gas expansion	LCG expansion shirt	Human subject	Industry	10 men, VO <sub>2</sub> max, work rate 465 W, treadmill, 523W for 12 min at 1.33 m/s, arm curls, 209W with 13.9 kg, hot, humid, rectal temperature, sweat rate, 3 skin temperatures, heart rate, t-shirt, short, jeans socks, and shoes, Air 30°C WBGT, 33°C DB, 29°C WB, 33°C Globe RH 75%, heat storage, sweat rate, sweat evaporation, heat storage, mean body temperature, thermal rating, thermal comfort, direct expansion compressed gas PCS LCG shirt, control no cooling

## **Chapter 3 - PCS Selection and Testing**

The initial priority of this research was to evaluate personal cooling systems for use by the dismounted U.S. Army soldier in order to mitigate heat stress. This task was split up into multiple phases comprising: database construction, PCS selection, thermal manikin testing, and human subjects testing. Eventually, this also comprised a modeling and analysis task much larger than the original Army project. The database contains more than 350 personal cooling systems. The equipment used in measuring PCS properties at each test will be described as well as the steps and setup of the PCS testing process.

### **3.1 PCS Selection**

The goal of this study was to find commercially ready, or nearly commercially ready PCS, evaluate and select the best systems for thermal manikin and human subject tests, and be able to justify the results. The initial task was finding as many commercial systems on the market as possible, including prototypes and military systems, then compiling them into a database. This created a pool of candidate systems from which to select the potentially best systems. To narrow down the over 300 systems in the database, a set of engineering metrics were developed and refined with input from the Army, consultation with active duty soldiers, and information found in literature. This PCS selection matrix included a novel method of selecting PCS and has been published in more detail in journal form (J. Elson & Eckels, 2015). The database creation and selection tool development and military applications are the focus of this section.

#### ***3.1.1 KSU PCS Database***

The KSU PCS Database was a significant outcome of this research. The database is built on the work of others. The original database was created by Walter Teal and Brad Laprise (2005)

as the Microclimate Cooling Database. This was updated and formed into the basic format used in this study during a previous study (E.A.; McCullough & Eckels, 2008). The database was expanded during this work by searching a number of keywords including body armor cooling, body armor heat, personal cooling system, personal temperature regulation system, temperature regulation body armor, microclimate cooling system, personal cooling device, air circulation system, phase change materials, individual cooling, wearable cooling device, and others.

The database contains over 390 systems, some are not unique, copies of other manufacturers' systems, or different re-sellers of the same systems. The database contains information about each system and contact information for the company in a cross referenced sheet. Many manufacturers did not provide vital statistics like size, weight, energy removal, and power requirements. The fields for each system are: Product Name, Company, Technology Classification, Product Description, Physical Description, Energy Removal, Size, System Weight, Power Requirements, Support System Requirements, Mobility Limitations, Unit Price, Price per Use, and Image. The Company fields are: company, Address Line 1, Address Line 2, City/State/Zip code, Telephone 1, Telephone 2, Fax, Company Contact, Web Address, and Notes. These were compiled in forms to allow for easy viewing and filtering based on fields. An example of a product from is shown in Figure 3.1 and the company form is shown in

Figure 3.2



---

## Entrak

---

www.ventilationvest.com

Energie- und Antriebstechnik GmbH und

90530 Wendelstein

+ 49 (0) 9129 40 35-0

---

### **iceCube**

**Technology Classification:** Active Evaporation

**Size:** One size fits all

**Product Description:**

The iceCube system contains phase change materials. Air is circulated over this phase change material to circulate cool air around the body.

**Weight:** 5.3 lb.

**Power:** 11.1 V battery

**Price:** Not given

**Physical Description:**

The iceCube system contains a phase change material in a placed on the front and the back with a battery powered fan to circulate air. The vest is held by shoulder and side straps.

**Support System Requirements:**

Extra freezer packs and batteries

**Mobility Limitations:** None



---

### **ventilationVest**

**Technology Classification:** Active Evaporation

**Size:** XS-3XL

**Product Description:**

The ventilationWear system contains two fans inside of a spacer vest to circulate air around the body.

**Weight:** 2.2 lb.

**Power:** 11.1 V battery

**Price:** Not given

**Physical Description:**

The ventilationWear system is a vest that contains two pockets on each hip that contains a fan module. These fans produce airflow under the vest at up to 400 liters of air per minute.

**Support System Requirements:**

Extra batteries

**Mobility Limitations:** None



---

Figure 3.1 KSU PCS Database product report form page

<b>Company:</b>	<i>Entrak</i>		
<b>Address:</b>	<i>Energie- und Antriebstechnik GmbH und 90530 Wendelstein www.ventilationvest.com + 49 (0) 9129 40 35-</i>		
<b>Product Name</b>	<b>Technology Classification</b>	<b>System Weight</b>	<b>Unit Price</b>
ventilationVest	Active Evaporation	2.2 lb.	Not given
iceCube	Active Evaporation	5.3 lb.	Not given

**Figure 3.2 KSU PCS Database company report form page**

### ***3.1.2 PCS Selection Criteria***

A significant component of the research was selecting the most appropriate cooling systems for the dismounted soldier. This is complicated by the many tasks and movements that are performed by the dismounted soldier over different periods of time and with varying equipment, clothing, and loads. At the beginning of the project there was not a reference for guidance in selecting PCS, however after the project was completed a reference on factors affecting submitted PCS was published by the Army (Laprise, 2012). Therefore, a set of criteria were developed to create a decision matrix using concepts from Ullman (1992). To create a useful tool, user requirements must be identified, grouped, and extrapolated into a scored system so they can facilitate a logical comparison between PCSs. This often presents a considerable challenge, as some user requirements are easily identified while others are much more difficult to define.

In this case, the first step was to identify necessary user requirements for the dismounted soldier by examining the research literature; standard operating procedures (SOPs); tactics, techniques, and procedures (TTPs); information on clothing and personal protective equipment (PPE) used by the soldier; and interviews with soldiers recently returned from deployment in the Middle East.

The basic requirements of a PCS intended for the dismounted soldier are that it should provide beneficial cooling effect without having a negative effect on the performance of the soldier. The list of other user requirements had to be narrowed down to reflect the level of information available on the PCS. A set of user requirements for the dismounted soldier discussed in this example are portable recharge supplies, bulk, weight, explosive, flammable, PPE compatible, safe, not tethered, simple maintenance, beneficially cool soldier.

### ***3.1.2.1 Factors***

User requirements needed to be refined into concrete terms and organized to reflect the interdependency of terms to create a score for each PCS identified. The degree to which each factor is important depends on the logistical scenario, which means the list had to be very general at this point in the process. In order to define the factors, user requirements had to undergo an evolution into engineering criteria, which are concrete and measurable terms. In some cases, multiple engineering criteria were formed out of one user requirement. It was important that engineering criteria were quantifiable and could be evaluated with the level of information available in the database

### ***3.1.2.2 Supply Portability Factor***

The length of time a PCS runs can often be altered by providing additional supplies. For example, extra batteries may provide additional life to the PCS. Therefore, the ability of the person to carry supplies or have immediate access to supplies is an important factor. All of these issues were incorporated into the supply portability rating. Technology such as phase-change materials (PCM) require an insulated cooler to maintain their effectiveness in storage over short periods of time, and a refrigeration system to stay frozen over longer periods. Extra PCM packs are something the end user could not easily carry, as the material would be losing significant

effectiveness while being transported unless incredibly insulated. Batteries or fuel cells are examples of supplies that are portable and will maintain their effectiveness over long periods of time. They are generally not very susceptible to temperature variation and do not require much additional space in an equipment pack. In the evaluation tool, a system where supplies did not take up minimal volume and were not portable by an individual without degradation in effectiveness would either allow the system to pass, or fail the logistical scenario defined. This is dependent on the importance of portable supplies on the application.

### ***3.1.2.3 Ergonomic Factor***

Personal protective equipment is very important for the end user in this application. Ideally, the personal cooling system should be worn under the soldier's body armor in order to interface with the large torso surface area. The PCS should be ergonomically compatible with the body armor and not impede the soldier's range of motion. Removal of body armor to recharge the system is a major issue for soldiers deployed in the field. Feedback from soldiers indicated they sometimes remove their body armor in the field to allow for cooling if in danger of heat stress, even when this decreases their protection from ballistic threats (Buller et al., 2008). Use of a PCS should reduce the need for the end user to remove his armor or other PPE. Obviously, if the end user must remove the PPE to recharge the system, then the benefit of the protective equipment has been lost.

The scoring system for the ergonomic factor could consider a wide range of issues, but with the limited amount of information available, only a couple of variables could be included. However, as more information becomes available, more ergonomic requirements can be included. In this example the pass fail criteria for a logistical scenario was set if the PCS compromised the effectiveness of the armor. If the system was not compatible with the body

armor, the system automatically was dropped, as this was a crucial factor. Incompatible could include systems too big to fit under body armor or not able to provide cooling when the body armor is worn.

#### ***3.1.2.4 Mobility Factor***

The mobility factor ranks the freedom of movement the soldier experiences when the PCS is being worn. This obviously is an extremely important factor for the soldier. The area-wide mobility of the soldier was considered in this factor – not the user’s flexibility or individual range of motion. Mobility is important, but it requires additional information to evaluate. For example, a system tethered to a stationary object limits the area of mobility of the soldier to the region of the tether. If user mobility was an important factor for a specific logistical scenario, this factor would be included to determine if a PCS were to be considered on other factors. It should also be recognized that the mobility documented by this factor was more important in some operational scenarios and less in others, which can be accounted for by using a weighting function discussed later.

#### ***3.1.2.5 User Maintenance Factor***

Another important factor is the ability of the end user to maintain the equipment in the field. A number of important criteria could be considered. For example, reliability of the system in different environments is difficult to determine at this level of analysis, but it is important. As the field of potential PCSs is narrowed, reliability could be incorporated into this factor as more information becomes known.

In this example, the main criterion considered was the maintenance time required for the end user to keep the system running while in the field without assistance. We estimated how fast the soldier could change out whatever part of the system was necessary to restore function. This

was limited to the power or cooling element in the PCS. This was an estimate based on pictures and descriptions of the systems provided by the manufacturers along with familiarity with the body armor systems on the part of the evaluator. The premise of the scoring for the application of the dismounted soldier was that minimum amount of maintenance time was most desirable. Therefore, the estimated time to restore cooling was broken up into three, 20-second increments. Each increment marked potential cutoff point when evaluating a PCS on a logistical scenario. In some scenarios, systems that were maintained in less than 20 seconds were allowed to pass, other scenarios systems estimated to require up to 0 seconds received passed, and in some logistical scenarios this factor was deemed unimportant.

#### ***3.1.2.6 Cooling Effectiveness Factor***

The cooling effectiveness factor was the most important, and novel part of the selection method. The score presented here is the same version published in the Journal of Applied Ergonomics (J. Elson & Eckels, 2015). Sections and equations have been quoted directly with permission from the publisher.

The primary purpose of the PCS is to protect the end user from heat stress by providing cooling to the body. In some cases, a PCS can be selected based only on its cooling rate, and this is relatively common. However, for the dismounted soldier, it is more complicated. The U.S. Army prefers to use cooling effectiveness as a variable consisting of the cooling (measured in Watts) divided by PCS weight to help account for the impact of the PCS weight on the soldier. However, duration of the cooling effect is as important as the cooling rate. The cooling rate itself may have other effects as discussed in Chapter 6. After systems are no longer effective, they become extra weight for the user to carry, thus adding to the physiological strain on the user.

Therefore, it was recognized that a time factor was needed to take into account effects of the limited run time of a PCS over longer mission times.

In developing a final numerical score for the cooling effectiveness factor, the three engineering criteria – cooling rate, duration, and system weight – needed to be combined in a logical manner. This was done by coupling existing equations for metabolic work rate with the first law of thermodynamics to calculate the time to heat stress for an average-sized man.

Physical aspects were defined as a slightly above average-sized man for this study at 81.6 kg (180 lbs.) and 1.8m tall, with 1.8 m<sup>2</sup> of surface for the purposes of thermal modeling.

Comparing the mission time required with the time to heat stress, with and without a PCS, gave a relative measure of effectiveness. Therefore, it was necessary to develop a logical way to incorporate the criteria of the PCS weight, supply weight, mission duration and cooling duration per cooling element into the evaluation tool in terms of the effect on heat generation.

This analysis begins with the energy balance of the human body with the personal cooling system presented in Equation ( 2.6 ) with a separate cooling time for the PCS to represent a shorter than mission time cooling ability. The storage term,  $St$ , represents the allowable energy storage in the body. Metabolic rate, again is the metabolic rate of the subject but includes the effects of carrying a PCS. The external work rate produced by the body is still  $Wr$ , the natural heat transfer term from the body,  $Ht$ , should be considered the natural heat transfer including the additional resistance caused by wearing the PCS. This is a difficult value to measure and will be discussed further throughout this work, and in detail in Chapter 5. The average PCS cooling power,  $Cl$ , over the PCS cooling time,  $\Delta t_{PCS}$ , is the effective cooling of the PCS. Finally, the maximum mission time is,  $\Delta t_{max}$ .

$$St = (Mr - Wr - Ht) * \Delta t_{max} - Cl * \Delta t_{PCS} \quad (3.1)$$

**Metabolic Rate**

The following section is excerpted from *Applied Ergonomics*, Vol. 48, pg. 33-41 J. Elson and Eckels (2015) used with permission from Elsevier Ltd. “To determine heat storage, metabolic work levels need to be estimated based on the tasks being performed by the wearer. Tables of metabolic rates for different activities can be found in the literature (Ainsworth et al., 2011; American College of Sports Medicine, 2010; K. Parsons, 2006) if the task metabolic rate is not known. Obviously, using direct measurement of metabolic rate during a task is preferable but not always possible. In the example of the dismounted soldier, activity levels provided in military publications FM 3-4 (Department of the Army, 1994) and TB-MED 507 (Sawka et al., 2003) can be used to determine possible work levels. In the selection done for the Army, the values for FM 3-4 were used solely because of the greater subdivision of work levels.

**Table 3.1- Selected work-rate levels for the dismounted soldier from Sawka et al. (2003)**

FM 3-4	TB-MED 50	KSU inputs to model
Very Light (VL) (105 - 175 W)	Easy Work (E) (< 250 W)	Very Light (VL) 175 W
Light (L) (172 - 325 W)	Moderate Work (M) (< 450 W)	Light (L) 325 W
Moderate (M) (325 - 500 W)	Heavy Work (H) (< 600 W)	Moderate (M) 500 W
Heavy (H) (500 W +)		Heavy (H) 600 W

Another option, in some situations, is to use the equation proposed by K. B. Pandolf et al. (1977) for standing or walking slowly. It can be used to estimate the base metabolic rate if the input parameters are known. These can be measured for many tasks by examining walking speed, grade, walking surface, mass of the subject, and extra load carried as shown in Equation ( 3.2 ).

$$Mw = 1.5 * Wt + 2.0 * (Wt + Lo) * (Lo/Wt)^2 + T * (Wt + Lo) * (1.5 * V^2 + 0.35 * V * G) \quad (3.2)$$



where  $M_w$  is the metabolic cost of walking (Watts),  $W_t$  is body mass (kg),  $L_o$  is load mass (kg),  $T$  is terrain coefficient,  $V$  is velocity or walk rate (m/sec), and  $G$  is slope or grade (%). The terrain coefficient was determined as follows: 1.0 = black top road; 1.1 = dirt road; 1.2 = light brush; 1.5 = heavy brush; 1.8 = swampy bog; 2.1 = loose sand; or snow, dependent on depth of depression ( $T = 1.30 + 0.082 * D$ , where  $D$  = depression depth in cm).

PCS system weight will change the metabolic energy generation as illustrated in Equation 3. Some systems may allow users to carry additional supplies but at the cost of higher increased metabolic generation. Other mechanical and physiological issues are also important that are not considered in this analysis. To compare PCS system performance, it is logical to assume the end user needs to perform a task at the same speed regardless of PCS weight. Equation 3 could be used to determine this shift in metabolic rate if the inputs are held constant but only the load mass is changed. If Equation ( 3.2 ) was used to find the baseline metabolic rate, the new metabolic rate with a PCS can be found by simply increasing the load carried by adding the weight of the PCS to the existing load.

Despite its limitations, Equation ( 3.2 ) is an empirical equation based on a very large data set. Assuming a general metabolic rate can be identified from published work or other methods, Equation ( 3.2 ) can provide a rough estimate of increased rates. Inputs to Equation 3 ( $M_t$ ,  $W_t$ ,  $T$ ,  $G$ , and  $L_o$ ) can be set without a PCS to match the desired metabolic rate to find the walking velocity,  $V$ . Once  $V$  is known, it can be use with the load increased by each PCS's weight to calculate the new metabolic rate. Additional information in this area is limited and additional experimental study would be useful.

### ***Natural Heat Loss***

The natural heat loss term in Equation ( 3.1 ) represents the ability of the body to expel heat to the environment, and is dependent on a number of environmental components including air temperature, air velocity, radiant load, and relative humidity. Fundamentally, natural heat transfer is the combination of many terms that can be thought of as energy loss from the body. First, is the energy loss from the skin due to conduction, convection, and radiation. Second is energy lost due to evaporation from the skin. Finally, losses due to respiration need to be included but are normally small. Two broad methods can be used to determine natural heat loss. One method uses thermal heat loss models such as those found in found in ASHRAE Fundamentals, Chapter 9 (ASHRAE, 2013). Another is use of various ISO thermal environment standards and supporting standards for hot conditions, such as ISO 7243 (ISO, 2003) and ISO 9920 (ISO, 2007) among others; or more advanced models such as Dusan Fiala et al. (1999). This uses estimates of the heat transfer coefficients and knowledge of clothing properties to estimate natural heat loss. The second method involves use of calorimetry to determine natural heat loss (Jay & Kenny, 2007). Natural heat loss values for the project were estimated using the highest metabolic rates in FM 3-4 and TB MED 507 where the soldiers were allowed a “no-limit” work time in MOPP 0 in the WBGT corresponding to the test environmental conditions.

### ***Storage***

The energy storage term,  $S_t$ , presented in Equations 1 and 2, represent energy stored in the body. This is surprisingly difficult to accurately measure as the complex distribution of temperatures and chemical reactions change the energy. Most assume a reasonable approximation can be made by assuming an average specific heat of tissue,  $C_{p_b}$ , and some bulk temperature change, usually core temperature,  $\Delta T_b$ . The value given for the average body specific heat,  $C_{p_b}$ , by ASHRAE is 3490 J/kg\*°C (ASHRAE, 2013). The first-law energy balance

can find the storage term, which is the fundamental principle behind calorimetry. However, determining which bulk temperatures to use, where they are located, and how many are required is still a topic of research, thus the reason for the summation in Equation 1 (Jay et al., 2006). It is widely accepted that the rise in core body temperature is the metric to be used when determining when heat stress will occur. The final core temperature, and as a result the allowable core temperature rise, depends on the application and safety protocols of each organization.

The maximum heat stress point of the human body can be generally set at a 2.8°C rise in core body temperature over a baseline core temperature of 37.2 °C, resulting in collapse. This correlates to body heat storage of 670 kJ for an average-sized man (ASHRAE, 2013). The international standard ISO 7243 WBGT for industrial work allows for a maximum rectal temperature of 38 °C over an eight-hour shift (ISO, 2003; K. Parsons, 2006). It is recommended civilian users apply occupational safety standards and international standards for work such as those from ISO to define limits. A helpful flow chart and description of the standards is found in K. Parsons (2006). It should be noted that the cooling effectiveness score developed in this paper is for ranking PCS, not for predicting work times. This should not be used to evaluate possible incidences of heat stress as humans are highly variable and this application requires intensive study by experts. The widely used equation for heat storage from human subject work is

$$St = Wt * Cp_b * (0.8 * T_c + 0.2 * T_{sk}) \quad (3.3)$$

which is a modified version from Equation ( 3.1 ), where two compartments of temperature are used with a mass weighting coefficient assuming a constant specific heat (M. J. Barwood et al., 2009).  $T_{sk}$  is mean skin temperature change and  $T_c$  is core temperature change. In this case, GI

temperature from a thermometric pill is used to evaluate the storage term. In the initial screening process, a less complicated set of assumptions can be made.

### ***Cooling Rate***

In the initial screening process, it can be difficult to determine the cooling rate of systems, but ideally, manufacturers have had systems measured according to ASTM Standard F2371-10. If this information is not available, the following background information can be used to help estimate system performance prior to validation with manikin or human subjects. Some systems are advertised by the manufacturer with a cooling rate that may or may not have been derived from physical testing. The testing standard and surface temperature can impact the cooling properties (Chuansi Gao et al., 2010). Open literature is also a potential source of estimating cooling rates. However, many systems do not have a cooling rate listed, so an engineering estimate is needed. Systems based on vapor-compression refrigeration technology, thermoelectric, and phase-change materials can be estimated reasonably well using thermodynamic first principles from their design parameter. Methods for evaluating cooling from thermoelectric and vapor-compression refrigeration technologies can be found commonly in many basic electrical and mechanical engineering texts. In practice, designers of the system should have a decent estimate of these values because they are required to design the systems, the evaluator must only check to make sure the claims are reasonable based on the laws of thermodynamics.

Air circulation systems, also seen in literature as body ventilation systems (BVS) present many problems when estimating cooling rates because of their dependence on fit, skin wettedness, environmental temperature and humidity, air flow, garments, etc. Essentially, manikin tests on air circulation systems can yield unrepresentative results compared with human

subjects. Work by Xu and Gonzalez (2011) has attempted to measure the effectiveness of air circulation systems. An air circulation system is used in the example presented later and is covered in detail in the discussion section. Estimating their cooling power could be performed using data from literature of similar systems, simple and advanced computer modeling, or standard or modified thermal manikins (Burke, Curran, & Hepokoski, 2009).

However, phase-change systems are commonly encountered on the market without a cooling estimate. The following is some general background on obtaining an estimate based on the technology used in phase-change materials, previous experience with these system types, and any material specifications available.

Phase-change materials, such as ice, are frozen and change phase to a liquid by absorbing heat when melting. Using the weight of the system provided by the manufacturer, and material properties such as the melting temperature or type of PCM used, allows for the estimation of the material's specific heat and latent heat of fusion. The latent heat of fusion multiplied by the mass of the material provides the energy required to change phase from a solid to a liquid. This can then be added to the amount of energy required to change the temperature of the material by multiplying the specific heat with the mass and the difference between melting temperature and body temperature. Most phase-change materials have variable cooling rates; they provide high initial cooling followed by a decline until the cooling stops. The cooling rate is dependent on a number of factors including composition of the PCM or packaging, in packs or microcapsules (Wittmers et al., 1998), the latent heat, thermal conductivity of PCM (Farid et al., 2004), and the gradient between skin temperature and PCM melting temperature (Chuansi Gao et al., 2010; James R. House et al., 2013), and many other issues. However, the cooling effect is usually complete in two hours for most PCSs containing phase-change components (McCullough and

Eckels, 2008). Because this analysis was path-independent until the PCS stopped cooling, the cooling rate in watts for phase-change material can be estimated as shown in Equation 4, where the total heat transfer is divided by the time, which is set at two hours. This way many of the variables can be factored out to simplify the calculations. It should be noted this is possibly at the expense of physiological effects, such as vasoconstriction and lowering skin temperature,  $T_{skin}$ , but these factors are not known, so cannot be included.

$$Cl = m_{PCM} * (Cp * (T_{sk} - T_{MP}) + LHF) / \Delta t_{pcs} \quad (3.4)$$

In this equation  $m_{PCM}$  is mass of PCM (kg),  $Cp$  is specific heat of the phase-change material (J/kg·K),  $LHF$  is latent heat of fusion of the phase-change material (J/kg),  $T_{skin}$  is skin temperature (K),  $T_{MP}$  is PCM melting temperature (K),  $t$  is PCM cooling time (2 hours), and  $Cl$  is cooling rate of PCS while active (W).

The goal of this section is to derive a numerical measure that objectively compares the thermal performance of two PCS for a given task scenario. Two steps are required. The first ensures the PCS provides a benefit to the wearer. The benefit can be seen if the heat storage of Equation ( 3.1 ) is less than if  $Cl$  is set to zero. This inequality is used to derive the mathematical expression in Equation ( 3.5 ). An important distinction is there are two terms for natural heat loss, one with the PCS and one without. This is important if the PCS allows for more or less natural heat loss in its inactive state than in the baseline, or possibly changes the natural heat loss because of the cooling effect of the PCS. The externally applied work was constant. The algebraically condensed inequality becomes

$$(Mr_w - Mr) * \Delta t_{TT} < Cl * \Delta t_{PCS} + (Ht_{PCS} - Ht) \quad (3.5)$$

where  $Mr$  is specified metabolic rate.  $Mr_w$  is weight-adjusted metabolic rate (W),  $\Delta t_{PCS}$  is cooling duration (sec),  $\Delta t_{TT}$  is task time (sec),  $Ht_{PCS}$  is natural heat transfer to/from the body with the PCS (W) and  $Ht$  is the heat transfer from the body without PCS (W), and  $Cl$  = cooling rate (W). If the inequality in Equation ( 3.5 ) is not true, then the PCS is predicted to be a net negative to the wearer and the system should not be considered for this scenario. For system screening applications, the cooling rate ( $Cl$ ) and natural heat transfer losses are the most difficult to estimate.

The next step was to determine if the PCS theoretically allowed the person to complete the task without reaching the specified heat-stress safety cutoff. This was accomplished by rearranging Equation 2 and solving for  $\Delta t_{TT}$  – the maximum time to heat stress.

$$\Delta t_{TTMAX} = (St + Cl * \Delta t_{PCS}) / (Mr_w - Wr - Ht_{PCS}) \quad (3.6)$$

where  $\Delta t_{PCS} \leq \Delta t_{TTMAX}$  and  $St$  is heat storage by the body (kJ),  $Mr_w$  is weight-adjusted metabolic rate (W),  $Wr$  is work rate performed on the environment (W),  $Ht$  is natural heat transfer to/from the body (W),  $\Delta t_{PCS}$  is PCS cooling duration (sec),  $\Delta t_{TTMAX}$  is maximum task time (sec), and  $Cl$  is cooling rate (W).

If the PCS allowed the user to complete the task time without dangerous heat stress,  $\Delta t_{TTMAX} > \Delta t_{TT}$ , the system received a maximum score of 100. In the case where the task time exceeded the time to heat stress, the percentage of the task time completed would be used to scale the score. This method, as shown in Equation 7, provides a relative measure between systems.

$$\text{Cooling Effectiveness Score} = (\Delta t_{TTMAX} / \Delta t_{TT}) * 100, \quad (3.7)$$

It should be noted here, the negative effect of the PCS system compared to the baseline will appear at the longer task times, even for otherwise high-performing systems. The effect of

carrying a depleted PCS eventually overcomes any benefit derived from the fixed cooling duration. Negative effects could also occur for systems with a high mass and relatively low cooling potential. As more information becomes available, such as the PCS cooling rate, duration, and weight will allow the scoring to be refined and better allow for comparison between PCSs. Satisfying the parameters in Equation ( 3.6 ) allows the calculation of the new cooling effectiveness score in Equation ( 3.7).”

### ***3.1.3 Scoring of Systems***

The desired outcome of the evaluation tool is a numerical score composed of a summation of the factors. If this methodology is being used to evaluate for one specific application where the task and all logistical support requirements are well known, the final score could be a simple summation of all the factor scores. However, if some factors were determined to be more important in a specific situation, a weighting function could be used that allows the scoring system to be tailored to each end-user application. In the example of the dismantled soldier, vastly different mission times and infrastructure support are possible when considering the range of missions a soldier can be assigned. This can be used to make something such as supply portability less important for a soldier standing guard on a fixed base.

An example of a final weighted score could be the general weighted score (GWS) shown in Equation ( 3.8 ) using the factors for the dismantled soldier. In this case, the score is intended to range from 0 to 100. Each function shown in Equation ( 3.8 ) could receive a 0 to 20 score in place of the pass/fail criteria for the five factors: supply portability (SP), ergonomics (EG), user maintenance (UM), mobility (MO), and cooling effectiveness (CE). The coefficients  $\theta_x$ , where  $x$  is the particular function designation, can then be used to scale the importance of that factor in the GWS for a certain logistical scenario. To keep the scoring uniform, the sum of the



coefficients must be equal to the number of factors, in this case 5. The GWS equation would then become:

$$GWS = SP * \theta SP + EG * \theta EG + UM * \theta UM + MO * \theta MO + CE * \theta CE \quad (3.8)$$

where  $\theta SP$  is Supply portability (SP),  $\theta EG$  is Ergonomics (EG),  $\theta UM$  is User maintenance (UM),  $\theta MO$  is Mobility (MO), and  $\theta CE$  is Cooling effectiveness (CE).

In continuation of the dismounted soldier example, the simple sum of all factors was be used because each factor could have an effect on the dismounted soldier. Soldiers would not be guaranteed access to additional supplies for the entire mission duration. As the soldiers are without logistical support, the ability to maintain the PCS cooling in the field was paramount. This included the capability to carry additional materials to extend PCS run time, if needed, and remain fully protected from other threats at all times. This made this scenario the most difficult to achieve.

#### List of Systems Selected for Thermal Manikin Testing:

- Ventilation Vest- Entrak
- Active Microclimate Cooling System (with body armor)- Mawashi
- Active Microclimate Cooling System (without body armor)- Mawashi
- Hummingbird I- Creative Thermal Solutions
- Hummingbird 1 (green version, on medium)- Creative Thermal Solutions
- PCVZ KM Zipper Front Vest- Polar Products
- Texas Cool Vest A (lightweight vest, standard packs)- Texas Cool Vest
- Texas Cool Vest B (modified lightweight vest, heavy packs) - Texas Cool Vest
- Cool UnderVest- Steele Inc.
- Hummingbird II- Creative Thermal Solutions
- Veskimo (with water and ice)- Veskimo
- Veskimo (20 oz. water to backpack full of ice)- Veskimo
- Blücher system IdZ (green version)- Blücher
- Blücher system IdZ (continuous turbo)- Blücher

## **3.2 Thermal Manikin Testing**

Thermal manikin testing provides an important standard, repeatable way of evaluating clothing ensembles and personal cooling systems. In this project, multiple PCS were evaluated on the thermal manikin. The base ensembles to use with the PCS in thermal manikin and human subject testing were also evaluated. These data were used later in the thermal modeling of component of this research, Chapter 5 and Chapter 6, as the boundary conditions for the simulations.

### ***3.2.1 Apparatus***

The thermal manikin is a Newton-type manikin, STAN, (MTNW, Seattle, WA) consisting of 20 independently controlled heated thermal zones shown in Figure 3.3 and Table 3.2. The manikin simulates the approximate size and shape of a typical western man (1.80 m<sup>2</sup>, 177.2 cm height). The manikin contains a fluid heater and is capable of full body sweating. All control, power, and sensor cables as well as fluid supply lines are connected to the manikin's face. The control system is the ThermDAC software sold with the manikin and is a 32-bit Windows based program that performs real-time data recording, control, data processing and numerical and graphical readout of the manikin.

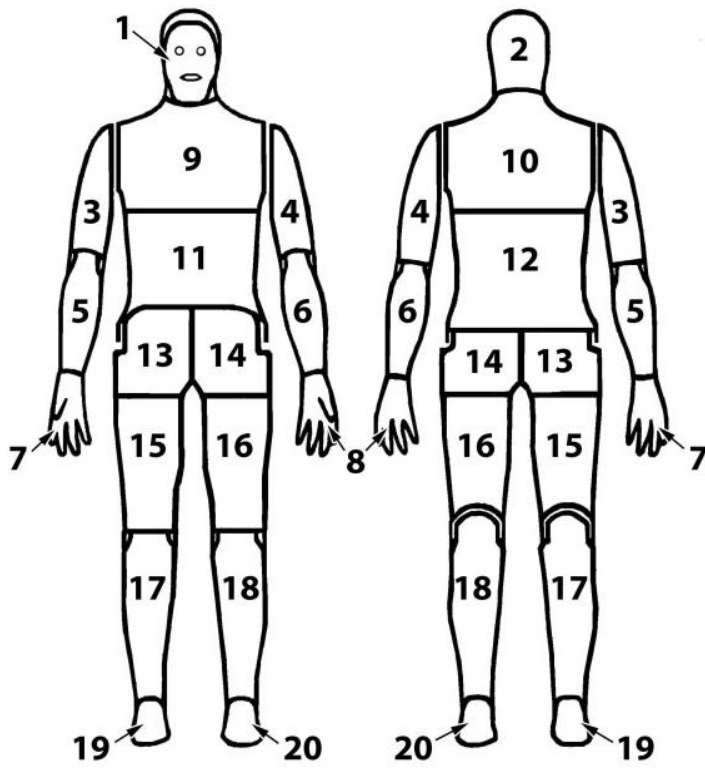


Figure 3.3 STAN, Newton-type sweating thermal manikin showing location of 20 zones

**Table 3.2 STAN, Newton-type sweating thermal manikin zone segment information**

<b>No.</b>	<b>Body Segments Marked on Stan</b>	<b>Surface Area of Each Part (m<sup>2</sup>)</b>	<b>% of Total Body Surface Area Represented by Each Segment</b>
1.	Face	0.0457	2.5
2.	Head	0.0962	5.3
3.	R Upper Arm	0.0817	4.5
4.	L Upper Arm	0.0817	4.5
5.	R Forearm	0.0648	3.6
6.	L Forearm	0.0648	3.6
7.	R Hand	0.0442	2.4
8.	L Hand	0.0442	2.4
9.	Chest	0.1201	6.7
10.	Shoulders	0.1007	5.6
11.	Stomach	0.1194	6.6
12.	Back	0.0930	5.2
13.	R Up Thigh	0.0777	4.3
14.	L Up Thigh	0.0777	4.3
15.	R Low Thigh	0.1509	8.4
16.	L Low Thigh	0.1509	8.4
17.	R Calf	0.1357	7.5
18.	L Calf	0.1357	7.5
19.	R Foot	0.0595	3.3
20.	L Foot	0.0595	3.3
<b>Total Body</b>		<b>1.8041</b>	<b>100.0</b>

The thermistors in the manikin are calibrated to +/- 0.15 °C yearly. The humidity sensor is calibrated by the vendor (Vaisala) to +/-1.3% RH. Any uncertainty in the power output is assumed a function of resistance and not voltage, which is measured and checked yearly.

### ***3.2.2 Base Ensemble Testing***

The base clothing used in this study was extremely important as it serves as the input to the modeling performed on the PCS. Four base ensembles were developed representing possible

clothing and PPE worn by dismounted soldiers. The component of these systems can be found in Table 3.3.

**Table 3.3 U.S. Army dismounted soldier base ensembles tested**

<p>Ensemble 1: Army Combat Ensemble with Basic Body Armor</p> <ul style="list-style-type: none"><li>• Total Weight: 17.425 kg (38 lbs. 7 oz.)</li><li>• ACH Advanced Combat Helmet (with cover, suspension system, and pads)</li><li>• Hanes Premium boxer briefs (75% cotton 25% polyester knit, fitted style)</li><li>• Gold Toe Ultra Tec crew socks (cushioned, antimicrobial, 79% cotton, 14% nylon, 6% polyester, 1% spandex)</li><li>• ACS Army Combat Shirt – Fire Resistant (knit portion on torso replaces T-shirt) shirt tucked into pants</li><li>• ACP Army Combat Pants – Fire Resistant (use the drawstrings at the bottom of the trousers to blouse around boots; when bloused, the trousers should not extend below the third eyelet from the top of the boot)</li><li>• Belt</li><li>• External Knee Protectors</li><li>• ACG Army Combat Gloves (worn under sleeve cuffs)</li><li>• MCB Mountain Combat Boots</li><li>• IOTV Improved Outer Tactical Vest with the following items in it:<ul style="list-style-type: none"><li>• ESAPI Enhanced Small Arms Protective Inserts (front and rear hard armor plates)</li><li>• ESBI Enhanced Side Ballistic Inserts (small side hard armor plates)</li><li>• Front and rear soft Kevlar inserts</li></ul></li></ul>
<p>Ensemble 2: Army Combat Ensemble with Enhanced Basic Body Armor (DAPS, groin and lower back protectors added)</p> <ul style="list-style-type: none"><li>• Total Weight: 20.324 kg (44 lbs. 13 oz.)</li><li>• ACH Advanced Combat Helmet (with cover, suspension system, and pads)</li><li>• Hanes Premium boxer briefs (75% cotton 25% polyester knit, fitted style)</li><li>• Gold Toe Ultra Tec crew socks (cushioned, antimicrobial, 79% cotton, 14% nylon, 6% polyester, 1% spandex)</li><li>• ACS Army Combat Shirt – Fire Resistant (knit portion on torso replaces T-shirt) shirt tucked into pants</li><li>• ACP Army Combat Pants – Fire Resistant (use the drawstrings at the bottom of the trousers to blouse around boots; when bloused, the trousers should not extend below the third eyelet from the top of the boot)</li></ul>

- Belt
- External Knee Protectors
- ACG Army Combat Gloves (worn under sleeve cuffs)
- MCB Mountain Combat Boots
- IOTV Improved Outer Tactical Vest with the following items in it:
  - ESAPI Enhanced Small Arms Protective Inserts (front and rear hard armor plates)
  - ESBI Enhanced Side Ballistic Inserts (small side hard armor plates)
  - Front and rear soft Kevlar inserts
  - DAPS Deltoid Axillary Pad System (attach to IOTV at the shoulders)
  - Lower back protector (attach to IOTV)
  - Groin protector (attach to IOTV)

Ensemble 3: Army Combat Ensemble with Soldier Plate Carrier System (lighter body armor)

- Total Weight: 15.054 kg (33 lbs. 3 oz.)
- ACH Advanced Combat Helmet (with cover, suspension system, and pads)
- Hanes Premium boxer briefs (75% cotton 25% polyester knit, fitted style)
- Gold Toe Ultra Tec crew socks (cushioned, antimicrobial, 79% cotton, 14% nylon, 6% polyester, 1% spandex)
- ACS Army Combat Shirt – Fire Resistant (knit portion on torso replaces T-shirt) shirt tucked into pants
- ACP Army Combat Pants – Fire Resistant (use the drawstrings at the bottom of the trousers to blouse around boots; when bloused, the trousers should not extend below the third eyelet from the top of the boot)
- Belt
- External Knee Protectors
- ACG Army Combat Gloves (worn under sleeve cuffs)
- MCB Mountain Combat Boots
- SPCS Soldier Plate Carrier System (lighter body armor with plates in place)
- ESAPI Enhanced Small Arms Protective Inserts (front and rear hard armor plates)
- ESBI Enhanced Side Ballistic Inserts (small side hard armor plates)

Ensemble 4: Army Combat Ensemble with Basic Body Armor – Using Lightweight Plates

- Total Weight: 10.419 kg (23 lbs. 0 oz.)
- ACH Advanced Combat Helmet (with cover, suspension system, and pads)
- Hanes Premium boxer briefs (75% cotton 25% polyester knit, fitted style)

- Gold Toe Ultra Tec crew socks (cushioned, antimicrobial, 79% cotton, 14% nylon, 6% polyester, 1% spandex)
- ACS Army Combat Shirt – Fire Resistant (knit portion on torso replaces T-shirt) shirt tucked into pants
- ACP Army Combat Pants – Fire Resistant (use the drawstrings at the bottom of the trousers to blouse around boots; when bloused, the trousers should not extend below the third eyelet from the top of the boot)
- Belt
- External Knee Protectors
- ACG Army Combat Gloves (worn under sleeve cuffs)
- MCB Mountain Combat Boots
- IOTV Improved Outer Tactical Vest with the following items in it:
  - Blue Board Lightweight ESAPI Enhanced Small Arms Protective Inserts (front and rear hard armor plates)
  - Blue Board Lightweight ESBI Enhanced Side Ballistic Inserts (small side hard armor plates)
  - Front and rear soft Kevlar inserts

Tests were conducted according to ASTM F1291, Standard Test Method for Measuring the Thermal Insulation of Clothing using a Heated Manikin, (ASTM, 2010b). The garments were hung on a rack before testing. The dry insulation tests were controlled to ambient air temperature, 20°C (68°F), air velocity, 0.3 m/s, (60ft/min), relative humidity 50%, manikin surface temperature 35°C (95°F). Wet testing for the evaporative resistance of the ensembles were performed according to ASTM F2370. Standard Test Method of Measuring the Evaporative Resistance of Clothing using a Sweating Manikin (ASTM, 2010a). The manikin was covered with a knitted skin that maintained complete saturation with the sweat simulant, distilled water, throughout the test. The manikin was dressed in the ensemble and excess water was allowed to run out of holes in his shoes and collect in a receptacle. The test was run until steady state, which was defined as a less than 1% coefficient of variation in the results over 30 minutes. The environmental conditions for the isothermal sweating manikin testing were: ambient air

temperature, 35°C (95°F), air velocity, 0.3 m/s (60 ft./min), relative humidity 40%, manikin surface temperature 35°C (95°F). The thermal and evaporative resistance values are pulled from the manikin.

Thermal resistance values are simply the resistance to heat transfer provided by the fabric during the dry test and is the inverse of the heat transfer coefficient, simply a rearrangement of Equation ( 2.17 ). It is the temperature difference between the outside air and the manikin's constant surface temperature divided by the heat flux applied to the surface. This is normalized if the total resistance,  $I_t$ , is not needed by subtracting out a nude run resistance without clothing,  $R_a$ , to remove the effects of the insulation of the air layer,  $I_{cl}$ . In literature a value of clo is used and one clo is  $6.45 \text{ W}/(\text{m}^2 \cdot ^\circ\text{C})$ .

In sweating tests, the thermal manikin and chamber are at isothermal conditions, leaving no ability for heat transfer by convection to occur. The process is similar to the dry ensemble test; a nude sweating test is performed to determine the evaporative resistance of the air layer,  $R_{ea}$ . The manikin is then dressed in the ensemble. In the isothermal sweating test, the manikin measures the heat flux necessary to maintain the manikin skin temperature based on the heat absorbed during the mass transfer evaporation process. This is the rearrangement of the heat mass transfer analogy cooling Equation ( 2.30 ). The value for the clothing with the air layer is  $R_{et}$ , and without the air layer is  $R_{ecl}$ . The permeability index,  $i_m$ , is the maximum evaporative heat transfer permitted by a clothing system compared to an uncovered surface.

$$i_m = \frac{R_t/R_{et}}{R_a/R_{ea}} \quad (3.9)$$

which after the application of the Lewis Ratio at sea level is:

$$i_m = 60.06 \left( \frac{R_t}{R_{et}} \right) \quad (3.10)$$



The results of the thermal insulation values are presented in Table 3.4 below and the evaporative insulation values are shown in Table 3.5.

**Table 3.4 Thermal insulation values for base ensembles**

Ensemble Code and Description	Total Insulation Value		Intrinsic Clothing Insulation Value <sup>a</sup>		Clothing Area Factor $f_{cl}$
	$R_t$ ( $m^2 \cdot ^\circ C/W$ )	$I_t$ (clo)	$R_{cl}$ ( $m^2 \cdot ^\circ C/W$ )	$I_{cl}$ (clo)	
#1. Army Combat Ensemble with Basic Body Armor	0.213	1.37	0.157	1.01	1.35
#2. Army Combat Ensemble with Enhanced Basic Body Armor (DAPS, groin and lower back protectors added)	0.228	1.47	0.174	1.13	1.40
#3. Army Combat Ensemble with Soldier Plate Carrier System (lighter body armor)	0.211	1.36	0.155	1.00	1.33
#4. Army Combat Ensemble with Basic Body Armor (with lightweight plate inserts replacing real ceramic plates)	0.217	1.40	0.161	1.04	1.35

**Table 3.5 Evaporative resistance data for base ensembles**

Ensemble Code and Description	Total Evaporative Resistance - $R_{et}$ ( $m^2 \cdot Pa/W$ )	Intrinsic Evaporative Resistance of Clothing - $R_{ecl}$ ( $m^2 \cdot Pa/W$ ) <sup>a</sup>	Total Moisture Permeability Index - $i_m$ <sup>b</sup>
#1. Army Combat Ensemble with Basic Body Armor	34.70	26.70	0.37
#2. Army Combat Ensemble with Enhanced Basic Body Armor (DAPS, groin and lower back protectors added)	36.98	29.27	0.37
#3. Army Combat Ensemble with Soldier Plate Carrier System (lighter body armor)	34.32	26.20	0.37
#4. Army Combat Ensemble with Basic Body Armor (with lightweight plate inserts replacing real ceramic plates)	34.92	26.92	0.37

Ensemble #3 was chosen as the test condition as it best represented the dismounted soldier under the study conditions.

### 3.2.3 PCS Manikin Testing

Testing PCS on a sweating thermal manikin is a repeatable and comparatively inexpensive method to determine a performance metric for each system. The direct application of the cooling values to human subjects and human subject modeling is a major topic of this work and can be found in detail in the following chapters.

Thermal manikin testing was carried out on the selected ensemble (#3) and was performed according to ASTM standard 2371, Standard Test Method for Measuring the Heat Removal Rate of Personal Cooling Systems Using a Sweating Heated Manikin (ASTM, 2010b).

Each PCS was also weighed to determine the W/lb. The same Newton-type thermal manikin described above was used. The environmental conditions are the same as the isothermal sweating test performed for ASTM F2370 standard: ambient air temperature, 35°C (95°F), air velocity, 0.3 m/s (60 ft./min), relative humidity 40%, manikin surface temperature 35°C (95°F). The tests were performed according to the standard. A baseline test is performed with the manikin wearing the ensemble and a PCS in the “OFF” condition. In the case of phase change material vests, melted packs at chamber temperature are used. Once steady state is reached for 30 minutes, data are taken. The PCS test is the exact same, the system is powered on, or charged PCM material is applied in accordance with the specifics of the PCS and the test is run for 2 hours. The standard only considers cooling rates above 50 W to be significant, but tests were run for the full 2 hours. Three replications of the baseline tests with the PCS off, followed by the heat difference test with the PCS turned on were conducted for each PCS. The results of the thermal manikin testing can be found in Table 3.6, the graphical results of the PCS thermal manikin testing, cooling power vs. time, can be found in Appendix D - Testing Results, Thermal Manikin.

**Table 3.6 Results of sweating heated manikin testing on PCS**

		120 Minute Test		50 Watt Cut-off Test		
PCS Name	Weight of PCS	Avg. Cooling Power Total (W)	Power Level at 120 min. (W)	Avg. Cooling Power to cutoff (W)	Time to 50 W cut-off (min)	Avg. Cooling power to cutoff Watts/Weight Ratio (W/lb.)
PCS #1: Ventilation Vest	0.995 kg 2.19 lb.	100.3	101.1	--	--	45.8
PCS #3A: Active Microclimate Cooling System (with body armor)	1.982 kg 4.37 lb.	22.4	22.4	Never reached 50 Watts	Never reached 50 Watts	Never reached 50 Watts
PCS #3B: Active Microclimate Cooling System (without body armor)	1.982 kg 4.37 lb.	48.5	48.2	51.7	25	11.8
PCS #7A: Hummingbird I	2.788 kg 6.15 lb.	43.4	42.8	Never reached 50 Watts	Never reached 50 Watts	Never reached 50 Watts
PCS #7C: Hummingbird I, with reciprocating green compressor on medium speed	2.778 kg 6.13 lb.	55.0	57.2	--	--	9.0
PCS #9: PCVZ-KM Zipper Front Vest by Polar Products	2.681 kg 5.91 lb.	96.9	62.9	--	--	16.4

PCS #10A: Texas Cool Vest A (Lightweight vest, standard packs)	1.870 kg 4.12 lb.	56.9	23.1	67.6	79.5	16.4
PCS #10B: Texas Cool Vest B (Modified lightweight vest, heavy packs)	3.433 kg 7.57 lb.	87.9	66.0	--	--	11.6
PCS #12: Cool UnderVest by Steele	3.499 kg 7.71 lb.	113.0	83.9	--	--	14.7
PCS #20 Hummingbird II	5.108 kg 11.26 lb.	124.6	125.6	--	--	11.1
Veskimo PCS #21 with backpack filled completely with water and ice	5.886 kg 12.98 lb.	121.2	51.3	-	-	9.3
Veskimo PCS #21 with 20 oz. water added to ice	4.843 kg 10.68 lb.	112.0	33.4	122.3	105	11.5
PCS #22: Blücher system IdZ version (green vest)	0.94 kg 2.07 lb.	36.6	37.0	Never reached 50 Watts	Never reached 50 Watts	--
PCS #22: Blücher system IdZ version #1 (green vest with continuous turbo modus) ventilation units on outside of body armor	0.826 kg 1.82 lb.	43.9	45.2	Never reached 50 Watts	Never reached 50 Watts	--

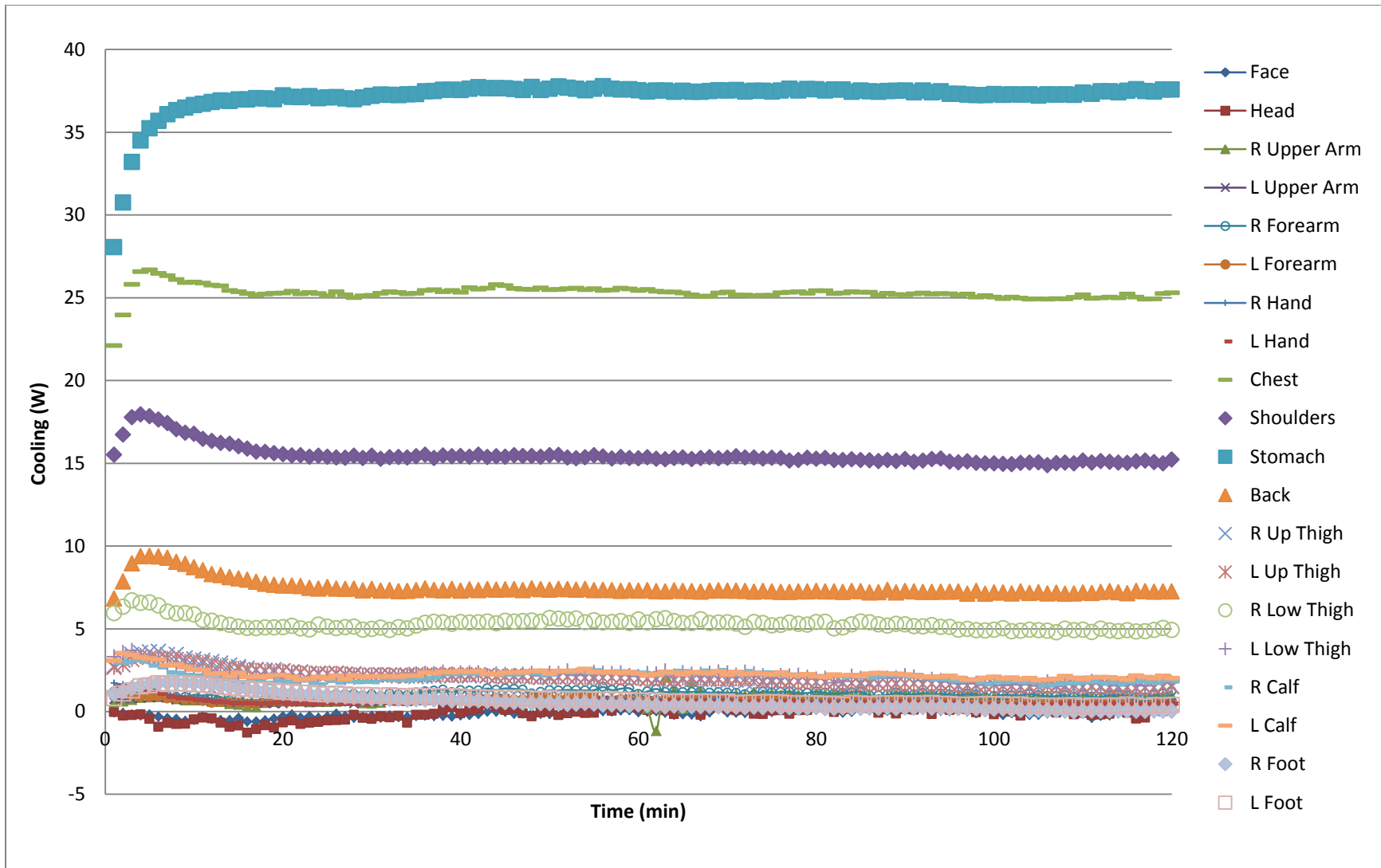


**Figure 3.4 PCS 1 cooling by thermal manikin segment**

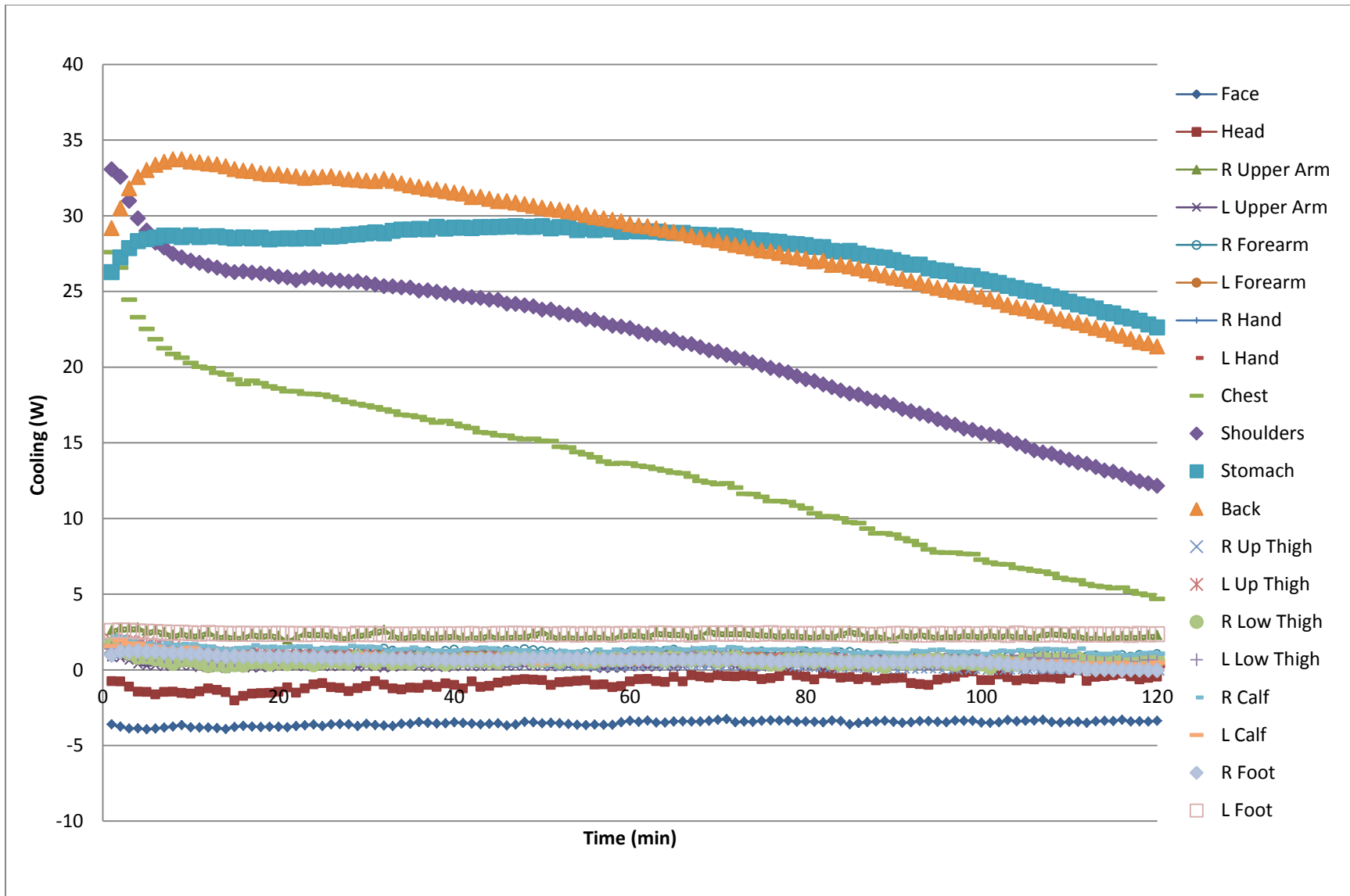


Figure 3.5 PCS 9 cooling by thermal manikin segment

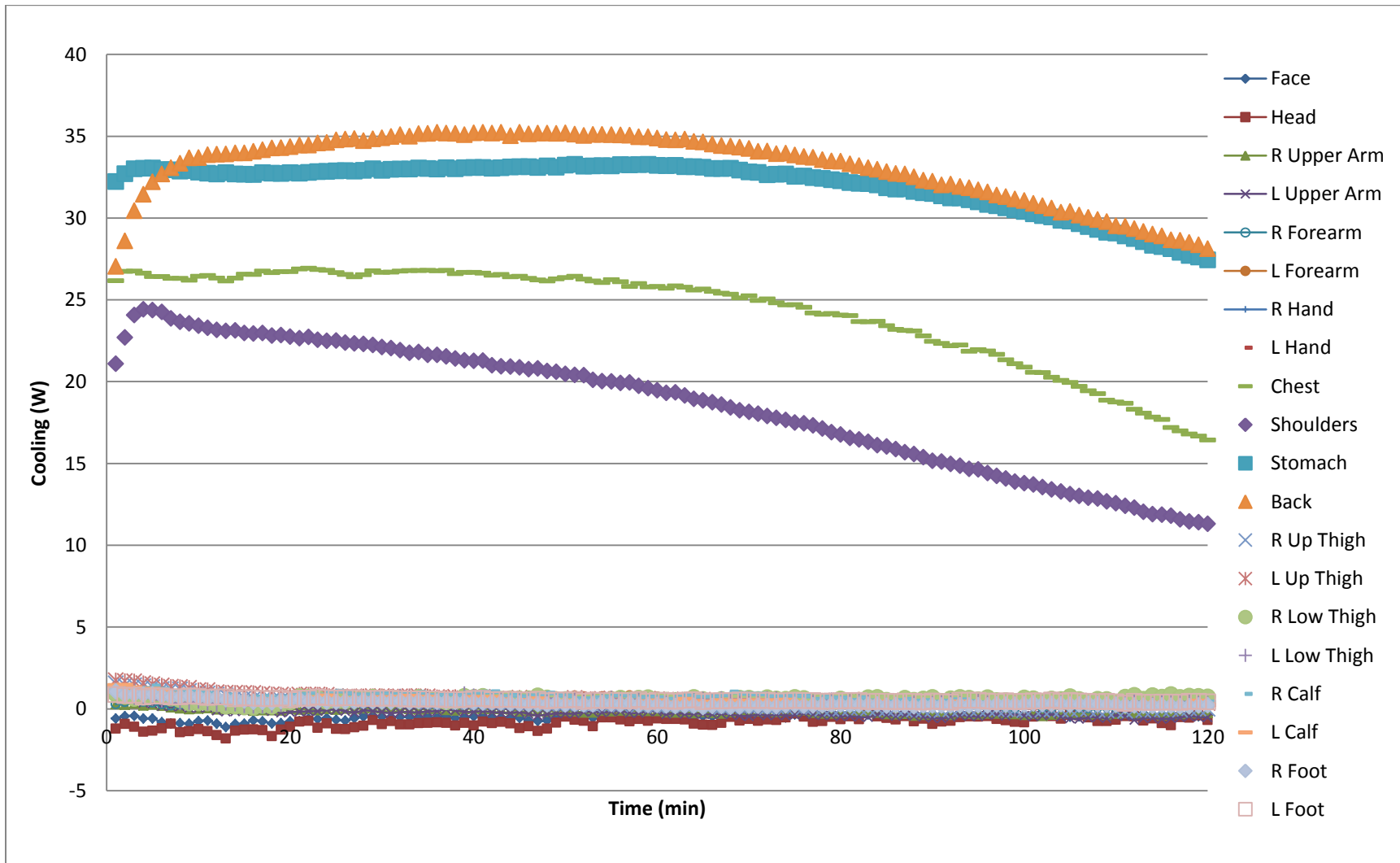


Figure 3.6 PCS 12 cooling by thermal manikin segment



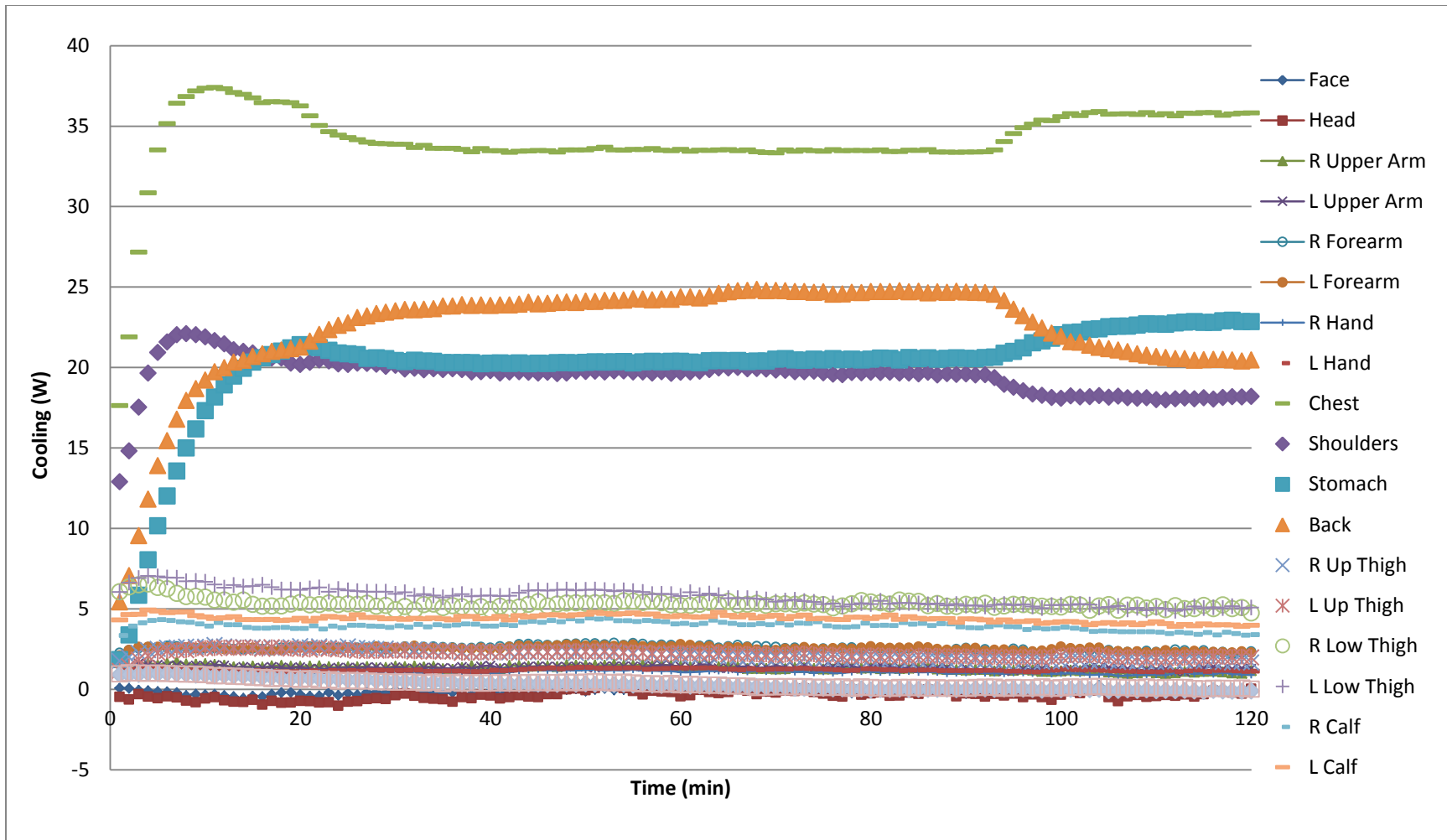


Figure 3.7 PCS 20 cooling by thermal manikin segment

The results of the heat difference tests by thermal manikin segment for four PCS have been included to show local effects. There is also a notable time dependence of cooling in PCS 9 and PCS 12 compared with the lack of time dependence in PCS 1 and PCS 20. In Figure 3.4, Figure 3.5, Figure 3.6, and Figure 3.7 most of the segments appear to show a very low cooling and some even show negative cooling. This is due to the uncertainty associated with the isothermal manikin testing. In these conditions, some segments do not come to steady state at 35°C before testing due to the impermeable nature of the ensemble. This introduces error in the tests that is most readily seen in segments that do not experience cooling from the PCS. This error is also dependent on the ability of the manikin segment to respond to the temperature changes. As seen in Figure 3.4 for PCS 1 the lower right thigh shows almost 5W of cooling, however, this segment is not near to the PCS only possibly getting airflow pulled past it by the intake fan. Considering the location of the segment this is the likely error associated with the testing.

PCS numbers 1, 3, 7, 9, 10, 12, 20 were selected for possible human subject testing. Some iterations or variations of PCS were tested at the request of the manufacturer and/or the project sponsor. Usually this involved different types of PCM, different amounts of PCM, or a change in how the system was configured. PCS #7 was part of a SBIR and was tested in multiple arrangements at the request of the sponsor. Specifically, #7A and #7 C as well as another version with a different compressor identified as #20. This PCS was a prototype system still in development and required more work. Numbers 1, 3, and 22 were Air Circulation systems with a fan located under the body armor. Systems 7 and 20 were direct expansion vapor compression refrigeration cycle system using R-134a and running on a military standard battery but in the developmental stage. The remainder of the systems tested were PCM based systems consisting of

a vest containing phase change packets of different materials providing a different melting temperatures and masses. The exception was system which was a backpack worn PCM based LCG.

### **3.3 Human Subject Testing**

Human subject testing was the most complex and expensive area of testing undertaken in this project. The goal of human subject testing was to provide an actual indication of the effectiveness of PCS on humans. Physiological data were monitored and collected for each subject. The test methods and analysis methods are discussed in this section.

#### ***3.3.1 Test methods***

Twenty-four subjects, 22 men and 2 women, took part in testing PCS over two three-week periods. KSU (Proposal 5633) and U.S. Army IRB approval was obtained for the test method. Volunteers were recruited from the population of active duty soldiers at Fort Riley, KS. The purpose of the testing was to use the basic procedures found in ASTM 2300, Standard test Method for Measuring the Performance of Personal Cooling Systems Using Physiological Testing (ASTM, 2010a). The standard was followed except the conditions in the chamber were much hotter to simulate a desert climate in the summer: air (dry bulb) temperature = 42.2°C (108°F), dew point temperature = 14.6°C (58.3°F), relative humidity = 20%, air velocity = 2 m/s (4.5 mph) average in chamber, mean radiant temperature = 54.4°C (130°F).

Each subject spent six days at the institute. The first three days were composed of instruction on testing procedures, mild acclimation, and familiarity with testing equipment. The second three days were composed of a 3 x 3 Latin square design where four subjects evaluated three PCS treatments on different days. This was repeated for a total of three days. In each

session, 12 subjects evaluated two PCS, equaling a total of four PCS evaluated on human subjects. Volunteers had to meet the following criteria to participate in the study.

1. Be an adult between 19-40 years of age.
2. Weigh between 65-100 kg (143-220 lb.) for males and between 55-90 kg (121-198 lb.) for females.
3. Have a height between 1.70-1.95 m (67-77 in.) for males and between 1.60-1.85 m (63-73 in.) for females.
4. Be free of chronic disease and generally in good health.
5. Have passed their most recent Army Physical Fitness Test.
6. Have no history of heat-related illness/injury (heat exhaustion, heat stroke, etc.)
7. Have no recent history of respiratory illness.
8. Have no history of orthopedic problems that could be made worse by walking in the combat uniform with body armor and helmet.
9. Have no recent history of skin disorder or disease.
10. Have no known allergy to adhesive tape.
11. Be willing to refrain from the use of any medications (prescription or over-the-counter) or dietary supplements throughout the length of the study, unless approved by both the Principal Investigator and staff providing medical coverage. Volunteers already taking medications or dietary supplements will not be admitted as test volunteers unless approved by both the Principal Investigator and staff providing medical coverage.
12. Refrain from the use of any caffeine or nicotine-containing product for at least 2 hours prior to the start of any test.
13. Refrain from the use of alcohol for at least 24 hours before the start of any test.
14. Have not had a vaccine in the preceding month.
15. Females must not be pregnant, and they must participate during the nine days after their menstrual period (follicular phase) to minimize hormonal effects (ASTM, 2010a).

Mark Lahan, a civilian employee of Ft. Riley, served as the ombudsman to assist Dr. McCullough in recruiting soldiers to ensure that participation was voluntary. The protocol was explained and literature was provided to the potential volunteers, including protocol and consent forms. Mr. Lahan arranged for the volunteers to be cleared by an Army physician who reviewed their file if a physical had been performed inside one year, or performed another physical. The physician provided the principal investigator, Dr. McCullough, written documentation about the fitness of each volunteer. Subjects who met the criteria were assigned a morning or afternoon

testing session. Subjects received no benefits for the testing, except for not being required to return to work during the week of testing.

The experiments took place in two environmental chambers at the Institute for Environmental Research at Kansas State University. One chamber served as a dressing room where subjects were preconditioned and instrumented. This chamber was maintained at approximately 28°C and 30% RH to expose subjects to slightly warm temperature before the test. The other chamber served as the main testing chamber. It contained two treadmills, two fans, and solar lights and measured 18 x 23 x 12.5 ft. This was maintained at the testing conditions that were designed to simulate summer in the middle east.

According to the ASTM (ASTM, 2010a) standard a metabolic energy expenditure between 250-400W was allowed. A target of 350W, independent of body mass and gender, was selected for this study and the subsequent treadmill speed was determined using the ASCM's guidelines for testing (American College of Sports Medicine, 2010). The basic equation consists of:

$$VO_2 = R + H + Vert \quad (3.11)$$

Where:

- VO<sub>2</sub> = rate of oxygen consumption (ml/kg/min)
- R = resting component of energy expenditure (3.5 ml/kg/min)
- H = horizontal component of energy expenditure (0.1 × walking speed in m/min × 26.8 to convert to mph = 2.68 mph)
- Vert = vertical component of energy expenditure (1.8 × walking speed in m/min × 26.8 to convert to mph × grade expressed as a decimal) In this study, grade was 1% (0.01), so V = 0.48.

Backing out of this equation for walking velocity requires using Equation ( 3.2 ) to estimate met rate, and then calculate the appropriate VO<sub>2</sub>. This also requires the mass of the subject and load carried. In this testing, the decision was made to normalize each system to test

for cooling potential at the same energy expenditure, therefore the weight of the PCS was added to the clothing and equipment worn by the subjects when calculating the targeted treadmill speed for each condition. This was in direct contradiction to the theory put forth in section 3.1.2.6 Cooling Effectiveness Factor. However, the goal of this testing was to determine the cooling ability of each PCS at 350W.

### ***3.3.1.1 Data Collection***

A HP VXI bus data acquisition system was used to measure all data from the chamber. A LabVIEW virtual instrument interface was created to display and store each instrument reading during testing. The VI was designed for real-time data monitoring to ensure the safety of the subjects.

Dry bulb temperatures were measured with two calibrated type-K thermocouples (Omega) which were shaded from solar loading. Two Optica 111H dew point hydrometers (General Eastern, MA, USA) measured the dew point and allowed for control of the relative humidity of the chamber. Seven skin temperatures were measured using calibrated type-T thermocouples (Omega). Each thermocouple was calibrated in a constant temperature bath and a fit curve was developed.

Before beginning the human subject testing session, the air velocity was set using a vane anemometer (Airflow Developments Limited, England) and a hot wire anemometer model 8475-03 (TSI Inc., MN, USA) positioned at chest level for a person standing on a treadmill. The speed of the fan was varied until an average velocity of 2 m/s was obtained for each subject. The solar loading in the chamber was set using the mean radiant temperature. The method described in the ASHRAE HVAC Applications Handbook was used to measure this temperature (ASHRAE, 2007). A 6-inch diameter black sphere composed of plastic was placed over the treadmill, under

the solar lights. The average temperature of the bulb was calculated from a type-T thermocouple (Omega) calibrated for the expected range using a constant temperature bath. The average temperature of the bulb, the dry bulb temperature, and air velocity were used to calculate the mean radiant temperature, and WBGT Index (ISO 1982).

Body core temperature and heart rate were recorded using a HQ Inc. CorTemp® data recorder that was attached to the soldier's equipment where a signal could be found. Two recorders were initially purchased, but eventually two more recorders were purchased to act as extra sensors to record data from multiple ingested pills if available to improve data fidelity. Two recorders were used corresponding to core temperature sensors transmitting in the 262 kHz range and two sensors transmitting in the 300 kHz range.

The core temperature sensors were scanned into the computer and cases of six core temperature sensor pills were provided to each subject to ensure the subjects took the appropriate pills each day. The cases contained holes 1.5" apart from one another to ensure the magnetized pills did not interact. Subjects were instructed to take their pills 5 hours in advance of the experiment so the pills would be in the intestinal track instead of the stomach. We did not have control over this portion of the experiment. Subjects were given water at 37°C during the experiment so that the water temperature would be less likely to affect the readings. The ingestible temperature sensor transmitted the internal body temperature continuously to the subject's recorder. A Polar® (Polar Products) heart rate chest strap with electrodes also transmitted to the CoreTemp® recorder. Recorders provided data to the DAQ every 20 seconds. The metabolic rate was determined from oxygen consumption, VO<sub>2</sub>, using a ParvoMedics True One 2400 Metabolic Measuring System.

### ***3.3.1.2 Test Schedule***

The test schedule for the familiarization sessions was different from the test days. Ft. Riley could not spare soldiers for two weeks to allow for extensive acclimatization. The heat familiarization tests were designed so subjects would not be completely shocked by the heat of the chamber. There was still the possibility that the subjects might change within the last three days of testing so this was included in the statistical design.

The first three days of testing were composed of subjects participating in two-hour work-rest cycles under the same environmental conditions used in the study. The protocol used is given below:

- 0-10 minutes: sitting for 10 minutes
- 10-55 minutes: walking for 45 minutes
- 55-65 minutes: sitting for 10 minutes
- 65-110 minutes: walking for 45 minutes
- 110-120 minutes: sitting for 10 minutes

The familiarization session began on Sunday, on the first day subjects were assigned a two-digit number that had been created to track their information separate from their identity and maintain their privacy. Demographic information was taken including age, gender, and race. Height and weight were measured and their body mass index, BMI, was calculated. Females took a pregnancy test and the first day of their most recent menstrual cycle was recorded. The appropriate sized ensemble garments were assigned to each subject. Subjects were given their supply of ingestible pills and a wristband were given to them to be worn stating “Warning: No MRI or NMR” for their safety when taking the ingestible pills. They performed their first familiarization session without body armor, helmet, knee pads, or gloves. In all test subjects were allowed to wear sunglasses if they wished. Oxygen consumption and skin temperature were not measured in the first two days. The second day the subjects completed their second familiarization session with the ensemble, minus the body armor. The final day of



familiarization, the subjects wore the complete ensemble; treadmill speed for each subject was lowered to account for the additional weight of the ensemble. All physiological variables were measured for this session.

The second set of three days comprised the actual PCS testing segment. The test protocol was the same each day, with only the PCS treatment as the variable, including the effects of its weight on walking speed. All of the garments were prepared and placed at the stations for the subject to wear. Male subjects were provided with a pair of boxer-briefs, female subjects wore their own underwear and bra for the duration of the tests.

The subjects would arrive at the institute and immediately go to the engineer who would scan to see which ingestible pills, if any, were still in the subjects. If the pill from the last day was still in the subject, that pill was used as the primary, because of its assured position in the GI tract. The engineer would prepare the correct monitors and input the information for the test into the computer.

The subjects voided their bladders and were weighed in their own underwear. They proceeded to the preconditioning chamber and were assisted in donning clothing if required. The nurse and technician attached thermocouples with transpore hospital tape, if the subject was excessively hairy, a small patch was shaved so the sensor would make contact with the skin. Skin temperature was measured in seven locations: forehead, right scapula, right upper chest, right upper arm, right lower arm, right anterior thigh, and right calf. Subjects also wore a wrist strap to form an electrical ground so they did not build up a static charge. Mean skin temperature was area weighted using the factors from ISO 9886 (ISO, 2004), but the hand's temperature was eliminated due to effects from the high radiant load. The hand's weighting factor was evenly

distributed over the other sensors to determine mean skin temperature. Subjects also put on their heart rate straps and then carried their thermocouple leads to the chamber.

At 45 minutes, the subjects proceeded to the testing chamber and drank 250 ml of water while the experimenter set up the treadmill and plugged in the instruments. When the experimenter determined the instruments were reading, the PCS was turned on, or the subject quickly donned a PCM vest under the body armor with assistance from the technician and nurse and the test began. The nurse stated a timer to provide 250 ml of water to the subjects every 30 minutes to prevent dehydrations. They were allowed to drink additional water when desired and were able to listen to music or watch a DVD on a shared flat screen TV. If the subjects needed to void their bladders, there was a hand held urinal, which did not need to be used. The subjects walked at a constant rate for 2 hours or until their core temperature or heart rate reached the cutoff values, illness, or wanted to quit. The removal criteria from ASTM standard F2300 were applied (ASTM, 2010a):

- The subject's body core temperature reached 39.0°C or increased 0.6°C in a 5-minute period (whichever occurred first).
- The subject's heart rate reached 90% of his or her age predicted maximum.
- The subject experienced heat exhaustion symptoms, including headache, extreme weakness, dizziness, vertigo, "heat sensations" on the head or neck, heat cramps, chills, "goose bumps", vomiting, nausea, and irritability (Hubbard & Armstrong, 1998).
- The subject wanted to quit the experiment.

Once the session was complete, the subjects were returned to the small chamber, and removed their clothing and equipment, with assistance if necessary. The subjects were weighed in their own underwear, put on their clothes and then were given cold water or Gatorade® to drink. If the subject's weight was not within 1% of their initial weight they were asked to stay for 15 minutes or until the target mass was reached.

Subject who were removed for reaching the cutoff or who experienced symptoms of heat stress were removed from the chamber immediately, core temperature and heart rate were measured using the handheld CoreTemp® data acquisition devices. Restrictive clothing and equipment were removed; the subjects were seated in front of a fan with cold water or Gatorade® to drink and monitored until their core temperature returned to safe levels.

### **3.3.2 PCS Results**

Most of the soldiers were able to complete the two-hour test session; however, there were nine instances where subjects either quit due to discomfort or were removed by the nurse when their core temperature reached 39.0°C. In the first session, the subjects that stopped the test early were as follows:

- Subject 1: male, wearing no PCS, 102 minutes (subject stopped experiment)
- Subject 5: female, wearing no PCS, 78 minutes (subject stopped experiment)
- Subject 6: female, wearing no PCS, 82 minutes (core temp reached 39°C)
- Subject 6: female, wearing PCS #01 Entrak, 61 minutes (core temp reached 39°C)
- Subject 6: female, wearing PCS #12 Steele, 84 minutes (subject stopped experiment)
- Subject 9: male, wearing no PCS, 95 minutes (subject stopped experiment)
- Subject 11: male, wearing no PCS, 99 minutes (core temp reached 39°C)

In the second session, there were fewer failures to complete the two hours of testing:

- Subject 13: male, wearing PCS #20, 71 minutes (system too heavy, shoulder/neck pain)
- Subject 15: male, wearing no PCS, 70 minutes (Experienced headache/lightheadedness)
- Subject 18: male, wearing no PCS, 102 minutes (Subject felt dizzy)

The average values of the core temperature (Figure 3.8, Figure 3.12), mean skin temperature (Figure 3.9, Figure 3.13), torso temperature (Figure 3.10, Figure 3.14), and heart rates (Figure 3.11, Figure 3.15) can be found below in the figures. Individual subject data by subject number can be found in Appendix D - Testing Results: Human Subject Testing. The average graphical results show the significant differences between the PCS results and the baseline results. In Figure 3.8 the differences in initial core temperatures complicate comparing

final core temperatures as called for in the ASTM Standard. However, the core temperature can be normalized by the using the change over the course of the test. Also of note is the slopes of the core temperatures for each PCS throughout the test, especially at the end. In PCS 9, 12 and 20 the core temperature rise has been attenuated.

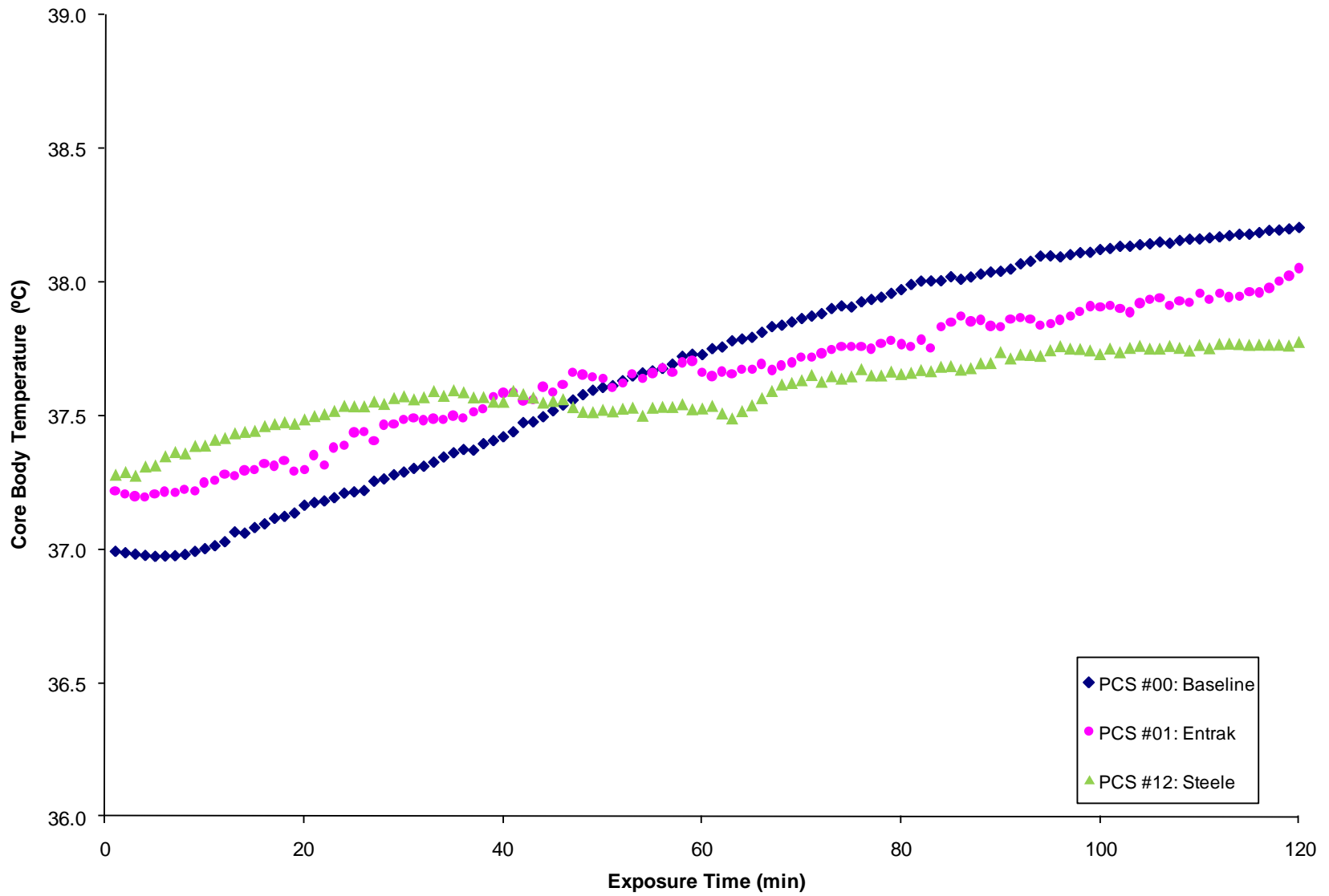
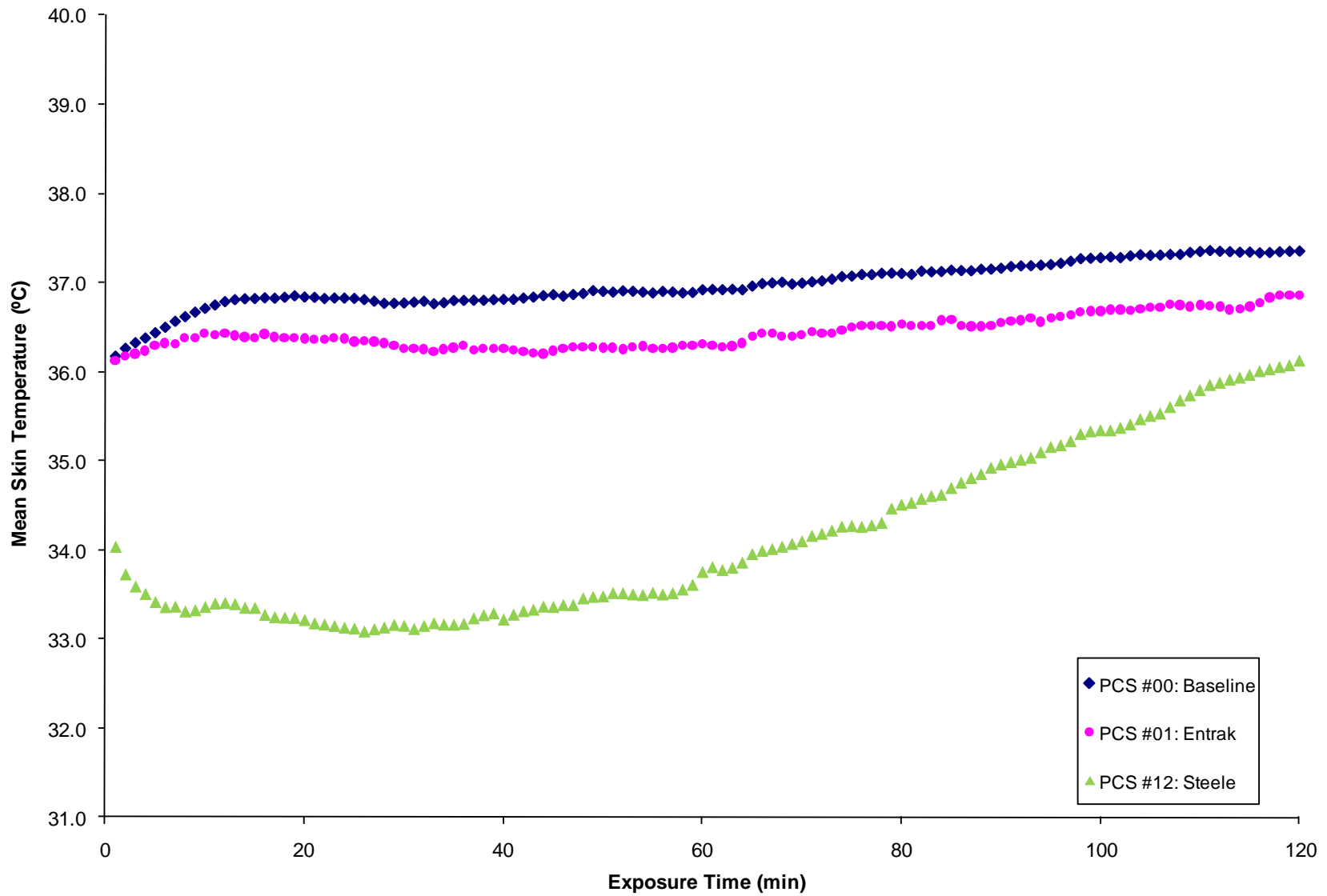
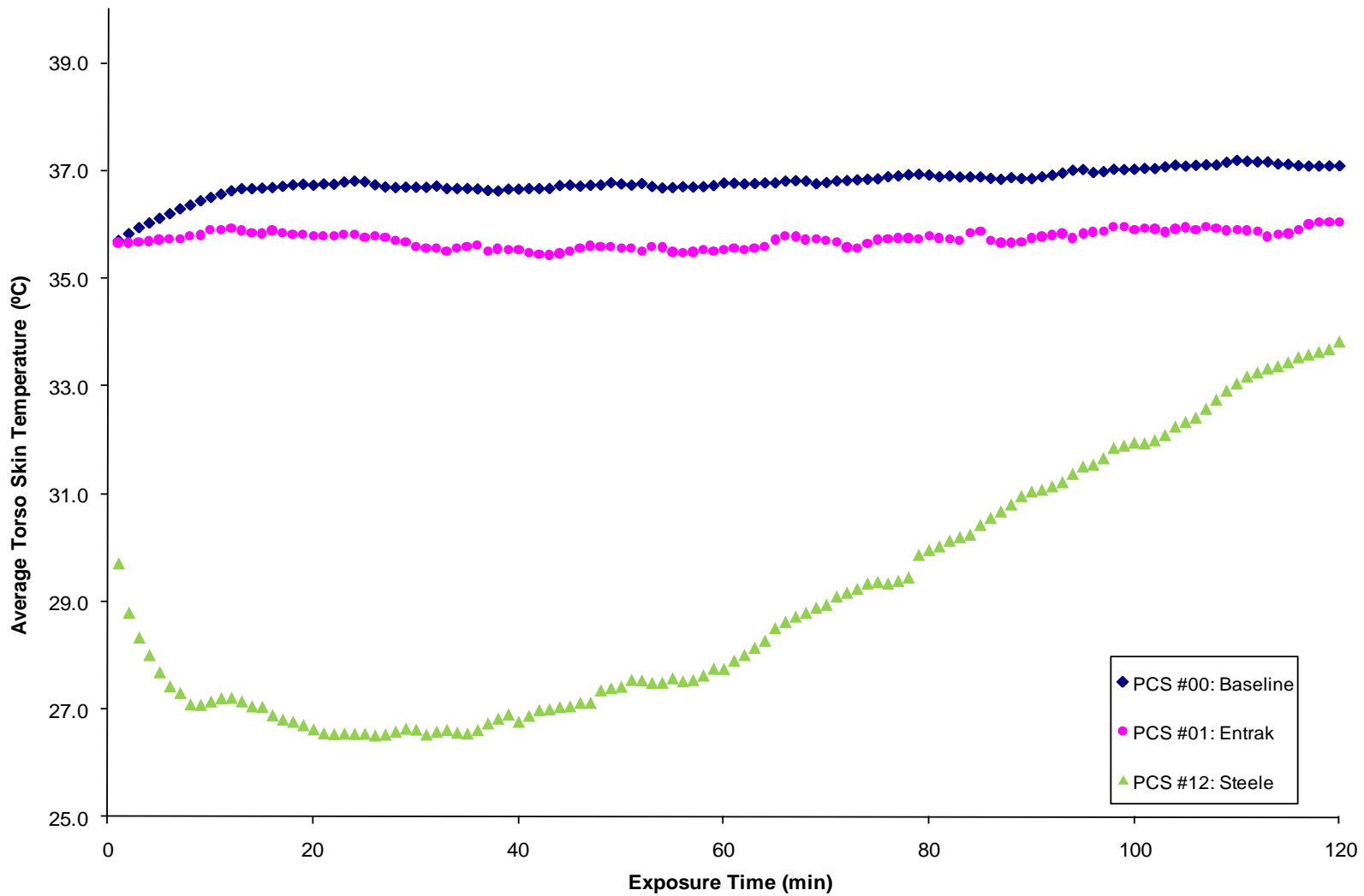


Figure 3.8 Average core temperatures of session 1 subjects while wearing different PCS



**Figure 3.9** Mean skin temperatures of session 1 subjects while wearing different PCS



**Figure 3.10** Average torso (back and chest) skin temperatures of session 1 subjects while wearing different PCS.

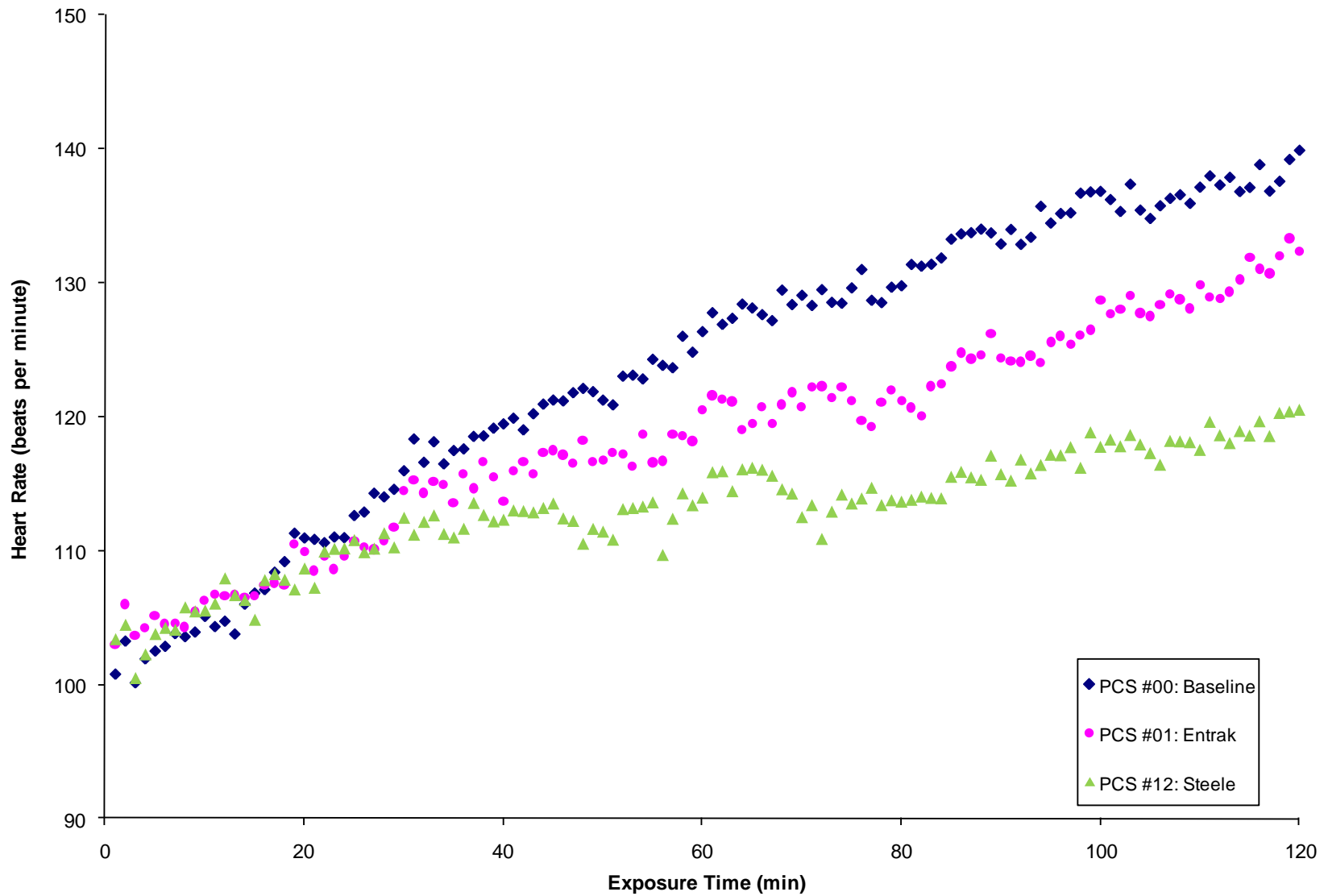


**Figure 3.11 Average heart rates of session 1 subjects while wearing different PCS.**



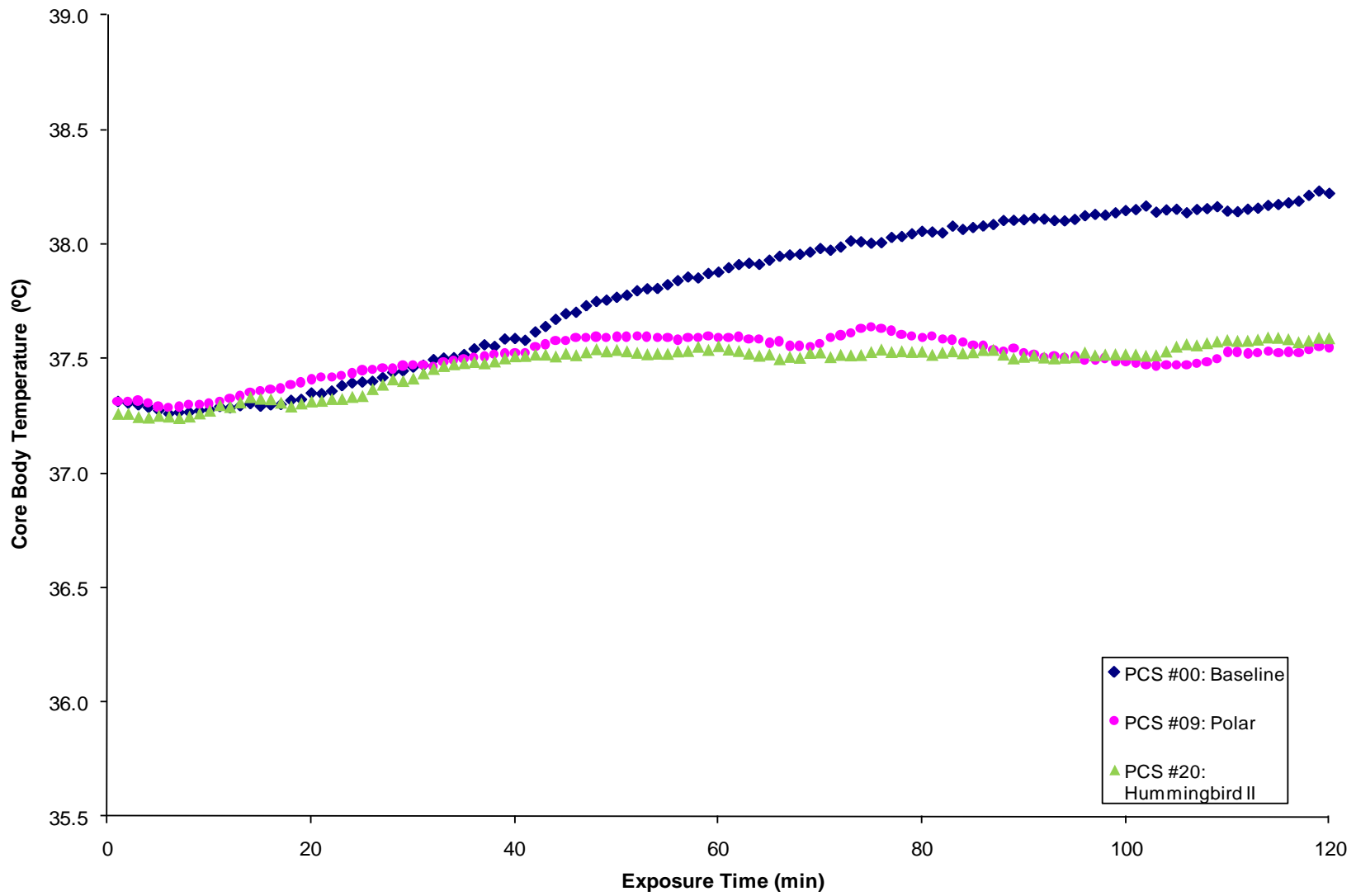


Figure 3.12 Average core temperatures of session 2 subjects while wearing different PCS

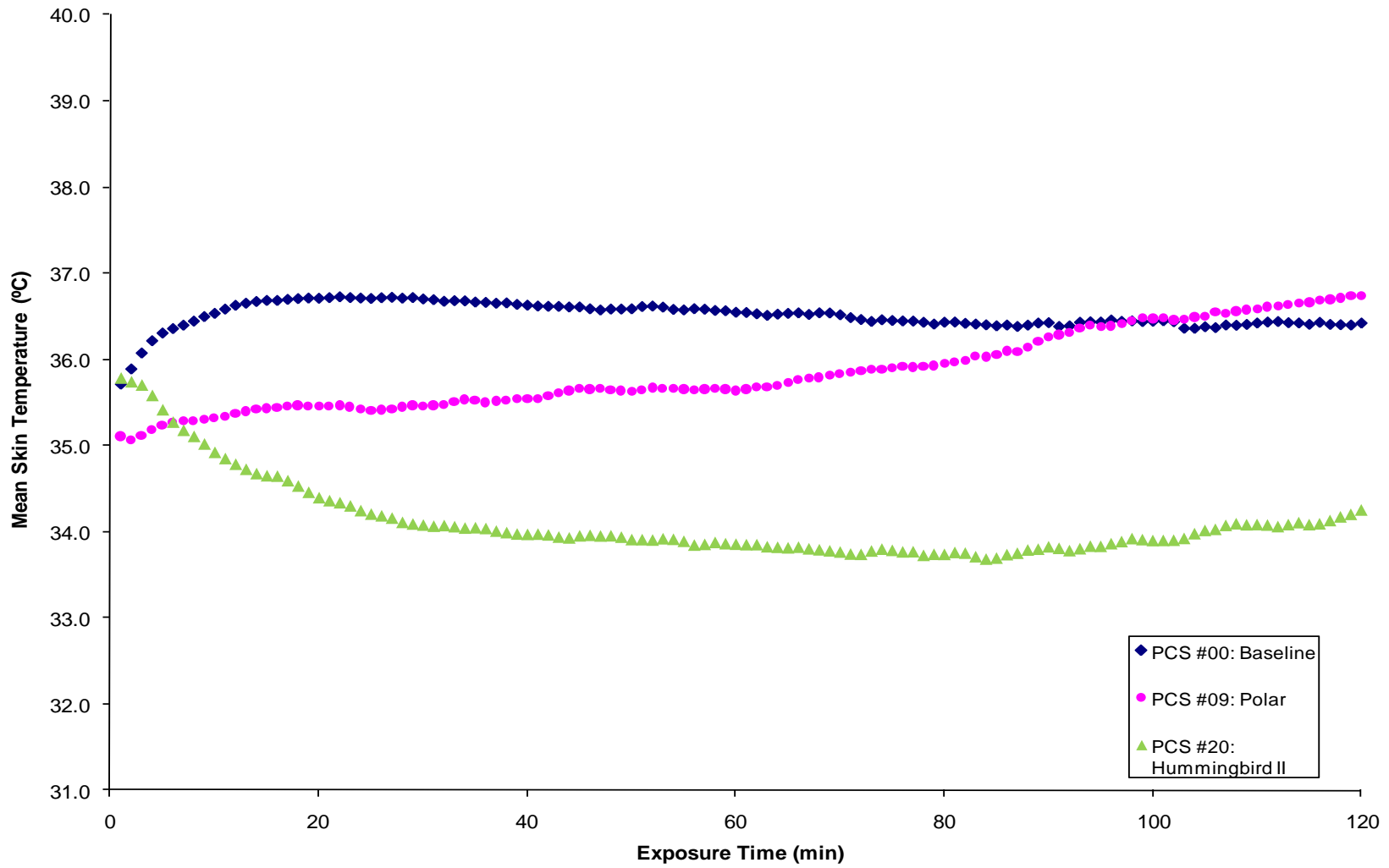
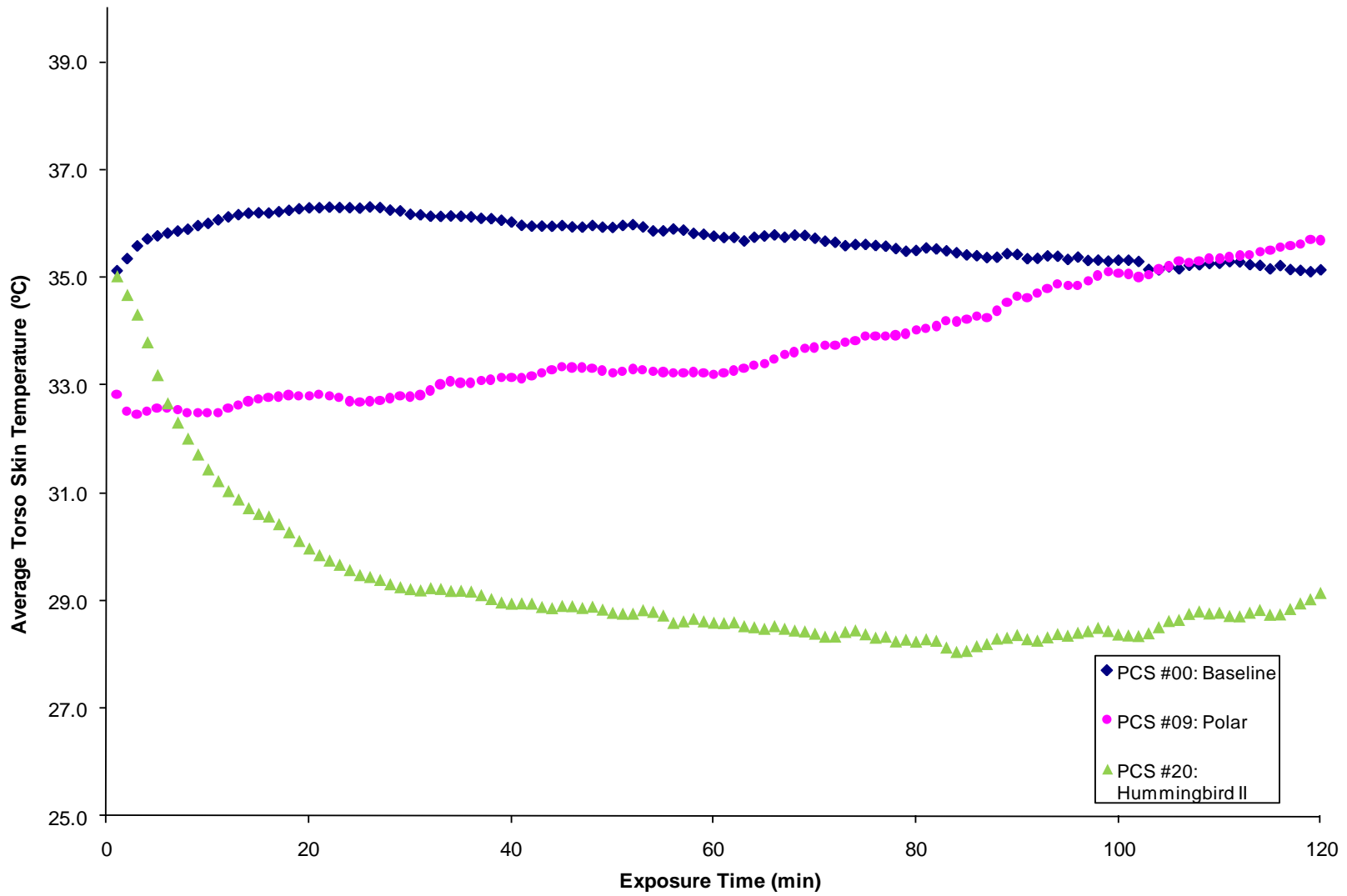
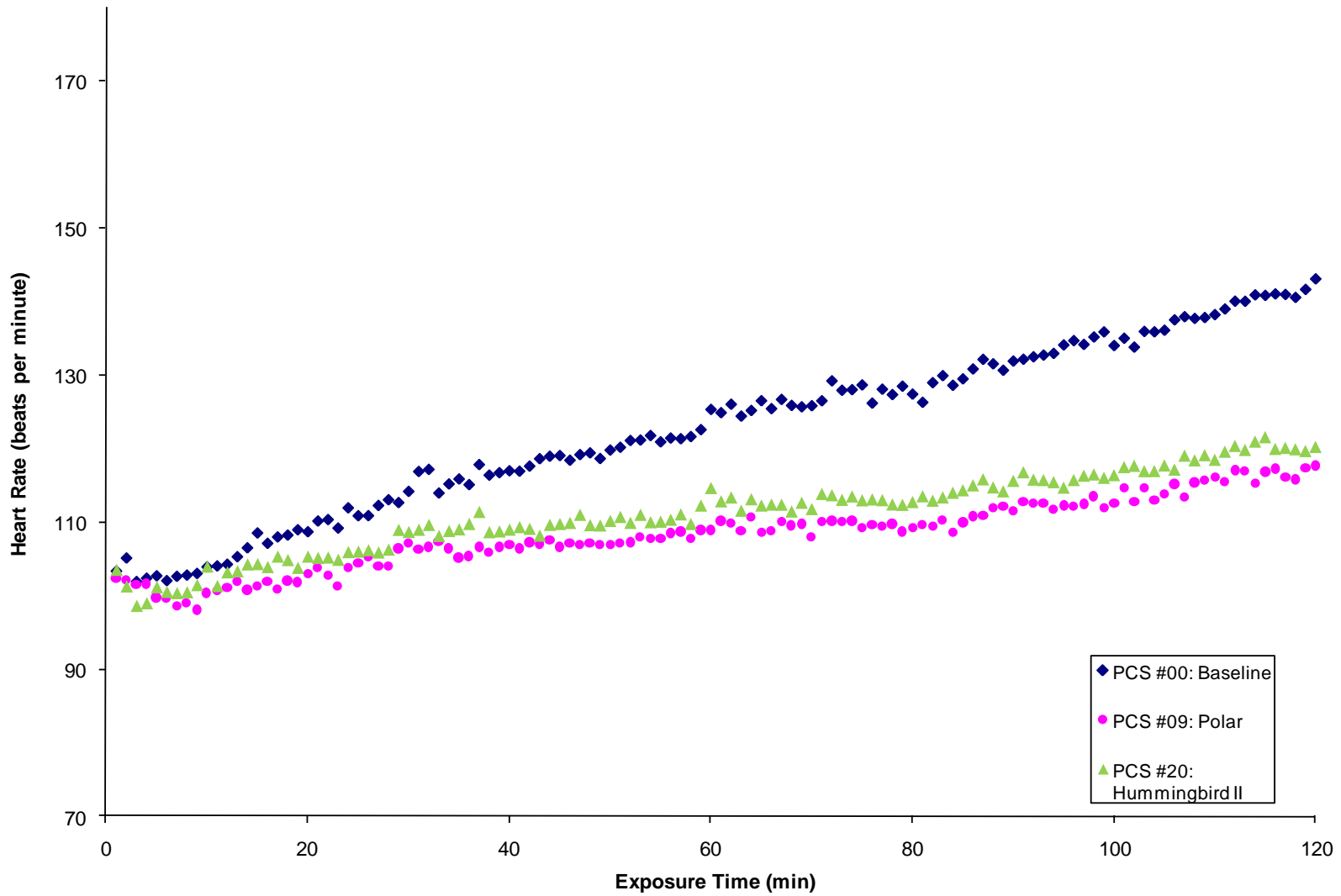


Figure 3.13 Mean skin temperatures of session 2 subjects while wearing different PCS.



**Figure 3.14 Average torso (back and chest) skin temperatures while wearing different PCS.**



**Figure 3.15 Average heart rates of session 2 subjects while wearing different PCS.**

Each session is presented separately because each group serves as their own control for the PCS tests. The statistics were run in SAS as a basic ANOVA. The significance level was set as  $p < 0.05$ . The effect of PCS on metabolic rate was not statistically significant because we adjusted each subject's treadmill speed so that the work rate was essentially the same for all subjects (i.e., 365-390 W at the end of the experiment). The average results for the graphed physiological variables are shown in Table 3.7.

**Table 3.7 Results for the Personal Cooling System human subject tests**

Personal cooling system	Final core temperature (°C)	Change in core temperature over test (°C)	Final heart rate (bpm)	Average torso skin temperature (°C)
First Session Baseline (no PCS)	38.21	1.21	139.8	37.08
#1 Ventilation Vest (Entrak)	38.07	0.83*	132.5*	36.03
#2 Cool UnderVest (Steele)	37.79*	0.50*	120.5*	33.83*
Next Session Baseline (no PCS)	38.30	0.97	141.8	36.61
#3 PCVZ-KM Vest (Polar)	37.56*	0.24*	117.8*	35.68
#4 Hummingbird II (CTS)	37.60*	0.33*	120.3*	29.13*

\*The PCS result was statistically different from the baseline ensemble with no PCS ( $p \leq 0.05$ ).

When the soldiers were wearing the phase change PCS (#2-3) and refrigeration PCS (#4), they had a significantly lower heart rate, final body core temperature, and change in core temperature over the two-hour test as compared to wearing no PCS. The air circulation system, PCS #1, significantly affected the heart rate and change in core temperature of the subjects, but not the final core temperature. The change in core temperature accounted for variability in the initial core body temperature. PCS #2 and #4 also produced a significantly lower skin temperature on the torso (under the body armor and PCS) than the baseline condition.

### 3.4 Human subject to thermal manikin PCS discussion

It is desirable to explore the ability of the thermal manikin to predict the cooling power of a system. The thermal manikin provides a standardized way of measuring PCS, but may not be an accurate representation of the cooling potential of a PCS on humans. The thermal manikin skin temperature is only limited by the heat flux provided by the heaters maintaining the temperature of the manikin's skin. It also has the advantage of having a fully saturated skin, which can affect the ability of air circulation PCS to provide cooling. Furthermore, the temperature of the thermal manikin chamber is lower than the human subject test chamber, resulting in less heat loss to the environment from cold boundary systems improving their efficiency. However, the relative cost and standard comparison capability make manikins an indispensable tool. The question remains how accurately the manikin predicts the effect of a cooling system on a human. This complex question was explored in depth validating the paper on PCS selection and is given in the following section (J. Elson & Eckels, 2015).

#### 3.4.1 Heat Storage

*The following section is excerpted from Applied Ergonomics, Vol. 48, pg. 33-41 J. Elson and Eckels (2015) used with permission from Elsevier Ltd.*

**Table 3.8 Percent difference between initial cooling power estimate and thermal manikin (Table 3 from Applied Ergonomics, Vol. 48, pg. 38 J. Elson and Eckels (2015) used with permission from Elsevier Ltd.)**

PCS and Manufacturers	Cooling Power (W)		
	Initial Estimate	Thermal Manikin	Percent Difference
Ventilation Wear	250.0	100.3	149.3
Cool UnderVest	94.9	113.0	16.0
PCVZ-KM Vest	126.5	96.9	30.5
Hummingbird II	125.0	124.6	0.3

**Table 3.9 Updated Cooling Effectiveness rating score using thermal manikin results (Table 4 from Applied Ergonomics, Vol. 48, pg. 38 J. Elson and Eckels (2015) used with permission from Elsevier Ltd.)**

Manikin Adjusted Screening PCS and Manufacturers	Time (hours)							
	1	2	3	4	5	6	7	8
Ventilation Wear	100	100	100	100	100	100	100	100
Cool UnderVest	100	100	100	100	92	76	66	57
PCVZ-KM Vest	100	100	100	100	88	73	63	55
Hummingbird II	100	100	100	100	90	75	64	56
Hummingbird II + 1 Battery	100	100	100	100	100	100	94	82

“Determining natural heat loss before obtaining manikin data or human subject data is a challenge. This value can be difficult to determine as it is dependent on environmental conditions, clothing, equipment, and individual subject variation. In the case of the dismounted soldier, the wet-bulb globe temperature (WBGT) charts showing work rates limits were used to estimate the natural heat loss. The selection of this value ultimately effects the calculation of the cooling power and effect of a PCS. The simplistic measure used the “no limit” work time for the corresponding metabolic rate of 400 W and WBGT temperature of 28 °C.

**Table 3.10 – Estimated and human subject heat storage results (Table 5 from Applied Ergonomics, Vol. 48, pg. 38 J. Elson and Eckels (2015) used with permission from Elsevier Ltd.)**

PCS system	Storage estimation from natural heat loss baseline and thermal manikin results, Watts	Human subject tests average (0.8Tc+0.2Tsk), Watts
Baseline	75	42.9
Ventilation Wear	-25.3	31.9
Cool UnderVest	-38	18.0
PCVZ-KM Vest	-21.9	26.7
Hummingbird II	-49.6	-1.0

The subjects worked at an average of 400 W for two hours, as measured by a VO2. Results of this experiment were reported in Elson et al. (2013). Table 4 [from the reference,

Table 3.9 in this work] predicts subjects should be able to finish the two-hour trial without heat stress. Using the final expected heat storage for each system from Equation 2 [in the reference, similar to Equation ( 3.1 ) in this work] , assuming the natural heat transfer to the environment is the same between PCS tests and baseline tests gives an additional way to rank the expected performance. Table 5 [from the reference, Table 3.10in this work] presents this estimate in the first column. The baseline result predicts heat storage of 75 W and the best system performance is the Hummingbird II, with a net energy loss of about 50 W to the subject. The second column in used the “no limit” work time for the corresponding metabolic rate of 400 W and WBGT temperature of 28 °C.

Table 3.10 Table 5 [from the reference, Table 3.10in this work] presents the measured energy storage from the human subject trial with the PCS. The human trial results are surprising, as the energy storage is significantly higher than expected. It is important to note, with the exception of the air circulation system, which has known measurement and estimation challenges, the rank order of the storage meets initial estimates. This provides an important level of validation to the proposed method. Although, the higher-than-expected heat storage suggests additional information is required to accurately estimate heat storage in humans.

Being able to directly calculate the cooling rate in Equation 2 [in the reference, similar to Equation ( 3.1 ) in this work] from human subject data would help diagnose the performance difference noted in the last paragraph. Natural heat loss from the subjects is the complicating factor, as it is not directly measured in the experiment. In previous studies, it has at least been implicitly assumed that the PCS does not significantly change natural heat loss from the body (M. J. Barwood et al., 2009; James R. House et al., 2013). For the current analysis, baseline data for each subject was used to estimate natural heat loss for the non-PCS case. Calculation of the



natural heat loss term can be found simply by rearranging Equation 1 and solving for  $Ht$ , with  $St$  from mean body temperature. The result of 356.5 W agrees relatively closely with our estimate from empirical data of 325 W prior to running the study. This represents approximately a 9% error, plus whatever uncertainty is associated with the mean body temperature calculation, which has significant potential errors (Jay & Kenny, 2007).

### ***3.4.2 Discussion***

The magnitude of the gap between the predictions and human subject results is troubling. For example, Table 5 [from the reference, Table 3.10 in this work] showed the Hummingbird II system should have caused the human subjects to lose 50 W over the two hours and human subjects results showed no change in storage after the two hours. This highlights the importance of using the most accurate PCS to human cooling rate and natural heat loss possible when using the cooling effectiveness factor.

Multiple issues affect natural heat loss estimation. Changes resulting from different coverage areas and possible physiological reactions to each PCS are the most obvious two impacts. In evaluating a PCS in the above example, the PCS was assumed to be covered by the PPE, while covering the same area with the same thermal and evaporative resistances. In this case, this assumption was deemed reasonable because of the insulated, vapor-impermeable nature of body armor and similar body coverage areas. In many cases, there may not be PPE, and it may cover different areas, or have different resistance values. For example, a firefighter's outerwear may have high evaporative resistance and a relatively high thermal resistance covering the body, not the extremely high thermal resistance of ceramic plate body armor over the torso. PCS systems can range from neck coolers, to vests, to complete body tube suits, so this area and resistances of the area can be a major factor.

In an ideal case, natural heat loss could be estimated using a thermal manikin to test the ensembles without a PCS and with an inactive PCS. This could be used to determine the thermal and evaporative resistances, and then used in a physiological model or a ratio to known data. However, this still requires the availability of good physiological information and models.

Physiological responses to natural heat loss mechanisms are another area that could affect the estimates used. Currently, there does not seem to be any published literature specifically quantifying natural heat loss differences between PCS tests and baseline tests due to physiological responses. There are two main areas where this could occur — dry heat exchange by convection, conduction, and radiation; and latent heat exchange, by evaporation.

In dry heat exchange, the first logical location to look at a difference in natural heat loss is because of the cooling effect of the PCS itself. If the PCS is working, then the body temperature should be lower than the baseline test. In this case, skin temperature is also likely lower. This will affect the temperature gradient from the skin, allowing for less beneficial heat exchange with the environment. A possibility that has been recognized in the literature is that a cold-boundary PCS could cause local vasoconstriction, which would lower the cooling experienced by the body (James R. House et al., 2013).

The latent heat exchange is the other aspect of the natural heat loss of the body that could be affected. It has been noted in literature by James R. House et al. (2013), and in our previous studies (E.A.; McCullough & Eckels, 2008), that there is a significantly lower ( $p \leq 0.05$ ) total sweat rate, in some cases, when using a PCS. This lowered sweat rate could have a major effect on the natural heat loss from the body and would need to be quantified to determine the effect. It is also possible there could be more sweating or more efficient use of sweat, as is the goal of air

circulation systems. These issues will affect the estimation and calculation of natural heat transfer with and without a PCS for use in this first principles analysis.

The second aspect that would improve the cooling-effectiveness factor is to define the cooling rate of each PCS as accurately as possible. Measuring the cooling rate of a PCS has been described in ASTM Standard F2371 (ASTM, 2010b), and is a reasonable estimate assuming a mean skin temperature of 35°C and good insulation between the PCS and the environment. Comparing the estimation methods presented in this paper to the manikin results, as shown in Table 3 [from the reference, Table 3.8 in this work], shows good agreement for all systems except the air circulation system. As was noted in section 2.6 [of the reference, Section 3.2.3 in this work], standard F2371 is not designed to work well with this type of system.

Two main issues must be considered when translating cooling power measured on a manikin to human subjects. It is important to remember that in ASTM Standard F2371 (ASTM, 2010b), the manikin surface temperature and ambient temperature are both held at 35°C.

Skin temperature on the human subjects is not constant at 35 °C, as in the manikin, and can drop significantly under the cooling system (James R. House et al., 2013). The manikin, being rigid, will also induce a different fit compared to human subject tests, which could create air gaps or make contact where none would occur on a human. The environment is typically more extreme than 35 °C, increasing the loss of cooling potential to the environment. Additional information on the effect of manikin surface temperature and different environments can be found in Chuansi Gao et al. (2010), Xu and Gonzalez (2011) and Jetté et al. (2004).

Estimating cooling power applied by the air circulation systems provides a different set of challenges. Currently, ASTM Standard F2371 (ASTM, 2010b) is not appropriate for testing these systems, but is used because there is no other standard. Air circulation systems can seem to

provide more or less cooling, during use in different environmental tests than Standard F2171. Flow rates necessary to maintain 100% skin wettedness of the manikin can be considered unrealistic in some scenarios, considering published maximum sweat rates (Gosselin, 1947; C. Smith & Havenith, 2011). Finally, there can be a different fit on the rigid manikin, which can change the cooling potential of the systems by creating and blocking potential airflow passages that may not exist on a malleable, moving human. There have been attempts to compensate for this effect by using physiological-controlled manikins to change the sweat rate of the manikin to better conform to human sweat rates (Burke et al., 2009). However, this can lead to a non-uniform sweat distribution on the manikin, which may affect results. This does solve the issue of 100% skin wettedness and deserves further study.

It is possible to define relatively accurately the natural heat loss with and without a PCS as well as the cooling rate of the PCS, using a thermal manikin and possibly thermal models. However, increasing the accuracy of the estimate will generally increase the cost, as extra information will be required. Therefore, a cost-benefit analysis is appropriate at this point to determine how well the natural heat loss and cooling rate need to be, and can be, defined.

This study also highlighted the need to take additional data during human subject testing. The data called out in ASTM Standard F2300 (ASTM, 2010a) is not sufficient to fully evaluate the physiological effect of a PCS on humans, and therefore validate the PCS cooling rate. A better understanding of the natural heat loss as discussed above would also benefit human subject trials. Perhaps the most significant is the ability to accurately calculate the energy storage from the human subject results.

As mentioned previously, Jay et al. (2006), Jay and Kenny (2007), and André L Vallerand et al. (1992) identified problems determining heat storage based on two compartment

mean body temperature estimations, such as those used in this validation. Jay and Kenny used a third compartment, which improved their estimate, but the procedure required invasive, intramuscular temperature measurement. Currently, there is not enough research to determine how many compartments form a reasonable estimate of the mean body temperature, where they could be located, or if the compartments vary in the population. The research by Jay et al. (2006) also shows a possible effect of temperature on the compartments. In the case of a PCS, this could conceivably cause variations between PCSs depending on cooling temperatures and locations on the body. Finally, the effect of exercise-induced core temperature rise is noted in the literature (Livingstone et al., 1983), where exercise causes an immediate core temperature increase even in cold weather. Conceivably, this could be a source of error in compartment models and impact comparisons of PCSs when using Standard F2300 (ASTM, 2010a). In addition, a smaller difference between the core temperatures of systems will result in the measurement uncertainty having a larger impact on the final results. If this method is to be fully validated, the cooling rate must be accurately calculated from the human subject data. This will require additions to the current standard, or a new standard, but will likely result in higher testing costs, more invasive procedures, or both.

Determining the necessary values to create an accurate model for heat stress and time, and then validating the model, is conceptually possible given the correct data. The information required for complete validation will require more information on the physiological effects of a PCS. Ultimately, if more accurate results are required, information is needed regarding the natural heat loss from both with and without a PCS, how clothing and a PCS interact, and how the body's physiology interacts with a PCS. This requires completing the energy and mass

balance equation, leaving only the storage term as the unknown. This may be done in the future on human subjects and possibly using advanced human thermal models.”

The above direct quote from J. Elson and Eckels (2015) included the initial exploration of the energy balance and discusses the possible sources of error in the energy storage analysis. What follows in this work is an analysis to determine the most significant sources of error and explain PCS effects. To explore the issue in depth, using the available information, basic and advanced validated human thermal models will be used in the next chapters to explore the effects of our results. Human thermal models provide a theoretical representation of some of the unknowns in the heat and mass transfer problem and can assist in identifying issues in thermal manikin and human subject testing protocols, data collection, and human modeling both with and without PCS.

## Chapter 4 - Modeling human subjects with and without PCS

It is desirable to understand the actual cooling effect of PCS on the human body. As discussed in the previous chapter, non-invasive human subject measurements do not necessarily allow for an accurate measure of the energy storage gradients in the body represented by temperature. The temperature gradient in the body with inflection points could be unrepresentative of the body storing energy, especially considering heat generation is taking place all over the body. Also, according to ASTM F-2300 (ASTM, 2010a) measurement of sweat evaporation and sweat production as separate measurements is not part of the standard test method. Without knowing the exact temperature distributions across the body, and the heat lost by evaporation, it would be difficult to determine the exact effects of the PCS on the human body by calorimetry alone.

There are numerous, validated models of human thermal physiology which use empirical equations and fundamental heat transfer effects to model the human body. In this research, there are baseline results for 24 subjects. This provides an important opportunity to explore the ability of human thermal models to predict the effects on human subjects. Two models were applied to predict the results of the baseline test: the ASHRAE two-node model (ASHRAE, 2013) and an commercial application of the Fiala model (Dusan Fiala et al., 2012; Dusan Fiala & Lomas, 2001; Dusan Fiala et al., 1999; D. Fiala et al., 2001). The version of Fiala's model, which is both multi-segmented and multi-layered integrated into a TAItherm module (Allen & Mark, 2013; A. Curran et al., 2006; A. R. Curran, Peck, Schwenn, & Hepokoski, 2009; Hepokoski et al., 2012) .

In preparation to modeling the effects of PCS, the baseline results are simulated to validate the usefulness of the models or assumptions made in the models. Modifications are made within the limits of the programs to improve the predictive capability of the models to

predict the baseline results. This chapter lays the groundwork for the comparison for discussing the models and the initial conditions, boundary conditions, and assumptions. Each model will be expanded upon in Chapter 5 when the models are compared to the baseline data, assumptions will be examined to determine their applicability, and modifications will be made to improve accuracy.

This chapter presents the models that will be applied later in this work in Chapter 5 and Chapter 6 to simulate the baseline and PCS tests respectively. It specifically details the setup, initial conditions, boundary conditions, and methods used in using the thermal models. The ASHRAE two-node model will be covered first in Section 4.1 followed by the human thermal model inside TAItherm in Section 4.2.

#### **4.1 Two Node Model**

The ASHRAE two-node model (ASHRAE, 2013), discussed in Subsection 2.3.2, Two Node Models, the simplest of the two human thermal models used in this analysis. The ASHRAE two-node model was used because of its ease of access- being published in the ASHRAE Fundamentals handbook- simplicity to program, ease of modification, and low cost to implement. If the ASHRAE model can provide a good estimate of the effects of the hot conditions in the baseline tests, it would be an inexpensive prediction tool for heat stress incidents and would provide for reasonable comparison by applying PCS effects to the model. The equations used in the model can be found in the ASHRAE Fundamentals Handbook, although versions from 2013 (with errata) and later are recommended as earlier handbooks are inconsistent in their applications of the two node model.

The two-node model was implemented in MathCad 15 (PTC Inc.). This model consists of two segments: core and skin. The core node is the majority of the body mass and the skin node



takes up the remainder. The two nodes can change their percentages of body mass depending on the temperatures of each node, according to the model corresponding to the blood allotted to each. A potential correction of the model accounting for the mass transfer from the skin and core proposed by Jones and Ogawa (1992) was explored and determined to have an insignificant effect in this application. The correction is not presented in this work as it has never been validated, but is likely more significant in transient cases where there is a rapid change in the environmental boundary conditions and metabolic rate. The skin interacts with the environment by convection, radiation, and evaporation. The core and skin interact by conduction and a common blood pool. The core node contains the metabolic heat generation source and interacts with the environment through respiration. In keeping with fundamental thermodynamic principles, it is necessary to properly define all the values required to setup a model: human properties, initial conditions, boundary conditions, and modeling environment.

#### ***4.1.1 Human conditions***

Human modeling and human subject testing are both complicated by the knowledge that all people are different in some way or another. This can create issues when testing on human subjects where different body types, metabolic rates, weights, muscle density, and other physiological factors can influence the human's response to different conditions. In a perfect world, with infinite resources it would be possible to quantify the exact reaction of each individual human. The use of validated models, such as the ASHRAE two-node model, provides a program based on the averages of large data sets spanning many physiological factors.

When testing both the baseline and PCS tests each subject's parameters were input directly into the program in order to get the closest possible individual effects. These values were the physiological parameters of height and weight to calculate the Dubois Area and provide mass

for the model. Initial conditions included initial core temperature, initial mean skin temperature, and metabolic rate.

#### ***4.1.2 Boundary conditions***

Boundary conditions are the second important aspect when performing simulations. The boundary conditions in this case are the ambient air temperature, mean radiant temperature, relative humidity, thermal and evaporative resistances of clothing, and convection coefficients. These conditions determine how the simulated human will exchange heat with the environment.

##### ***4.1.2.1 Temperature and humidity***

The temperature of the environment from the human subject tests is used as the boundary condition in the simulations. The same environmental values for air temperature, air velocity, mean radiant temperature, and relative humidity from Section 3.3.1 are used in the simulations. The radiation coefficient used was  $4.7 \text{ W/m}^2\text{K}$  corresponding to an indoor environment. The relative humidity was multiplied by the saturated pressure at the ambient air temperature calculated from the multivariable saturated pressure approximation equation from Chapter 1 of the ASHRAE Fundamentals (ASHRAE, 2013).

##### ***4.1.2.2 Heat and mass transfer***

The convection coefficient is used for both the convection and evaporative heat and mass transfer calculation to and from the body. The choice of a convection coefficient is an extremely important factor. To calculate the convection coefficient,  $h_c$ , an empirical correlation was used for a clothed soldier walking on a treadmill in wind velocity,  $v_{\text{wind}}$ , at 2.0 m/s (4.5 mph) taken from the work of Danielsson (1993) in SI Units.

$$h_c = 11.7 \cdot v_{\text{wind}}^{0.57} \quad (4.1)$$

In keeping with the application of the heat and mass transfer analogy, the Lewis Ratio, is used to directly calculate the equation the evaporative heat transfer coefficient. The conditions in the chamber resulted in a calculated Lewis Ratio of 17.15 K/kPa.

$$h_e = h_c \cdot LR \quad (4.2)$$

Using Equation ( 4.2 ) yields an evaporative heat transfer coefficient of 0.2979 W/(m<sup>2</sup> Pa)

#### 4.1.2.3 Clothing

The clothing information was taken from the thermal manikin tests. This provides the measured thermal and evaporative resistance of the whole body-clothing ensemble given in Table 3.4 and Table 3.5. The intrinsic thermal resistance is 0.155 m<sup>2</sup>C/W (1.00 clo) and the evaporative thermal resistance is 26.2 (m<sup>2</sup> Pa)/W. The clothing is applied to the human using series thermal resistance with a clothing area factor of 1.33. The equation for the dry heat transfer convection and radiation:

$$C + R = \frac{T_{sk} - T_o}{R_{cl} + 1/f_{cl} \cdot h_t} \quad (4.3)$$

where skin temperature, T<sub>sk</sub>; operative temperature, T<sub>o</sub>; intrinsic dry clothing resistance, R<sub>cl</sub>; clothing area factor, f<sub>cl</sub>; and total dry heat transfer coefficient, h<sub>c</sub> + h<sub>r</sub>=h<sub>t</sub> are the variables.

The evaporative heat transfer is dependent on sweat rate that is expressed as a skin wettedness coefficient. A main assumption of the standard model is that sweat can increase until reaching 100% body surface area and then drips with no energy losses and the clothing does not wet. This will be discussed in more detail in Chapter 5 when comparing the baseline results of the modeling and human subject tests. This is a likely source of error in modeling these conditions. The maximum evaporation available to the simulated person, E<sub>max</sub>, is given by:

$$E_{max} = \frac{P_{sat}(T_{sk}) - \phi \cdot P_{sat}(T_a)}{Re_{cl} + 1/f_{cl} \cdot h_e} \quad (4.4)$$

where  $P_{sat}$  is listed twice as a function of first the skin temperature,  $T_{sk}$ , and as the ambient air temperature,  $T_a$ . The percent relative humidity (in decimal form),  $\phi$ , is used to solve for the partial pressure. The skin is assumed fully saturated under the maximum condition. The saturated pressure curve equation used can be found in the ASHRAE HVAC Applications Handbook (ASHRAE, 2007). The remaining terms are the intrinsic evaporative resistance,  $Re_{cl}$ : clothing area factor,  $f_{cl}$ ; and total evaporative heat transfer coefficient,  $h_e$ . The skin wettedness factor is computed based on the model's prediction for sweat production, and evaporation related to the maximum evaporation.

#### ***4.1.3 Modeling Environment***

The differential equations governing the transient energy balance in the body were solved numerically using a time step of ten seconds. In previous tests, this was determined to be sufficiently small enough to not see a change in results, but is not optimized for computer usage. This is the minimum time step called out in Chapter 9 of the Handbook (ASHRAE, 2013). The program used such little memory and completed calculations in less than a second, so this was deemed a reasonable tradeoff.

#### **4.2 Multi-Node Model**

The other model used by in the evaluation was a commercial application of the Fiala Model (Dusan Fiala et al., 2012; Dusan Fiala & Lomas, 2001; Dusan Fiala et al., 1999; D. Fiala et al., 2001) inside an existing finite element thermal solver TAItherm program, produced by ThermoAnalytics Inc. (Calumet, MI). This will be hereafter referred to as the multi-node model or TAItherm model. This program is primarily set up to allow solving complex thermal

environments involving the need for accurate thermal radiation modeling. Conduction can be modeled in homogenous materials, and conduction boundaries can be applied to model non-homogenous materials. Convection boundary conditions, and limited evaporation effects, can also be applied to surfaces. The movement of fluids can be simulated using fluid nodes; applying convection coefficients using an empirical formula; or by importing results from a CFD analysis once, or at each time step passed back and forth to the CFD program. Radiation is modeled in two components, thermal long-wave radiation and solar short-wave radiation. Long-wave is in the infrared spectrum and assumes a black body source. Short-wave radiation is the assumed solar component. The division between these two components is up to the user to define the different thermal properties of the materials and properties of the sources. This procedure is described in more detail in the next section.

The human thermal model is a shell element model of a human, which can be split up into multiple parts, independent of physiology. This is useful when modeling areas of the body with different boundary conditions such as fabric coverage, convection, conduction, and radiation. These must then be defined to belong to one of 16 compartments associated with the human thermal model. Multiple parts can be defined as a part in the model and then are defined as a part in the Berkeley Comfort Model, if that is going to be implemented. An example of the setup file as can be seen in Figure 4.1

```

#####
# Human Comfort Module - Body Part Map File #
#####
# Description: This tab-delimited data file relates part numbers to body
# compartments.
#
# For example:
# Part Name Compartment
# 18 Right Upper Leg Legs
#
# WARNING: Both the command line utility (physiogen.exe) AND the human
# comfort library use this file, so it is imperative that the
# physiogen.exe utility is run after making any changes to the
# bodypartmap.txt. INCORRECT RESULTS will most likely be obtained
# from a human comfort analysis being performed in which the current
# bodypartmap.txt does not properly correlate to the current TDF file.
#
# NOTE: Since this file relates part numbers to boundary conditions,
# this file may need to be revisited and modified if parts are added
# or deleted from the TDF file. To avoid this potential problem, it
# is always a good idea to start with a fully parted out human, and
# append the environmental geometry (vehicle or building). This way
# parts can be added to or removed from the surroundings without
# affecting the part numbers associated with the human
# thermoregulatory model.
#
#####

Part Name Compartment BerkeleySegment
1 Face Face Head
2 Head Head
3 R Upper Arm RightUpperArm RightUpperArm
4 L Upper Arm LeftUpperArm LeftUpperArm
5 R Forearm RightLowerArm RightLowerArm
6 L Forearm LeftLowerArm LeftLowerArm
7 R Hand RightHand RightHand
8 L Hand LeftHand LeftHand
9 Chest Chest Chest
10 Shoulders Back Back
11 Stomach Abdomen Pelvis
12 Back Abdomen Pelvis
13 R Hip Front Abdomen Pelvis
14 R Hip Back Abdomen Pelvis
15 L Hip Front Abdomen Pelvis
16 L Hip Back Abdomen Pelvis
17 R Thigh Front RightThigh RightThigh
18 R Thigh Back RightThigh RightThigh
19 L Thigh Front LeftThigh LeftThigh
20 L Thigh Back LeftThigh LeftThigh
21 R Calf Front RightLowerLeg RightLowerLeg
22 R Calf Back RightLowerLeg RightLowerLeg
23 L Calf Front LeftLowerLeg LeftLowerLeg
24 L Calf Back LeftLowerLeg LeftLowerLeg
25 R Foot RightFoot RightFoot
26 L Foot LeftFoot LeftFoot

#WARNING: PHYSIOLOGICAL RESPONSE OF NECK AND SHOULDERS ARE NOT ACCOUNTED FOR
27 Virtual:Face Neck Head
28 Virtual:L Upper Arm LeftShoulder LeftUpperArm
29 Virtual:R Upper Arm RightShoulder RightUpperArm

```

**Figure 4.1** TAItherm body part map file assigning virtual manikin segments to human simulation body parts

### 4.2.1 Chamber Setup

The virtual manikin was placed on a model of a treadmill in a model of the chamber, which can be seen below in Figure 4.2 and Figure 4.3. The size of the chamber is the same as the actual chamber at 18 x 23 x 12.5 ft. The walls are the supply and exhaust plenums for the airflow in the chamber, and are set to the supply temperature of 40°C, which was what was used in the tests, as the circulating air in the chamber was further warmed by the radiation load. There are two fans; one was placed in front of each subject. The effects are modeled on the person from the measured air velocity but the fans were not included. The solar load was provided by a bank of 140 lights suspended below the ceiling at a distance of 110 inches from the floor. Rows 8 through 14 are angled at 30° to better face the human subject model as they are in the chamber.

Each door is estimated in composition and comprises steel with a 1.5mm steel shell,  $k = 52.019 \text{ W}/(\text{m}^2\text{K})$ , filled with 25.4 mm of fiberglass wool,  $k = 0.2994 \text{ W}/\text{mK}$ , and painted white on both sides,  $\epsilon=0.87$ . Each door has a small square window 1.5 mm thick, “Glass, Conventional Automotive,  $k=1.1717 \text{ W}/\text{mK}$ ,  $t = 0.0888789$ ,  $\rho_f = 0.861763$ . The garage door is two 1.5mm thick steel plates with air modeled between them, 12.7mm apart with 20% contact area to represent the panels on the door. The values for thermal insulation and radiation properties were taken from the internal TAItherm program library. The floor is modeled to represent the actual floor in the chamber. From the inside to the outside of the chamber it is composed of 25.4 mm of green painted plywood,  $k=0.12 \text{ (W}/\text{m}^2\text{K)}$  and  $\epsilon=0.89$ , followed by 101.6 mm of fiberglass wool,  $k=0.037 \text{ W}/(\text{mK})$ , and then 25.4 mm of plywood,  $k=0.12 \text{ (W}/\text{m}^2\text{K)}$ . The outside of the chamber floor is a concrete block,  $k=1.28 \text{ W}/(\text{mK})$ , 1m thick to represent the foundation of the building, and starts at an initial temperature of 25°C. The ceiling composition is the same as the floor, without the concrete slab, and the inside paint is white,  $\epsilon=0.87$ ; the outside is asphalt,  $\epsilon=0.93$ , The outside of roof experiences convection at  $5 \text{ W}/(\text{m}^2 \text{K})$ , to 27°C ambient air. The outside of all

doors also experience  $5 \text{ W}/(\text{m}^2 \text{ K})$  of convection at  $27^\circ\text{C}$ . On the inside of the chamber the doors experience convection at  $7 \text{ W}/(\text{m}^2 \text{ K})$  while the ceiling, and floor use a built in convection coefficient in TAITherm for plates using a velocity of  $2 \text{ m/s}$  resulting in a convection coefficient of  $7 \text{ W}/(\text{m}^2 \text{ K})$ . The treadmill is a shell composed of grey plastic, “Dark PVC”  $k=0.15 \text{ W}/(\text{mK})$  and  $\epsilon=0.95$ , while the treadmill belt is a radiation patched, surface with the properties of rubber, “Rubber Tire”,  $k=0.1558 \text{ (W}/\text{m}^2 \text{ K})$  and  $\epsilon=0.99$ , to represent the spinning belt. The chamber model is placed in a bounding box with a fixed temperature of  $27^\circ\text{C}$ .

Model Size (mm):  
X = 7010.4  
Y = 5486.4  
Z = 3759.2

Visible Size (mm):  
X = 7010.4  
Y = 5486.4  
Z = 3759.2

Visible Counts:  
Parts = 39  
Elements = 10849

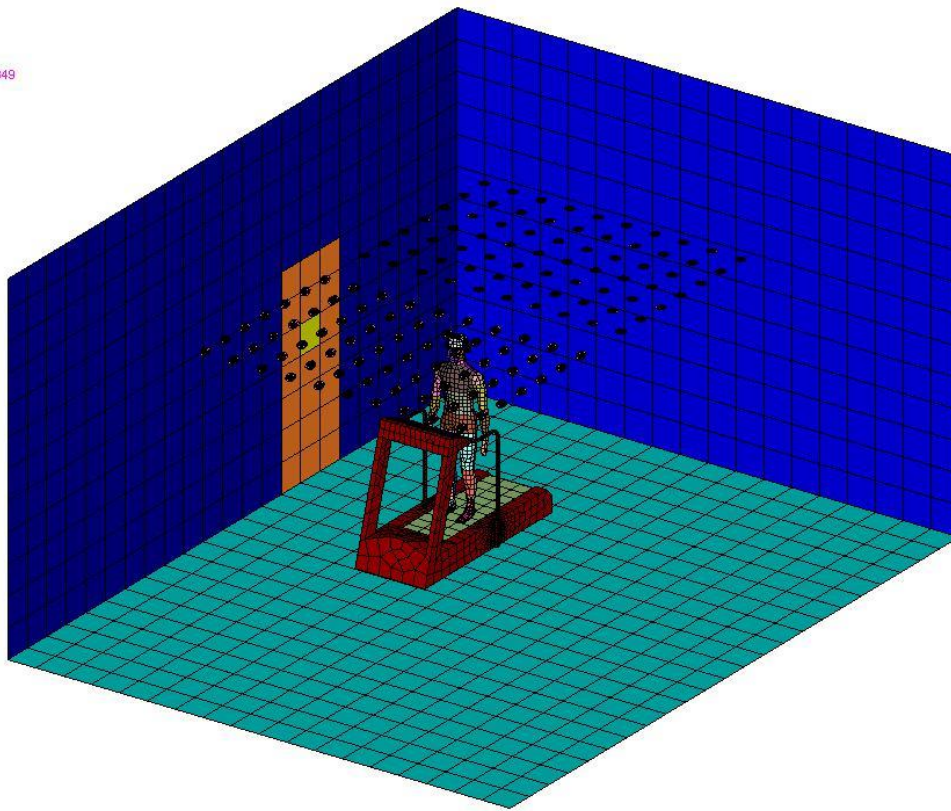


**Figure 4.2 Isometric view of human model in chamber with two walls, light reflectors, and ceiling hidden**



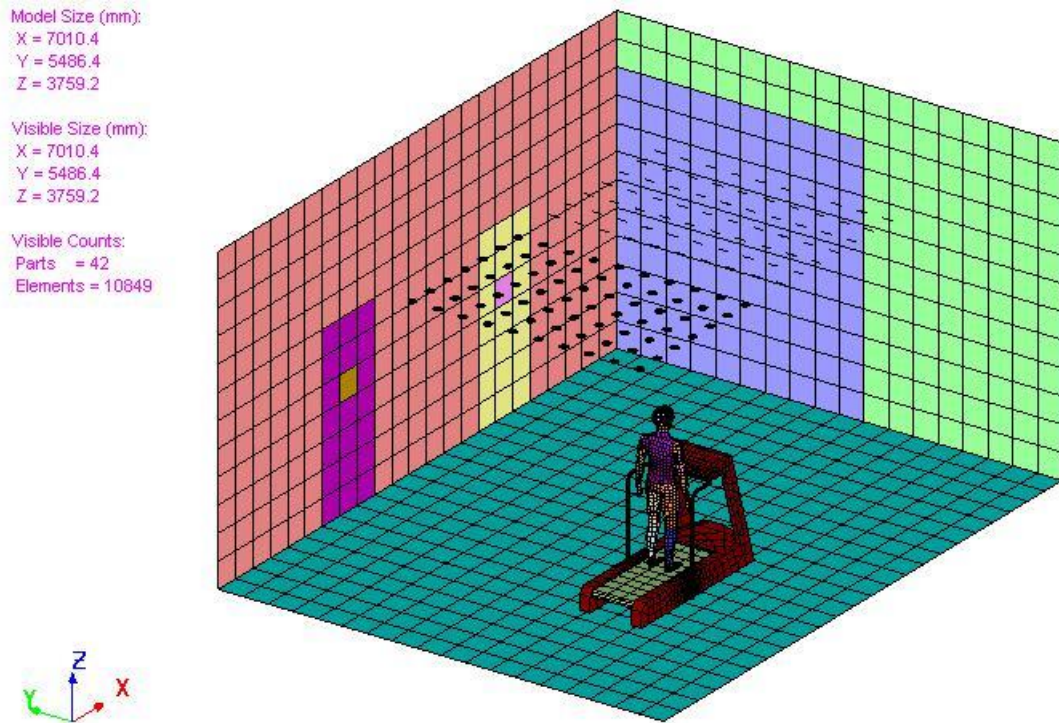


**Figure 4.3 Reversed isometric view of human model in chamber with two walls, light reflectors, and ceiling hidden**

#### **4.2.2 Solar lamps**

Modeling of the chamber lights in TAItherm was difficult because the use of spotlights in the chamber. Each light was a GE PAR38 (General Electric) with a 9° nominal beam spread spotlight at a light temperature of 2800 K. These were arrayed in 14 banks of 10 lights. The four banks furthest from the subjects were angled approximately 30° to point at the subject; this was modeled at 30°. The version of TAItherm used provided the capability to model solar lights, however the included lights are defuse sources not spotlights. Providing the correct radiant load necessitated knowing the angular intensity distribution of the lights. A pyrometer was used in the chamber to determine the intensity response as a function of angle for the lights.

A light was selected out of the bank to be tested and a pyranometer was used to measure the total intensity over a spectral range, specifically the solar spectrum. The spectrum range depends on the type of pyranometer. An Apogee Instruments, Inc. (Logan, Utah) silicon-cell pyranometer with a range of 300 to 1100 nm, which is representative of a shorter-wave light peak than was used, and adjustment methods are discussed below. A Grid with 1" spacing was laid out on the floor and the pyrometer was moved under one light in plus and minus x and y directions to determine to determine the incident intensity.

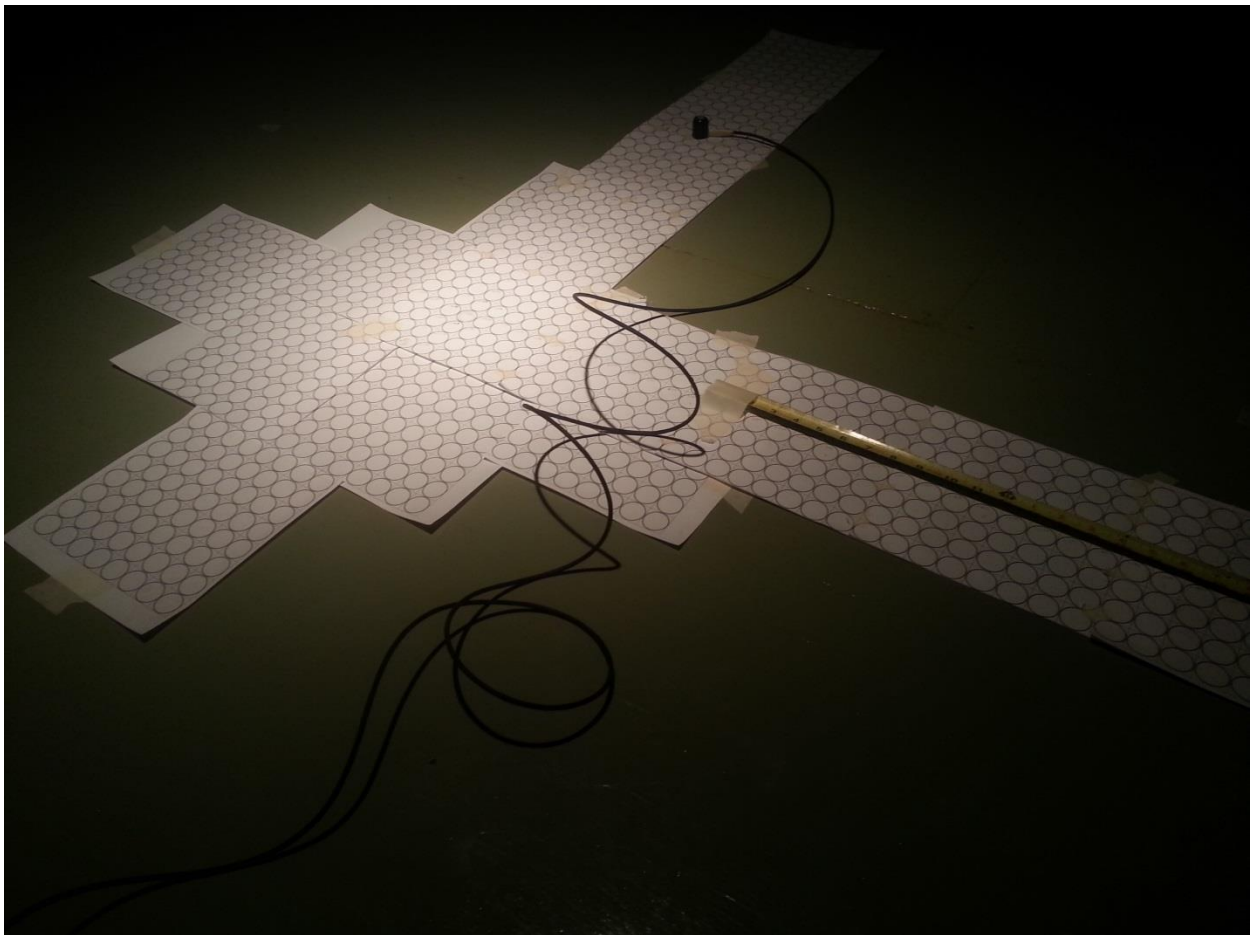


**Figure 4.4 Two axis of four-direction light intensity study with 1-inch movement of pyranometer**

The result of this was an intensity at each point which could then be converted into an angle off of the center focus of the light out to 38° on one side and 32° on the three other axis. The resulting data, in Figure 4.5 showed a good agreement between each axis that the light was pointed straight downward and the intensity was radially similar.

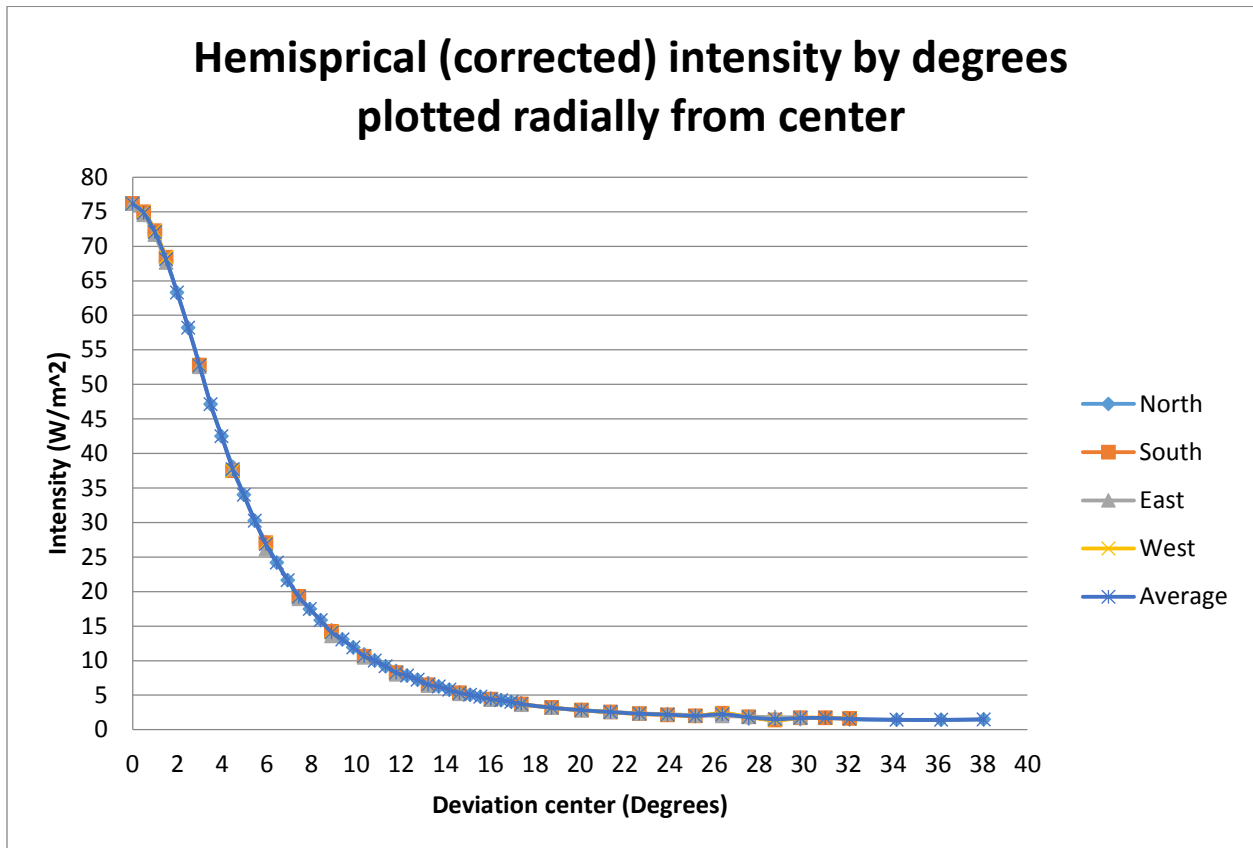


**Figure 4.5 Hemispherical intensity by degrees of one light plotted radially from center**

The next step was to come up with a method of applying the measured hemispherical distribution to the diffuse lights in TAItherm. The initial idea used a blackbody cylinder which was set up to provide the intensity at the center of the light, as an average of the hot spot location and then provide a ring around the light to create the diffuse element. After discussion with the manufacturer of TAItherm, it was decided to make the inside surface of the lights cylinder specular, to reflect the solar component. The outside and inside of the lights were set at the

ambient air temperature and the outside surface was a black body to minimize their impact on longwave radiation transfer. The tube shaped light reflectors provided a curve similar to the measured values and a series of studies were undertaken to determine the size and shape of the light, length of can reflector, and proper intensity. This yielded a series of data points taken from the element on the floor of the simulated chamber. The TAITherm test setup can be found in Figure 4.6 and Figure 4.7 and the intensity results of different lengths of reflective cans can be seen in Figure 4.8.

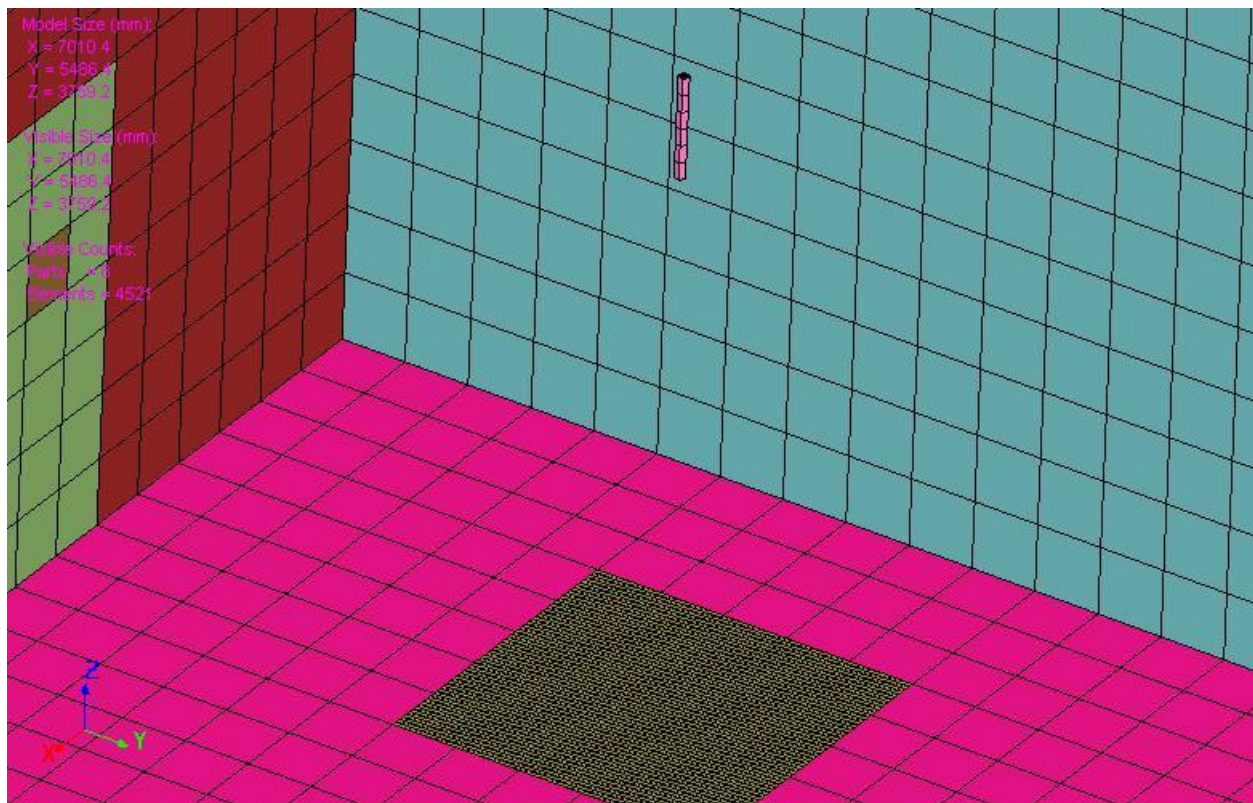


**Figure 4.6 Isometric view of light study with can reflector and light**

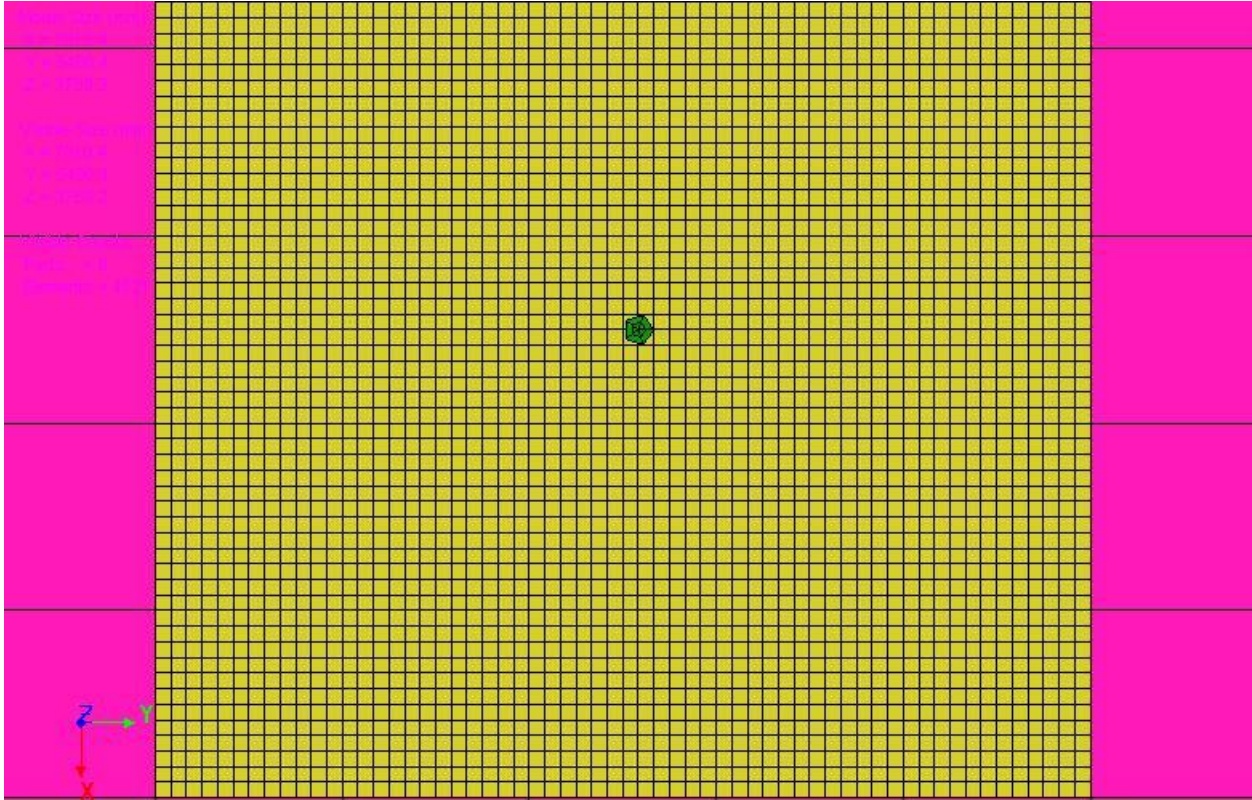


**Figure 4.7 Top view of light study with light shape and view of floor elements**

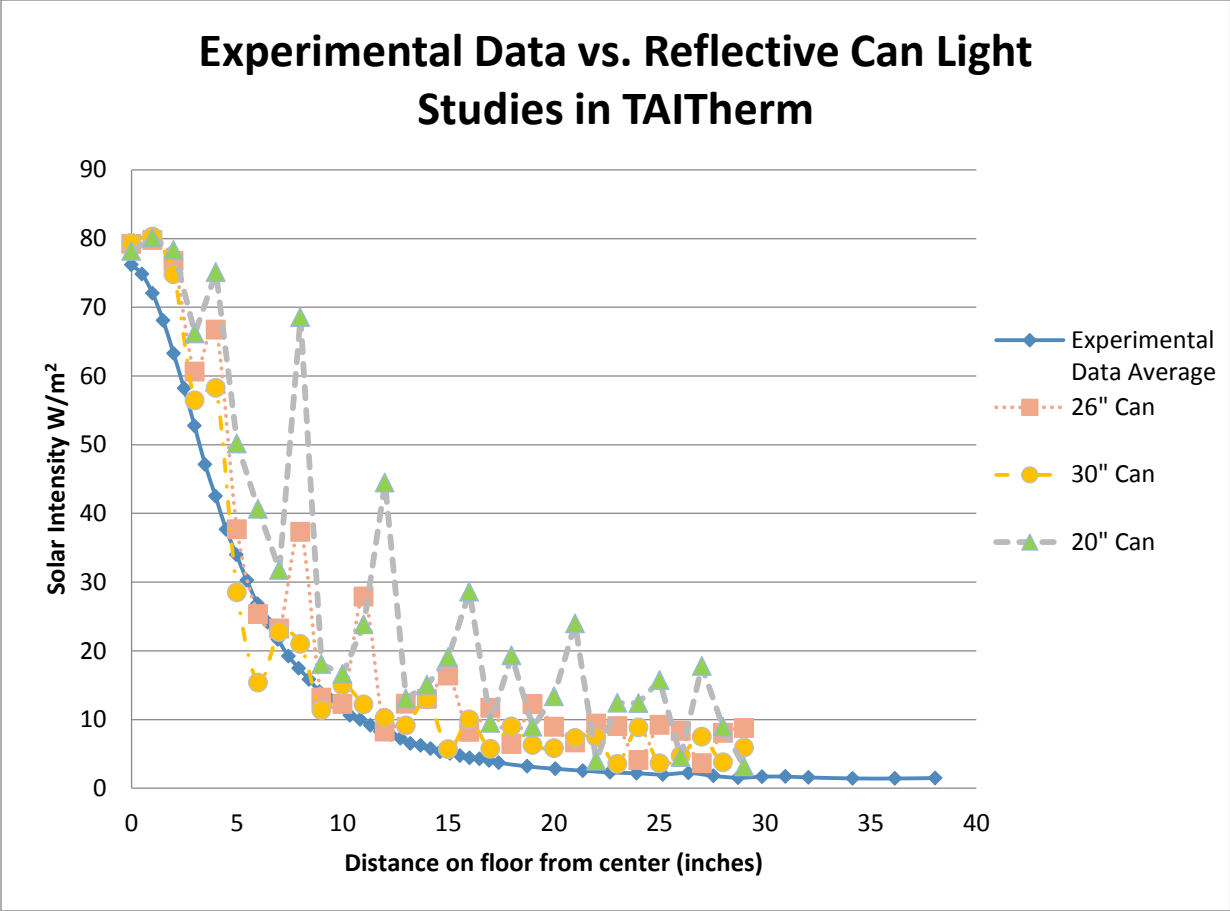


**Figure 4.8 Solar intensity at distances on floor for different reflective can lengths in TAITherm compared to the experimental floor average**

The 30-inch cans provided the closest value with a small amount of noise. They were ultimately restricted with a length requirement to ensure they did not overlap with the subject's body. This was balanced against the light size that had to have enough sources to allow for ray tracing but not be too fine to seriously affect solving time. A study on light sizes was not used to optimize the ideal length because of the limited number of simulations being run. Only a study on the specular apparent area was performed to decrease simulation time without significantly affecting accuracy.

These results were complicated because the spectral response of the apogee pyrometer used was not uniform across the spectral range, unlike a glass shielded thermopile pyranometer. The photovoltaic pyranometer's response is adjusted by the pyranometer to account for this response when measuring the solar spectrum. However, because the lights in the chamber peak at 2950K, the pyranometer is adjusting to a peak at 5762 K, the blackbody temperature of the sun. Originally, it would have been possible to use the pyranometer result, if it was of the glass shielded thermopile type, to set the short wave light output, and then adjust the blackbody temperature of the lights to adjust the longwave output of the lights, if the pyranometer was correctly measuring indoor light. In this case, the pyranometer was only useful for determining the proper intensity distribution on the floor with the assumption that there were no angular effects on the output spectrum.

In order to estimate the proper solar spectrum light intensity value, the black globe was used with one light. The globe was placed directly under the light and was experiencing convection from a small fan. A ring was added around the light on the outside of the can to represent the long wave radiation component of the light area forming a total diameter with the rest of the light of 4 in. The fan velocity was measured as 0.63 m/s using the same hotwire anemometer from the human subject tests. The air temperature and the temperature of the light were also measured. This was modeled in the TAITherm program and used to determine the flux of the globe in the solar spectrum. With the knowledge of the air temperature, wall temperatures an estimate for the convection coefficient, the solar component could be solved for numerically through iteration by changing the solar emissive power until the black globe temperature matched the experimental results. The model setup can be seen in Figure 4.9 with the one light and the black globe. The walls were set to the ambient air temperature. The convection

coefficient used on the globe was  $5.7 \text{ W/m}^2\text{K}$  and calculated from the Nusselt number given in their Equation 7.56 of the reference for a sphere in crossflow (Incropera et al., 2007). This provided an estimate of the hemispherical solar spectrum intensity of the light.

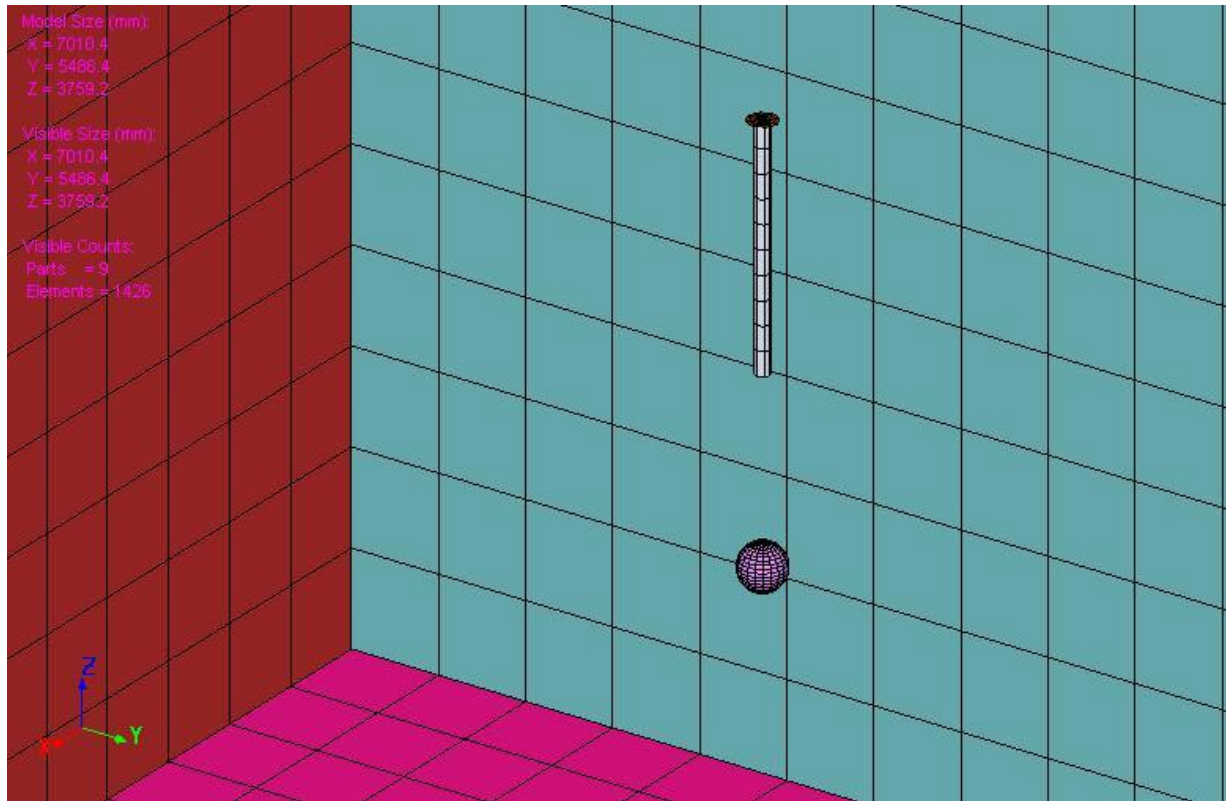


**Figure 4.9 Model of black globe in chamber under convection to determine solar component of load**

The next step was to recreate the Mean Radiant Temperature (MRT) Test in the simulated chamber to confirm our model was correct or make further adjustments. When the intensity from the pyranometer was used in the simulation with the globe located over the treadmill the air temperature of the globe was higher than the experimental results. This confirmed the pyranometer did not correctly measure the solar incidence with the incandescent lights and was supported by the manufacturer's literature. The final hemispherical solar lamp intensity was found to be  $67,000 \text{ W/m}^2\text{sr}$  based on the previous calibration. This is an order of



magnitude less than the value calculated for the pyranometer result of  $736,926 \text{ W/m}^2\text{sr}$ . The new lamp intensity was used in the full bank of lights with the globe suspended over the treadmill as it was in the MRT test as shown in Figure 4.10.

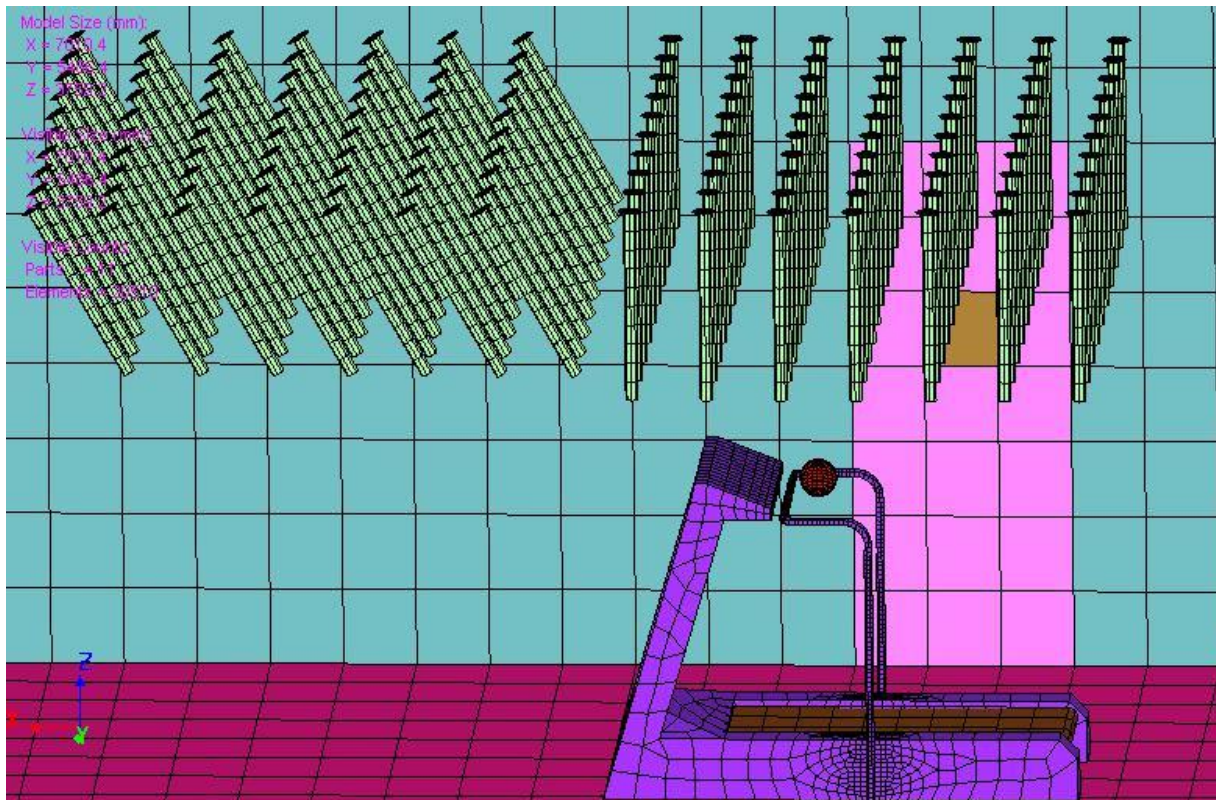


**Figure 4.10 Mean Radiant Temperature black globe test recreation**

The black body temperature of the lights were increased until the black globe reached the test condition  $47.5^\circ\text{C}$ . Increasing the black body temperature increased the long wave component of the lights. The result was the best approximation of the longwave and shortwave components of the spot lights used in the test. The uniform of the soldier provides distinctly different long and short wave absorptivity, given in the next section, so the correct split is an important factor. This resulted in a light temperature of  $210^\circ\text{C}$  finalizing the last piece of the simulation setup and creating a reasonable representation of the thermal radiation in the chamber.

### ***4.2.3 Human boundary conditions***

The human model shell and part distribution used was the same as the thermal manikin STAN used for the dry and wet clothing tests and was provided by TAITherm. Therefore, it was possible to directly import the clothing properties as measured on the manikin into the program to set the clothing conditions. Importing clothing information from the results of a Thermetrics Newton manikin is built into the TAITherm program and simplified the integration of clothing on each segment. The clothing area factor,  $f_{cl}$ , was estimated to be 1.33. The standard clothing measurements for each part of the manikin is shown in the Table 4.1. In the model, there are slightly different segments and the face remains uncovered, and is not included in the table, thus the modification to the  $f_{cl}$  value of 1.326 that removes that surface area from the area factor in the program. This results in an average  $R_{cl}$  of 0.153 ( $m^2K$ )/W and a  $Re_{cl}$  of 26.9, a slightly average lower thermal resistance and a slightly higher evaporative resistance than used in the two-node model. However, this does take into account the local effects unlike the two-node model.

**Table 4.1 Army Ensemble 3 clothing resistances by manikin/model segment in TAItherm**

Name	$R_{cl}$ ( $m^2K/W$ )	$Re_{cl}$ ( $m^2kPa/W$ )	$f_{cl}^*$
L Up Thigh	0.303	0.030	1.327
L Low Thigh	0.166	0.027	1.327
R Foot	0.170	0.061	1.327
Head	0.117	0.022	1.327
R Forearm	0.097	0.012	1.327
L Hand	0.074	0.012	1.327
R Hand	0.076	0.011	1.327
L Forearm	0.114	0.014	1.327
R Calf	0.129	0.019	1.327
Stomach	0.173	0.092	1.327
Chest	0.167	0.031	1.327
Shoulders	0.128	0.023	1.327
L Foot	0.136	0.021	1.327
L Upper Arm	0.164	0.024	1.327
R Upper Arm	0.262	0.032	1.327
Back	0.292	0.057	1.327
L Calf	0.186	0.041	1.327
R Low Thigh	0.262	0.095	1.327
R Up Thigh	0.284	0.051	1.327

Conduction as a mode of heat transfer was safely ignored as the subjects were constantly walking on the treadmill providing limited contact with the belt. Radiation was applied in the chamber as part of the TAItherm program as detailed in the previous subsections. The clothing radiation properties were provided by Thermoanalytics who had measured the digital pattern uniform fabric for a previous study (Hepokoski et al., 2012). The provided values were 0.92 for the thermal emissivity,  $\epsilon$ , and 0.66 for the solar absorptivity,  $\alpha$ .

Convection was applied to the manikin's surface using two different formulas to explore if there were any significant differences in the results of the built in human convective coefficients in TAItherm at  $v=2.0$  m/s. The first was the formula from Danielsson (1993) as was used with the segmental equations. For a walking and air velocity using the equation on page 82, Table 3.4 the convection coefficients from Danielsson are as follows:

**Table 4.2 Body convection coefficients Danielsson (1993) pg82 table 3.4, velocity 2.0 m/s**

Body Area	Convection Coefficient
	W/m <sup>2</sup> K
Lower leg	21.04
Lower trunk	21.73
Mid trunk	14.04
Upper trunk	14.77
Lower arm	15.27
Upper arm	18.18
whole body	17.37

The second convection coefficient considered is built into the human comfort module in TAItherm and is based on the work of X. Wang (1994). The two convective coefficients produced such similar results so those of Wang et al. were chosen as they had more segmental refinement. The visual depiction of the convection coefficients used can be seen in Figure 4.11.

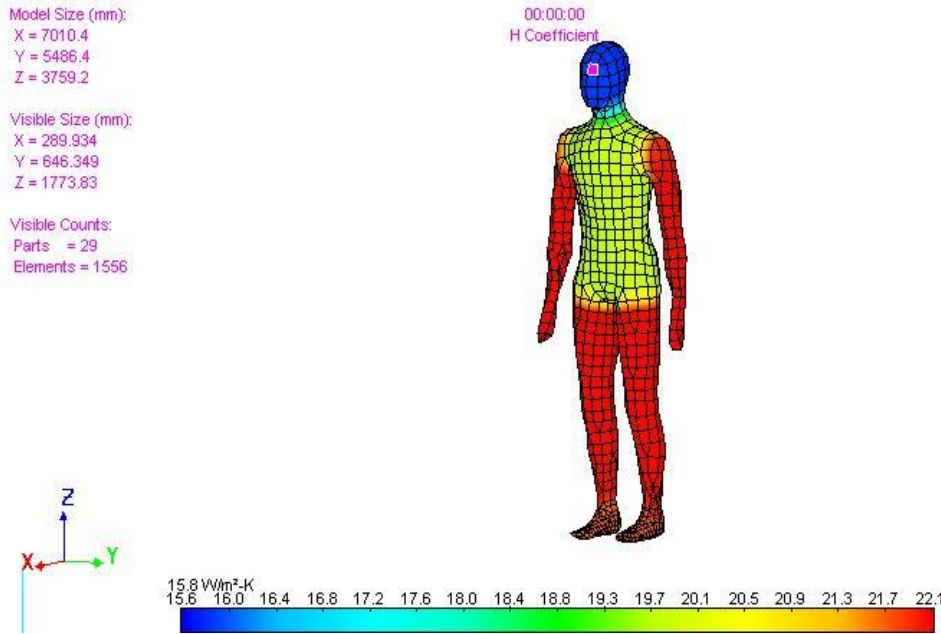


**Figure 4.11 TAItherm convection coefficients on manikin using built in Human Comfort Convection Module, velocity 2.0 m/s**

The simulation uses the applied convection coefficient with the thermal and evaporative resistance to determine the heat loss by convection and evaporation with the heat and mass transfer analogy. The simulation does not take into account clothing wetting and uses the same heat transfer equation from the skin surface as the two node model in Equations ( 4.1 ), ( 4.2 ), ( 4.3 ), ( 4.4 ), and therefore is subject to the same limitation on clothing wetting and sweat drip.

#### ***4.2.4 Initial conditions***

The final component for the simulation is providing reasonable initial conditions to the chamber for the test. A two-hour precondition of the chamber takes place using the setup previously described. This was the same as the beginning of a day's testing. The results of the two-hour preconditioning simulation are used as the starting chamber temperatures of the human modeling runs using the transient restart function in TAItherm. This was done to reflect the

chamber being started 2 hours before the first subjects entered in order for the chamber to come to steady state and the complications of the radiant environment in the chamber.

The human initial conditions and parameters are much more complicated. Models are not perfect simulations of human thermoregulation, so a decision had to be made how to initialize the humans in the chamber. The highly invasive and unpractical measurement techniques required to get multilayer, segmental body temperatures make it impossible to perfectly set up a human for a multilayer model. Therefore, the human was preconditioned in a comfortable chamber until their core temperature became steady state. A comfortable chamber is defined in the literature as achieving thermal neutrality and was the goal of preconditioning subjects before the start of the test. An algorithm inside TAItherm is used to set the conditions, or reference variables, for a nude man of a specified body type when it differs from the average height 50%, weight 50%. In this test, a man of height 50% and weight 75% was used to better match our human subjects, therefore new reference variables had to be created. The result of this setup procedure produced a core temperature that was approximately equal to the human subject results. This value was used to initialize each human subject test as there was no need to modify it further. The spreadsheet of the model initial temperature can be found in Appendix B - Modeling Initial Values.

## **Chapter 5 - Comparison of baseline results to models**

The focus of this chapter is the comparison of the human subject results of the baseline test, performed without PCS, to the human thermal models. A major emphasis is to evaluate the ability of these models to predict the core temperature change and sweat rate of the human subjects using the clothing data measured on the thermal manikin. This will provide a solid foundation with which to examine the effects of PCS on the simulated humans.

The assumption that clothing wetting does not occur in the human thermal models is found to be an error in both models. A model is proposed for the wetting of the fabric and increasing the sweat rate which improves two-node model predictions. The more complicated, multi-node model is compared to the baseline results with and without clothing modifications to determine if it provides any improvement in modeling baseline effects. The knowledge of how these models work in the baseline will set a foundation for PCS modeling in the next chapter.

### **5.1 Two node model comparison**

The two-node model is simplest of the two models being utilized in this work. The main values compared between the simulation and the actual results are the core body temperature and sweat production. However, mean skin temperature is also shown in the graphs to determine if the mean skin temperature can be predicted with accuracy in these conditions.

The ASHRAE two node model introduced in Section 4.1 is compared to the human subject test results for each of 21 subjects and then the average of those subjects. Three subjects 5, 6, 15 were removed from the comparison because metabolic cart data was not taken for their baseline runs, therefore the metabolic production is not known. In all of the two-node models, a skin dilation coefficient,  $c_{dil}$ , of 150 was chosen to represent the higher skin dilation in the hot environment. Models of the subjects, when compared individually, ran for the amount of time

they did in the baseline test. An average subject was also run to determine the ability of the models to predict the group average.

In the second subsection, modifications to the clothing heat transfer in the two node model are described, and the modified two-node model is compared to each individual subject and then to the average subject. The ability to correctly predict the baseline results is required in order to have any confidence in the prediction of the two-node model in the next chapter when PCS cooling is included.

### ***5.1.1 Comparison of ASHRAE two node model to human subject results***

The modeling of the baseline human subject results was performed as described in the previous chapter. The comparison of the subjects is between the predicted and measured final core temperature and the total sweat production for each subject, the average of all subjects, and the average subject. The average subject was set to complete the 120 min test as the mode of test times was 120 minutes, while the average was 116 minutes. This was done for uniformity of ending time and had little effect of the ending core temperature. Core temperature of the human subjects is  $T_{coreHS}$ , two-node simulated core temperature is  $T_{coreTN}$ , Sweat total of the human subjects is  $SWHS$ , and simulated sweat rate is  $SWTN$ , and the predicted total evaporation from the two-node model is  $TN\ Evap\ Sweat$ .



**Table 5.1 Baseline data comparison: Two-Node Model (TN) vs. Human Subject (HS)**

Subject #	TcoreHS °C	TcoreTN °C	TcoreTN-		SWTN kg	SWTN- SWHS Kg	TN Evap Sweat kg
			TcoreHS °C	SWHS kg			
1	39.02	39.77	0.75	1.557	1.804	0.248	0.813
2	37.67	39.21	1.54	1.976	1.710	-0.266	0.905
3	37.05	39.07	2.02	2.823	1.660	-1.163	0.929
4	37.71	39.58	1.87	2.749	2.094	-0.655	0.986
7	38.48	39.29	0.81	2.542	2.087	-0.455	1.073
8	38.00	39.28	1.28	2.328	1.994	-0.335	1.039
9	37.91	39.23	1.32	1.764	1.468	-0.297	0.788
10	37.85	38.97	1.12	2.407	1.680	-0.727	0.971
11	39.01	39.86	0.84	1.363	1.815	0.452	0.796
12	38.21	39.70	1.49	2.381	2.015	-0.366	0.909
13	38.70	39.63	0.92	2.000	2.124	0.124	0.985
14	38.41	38.68	0.26	1.726	1.641	-0.085	1.031
16	38.27	39.60	1.33	2.156	2.217	0.061	1.037
17	37.95	39.80	1.84	2.725	2.266	-0.459	1.002
18	38.91	39.53	0.62	2.048	1.492	-0.556	0.724
19	38.27	39.10	0.82	2.274	1.964	-0.310	1.077
20	37.95	39.19	1.24	2.634	1.941	-0.694	1.004
21	37.88	40.19	2.31	2.877	2.531	-0.346	1.006
22	38.37	40.70	2.33	2.421	2.609	0.188	0.959
23	37.90	39.02	1.12	2.816	2.084	-0.732	1.116
24	38.14	39.84	1.70	2.317	2.634	0.317	1.060
Average of subjects	38.17	39.49	1.31	2.280	1.992	-0.288	0.962
Standard Deviation	0.482	0.463	0.557	0.4346	0.3362	0.4097	0.1062
Average Subject	38.17	39.48	1.30	2.280	2.059	-0.222	1.090

The average subject characteristics, with the previously described 120 min work time, was also applied and calculated in the two-node model. Core temperature data is shown in Figure 5.1. It clearly shows the very high prediction of the subject core temperature compared to the average of all modeled subjects.

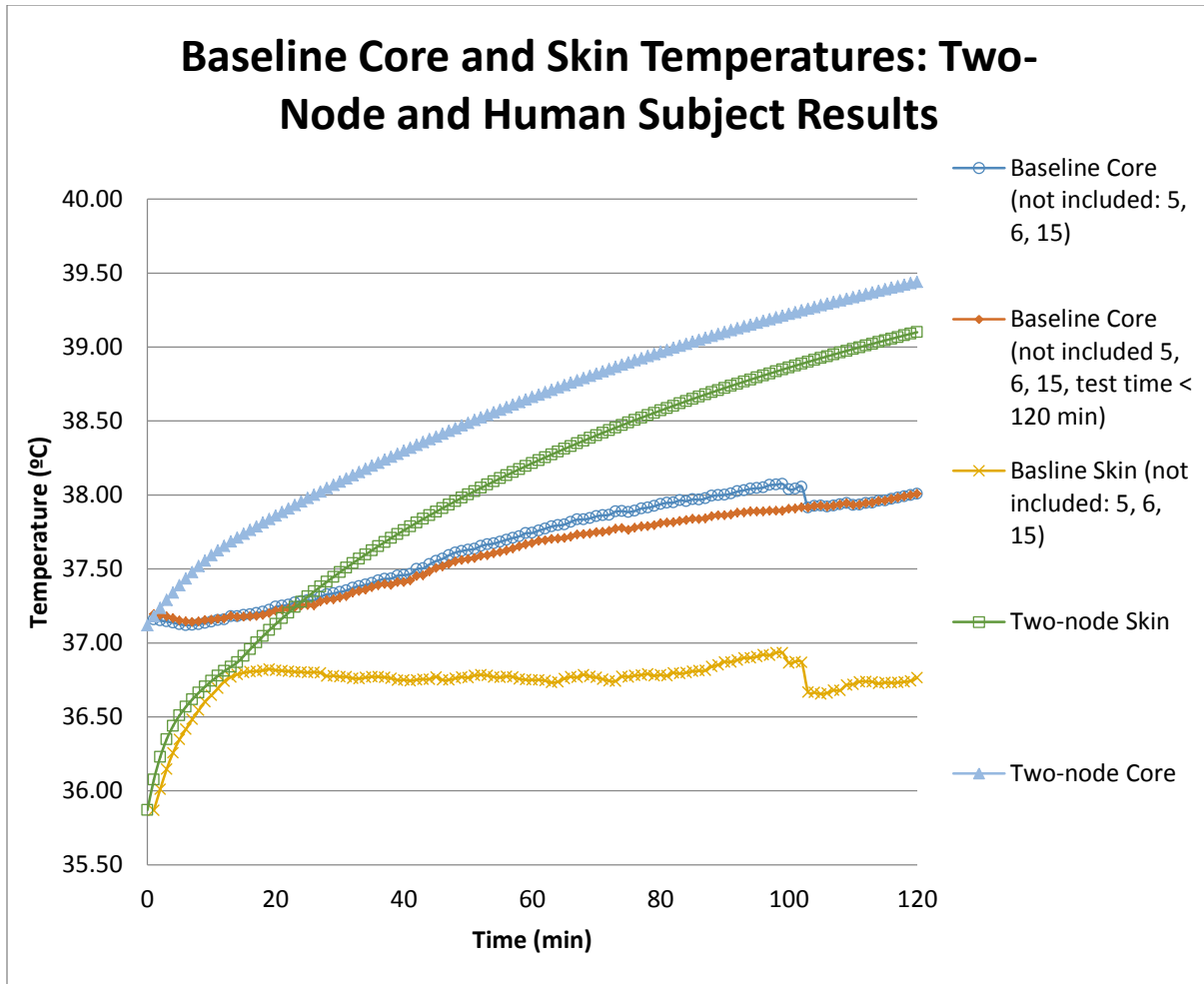


**Figure 5.1 Baseline core temperature comparison graph average subject Two-Node Model (TN) and Human Subject (HS) Results with two data sets for human subject results to show impact of ending time on average core temperature**

The comparison between the two runs shows the negligible effect on the core temperature of removing the subjects who dropped out before reaching the end of the test. More importantly, it also demonstrates the distinct inability of the standard two-node model, even with the beneficial enhanced  $c_{dil}$  factor, to predict core temperature. The problem is not limited to the average subject as shown in Table 5.1, where the average subject very closely matched the average of the individual subjects modeled results. The table also shows the two-node model under-predicting the sweat when compared to measurements. The average model predicts the

amount of the test that the skin wettedness was at 100% is 89% of the subjects' runtimes. The high skin wettedness,  $\omega = 1$ , percentage coupled with the amount of sweat not evaporated in the two node model, on average 0.962 kg, it is likely that this sweat is providing useful cooling and not dripping on the ground. This is the likely source of error in the model. The sweat rate of the two-node model is, on average, 0.222 to 0.288 kg less than that of the human subjects, but due to error in skin and core temperature not much can be said about this model. The skin temperature is also higher in the model than experienced by the human subjects.

The drastic differences in core temperature and skin temperature prediction of the model indicate that the simulated human is not being cooled sufficiently. Another cooling mechanism must be present in the human subject tests that is lacking in the model. The assumption that the clothing does not wet, inherent in the two-node model, is a likely cause of this error. This is supported by observations during the human subject testing where wet, often soaked clothing was observed. In addition, considering the almost full encapsulation of the body there is no place where the skin cannot drip without wetting fabric, with the possible exception of the face. Finally, because the subjects were in motion their somewhat loose fitting clothing made contact with their skin and had the ability to adsorb moisture. Wet fabric will change the heat and mass transfer equations for the body system and the respective resistance values will need to be modified to account for this effect.

### ***5.1.2 Modification of ASHRAE two node model***

Section 5.1.1 made it clear that for this application the standard two-node model did not work, likely because of the clothing wetting during testing. Therefore, it was necessary to modify the clothing models to account for the clothing wetting using fundamental heat and mass transfer principles and reasoned assumptions. Although the two-node model does not account for unequal

clothing coverage and environmental exposure on different segments, for the sake of simplicity of modeling the standard two node average surface was used in order to deal with only one factor. The model required two broad adjustments: 1) partitioning the clothing to a wetted area and a non-wetted clothing and developing a spot model and 2) changes to the overall sweat production.

### 5.1.2.1 Spot Creation

A method to include fabric wetting in the model is described in this section. The creation of a wetted spot is the most straightforward manner in the two-node model to account for the cooling being experienced by the human subjects by wetted clothing in the single surface node of the two-node model. Accounting for the clothing wetting was accomplished by splitting the clothing into two sections averaged over the entire surface area, one dry and one wet. The dry area heat and mass transfer takes place according to the same principles and assumptions as the two-node model. On the wetted area, it is assumed that the clothing wets to 100% over a distributed wetted spot on the body and a mass and energy balance is applied to the wetted spot. The spot grows when excess sweat that is produced, i.e. that sweat that is greater than that used to maintain 100% skin wettedness,  $\omega = 1$ . The sweat rate given in the ASHRAE two-node model, in power units, is governed by Equation (5.1).

$$E_{rsw} = \dot{m}_{rsw} \cdot h_{fg} = c_{sw} \cdot (T_b - T_{bset}) \cdot \exp\left[\frac{T_{sk} - 34^{\circ}\text{C}}{10.7}\right] \quad (5.1)$$

The sweat rate coefficient,  $c_{sw}$  given in energy terms, as 116 W/(m<sup>2</sup>K) in the ASHRAE model (ASHRAE, 2013) is in terms of power units. In the original source, Gagge, Fobelets, and Berglund (1986),  $c_{sw}$  is 170 g/(hr•m<sup>2</sup>•K). Converting using a latent heat of vaporization of 2430 kJ/kg and 3600s/hr results in the  $c_{sw}$  given in the ASHRAE chapter shows  $E_{rsw}$  is the power converted sweat rate. The value  $T_b$  is the mean body temperature and  $T_{bset}$  is the mean body set

point temperature both governed by equations in the two-node model that were not modified in this analysis.

In the unmodified model, any excess sweat  $\omega > 1$  is assumed to drip off and not wet clothing. However, in the modification part of this excess sweat is added to the wetted area spot. The spot mass balance can be stated as:

$$dm_{spot}/dt = (\dot{m}_{spot,in} - \dot{m}_{spot,out}) \quad (5.2)$$

The change balance of the spot mass,  $m_{spot}$  and the mass entering the spot from excess sweat  $\dot{m}_{spot,in}$  and the mass leaving the spot by evaporation,  $\dot{m}_{spot,out}$ . Therefore, the net exchange of the spot at any instant,  $\dot{m}_{spot,net}$ , is:

$$\dot{m}_{spot,net} = (\dot{m}_{spot,in} - \dot{m}_{spot,out}) \quad (5.3)$$

The two-node model is run on a computer by converting the partial derivative form of the energy balance of the skin and core nodes into an iterative program through the fundamental theorem of calculus, using an appropriate time step,  $\Delta t$ , which will allow for a discrete approximation of a continuous function. The recommended time step is between 10 and 60 seconds according to the Fundamentals Handbook; 10 seconds was chosen for all the simulations (ASHRAE, 2013). The equation for the next time step in the program,  $m_{spot,i+1}$ , is given by the current mass,  $m_{spot,i}$ , plus the net change in the spot mass from evaporation and excess sweat for that time step,  $\dot{m}_{spot,net} \cdot \Delta t$ .

$$m_{spot,i+1} = m_{spot,i} + \dot{m}_{spot,net} \cdot \Delta t \quad (5.4)$$

The mass balance of the spot is the difference between the regulatory sweat rate term,  $E_{rsw}$ , minus the sweat evaporated by the 100% skin wettedness,  $E_{sk}$ . Both of these control equations are given in terms of energy units and must be divided by the latent heat of vaporization,  $h_{fg}$ , to get the mass of excess sweat. A certain portion of the sweat will remain unavailable for spot size

creation in a location where evaporation will occur. The variable  $\phi_w$  is introduced as the percentage of sweat available for spot size creation. Based on surface area measurements of the body armor on the manikin, a conservative estimate is that 32% of the body surface is covered by the body armor, which is assumed to be impermeable; therefore, only 68% of the excess sweat goes into spot size creation,  $\phi_w = 0.68$ , which is available for evaporation. The effect of the knee pads is ignored as the attachment points on the legs is very likely to cause sweat to wet the clothing and their surface area was small. The remaining excess sweat, 32%, is assumed trapped under the body armor. Therefore, the wetted spot is defined as only the wetted area that is available for evaporation. The term,  $w_c$ , is the wettedness coefficient, which is the percentage of the surface area of the body that is considered wetted by the spot.

$$\dot{m}_{spot,in} = \phi_w \cdot \frac{E_{rsw} - (1 - w_c) \cdot E_{sk}}{h_{fg}} \quad (5.5)$$

The evaporation component out of the spot is the amount of evaporation from the spot,  $w_c \cdot E_{spot}$ , divided by the latent heat of vaporization to get the mass component.

$$\dot{m}_{spot,out} = \frac{w_c \cdot E_{spot}}{h_{fg}} \quad (5.6)$$

The possible energy that can be removed by the spot is given by  $E_{spot}$  for 100% wetted surface of clothing. The values are the same as presented in the Newton's Law of Cooling, heat and mass transfer analogy presented in Equation ( 2.30 ), where  $P_{sk}$  is the partial pressure of the 100% wetted skin surface and  $P_a$  is the partial pressure of the air at their respective temperatures.

$$E_{spot} = \frac{P_{sat}(T_{sk}) - P_{sat}(T_a)\phi}{\frac{1}{f_{cl}h_e}} \quad (5.7)$$

In this case, the  $E_{spot}$  value is used due to convenience because the heat and mass transfer analogy has already been solved with the appropriate Lewis Ratio for these conditions. In addition, this equation will also be used in the energy balance with another further refinement to calculate the energy removed by the spot.

The remaining term not defined in the mass balance equations is that of the wetted area, already introduced as the percentage of surface area comprising the wetted spot,  $w_c$ . To determine a reasonable  $w_c$  it was necessary to determine liquid mass per unit surface area of the clothing. The wetted surface area is a function of the mass of water, and thus is analogous to the water adsorption capacity of the clothing layer. To determine the surface area ratio per liquid mass, a series of tests were performed on the uniform used in the human and manikin tests. A titration burette was used to drip precise quantities of water onto a single layer section of the clothing. The clothing fabric was backed by impermeable plastic to ensure all the liquid was absorbed into the spot. Eight different quantities of water were measured on the fabric and a new spot was made for each quantity of liquid. The spot size was measured visually using the difference in the shade of the saturated portion. This was done at 30-second intervals to look for large changes in spot size as seen in Figure 5.2. when length change in both directions was less than 0.25 inches data was recorded.

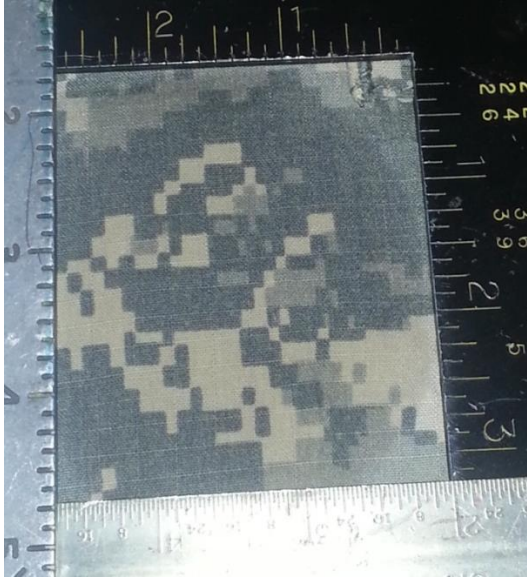


**Figure 5.2 Spot size measurement on fabric using wetted discoloration**

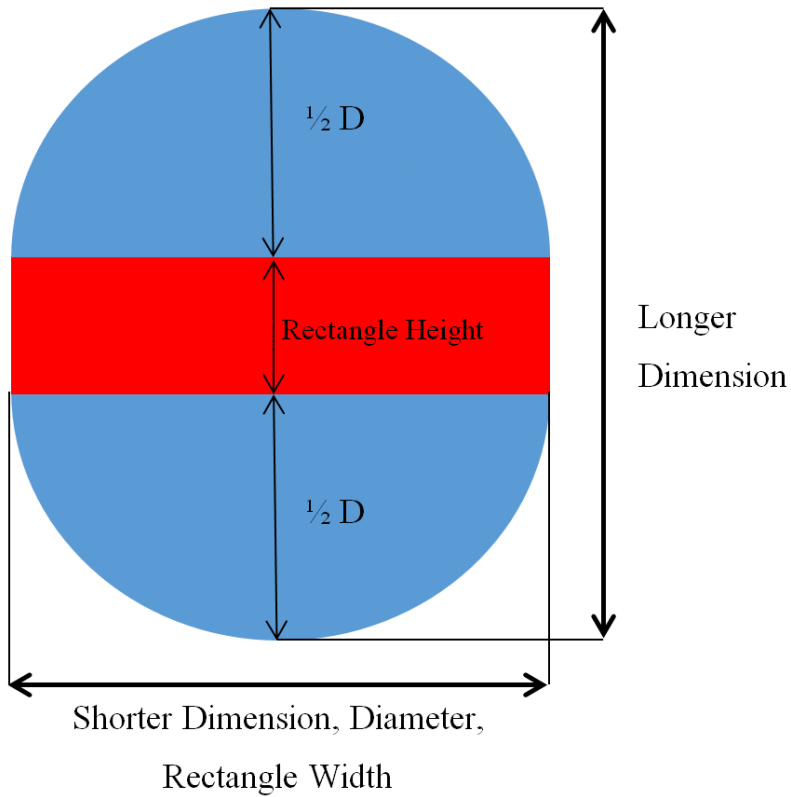


**Figure 5.3 Depiction of area calculation in spot size per area calculations. Area was calculated by two semi circles tangent to a central rectangle.**



The adsorption of the fabric did not take place perfectly radially due to flow direction, levelness of the table, etc. However, when the steady state approximation was reached the shapes were rounded and were assumed to resemble Figure 5.3 with a rectangular area and two semicircular halves. The shorter of the two distances measured was used as the diameter of the two semi circles and the long edge of the rectangle, width as portrayed in the figure. The longer dimension was used to calculate the shorter side of the rectangle, height as portrayed, by subtracting the longer dimension by one diameter. This provided a straightforward way to calculate the area of saturation per unit mass. The calculated values per mass equation and linear approximation can be seen in Figure 5.4

Figure 5.4. The linear approximation is set to have an intercept at zero.

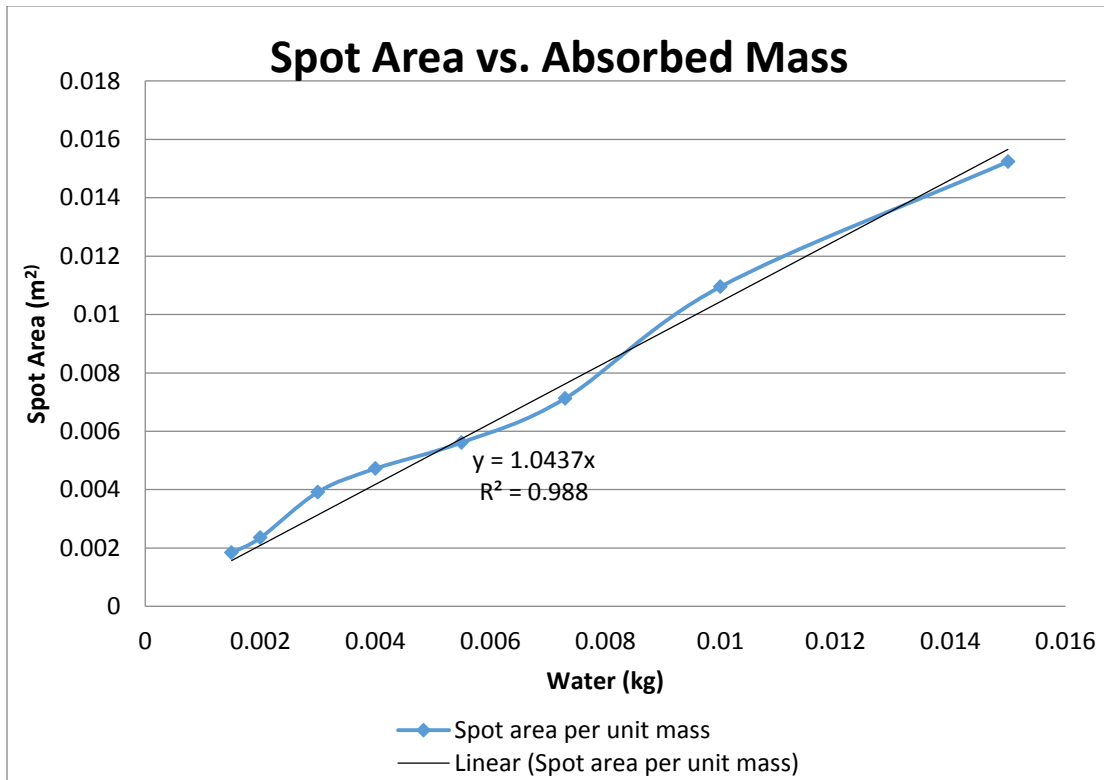


Figure 5.4 Graph of plotted absorbed mass and resulting spot area showing linear approximation overlay

The linear curve fit provides a good representation,  $R^2 = 0.988$ , of the tested data points and yields an equation to determine the surface area of a wetted area given the mass on the clothing worn by the subjects. Dividing this area by the Dubois Area of the subject provides the percent wetted surface area of the body,  $w_c$  at any time step,  $i$ , is the wetted spot area  $A_w$  over the body surface area,  $A_D$ .

$$w_c = \frac{A_w}{A_D} = \frac{m_{spot,i} * x_c(m^2/kg)}{A_D} \quad (5.8)$$

This approximation provides a starting point in determining a reasonable spot size, but would require further testing to determine exact relationships of the spot size to textile properties. The next step is the energy balance.

### 5.1.2.2 Spot Energy Balance

The previous section defined the mass balance that takes place in the spot; however, it is necessary to determine the energy entering and leaving the spot. First, it was assumed that the mass of the spot did not store energy and change with each time step. This greatly simplifies the calculations. The original energy removal term from the skin via evaporation is by the two-node model's evaporation term, with the assumption of no clothing wettedness,  $E_{sk}$ . It was decided to cast the spot model in a form similar to the evaporation loss from the human. This makes implementation by the broader community more practical. The modification replaces this term with the two areas, dry clothing and wet clothing:

$$Q_{evap} = (1 - w_c) \cdot E_{sk} + \epsilon_s \cdot w_c \cdot E_{spot} \quad (5.9)$$

Unless the wetted area has perfect contact with the skin, there will be impedance to the transfer of heat from the body by the air layer, fabric resistance, and any heat gain from the environment. Therefore, not all the energy gained from evaporation on the clothing will transfer to the person. Therefore, it is essential to calculate an efficiency value,  $\epsilon_s$  of the wetted clothing.

This was done based on the average body temperature, taken from human subject baseline tests, together with a decreased thermal resistance value to account for fabric saturation. Placing a control volume around the spot (as seen in Figure 5.5.) and simplifying using the same idealizations used in the  $Q_{evap}$  results in Equation ( 5.10 ).

$$0 = Q_{body} + Q_{evap} + Q_{C+R} \quad (5.10)$$

In this equation  $Q_{body}$  represents the heat transfer from the body to the wetted spot through the clothing and air layer,  $Q_{evap}$  is the evaporative losses from the spot, and  $Q_{C+R}$  is the energy gained in the spot due to convection and radiation. Substituting the proper heat transfer equations provides a per unit area calculation of the temperature,  $T_{spot}$  through numerical iteration of the current study.

$$F(T_{spot}) = 0 = \frac{T_{sk} - T_{spot}}{R_{cl,w}} + h_e \cdot (P_{sat}(T_{sk}) \cdot \phi - P_{sat}(T_{spot})) + h_t \cdot (T_o - T_{spot}) \quad (5.11)$$

The values used in the efficiency calculation to determine  $T_{spot}$  are as follows and are mostly taken from the environmental chamber conditions. The skin temperature was the average mean skin temperature of the human subjects across the baseline tests. The convective and radiant exchange between body and spot is found from the resistance value of the clothing with air layer of the non-armor covered segments that are allowed to wet and is given as  $R_{cl,wet} = 0.133 \text{ (m}^2\text{K/W)}$ . This was modified based on the concept that the insulation resistance of a wet garment can be reduced by 1/3 resulting in the wet resistance yielding:  $R_{cl,w} = 0.04433 \text{ (m}^2\text{K/W)}$  (Crow, 1974). The other values used in the calculation are given in the list below, unless otherwise specified above, are the same as those used in the two-node model calculations:

- $T_a = 42.2 \text{ }^\circ\text{C}$

- $T_r = 54.4 \text{ }^\circ\text{C}$
- $R_{cl,w} = 0.0443$
- $T_{sk} = 36.7 \text{ }^\circ\text{C}$
- $h_r = 4.7 \text{ W/m}^2\text{K}$
- $h_c = 17.37 \text{ W/m}^2\text{K}$
- $h_e = 0.29793 \text{ W/m}^2\text{Pa}$
- $h_t = 22.069 \text{ W/m}^2\text{K}$
- Relative Humidity = 20%

Equation ( 5.11 ) was iterated as a function of  $T_{spot}$ , which resulted in  $T_{spot} = 27.4 \text{ }^\circ\text{C}$ . To

determine the efficiency of cooling from the evaporating spot,  $\varepsilon_s$  the equation for the efficiency is simply the heat removed from the body,  $Q_{body}$  over the energy removed from the spot  $Q_{evap}$  at  $T_{spot} = 27.4 \text{ }^\circ\text{C}$ .

$$\varepsilon_s(T_{spot} = 27.4 \text{ }^\circ\text{C}) = \frac{Q_{body}}{Q_{evap}} = \frac{\frac{T_{sk} - T_{spot}}{R_{cl,w}}}{h_e \cdot (P_{sat,air} \cdot \phi - P_{sat,spot})} = 35\% \quad (5.12)$$

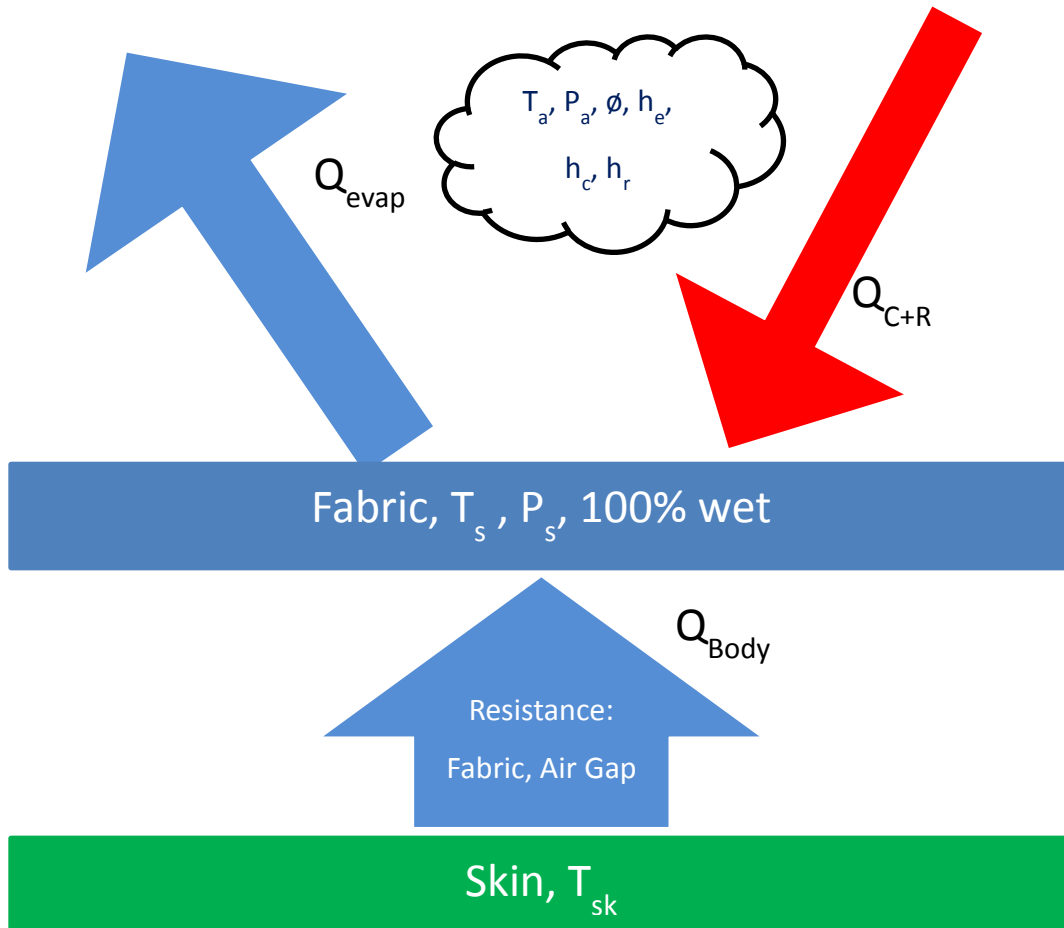


**Figure 5.5 Energy balance on the wetted fabric**

Since  $E_{spot}$  can be calculated, the efficiency controls how much energy is removed from the body

The convection and radiation component of the wetted area are included when calculating the spot efficiency using the average skin temperature. Therefore, the total C+R to the body must be reduced by the spot size. The remaining non-wetted clothed area is subject to the conduction and radiation and evaporation as expected. The energy equation for the non-wetted area is:

$$(1 - w_c) \cdot [(C + R) + E_{sk}] \quad (5.13)$$

### 5.1.2.3 Sweat Rate Modification

Section 5.1.1 showed that there was a drastic core temperature difference, 1.2 °C, and skin temperature between the two-node model simulations and the human subject tests. It was also discussed that for the majority of the subjects the two node model under predicted the total

sweat. Sweat rate can vary from person to person based on fitness level, genetics, acclimatization, among other factors (K. Parsons, 2002). As the spot cooling effect is added, the sweat rate will continue to drop as predicted skin and core temperature fall. This effect required that the sweat rate be tuned to match subject data.

Specifically, the sweat rate coefficient,  $c_{sw}$ , was modified by the inclusion of a multiplier specifically tailored for each subject,  $SW_{mod}$ . Each subject's sweat rate multiplication factor was iterated until the difference between the total sweat production from the model and human subject results was less than 0.01 kg with the spot model implemented. This resulted in an average sweat rate 1.859 times the current sweat rate coefficient with a reasonable skin and core prediction. To constrain the sweat rate within reasonable bounds the sweat rate was set at a threshold of producing 670 W/(m<sup>2</sup>K) of energy from sweat (ASHRAE, 2013). The modified equation for sweat Equation (5.1), given in units of Watts, can be seen in Equation ( 5.14 ).

$$E_{rsw} = SW_{mod} \cdot c_{sw} \cdot (T_b - T_{bset}) \cdot \exp \left[ \frac{T_{sk} - 34^{\circ}\text{C}}{10.7} \right] \quad (5.14)$$

The spot size creation and sweat rate modification proposed in this section are inserted in the ASHRAE two-node model as described. The skin energy balance contains the modifications through the equations discussed in this chapter and the calculation of the next skin temperature step  $T_{sk,i+1}$  by Equation ( 5.15 ).

$$T_{sk,i+1} = \frac{-[(1 - w_c) \cdot [(C + R) + E_{sk}] + \epsilon_s \cdot w_c \cdot E_{spot} + (K + \rho_{bl} \cdot Q_{bl} \cdot Cp_{bl}) \cdot (T_{cr,i} - T_{sk,i})]}{\frac{\alpha_{sk} \cdot m_b \cdot C_{sk}}{A_D \cdot \Delta t}} + T_{sk,i} \quad (5.15)$$

The next step is to demonstrate the improved prediction results of the modified two-node model over the standard model for the application of encapsulating and adsorptive clothing.

### ***5.1.3 Comparison of modified ASHRAE two node model to human subject results***

This section presents the results of the wetted clothing spot and sweat rate modification discussed in the previous subsection 5.1.2. The procedure to individually match the sweat total of the two-node model to the individual subjects was discussed in the previous section and an individual sweat rate modification multiplier,  $SW_{mod}$ , was developed which is one of the additions to the results table. The other addition to the results table is the inclusion of an average ReCl value for each subject's test. The average ReCl is the thermal resistance of the spot plus the rest of the clothing evaporative resistance with using their associated area percentages. Core temperature of the human subjects is  $T_{coreHS}$ , modified two-node simulated core temperature is  $T_{coreTNM}$ , Sweat total of the human subjects is  $SW_{HS}$ , and simulated sweat rate is  $SW_{TNM}$ , the predicted total evaporation from the modified two-node model is  $TNM\ Evap\ Sweat$ , and  $Sw_{mod}$  is the gain factor for each subject in the two-node model.

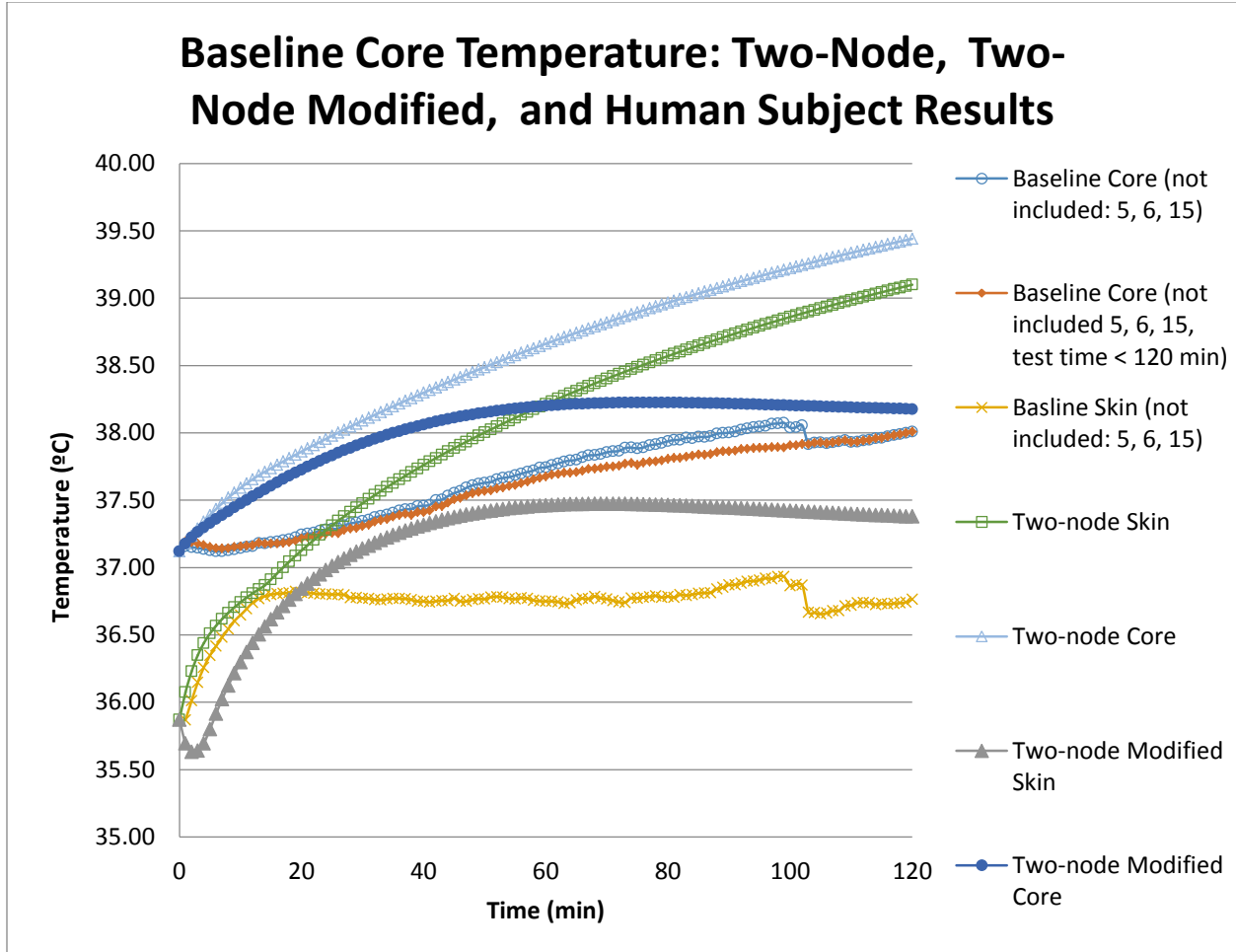
**Table 5.2 Baseline data comparison: Modified Two-Node Model (TNM) vs. Human Subject (HS)**

Subject #	Tcore HS °C	Tcore TNM °C	TcoreTNM -TcoreHS °C	SWH S kg	SWTN kg	SWTNM -SWHS kg	ReCl Adj Avg. Pa*m <sup>2</sup> / W	TNM Evap Sweat kg	Swmod kg
1	39.02	39.07	0.05	1.557	1.566	0.010	25.24	1.12	1.00
2	37.67	38.16	0.50	1.976	1.969	-0.007	24.80	1.39	1.70
3	37.05	37.57	0.52	2.823	2.825	0.002	23.61	1.83	3.90
4	37.71	37.97	0.26	2.749	2.744	-0.005	23.76	1.83	2.45
7	38.48	38.15	-0.33	2.542	2.538	-0.004	24.46	1.76	1.85
8	38.00	38.27	0.27	2.328	2.331	0.002	24.71	1.63	1.67
9	37.91	38.47	0.56	1.764	1.755	-0.009	24.93	1.19	1.55
10	37.85	37.81	-0.04	2.407	2.410	0.002	24.35	1.64	2.50
11	39.01	39.38	0.36	1.363	1.368	0.005	25.51	1.01	0.79
12	38.21	38.13	-0.08	2.381	2.373	-0.008	24.02	1.61	2.05
13	38.70	38.70	0.00	2.000	2.000	0.000	25.00	1.43	1.20
14	38.41	38.18	-0.24	1.726	1.721	-0.005	25.44	1.33	1.27
16	38.27	38.70	0.43	2.156	2.148	-0.009	24.93	1.53	1.23
17	37.95	38.19	0.24	2.725	2.719	-0.006	23.93	1.82	2.07
18	38.91	38.07	-0.83	2.048	2.046	-0.002	24.02	1.32	2.35
19	38.27	38.17	-0.10	2.274	2.283	0.009	24.84	1.63	1.65
20	37.95	37.81	-0.15	2.634	2.638	0.004	23.82	1.80	2.50
21	37.88	38.36	0.48	2.877	2.878	0.001	23.67	1.90	1.97
22	38.37	39.12	0.75	2.421	2.428	0.007	24.27	1.64	1.25
23	37.90	37.82	-0.08	2.816	2.815	-0.001	23.97	1.95	2.30
24	38.14	38.75	0.61	2.317	2.326	0.010	24.61	1.66	1.17
Average of subjects	38.17	38.33	0.15	2.280	2.280	0.000	24.47	1.57	1.830
Standard Deviation	0.482	0.473	0.383	0.434 6	0.434 2	0.0061	0.59	0.27	0.705
Average Subject	38.17	38.24	0.07	2.280	2.387	0.107	24.43	1.74	1.830

Figure 5.6 shows the graph of the average subject modeled core temperatures, with and without modification, compared to the human subject results. The human subject results are shown with all subjects that were modeled, i.e. not 5, 6, and 15. There is also a second human subject data set presented, as in section 5.1, only including the subjects that lasted the full 120



minutes, (120 min only). This information is added to highlight the effect of the subjects that did not finish had in influencing the results.



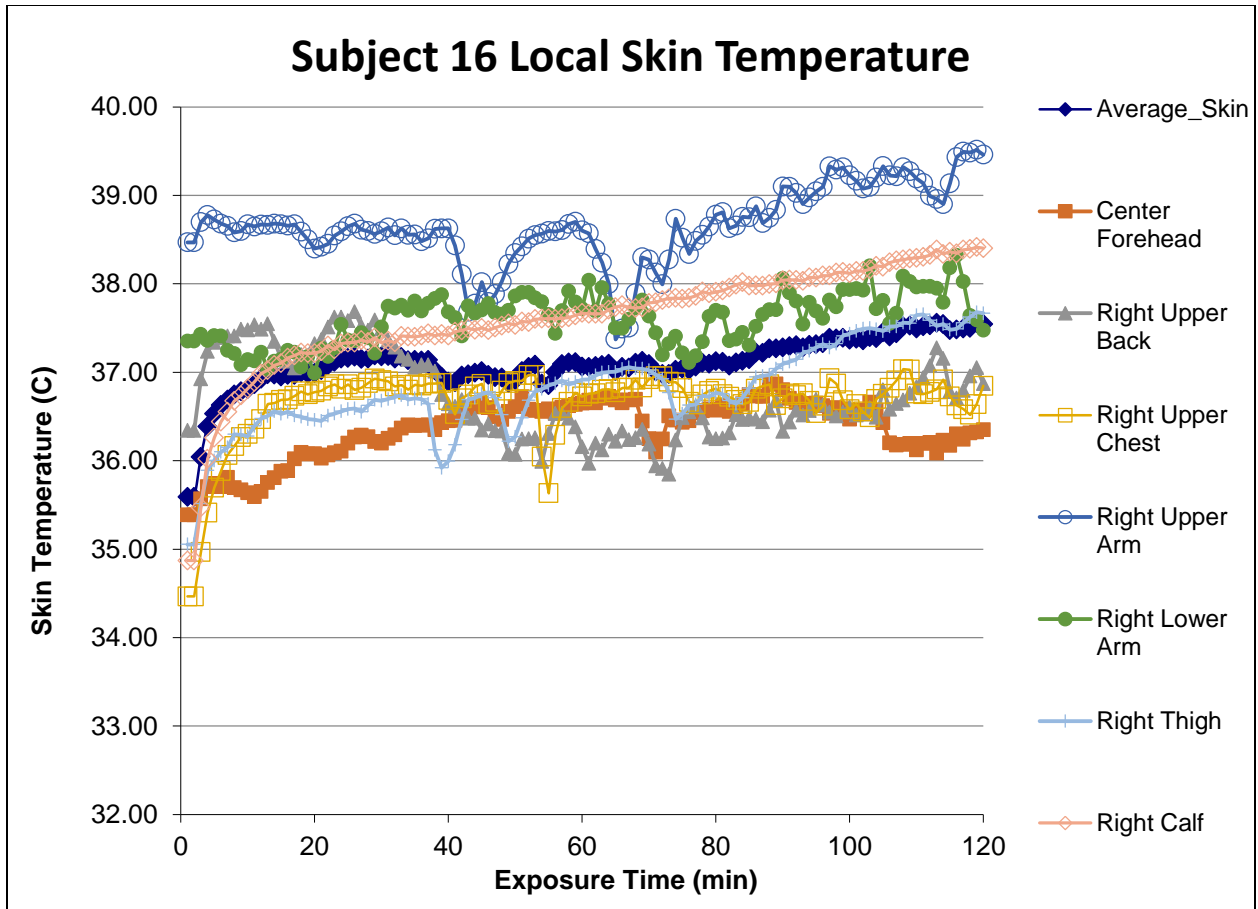
**Figure 5.6 Baseline core temperature comparison graph average subject Two-Node Model (TN), Modified Two-Node Model (TNM) and Human Subject (HS) Results with two data sets for human subject results to show impact of ending time on average core temperature**

Table 5.2, Figure 5.6 and Table 5.2 are interesting in a number of different ways. The most striking is that the modeled core temperatures have a concave down shape at the beginning of the test while the human subject results are slightly concave up at the beginning of the test and then switch inflection roughly half way through to concave down. One possible reason for this shape in the model is because  $T_{sk}$  and  $T_c$  starting points are fixed to the starting points of the subjects. This could have conflicts with the control algorithms built into the two-node model causing them to react quickly, or not react quickly enough because of the odd set points. The algorithms themselves are also possibly a source of error as they are generalized for a large subset of the population and may not react well to directly mapping individuals. Another issue could be the blood flow value,  $Q_{bl}$ , and the location of energy in the body. The lack of resolution using a two-node model opens the possibility that there is the opportunity for energy to be located in many different compartments and layers. This is the same issue that prevents truly accurate partial calorimetry from being practical as discussed in the literature review in Section 2.2.1.

It is also possible, and likely, that the subjects started sweating before the data recording started while they were in the chamber getting ready to start the test. Unfortunately, there is no way to quantify this. The subject procedure in the chamber before the test was usually reasonably fast, but sweating, especially while at a lower metabolic rate would have provided an opportunity to accumulate sweat and begin cooling before the test started. The decision was made to use the starting points as their metabolic rates, times before the test started, and other factors are unknown. Another issue relating to the study structure is that in the human subject test design, each subject acted as his or her own control. Although the subjects dressed, were instrumented, and sat in a slightly warm, thermally neutral chamber, they were not measured to see if they had

reached thermal neutrality (i.e. steady state) before entering the test chamber and starting the experiment. This will also present an issue when comparing PCS core temperature data according to ASTM standards, which will be discussed in the next section.

In both the modified and unmodified two-node models both convection and radiation added energy to the body throughout the test. As the body temperature rose, this value decreased from 94 W at the beginning of the test to 60 W at the end. Both convection and radiation are playing a near equal role as the radiation heat transfer coefficient is 3 times less than the convective heat transfer coefficient. However, the difference between the mean radiant temperature and the skin temperature is approximately 3 times higher than the difference between the skin temperature and air temperature. As the skin temperature rises the radiant load is a larger quantity of the energy entering the body.



**Figure 5.7 Subject 16 local skin temperatures as example of human subject baseline data**

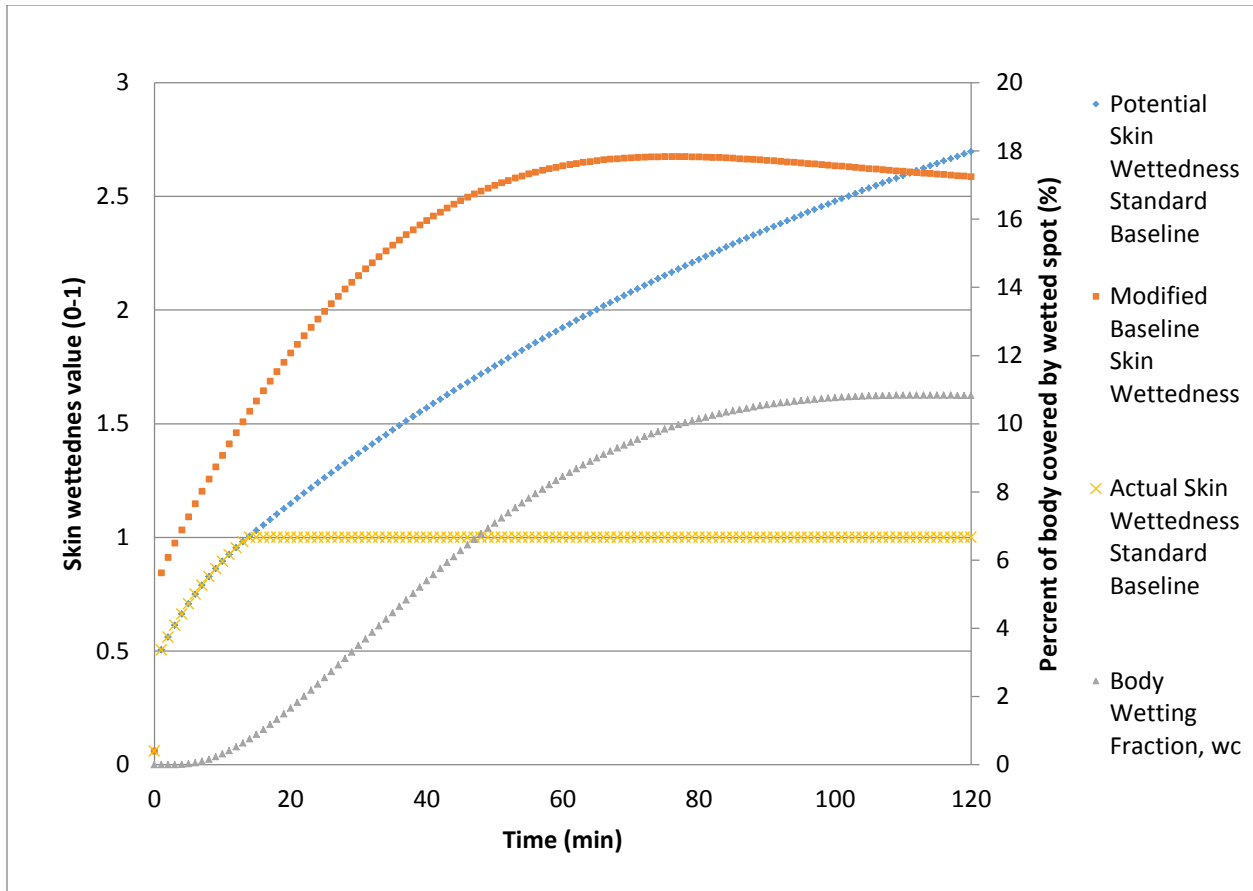


**Figure 5.8 Skin wettedness on left axis for unmodified and modified two-node models. Percent of body surface covered by wetted spot in the modified two-node model is on right axis**

Overall, the modification to the clothing model and sweat rate provide a much higher degree of core temperature accuracy than the standard two node model. The model did not track the core temperature well at the beginning of the test possibly for reasons discussed. However, the essential aspect of the modified two-node model is that it allows for reasonable sweat and final core temperature prediction. As previously discussed core temperature and sweat rate have significance in predicting and mitigating heat stress in the test conditions. As the motivation of this work is to better understand the effects of PCS, the two node models, with the baseline end results established as reasonably predictive, the PCS effect can be explored through the use of

the two-node and modified two-node model in the first section of Chapter 6. As a point of comparison the baseline skin temperature values for subject 16 are presented showing different segment temperatures in Figure 5.7. The effect of the wetted spot and sweat rate difference can be seen in Figure 5.8. In this figure it is possible to see that the sweat rate starts out high and continues for the entire test, however in the unmodified two-node model the skin wettedness is capped at 1 shown in the actual Skin Wettedness Standard Baseline plot, so the potential skin wetting percentage is wasted. In the modified two-node model the excess sweat becomes part of the wetted spot area leading to a decrease in the sweat production. It is possible that a better prediction could be obtained by using a multi-node model to better represent boundary conditions, and body layers, as in the next section.

## **5.2 Multi-node Model**

The multi-node model utilized TAItherm v.12.0.3 by ThermoAnalytics Inc. as was described in Section 4.2. Just like in the two-node model, values to be compared between the model and the human subject results include sweat rate as well as core and mean skin temperatures. Unlike in the two-node model, only an average subject is modeled and compared to the average of the subjects. The TAItherm model has the ability to scale models to match different subjects and provide local temperatures. However, the initialization requires knowledge of the state of 16 layers in the model in order to start each subject correctly. Furthermore, the model is currently oriented at comfort and the extreme boundary conditions that are being used are parameters that have not been validated or optimized in this model at the time of this work.

This section will follow the same layout of the previous section, but the section presenting the modifications of the model has been shortened because the modifications of this advanced model is outside of the focus of this research. It is prudent to point out here that the

fundamental principles behind the wetted fabric modifications made to the two-node model can also be made to this model, and similar models on a segmental or nodal basis. The final subsection will include the limited changes made to the model.

### ***5.2.1 Comparison of the standard multi-node model to human subject results***

The use of the multi-node model allowed the application of local boundary conditions including clothing properties. The multi-node model also distributes sweat to each body segment using data from (C. Smith & Havenith, 2011). The model has much finer resolution on the boundary conditions, accounting for the averaging issues inherent in the two-node model. The measured human body segment starting and ending temperatures and sweat totals can be found in Table 5.3 and Table 5.4 and graphs of mean skin temperature and core temperature are compared in Figure 5.9. Results with two data sets for human subject results to show impact of ending time on average core temperature

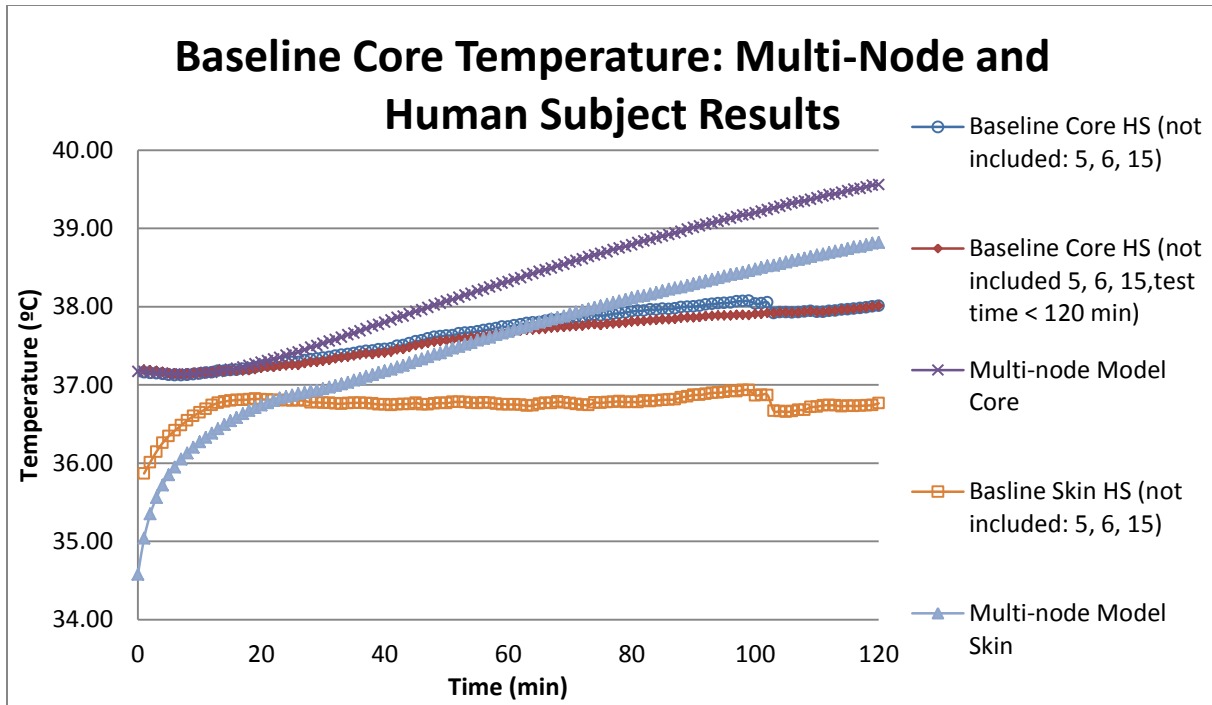


**Figure 5.9** Baseline core temperature comparison graph average subject Standard Multi-Node Model and average Human Subject (HS) mean skin temperature and core temperatures.

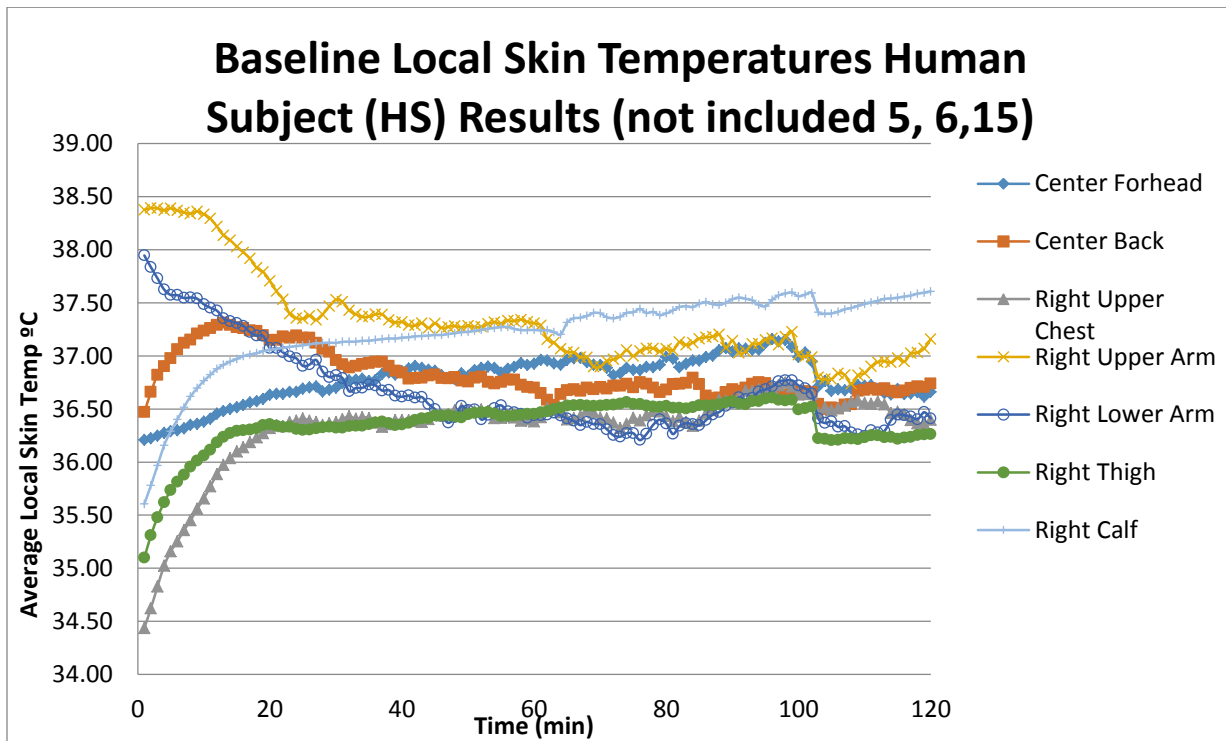


**Figure 5.10** Baseline local skin temperature graph of average of subject Human Subject (HS) to show trends in external skin temperatures.



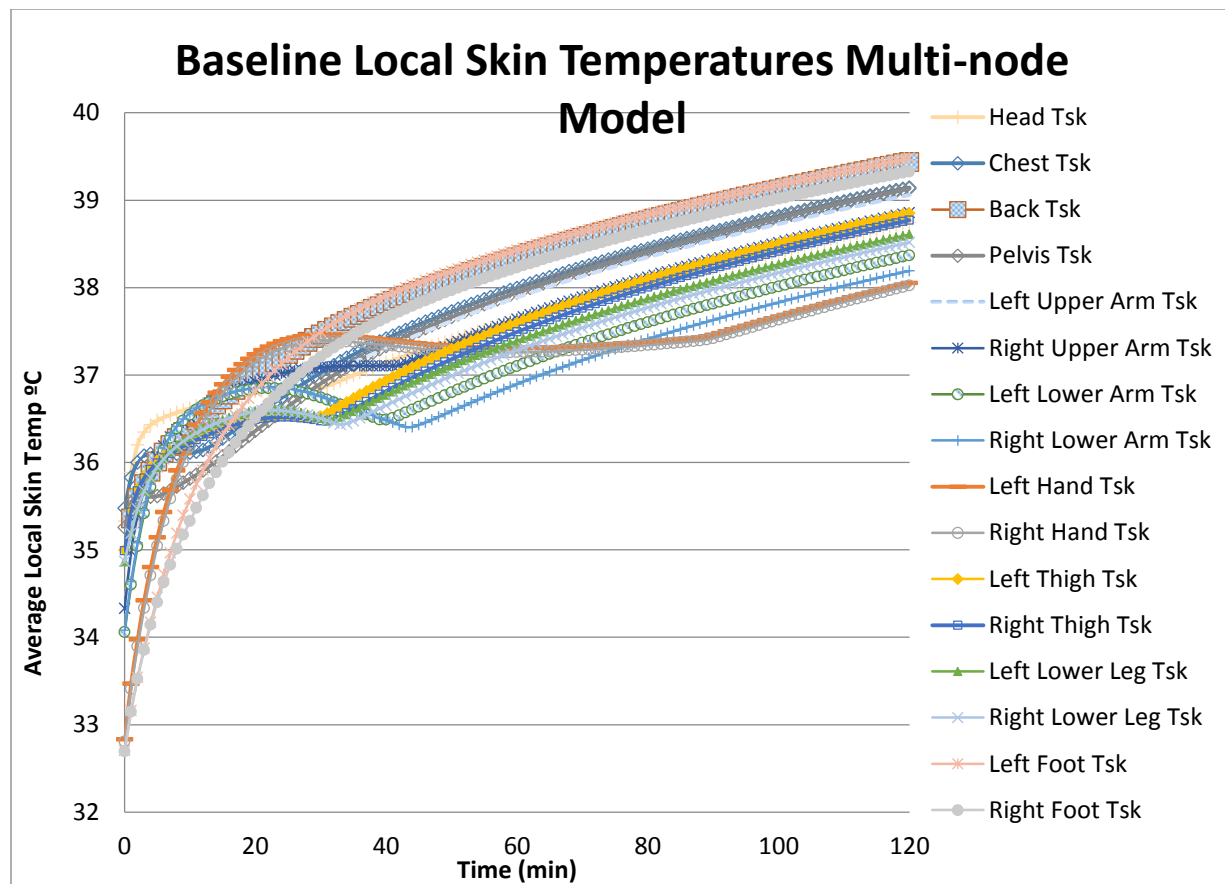


**Figure 5.11** Baseline local skin temperature graph of average of subject Standard Multi-Node Model to show trends in external skin temperatures.

The results of the multi node model do not appear to be any better than those of the two-node model. The core and mean skin temperature predictions are much higher than those of the human subjects' averages and are at a much higher slope as can be seen in Figure 5.10 and Figure 5.11. It is interesting that the multi-node model inflection matches that of the human subject results slightly better than that of the two-node model, especially at the beginning of the test. This is likely because there was no attempt made to initialize the mean skin and core temperatures to the exact averages of the human subject results. In addition, the multi-node model has a more complicated control algorithm and multiple layers to better approximate the human. The results for the temperature change in Table 5.3 of the measured right arm

temperatures, which can be seen in Figure 5.10, show the skin temperatures going down over the course of the test. There are two likely causes for this result. The first is that the temperature sensors may have come detached from the skin's surface and been measuring the temperature in the space between the skin and the uniform blouse. The second reason, which was the conclusion from the two-node model covering the same data, is that the wetted fabric lowers the skin or environment temperature and supports the conclusions from the previous chapter.

The closest approximation to the average human subjects that could be made in TAItherm was a man at 50% weight, 75% height. The results of placing the simulated human in thermally neutral conditions with the clothing and equipment resulted in almost exactly the same core temperature as the measured average. Therefore, the human parameters from the steady state, thermal neutral simulation were used as the starting values for the simulated human.

The likely reason for the discrepancy in core temperature is that the multi-node model used is not intended for the extreme application modeled here. Like the two-node model, the multi-node model uses the assumption that the clothing does not wet. Again, this is not in keeping with the observed state of the subjects clothing and will likely cause disparity in the measured values.

**Table 5.3 Baseline data comparison: Standard Multi-Node Model vs. Human Subject core, mean skin, and local skin temperatures.**

Segments	Standard Multi-Node Model			Human Subjects (not included: 5, 6, 15)			Human Subjects (not included: 5, 6, 15), >120 min only			Starting Conditions Difference		Delta T Error Value	
	Initial Value (°C)	Final Value (°C)	Delta T (°C)	Initial Value (°C)	Final Value (°C)	Delta T (°C)	Initial Value (°C)	Final Value (°C)	Delta T (°C)	HS(not included: 5, 6, 15)	HS (not included: 5, 6, 15), >120 min only	HS(not included: 5, 6, 15)	HS (not included: 5, 6, 15), >120 min only
Mean Skin	35.04	38.82	3.78	35.87	36.76	0.90	35.81	36.76	0.96	-0.83	-0.77	2.88	2.82
Core	37.17	39.56	2.39	37.16	38.01	0.85	37.20	38.01	0.81	0.01	-0.02	1.54	1.58
Head Tsk	35.88	38.75	2.86	36.21	36.66	0.45	34.47	36.66	2.19	-0.33	1.41	2.41	0.68
Chest Tsk	35.83	39.14	3.32	34.44	36.40	1.96	34.47	36.40	1.92	1.39	1.35	1.36	1.40
Back Tsk	35.59	39.45	3.86	36.47	36.74	0.27	36.30	36.74	0.43	-0.88	-0.71	3.59	3.42
Pelvis Tsk	35.54	39.13	3.60	N/A	N/A	N/A	N/A	N/A	N/A	N/A	N/A	N/A	N/A
Left Upper Arm Tsk	34.94	39.06	4.12	N/A	N/A	N/A	N/A	N/A	N/A	N/A	N/A	N/A	N/A
Right Upper Arm Tsk	34.99	38.86	3.87	38.38	37.16	-1.22	38.44	37.16	-1.28	-3.39	-3.46	5.09	5.16
Left Lower Arm Tsk	34.60	38.37	3.77	N/A	N/A	N/A	N/A	N/A	N/A	N/A	N/A	N/A	N/A
Right Lower Arm Tsk	34.64	38.19	3.56	37.95	36.41	-1.53	37.88	36.41	-1.47	-3.31	-3.25	5.09	5.03
Left Hand Tsk	33.47	38.05	4.58	N/A	N/A	N/A	N/A	N/A	N/A	N/A	N/A	N/A	N/A
Right Hand Tsk	33.41	38.02	4.61	N/A	N/A	N/A	N/A	N/A	N/A	N/A	N/A	N/A	N/A
Left Thigh Tsk	35.45	38.85	3.40	N/A	N/A	N/A	N/A	N/A	N/A	N/A	N/A	N/A	N/A
Right Thigh Tsk	35.43	38.77	3.34	35.10	36.26	1.16	34.96	36.26	1.30	0.33	0.48	2.18	2.03
Left Lower Leg Tsk	35.19	38.61	3.42	N/A	N/A	N/A	N/A	N/A	N/A	N/A	N/A	N/A	N/A
Right Lower Leg Tsk	35.19	38.52	3.33	35.61	37.61	2.00	35.59	37.61	2.02	-0.41	-0.39	1.32	1.30
Left Foot Tsk	33.16	39.48	6.32	N/A	N/A	N/A	N/A	N/A	N/A	N/A	N/A	N/A	N/A
Right Foot Tsk	33.15	39.33	6.18	N/A	N/A	N/A	N/A	N/A	N/A	N/A	N/A	N/A	N/A

Through Table 5.3 it is possible to see the initial values used in the model and how they relate to the human subject measured values. This gives an indication of how well the thermal neutral model corresponded to the human subjects. It is clear that the skin temperature of the model was significantly lower than the human subjects with the exception of one segment. This discrepancy may be due to the delay from plugging in thermocouples and beginning the tests in the human subject tests coupled with the quick response of the modeled skin temperature to the conditions seen in Figure 5.9. Again, the human subject data is divided into two groups the first being all subjects except subjects 5, 6, and 15, for which there was no metabolic data to use in modeling activity level. Second, there are only the subjects who finished the entire 120-minute test, which also excludes subjects: 1, 9, 11, 13, and 18 to show the effect those subjects dropping have on the test. It is likely if those subjects had been allowed to continue for the entire test past the safety cutoff the model would agree more favorably with the empirical data.

The thermal neutral condition setup at from the TAItherm reference variables procedure produced a core temperature (rectal) within 0.02 °C of the average human subjects. However, the difference between the final average human subject results and the standard multi-node model show an alarming error in core temperature of 1.54 °C and 2.82 °C in mean skin temperature. The likely cause is again the inability of the sweat to wet the clothing resulting in a loss of potential cooling as discussed in Section 5.1.2.

**Table 5.4 Baseline sweat total comparison: Standard Multi-Node Model vs. Human Subject (HS) sweat rates with human subject results as the comparator.**

Sweat Totals	Standard Multi-Node Model	Human Subjects (not included: 5, 6, 15)	Human Subjects (not included: 5, 6, 15), >120 min only
Total Sweat (kg)	2.23	2.28	2.45
Error Value (kg)	N/A	-0.05	-0.22
% Error	N/A	-2.31	-8.98

The sweat total of the model, as seen in Table 5.4 agreed well with the average of the human subjects with 2.31% error and the subjects who finished the test with a worse 8.98% error. The sweat total of the model matched the human subject results however, one must still account for the discrepancy between the core temperature values as those values drive the sweat rate in the model. The sweat produced in the model is at much higher core and skin temperatures than are seen in in the human subject test and thus would likely under estimate the sweat rate if the core temperatures were predicted correctly.

### ***5.2.2 Comparison of the modified multi-node model to human subjects results***

The results of the previous section illustrate again that there is a heat transfer mechanism missing from the multi-node model. It has also been hypothesized and proven in the previous section that the assumption that the clothing does not wet is part of the problem. The implementation of the same procedure outlined in section 5.1.2 could be performed in this model, but will be much more complex and require access to specialized information from the program and is ultimately outside the scope of this research.

The previous section also highlighted the difference in sweat rate between the average of the human subjects and the multi-node model. The multimode model provides different amounts of sweat to different segments based on values from literature. There is no way to know how this sweat is being used in local segments without a deeper analysis of the program that is not

available in the standard output. The argument could be made that the distribution is incorrect and that the local sweat values may also be a cause of the prediction problems. Therefore, a possible immediate area for improvement that could be explored is to see if increasing the sweat rate to match or exceed that of the human subjects will improve the modeled core temperature. This provides a good starting point to diagnose the differences in the next subsection. However, the hypothesis is that the wetted clothing will have an effect on the subjects so the final subsection will supplement increased sweat rate and use an average  $Re_{Cl}$  value from the modified two-node model. This is applied to lower the  $Re_{Cl}$  values on the segments not covered in body armor to make an approximation at improving the model.

#### ***5.2.2.1 Sweat Rate Modification of the multi-node model***

The sweat rate modification of the multi-node model uses a modification to the physiology.txt file, provided by the manufacturer, to allow the changes to be applied in TAItherm version 12.0.3. The sweat rate controller gain was doubled based on the average  $SW_{mod}$  value, 1.83 from Table 5.2 of the two-node model and because the version of TAItherm does not account for sweat rate scaling on body types that are not the 50 percentile man. The results from the model can be seen in Figure 5.12, Table 5.5, Table 5.6, and Table 5.7.

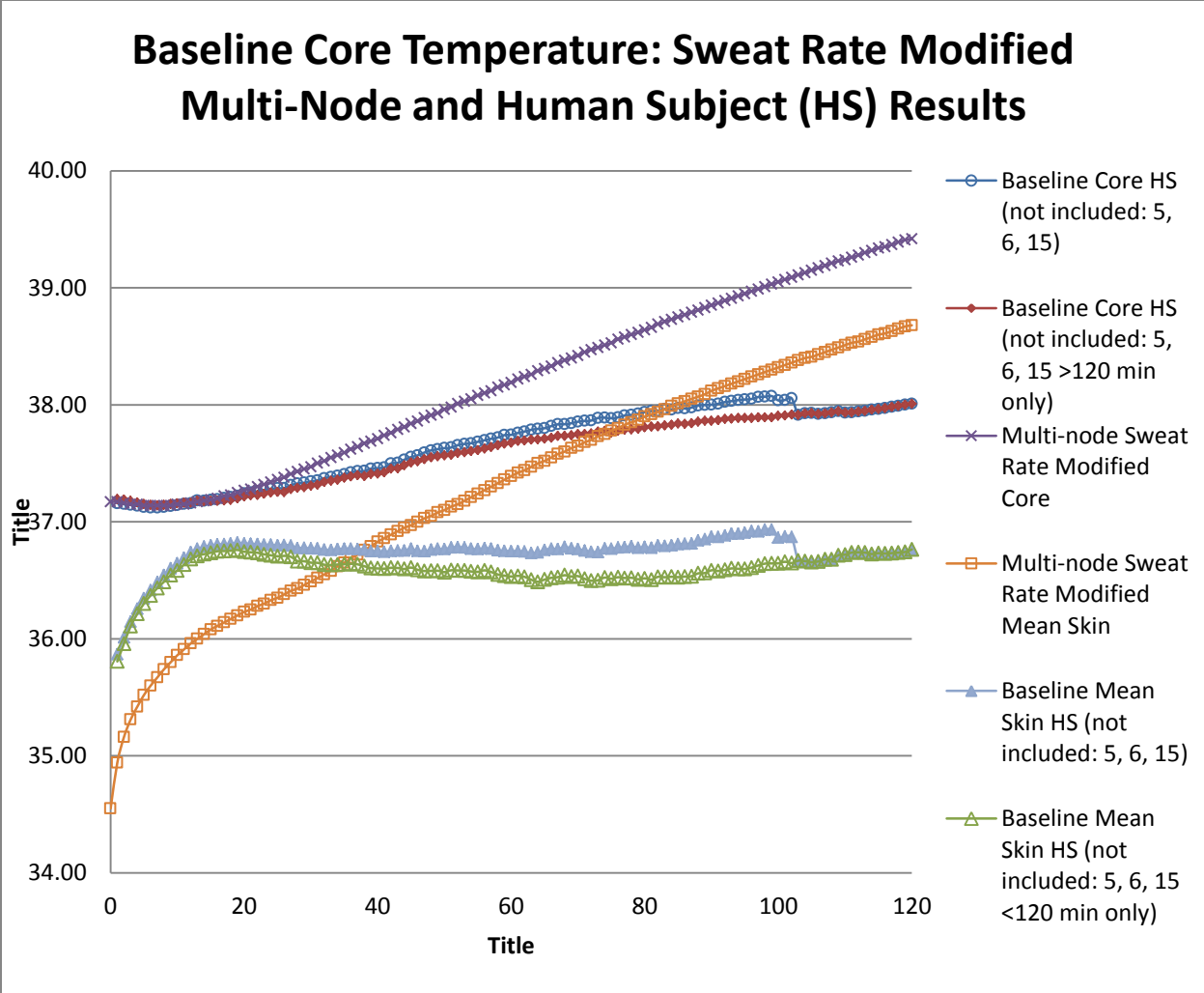


**Figure 5.12 Baseline core temperature comparison graph average subject Sweat Rate Modified Multi-Node Model and average Human Subject mean skin temperature and core temperatures. Results with two data sets for human subject results to show impact of ending time on average core temperature**

**Table 5.5 Baseline data comparison: Sweat Rate Modified Multi-Node Model vs. Human Subject (HS) core, mean skin, and local skin temperatures.**

Segments	Sweat Rate Modified Multi-Node Model			Human Subjects (not included: 5, 6, 15)			Human Subjects (not included: 5, 6, 15), >120 min only			Starting Conditions Difference		Delta T Error Value	
	Initial Value (°C)	Final Value (°C)	Delta T (°C)	Initial Value (°C)	Final Value (°C)	Delta T (°C)	Initial Value (°C)	Final Value (°C)	Delta T (°C)	HS(not included: 5, 6, 15)	HS (not included: 5, 6, 15), >120 min only	HS(not included: 5, 6, 15)	HS (not included: 5, 6, 15), >120 min only
Mean Skin	34.94	38.68	3.74	35.87	36.76	0.90	35.81	36.76	0.96	-0.93	-0.87	2.84	2.78
Core	37.17	39.42	2.25	37.16	38.01	0.85	37.20	38.01	0.81	0.01	-0.02	1.40	1.44
Head Tsk	35.79	38.61	2.82	36.21	36.66	0.45	34.47	36.66	2.19	-0.42	1.31	2.37	0.64
Chest Tsk	35.69	39.01	3.32	34.44	36.40	1.96	34.47	36.40	1.92	1.26	1.22	1.36	1.40
Back Tsk	35.51	39.32	3.82	36.47	36.74	0.27	36.30	36.74	0.43	-0.96	-0.80	3.55	3.38
Pelvis Tsk	35.36	39.00	3.64	N/A	N/A	N/A	N/A	N/A	N/A	N/A	N/A	N/A	N/A
Left Upper Arm Tsk	34.84	38.93	4.08	N/A	N/A	N/A	N/A	N/A	N/A	N/A	N/A	N/A	N/A
Right Upper Arm Tsk	34.89	38.72	3.83	38.38	37.16	-1.22	38.44	37.16	-1.28	-3.48	-3.55	5.04	5.11
Left Lower Arm Tsk	34.50	38.22	3.73	N/A	N/A	N/A	N/A	N/A	N/A	N/A	N/A	N/A	N/A
Right Lower Arm Tsk	34.53	38.05	3.51	37.95	36.41	-1.53	37.88	36.41	-1.47	-3.41	-3.35	5.05	4.98
Left Hand Tsk	33.42	37.90	4.48	N/A	N/A	N/A	N/A	N/A	N/A	N/A	N/A	N/A	N/A
Right Hand Tsk	33.36	37.86	4.51	N/A	N/A	N/A	N/A	N/A	N/A	N/A	N/A	N/A	N/A
Left Thigh Tsk	35.34	38.71	3.37	N/A	N/A	N/A	N/A	N/A	N/A	N/A	N/A	N/A	N/A
Right Thigh Tsk	35.33	38.63	3.30	35.10	36.26	1.16	34.96	36.26	1.30	0.23	0.37	2.14	2.00
Left Lower Leg Tsk	35.10	38.47	3.37	N/A	N/A	N/A	N/A	N/A	N/A	N/A	N/A	N/A	N/A
Right Lower Leg Tsk	35.10	38.38	3.28	35.61	37.61	2.00	35.59	37.61	2.02	-0.51	-0.49	1.28	1.26
Left Foot Tsk	33.08	39.36	6.28	N/A	N/A	N/A	N/A	N/A	N/A	N/A	N/A	N/A	N/A
Right Foot Tsk	33.06	39.20	6.14	N/A	N/A	N/A	N/A	N/A	N/A	N/A	N/A	N/A	N/A



**Table 5.6 Baseline sweat total comparison: Sweat Rate Modified Multi-Node model vs. Human Subject (HS) sweat rates with human subject results as the comparator.**

Sweat Totals	Sweat Rate Modified Multi-Node Model	Human Subjects (not included: 5, 6, 15)	Human Subjects (not included: 5, 6, 15), >120 min only
Total Sweat (kg)	2.67	2.28	2.45
Error Value (kg)	N/A	0.39	0.22
% Error	N/A	17.16	9.16

**Table 5.7 Improvement in core temperature change between Sweat Rate Modified Multi-Node Model vs. Human Subjects (HS) results.**

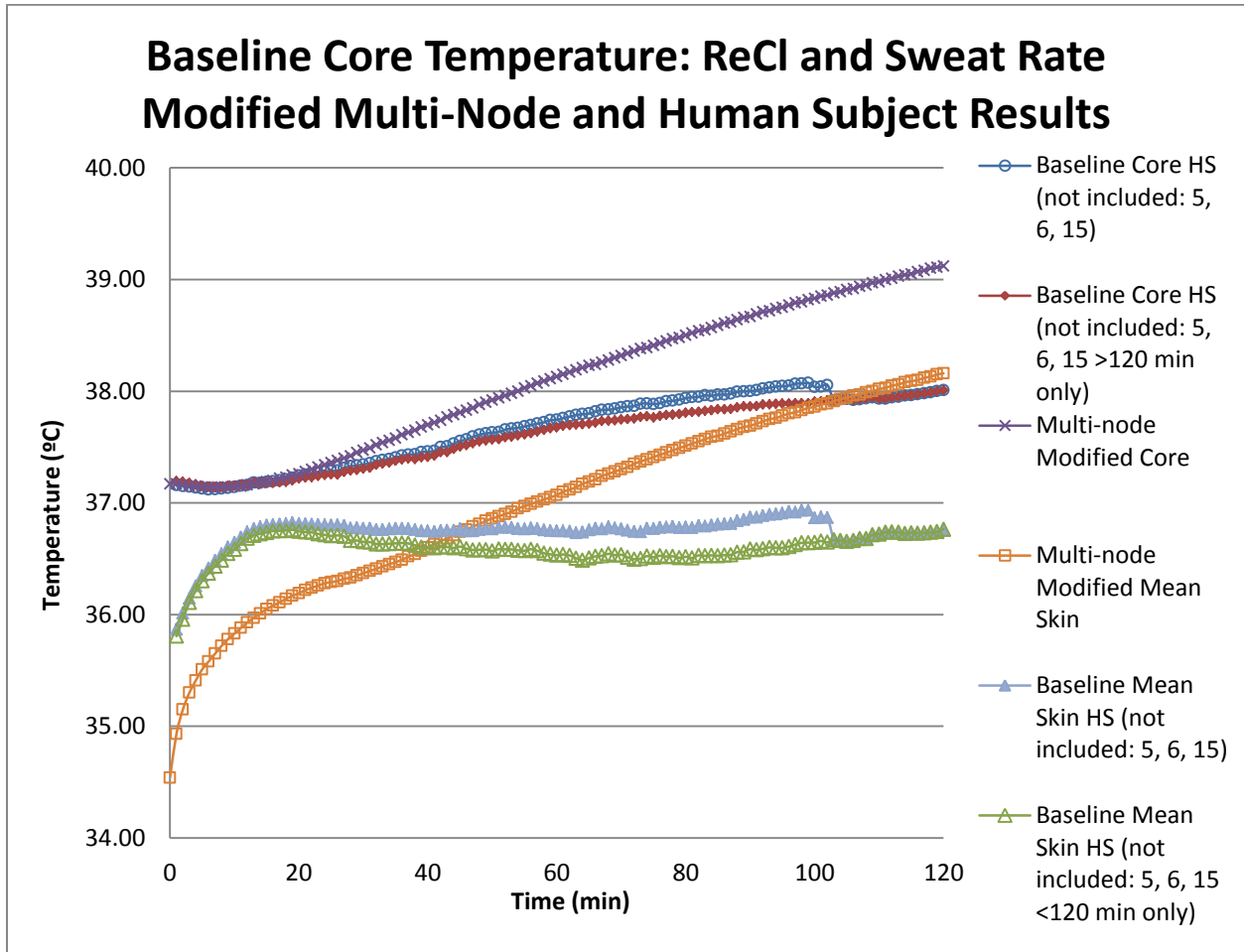
	Human Subjects (not included: 5, 6, 15)	Human Subjects (not included: 5, 6, 15), >120 min only
Standard Multi-Node to Human Subject Error °C	1.54	1.58
Sweat Rate Modified Multi-node Change to Human Subject Error °C	1.40	1.44
Difference °C	0.14	0.14
% Difference	9.09	8.87

Table 5.5 and Table 5.6 show virtually the same data as Table 5.3 and Table 5.4 from the previous section. Table 5.7 shows the core temperature differences between the standard multi-node model to the doubled sweat gain factor multi-node model. Overall, increasing the sweat gain shows that there is an improvement in the core temperature prediction ability of the model by 24.7% to 24.9% out of original percent errors of 189.6% and 194.2% respectively so the predicted core temperature is still drastically different from that of the human subjects.

There remains the possibility that the subjects may have started sweating in the few minutes they were in the chamber prior to the test or may have started sweating at a higher rate than is being modeled at the beginning of the test. However, this is also offset by the fact that an extra 400 to 500 grams of potential sweat were added to the model over that seen in the human subject results and the core temperature predictions were still not close to the measured results. This section highlights the need to implement the wet clothing model in the multi-node mode.

#### ***5.2.2.2 Sweat Rate and Evaporative Resistance Modification of the Multi-Node Model***

The more complex nature of the multi-node model and the proprietary nature of the algorithms make the application of the wetted fabric model to the human subject results outside the scope of this work. To approximate wetting clothing a simple method to allow more evaporation to occur was implemented. The evaporative resistance values of the clothes segments other than the chest, back, stomach, and shoulders were modified until the total resistance of the ensemble equaled that of the average value from the modified two-node model. The average body value used can be found in Table 5.2 and is approximately  $24.47 \text{ Pa}\cdot\text{m}^2/\text{W}$  and the specific modifications can be found in Appendix B- Modeling Initial Values. The same model was run again and the results can be found in, Figure 5.13, Table 5.8, Table 5.9, and Table 5.10.



**Figure 5.13 Baseline core temperature comparison graph average subject ReCl and Sweat Rate Modified Multi-Node Model and average Human Subject (HS) mean skin temperature and core temperatures. Results with two data sets for human subject results to show impact of ending time on average core temperature**

**Table 5.8 Baseline data comparison: ReCl and Sweat Rate Modified Multi-Node Model vs. Human Subject core, mean skin, and local skin temperatures.**

Segments	ReCl and Sweat Rate Modified Multi-Node Model			Human Subjects (not included: 5, 6, 15)			Human Subjects (not included: 5, 6, 15), >120 min only			Starting Conditions Difference		Delta T Error Value	
	Initial Value (°C)	Final Value (°C)	Delta T (°C)	Initial Value (°C)	Final Value (°C)	Delta T (°C)	Initial Value (°C)	Final Value (°C)	Delta T (°C)	HS(not include d: 5, 6, 15)	HS (not included: 5, 6, 15), >120 min only	HS(not include d: 5, 6, 15)	HS (not included: 5, 6, 15), >120 min only
Mean Skin	34.93	38.16	3.23	35.87	36.76	0.90	35.81	36.76	0.96	-0.94	-0.88	2.33	2.27
Core	37.17	39.12	1.95	37.16	38.01	0.85	37.20	38.01	0.81	0.01	-0.02	1.10	1.14
Head Tsk	35.79	38.18	2.39	36.21	36.66	0.45	34.47	36.66	2.19	-0.42	1.31	1.94	0.21
Chest Tsk	35.70	38.61	2.91	34.44	36.40	1.96	34.47	36.40	1.92	1.26	1.22	0.95	0.99
Back Tsk	35.51	38.94	3.43	36.47	36.74	0.27	36.30	36.74	0.43	-0.96	-0.79	3.16	3.00
Pelvis Tsk	35.36	38.51	3.16	N/A	N/A	N/A	N/A	N/A	N/A	N/A	N/A	N/A	N/A
Left Upper Arm Tsk	34.83	38.36	3.53	N/A	N/A	N/A	N/A	N/A	N/A	N/A	N/A	N/A	N/A
Right Upper Arm Tsk	34.88	38.10	3.23	38.38	37.16	-1.22	38.44	37.16	-1.28	-3.50	-3.57	4.44	4.51
Left Lower Arm Tsk	34.48	37.52	3.04	N/A	N/A	N/A	N/A	N/A	N/A	N/A	N/A	N/A	N/A
Right Lower Arm Tsk	34.51	37.31	2.80	37.95	36.41	-1.53	37.88	36.41	-1.47	-3.43	-3.37	4.33	4.27
Left Hand Tsk	33.40	37.40	4.00	N/A	N/A	N/A	N/A	N/A	N/A	N/A	N/A	N/A	N/A
Right Hand Tsk	33.34	37.36	4.02	N/A	N/A	N/A	N/A	N/A	N/A	N/A	N/A	N/A	N/A
Left Thigh Tsk	35.33	38.09	2.76	N/A	N/A	N/A	N/A	N/A	N/A	N/A	N/A	N/A	N/A
Right Thigh Tsk	35.31	37.99	2.68	35.10	36.26	1.16	34.96	36.26	1.30	0.21	0.36	1.52	1.38
Left Lower Leg Tsk	35.09	37.82	2.74	N/A	N/A	N/A	N/A	N/A	N/A	N/A	N/A	N/A	N/A
Right Lower Leg Tsk	35.08	37.71	2.63	35.61	37.61	2.00	35.59	37.61	2.02	-0.52	-0.50	0.62	0.60
Left Foot Tsk	33.08	38.99	5.91	N/A	N/A	N/A	N/A	N/A	N/A	N/A	N/A	N/A	N/A
Right Foot Tsk	33.06	38.81	5.75	N/A	N/A	N/A	N/A	N/A	N/A	N/A	N/A	N/A	N/A

**Table 5.9 Baseline sweat total comparison: ReCl Sweat Rate Modified Multi-Node Model vs. Human Subject sweat rates with human subject results as the comparator.**

Sweat Totals	ReCl and Sweat Rate Modified Multi-Node Model	Human Subjects (not included: 5, 6, 15)	Human Subjects (not included: 5, 6, 15), >120 min only
Total Sweat (kg)	2.60	2.28	2.45
Error Value (kg)	N/A	0.32	0.16
% Error	N/A	14.20	6.40

**Table 5.10 Improvement in core temperature change between ReCl Sweat Rate Modified Multi-Node Model vs. Standard multi-node model.**

	Human Subjects (not included: 5, 6, 15)	Human Subjects (not included: 5, 6, 15), >120 min only
Standard Multi-Node to Human Subject Error °C	1.54	1.58
ReCl and Sweat Rate Modified Multi-node Change to Human Subject Error °C	1.10	1.14
Difference °C	0.44	0.44
% Difference	28.56	27.89

The addition of the  $Re_{Cl}$  change to the multi-node model with the doubled sweat gain factor showed an approximately 60.0% to 60.2% improvement the core temperature prediction over the standard model, however the model is still off by 1.10 °C to 1.14 °C. As can be seen in Figure 5.13 the core temperature closely approximates that of the human subject results better than any other simulation in the initial stage where sweating occurs. However, because the clothing wetting is a reaction to the sweat soaking the fabric this cooling would occur later in the test, likely where the simulated core temperature diverges from the measured average. Another issue with this approximation is that the uniform distribution when lowering the evaporative resistance does not account for the local sweating effects. One advantage of the multi-node model is the local sweating and convection coefficients, but without the knowledge of the sweat

rate at each segment the evaporative resistance cannot be properly scaled to match the potential fabric saturation. However, an implementation of the wetted fabric cooling model presented in the previous chapter would be hypothetically feasible.

Considering the fact that the local effects complicate the model, it was decided to change the evaporative resistance of all segments to the average  $Re_{Cl}$  from the modified two-node model to determine if this might allow for more of the sweat under the body armor to evaporate. The results were only a slight improvement over the  $Re_{Cl}$  and sweat rate modified multi-node model and can be seen below in Figure 5.14, Table 5.11, Table 5.12, and Table 5.13.

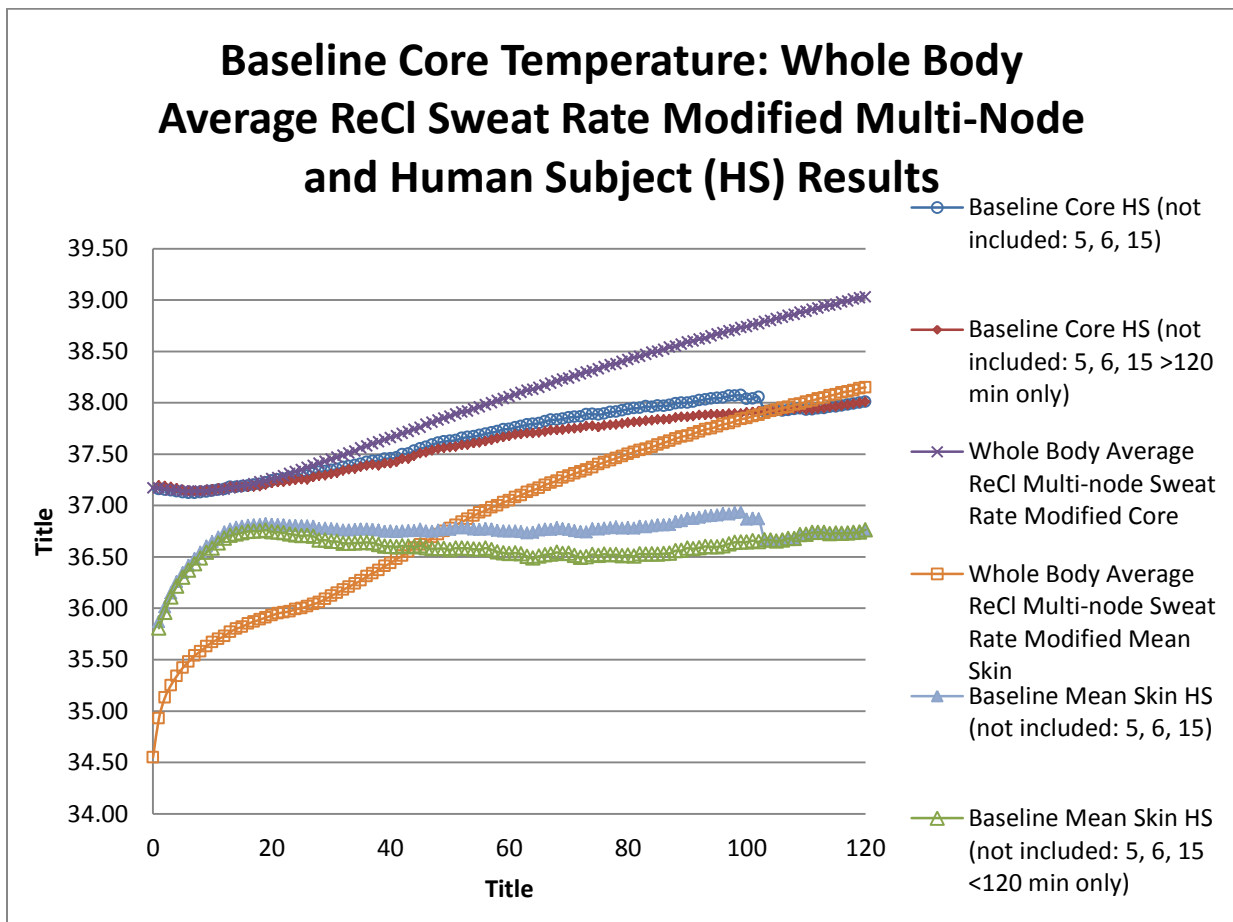


**Figure 5.14 Baseline core temperature comparison graph average subject Whole Body Average  $Re_{Cl}$  Sweat Rate Modified Multi-Node Model and average Human Subject (HS) mean skin temperature and core temperatures. Results with two data sets for human subject results to show impact of ending time on average core temperature**

**Table 5.11 Baseline data comparison: Whole Body Average ReCl Sweat Rate Modified Multi-Node Model vs. Human Subject core, mean skin, and local skin temperatures.**

Segments	ReCl and Sweat Rate Modified Multi-Node Model			Human Subjects (not included: 5, 6, 15)			Human Subjects (not included: 5, 6, 15), >120 min only			Starting Conditions Difference		Delta T Error Value	
	Initial Value (°C)	Final Value (°C)	Delta T (°C)	Initial Value (°C)	Final Value (°C)	Delta T (°C)	Initial Value (°C)	Final Value (°C)	Delta T (°C)	HS(not included: 5, 6, 15)	HS (not included: 5, 6, 15), >120 min only	HS(not included: 5, 6, 15)	HS (not included: 5, 6, 15), >120 min only
Mean Skin	34.93	38.15	3.22	35.87	36.76	0.90	35.81	36.76	0.96	-0.94	-0.88	2.32	2.26
Core	37.17	39.03	1.86	37.16	38.01	0.85	37.20	38.01	0.81	0.01	-0.02	1.01	1.05
Head Tsk	35.79	38.16	2.37	36.21	36.66	0.45	34.47	36.66	2.19	-0.42	1.32	1.92	0.18
Chest Tsk	35.67	38.11	2.44	34.44	36.40	1.96	34.47	36.40	1.92	1.23	1.19	0.48	0.51
Back Tsk	35.25	38.03	2.78	36.47	36.74	0.27	36.30	36.74	0.43	-1.22	-1.06	2.51	2.35
Pelvis Tsk	35.33	38.08	2.75	N/A	N/A	N/A	N/A	N/A	N/A	N/A	N/A	N/A	N/A
Left Upper Arm Tsk	34.83	38.22	3.39	N/A	N/A	N/A	N/A	N/A	N/A	N/A	N/A	N/A	N/A
Right Upper Arm Tsk	34.90	38.23	3.33	38.38	37.16	-1.22	38.44	37.16	-1.28	-3.48	-3.55	4.55	4.62
Left Lower Arm Tsk	34.54	38.31	3.77	N/A	N/A	N/A	N/A	N/A	N/A	N/A	N/A	N/A	N/A
Right Lower Arm Tsk	34.59	38.31	3.72	37.95	36.41	-1.53	37.88	36.41	-1.47	-3.35	-3.29	5.26	5.19
Left Hand Tsk	33.48	38.27	4.79	N/A	N/A	N/A	N/A	N/A	N/A	N/A	N/A	N/A	N/A
Right Hand Tsk	33.42	38.23	4.81	N/A	N/A	N/A	N/A	N/A	N/A	N/A	N/A	N/A	N/A
Left Thigh Tsk	35.34	38.10	2.76	N/A	N/A	N/A	N/A	N/A	N/A	N/A	N/A	N/A	N/A
Right Thigh Tsk	35.33	38.10	2.77	35.10	36.26	1.16	34.96	36.26	1.30	0.23	0.37	1.60	1.46
Left Lower Leg Tsk	35.11	38.13	3.02	N/A	N/A	N/A	N/A	N/A	N/A	N/A	N/A	N/A	N/A
Right Lower Leg Tsk	35.12	38.13	3.01	35.61	37.61	2.00	35.59	37.61	2.02	-0.49	-0.47	1.01	0.99
Left Foot Tsk	33.03	38.06	5.02	N/A	N/A	N/A	N/A	N/A	N/A	N/A	N/A	N/A	N/A
Right Foot Tsk	33.03	38.05	5.03	N/A	N/A	N/A	N/A	N/A	N/A	N/A	N/A	N/A	N/A

**Table 5.12 Baseline sweat total comparison: Whole Body Average ReCl Sweat Rate Modified Multi-Node Model vs. Human Subject sweat rates with human subject results as the comparator.**

Sweat Totals	Whole Body Average ReCl Sweat Rate Modified Multi-Node Model	Human Subjects (not included: 5, 6, 15)	Human Subjects (not included: 5, 6, 15), >120 min only
Total Sweat (kg)	2.50	2.28	2.45
Error Value (kg)	N/A	0.22	0.05
% Error	N/A	9.44	1.96

**Table 5.13 Improvement in core temperature change between Whole Body Average ReCl Sweat Rate Modified Multi-Node Model vs. Standard multi-node model.**

	Human Subjects (not included: 5, 6, 15)	Human Subjects (not included: 5, 6, 15), >120 min only
Multi-node to Human Subject Error °C	1.54	1.58
Whole Body Average ReCl Sweat Rate Modified Multi-Node Change to Human Subject Error °C	1.01	1.05
Difference °C	0.53	0.53
% Difference	34.40	33.60

The average  $Re_{cl}$  value does help improve the sweat rate prediction slightly bringing the core temperature change to within 1.01 °C to 1.05 °C. The sweat rate prediction is still very close to that of the human subject results differing by from 0.22 kg to 0.05 kg. However, the average  $Re_{cl}$  value applied over the entire body surface does not take into account the local effects from convection coefficients to sweat rates.

The TAItherm model does provide the ability to define and simulate the radiant conditions with more precision than in the two-node model. This is also coupled with the unrealistic skin and core temperatures in the multi-node model. From the results, the solar



spectrum radiation dominated both convection and long wave radiation. The solar spectrum provided a constant 57.7 W of energy to the body, compared with the approximately 25 W from long wave radiation and 8 W from convection. The increase in the temperature of the clothing surface and skin temperature eventually turn the convection coefficient into -25 W, where convection is removing heat from the body. With the skin temperature not calculated correctly by the multi-node model, and the interference with clothing, the convective value may or may not be representative of the actual total energy transfer in the human subject tests.

### **5.3 Conclusions**

The Elson spot model presented here in Section 5.1.2 allowed for the use of the ASHRAE two-node model in simulating human subject results where fabric wetting is a known possibility. The standard two-node model was not capable of simulating the tested conditions because of the sweat rate and non-wetting clothing assumption. This created unrealistic core and skin temperatures. The presented wetted clothing model is capable of handling the baseline simulation total energy balance over the course of the test. A time dependent sweat rate gain factor may provide a better fit to the human subject results, but more information is required to implement that feature. Breaking the model down into different surface segment areas with strictly defined properties is another possible way forward to incorporating the lowered  $Re_{Cl}$  value or the wetted spot model.

The multi node model has been validated many times covering thermal comfort and thermal sensation related activities. The clothing and equipment in the application have pushed the model to its boundaries with the unique case of the soldier. The advantages of employing a complex model are unfortunately also its downfalls. The local sweat rates, thermal and evaporative resistances, as well as convection coefficients make knowledge of the exact

conditions on a segment extremely important. Similarly, the time dependent sweat rate is an important feature for accuracy in both models. However, in the multi-node model not allowing that sweat to wick and/or drip outside the relatively impermeable coverage area does not allow for a reasonable estimate of a reduced  $Re_{Cl}$  value. Also, the lowered  $Re_{Cl}$  value is closer to the human subject results demonstrating that the local sweat rates coupled with local clothing wettedness is the likely cause of the poor prediction capability. Accounting for differences in fitment between the thermal manikin and humans and the possibility of movement related pumping under the armor remain possibilities to improve the prediction capabilities. Although both models have some limitations, it will be illustrative to model the two-node model and the more advanced multi-node model to compare PCS results and examine the effects of the PCS, the main focus of this work.

## **Chapter 6 - Comparison of PCS results to models**

The focus of this work has been to analyze the effects of PCS on humans in order to determine their usefulness and areas for improvement. The previous chapter illustrated the ability of two different human thermal models to predict primary indicators of heat stress: core temperature and sweat rate. In that chapter, it was shown that wet clothing must be included in this case. The introduction of a clothing wetting effect resolved the energy balance on the body and improved model predictions. The sweat rate of the model was also adjusted to match the human subject results to ensure the water mass balance was accurate. Although, the core temperature does not track precisely in the baseline, the theoretical total energy exchange has been improved and predicts these values well in the modified baseline tests, thus allowing the PCS modeling to proceed with reasonable confidence.

Using the modified and unmodified baseline human models, the PCS systems will be simulated and the results compared to the human subjects to observe how the cooling systems are affecting the body. Our hypothesis, from previous work, was that the body had lessened its active cooling mechanisms when provided with cooling from the PCS. Thanks to the work on the baseline models in Chapter 5, the human models can incorporate the cooling effects from the thermal manikin tests and be expected to predict the core temperature with reasonable accuracy. This chapter is similar in structure to Chapter 5 where the two-node model will be presented first followed by the multi-node TAItherm model. In the respective sections, the four PCS will be compared to its respective human subject result. As a reminder, a brief description can be found in below in a modified version of Table 3.6. A more detailed description can be found in Chapter 3 followed by the discussion of the findings of this complete work in Section 6.3.

**Table 6.1 Personal cooling systems (PCS) tested on human subject and to be compared to human thermal models**

<b>PCS Name</b>	<b>Weight of PCS</b>	<b>Avg. Cooling Power Total (W)</b>	<b>PCS System Description</b>
PCS #1: Ventilation Vest	0.995 kg 2.19 lb.	100.3	Air Circulation vest worn under the body armor with two front mounted, battery-powered blowers at the bottom of the vest. Blowers force ambient air under the vest into passages maintained by flexible mesh material.
PCS #9: PCVZ-KM Zipper Front Vest by Polar Products	2.681 kg 5.91 lb.	96.9	Phase Change Material (PCM) vest worn under the body armor with four packages of PCM two in front and two in the back of the vest. PCM material freezing temperature < 0 °C but different from PCS# 12.
PCS #12: Cool UnderVest by Steele	3.499 kg 7.71 lb.	113.0	Phase Change Material (PCM) vest worn under the body armor with four packages of PCM two in front and two in the back of the vest. PCM material freezing temperature < 0 °C but different from PCS# 9.
PCS #20 Hummingbird II	5.108 kg 11.26 lb.	124.6	Vapor Compression Refrigeration Cycle system with a liquid cooling garment (LCG) acting as the evaporator section of the cycle. Compressor and heat exchanger worn in a box attached to the back of the body armor and the battery was attached to the front of the armor.

The general approach in both models was the same with the exception of having control of the location and intensity of cooling in the multi-node TAITherm model. The PCS were measured on the thermal manikin as described in Section 3.2.3. The manikin was wearing the base ensemble and was tested at isothermal conditions. Although the conditions in the human subject testes were different from those in the manikin tests, it was assumed that due to the resistance of the plate body armor the cooling effect on the humans in terms of heat flux would

be similar. A likely discrepancy in the cooling effects of the cold boundary systems; 9, 12, and 20 would be slightly less cooling to the body due the PCS gaining more energy from the environment than in the isothermal tests. There is also an uncertainty created by the human skin temperature, which could be higher or lower than the isothermal manikin surface temperature of 35 °C. Although, the torso skin temperature was measured, sometimes the thermocouple was located directly against a cooling packet or evaporator tube, which can cause a lower measured skin temperature. The torso temperature of PCS 1 is only exposed to ambient conditions and therefore this discrepancy is not expected from this system. The thermal manikin results were applied as a function of time to the PCS simulations.

## 6.1 Two-node model PCS comparison

The two-node model used our thermal manikin PCS results as the PCS cooling input. The time resolved PCS cooling was applied in the skin energy equation, because that is where the PCS interacts with the body. In the unmodified two-node model, the addition of the cooling term for a time step,  $E_{PCS,i}$ , can be seen in Equation ( 6.1 ) and the modified two-node model in Equation ( 6.2 ).

$$T_{sk, i+1} = \frac{-[(C + R) + E_{sk} + E_{PCS,i} + (K + \rho_{bl} \cdot Q_{bl} \cdot Cp_{bl}) \cdot (T_{cr,i} - T_{sk,i})]}{\frac{\alpha_{sk} \cdot m_b \cdot C_{sk}}{A_D \cdot \Delta t}} + T_{sk,i} \quad (6.1)$$

$$T_{sk, i+1} = \frac{-[(1 - w_c) \cdot [(C + R) + E_{sk}] + \epsilon_s \cdot w_c \cdot E_{spot} + E_{PCS,i} + (K + \rho_{bl} \cdot Q_{bl} \cdot Cp_{bl}) \cdot (T_{cr,i} - T_{sk,i})]}{\frac{\alpha_{sk} \cdot m_b \cdot C_{sk}}{A_D \cdot \Delta t}} + T_{sk,i} \quad (6.2)$$

### 6.1.1 PCS #1 Entrak Ventilation Vest

The Ventilation Vest from Entrak showed an average of 125 W of cooling on the thermal manikin. The average subject two-node models are compared to the average of the subjects in the

graph showing the core and mean skin temperatures.

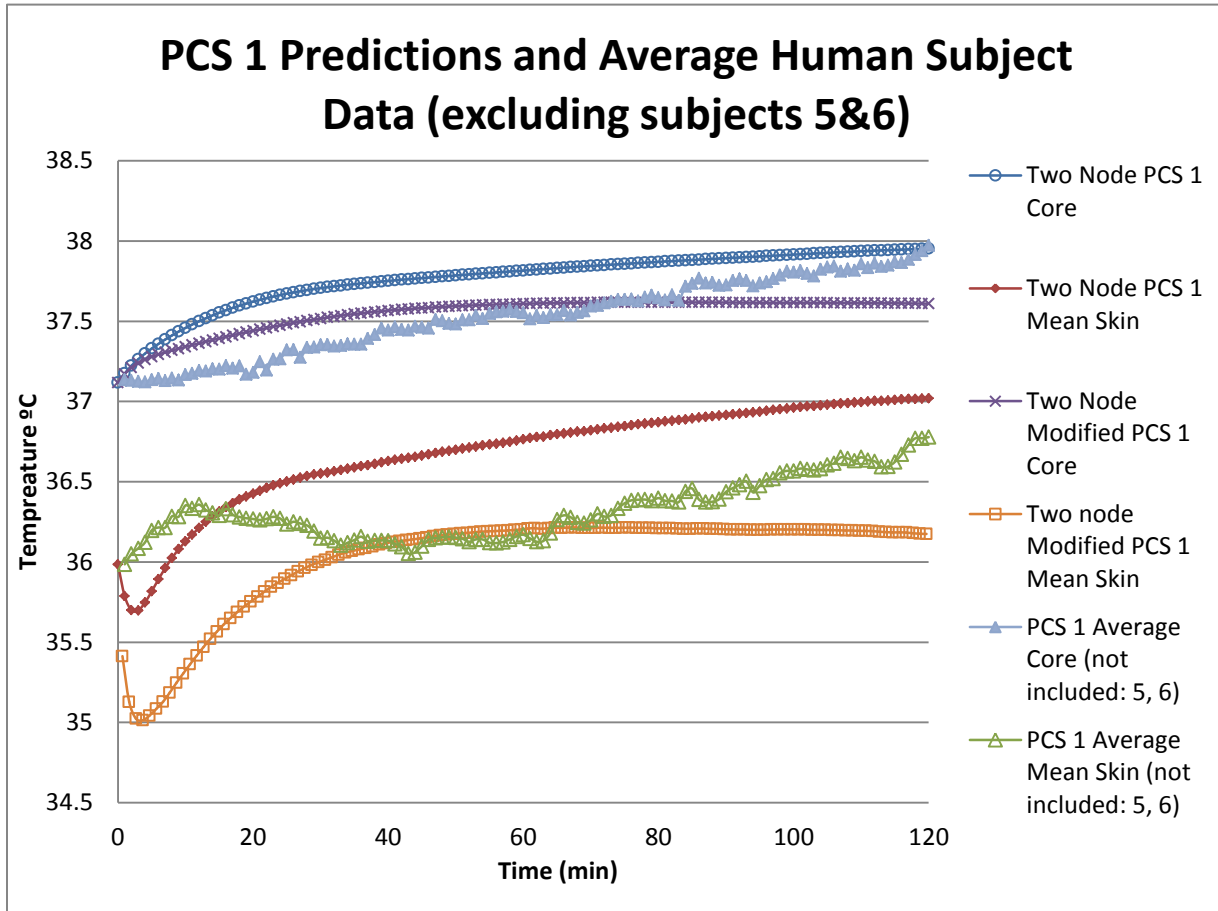


**Figure 6.1 PCS #1 Ventilation Vest by Entrak core and mean skin temperature results of the Unmodified (TN) and Modified Two-Node Model (TNM) compared to the average Human Subject (HS) results, not including subjects 5 and 6**

The graph shows the remarkable similarity between the two-node models and the average human subject results for both skin and core temperature. This is one of the closest matching skin temperatures, likely because of the measured torso skin temperatures are on a neutral location as mentioned early in the chapter. A comparison of the core temperature and total sweat production of the unmodified two-node is shown on the table for each subject. Average results are shown on the bottom of the table.

**Table 6.2 PCS #1 Ventilation Vest by Entrak results of Unmodified Two-Node Model (TN)**

Subject #	TcoreHS	TcoreTN	TcoreTN- TcoreHS	SWHS	SWTN	SWTN- SWHS	TN Evap Sweat
	°C	°C	°C	kg	kg	kg	kg
1	39.02	38.82	-0.20	1.724	1.392	-0.332	0.891
2	37.67	37.86	0.19	1.690	0.785	-0.905	0.718
3	37.05	36.74	-0.31	2.324	1.028	-1.296	0.932
4	37.71	38.17	0.46	2.732	1.054	-1.678	0.882
7	38.48	38.94	0.46	2.090	0.978	-1.112	0.891
8	38.00	37.93	-0.07	2.290	1.088	-1.202	0.967
9	37.91	37.48	-0.43	2.898	1.260	-1.638	0.957
10	37.85	37.47	-0.38	2.272	0.900	-1.372	0.823
11	39.01	39.06	0.05	1.568	1.300	-0.268	0.852
12	38.21	39.33	1.13	2.070	1.355	-0.715	0.830
Average of subjects	38.09	38.18	0.09	2.166	1.114	-1.052	0.874
Standard Deviation	0.613	0.839	0.486	0.4349	0.2044	0.4934	0.0738
Average Subject	38.17	38.12	-0.05	2.166	1.066	-1.100	0.885

The unmodified two-node model provides a reasonable average prediction of the final core temperature, but not for individual human subjects, specifically subject #12. The predicted sweat rate for the two-node model is lower than that measured in the human subject tests by about 1 kg. This may be due to the effect of modeling ambient air circulation system as a heat flux device. The results of the modified two-node PCS model are shown in the table below including the wetted spot and sweat rate additions.

**Table 6.3 PCS #1 Ventilation Vest by Entrak results of Modified Two-Node Model (TNM)**

Subject #	TcoreHS °C	TcoreTN °C	TcoreTN-TcoreHS °C	SWHS kg	SWTN kg	SWTN-SWHS kg	TN Evap Sweat kg
1	39.02	38.53	-0.49	1.724	1.287	-0.437	1.029
2	37.67	37.62	-0.05	1.690	0.906	-0.784	0.793
3	37.05	36.29	-0.77	2.324	2.034	-0.290	1.443
4	37.71	37.72	0.01	2.732	1.627	-1.105	1.211
7	38.48	38.71	0.23	2.090	1.281	-0.809	1.042
8	38.00	37.70	-0.30	2.290	1.443	-0.847	1.164
9	37.91	37.12	-0.79	2.898	1.549	-1.349	1.203
10	37.85	37.15	-0.70	2.272	1.325	-0.947	1.039
11	39.01	38.97	-0.05	1.568	1.082	-0.486	0.906
12	38.21	38.47	0.26	2.070	1.760	-0.310	1.243
Average of subjects	38.09	37.83	-0.26	2.166	1.430	-0.736	1.107
Standard Deviation	0.613	0.843	0.404	0.4349	0.3294	0.3510	0.1852
Average Subject	38.17	37.83	-0.34	2.166	1.402	-0.763	0.875



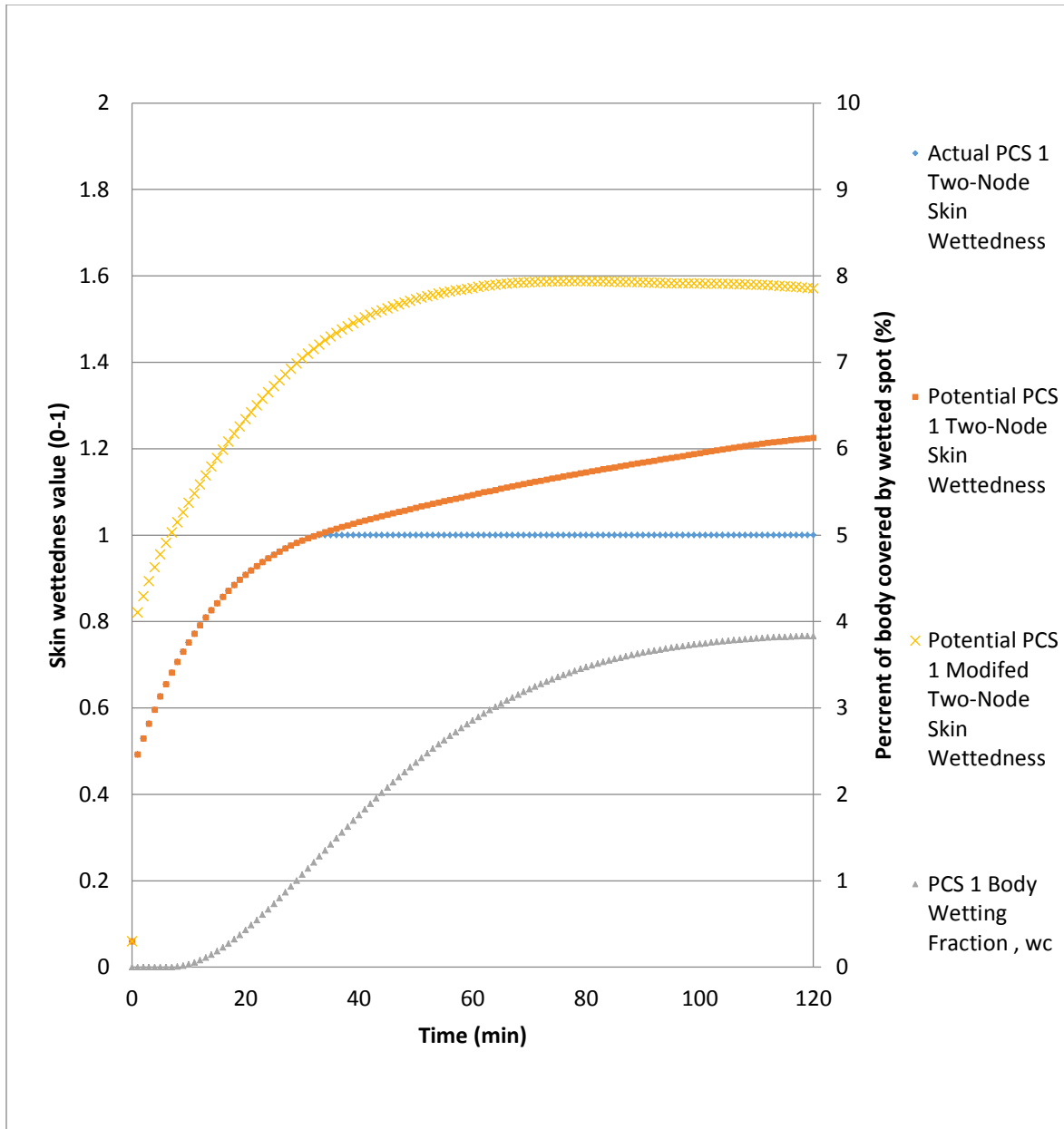


**Figure 6.2 PCS #1 skin wettedness on left axis for unmodified and modified two-node models including potential and actual skin wettedness for unmodified two-node model. Percent of body surface covered by wetted spot in the modified two-node model is on right axis**

The modified two-node model with PCS #1 predicts the average of the subjects within 0.26 °C for core temperature, but predicts 0.763 kg less sweat than was produced on average by the subjects. Furthermore, prediction of the individual subject temperature improved with the inclusion of the wetted spot and sweat function. However, the significant difference in the ability

to predict the total sweat of the subjects in the modified two-node model still exists. Again, this may be due to how the cooling was applied in the model from the manikin results. The thermal manikin measured the heat removal from an unrealistic 100% saturation of the manikin surface. This condition is not reasonably feasible for a human under steady state conditions without supplementary water added. The simulated human may have reduced the sweat rate in reaction to the over prediction of heat removal by the thermal manikin. As shown in Figure 6.2, the potential sweat of the unmodified test was lower than that of the baseline, and only slightly higher than the actual 100% wetted case. However, with the modified two-node mode, the skin wettedness would have been at 100% for most of the test, causing the spot to appear and grow to approximately 3.8% of the body surface area, seen on the right axis. Of note is that the unmodified and modified two-node models bracketed the measured core temperature indicating that the actual solution is between the two. In the case of the Air Circulation system, some, or all of the lack in sweat predicted in the two-node model compared to the human subjects was actually used to provide the cooling to the humans.

### ***6.1.2 PCS #9 PCVZ-KM Zipper Front Vest by Polar Products***

The PCVZ-KM Zipper Front Vest by Polar Products predicted an average of 96.9 W. PCS #9 is a PCM based system. As the PCM systems begin to change phase, the side of the PCM packet exposed to the body melts creating a thermal resistance between the frozen, constant temperature material and the body, raising the surface temperature of the packet and lowering the heat flux. The time dependent heat removal values from the manikin were used to help compensate for this effect. The modified and unmodified two-node model predictions are compared to the human subject skin and core results in the figure below.

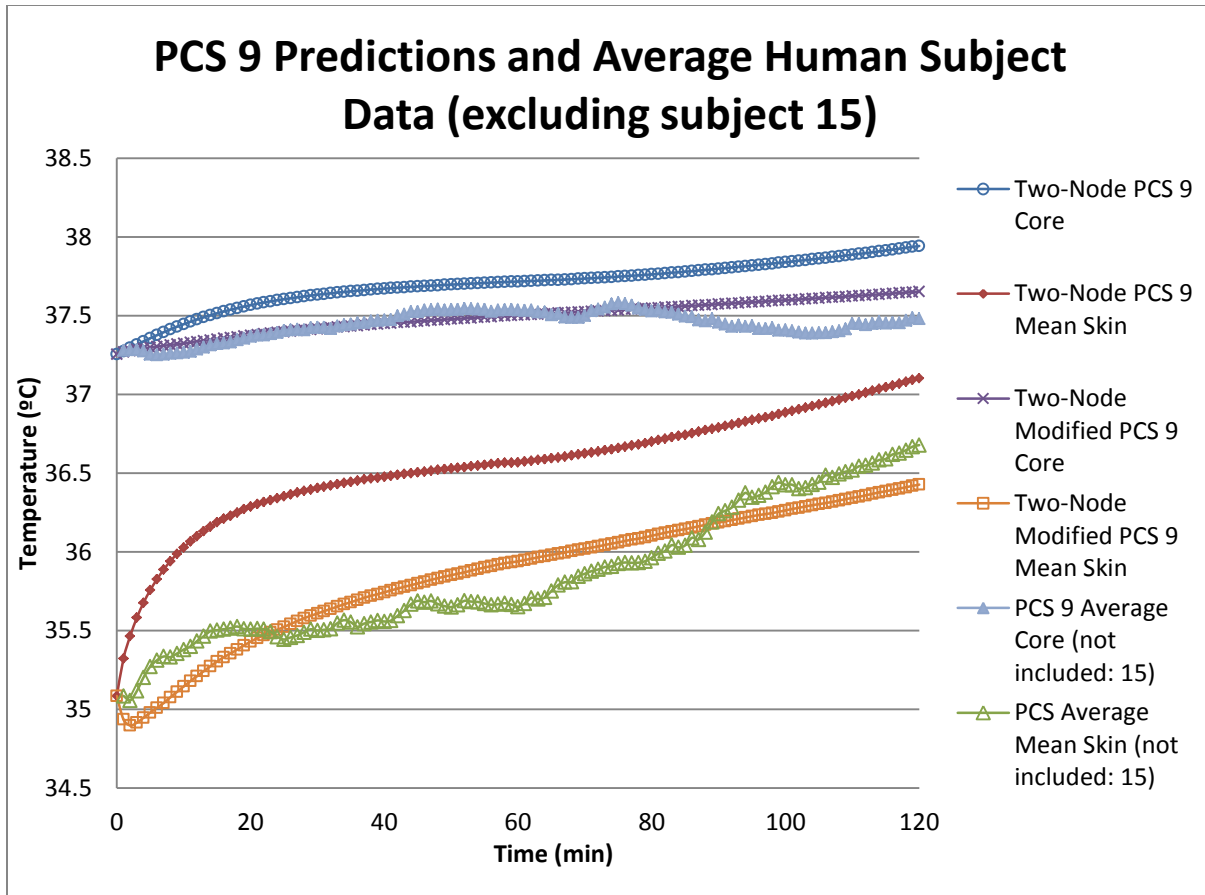


**Figure 6.3 PCS #9 PCVZ-KM Zipper Front Vest by Polar Products core and mean skin temperature results of the Unmodified (TN) and Modified (TNM) Two-Node Model compared to the average Human Subject (HS) results, not including subjects 5 and 6.**

The graph shows reasonable agreement between the predicted and measured skin and core temperatures. For the unmodified two-node model, the lowered measured skin temperature shown may be due to the sensors being located under a frozen ice pack as described previously. However, the modified two-node model tracks well with the human subject results. The subject-by-subject unmodified two node model results can be seen in Table 6.4.

**Table 6.4 PCS #9 PCVZ-KM Zipper Front Vest by Polar Products results of Unmodified Two-Node Model (TN)**

Subject #	TcoreHS	TcoreTN	TcoreTN- TcoreHS	SWHS	SWTN	SWTN- SWHS	TN Evap Sweat
	°C	°C	°C	kg	kg	kg	kg
13	39.02	39.31	0.29	1.836	1.096	-0.740	0.846
14	37.67	38.00	0.33	1.414	0.901	-0.513	0.828
16	37.05	37.45	0.40	1.772	1.043	-0.729	0.901
17	37.71	39.12	1.41	2.362	1.202	-1.160	0.888
18	38.48	38.64	0.16	1.544	1.075	-0.469	0.778
19	38.00	38.24	0.24	2.466	0.936	-1.530	0.860
20	37.91	38.38	0.47	1.954	0.957	-0.997	0.861
21	38.91	39.69	0.78	2.136	1.157	-0.979	0.862
22	37.85	39.25	1.40	1.772	0.843	-0.929	0.752
23	39.01	39.00	-0.01	2.180	1.133	-1.047	1.007
24	38.21	38.88	0.67	1.772	0.933	-0.839	0.839
Average of subjects	38.17	38.72	0.56	1.928	1.025	-0.903	0.856
Standard Deviation	0.632	0.656	0.472	0.3284	0.1174	0.2993	0.0664
Average Subject	38.17	38.66	0.49	1.928	0.987	-0.941	0.860

The unmodified two-node model over-predicts the core temperature by 0.49-0.56 °C. More significantly the unmodified two node model under-predicts the production of sweat compared to the human subjects by approximately 0.90-0.94 kg. Therefore, it should be expected that the increase in sweat rate and the spot model used in the modified two-node model will improve prediction capabilities.

**Table 6.5 PCS #9 PCVZ-KM Zipper Front Vest by Polar Products results of Modified Two-Node Model (TNM)**

Subject	TcoreHS	TcoreTN	TcoreTN-TcoreHS	SWHS	SWTN	SWTN-SWHS	TN Evap Sweat
#	°C	°C	°C	kg	kg	kg	kg
13	39.02	39.10	0.08	1.836	1.165	-0.671	0.945
14	37.67	37.86	0.20	1.414	0.944	-0.470	0.861
16	37.05	37.33	0.27	1.772	1.128	-0.644	0.962
17	37.71	38.53	0.82	2.362	1.666	-0.696	1.211
18	38.48	37.94	-0.54	1.544	1.569	0.025	1.113
19	38.00	38.04	0.04	2.466	1.065	-1.401	0.934
20	37.91	38.02	0.11	1.954	1.498	-0.456	1.136
21	38.91	39.14	0.23	2.136	1.567	-0.569	1.151
22	37.85	39.14	1.29	1.772	0.905	-0.867	0.788
23	39.01	38.65	-0.36	2.180	1.799	-0.381	1.365
24	38.21	38.80	0.59	1.772	0.976	-0.796	0.865
Average of subjects	38.17	38.41	0.25	1.928	1.298	-0.630	1.030
Standard Deviation	0.632	0.613	0.512	0.3284	0.3251	0.3514	0.1771
Average Subject	38.17	38.37	0.20	1.928	1.291	-0.637	0.868

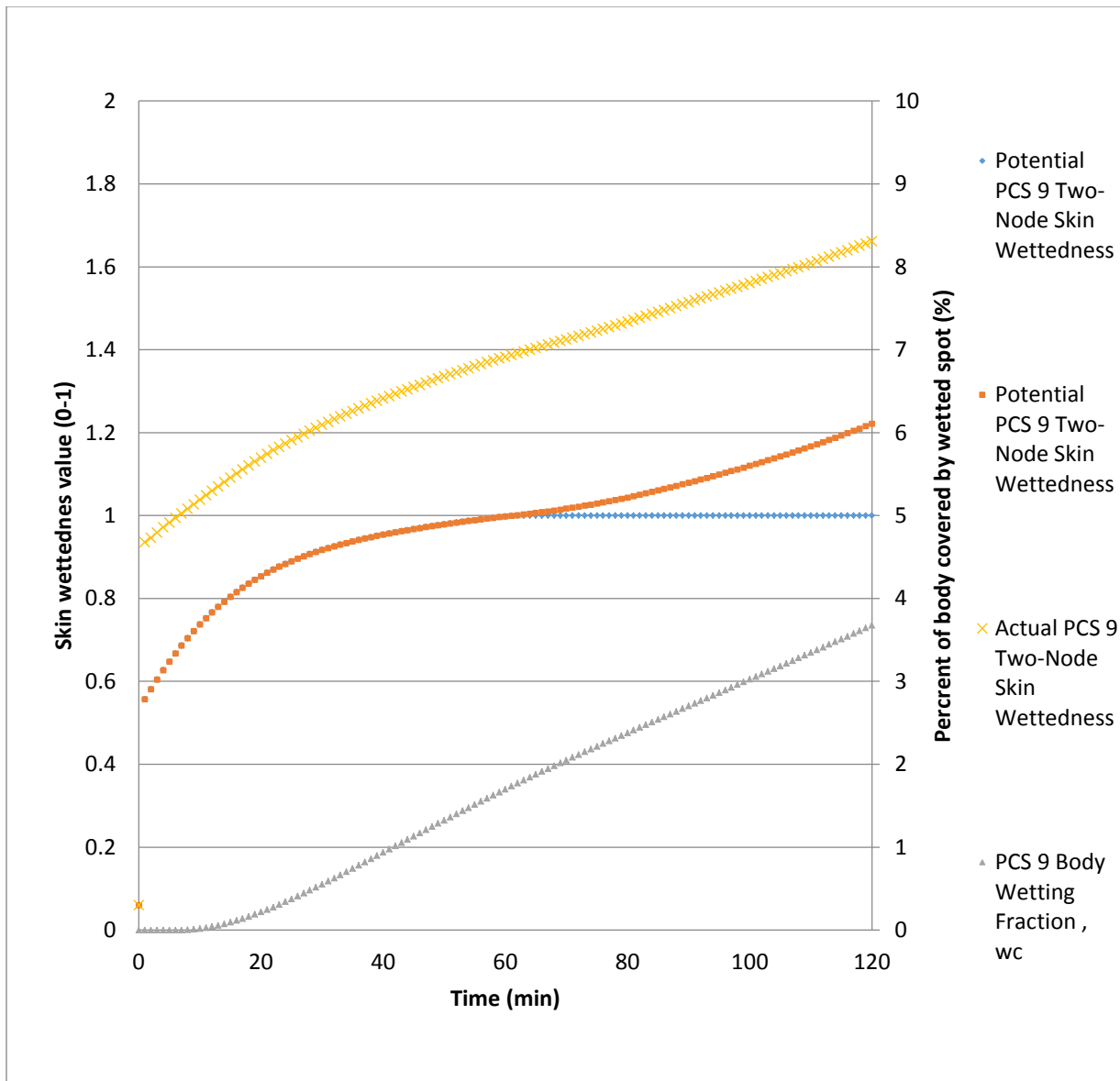


**Figure 6.4 PCS #9 skin wettedness on left axis for unmodified and modified two-node models including potential and actual skin wettedness for unmodified two-node model. Percent of body surface covered by wetted spot in the modified two-node model is on right axis**

The modified two-node model improves the prediction ability over the unmodified two-node model for PCS #9. This The core temperature prediction is closer, and the sweat rate prediction improves, this is because the skin wettedness level exceeds one for most of the test as seen in Figure 6.4 and the spot is able to grow because of the sweat rate modification. The

difference between the potential sweat and actual sweat seen in the difference between the skin wettedness for the unmodified two-node model further reinforces that the sweat rate is the issue in the program. The addition of the sweat rate and spot model allowed the skin wettedness to stay at 100% longer and for the spot size to grow to about 3.7% of the body surface, seen on the right axis. The PCS cooling in the two-node model uses the values from the thermal manikin, which maintained a constant 35 °C skin temperature in a 35 °C environment. The body does not maintain a constant skin temperature and some energy was likely lost to the environment from the PCM based system. The two-node model still under predicted the sweat rate by 0.637 kg. It is not surprising that the sweat rate is under-predicted. The modified two-node model over predicts the core and skin temperatures for much of the baseline tests while correctly predicting total sweat. A proportional gain factor was used to modify the sweat rate in the baseline data because there were no time dependent sweat results. This result is also seen in the predictions of the other cold-boundary PCS to follow. The modified two-node model over predicted the core temperature by 0.20 °C PCS demonstrating that more complex interactions are taking place that are not captured in the two node model. It is possible that further increasing the sweat gains would increase the ability of the modified two-node model to simulate the PCS results. Overall, this is a reasonably accurate simulation of PCS systems.

### ***6.1.3 PCS #12 Cool UnderVest by Steele***

The Cool UnderVest by Steele provided an average of 113 W over the two-hour thermal manikin tests. The Cool UnderVest is a PCM based system which started at a very high cooling rate and the rate decreased as the test proceed due to the development of a thermal resistance from the melting liquid in the PCM pack as described for PCS #9. The modified and unmodified

two-node model skin and core temperatures are compared to the average human subject results in Figure 6.5 as well as Table 6.6 and Table 6.7.

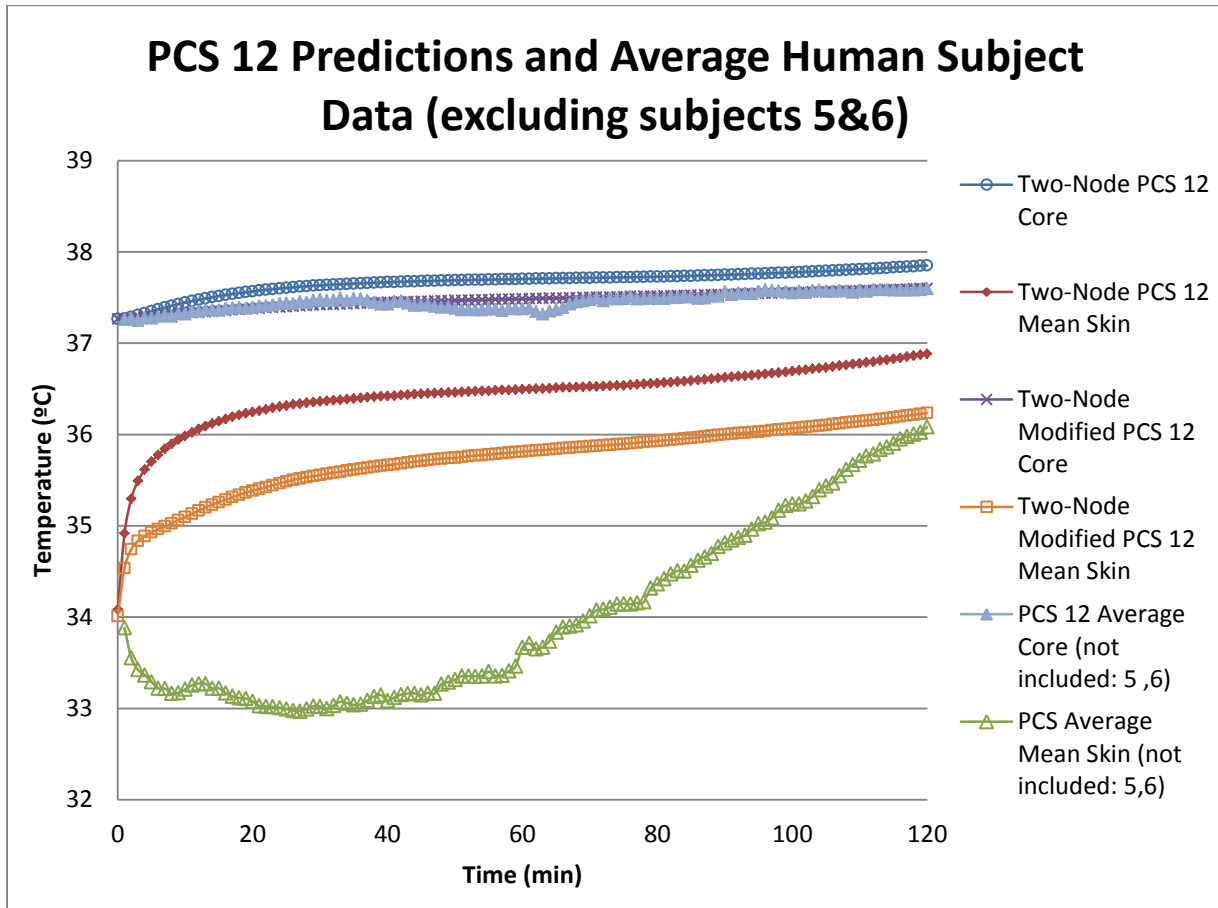


**Figure 6.5 PCS #12 Cool UnderVest by Steele core and mean skin temperature results of the Unmodified (TN) and Modified \*(TNM) Two-Node Model compared to the average Human Subject (HS) results, not including subjects 5 and 6.**

The average simulations for the unmodified and modified two-node model show a good agreement with the core temperature with the modified two-node model showing the better simulation of the measured results. The skin temperature predictions do not appear to match very closely. It is very likely that one or more of the skin temperature sensors under the PCS were in direct contact with the PCM pack, lowering the temperature of the sensor(s). It is also possible that PCS #12 caused more vasoconstriction than PCS #9 causing the models to lose fidelity. The



results of the unmodified two-node model for the Steele Cool UnderVest can be seen below in Table 6.6.

**Table 6.6 PCS #12 Cool UnderVest by Steele results of Unmodified Two-Node Model (TN)**

Subject #	TcoreHS °C	TcoreTN °C	TcoreTN-TcoreHS °C	SWHS kg	SWTN kg	SWTN-SWHS kg	TN Evap Sweat kg
1	39.02	39.43	0.41	1.430	1.093	-0.337	0.825
2	37.67	37.70	0.03	1.404	0.778	-0.626	0.710
3	37.05	37.65	0.60	1.936	0.924	-1.012	0.838
4	37.71	38.58	0.87	2.208	0.957	-1.251	0.857
7	38.48	38.94	0.46	1.764	0.884	-0.880	0.803
8	38.00	38.35	0.35	1.832	1.000	-0.832	0.897
9	37.91	37.92	0.01	1.636	0.998	-0.638	0.882
10	37.85	38.19	0.34	1.862	0.897	-0.965	0.818
11	39.01	39.98	0.97	1.254	1.162	-0.092	0.824
12	38.21	37.83	-0.37	1.790	1.374	-0.416	0.871
Average of subjects	38.09	38.46	0.37	1.712	1.007	-0.705	0.832
Standard Deviation	0.613	0.783	0.405	0.2852	0.1685	0.3517	0.0527
Average Subject	38.17	38.42	0.24	1.712	0.952	-0.759	0.848

The predicted core temperature results of the unmodified two-node model show good agreement on average with the human subject results giving a 0.24°C-0.37°C average difference between the unmodified two-node model and human subject results. The sweat rate predicted by the simulation shows the same lower values as the other PCS two node results, coming in about 0.7 to 0.76 kg lower than that produced by the human subject, although slightly better overall than the unmodified two-node models of PCS 1 and 9. The modified two-node model is shown below in Table 6.7.

**Table 6.7 PCS #12 Cool UnderVest by Steele results of Modified Two-Node Model (TNM)**

Subject #	TcoreHS °C	TcoreTN °C	TcoreTN-TcoreHS °C	SWHS kg	SWTN kg	SWTN-SWHS kg	TN Evap Sweat kg
1	39.02	39.30	0.28	1.430	1.060	-0.370	0.883
2	37.67	37.47	-0.19	1.404	0.886	-0.518	0.774
3	37.05	37.21	0.16	1.936	1.715	-0.221	1.221
4	37.71	38.23	0.52	2.208	1.487	-0.721	1.125
7	38.48	38.72	0.24	1.764	1.095	-0.669	0.911
8	38.00	38.15	0.15	1.832	1.234	-0.598	1.016
9	37.91	37.72	-0.19	1.636	1.203	-0.433	0.991
10	37.85	37.87	0.02	1.862	1.285	-0.577	1.017
11	39.01	39.95	0.94	1.254	0.999	-0.255	0.849
12	38.21	37.20	-1.00	1.790	1.763	-0.027	1.297
Average of subjects	38.09	38.18	0.09	1.712	1.273	-0.439	1.009
Standard Deviation	0.613	0.906	0.509	0.2852	0.2964	0.2210	0.1663
Average Subject	38.17	38.17	-0.01	1.712	1.240	-0.471	0.858

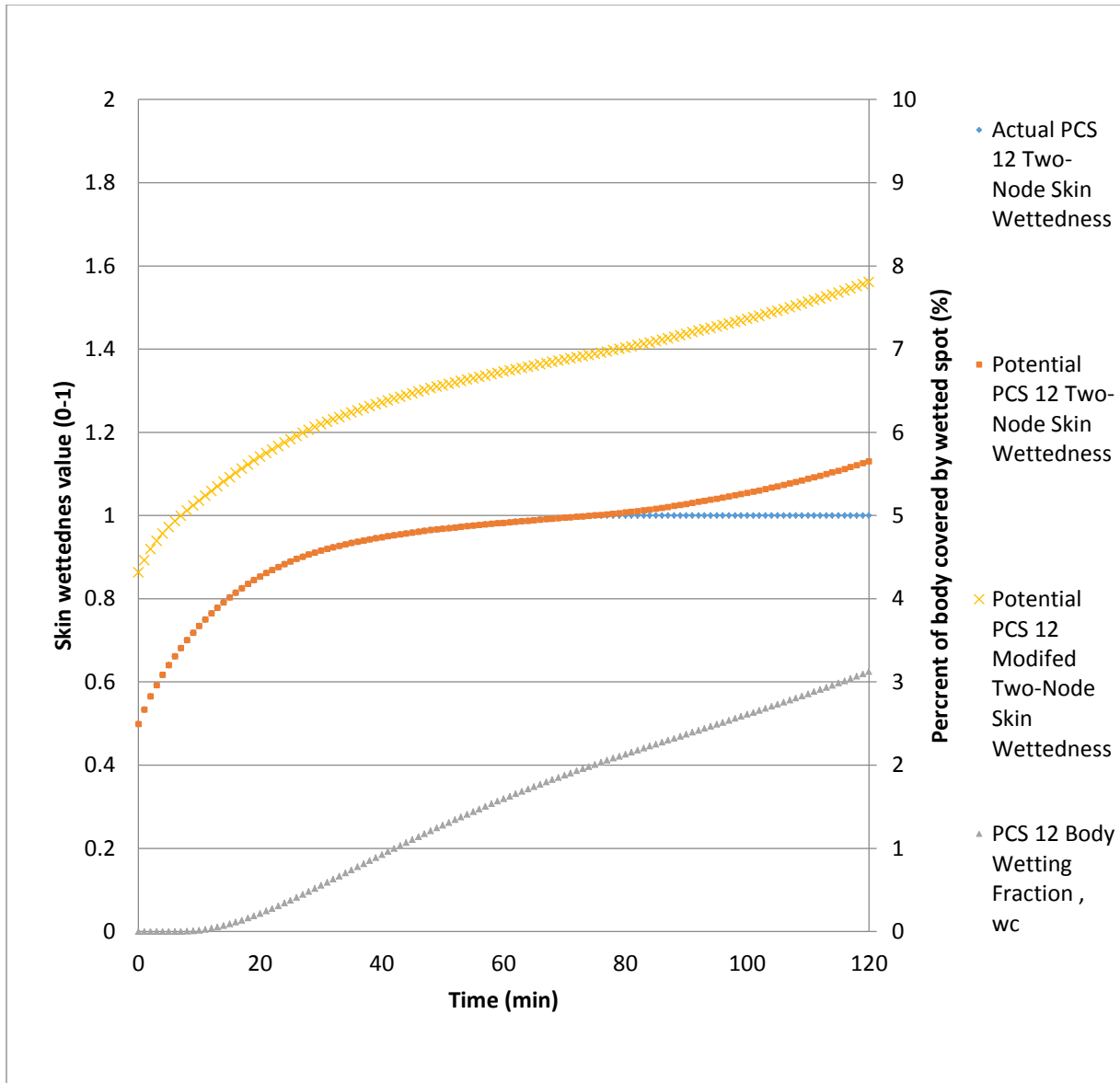


**Figure 6.6 PCS #12 skin wettedness on left axis for unmodified and modified two-node models including potential and actual skin wettedness for unmodified two-node model. Percent of body surface covered by wetted spot in the modified two-node model is on right axis**

The modified two-node model improves on the core temperature prediction over the unmodified model with an average difference to the measured results from 0.09 °C-0.01 °C. There is also an improvement in prediction of sweat rate, but the sweat production is still on average 0.439 kg to 0.0471 kg. Again, as described in the results for PCS #9, the Steele Cool

UnderVest is a PCM based system and does not provide a constant cooling rate. The lowering of the skin temperature will reduce heat transfer to the body by conduction. In addition, the packs may gain more energy from the environment in the higher temperature human subject tests than in the manikin testing. The single node skin temperature does not take into account possible local effects on the human body. However, both two-node models do an excellent job of predicting the core body temperature response of the Steele Cool UnderVest. The primary reason for the improvement of the modified two node model is because of the high skin wettedness and spot model shown in Figure 6.6. The modified two-node model allows the skin wettedness to remain at 100% for most of the test and for the spot to also grow for most of the test. Again, the modified two-node model is providing a good prediction of core temperatures for cold boundary PCS.

#### ***6.1.4 PCS #20 Hummingbird II by Creative Thermal Solutions (CTS)***

The Hummingbird II by Creative Thermal Solutions (CTS), PCS # 20, was the only vapor compression refrigeration cycle system evaluated. This system was unique compared to many vapor compression refrigeration cycle systems tested in the literature and in previous studies at Kansas State University. In many of these a liquid cooling garment filled circulating water was used, which exchanged heat with the refrigeration system through a heat exchanger. In the Hummingbird II, the vest was the evaporator of the cycle and acted as the heat exchanger as the refrigerant changed phase and expanded in the vest, absorbing energy. In the standard two-hour manikin tests it provided an average total of 124.6 W of cooling to the thermal manikin. The cooling from the Hummingbird II was almost steady providing a relatively constant heat flux to the fixed skin temperature of the manikin. The comparison of the modified and unmodified two-

node model skin and core temperatures to that of the human subject averages are shown in Figure 6.7.

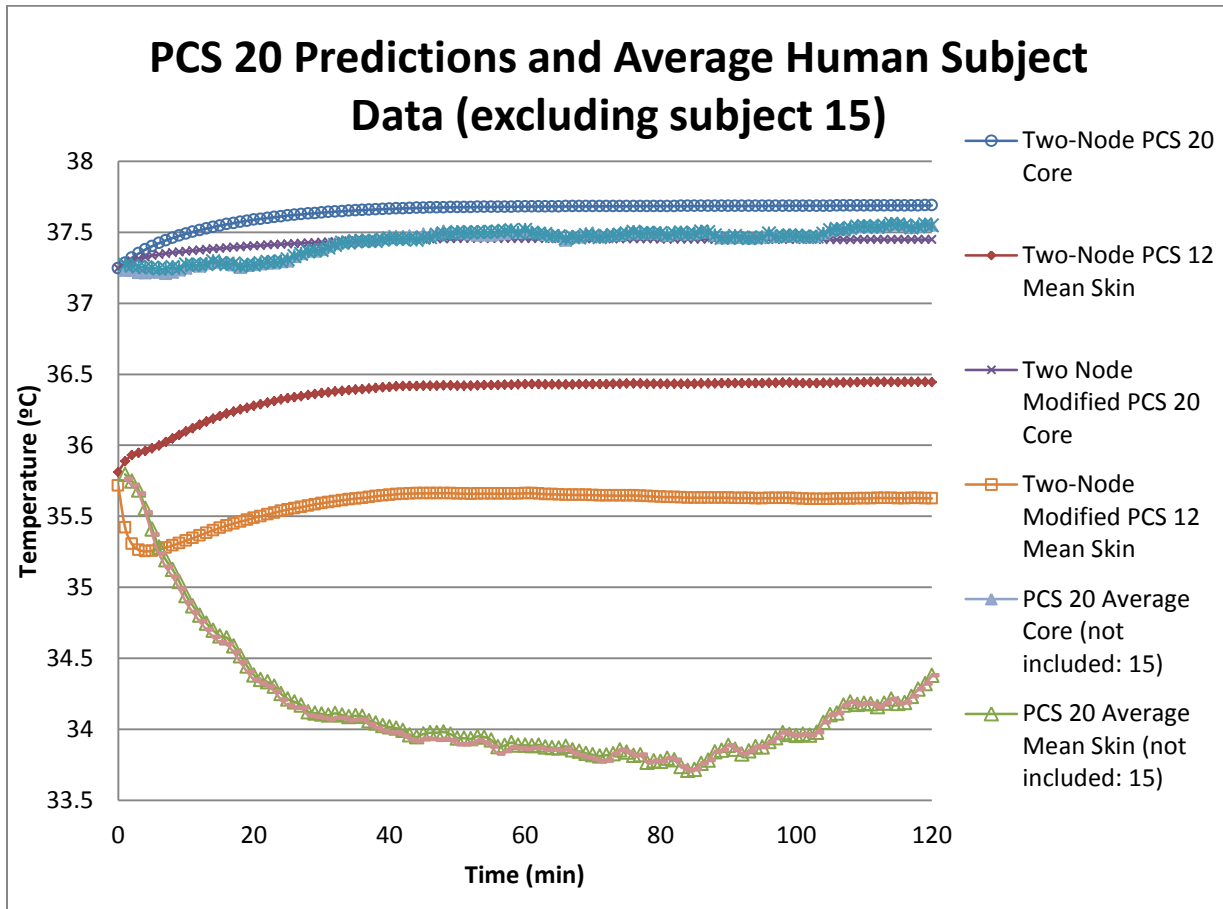


**Figure 6.7 PCS #20 Hummingbird II by Creative Thermal Solutions (CTS) core and mean skin temperature results of the Unmodified (TN) and Modified (TNM) Two-Node Model compared to the average Human Subject (HS) results, not including subject 15.**

As with the other systems, the cooling power at each minute was used in the calculation of the skin temperature by removing the energy from the skin node. The prediction of the core temperature for both the modified and unmodified two-node models compares well with the average of the human subjects. Again, as with the other cold boundary systems, the PCS can affect the sensors under the system coming by into contact with the temperature sensors. This

cannot be ruled out as the cause of the low measured skin temperatures. Another, possibility is that vasoconstriction occurred outside of the ability of the model to predict. In addition, the single skin node of the two-node model spreads out the effect of the cooling across the entire surface, and does not take into account intense local effects. The results of the unmodified two-node model can be seen in Table 6.8.

**Table 6.8 PCS #20 Hummingbird II by Creative Thermal Solutions (CTS) results of Unmodified Two-Node Model (TN)**

Subject #	TcoreHS °C	TcoreTN °C	TcoreTN-TcoreHS °C	SWHS kg	SWTN kg	SWTN-SWHS kg	TN Evap Sweat kg
13	39.02	39.29	0.27	1.136	0.486	-0.650	0.438
14	37.67	37.83	0.16	1.432	0.811	-0.621	0.744
16	37.05	37.46	0.40	1.538	0.911	-0.627	0.828
17	37.71	38.46	0.75	2.238	0.914	-1.324	0.829
18	38.48	38.40	-0.08	1.726	0.887	-0.839	0.755
19	38.00	37.39	-0.61	2.044	0.972	-1.072	0.885
20	37.91	37.98	0.07	2.768	0.883	-1.885	0.805
21	38.91	39.37	0.46	2.254	1.009	-1.246	0.840
22	37.85	38.72	0.87	1.954	1.183	-0.771	0.826
23	39.01	39.08	0.06	2.272	0.999	-1.273	0.912
24	38.21	38.49	0.28	1.956	0.905	-1.051	0.826
Average of subjects	38.17	38.41	0.24	1.938	0.905	-1.033	0.790
Standard Deviation	0.632	0.686	0.402	0.4589	0.1692	0.3877	0.1263
Average Subject	38.17	38.30	0.13	1.938	0.845	-1.093	0.833

The unmodified two node model core temperature came within 0.24 °C for the average of modeled subjects and 0.13 °C for the average subject compared to the average of human subjects. The sweat rate difference between the two-node model and the human subjects was 1.03 kg

lower than the human subjects for the average of modeled subjects and 1.093 lower for the average subject.

**Table 6.9 PCS #20 Hummingbird II by Creative Thermal Solutions (CTS) results of Modified Two-Node Model (TNM)**

Subject #	TcoreHS °C	TcoreTN °C	TcoreTN-TcoreHS °C	SWHS kg	SWTN kg	SWTN-SWHS kg	TN Evap Sweat kg
13	39.02	39.21	0.19	1.136	0.51686	-0.619	0.455
14	37.67	37.71	0.04	1.432	0.84700	-0.585	0.776
16	37.05	37.33	0.27	1.538	0.94420	-0.594	0.858
17	37.71	38.19	0.48	2.238	1.25191	-0.986	1.001
18	38.48	38.01	-0.47	1.726	1.32062	-0.405	0.992
19	38.00	37.16	-0.84	2.044	1.12004	-0.924	0.977
20	37.91	37.66	-0.25	2.768	1.29397	-1.474	1.033
21	38.91	39.02	0.11	2.254	1.37968	-0.874	1.060
22	37.85	38.38	0.53	1.954	1.25010	-0.704	0.983
23	39.01	38.76	-0.25	2.272	1.45085	-0.821	1.171
24	38.21	38.39	0.19	1.956	0.92940	-1.027	0.847
Average of subjects	38.17	38.16	0.00	1.938	1.119	-0.819	0.923
Standard Deviation	0.632	0.668	0.415	0.4589	0.2806	0.2905	0.1897
Average Subject	38.17	38.06	-0.11	1.938	1.08903	-0.849	0.852

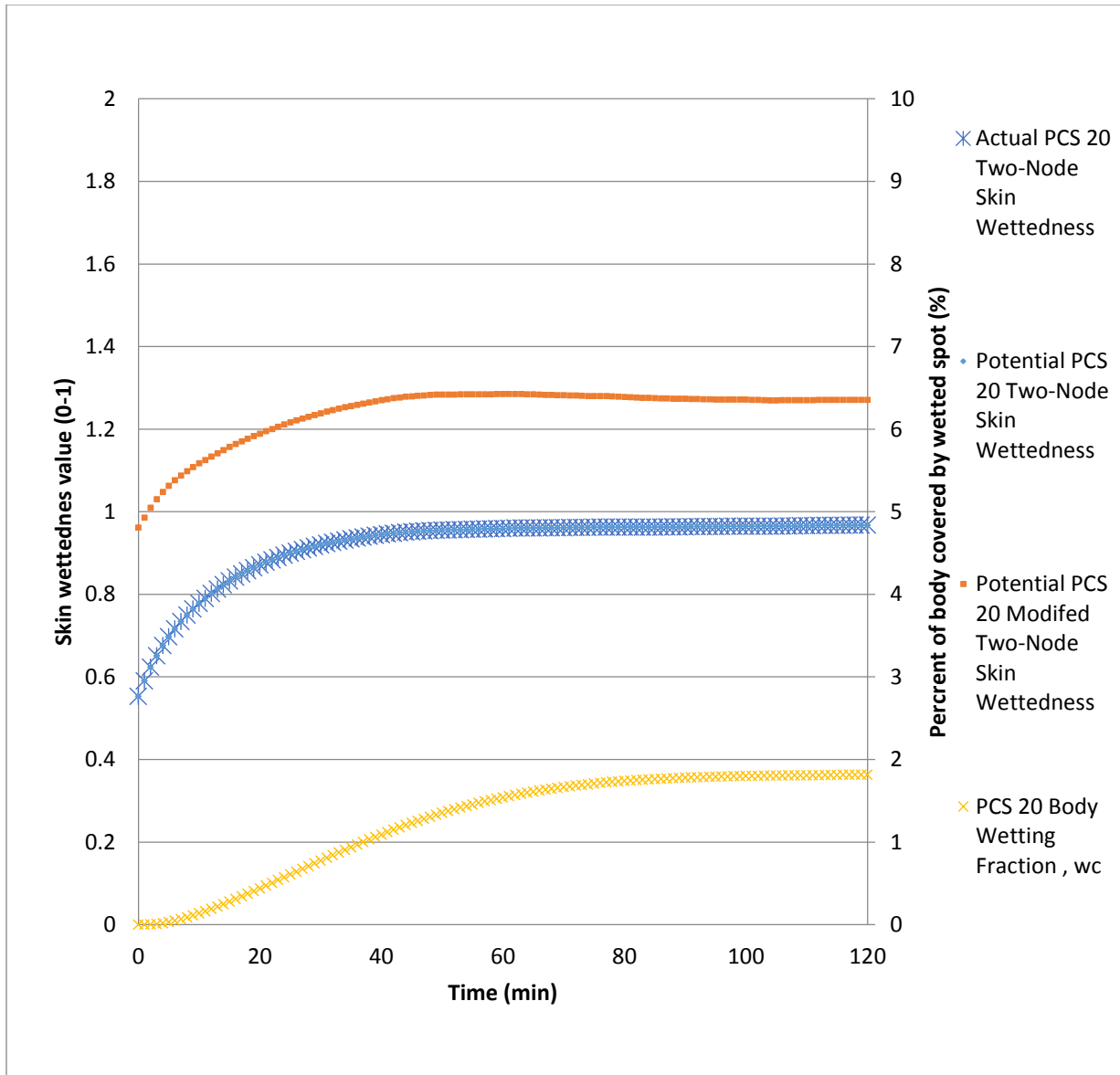


**Figure 6.8 PCS# 20 skin wettedness on left axis for unmodified and modified two-node models including potential and actual skin wettedness for unmodified two-node model. Percent of body surface covered by wetted spot in the modified two-node model is on right axis**

The modified two-node model results for core temperature and sweat rate compared to the human subject results are shown in Table 6.9. The modified two-node model core temperature change improved compared with the standard model. The difference in core temperature between the measured results and predicted results is 0.00°C for the average of the



subjects and 0.11 °C for the representative average subject. As seen in Figure 6.8, the predicted skin wettedness in the modified two-node model allows a wetted spot to form throughout the test. The unmodified two-node model never reaches 100% skin wettedness in the simulation so the potential and actual skin wettedness values are the same in this run. Again, the sweat rate term seems to be the unknown. Also, the PCS is likely not as efficient in the human subject test due to gains from the environment and the effects lowering the skin temperature has on the capacity and efficiency of the refrigeration unit. There may be a tradeoff between excess sweat contributing to the spot resulting from these efficiencies if known. This would help narrow the gap between the measured and simulated sweat rates. The modified two-node model predicts the core temperature PCS #20 well, but there is room for improvement in sweat rate and mean skin temperature predictions. This does provide confidence in using the modified two-node model for prediction of PCS capabilities.

## **6.2 Multi-Node Model PCS Comparison**

In section 5.2 the baseline results from the human subject tests were compared to a baseline multi-node model with multiple modifications. In this chapter, the multi-node model is compared against the PCS human subject results. The multi-node model allows for more precise application of cooling to the body on a segment or even element basis. The same initial conditions from the standard baseline tests were used in this case to simplify the modeling and to explore the ability of the standard multi-node model to PCS results.

Each section contains a table showing the differences between the simulated initial conditions and average human subject values. The cooling data from the thermal manikin results for the chest, shoulders, back, and stomach were used to simulate the cooling effect. In the case of PCS #9, #12, and #20 the cooling value removed from the segment was the same value

measured by the manikin, applied as a heat removal from the surface. As in the two-node model, the time dependent curve for each PCS head adsorption was loaded into TAITherm and used as the removal value but on a segmental basis. However, on PCS #1 it was possible to calculate the approximate convective heat transfer coefficients produced by the air circulation system under the body armor. This method was used as it would better represent the actual conditions. The results of each PCS tests and comparison to the multi-node model are provided in each subsection.

### **6.2.1 PCS #1 Entrak Ventilation Vest**

The Entrak system is an air circulation system forcing ambient air under the body armor and this provided a unique opportunity to use the sweating thermal manikin's ability to measure boundary conditions in a fundamental manner. The ASTM heat differential test determines the cooling power on the thermal manikin. The manikin surface temperature and air temperature are equal and the relative humidity is maintained at a constant value. The measured cooling power is the difference in heat flux from the PCS turned on over the when it turned off and only results from evaporation or conduction. Unlike the other PCS tested, this system did not provide a cold boundary and instead relied on evaporation. It was introduced in Section 2.2.2.4 that heat transfer under these test conditions involved mass transfer only. Therefore, it was possible to use Equation ( 2.30 ) to per segment calculate the evaporative heat transfer coefficient of the system from the heat flux difference and other measured conditions.

$$h_c = \frac{h_e}{LR} = \frac{q''}{LR \cdot (P_{sat}(T_{sk}) - \phi P_{sat}(T_a))} \quad ( 6.3 )$$

With the assumption that the surface was 100% wet and the knowledge of the incoming air at 40% relative humidity, the saturated pressure was calculated as a function of air temperature. Using the calculated Lewis Ratio, it was possible to calculate the convection

coefficients for the areas previously covered by body armor from the thermal manikin results using Equation ( 6.3 ).

In order to apply the convection coefficients to the torso area, the fabric layer was removed on the stomach, back, shoulders, and chest. The ambient air was applied to those segments with the convective heat transfer coefficients calculated for each found below in Table 6.10. This application method was possible because the thermal resistance of the shirt worn between the skin and the PCS is assumed included in heat transfer coefficient as shown in Equation ( 5.7 ).

**Table 6.10 Convection coefficients under the body armor including fabric resistance**

Segment	hc (W/m <sup>2</sup> K)
Chest	3.940664
Shoulders	2.682852
Stomach	5.459727
Back	1.391854
Front Average	4.700196
Back Average	2.037353

This leaves the possibility for these areas to be potentially impacted by radiation at a higher rate due to the removal of the high thermal resistance of the body armor. In order to simulate the insulation effects of the body armor the chest, stomach, back, and shoulder segments were offset by 10 mm away from the body to simulate the body armor and the armor's separation from the body formed by the PCS. The newly created body armor is modeled as 2 mm of canvas  $k = 0.3998 \text{ W/(mK)}$  on the either side of 25.4 mm of Kevlar  $k = 0.2596 \text{ W/(mK)}$ . The body armor interacts with the body and environment by radiation at the military clothing values given in Section 4.2.3. The outside of the armor experiences the same convection as the torso on the front and back as  $18.75 \text{ W/m}^2\text{K}$ . The inside of the body armor experiences convection on the

front and back as shown in Table 6.10 under front average and back average. Presented here are the core, mean skin, local skin, and torso temperatures in Figure 6.9, Figure 6.10, Figure 6.11, Figure 6.12, Table 6.10, and Table 6.11.

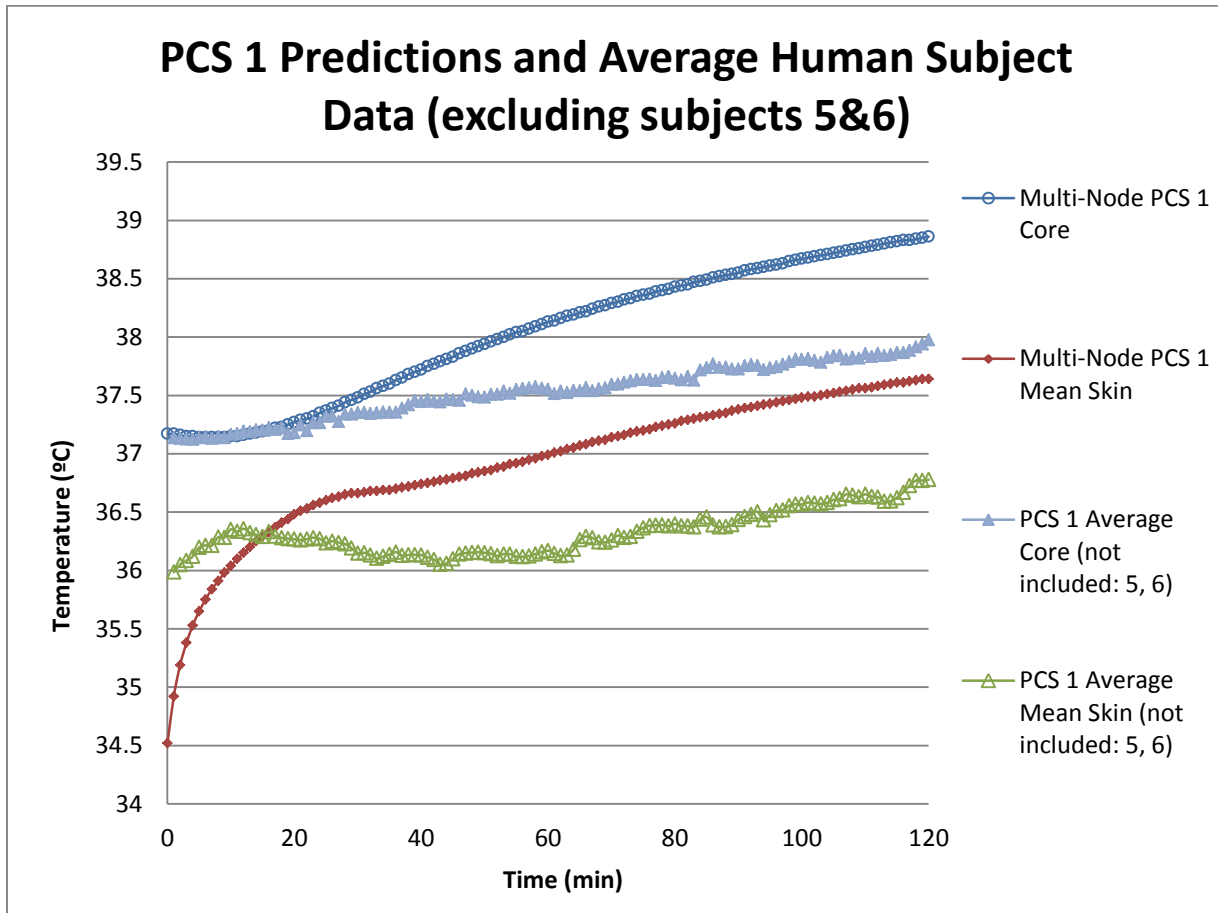


**Figure 6.9 PCS 1 Ventilation Vest by Entrak core temperature and mean skin temperature comparison graphs between average subject Standard Multi-Node Model and average Human Subject (HS) results.**

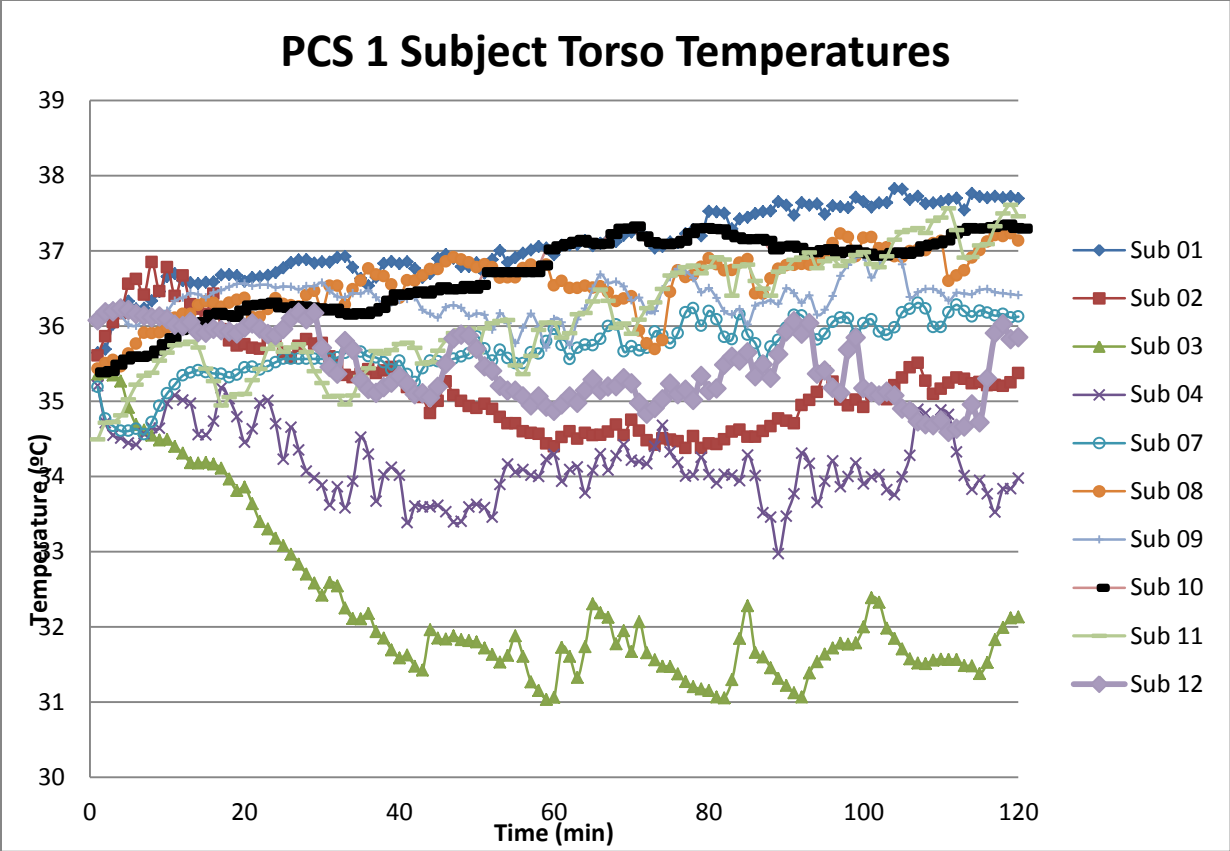


**Figure 6.10 PCS #1 Ventilation Vest by Entrak torso skin temperatures graphs of subject Human Subject (HS) to show trends in skin temperatures contacting PCS.**

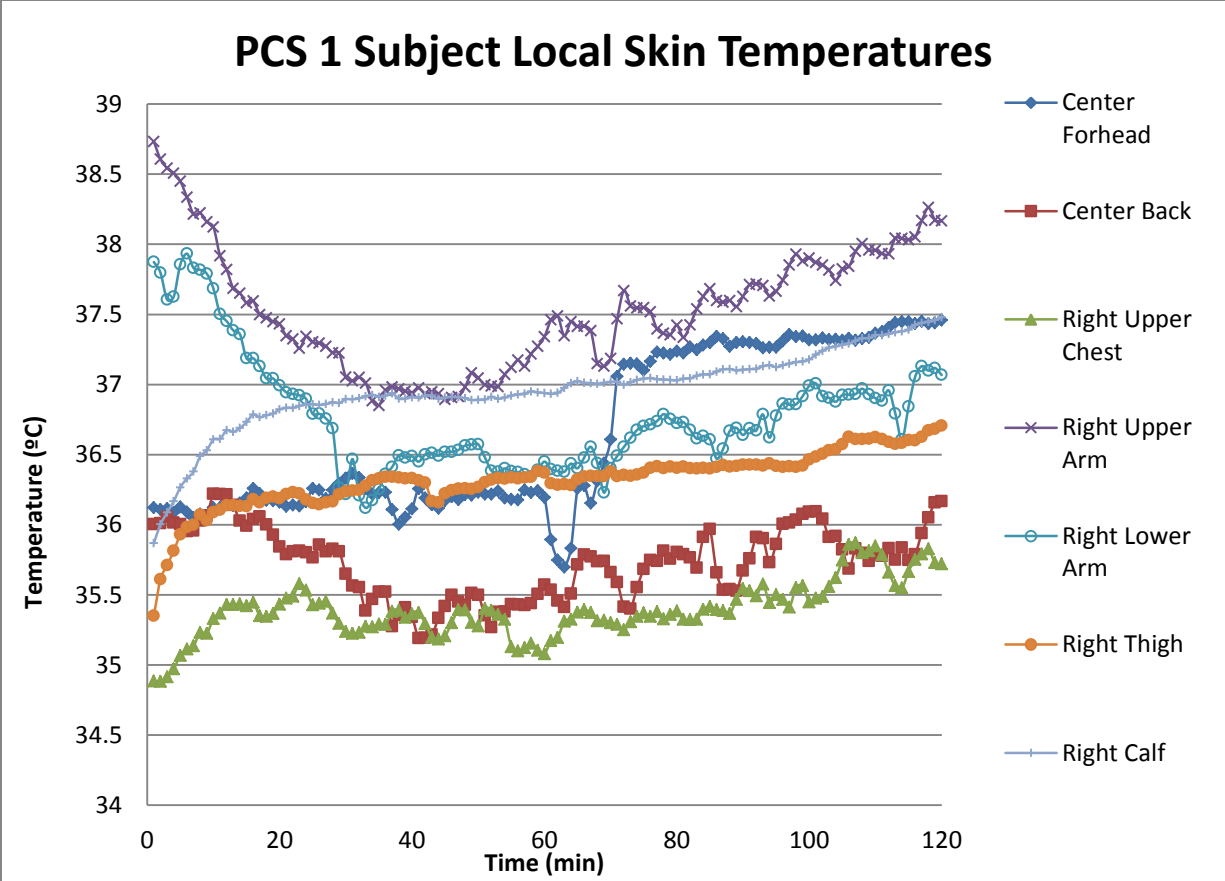


**Figure 6.11 PCS #1 Ventilation Vest by Entrak local skin temperature graph of average of Human Subject (HS) to show trends in external skin temperatures.**

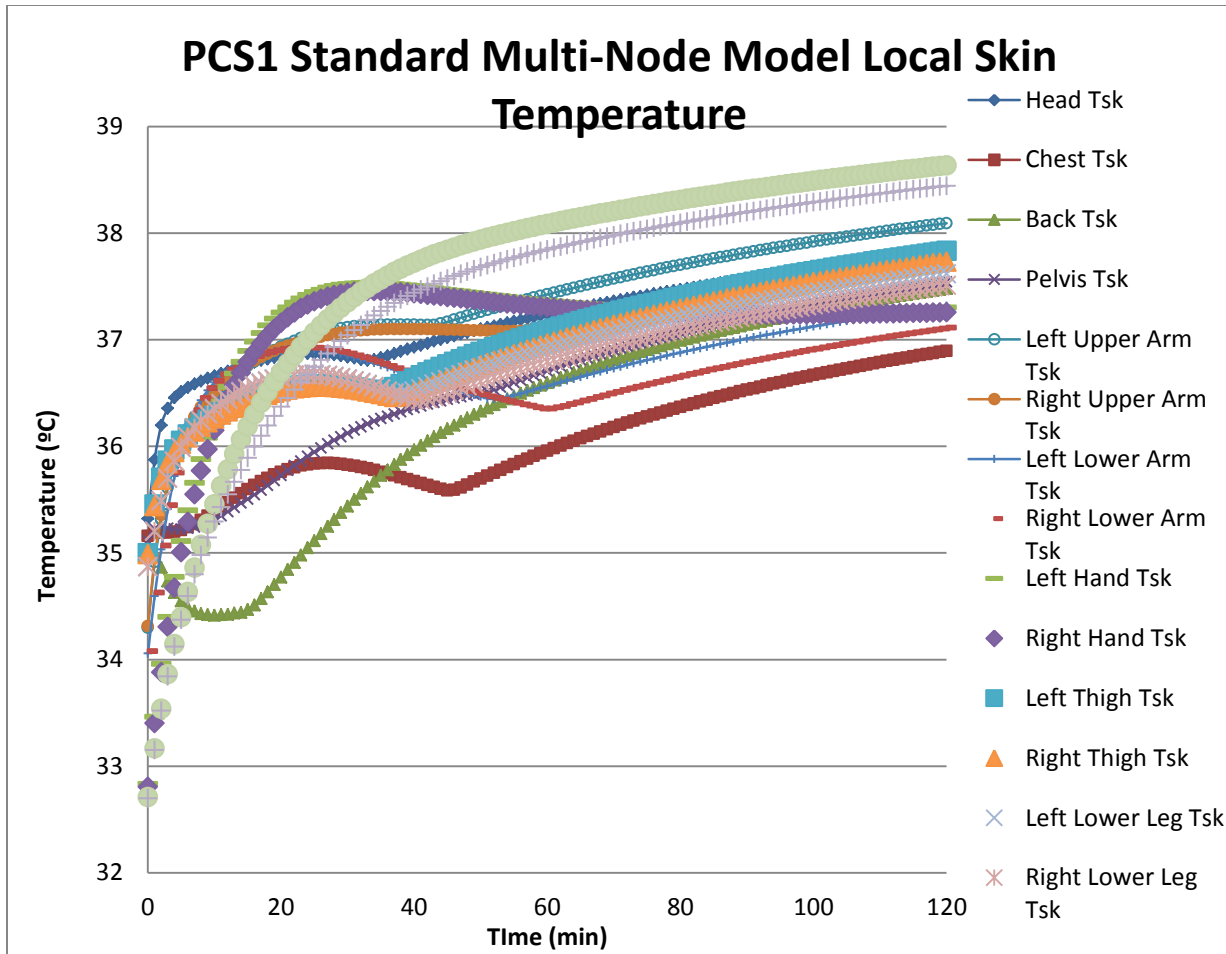


**Figure 6.12 PCS #1 Ventilation Vest by Entrak Standard Multi-Node Model predicted local skin temperature graph showing trends in external skin temperatures.**

The graphs show that PCS #1 was able to be modeled, but with large amounts of error compared to the PCS tests with regards to skin temperature, and the predicted core temperature was much higher than seen in the human subject results. The multi-node core temperature tracks well at the beginning of the test with the human subject results and the modeled mean skin temperature difference maintains a solid level, which does mimic, to some extent, what happens in the human subject results. The values in Figure 6.10 show the incredible variation between subjects' torso temperatures and this makes the ability of the model to predict the average even more impressive.

**Table 6.11 PCS #1 Ventilation Vest by Entrak Standard Multi-Node Model vs. Human Subject (HS) core, mean skin, and local skin temperatures including initial and final conditions.**

Segments	Standard Multi-Node Model			Human Subjects (not included: 5, 6)			Starting Conditions Difference	Delta T Error Value
	Initial Value (°C)	Final Value (°C)	Delta T (°C)	Initial Value (°C)	Final Value (°C)	Delta T (°C)	HS (not included: 5, 6)	HS (not included: 5, 6)
Mean Skin	34.92	37.64	2.72	35.99	36.78	0.79	-1.07	1.93
Core	37.17	38.86	1.69	37.14	37.97	0.84	0.03	0.85
Head Tsk	35.87	37.81	1.94	36.12	37.46	1.34	-0.25	0.60
Chest Tsk	35.19	36.89	1.71	34.88	35.72	0.84	0.30	0.87
Back Tsk	35.00	37.48	2.48	36.00	36.17	0.17	-1.00	2.31
Pelvis Tsk	35.23	37.54	2.32	N/A	N/A	N/A	N/A	N/A
Left Upper Arm Tsk	34.91	38.09	3.18	N/A	N/A	N/A	N/A	N/A
Right Upper Arm Tsk	34.95	37.84	2.89	38.73	38.17	-0.57	-3.78	3.46
Left Lower Arm Tsk	34.59	37.32	2.72	N/A	N/A	N/A	N/A	N/A
Right Lower Arm Tsk	34.63	37.11	2.49	37.87	37.07	-0.81	-3.25	3.29
Left Hand Tsk	33.46	37.30	3.84	N/A	N/A	N/A	N/A	N/A
Right Hand Tsk	33.40	37.26	3.85	N/A	N/A	N/A	N/A	N/A
Left Thigh Tsk	35.45	37.83	2.38	N/A	N/A	N/A	N/A	N/A
Right Thigh Tsk	35.44	37.73	2.30	35.35	36.71	1.35	0.09	0.94
Left Lower Leg Tsk	35.20	37.62	2.41	N/A	N/A	N/A	N/A	N/A
Right Lower Leg Tsk	35.20	37.51	2.31	35.87	37.48	1.61	-0.67	0.70
Left Foot Tsk	33.17	38.64	5.47	N/A	N/A	N/A	N/A	N/A
Right Foot Tsk	33.15	38.44	5.29	N/A	N/A	N/A	N/A	N/A



**Table 6.12 PCS #1 Ventilation Vest by Entrak Standard Multi-Node Model vs. Human Subject (HS) sweat rates with human subject results as the comparator.**

Sweat Totals	Standard Multi-Node Model	Human Subjects (not included: 5, 6)
Total Sweat (kg)	1.61	2.28
Error Value (kg)	N/A	-0.67
% Error	N/A	-29.60

The values from the table show that there was 0.03 °C difference in the initial core temperature of the human subjects' average compared to the modeled conditions. The multi-node model final core temperature exceeds the average value by 0.85 °C, which is closer than the baseline tests. The modeled sweat value was 0.67 kg less than the average subject water loss seen in the human subject tests. This system removed heat by evaporation and may have dried out the surfaces under the body armor. In addition, the lower predicted sweat total may have contributed to the difference from the measured results. The whole body skin wettedness can be seen in Figure 6.13.

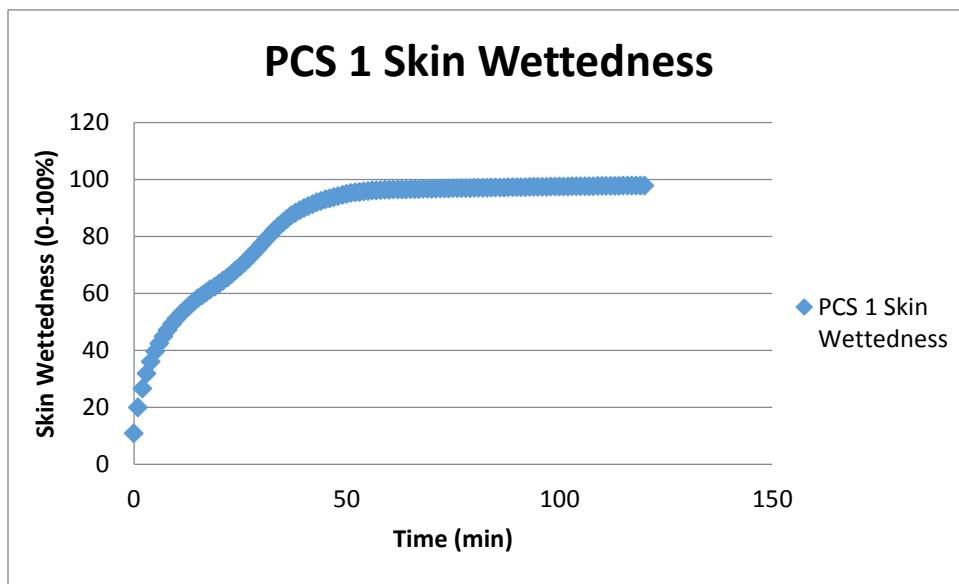


**Figure 6.13 Skin wettedness of the Standard Multi-Node Model with PCS 1**

This is the average value for the whole body, and it is possible that the segments under the PCS have further cooling potential available. Furthermore, sweat does not transfer from segment to segment further complicating the simulation. Therefore it would be illustrative to use the doubled sweat rate gain from the sweat rate modified multi-node simulations of Section 5.2.2.1 because sweat rate is incredibly important to the functioning of this system and there are no large cooling effects applied to these segments as in the other PCS simulated.

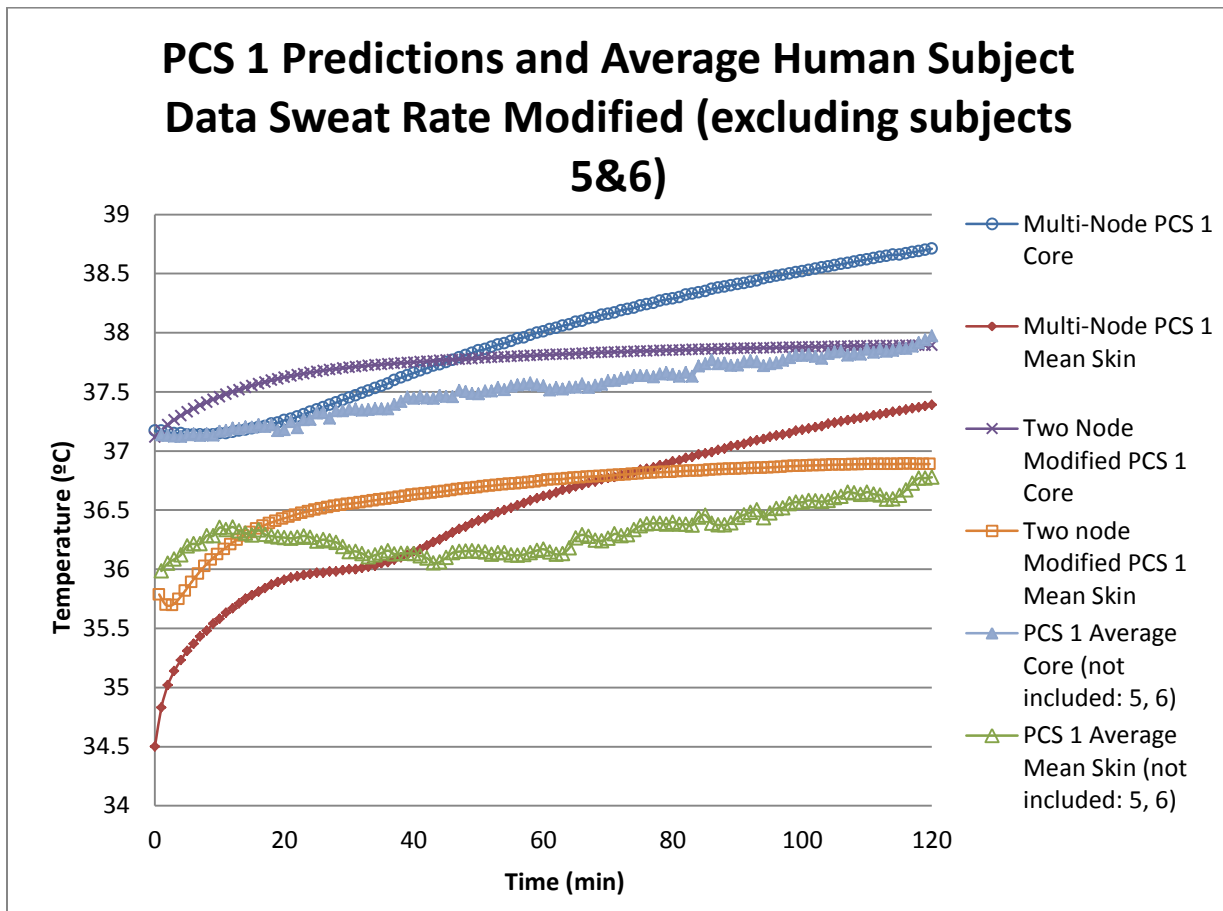


**Figure 6.14 PCS 1 Ventilation Vest by Entrak core temperature and mean skin temperature comparison graphs between average subject Standard Multi-Node Model and average Human Subject (HS).**

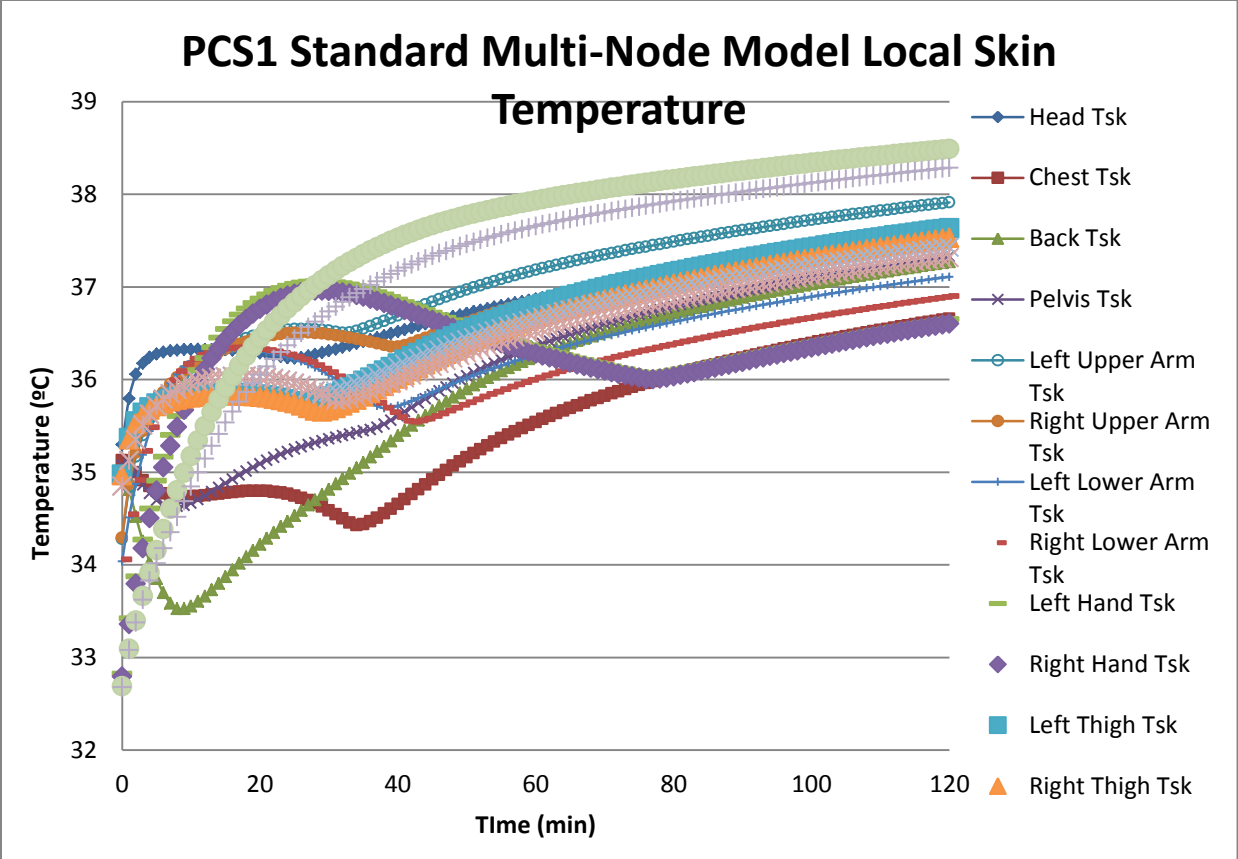


**Figure 6.15 PCS #1 Ventilation Vest by Entrak Sweat Rate Modified Multi-Node Model predicted local skin temperature graph showing trends in external skin temperatures.**

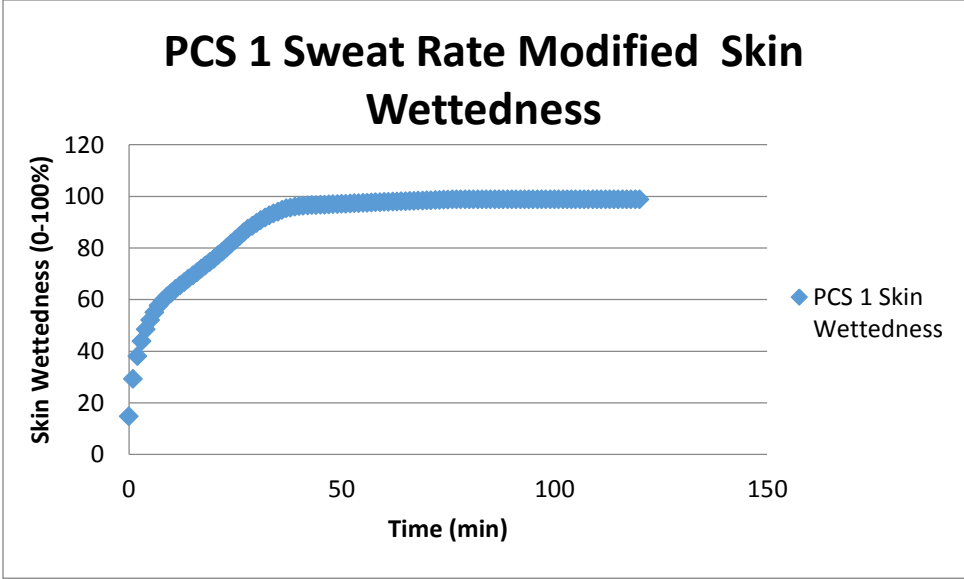


**Figure 6.16 Skin wettedness of the Sweat Rate Modified Multi-node Model with PCS 1**

**Table 6.13 PCS #1 Ventilation Vest by Entrak Sweat Rate Modified Multi-Node Model vs. Human Subject (HS) core, mean skin, and local skin temperatures including initial and final conditions.**

Segments	ReCl and Sweat Rate Modified Multi-Node Model			Human Subjects (not included: 5, 6)			Starting Conditions Difference	Delta T Error Value
	Initial Value (°C)	Final Value (°C)	Delta T (°C)	Initial Value (°C)	Final Value (°C)	Delta T (°C)	HS (not included: 5, 6)	HS (not included: 5, 6)
Mean Skin	34.83	37.39	2.56	35.99	36.78	0.79	-1.16	1.77
Core	37.17	38.71	1.54	37.14	37.97	0.84	0.03	0.70
Head Tsk	35.79	37.56	1.77	36.12	37.46	1.34	-0.33	0.43
Chest Tsk	35.08	36.66	1.58	34.88	35.72	0.84	0.20	0.74
Back Tsk	34.81	37.27	2.46	36.00	36.17	0.17	-1.19	2.29
Pelvis Tsk	35.08	37.33	2.24	N/A	N/A	N/A	N/A	N/A
Left Upper Arm Tsk	34.84	37.91	3.08	N/A	N/A	N/A	N/A	N/A
Right Upper Arm Tsk	34.87	37.65	2.78	38.73	38.17	-0.57	-3.86	3.34
Left Lower Arm Tsk	34.51	37.11	2.60	N/A	N/A	N/A	N/A	N/A
Right Lower Arm Tsk	34.55	36.90	2.36	37.87	37.07	-0.81	-3.33	3.16
Left Hand Tsk	33.42	36.65	3.23	N/A	N/A	N/A	N/A	N/A
Right Hand Tsk	33.36	36.60	3.24	N/A	N/A	N/A	N/A	N/A
Left Thigh Tsk	35.37	37.63	2.27	N/A	N/A	N/A	N/A	N/A
Right Thigh Tsk	35.35	37.53	2.18	35.35	36.71	1.35	0.00	0.82
Left Lower Leg Tsk	35.13	37.43	2.30	N/A	N/A	N/A	N/A	N/A
Right Lower Leg Tsk	35.13	37.32	2.19	35.87	37.48	1.61	-0.74	0.58
Left Foot Tsk	33.10	38.49	5.40	N/A	N/A	N/A	N/A	N/A
Right Foot Tsk	33.08	38.29	5.21	N/A	N/A	N/A	N/A	N/A

**Table 6.14 PCS #1 Ventilation Vest by Entrak Sweat Rate Modified Multi-Node Model vs. Human Subject (HS) sweat rates with human subject results as the comparator.**

Sweat Totals	Multi-node Model	Human Subjects (not included: 5, 6)
Total Sweat (kg)	2.36	2.28
Error Value (kg)	N/A	0.08
% Error	N/A	3.43

The addition of the doubled sweat rate gain resulted in better agreement with the human subject results with a core temperature difference of 0.70 °C compared to the human subjects as can clearly be seen in Table 6.14. The addition of the extra sweat did not change the final skin wettedness value significantly comparing Figure 6.16 to the standard sweat rate in Figure 6.13, but lowered the core temperature by 0.13 °C compared to the standard model. The simulated sweat rate closely match the human subjects, under predicting the sweat by 0.08 kg as seen in Figure 6.14 and resulting in percent error of under 5%.

This core difference is still quite large, but unlike the two-node model, there are complicated local effects. Those local effects do allow for the fundamental-based application of the local convection simulation to this PCS instead of the heat removal from the skin surface from the thermal manikin measurements, as were used in the two-node model. Increasing the overall sweat gain provided a slightly better result, however this only affects the proportional values, the local effects are not known.

Using this simulation, it is possible to estimate the effect of the PCS on the human, if we assume that the torso area is impermeable as modeled. The best case modeled baseline test was used,  $Re_{cl}$  Sweat rate modified as the comparison, and the total of the external heat losses was calculated by comparing the convection, radiation, evaporation, and evaporation exchange values. The predicted actual cooling provided by the PCS system can be found in Figure 6.17. This is a new way to look at PCS evaluation. However, it is dependent on accurate local values

and on the ability to properly predict the local sweat response. The cooling difference can clearly be seen in the figure as to what adding the sweat rate gain did to increase the cooling power.

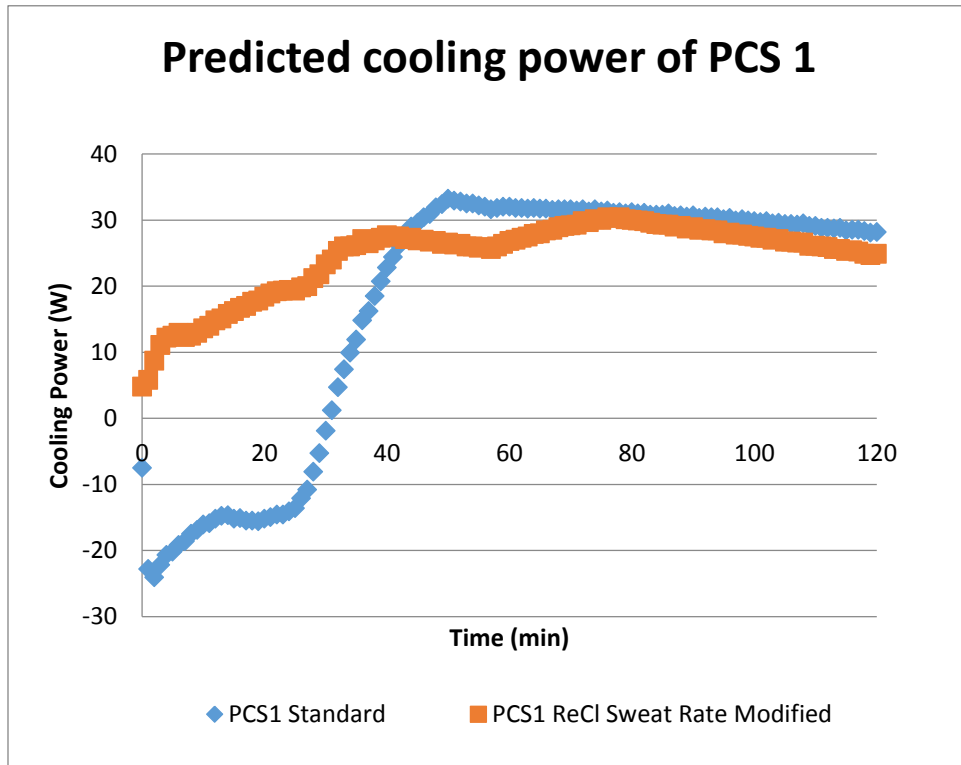


**Figure 6.17 Predicted cooling power of PCS1 based on predicted body external energy balance.**

Given the high skin wettedness percentage predicted, it is likely that the clothing was becoming saturated as well introducing the error from that assumption as previously discussed. In addition, there are fitment issues between the human subjects and thermal manikin, including the effects of movement on the air gap provided by the PCS. These are especially important considering the mechanism of cooling is dependent on air exchange. A different air path or a pumping effect would change and increase the convective coefficients respectively and making modeling difficult. Accounting for local effects of the sweat wetting, the fabric on the other

segments and matching the total sweat to match the measured values would likely result in an even closer agreement with the human subject results and leaves room for future study.

### ***6.2.2 PCS #9 PCVZ-KM Zipper Front Vest by Polar Products***

PCS #9 PCVZ-KM was one of two PCM based personal cooling systems tested. The cooling in this case was provided directly to the model surface using the manikin cooling rates as can be seen in Figure 3.5. The cooling from PCS #9 when tested on the manikin drops off as the PCM melts and there is a barrier between the PCM formed by the melted liquid. The core and mean skin graph is found in Figure 6.18 followed by human subject's torso skin temperatures and average local skin temperatures by segment in Figure 6.19, Figure 6.20 and Figure 6.21. The comparison between the models initial and final core and skin temperatures are found In Table 6.15 and the sweat rates in Table 6.16.

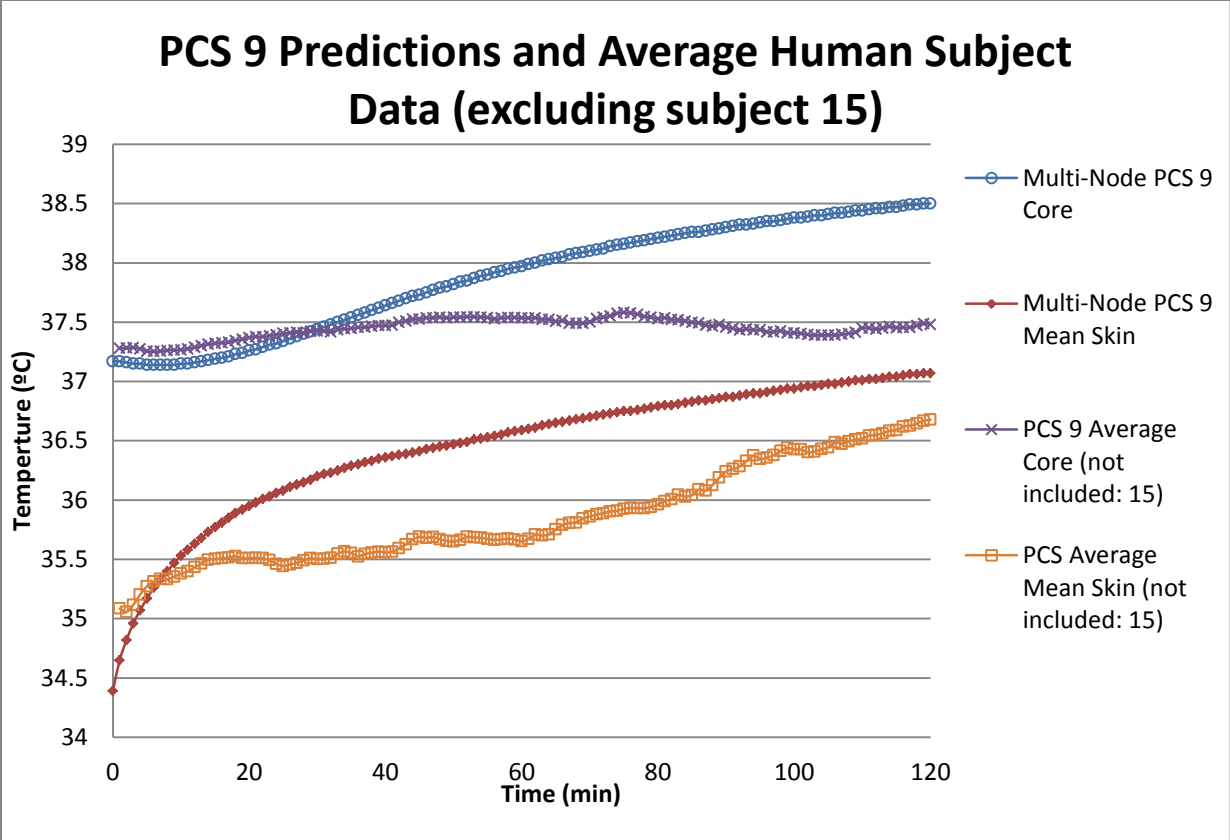


**Figure 6.18 PCS #9 PCVZ-KM Zipper Front Vest by Polar Products core and mean skin temperature comparison graphs between average subject Standard Multi-Node Model and average Human Subject (HS).**



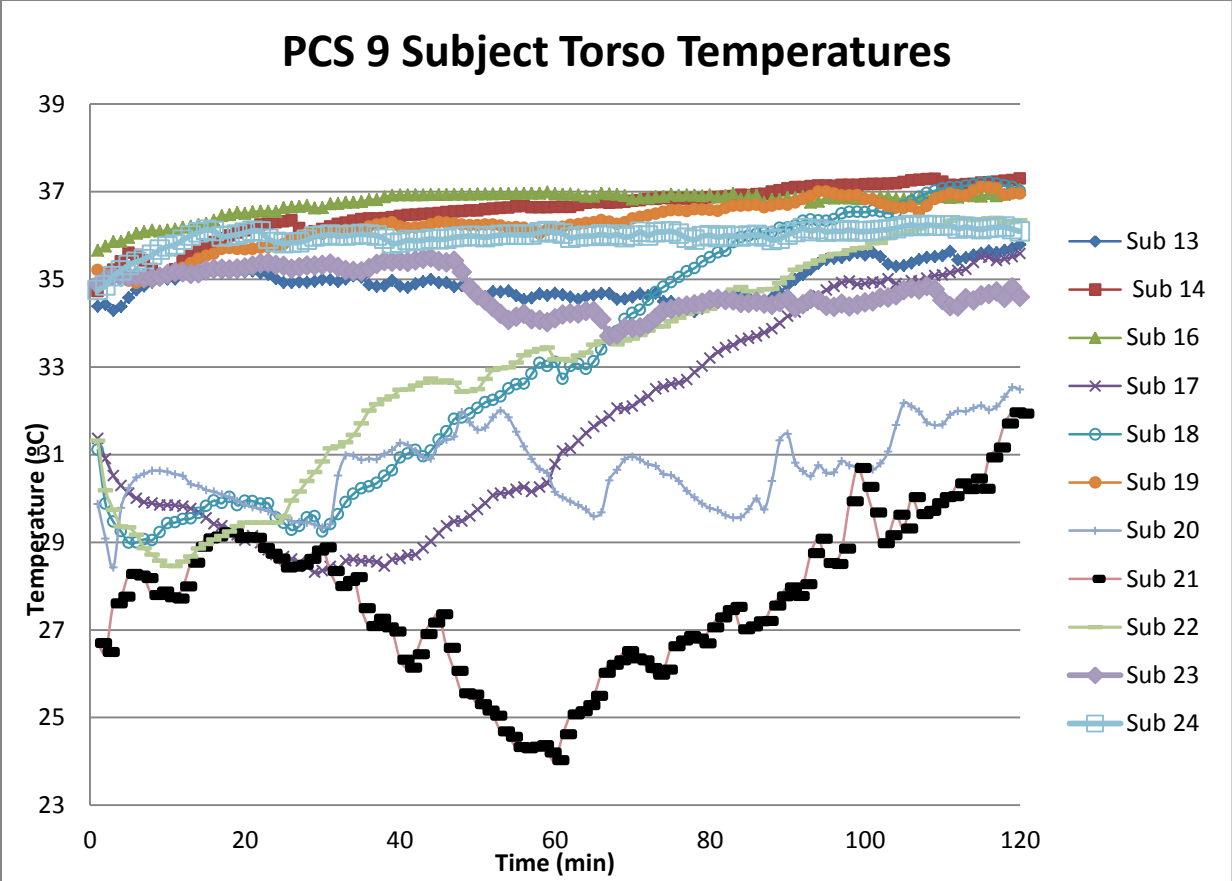


**Figure 6.19 PCS #9 PCVZ-KM Zipper Front Vest by Polar Products torso skin temperatures graphs of subject Human Subject (HS) to show trends in skin temperatures contacting PCS.**

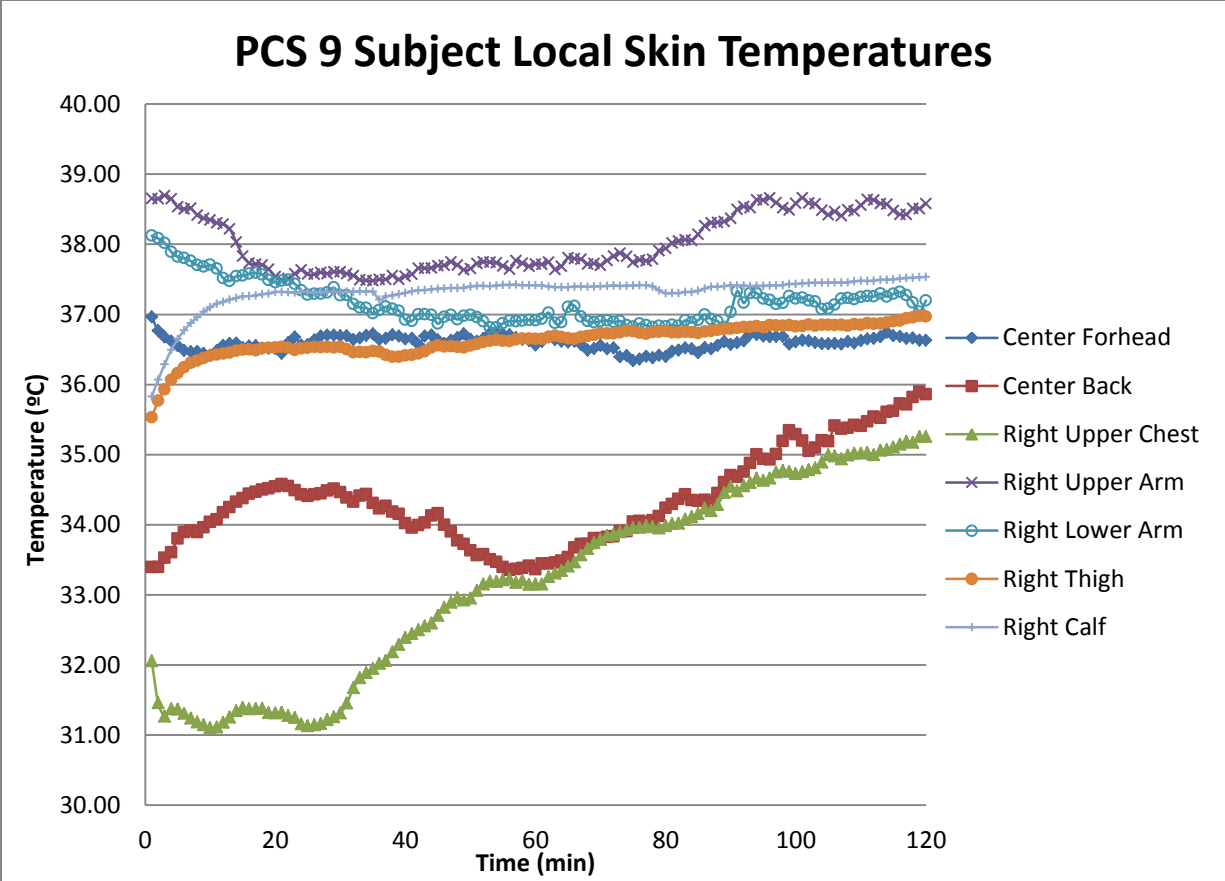


**Figure 6.20 PCS #9 PCVZ-KM Zipper Front Vest by Polar Products local skin temperature graph of average of subject Human Subject (HS) to show trends in external skin temperatures.**

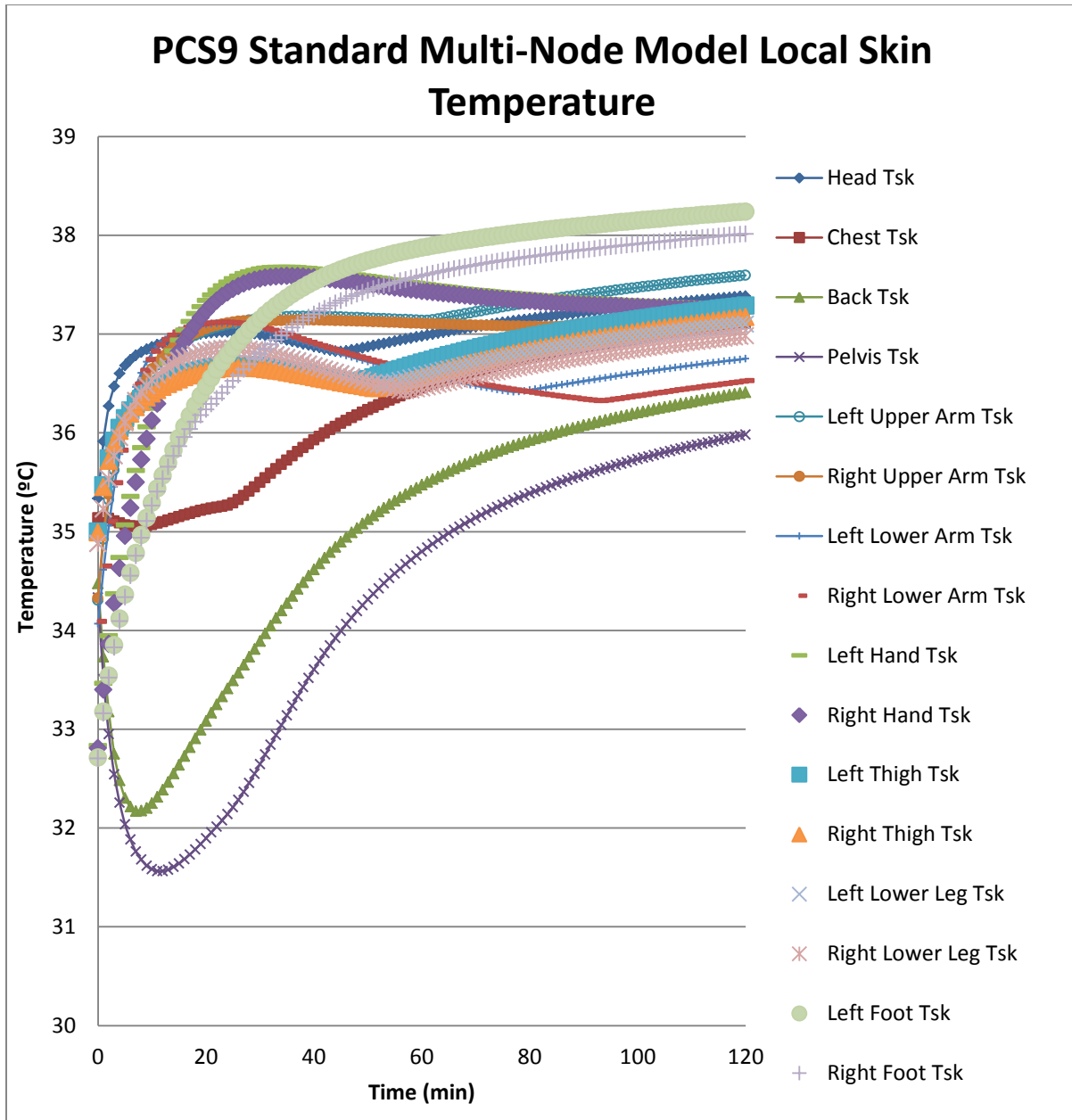


**Figure 6.21 PCS #9 PCVZ-KM Zipper Front Vest by Polar Products Standard Multi-Node Model predicted local skin temperature graph showing trends in external skin temperatures.**

The simulated core temperature with for PCS #9 with the standard multi-node model predicts the core temperature worse than PCS #1, and not as well as the sweat rate modified multi-node results PCS#1. Again, the multi-node model predicted a value higher than the human

subject average. The mean skin temperature is lower in the thermal model possibly because the core is reacting to the large energy losses. In Figure 6.20 there are very low skin temperatures for the “Right Upper Chest” and “Center Back”. In some cases, the thermocouple was situated directly under a PCM pack causing low skin temperatures. Figure 6.19 shows that subjects 20 and 21 contributed highly to driving the mean skin temperature down for the human subjects. Figure 6.21 does show the same average low skin temperatures on the human subjects standing somewhat in opposition to this theory.

**Table 6.15 PCS #9 PCVZ-KM Zipper Front Vest by Polar Products Standard Multi-Node Model vs. Human Subject (HS) core, mean skin, and local skin temperatures including initial and final conditions.**

Segments	Standard Multi-Node Model			Human Subjects (not included: 5, 6)			Starting Conditions Difference	Delta T Error Value
	Initial Value (°C)	Final Value (°C)	Delta T (°C)	Initial Value (°C)	Final Value (°C)	Delta T (°C)	HS (not included: 5, 6)	HS (not included: 5, 6)
Mean Skin	34.65	37.07	2.42	35.09	36.68	1.59	-0.44	0.83
Core	37.17	38.50	1.33	37.28	37.48	0.20	-0.11	1.13
Head Tsk	35.91	37.38	1.47	36.96	36.63	-0.33	-1.05	1.80
Chest Tsk	35.15	37.11	1.96	32.06	35.26	3.20	3.09	-1.24
Back Tsk	33.73	36.41	2.68	33.39	35.86	2.46	0.34	0.21
Pelvis Tsk	33.51	35.98	2.47	N/A	N/A	N/A	N/A	N/A
Left Upper Arm Tsk	34.92	37.59	2.67	N/A	N/A	N/A	N/A	N/A
Right Upper Arm Tsk	34.97	37.32	2.35	38.65	38.58	-0.07	-3.68	2.42
Left Lower Arm Tsk	34.61	36.75	2.14	N/A	N/A	N/A	N/A	N/A
Right Lower Arm Tsk	34.65	36.53	1.88	38.12	37.20	-0.92	-3.47	2.80
Left Hand Tsk	33.46	37.30	3.83	N/A	N/A	N/A	N/A	N/A
Right Hand Tsk	33.40	37.24	3.84	N/A	N/A	N/A	N/A	N/A
Left Thigh Tsk	35.47	37.29	1.82	N/A	N/A	N/A	N/A	N/A
Right Thigh Tsk	35.45	37.17	1.72	35.53	36.97	1.44	-0.08	0.28
Left Lower Leg Tsk	35.23	37.10	1.87	N/A	N/A	N/A	N/A	N/A
Right Lower Leg Tsk	35.23	36.98	1.75	35.83	37.53	1.71	-0.60	0.05
Left Foot Tsk	33.18	38.24	5.06	N/A	N/A	N/A	N/A	N/A
Right Foot Tsk	33.16	38.01	4.85	N/A	N/A	N/A	N/A	N/A

**Table 6.16 PCS #9 PCVZ-KM Zipper Front Vest by Polar Products Standard Multi-Node Model vs. Human Subject (HS) sweat rates with human subject results as the comparator.**

Sweat Totals	Standard Multi-Node Model	Human Subjects (not included: 5, 6)
Total Sweat (kg)	1.12	2.28
Error Value (kg)	N/A	-1.16
% Error	N/A	-50.98

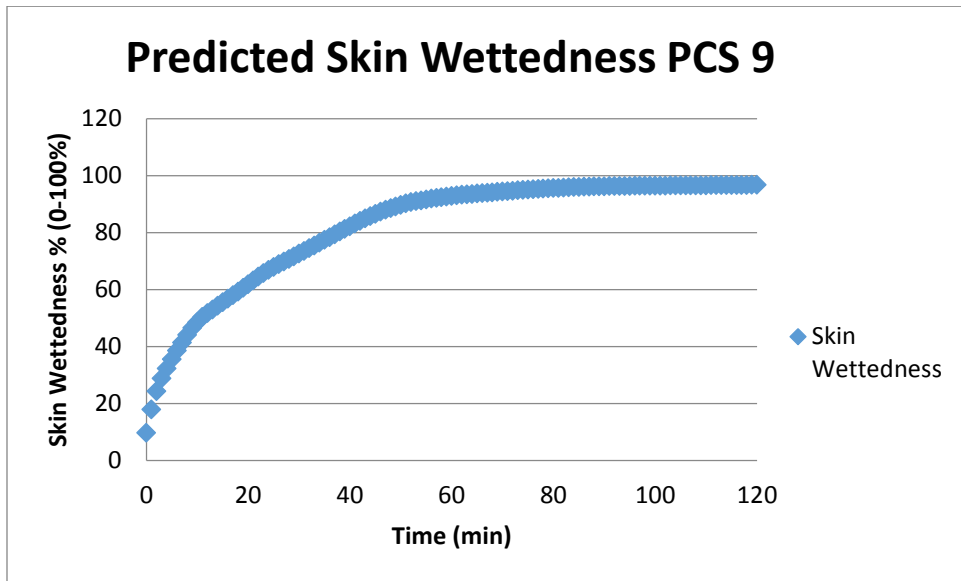


**Figure 6.22 Skin wettedness of the Standard Multi-Node Model with PCS 9**

The initial core temperature was 0.11 °C lower than the human subject average for this test, however the final core temperature was 1.13 °C higher. Examining the sweat rate shows that the model under predicted the sweat rate by 1.16 kg, for an error of 50.98%. This is a likely cause of the discrepancy between the human subject average and the multi-node model. The sweat control algorithm may need to be adapted to fit this type of scenario or other changes may need to be made to the model. If the sweat rate gain was increased, the wetted clothing may still become an issue and have to be addressed as well. The skin wettedness graph shown in Figure 6.22 where skin wettedness approaches 100% with cooling applied, however it may increase the

sweat rate gain may increase the natural cooling at the beginning of the test. It should be noted that the model was never intended to be used with such intense, local cooling and it is likely that this has caused the cooled segments to stop sweating. The body's reaction to this type of cooling is largely unknown is a part of this research, the literature review of Chapter 2 and a PCS model does not yet exist.

### ***6.2.3 PCS #12 Cool UnderVest by Steele***

The Cool UnderVest was the second of the two PCM based PCS tested on the human subjects. The cooling provided to the manikin from the ASTM heat differential test was applied to the simulated human on the chest, back, shoulders, and stomach segments in TAITherm. The cooling intensity of PCS #12 decreased over time as the PCM melted and a liquid resistance barrier was formed. The time dependent curve used in the model can be found in Figure 3.6. The comparison graphs between the multi-node model and the human subject core and mean skin temperatures is in Figure 6.23. The torso temperature of the individual subjects is found in Figure 6.24 and the average local skin temperature by segment is in Figure 6.25 and Figure 6.26. A comparison between the initial conditions and the final conditions of the multi-node model and human subject average skin and core temperatures is in Table 6.17 and sweat rate in Table 6.18.

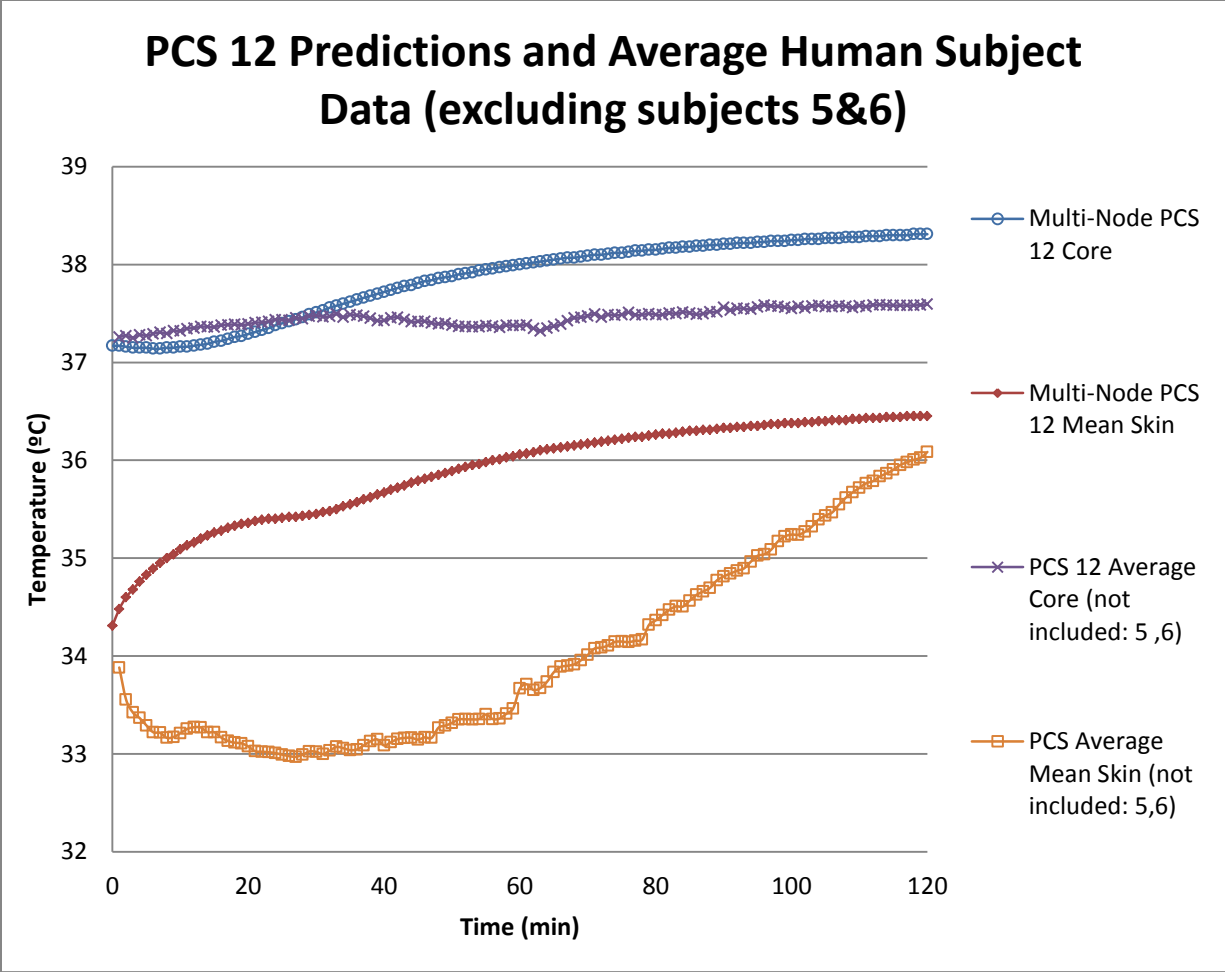


**Figure 6.23 PCS #12 Cool UnderVest by Steele core and mean skin temperature comparison graphs between average subject Standard Multi-Node Model and average Human Subject (HS).**



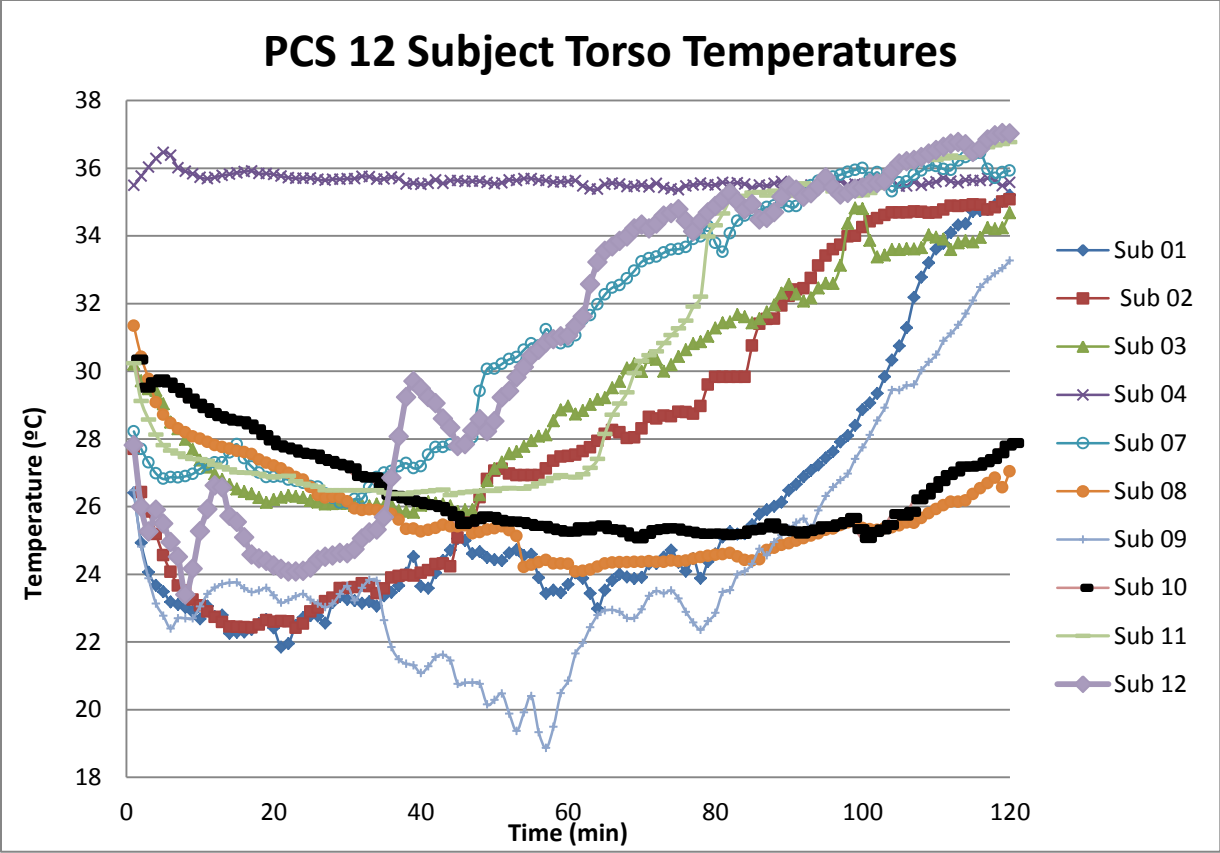
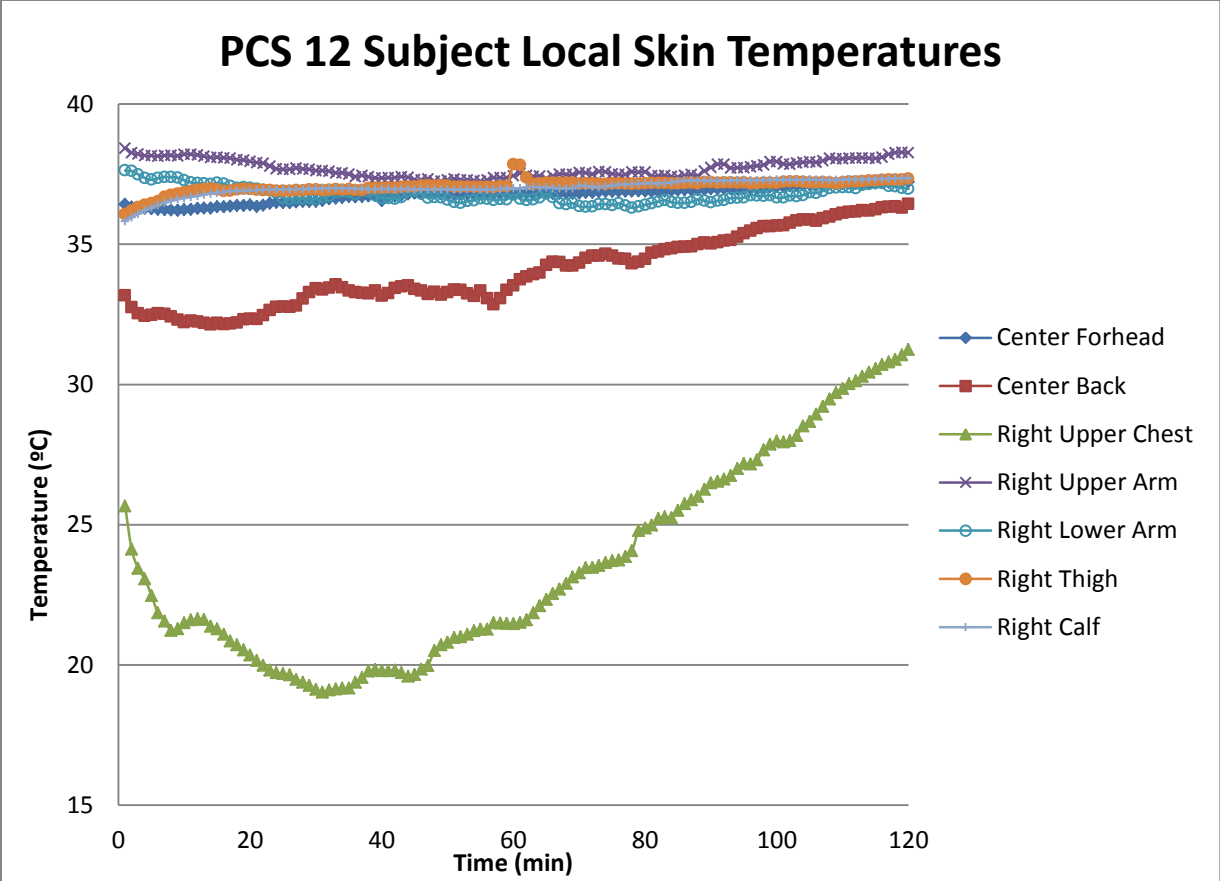
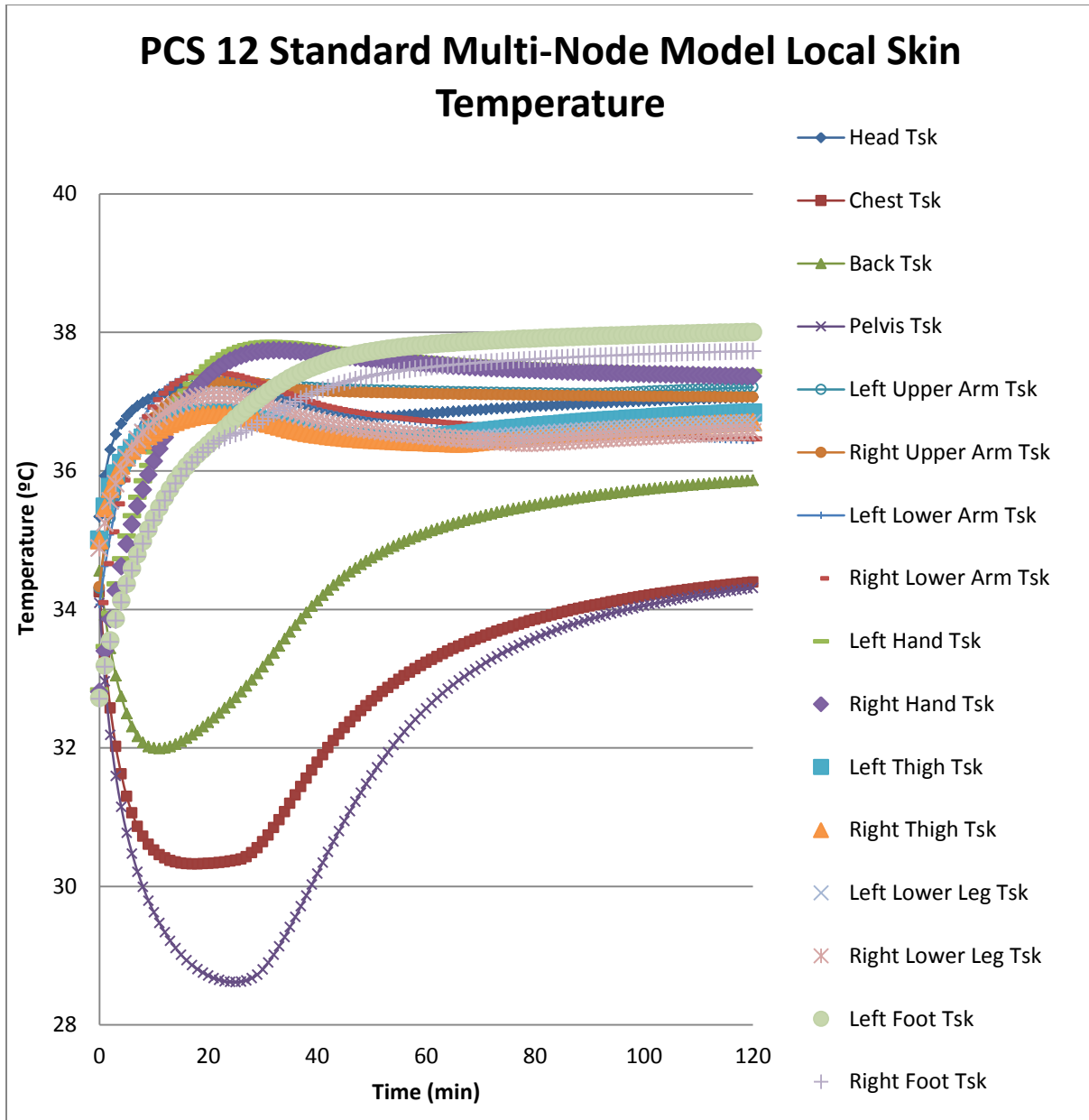


Figure 6.24 PCS #12 Cool UnderVest by Steele torso skin temperatures graphs of subject Human Subject (HS) to show trends in skin temperatures contacting PCS.



**Figure 6.25 PCS #12 Cool UnderVest by Steele local skin temperature graph of average of subject Human Subject (HS) to show trends in external skin temperatures.**



**Figure 6.26 PCS #12 Cool UnderVest by Steele Standard Multi-Node Model predicted local skin temperature graph showing trends in external skin temperatures.**

The agreement of the core and mean skin temperature is not very close as seen in Figure 6.23. The initial mean lowered mean skin temperature of the human subjects can partly be because the skin thermocouples were located directly under a cooling pack. In Figure 6.25, the average right upper chest is incredibly low and the individual mean skin temperature breakdown in

Figure 6.24 indicates that this was the case in many subjects. Comparing the human subject results to the graphs of predicted local skin temperatures from the standard multi-node model as seen in Figure 6.26, the skin temperatures do not reach the same low temperatures as seen in the human subjects' results. The initial increase in the multi-node mean skin temperature is likely caused by the intense, local cooling, for which the model was not designed.

**Table 6.17 PCS #12 Cool UnderVest by Steele Standard Multi-Node Model vs. Human Subject (HS) core, mean skin, and local skin temperatures including initial and final conditions.**

Segments	Standard Multi-Node Model			Human Subjects (not included: 5, 6)			Starting Conditions Difference	Delta T Error Value
	Initial Value (°C)	Final Value (°C)	Delta T (°C)	Initial Value (°C)	Final Value (°C)	Delta T (°C)	HS (not included: 5, 6)	HS (not included: 5, 6)
Mean Skin	34.48	36.45	1.97	33.88	36.09	2.20	0.60	-0.23
Core	37.17	38.31	1.14	37.26	37.60	0.34	-0.09	0.80
Head Tsk	35.93	37.06	1.14	36.42	37.22	0.80	-0.50	0.34
Chest Tsk	33.27	34.39	1.12	25.66	31.25	5.58	7.60	-4.46
Back Tsk	33.92	35.86	1.95	33.18	36.43	3.26	0.74	-1.31
Pelvis Tsk	32.96	34.31	1.35	N/A	N/A	N/A	N/A	N/A
Left Upper Arm Tsk	34.92	37.21	2.29	N/A	N/A	N/A	N/A	N/A
Right Upper Arm Tsk	34.97	37.06	2.10	38.43	38.26	-0.17	-3.46	2.26
Left Lower Arm Tsk	34.62	36.44	1.82	N/A	N/A	N/A	N/A	N/A
Right Lower Arm Tsk	34.66	36.46	1.80	37.63	36.98	-0.66	-2.97	2.46
Left Hand Tsk	33.46	37.43	3.97	N/A	N/A	N/A	N/A	N/A
Right Hand Tsk	33.40	37.36	3.96	N/A	N/A	N/A	N/A	N/A
Left Thigh Tsk	35.48	36.84	1.36	N/A	N/A	N/A	N/A	N/A
Right Thigh Tsk	35.46	36.70	1.24	36.07	37.33	1.27	-0.61	-0.03
Left Lower Leg Tsk	35.25	36.70	1.45	N/A	N/A	N/A	N/A	N/A
Right Lower Leg Tsk	35.25	36.56	1.32	35.82	37.36	1.54	-0.58	-0.22
Left Foot Tsk	33.19	38.00	4.82	N/A	N/A	N/A	N/A	N/A
Right Foot Tsk	33.17	37.73	4.56	N/A	N/A	N/A	N/A	N/A

**Table 6.18 PCS #12 Cool UnderVest by Steele Standard Multi-Node Model vs. Human Subject (HS) sweat rates with human subject results as the comparator.**

Sweat Totals	Standard Multi-Node Model	Human Subjects (not included: 5, 6)
Total Sweat (kg)	0.84	2.28
Error Value (kg)	N/A	-1.44
% Error	N/A	-62.99

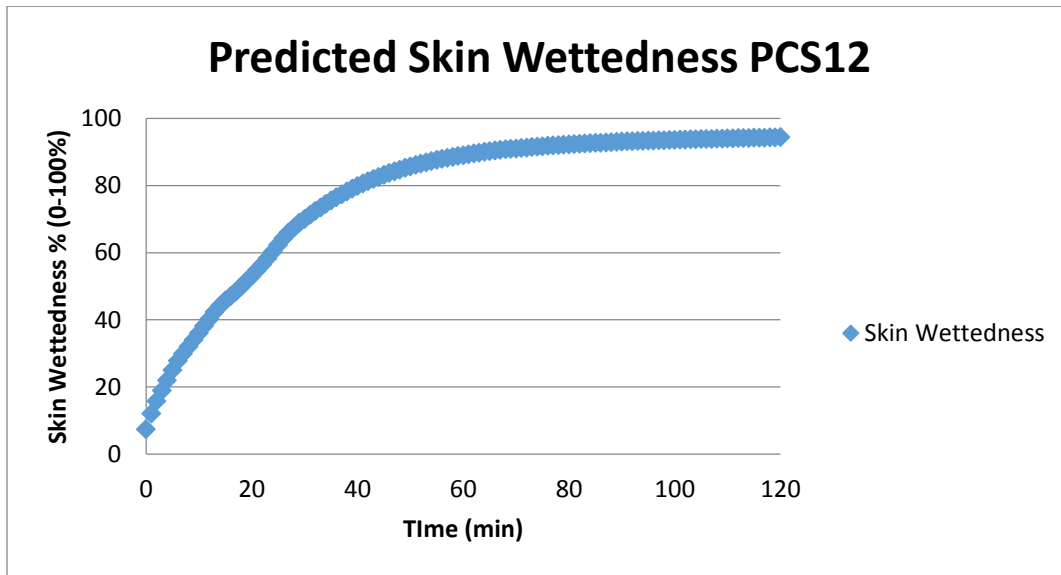


**Figure 6.27 Skin wettedness of the Standard Multi-Node Model with PCS 12**

The initial conditions for the multi-node were started 0.09 °C lower than the average of the human subjects. The final core temperature was predicted by the multi-node to be 0.80 °C higher than the human, which is not ideal. While this is not acceptable, it is certainly much closer to the human results than the multi-node baseline prediction. The sweat rate was under predicted by the model, as shown in Table 6.18, by 1.44 kg of sweat. The key finding is, this is a significant amount of potential cooling and likely is the cause of the multi-node model high core prediction. This value would need to be adjusted to match the human subjects and the wetting

clothing conditions may need to be applied if the skin wettedness reached 100% in areas, which is likely given the whole body prediction for the standard multi-node results in Figure 6.27.

#### ***6.2.4 PCS #20 Hummingbird II by Creative Thermal Solutions***

The battery powered Hummingbird II provided a relatively constant heat removal rate from the thermal manikin. The time dependent heat flux measured from the thermal manikin heat differential test was applied to the chest, back, stomach, and shoulders segments in TAITherm. The cooling for each segment can be found in Figure 3.7. The Hummingbird II system was unique because it was the only system where a subject outside of those already excluded, failed to finish the test. The reason for not finishing the test was not due to heat reasons, but this does change the average results somewhat, so data will be presented with and without that subject. The comparison between the multi-node and human subject core and mean skin temperatures are found in the graph of Figure 6.28. The torso temperatures of individual subjects are located in Figure 6.29 and the average local skin temperatures of all subjects are in Figure 6.30. The local simulated skin temperatures are in Figure 6.31. The initial and final temperatures for core and skin and a comparison between the human subjects and multi-node model are in Table 6.19. The comparison between the multi-node and human subject total sweat produced is found in Table 6.20.

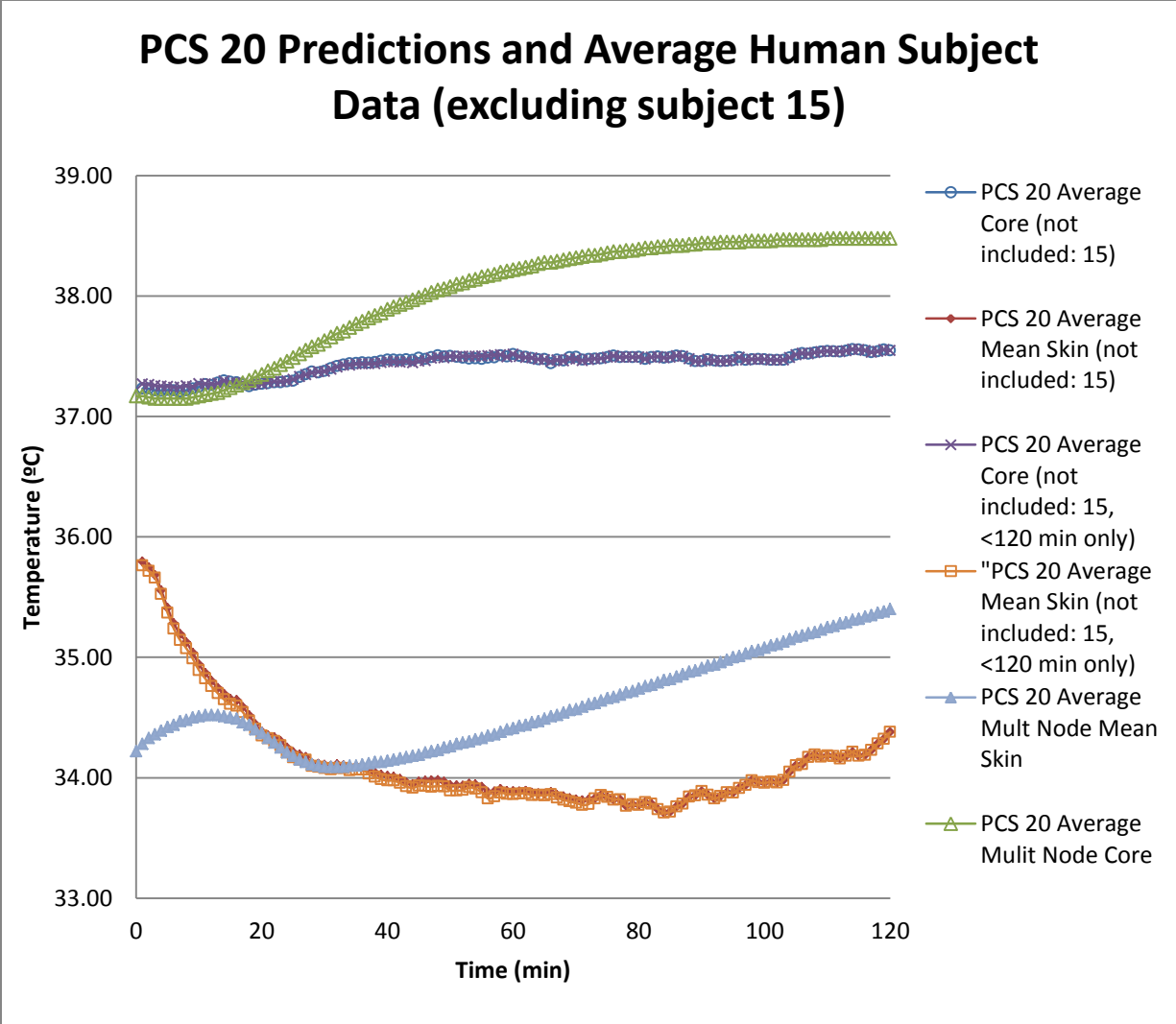


**Figure 6.28 PCS #20 Hummingbird II by Creative Thermal Solutions core and mean skin temperature comparison graphs between average subject Standard Multi-Node Model and average Human Subject (HS). Included are the mean skin and core temperature averages with and without the subjects who did not finish the test.**



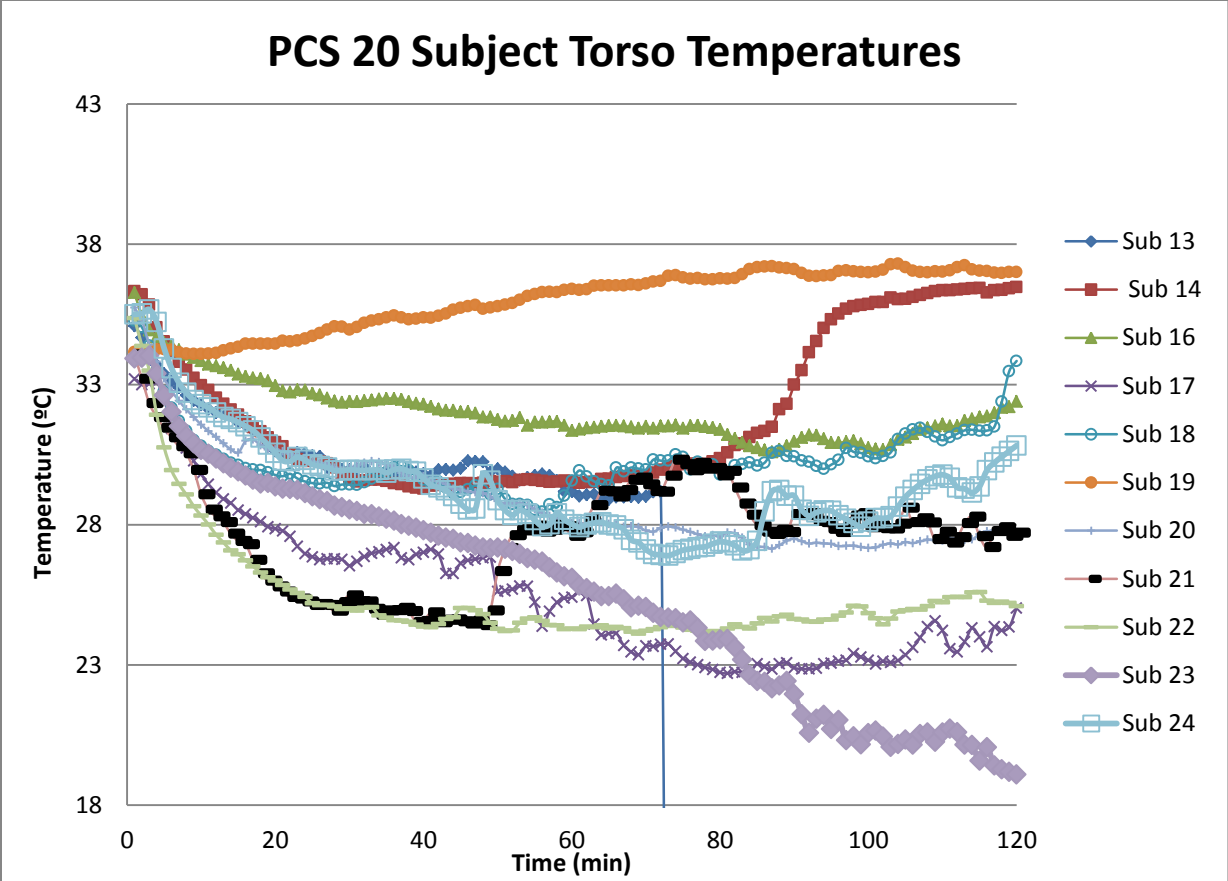


**Figure 6.29 PCS #20 Hummingbird II by Creative Thermal Solutions torso skin temperatures graphs of subject Human Subject (HS) to show trends in skin temperatures contacting PCS.**

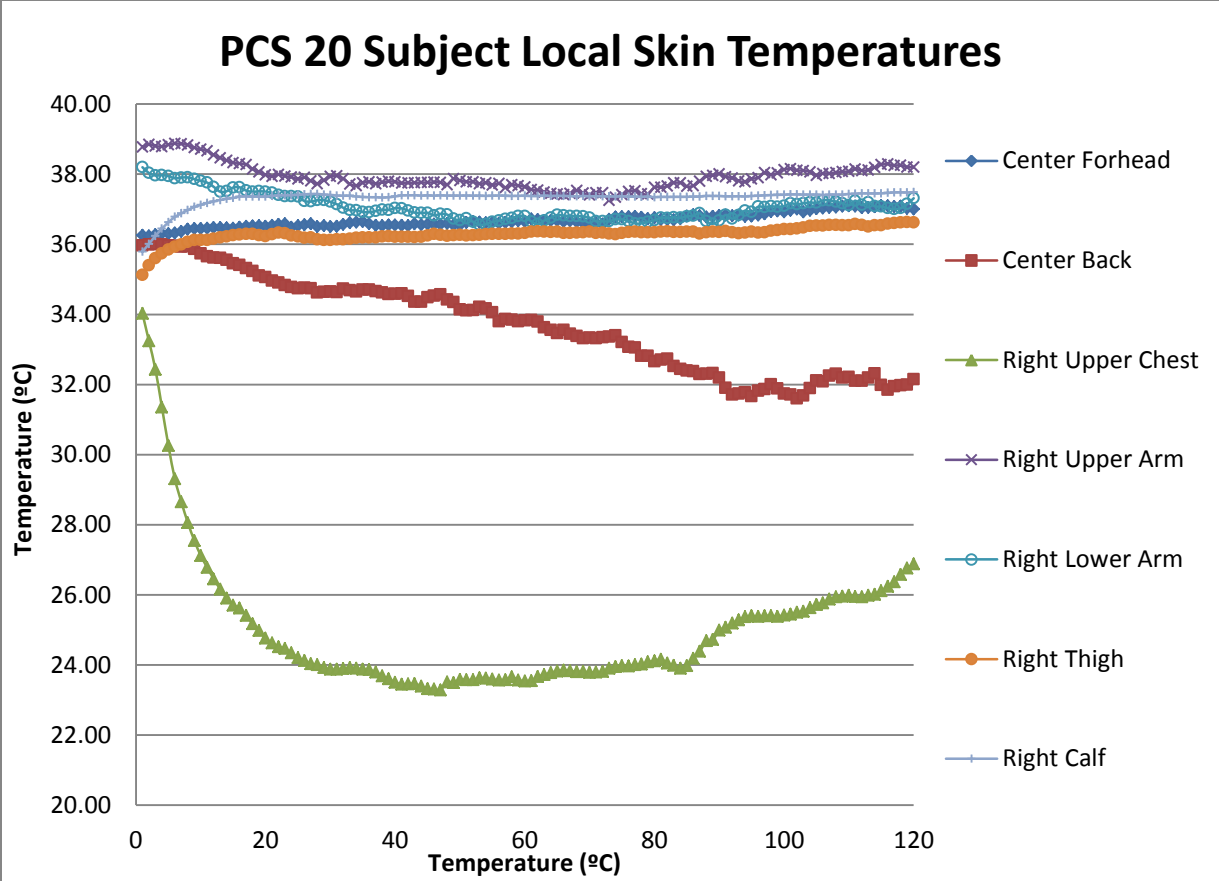


**Figure 6.30 PCS #20 Hummingbird II by Creative Thermal Solutions local skin temperature graph of average of subject Human Subject (HS) to show trends in external skin temperatures.**

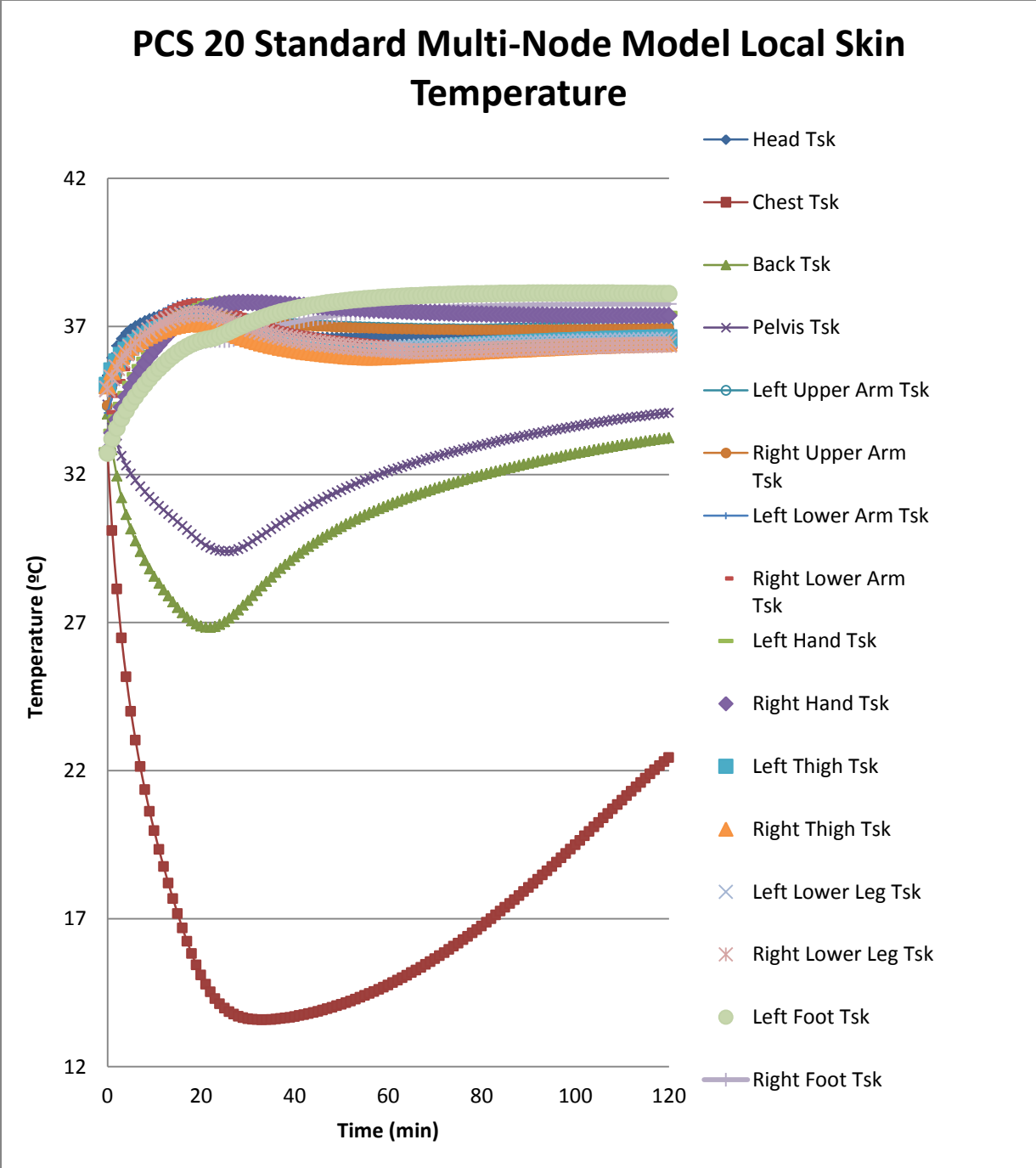


**Figure 6.31 PCS #20 Hummingbird II by Creative Thermal Solutions Standard Multi-Node Model predicted local skin temperature graph showing trends in external skin temperatures.**

The core temperature of the multi-mode model tracks well with the human subjects for the beginning of the test as seen in Figure 6.28. However, the core temperature begins to rise in

excess of that seen in the human subject tests. The multi-node mean skin temperature rises and then falls, remaining relatively constant until the end of the test. This is compared with the mean skin temperature of the human subjects, which falls rapidly and then begins to rise at the end. In Figure 6.30 the “Right Upper Chest” and “Center Back” segments can be seen to be driving this response similar to the other cold boundary PCS. In this case, the thermocouple may be located underneath the refrigerant tube and produce an artificially low skin temperature this hypothesis is supported in part by the widely varying torso skin temperatures in Figure 6.29. Another reason that the skin temperature is low could be due to vasoconstriction removing the blood flow and preventing the heat from reaching the skin, except through conduction. However, unlike other systems modeled the predicted chest skin temperature reaches approximately 13 °C as seen in Figure 6.31. The extremely low predicted chest temperature could be from using the cooling values from the thermal manikin in this direct expansion vapor compression system because the manikin is capable of producing a high heat flux to maintain the 35 °C skin temperature. In the direct expansion system, the refrigerant is changing phase and expanding throughout its path through the tube suit vest. Therefore, a large quantity of refrigerant may be evaporating in the chest portion, possibly the tube suit entrance, thanks to the fixed manikin skin temperature. This would produce the high heat transfer rates seen in Figure 3.7. On the human, as the skin temperature decreased there would be less energy available for the latent heat transfer process to occur in the chest area likely spreading out the cooling more evenly across the tube suit. A second effect is that the refrigeration cycle loses capacity as the evaporator temperature lowers. This is a complex issue and is notable when using the sweating thermal manikin to model PCS with multi-segment/multi-node models.

**Table 6.19 PCS #20 Hummingbird II by Creative Thermal Solutions Standard Multi-Node Model vs. Human Subject core, mean skin, and local skin temperatures including initial and final conditions.**

Segments	Standard Multi-Node Model			Human Subjects (not included: 5, 6, 15)			Human Subjects (not included: 5, 6, 15), >120 min only			Starting Conditions Difference		Delta T Error Value	
	Initial Value (°C)	Final Value (°C)	Delta T (°C)	Initial Value (°C)	Final Value (°C)	Delta T (°C)	Initial Value (°C)	Final Value (°C)	Delta T (°C)	HS(not included: 5, 6, 15)	HS (not included: 5, 6, 15), >120 min only	HS (not included: 5, 6, 15)	HS (not included: 5, 6, 15), >120 min only
Mean Skin	34.28	35.40	1.12	35.80	34.38	-1.42	35.76	34.38	-1.38	-1.52	-1.48	2.54	2.50
Core	37.17	38.48	1.31	37.23	37.55	0.32	37.27	37.55	0.28	-0.06	-0.10	0.99	1.03
Head Tsk	35.94	36.91	0.97	36.26	37.00	0.74	34.07	37.00	2.94	-0.32	1.87	0.23	-1.96
Chest Tsk	30.10	22.44	-7.66	34.02	26.88	-7.14	34.07	26.88	-7.18	-3.93	-3.97	-0.52	-0.47
Back Tsk	32.83	33.24	0.41	35.96	32.14	-3.82	35.90	32.14	-3.75	-3.14	-3.07	4.23	4.16
Pelvis Tsk	33.58	34.08	0.51	N/A	N/A	N/A	N/A	N/A	N/A	N/A	N/A	N/A	N/A
Left Upper Arm Tsk	34.92	37.06	2.14	N/A	N/A	N/A	N/A	N/A	N/A	N/A	N/A	N/A	N/A
Right Upper Arm Tsk	34.97	36.94	1.97	38.77	38.20	-0.57	38.67	38.20	-0.47	-3.80	-3.70	2.54	2.44
Left Lower Arm Tsk	34.63	36.30	1.66	N/A	N/A	N/A	N/A	N/A	N/A	N/A	N/A	N/A	N/A
Right Lower Arm Tsk	34.67	36.32	1.65	38.20	37.31	-0.88	38.21	37.31	-0.89	-3.53	-3.54	2.54	2.55
Left Hand Tsk	33.46	37.45	3.98	N/A	N/A	N/A	N/A	N/A	N/A	N/A	N/A	N/A	N/A
Right Hand Tsk	33.40	37.36	3.96	N/A	N/A	N/A	N/A	N/A	N/A	N/A	N/A	N/A	N/A
Left Thigh Tsk	35.49	36.61	1.12	N/A	N/A	N/A	N/A	N/A	N/A	N/A	N/A	N/A	N/A
Right Thigh Tsk	35.47	36.43	0.96	35.13	36.62	1.49	35.05	36.62	1.57	0.34	0.42	-0.53	-0.60
Left Lower Leg Tsk	35.26	36.54	1.28	N/A	N/A	N/A	N/A	N/A	N/A	N/A	N/A	N/A	N/A
Right Lower Leg Tsk	35.26	36.38	1.12	35.79	37.49	1.70	35.74	37.49	1.75	-0.53	-0.48	-0.57	-0.63
Left Foot Tsk	33.19	38.10	4.91	N/A	N/A	N/A	N/A	N/A	N/A	N/A	N/A	N/A	N/A
Right Foot Tsk	33.18	37.75	4.58	N/A	N/A	N/A	N/A	N/A	N/A	N/A	N/A	N/A	N/A

**Table 6.20 PCS #20 Hummingbird II by Creative Thermal Solutions Standard Multi-Node Model vs. Human Subject (HS) sweat rates with human subject results as the comparator.**

Sweat Totals	Standard Multi-Node Mode	Human Subjects (not included: 5, 6, 15)	Human Subjects (not included: 5, 6, 15), >120 min only
Total Sweat (kg)	0.87	2.28	2.45
Error Value (kg)	N/A	-1.41	-1.58
% Error	N/A	-61.84	-64.45

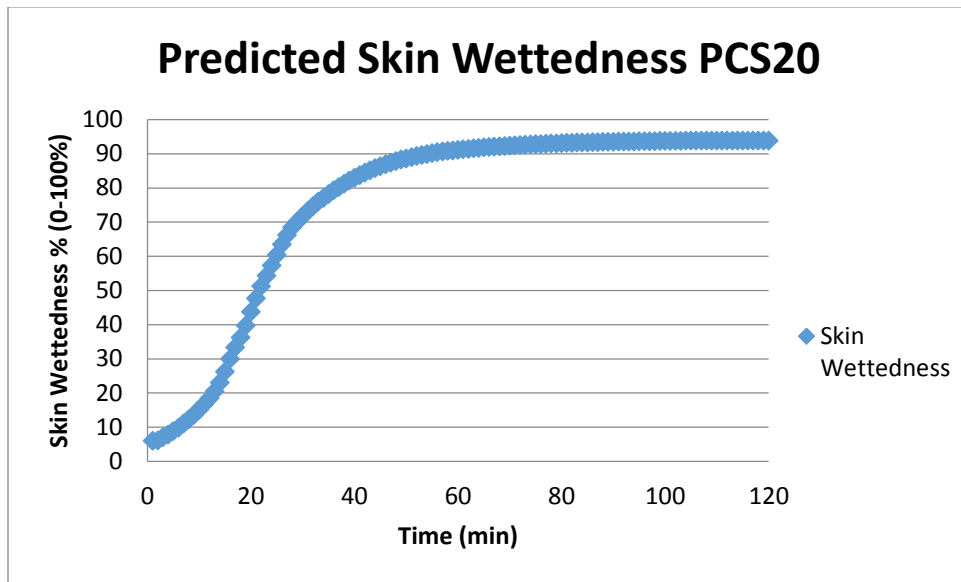


**Figure 6.32 Skin wettedness of the Standard Multi-node Model with PCS 20**

The multi-node initial core temperature ranged from 0.06 °C to 0.10 °C lower than the human subjects depending on the data set used. The multi-node predicted a 0.99 °C to 1.03 °C higher core temperature than the human subject average for PCS #20. It also predicted the largest sweat rate difference with a sweat rate 1.41 kg to 1.58 kg lower than the human subject average. The lack of evaporative cooling from sweat is a likely reason for the multi-node model high core temperature prediction. Again, if the sweat was produced in similar quantities to the human subjects, some accounting for the wetting clothing would be needed. The sweat rate gain increase would be more important early on in the prediction and may cause the skin wettedness to reach

our exceed one hundred percent as this would be in excess of that seen in the standard multi-node prediction in Figure 6.31.

### **6.3 Conclusions**

The standard versions of the models predicted the PCS results better than the baseline data presented in the previous chapter. However, that was not difficult because of large core differences in the standard baseline models compared to the measured results. The improvement in the prediction ability of the models does support the theory that the wetted clothing is to blame for the poor prediction ability of the baseline results as the lowered sweat rate in the PCS tests makes wetted clothing less important. Sweat rates under cooling and exercise are vital factor in the accuracy of both models, but do not appear to be a validated aspect of either model.

The modified two-node model provides the best core temperature PCS prediction capabilities and is significantly better than the standard model. It is clear, as the PCS lowered sweat rates and prevented the serious wetted clothing conditions in some of the cases. In the two-node model, all the PCS energy was removed from the skin node, which was not necessarily realistic in the case of PCS 1, the air circulation system because of the unrealistic sweat rate of the thermal manikin discussed previously. This was possibly reflected in the large discrepancies of predicted sweat compared with measured results. It is likely that this system cooled less and the remaining cooling was provided by sweat, including wetted clothing. A separate skin node would be needed to use a similar analysis to the multi-node PCS 1 evaluation. Modeling the cold boundary systems also resulted in reasonable core temperatures, but lower total sweat rates, even in the case of the modified-two node model. This effect is likely because of the large amounts of artificial cooling applied. The mean skin temperatures of the modified two-node models did not track well with the human subject results in two cases, PCS #12 and PCS #20, possibly because

of artificially cold thermocouples contacting the PCS in the trials and or vasoconstriction. The other possibility is that the ideal cooling on the thermal manikin is not seen in the human subjects. As a result, the PCS cool less and missing sweat in the prediction will make up the difference. Either way, more information is required to solve this dilemma.

The multi-node model prediction capabilities for the cold boundary systems were closer that baseline prediction but still not acceptable. As mentioned in Chapter 5, this model is intended and validated for comfort and sensation studies, although it has been used in some PCS validation and testing. The conditions that the simulated human is subjected to in this study result are conditions outside the validation range. The local segment boundary condition definition allows for the more accurate assignment of cooling to a segment, but may have the result of shutting off sweating to that segment, or significantly reducing it for the whole body. The application of the convection coefficients to model the ambient air circulation system, PCS 1, was the most accurate, however it appears that using this system clothing wetting still occurred, and/or the local sweat rates were not reflective of the values of the actual humans. The sweat rate in the multi-node model needs to be better defined for exercise related issues, and the local sweating values need to be known in order to determine the effects of sweating under these conditions as overall gain control is the only mechanism to modify the sweat. To improve the sweat model in both models will likely require further study to determine the proper rates and distributions, where applicable, under exercise, intense local cooling, and uncompensable heat conditions.



## **Chapter 7 - Discussion**

### **7.1 Introduction**

This chapter interprets and discusses the data taken from thermal manikin tests, human subject results, and human thermal modeling work performed. At the beginning of the project, the goal was to find an ‘off the shelf’ solution to mitigate the problem of heat stress on soldiers. With the completion of the initial selection and testing project, the focus shifted to research in an attempt to understand the effects of PCS on humans and the applicability of PCS test methods. The previous sections contain the information on the PCS testing performed and analysis of the data. However, after the completion of the testing and modeling it is instructive to include a chapter discussing PCS effects, testing methodology, and PCS testing. Discussing these results in more detail and exploring the issues is the focus of this chapter.

### **7.2 PCS Effects**

The first step performed in the analysis of the PCS effects was to perform an energy balance on the human. This took into account the metabolic rate, specific heats of the body, mean body temperature, and the cooling rate of the PCS. It was generally assumed, that the PCS effects would be purely subtractive to energy storage based on the test methodology in ASTM 2370, and literature. However, this was not seen in this analysis (ASTM, 2010a; M. Barwood et al., 2009; James R. House et al., 2013). Chapter 5 and Chapter 6 contain the results of the human subject tests baseline and PCS tests respectively compared to human thermal models. The energy balance completed at the end of the human subject results in Section 3.4 identified a possible oversight in comparing the baseline tests to the PCS tests. The human body is an integrated system and it is impossible to separate the different factors with the data available. Therefore, it is illustrative to discuss the different factors affecting the response of the human to PCS.

### ***7.2.1 Core Temperature***

When examining the mean body temperature, the core temperature accounts for a large percentage of the mean value. A key reason that the mean body temperature may not match precisely is due to the observed rise in core body temperature during exercise (M. Barwood et al., 2009; James R. House et al., 2013) . This effect is relatively short and generally seems to result in a core temperature plateau when exercising in thermally compensable conditions. It is likely related to the establishment of a conduction gradient inside the body to pass energy out of the body, a control point triggering body cooling measures, or the combination of the two. Therefore, exercise effects are likely to cause uncertainty, but in theory should not affect the overall energy balance. The theory is complicated if the body naturally raises the core temperature, which would require a path dependence function to ensure complete knowledge of the heat transfer pathways.

Similarly, core temperature rise alone does not indicate heat stress. This rise complicates comparing systems based on core temperature for a number of reasons. First, the natural core temperature rise and the core temperature safety limit of 39 °C used in these experiments decrease the temperature range where systems can be compared to approximately 1-2°C. This small difference can make it more difficult to show statistical variances between PCS core temperatures, which are set by the standard to be 0.3 °C core temperature drop compared to the baseline test.

The even more important issue is that the total core temperature rise is not important unless it exceeds the safety limit temperature for the specific application. Section 3.1.2 the importance of task time and choosing a PCS for a specific end use was covered in depth. Evaluating systems based off the total core temperature rise or fall compared to the baseline, when taken at the end of the two-hour standardized human subject tests, can artificially benefit

PCS that can bring the core temperature the lowest during that timeframe regardless of their longer term effects, e.g. carrying a heavy, depleted system for a long time period. This type of evaluation may be beneficial to the user in scenarios where a defined work time, with the PCS driving core temperature down, is followed by a period where there is the possibility of dramatic energy storage. The slope of the core temperature change with respect to time, especially at the end of the test, is what determines if the combination of work rate, ensemble, and conditions is sustainable. A core temperature slope  $\leq 0$  indicates that the PCS effect on the person is enough to prevent heat stress. The purpose of the PCS can, and perhaps should be in some circumstances, to restore conditions where the body can expel enough energy with the help of the PCS as to stop the core temperature rise and return the body to compensable energy loss. Therefore, as long as the PCS is functioning, the body is experiencing compensable heat exchange with the environment. This does not mean that the PCS is necessarily more efficient or a better system for each application, which requires the exploration of other PCS effects. The PCS has multiple effects on the human and these should be considered with the energy storage when evaluating systems for their desired end use.

### ***7.2.2 Sweat Rate***

As discussed throughout this work, sweating is the only natural mechanism for the body to remove energy in these conditions. Although the core temperature effects discussed in the previous section indicates the thermal state of the body, it does not resolve the energy balance. The most promising theory to resolve the energy balance for the PCS tests was that lower sweat production decreased the body's natural heat loss compared to the baseline tests. In the human subject test conditions a significantly lower sweat production was seen in the PCS tests

compared to the baseline tests, which returned the sweat rate. The previous sections detailed the performance of human thermal simulations on the baseline and four PCS conditions.

The human thermal models required validation and comparison to the human subjects at the baseline test conditions but this has not been done for the conditions used in this study. The models of the baseline tests produced core temperatures higher than the human subject results and sweat totals significantly lower than the human subject results. The theory was validated where the excess sweat was not dripping off the body without removing energy from the body, but was instead wetted the clothing. This provided an extra cooling mechanism resulting from over sweating. Interestingly enough, the dripped sweat was not wasted, but it was not used as efficiently as possible.

An implicit assumption in the models: the clothing does not wet, absorb moisture, and interact via evaporation with the surroundings; had a large effect on the simulated heat transfer accuracy of both models. A method to incorporate the wetting of the clothing using a wetted area as a percentage of the overall surface area, was presented and then formulated specifically for the human subjects in these conditions. There have been multiple models created to address the issue of moisture transport through fabric including absorption in some cases (Crow, 1974; Lotens, 1993; K. C. Parsons, Havenith, Holmér, Nilsson, & Malchaire, 1999). However, the method developed in this research looks at liquid wetting of the fabric and has the advantage of requiring only a few empirical measurements, and one variable, to achieve final core temperatures and sweat totals in a reasonable range. This is different from the other models in the literature, accounts for the dripping moisture, and provides an energy balance to determine the efficiency of evaporation from the fabric.

Simulating PCS results without the sweat rate model or spot size modification, in the two-node model, the core temperature results were surprisingly close to the measured results. This is significant compared to the large differences in core temperature when modeling the baseline results without modification. In the two-node PCS simulations, like in the baseline simulations, the clothing did become significantly saturated and add a new heat transfer pathway. Similarly, the multi-node model is much more complicated as it incorporates local effects. This makes it powerful, but more precise knowledge of the local sweat rates, and their clothing wetting effects is needed. Furthermore, the local sweating does not transfer from segment to segment, unlike in the human subject tests where both wicking and gravity have the ability to move moisture around the clothing. It was difficult to properly replicate the wetted conditions by using an average  $Re_{Cl}$  value as was hoped because of the local effects.

The ability to define the local values does provide the ability to apply the local cooling from the thermal manikin. It also allows the use of the thermal manikin to calculate the heat transfer coefficients for ambient air circulation systems as was performed in this work for the first time in the author's knowledge. This has the potential to provide a much more accurate value for thermal modeling of air circulation systems as it uses heat and mass transfer fundamentals to determine the proper boundary conditions that are largely independent of the artificial thermal manikin properties.

The sweat rate and distribution in the two-models was also an important issue. The two-node model performed the best out of both systems after the application of the presented wetted clothing model. However, both systems did not sweat enough for the baseline case. The standard multi-node model sweat was much lower than the measured results and reached 100% skin wettedness in most of the simulations. In the simulations where a cold boundary for a PCS was

applied, the simulation lowered the sweat rate even more. Nevertheless, it is likely from the predicted skin wettedness graphs that clothing wetting occurred.

Similarly, the lowered sweat production in the PCS tests decreased the amount of sweat required to achieve a similar or better core temperature compared to the baseline result. This highlighted a further effect of the PCS when addressing uncompensable conditions. The complete saturation of the body, where skin wettedness,  $\omega=1$ , indicates at least the boundary of uncompensable heat stress conditions if not completely into the region. It is hypothetically possible for the wetted clothing to reach a point of compensable conditions under this theory, but the larger spot size, or excess sweat in the case of a relatively impermeable system, points to the presence of uncompensable heat stress and the wasting of the body's water supply in an inefficient attempt to cool itself.

### ***7.2.3 Heart Rate***

Another physiological benefit of PCS was significant lowering of heart rate in some of the systems. What causes the decrease in heart rate remains to be a topic of investigation. Heart rate has been shown to be an important measurement value when investigating high stress decision making (Hope et al., 2015). A decrease in the heart rate could be seen as desirable, despite the physiological cause, which may be linked to other factors, such as core temperature. In any case, the lower heart rate provides a benefit to the wearer, especially if it has an effect on high stress decision-making ability.

### ***7.2.4 Tradeoff***

In order to determine the best PCS for the wearer, a series of tradeoffs are essential. The lowest core temperature is not necessarily the main goal of a PCS, nor is lowest sweat rate or heart rate. The goal is to make provisions for activity over a certain time in a specified ensemble.

Reasonable selection criteria must be made the exact needs of the end user must be quantified. Comparing PCS based on ASTM thermal manikin and human subject testing is rife with issues, but does exist to standardize comparison of systems. However, the PCS system will also incur logistical and time penalties in practical use. Therefore, if a system can restore compensable heat exchange conditions with the environment, this may be good enough for use, or even better than a system that creates a larger logistical or operational burden on the end user.

The most logical example is the lowered sweat rate seen on the soldiers in the simulated desert conditions. Soldiers are already overburdened and must carry enough water to not enter dehydration (Committee, 2007). Therefore, a 0.5 kg PCS that reduces the sweat produced by the soldier by 1 kg over a 2-hour mission has saved that soldier 0.5 kg that needed to be carried. However, in the case where a high metabolic output is to be expected during or after cooling with little to no evaporative component, for example firefighting, it may be desirable to provide the lowest core temperature.

### **7.3 Testing Methodology**

In practice and the literature, thermal manikin testing of personal cooling systems according to ASTM Standard 2371, is considered to be a reasonable predictor of the ability of a PCS to cool a human subject (ASTM, 2010b; Mokhtari Yazdi & Sheikhzadeh, 2014). There are three main areas where the standardized test creates uncertainty in comparing thermal manikin results and human thermal results/predictions. The three areas to consider are losses to the environment, constant manikin skin temperature, and manikin sweat rate.

#### ***7.3.1 Losses to the environment***

In the ASTM thermal manikin test ASTM F2371 (ASTM, 2010b) the manikin and the environment are at isothermal conditions. However, the human subject tests in this study take

place at an ambient temperature of 42.2 °C air temperature and 54.4 °C radiant load. Actual end use for a soldier will encompass many different conditions. In the human subject tests, the cooling systems had at least a 7.2 °C temperature differential with the environment over the thermal manikin tests. However, the environment losses are generally ignored when comparing the thermal manikin results to human subjects. This is often partially justified because the skin temperature of 35 °C used by the thermal manikin can be lower than that seen on human subjects. PCS could perform longer on the thermal manikin under isothermal conditions because there is less energy removed from the system. If a system is limited in cooling time, which is very common among portable systems this can be a major factor. Unfortunately, without knowing the heat flux from the human, representative skin temperatures under the PCS, and or losses to the environment, it is difficult to predict the cooling provided to the human at any time step.

A theoretical method to model PCM systems PCS #9 and PCS #12 would involve creating a conduction, thermal capacity, and phase change model of the PCM material. This would involve defining moving phase change boundary conditions in the packet and allowing for a time and temperature dependent resistance model where the fluid level can grow. In this method, a number of definitions are required: conduction model of the body armor, the thermal mass of both systems and their convective, conductive, radiative, and evaporative boundary conditions, including the possibly proprietary properties of the PCM materials, and an accurate model of PCM shape changes during melting.

The vapor compression system has an advantage of applying a relatively constant energy removal capacity to the body because of the nature of the vapor-compression refrigeration cycle, but only as long as skin temperature is maintained. Therefore, a conduction model would be needed of the body armor with an available mass flow rate of liquid refrigerant changing phase



in evaporator vest assuming all the refrigerant evaporates, a value for the fraction absorbed by the body could then be calculated. However, the capacity of the system changes with relation Carnot cycle. As the skin temperature decreases, the capacity of the system goes down.

### ***7.3.2 Maximum thermal manikin heat flux***

The constant skin temperature of 35 °C can create a situation where the manikin can provide more energy than would be seen on a human. The high available heat flux from the thermal manikin allows the manikin's skin temperature to remain at 35 °C even when exposed to extremely cold conditions. The skin temperature of the human decreases when exposed to low temperature, cold boundary PCS, as seen in our tests, therefore this does not necessarily represent the correct heat flux from a PCS. A PCS could be expected to run for different periods of time or with different cooling intensity when interacting with a human based skin temperature. The standard does exist as a way to compare PCS, however it may not always be representative of the how the PCS operates on a human in different applications.

### ***7.3.3 Manikin sweat rate***

The air circulation system presents a special circumstance when applying the thermal manikin results to the human subjects. The 100% wetted surface of the manikin skin provides a sweat quantity across the evaporation area that is higher than can be maintained by the human subject. The other aspect is that the thermal manikin test takes place under isothermal conditions where the only heat loss from the manikin comes from evaporation. In the human subject tests, the ambient air temperature is higher than the skin temperature adding energy to the body by convection while removing it via evaporation, causing a net decrease in the evaporation value. The logical way to do an air circulation type PCS is to use the thermal manikin to determine the effective convective and evaporative heat transfer coefficient created by the PCS, and then use

that with the skin temperature, sweat rate, and possibly spot size to solve the mass and energy balance.

## 7.4 Wetted Clothing Model

This work has presented a complete overview of PCS selection, testing, and evaluation. The focus was on the dismounted soldier however, the same concepts can be applied to many other uses. To evaluate the results in the two-node model, and resolve the assumption that the clothing does not wet, required the creation of a modified two-node model to address uncompensable conditions. The modification to the two-node model was discussed in detail in Section 5.1.2 and provides two scalable factors that can be modified to fit a set of empirical data and improve the accuracy of the two-node mode when clothing wetting is likely. The values presented could also be used in military applications for an active group of soldiers where the clothing and equipment coverage are similar to our tests using the coefficients from this work. The general version of the model for use is presented below. The model contains two features that modify the sweat rate term: the wetted spot model and sweat rate modification term.

### 7.4.1 Spot Size

The spot grows when excess sweat that is produced, i.e. that sweat that is greater than that used to maintain 100% skin wettedness,  $\omega = 1$ . The sweat rate given in the ASHRAE two-node model, in power units, is governed by Equation (5.1).

$$E_{rsw} = \dot{m}_{rsw} \cdot h_{fg} = c_{sw} \cdot (T_b - T_{bset}) \cdot \exp \left[ \frac{T_{sk} - 34^{\circ}\text{C}}{10.7} \right] \quad (7.1)$$

The sweat rate coefficient,  $c_{sw}$  given in energy terms, as 116 W/(m<sup>2</sup>K) in the ASHRAE model (ASHRAE, 2013) is in terms of power units.  $E_{rsw}$  is the power converted sweat rate. The value  $T_b$  is the mean body temperature and  $T_{bset}$  is the mean body set point temperature, both governed by equations in the two node model that were not modified in this analysis. In the

sweat rate, spot creation the excess sweat is added to the wetted area spot. The spot mass balance can be stated as:

$$d\mathbf{m}_{spot}/dt = (\dot{\mathbf{m}}_{spot,in} - \dot{\mathbf{m}}_{spot,out}) \quad (7.2)$$

The spot mass change with respect to time is the balance of the spot mass,  $m_{spot}$ , the mass entering the spot from excess sweat  $\dot{m}_{spot,in}$ , and the mass leaving the spot by evaporation,  $\dot{m}_{spot,out}$ . Therefore, the net exchange of the spot at any instant,  $\dot{m}_{spot,net}$ , is:

$$\dot{\mathbf{m}}_{spot,net} = (\dot{\mathbf{m}}_{spot,in} - \dot{\mathbf{m}}_{spot,out}) \quad (7.3)$$

Using an appropriate time step,  $\Delta t$ , will allow for a discrete approximation of a continuous function. The equation for the next time step in the program,  $m_{spot,i+1}$ , is given by the current mass,  $m_{spot,i}$ , plus the net change in the spot mass from evaporation and excess sweat for that time step,  $\dot{m}_{spot,net} \cdot \Delta t$ .

$$\mathbf{m}_{spot,i+1} = \mathbf{m}_{spot,i} + \dot{\mathbf{m}}_{spot,net} \cdot \Delta t \quad (7.4)$$

The wetted spot is defined as only the wetted area that is available for evaporation. The term,  $w_c$ , is the wettedness coefficient, which is the percentage of the surface area of the body that is considered wetted by the spot. The percentage of the body's sweat that is available to contribute the wetted spot is  $\phi_w$ .

$$\dot{\mathbf{m}}_{spot,in} = \phi_w \cdot \frac{E_{rsw} - (1 - w_c) \cdot E_{sk}}{h_{fg}} \quad (7.5)$$

The evaporation component out of the spot is the amount of evaporation from the spot,  $w_c \cdot E_{spot}$ , divided by the latent heat of vaporization to get the mass component.

$$\dot{\mathbf{m}}_{spot,out} = \frac{w_c \cdot E_{spot}}{h_{fg}} \quad (7.6)$$

The possible energy that can be removed by the spot is given by  $E_{spot}$  for 100% wetted surface of clothing. The value  $P_{sk}$  is the partial pressure of the 100% wetted spot surface and  $P_a$  is the partial pressure of the air at their respective temperatures. The relative humidity percentage is  $\phi$ .

$$E_{spot} = \frac{P_{sat}(T_{sk}) - P_{sat}(T_a)\phi}{\frac{1}{f_{cl}h_e}} \quad (7.7)$$

In this case, the  $E_{spot}$  value is used to maintain the same solving methodology used with the heat and mass transfer analogy and the appropriate Lewis Ratio for these conditions has already been calculated to use the two-node model. In addition, this equation will also be used in the energy balance with another further refinement to calculate the energy removed by the spot. The remaining term not defined in the mass balance equations is that of the wetted area, already introduced as the percentage of surface area comprising the wetted spot,  $w_c$ . To determine a reasonable  $w_c$  it is necessary to determine liquid mass per unit surface area of the clothing. The wetted surface area is a function of the mass of water, and thus is analogous to the water adsorption capacity of the clothing layer. To determine the surface-area ratio per liquid mass, a series of tests can be performed on the clothing material that is expected to wet. A titration burette should be used to drip precise quantities of water onto a single layer section of the clothing fabric. The clothing fabric should also be backed by an impermeable layer to ensure all

the liquid is absorbed into the spot.

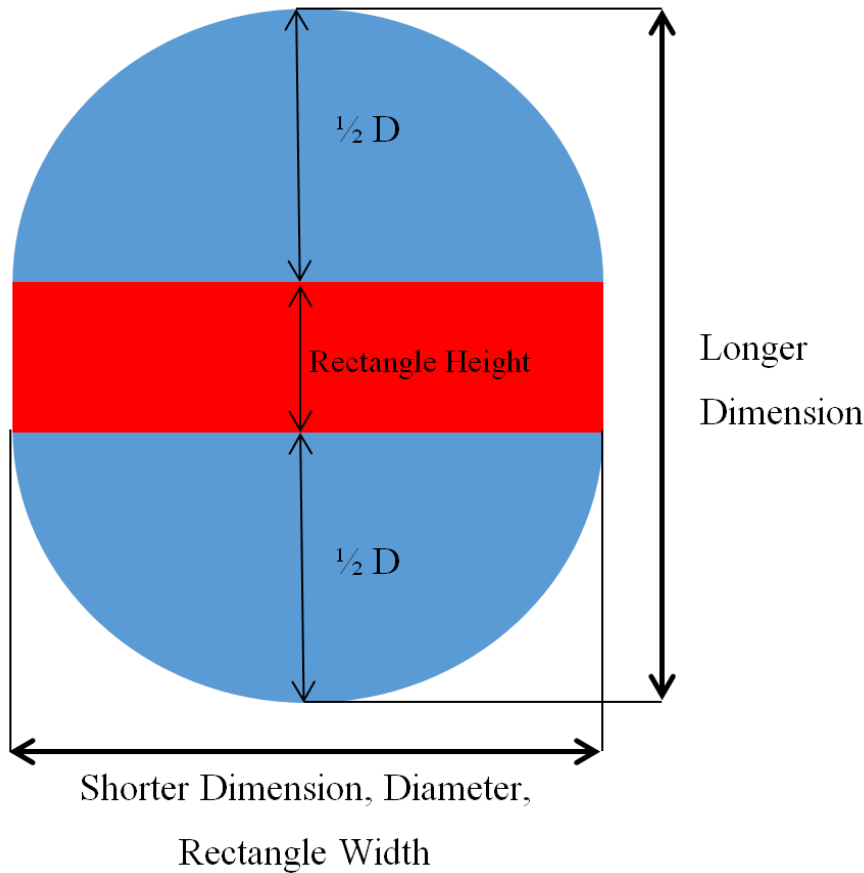


**Figure 7.1 Depiction of area calculation in spot size per area calculations. Area was calculated by two-semi circles tangent to a central rectangle.**

When steady state approximation was reached, the shapes can be rounded and were assumed to resemble Figure 5.3 with a rectangular area and two semicircular halves. The shorter of the two distances measured is used as the diameter of the two semi circles and the long edge of the rectangle, width as portrayed in the figure. The longer dimension is used to calculate the shorter side of the rectangle, height as portrayed, by subtracting the longer dimension by one diameter. The linear approximation is set to have an intercept at zero and the slope,  $x_c$ , becomes the mass/unit area term. Therefore, the wetting coefficient,  $w_c$  at any time step,  $i$ , is the wetted spot area  $A_w$  over the body surface area,  $A_D$ .

$$w_c = \frac{A_w}{A_D} = \frac{m_{spot,i} * x_c (m^2/kg)}{A_D} \quad (7.8)$$

Mass of the spot is assumed to not store energy and change with each time step. The original energy removal from the skin via evaporation is by the two-node model's evaporation term, with the assumption of no skin wettedness,  $E_{sk}$ . The modification replaces this term with the two areas, dry clothing and wet clothing:

$$Q_{evap} = (1 - w_c) \cdot E_{sk} + \varepsilon_s \cdot w_c \cdot E_{spot} \quad (7.9)$$

Unless the wetted area has perfect contact with the skin, there will be impedance to the transfer of heat from the body by the air layer, fabric resistance, and any heat gain from the environment. The efficiency value,  $\varepsilon_s$  of the wetted clothing, corrects for this exchange. This can be done based on the average body temperature, taken from human subject baseline tests, together with a decreased thermal resistance value to account for fabric saturation. The energy balance can be seen in Figure 5.5. The massless temperature of the fabric is calculated by solving the energy balance of Equation ( 5.10 ).

$$0 = Q_{body} + Q_{evap} + Q_{C+R} \quad (7.10)$$

In this equation  $Q_{body}$  represents the heat transfer from the body to the wetted spot through the clothing and air layer,  $Q_{evap}$  is the evaporative losses from the spot, and  $Q_{C+R}$  is the energy gained in the spot due to convection and radiation. Substituting the proper heat transfer equations provides a per unit area calculation of the temperature,  $T_{spot}$  through numerical iteration of the input variables.

$$F(T_{spot}) = 0 = \frac{T_{sk} - T_{spot}}{R_{cl,w}} + h_e \cdot (P_{sat}(T_a) \cdot \phi - P_{sat}(T_{spot})) + h_t \cdot (T_o - T_s) \quad (7.11)$$

The variables used in the efficiency calculation to determine  $T_{spot}$  are as follows and are mostly taken from the environmental chamber conditions. The skin temperature was the average mean skin temperature of the human subjects across the baseline tests. The wet resistance value of the clothing with air layer,  $R_{cl,w}$ , can be estimated using resistance of the segments that are allowed to wet and evaporate and is given as  $R_{cl,wet}$ . This can be modified based on the concept that the insulation resistance of a wet garment can be reduced by 1/3 (Crow, 1974). The other values that need to be determined prior to calculation are given in the list below and unless otherwise specified for some valid reason, should be the same as those used in the two-node model calculations:  $T_a$ ,  $T_r$ ,  $R_{cl,w}$ ,  $T_{sk}$ ,  $h_r$ ,  $h_c$ ,  $h_e$ ,  $h_t$ ,  $\phi$ .

Equation ( 5.11 ) can then be iterated as a function of  $T_{spot}$ , which will result in the  $T_{spot}$  where the energy balance exists. To determine the efficiency of cooling from the evaporating spot,  $\epsilon_s$ , the equation for the efficiency is simply the heat removed from the body,  $Q_{body}$  over the energy removed from the spot  $Q_{evap}$  at the energy balanced temperature,  $T_{spot}$  .

$$\epsilon_s(T_{spot} = 27.4 \text{ }^\circ\text{C}) = \frac{Q_{body}}{Q_{evap}} = \frac{\frac{T_{sk} - T_{spot}}{R_{cl,w}}}{h_e \cdot (P_{sat}(T_a) \cdot \phi - P_{sat}(T_{spot}))} = 35\% \quad (7.12)$$

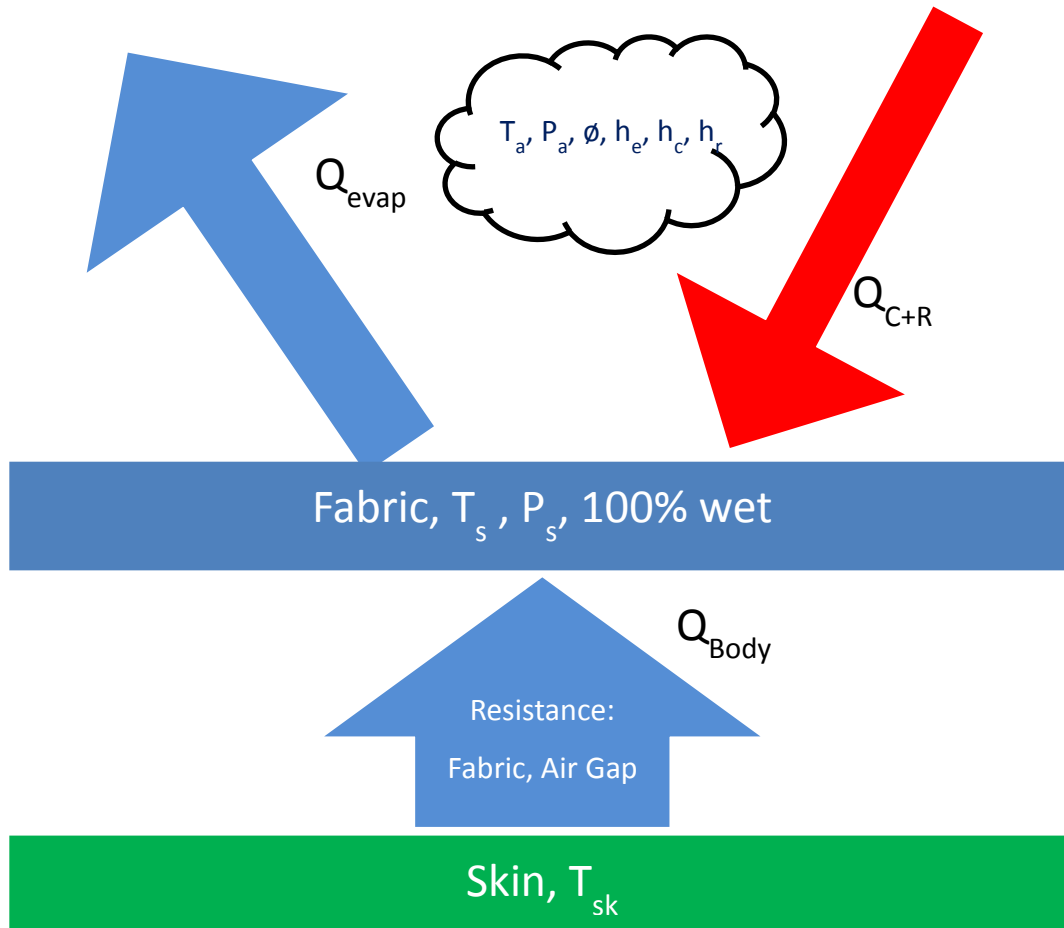


**Figure 7.2 Energy balance on the wetted fabric**

The total C+R to the body must be reduced by the spot size. The remaining non-wetted clothed area is subject to conduction, radiation, and evaporation as expected. The energy equation for the non-wetted area is:

$$(1 - w_c) \cdot [(C + R) + E_{sk}] \tag{7.13}$$

#### **7.4.2 Sweat Rate**

Applying the additional cooling from the spot size artificially decreases the sweat rate in uncompensable conditions compared to the results seen in human subject testing. The sweat rate should be constrained the within reasonable bounds from literature and set at a threshold of



producing 670 W/(m<sup>2</sup>K) of energy from the sweat (ASHRAE, 2013), or approximately 16.5 g/(m<sup>2</sup>min) or 29.7 g/min for the average Dubois Area, A<sub>D</sub> of 1.8 m<sup>2</sup>. The modified equation for sweat with the linear sweat modification term SW<sub>mod</sub>, Equation (5.1), given in power units, can be seen in use Equation (5.14).

$$E_{rsw} = SW_{mod} \cdot c_{sw} \cdot (T_b - T_{bset}) \cdot \exp \left[ \frac{T_{sk} - 34^{\circ}\text{C}}{10.7} \right] \quad (7.14)$$

Once the SW<sub>mod</sub> term and spot size have been included in the standard ASHRAE model, the sweat rate modification term should be iterated until the total sweat predicted by the model is equal to that seen in human subject tests. The proportional sweat modification term SW<sub>mod</sub> is acceptable for modeling the energy storage in the subjects over a measured and specified time period. As discussed, this is likely a function of time and with data on human subject sweat rates as a function of time it would be logical to scale SW<sub>mod</sub> as a time function: SW<sub>mod</sub>(t), to account for these changes. This could be performed either as by adding an equation or referenceable matrix.

The spot size creation and sweat rate modification proposed in the presented wetted clothing model interfaces in the model as part of the skin node. The skin energy balance contains the new values and the next skin temperature at time step i+1, T<sub>sk, i+1</sub>, is shown in Equation (5.15).

$$T_{sk, i+1} = \frac{-[(1 - w_c) \cdot ((C + R) + E_{sk}) + \varepsilon_s \cdot w_c \cdot E_{spot} + (K + \rho_{bl} \cdot Q_{bl} \cdot Cp_{bl}) \cdot (T_{cr, i} - T_{sk, i})]}{\frac{\alpha_{sk} \cdot m_b \cdot C_{sk}}{A_D \cdot \Delta t}} + T_{sk, i} \quad (7.15)$$

## 7.5 Conclusions

Based on the PCS research performed, a number of topics have been discussed and a series of conclusions can be drawn. Overall, the more information that can be gathered from

human subject tests will allow for the best comparison of PCS. Current testing according to the PCS standards does not provide enough information to compare PCS for the application of dismounted soldiers. Measuring local sweating, and the sweat stored in clothing would allow PCS to be better quantified in human subject tests.

With more information regarding local sweat rates and wetting, the next logical step is to expand the spot model to cover multiple clothing types and with multiple spots. The success of the presented wetted clothing model application of the ASHRAE two-node model makes another similar derivation a logical starting place. This would likely use the two-node implementation of (Jones & Ogawa, 1992) with multiple clothing segments and a subdivided sweat rate, convection coefficients, etc.

PCS were studied in uncompensable conditions for use in extreme environments. The known benefits of PCS are that they can extend work time and improve recovery from heat stress. However, a key benefit of PCS seems to be the return the body to more compensable conditions, decreasing sweat rate and heart rate in addition to core temperature. The best course of action is to encourage the natural cooling of the body wherever possible. PCS lowered the sweat rates in many cases, which would potentially result in less water that needed to be carried. This is important because in compensable conditions, dehydration becomes the key limit to work and a tradeoff could be made between carrying a PCS and water. Achieving dehydration has the possibility to create uncompensable thermal conditions in addition to the other physiological detriments associated with the condition.

The future of PCS requires a design goal in order to determine the best system for a given task. Traditionally, the target has been the lowering of the core body temperature as much as possible, however it has been argued here this is not necessarily the best goal when searching for

or designing a PCS. When examining and modeling the data from the human subject tests it became clear that dripping sweat was an important indication of the body's inability to properly cool the body in uncompensable thermal conditions. Moreover, when sweat dripping occurs at  $w > 1$ , in semi-permeable, encapsulating clothing it is wasted potential energy that could be used in cooling the body later in the activity. Therefore, the role of the PCS should be to return the body to the compensable conditions, if possible, and relying on the human body to make up the remainder of the energy loss to the environment. Sweating more than necessary is not an efficient use of resources, although neither is overcooling the body, so finding the right balance of cooling to achieve compensable conditions with the lowest sweat rate is a worthy target of PCS design endeavors. This work has been an important first step in exploring the design goals of PCS, however to find the balance between different cooling types and methods in terms of sweat rate, core temperature, heart rate, and weight will require more empirical research and analysis.

## Chapter 8 - Conclusions

The current research initially set out to select and test personal cooling systems (PCS) for use on dismounted U.S. Army soldiers in a desert combat environment. The goal was to address heat stress in conditions where environmental variables, activity level, clothing and/or equipment limit the removal of metabolic energy from the body. The dismounted soldier provides a unique and challenging area for study as military operations often dictate these factors, requiring mitigation for the resultant heat stress through another means. The inability to expel enough metabolic energy, plus any energy gained from the environment, is also common in recreational activities, occupations, and sports; PCS may be a viable mitigation strategy for the resulting heat stress in those areas as well. After, the completion of the standardized testing and initial analysis, the project sought to understand the effects of PCS on humans and develop a set of design goals to direct future work in creating and selecting efficient and workable PCS.

This work has provided an intensive review of heat stress, thermal models, PCS cooling technology, and PCS literature to aid in the further research and design of PCS. The thermodynamics associated with human heat exchange and storage has been presented along with the current understanding in literature of PCS effects, which has yet to be codified in one piece of work. Furthermore, a table suitable for searching for similar PCS systems, applications, variables studied, and a number of other factors has been created to aid further research and design on PCS in addition to a detailed review and discussion of PCS.

PCS testing required the development of a selection method based on sound engineering, scientific, and logistical principles to ensure the best possible systems were chosen. This task was completed and selection of a suitable number of PCS systems for thermal manikin and human subject testing were picked. The PCS selection methodology was published, including the

innovative cooling effectiveness value. The cooling effectiveness is based on the expected cooling provided by a system at the same walking conditions, incorporating the effects of PCS weight and cooling time; compared to the desired mission time. The heat stress cutoff for the subject is a user supplied variable, along with the other physiological and environmental conditions to create a matrix of predicted cooling effectiveness for a range of variables. With this method, the selection of PCS can begin to account for these variables if multiple end use cases exist, as was the case with the dismounted soldier.

The testing methodology for evaluating PCS on the sweating thermal manikin and on human subjects was detailed to provide scientific continuity. The average results of the human subject testing were also presented and an energy balance was performed on the human system to explore the PCS effects on humans. During this analysis, it was discovered that the cooling systems seemed to perform much worse on the human subjects than predicted by the thermal manikin testing. The core and mean body temperatures were higher than the expected results, which used the natural heat loss from the baseline test and the cooling values from the thermal manikin. The lower sweat rate of the PCS tests compared to the baseline results seemed to indicate that the natural heat loss term might be lower in the PCS tests due to less evaporation. In order to determine the breakdown of the energy balance, more information was required. It was determined that human thermal modeling and or further empirical experiments needed to be performed to provide evidence to support this theory.

Two thermal models were selected to simulate the baseline and human subject tests: the ASHRAE two-node model and the multi-node human thermal model in TAITherm by Thermoanalytics. The initial and boundary conditions of both models were presented with the human subject data used in each model. To define the more specific radiation boundary

conditions on the human, a complex model was developed for simulating the chamber's solar lamps. Other boundary conditions such as convection and clothing properties also required definition to properly set up the multiple skin segments and clothing layers.

Baseline human subject results for each model were simulated to validate that both models were working properly before application to the PCS tests. Both models predicted core temperatures, on average, over 1 °C higher than seen on the human subjects. After further study, it was discovered that the models were both not designed for the severe, uncompensable thermal conditions because they assumed that the clothing could not wet, hold, and evaporate moisture. The human subjects were sweating at a very high rate and were exceeding a skin wettedness of 100% resulting in sweat dripping off. In the original model validation, this held true as the tests were performed on men clad only in running shorts and shoes, allowing sweat to drip off and not be absorbed over the majority of the body. The nature of the clothing and equipment worn by the soldiers were almost the complete opposite. It ensured that most of the dripping sweat was captured by the clothing and equipment covering the majority of the body, with the exception of the face and neck. In the human subject baseline tests the clothing was becoming saturated, and due to the low humidity levels, the clothing was allowing for more evaporative cooling. A method was formulated for simulating the clothing wettedness area by creating a wetted spot, which was fed by the excess sweat produced in the model. The wetted clothing evaporated to the environment with a lower evaporative resistance than the unwetted sections; splitting the surface node into wetted and unwetted areas. The simulation was performed for each human subject to determine how well the values matched. The addition of the cooling provided by the wetting fabric caused the human thermal model to decrease the sweat rate even though the conditions were uncompensable. Therefore, a modification value was added to increase or decrease the

sweat rate by a single proportional factor to match the measured result from the human subject tests. The ability of the model to predict the baseline core temperature was improved by 95% and the sweat production by 51% when the average subject was simulated. The multi-node model shared this issue, however there was no way to apply the spot model without creating a code package to interface with a proprietary program, which was outside the scope of this work. Therefore, the average evaporative resistance of the clothing was modified to match the average resistance from the two-node model and an increased sweat rate was employed to only minor improvements in core temperature accuracy. The local segments of the multi-node model make it more precise, but make the knowledge of individual segment sweat rates and saturation impossible in the version of the model used.

With the validation of the Elson version of the ASHRAE two-node model, the personal cooling systems were modeled and compared to the human subject results. The results of these models were a reasonable prediction of final core temperatures and a low prediction of sweat production compared to the human subject results. The sweat rate reaction to the PCS remains an area for further study, however it is possible that by using the cooling values from the thermal manikin results more cooling was applied in the simulations. This excess PCS cooling may have offset the loss of the cooling that would have been produced at the sweat production rate seen in the human subject tests. The PCS simulations were also performed using the multi-node model. This was justified as the PCS decreased the sweat rate enough that the clothing may not have wet significantly. Therefore, the non-wetted clothing assumption would hold true and the model was free to function as designed. As was observed in the literature, in previous PCS tests, the multi-node model performed better when predicting PCS cooling, especially the ambient air circulation system, but not as well as the presented wetted clothing model. The local cooling effects are still

not understood and the sweat rate algorithm needs to be modified for exercise, uncompensable heat stress, and local cooling effects.

This work has included unique thermal manikin and human subject data into the literature for future use in evaluating, selecting, and modeling PCS. Even more importantly, this research has provided a unique engineering and thermodynamic insight into human thermoregulation and the selection and use of PCS based on the end-use application. Although the core temperature is the important factor in determining heat illness, sweat rate was recognized as the factor affected by the PCS that had the most impact on the actual performance of the PCS. Furthermore, the presented wetted clothing model, a modification of the ASHRAE two-node model was created for use in exploring the effects of heat stress on active soldiers in encapsulating, semi-permeable, wetting garments. This unique system included a modification to the sweat rate of the modeled human subjects to account for high sweat rates during the uncompensable baseline tests as well as a wetted spot size calculation method that can be scaled easily into other thermal models with the non-wetting clothing assumption.

Additionally, dripping sweat, occurring when skin wettedness is greater than 100%,  $\omega > 1$ , represents wasted sweat that could be used later in task performance. Complete skin wettedness also represents the transition region from barely compensable thermal conditions into the uncompensable range. The ability to maintain sweat production is essential where evaporation heat loss is an option. When the available water in the body used for sweating is exhausted, dehydration can quickly turn a compensable thermal condition into an uncompensable thermal condition in addition to the other detrimental effects of dehydration. This further reinforces the important role of sweat in PCS applications where evaporative cooling is possible. Decreasing



wasted sweat and increasing the time to dehydration is a distinct benefit and is a unique outlook on PCS effects.

The role of the PCS requires a redefinition where personal cooling systems provide an efficient and targeted benefit to the wearer. This work has been a significant step in determining how the PCS affects the body, future areas of study, and articulating how PCS should be designed and selected. As in many engineering endeavors, there are tradeoffs that must be made, and there is not a “one size fits all” cooling method. The needs of the end users must dictate the requirements of the PCS, which are not only limited to a low core temperature, but include logistical and safety issues, water replenishment needs, efficiency of sweating, heart rate, and many other factors. Determining the proper balance between the PCS effects and defining the design goals of PCS through further research and testing will allow for system designs that efficiently meet the needs of the end user rather than targeting an artificial value without perspective on the end-use scenario.

## Bibliography

- Adolph, E. F. (1947). Physiology of Man in the Desert. *Physiology of Man in the Desert*.
- Ainsworth, B. E., Haskell, W. L., Herrmann, S. D., Meckes, N., Bassett Jr, D. R., Tudor-Locke, C., . . . Leon, A. S. (2011). *The Compendium of Physical Activities Tracking Guide*. (March 20, 2014). Healthy Lifestyles Research Center, College of Nursing & Health Innovation, Arizona State University.
- Aitken, A., Hamilton, J., Redortier, B., Robbie, M., Spindler, U., & Thwaites, C. (2002). *Performance tests of a novel cooling vest providing cooling by the means of a cryogenic fluid*. Paper presented at the Environmental ergonomics: The 10th International Conference on Environmental Ergonomics, Fukuoka, Japan: Kyushu Institute of Design.
- ALGERA, R. (1985). *Development of an improved liquid cooling system((in protective clothing))*. Paper presented at the SAFE Association, Annual Symposium, 22 nd, Las Vegas, NV.
- Allen, C., & Mark, H. (2013). Assessment of Modeling Individual Physiological Differences when Predicting Thermal Comfort *Proceedings of the FISITA 2012 World Automotive Congress* (Vol. 195, pp. 393-398): Springer Berlin Heidelberg.
- American College of Sports Medicine. (2010). *ACSM's resource manual for Guidelines for Exercise Testing and Prescription* (8th ed.). New York: Lippincott Williams & Wilkins.
- Amorim, F., Yamada, P., Robergs, R., & Schneider, S. (2007). Effect of Palm Cooling on Heat Extraction During Exercise in a Hot Dry Environment: 1840: Board# 128 May 31 8: 00 AM 9: 30 AM. *Medicine & Science in Sports & Exercise*, 39(5), S309.
- Arens, E., Xu, T., Miura, K., Hui, Z., Fountain, M., & Bauman, F. (1998). A study of occupant cooling by personally controlled air movement. *Energy and Buildings*, 27(1), 45-59. doi:[http://dx.doi.org/10.1016/S0378-7788\(97\)00025-X](http://dx.doi.org/10.1016/S0378-7788(97)00025-X)
- Arkin, H., Xu, L. X., & Holmes, K. R. (1994). Recent developments in modeling heat transfer in blood perfused tissues. *Biomedical Engineering, IEEE Transactions on*, 41(2), 97-107. doi:10.1109/10.284920
- ASHRAE. (2007). HVAC Applications (Vol. SI Edition). Atlanta, GA: ASHRAE.
- ASHRAE. (2013). Fundamentals. Atlanta, GA: ASHRAE.
- ASTM. (2010a). Standard F2300-10 *Standard Test Method for Measuring the Performance of Personal Cooling Systems Using Physiological Testing*. West Conshohoken, PA, USA: ASTM International.
- ASTM. (2010b). Standard F2371-10 *Standard Test Method for Measuring the Heat Removal Rate of Personal Cooling Systems Using a Sweating Heated Manikin*. West Conshohocken, PA, USA: ASTM International.
- ASTM. (2011). Standard Practice for Determining Temperature Ratings for Cold Weather Protective Clothing (Vol. F2732-11). West Conshohocken, PA: ASTM International.
- Azer, N., & Hsu, S. (1977). The prediction of thermal sensation from a simple model of human physiological regulatory response. *ASHRAE Transactions*, 83(1), 88-102.
- Bansevičius, R., Račkienė, R., & Virbalis, J. (2007). The body cooling system integrated into the clothes. *Electronics and Electrical Engineering.–Kaunas: Technologija*(5), 77.

- Barbosa, J. R., Ribeiro, G. B., & de Oliveira, P. A. (2011). A State-of-the-Art Review of Compact Vapor Compression Refrigeration Systems and Their Applications. *Heat Transfer Engineering*, 33(4-5), 356-374. doi:10.1080/01457632.2012.613275
- Bartkowiak, G., Dabrowska, A., & Marszalek, A. (2014). Assessment of the human responses to the influence of personal liquid cooling system in the hot environment. *International Journal of Clothing Science and Technology*, 26(2), 145-163.
- Barwood, M., Davey, S., House, J., & Tipton, M. (2009). Post-exercise cooling techniques in hot, humid conditions. *European Journal of Applied Physiology*, 107(4), 385-396. doi:10.1007/s00421-009-1135-1
- Barwood, M. J., Newton, P. S., & Tipton, M. J. (2009). Ventilated vest and tolerance for intermittent exercise in hot, dry conditions with military clothing. *Aviation, space, and environmental medicine*, 80(4), 353-359.
- Bennett, B. L., Hagan, R. D., Huey, K. A., Minson, C., & Cain, D. (1995). Comparison of two cool vests on heat-strain reduction while wearing a firefighting ensemble. *European Journal of Applied Physiology and Occupational Physiology*, 70(4), 322-328. doi:10.1007/BF00865029
- Biermann, P. J. (2005). *Improved Thermal Control Body Armor*. Johns Hopkins University United States of America: National Institute of Justice.
- Bishop, P., Ray, P., & Reneau, P. (1995). A review of the ergonomics of work in the US military chemical protective clothing. *International Journal of Industrial Ergonomics*, 15(4), 271-283. doi:[http://dx.doi.org/10.1016/0169-8141\(94\)00041-Z](http://dx.doi.org/10.1016/0169-8141(94)00041-Z)
- Bishop, P. A., Nunneley, S. A., & Constable, S. H. (1991). Comparisons of air and liquid personal cooling for intermittent heavy work in moderate temperatures. *American Industrial Hygiene Association Journal*, 52(9), 393-397. doi:10.1080/15298669191364929
- Bogerd, N., Psikuta, A., Daanen, H. A., & Rossi, R. M. (2010). How to measure thermal effects of personal cooling systems: human, thermal manikin and human simulator study. *Physiol Meas*, 31(9), 1161-1168. doi:10.1088/0967-3334/31/9/007
- Bolster, D. R., Trappe, S. W., Short, K. R., Scheffield-Moore, M., Parcell, A. C., Schulze, K. M., & Costill, D. L. (1999). Effects of precooling on thermoregulation during subsequent exercise. *Medicine and science in sports and exercise*, 31(2), 251-257. doi:10.1097/00005768-199902000-00008
- Bomalaski, S., Chen, Y., & Constable, S. (1995). Continuous and intermittent personal microclimate cooling strategies. *Aviation, space, and environmental medicine*, 66(8), 745-750.
- Bouskill, L., & Parsons, K. (1996). Effectiveness of a neck cooling personal conditioning unit at reducing thermal strain during heat stress. *Contemporary Ergonomics*, 196-201.
- Branson, D. H., Farr, C. A., Peksoz, S., Nam, J., & Cao, H. (2005). Development of a Prototype Personal Cooling System for First Responders: User Feedback. *Journal of ASTM International*, 2(2).
- Budd, G. M. (2008). Wet-bulb globe temperature (WBGT)—its history and its limitations. *Journal of Science and Medicine in Sport*, 11(1), 20-32. doi:<http://dx.doi.org/10.1016/j.jsams.2007.07.003>
- Buller, M., Wallis, D., Karis, A., Herbert, N., Cadarette, B., Blanchard, L., . . . Hoyt, R. (2008). *Thermal-work strain during Marine rifle squad operations in Iraq (Summer 2008)* (USARIEM Technical Report T09-01). Retrieved from Natick, MA:

- Burke, R., Curran, A., & Hepokoski, M. (2009). *Integrating an active physiological and comfort model to the Newton sweating thermal manikin*. Paper presented at the The 13th International Conference on Environmental Ergonomics, Boston.
- Cadarette, B. S., Blanchard, L., Staab, J. E., Kolka, M. A., & Sawka, M. N. (2001). *Heat stress when wearing body armor* (USARIEM Technical Report T-01/9). Retrieved from Natick, MA:
- Cadarette, B. S., Levine, L., Kolka, M. A., Proulx, G. N., Correa, M. M., & Sawka, M. N. (2002). Heat strain reduction by ice-based and vapor compression liquid cooling systems with a toxic agent protective uniform. *Aviation, space, and environmental medicine*, 73(7), 665-672.
- Cadarette, B. S., Levine, L., Staab, J. E., Kolka, M. A., Correa, M., Whipple, M., & Sawka, M. N. (2001). Heat strain imposed by toxic agent protective systems. *Aviation, space, and environmental medicine*, 72(1), 32-37.
- Cadarette, B. S., Levine, L., Staab, J. E., Kolka, M. A., Correa, M. M., Whipple, M., & Sawka, M. N. (2003). Upper Body Cooling During Exercise-Heat Stress Wearing the Improved Toxicological Agent Protective System for HAZMAT Operations. *AIHA Journal*, 64(4), 510-515. doi:10.1080/15428110308984847
- Cadarette, B. S., Matthew, W. T., & Sawka, M. N. (2005). *WBGT index temperature adjustments for work/rest cycles when wearing NBC protective clothing or body armor* (Technical Note TN05-04). Retrieved from Natick, MA:
- Cadarette, B. S., Santee, W. R., Robinson, S. B., & Sawka, M. N. (2007). Reflective Inserts to Reduce Heat Strain in Body Armor: Tests With and Without Irradiance. *Aviation, space, and environmental medicine*, 78(8), 809-813.
- Caldwell, J., Patterson, M., & Taylor, N. S. (2012). Exertional thermal strain, protective clothing and auxiliary cooling in dry heat: evidence for physiological but not cognitive impairment. *European Journal of Applied Physiology*, 112(10), 3597-3606. doi:10.1007/s00421-012-2340-x
- Cao, H., Branson, D. H., Nam, J., Peksoz, S., & Farr, C. A. (2005). Development of a Cooling capability test Method for liquid cooled textile systems. *Journal of ASTM International*, 2(1), 1-10.
- Cao, H., Branson, D. H., Peksoz, S., Nam, J., & Farr, C. A. (2006). Fabric Selection for a Liquid Cooling Garment. *Textile Research Journal*, 76(7), 587-595. doi:10.1177/0040517506067375
- Chen, Y. T., Constable, S. H., & Bomalaski, S. H. (1997). A Lightweight Ambient Air-Cooling Unit for Use in Hazardous Environments. *American Industrial Hygiene Association Journal*, 58(1), 10-14. doi:10.1080/15428119791013017
- Chevront, S. N., Goodman, D. A., Kenefick, R. W., Montain, S. J., & Sawka, M. N. (2008). Impact of a protective vest and spacer garment on exercise-heat strain. *European Journal of Applied Physiology*, 102(5), 577-583. doi:10.1007/s00421-007-0632-3
- Chevront, S. N., Kolka, M. A., Cadarette, B. S., Montain, S. J., & Sawka, M. N. (2003). *Efficacy of intermittent, regional microclimate cooling* (Vol. 94).
- Chevront, S. N., Montain, S. J., Stephenson, L. A., & Sawka, M. N. (2009). *Skin Temperature Feedback Increases Thermoregulatory Efficiency and Decreases Required Microclimate Cooling Power*. Retrieved from
- Chinevere, T., Cadarette, B., Goodman, D., Ely, B., Chevront, S., & Sawka, M. (2008). Efficacy of body ventilation system for reducing strain in warm and hot climates.

- European Journal of Applied Physiology*, 103(3), 307-314. doi:10.1007/s00421-008-0707-9
- Choi, J.-W., Kim, M.-J., & Lee, J.-Y. (2008). Alleviation of Heat Strain by Cooling Different Body Areas during Red Pepper Harvest Work at WBGT 33&#8451. *Industrial Health*, 46(6), 620-628. doi:10.2486/indhealth.46.620
- Chou, C., Tochihara, Y., & Kim, T. (2008). Physiological and subjective responses to cooling devices on firefighting protective clothing. *European Journal of Applied Physiology*, 104(2), 369-374. doi:10.1007/s00421-007-0665-7
- Cilen, N., Ultman, J. S., & Kamon, E. (1983). *Simulation of personal cooling by frozen materials*. Paper presented at the AIChE Symposium Series.
- Clark, J. A., McArthur, A. J., Monteith, J. L., & Wheldon, A. E. (1981). Chapter 1 the Physics of the Microclimate. In K. Cena & J. A. Clark (Eds.), *Studies in Environmental Science* (Vol. Volume 10, pp. 13-27): Elsevier.
- Colburn, D., Suyama, J., Reis, S. E., Morley, J. L., Goss, F. L., Chen, Y.-F., . . . Hostler, D. (2011). A comparison of cooling techniques in firefighters after a live burn evolution. *Prehospital Emergency Care*, 15(2), 226-232.
- Coleman, S. R. (1989). Heat Storage Capacity of Gelled Coolants in ice Vests. *American Industrial Hygiene Association Journal*, 50(6), 325-329. doi:10.1080/15298668991374741
- Colvin, D. P., Hayes, L. J., Bryant, Y. G., & Myers, D. (1993). Thermal analysis of PCM cooling garments. *ASME-PUBLICATIONS-HTD*, 268, 73-73.
- Colvin, D. P., & Lokody, T. (2003). *Development of a MacroPCM Neck Cooling Collar for Athletes and Runners*. Paper presented at the ASME 2003 International Mechanical Engineering Congress and Exposition.
- Committee, N. R. A. (2007). *Lightening the Load. briefing to Honorable Delores M. Etter, Assistant Secretary of the Navy for Research, Development and Acquisition*.
- Constable, S. H. (1993). *USAF physiological studies of personal microclimate cooling: A review*. Retrieved from
- Constable, S. H., Bishop, P. A., Nunneley, S. A., & Chen, T. (1994). Intermittent microclimate cooling during rest increases work capacity and reduces heat stress. *Ergonomics*, 37(2), 277-285. doi:10.1080/00140139408963645
- Corcoran, S. (2002). Why some workers boil over wearing cooling garments. *Occup Health Saf*, 71(5), 104-106.
- Cotter, J. D., Sleivert, G. G., Roberts, W. S., & Febbraio, M. A. (2001). Effect of pre-cooling, with and without thigh cooling, on strain and endurance exercise performance in the heat. *Comparative Biochemistry and Physiology Part A: Molecular & Integrative Physiology*, 128(4), 667-677. doi:[http://dx.doi.org/10.1016/S1095-6433\(01\)00273-2](http://dx.doi.org/10.1016/S1095-6433(01)00273-2)
- Crow, R. M. (1974). *Heat and Moisture Transfer in Clothing Systems. Part 1. Transfer Through Materials, A Literature Review*. Retrieved from Ottawa, Canada:
- Curran, A., Hepokoski, M., Curlee, J., Nelson, D., & Biswas, A. (2006). Adapting segmental models of human thermoregulation and thermal sensation for use in a thermal simulation of a vehicle passenger compartment, F2006D129T, FISITA transactions 2006. *International Federation of Automotive Engineering Societies, London*.
- Curran, A. R., Peck, S. D., Schwenn, T. J., & Hepokoski, M. A. (2009). *Improving cabin thermal comfort by controlling equivalent temperature*. Retrieved from

- D'Angelo, S. (2009). *The Cooling Vest-Evaporative Cooling*. WORCESTER POLYTECHNIC INSTITUTE.
- Danielsson, U. (1993). *Convection coefficients in clothing air layers*. (Doctoral), The Royal Institute of Technology, Stockholm.
- Delkumburewatte, G. B., & Dias, T. (2011). Wearable cooling system to manage heat in protective clothing. *The Journal of The Textile Institute*, 103(5), 483-489. doi:10.1080/00405000.2011.587647
- Department of the Army. (1994) *FM 3-7 NBC Field Handbook*. Fort McClellan, AL: U.S. Army Chemical School.
- Dionne, J., Makris, A., Semeniuk, K., Teal, W., & Laprise, B. (2003). *Thermal manikin evaluation of liquid cooling garments intended for use in hazardous waste management: United States*. Department of Energy. Office of Scientific and Technical Information.
- Doerr, D. (2001). Development of an advanced rocket propellant handler's suit. *Acta Astronautica*, 49(3-10), 463-468. doi:[http://dx.doi.org/10.1016/S0094-5765\(01\)00122-9](http://dx.doi.org/10.1016/S0094-5765(01)00122-9)
- Drost, M. K., & Friedrich, M. (1997, 27 Jul-1 Aug 1997). *Miniature heat pumps for portable and distributed space conditioning applications*. Paper presented at the Energy Conversion Engineering Conference, 1997. IECEC-97., Proceedings of the 32nd Intersociety.
- Duffield, R., Green, R., Castle, P., & Maxwell, N. (2010). Precooling can prevent the reduction of self-paced exercise intensity in the heat. *Medicine and science in sports and exercise*, 42(3), 577-584. doi:10.1249/mss.0b013e3181b675da
- Duffield, R., & Marino, F. (2007). Effects of pre-cooling procedures on intermittent-sprint exercise performance in warm conditions. *European Journal of Applied Physiology*, 100(6), 727-735. doi:10.1007/s00421-007-0468-x
- Duncan, J., & Konz, S. (1975). Design and Evaluation of a Personal Dry-Ice Cooling Jacket. *Proceedings of the Human Factors and Ergonomics Society Annual Meeting*, 19(3), 359-363. doi:10.1177/154193127501900316
- Elson, J., & Eckels, S. (2015). An objective method for screening and selecting personal cooling systems based on cooling properties. *Applied Ergonomics*, 48, 33-41. doi:<http://dx.doi.org/10.1016/j.apergo.2014.10.019>
- Elson, J. C., McCullough, E. A., & Eckels, S. (2013). *Evaluation of personal cooling systems for military use*. Paper presented at the 15th International Conference on Environmental Ergonomics, Queenstown, New Zealand.
- EN. (2012). Requirements for sleeping bags (Vol. EN 13537:2012-05). Heinestraße: Austrian Standards Institute.
- Endrusick, T., Gonzalez, J., & Berglund, L. (2007). *Thermal Manikin Evaluation of Passive and Active Cooling Garments to Improve Comfort of Military Body Armor* (USARIEM Technical Report M07-38). Retrieved from Natick, MA:
- Endrusick, T. L., Berglund, L. G., Gonzalez, J. A., Gallimore, R., & Zheng, J. (2006). *Use of a spacer vest to increase evaporative cooling under military body armor*. Retrieved from
- Ernst, T. C., & Garimella, S. (2013). Demonstration of a wearable cooling system for elevated ambient temperature duty personnel. *Applied Thermal Engineering*, 60(1-2), 316-324. doi:<http://dx.doi.org/10.1016/j.applthermaleng.2013.06.019>
- Fanger, P. O. (1973). Assessment of man's thermal comfort in practice. *British Journal of Industrial Medicine*, 30(4), 313-324. doi:10.1136/oem.30.4.313

- Farid, M. M., Khudhair, A. M., Razack, S. A. K., & Al-Hallaj, S. (2004). A review on phase-change energy storage: materials and applications. *Energy Conversion and Management*, 45(9–10), 1597-1615. doi:<http://dx.doi.org/10.1016/j.enconman.2003.09.015>
- Fiala, D., Havenith, G., Bröde, P., Kampmann, B., & Jendritzky, G. (2012). UTCI-Fiala multi-node model of human heat transfer and temperature regulation. *International Journal of Biometeorology*, 56(3), 429-441. doi:10.1007/s00484-011-0424-7
- Fiala, D., & Lomas, K. (2001). *The dynamic effect of adaptive human responses in the sensation of thermal comfort*. Paper presented at the Proceedings Windsor Conference.
- Fiala, D., Lomas, K. J., & Stohrer, M. (1999). A computer model of human thermoregulation for a wide range of environmental conditions: the passive system. *Journal of Applied Physiology*, 87(5), 1957-1972.
- Fiala, D., Lomas, K. J., & Stohrer, M. (2001). Computer prediction of human thermoregulatory and temperature responses to a wide range of environmental conditions. *International Journal of Biometeorology*, 45(3), 143-159. doi:10.1007/s004840100099
- Flouris, A. D., & Cheung, S. S. (2006). Design and Control Optimization of Microclimate Liquid Cooling Systems Underneath Protective Clothing. *Annals of Biomedical Engineering*, 34(3), 359-372. doi:10.1007/s10439-005-9061-9
- Frim, J. (1989). Head cooling is desirable but not essential for preventing heat strain in pilots. *Aviation, space, and environmental medicine*, 60(11), 1056-1062.
- Frim, J., & Glass, K. (1991). *Alleviation of thermal strain in engineering space personnel aboard CF ships with the Exotemp personal cooling system*. Retrieved from
- Frim, J., Michas, R. D., & Cain, B. (1996). Personal cooling garment performance: a parametric study. *Environmental Ergonomics. Recent Progress and New Frontiers*. London and Tel Aviv: Freund Publishing House, Ltd.
- Frim, J., & Morris, A. (1992). *Evaluation of personal cooling systems in conjunction with explosive ordnance disposal suits*. Retrieved from
- Fu, G. (1995). *A transient 3-D mathematical thermal model for the clothed human (PhD)*. (Ph.D. Dissertation), Kansas State University, Manhattan, KS, USA.
- Fujii, R. K., Horie, S., Tsutsui, T., & Nagano, C. (2008). Effectiveness of a Head Wash Cooling Protocol Using Non-Refrigerated Water in Reducing Heat Stress. *Journal of Occupational Health*, 50(3), 251-261. doi:10.1539/joh.L7097
- Furtado, A. L., Craig, B. N., Chard, J. T., Zaloom, V. A., & Chu, H. (2007). Cooling suits, physiological response, and task performance in hot environments for the power industry. *International Journal of Occupational Safety and Ergonomics*, 13(3), 227-239.
- Gage, A. P., Burton, A. C., & Bazett, H. C. (1941). A practical system of units for the description of the heat exchange of man with his environment. *Science*, 94(2445), 428-430.
- Gage, A. P., Fobelets, A. P., & Berglund, L. G. (1986). *A standard predictive index of human response to the thermal environment*.
- Gage, A. P., & Gonzalez, R. R. (1996). Mechanisms of heat exchange: biophysics and physiology. In a. C. M. B. M.J. Fregly (Ed.), *Environmental Physiology* (pp. 45-84). New York: Oxford University Press.
- Gage, A. P., & Nishi, Y. (1977). Heat exchange between human skin surface and thermal environment: biophysics and biophysiology. In H. L. Falk & S. D. Murphy (Eds.), *Reactions to Environmental Agents*.

- Gagge, A. P., Stolwijk, J. A. J., & Hardy, J. D. (1967). Comfort and thermal sensations and associated physiological responses at various ambient temperatures. *Environmental Research*, 1(1), 1-20. doi:[http://dx.doi.org/10.1016/0013-9351\(67\)90002-3](http://dx.doi.org/10.1016/0013-9351(67)90002-3)
- Gao, C., Kuklane, K., & Holmér, I. (2010). Cooling vests with phase-change material packs: the effects of temperature gradient, mass and covering area. *Ergonomics*, 53(5), 716-723. doi:10.1080/00140130903581649
- Gao, C., Kuklane, K., & Holmér, I. (2011). Cooling vests with phase change materials: the effects of melting temperature on heat strain alleviation in an extremely hot environment. *European Journal of Applied Physiology*, 111(6), 1207-1216. doi:10.1007/s00421-010-1748-4
- Gao, C., Kuklane, K., Wang, F., & Holmér, I. (2012). Personal cooling with phase change materials to improve thermal comfort from a heat wave perspective. *Indoor Air*, 22(6), 523-530. doi:10.1111/j.1600-0668.2012.00778.x
- Gentile, M. H. (2006). *A novel personal cooling system for use by soldiers in hot climates*. (Bachelor of Science), Massachusetts Institute of Technology.
- Glitz, K. J., Seibel, U., Rohde, U., Gorges, W., G., K., Piekarski, C., & Leyk, D. (2011). *Sustaining performance under thermal insulation: Reducing heat stress by physiological microclimate cooling*. Paper presented at the 2nd International Congress on Soldiers' Physical Performance, Jyväskylä, Finland.
- Gonzalez, J. A., Berglund, L. G., Endrusick, T. L., & Kolka, M. A. (2006). *Forced ventilation of protective garments for hot industries*. Retrieved from Natick, MA USA:
- Goodman, D. A., Diaz, J., Cadarette, B. S., & Sawka, M. N. (2008). *Soldier Protection Demonstration III-Field Testing and Analysis of Personal Cooling Systems for Heat Mitigation* (USARIEM Technical Report . TN09-01). Retrieved from Natick, MA:
- Gordon, R. G., Roemer, R. B., & Horvath, S. M. (1976). A Mathematical Model of the Human Temperature Regulatory System - Transient Cold Exposure Response. *Biomedical Engineering, IEEE Transactions on, BME-23*(6), 434-444. doi:10.1109/TBME.1976.324601
- Gosselin, R. E. (1947). Rates of Sweating in the Desert. In E. F. Adolph (Ed.), *Physiology of Man in the Desert* (pp. 44-76). New York, N.Y.: Hafner Publishing Company, Inc. (Reprinted from: 1969).
- Grahn, D. A., Cao, V. H., & Heller, H. C. (2005). *Heat extraction through the palm of one hand improves aerobic exercise endurance in a hot environment* (Vol. 99).
- Grahn, D. A., Dillon, J. L., & Heller, H. C. (2009). Heat Loss Through the Glabrous Skin Surfaces of Heavily Insulated, Heat-Stressed Individuals. *Journal of Biomechanical Engineering*, 131(7), 071005-071005. doi:10.1115/1.3156812
- Grzyll, L. R., & Balderson, W. C. (1997, 27 Jul-1 Aug 1997). *Development of a man-portable microclimate adsorption cooling device*. Paper presented at the Energy Conversion Engineering Conference, 1997. IECEC-97., Proceedings of the 32nd Intersociety.
- Grzyll, L. R., & McLaughlin, T. (1997). *A crew cooling system for the M9 armored combat earthmover (ACE)*. Paper presented at the Proceedings of the Intersociety Energy Conversion Engineering Conference.
- Guo, X., Zhang, X., & Yuan, X. (2014). Design and Development of Novel Ventilated Clothing. In S. Long & B. S. Dhillon (Eds.), *Proceedings of the 13th International Conference on Man-Machine-Environment System Engineering* (Vol. 259, pp. 451-459): Springer Berlin Heidelberg.



- Hadid, A., Yanovich, R., Erlich, T., Khomenok, G., & Moran, D. S. (2008). Effect of a personal ambient ventilation system on physiological strain during heat stress wearing a ballistic vest. *European Journal of Applied Physiology*, *104*(2), 311-319. doi:10.1007/s00421-008-0716-8
- Hagan, R., Huey, K., & Bennett, B. (1994). *Cool Vests Worn Under Firefighting Ensemble Increase Tolerance to Heat*. Retrieved from
- Harrison, M. H., & Belyavin, A. J. (1978). Operational characteristics of liquid-conditioned suits. *Aviation, space, and environmental medicine*, *49*(8), 994-1003.
- Heled, Y., Epstein, Y., & Moran, D. S. (2004). Heat Strain Attenuation While Wearing NBC Clothing: Dry-Ice Vest Compared to Water Spray. *Aviation, space, and environmental medicine*, *75*(5), 391-396.
- Hepokoski, M., Packard, C., Curran, A., & Rothschild, J. (2012). *Evaluation of a Personal Cooling System using a Physiologically Controlled Sweating Thermal Manikin*. Paper presented at the The 9th International Meeting for Manikins and Modeling, Tokyo, Japan.
- Hexamer, M., & Werner, J. (1995). Control of liquid cooling garments: subjective versus technical control of thermal comfort. *Applied Human Science*, *14*(6), 271-278.
- Hexamer, M., & Werner, J. (1998). *Automatic control of liquid cooling garments: What is the ideal control mode?* Paper presented at the 8th International Congress on Environmental Ergonomics, San Diego, CA.
- Hexamer, M., Xu, X., & Werner, J. (1996). Automatic multi-loop control of cooling garments. *Environmental ergonomics: Recent progress and new frontiers*(Recent progress and new frontiers), 343-346.
- Hope, L., Blocksidge, D., Gabbert, F., Sauer, J. D., Lewinski, W., Mirashi, A., & Atuk, E. (2015). Memory and the Operational Witness: Police Officer Recall of Firearms Encounters as a Function of Active Response Role. *Law and human behavior*.
- House, J. R. (1996). *Reducing heat strain with ice-vests or hand immersion*. Paper presented at the Proceedings of the 7th international conference on environmental ergonomics, Jerusalem, Israel, October.
- House, J. R., Groom, J. A. S., Hodgdon, J. A., Heaney, J. H., & Buono, M. J. (1998). *The alleviation of heat strain using water perfused forearm cuffs*. Paper presented at the 8th International Environmental Ergonomics Conference, San Diego, USA.
- House, J. R., Lunt, H., Lyons, J., Holmér, I., Kuklane, K., & Gao, C. (2005). *Extending safe working times in the heat by combined use of hand cooling and ice-vests*. Paper presented at the Proceedings of the 11th international conference on environmental ergonomics, Lund University, Lund, Sweden, ISBN.
- House, J. R., Lunt, H. C., Taylor, R., Milligan, G., Lyons, J. A., & House, C. M. (2013). The impact of a phase-change cooling vest on heat strain and the effect of different cooling pack melting temperatures. *European Journal of Applied Physiology*, *113*(5), 1223-1231. doi:10.1007/s00421-012-2534-2
- Hu, J. S., & Chao, C. Y. H. (2008). Development of an Electroosmotic Pump-Driven Micro LiBr Absorption Heat Pump System for Controlling Microclimate in Protective Clothing: Feasibility Review and Role of the Pump. *HVAC&R Research*, *14*(3), 467-487. doi:10.1080/10789669.2008.10391020
- Incropera, F. P., DeWitt, D., Bergman, T. L., & Lavine, A. S. (2007). *Fundamentals of Heat and Mass Transfer* (6th ed.): John Wiley and Sons, ISBN.

- ISO. (2003). ISO 7243 *Hot Environments -- Estimation of the heat stress on working man, based on the WBGT-index (wet bulb globe temperature)*. Geneva: International Standards Organization.
- ISO. (2004). ISO 8996 *Ergonomics--Determination of metabolic rate*. Geneva: International Standards Organization.
- ISO. (2007). ISO 9920:2007 *Ergonomics of the thermal environment -- Estimation of thermal insulation and water vapour resistance of a clothing ensemble*. Geneva: International Standards Organization.
- Jay, O., Gariépy, L. M., Reardon, F. D., Webb, P., Ducharme, M. B., Ramsay, T., & Kenny, G. P. (2006). A three-compartment thermometry model for the improved estimation of changes in body heat content. *American Journal of Physiology - Regulatory, Integrative and Comparative Physiology*, 292(1), R167-R175. doi:10.1152/ajpregu.00338.2006
- Jay, O., & Kenny, G. P. (2007). The Determination of Changes in Body Heat Content during Exercise Using Calorimetry and Thermometry. *Journal of the Human-Environment System*, 10(1), 19-29.
- Jay, O., Reardon, F. D., Webb, P., DuCharme, M. B., Ramsay, T., Nettlefold, L., & Kenny, G. P. (2007). *Estimating changes in mean body temperature for humans during exercise using core and skin temperatures is inaccurate even with a correction factor* (Vol. 103).
- Jette, F.-X., Dionne, J.-P., Semeniuk, K., & Makris, A. (2003). *Thermal manikin investigation of personal cooling systems worn under protective clothing with various permeability and insulation properties*. Paper presented at the SAFE Association 41 st Annual Symposium.
- Jetté, F. X., Dionne, J. P., Rose, J., & Makris, A. (2004). Effect of thermal manikin surface temperature on the performance of personal cooling systems. *European Journal of Applied Physiology*, 92(6), 669-672. doi:10.1007/s00421-004-1112-7
- Jones, B. W., & Ogawa, Y. (1992). Transient interaction between the human body and the thermal environment. *ASHRAE Transactions*, 98(1), 189-195.
- Jones, B. W., & Ogawa, Y. (1993). Transient response of the human-clothing system. *Journal of Thermal Biology*, 18(5-6), 413-416. doi:[http://dx.doi.org/10.1016/0306-4565\(93\)90068-5](http://dx.doi.org/10.1016/0306-4565(93)90068-5)
- Jovanović, D., Karkalić, R., Tomić, L., Veličković, Z., & Bajić, Z. (2012). Effects of the Liquid Circulation Cooling Vest on a Physiological Strain Level in Solders During Exertional Heat Stress. *Scientific Technical Review*, 62(2), 76-83.
- Jovanović, D., Karkalić, R., Zeba, S., Pavlović, M., & Radaković, S. S. (2014). Physiological tolerance to uncompensated heat stress in soldiers: effects of various types of body cooling systems. *Vojnosanitetski pregled*, 71(3), 259-264.
- Kamon, E., Kenney, W. L., Deno, N. S., Soto, K. I., & Carpenter, A. J. (1986). Readdressing Personal Cooling With Ice. *American Industrial Hygiene Association Journal*, 47(5), 293-298. doi:10.1080/15298668691389784
- Katica, C. P., Pritchett, R. C., Pritchett, K. L., Del Pozzi, A. T., Balilionis, G., & Burnham, T. (2011). Effects of Forearm vs. Leg Submersion in Work Tolerance Time in a Hot Environment While Wearing Firefighter Protective Clothing. *Journal of Occupational and Environmental Hygiene*, 8(8), 473-477. doi:10.1080/15459624.2011.590743
- Kaufman, J. W. (2001). Estimated ventilation requirements for personal air-cooling systems. *Aviation, space, and environmental medicine*, 72(9), 842-847.
- Kaufman, J. W. (2002). Cooling individuals using encapsulating protective clothing in a hot humid environment. *Blowing Hot and Cold: Protecting Against Climatic Extremes*, 6.

- Kaufman, J. W., & Fatkin, L. T. (2001). *Assessment of advanced personal cooling systems for use with chemical protective outer garments*. Retrieved from
- Kenny, G. P., Schissler, A. R., Stapleton, J., Piamonte, M., Binder, K., Lynn, A., . . . Hardcastle, S. G. (2011). Ice Cooling Vest on Tolerance for Exercise under Uncompensable Heat Stress. *Journal of Occupational and Environmental Hygiene*, 8(8), 484-491. doi:10.1080/15459624.2011.596043
- Khomenok, G. A., Hadid, A., Preiss-Bloom, O., Yanovich, R., Erlich, T., Ron-Tal, O., . . . Moran, D. (2008). Hand immersion in cold water alleviating physiological strain and increasing tolerance to uncompensable heat stress. *European Journal of Applied Physiology*, 104(2), 303-309. doi:10.1007/s00421-008-0693-y
- Kim, J.-H., Coca, A., Williams, W. J., & Roberge, R. J. (2011). Subjective perceptions and ergonomics evaluation of a liquid cooled garment worn under protective ensemble during an intermittent treadmill exercise. *Ergonomics*, 54(7), 626-635. doi:10.1080/00140139.2011.583362
- Kim, J., & Cho, G. (2002). Thermal Storage/Release, Durability, and Temperature Sensing Properties of Thermostatic Fabrics Treated with Octadecane-Containing Microcapsules. *Textile Research Journal*, 72(12), 1093-1098. doi:10.1177/004051750207201209
- Konz, S. (1984). Personal cooling garments: a review. *ASHRAE Transactions*, 90(1B), 499-518.
- Konz, S., Hwang, C., Perkins, R., & Borell, S. (1974). Personal Cooling With Dry Ice. *American Industrial Hygiene Association Journal*, 35(3), 137-147. doi:10.1080/0002889748507015
- Kuennen, M., Gillum, T., Amorim, F., Kwon, Y., & Schneider, S. (2010). Palm cooling to reduce heat strain in subjects during simulated armoured vehicle transport. *European Journal of Applied Physiology*, 108(6), 1217-1223. doi:10.1007/s00421-009-1335-8
- Kuznetz, L. H. (1980). Automatic Control of Human Thermal Comfort by a Liquid-Cooled Garment. *Journal of Biomechanical Engineering*, 102(2), 155-161. doi:10.1115/1.3138213
- Kwon, Y. S., Robergs, R. A., KRAVITZ, L., Gurney, B. A., Mermier, C. M., & Schneider, S. M. (2010). Palm cooling delays fatigue during high-intensity bench press exercise. *Medicine and science in sports and exercise*, 42, 1557-1565.
- Laprise, B. (2012). *Proposed Standard for a Microclimate Cooling System for Emergency Responder Operations* (NATICK/TR-12/012). Retrieved from Natick, MA:
- Laprise, B., Teal, W., Zuckerman, L., & Cardinal, J. (2005). *Evaluation of Commercial Off-the-Shelf and Government Off-the-Shelf Microclimate Cooling Systems*. Retrieved from Natick, MA:
- LeDuc, P. A., Reardon, M. J., Persson, J. L., Gallagher, S. M., & Dunkin, S. L. (2002). *Heat Stress Evaluation of Air Warrior Block I MOPPO and MOPP4 Ensembles With and Without Microclimate Cooling* (2002-19). Retrieved from Fort Rucker, AL:
- Lee, D. T., & Haymes, E. M. (1995). *Exercise duration and thermoregulatory responses after whole body precooling* (Vol. 79).
- Levine, L., Cadarette, B. S., & Kolka, M. A. (2003). *Endurance time in the self-contained toxic environment protective outfit (STEPO) with personal ice-cooled microclimate cooling system (PICS) in three environments*. Retrieved from
- Leyva, F. F., & Goehring, G. S. (2004). *Evaluation of a Diver Cooling System for Use With Personal Protective Equipment in Contaminated Water Diving* (NEDU TR 04-07). Retrieved from Washington D.C.:

- Lim, C. L., Song, E., Law, L., Sng, S., & Soh, B. K. (2002). *Evaluation of field based body cooling systems*. Paper presented at the Environmental ergonomics: The 10th International Conference on Environmental Ergonomics, Fukuoka, Japan: Kyushy Institute of Design. .
- Livingstone, S., Grayson, J., Frim, J., Allen, C., & Limmer, R. (1983). Effect of cold exposure on various sites of core temperature measurements. *Journal of applied physiology: respiratory, environmental and exercise physiology*, *54*, 1025-1031.
- Lomas, K., Fiala, D., & Stohrer, M. (2003). First principles modeling of thermal sensation responses in steady-state and transient conditions.
- Lotens, W. A. (1993). *Heat transfer from humans wearing clothing*. (PhD), TU Delft, Delft University of Technology, Netherlands.
- Luechtefeld, R., Laprise, B., Teal, W., Fischbach, D., Sopko, T., & Frampton, R. (2003). *Air Warrior Microclimate Cooling System for US Army Helicopter Aircrew*. Paper presented at the SAFE Association 41 st Annual Symposium.
- Luomala, M. J., Oksa, J., Salmi, J. A., Linnamo, V., Holmér, I., Smolander, J., & Dugué, B. (2012). Adding a cooling vest during cycling improves performance in warm and humid conditions. *Journal of Thermal Biology*, *37*(1), 47-55.  
doi:<http://dx.doi.org/10.1016/j.jtherbio.2011.10.009>
- Machle, W., & Hatch, T. F. (1947). *HEAT: MAN'S EXCHANGES AND PHYSIOLOGICAL RESPONSES* (Vol. 27).
- Maier-Laxhuber, P., Schmidt, R., & Grupp, C. (2002). *Air Ventilated Heating and Cooling Based on Zeolite Technology*: DTIC Document.
- Martini, S. (2011, 24, October 11 ). *Cooling vests/clothing tested in the climate chamber at FFI*. Paper presented at the CCIEP Amsterdam.
- McClure, C. M., McClure, C. D., & Melton, M. (1991). Breathing air cooling system combats respiratory contamination, heat stress. *Occupational health & safety*, *60*(8), 33-35.
- McCullough, E. (2001). Phase change and protective possibilities What are phase change materials and how can they enhance fabric performance? Here are the basics and the applications where phase change will work best. *Industrial Fabric Products Review*, *78*(1), 64-67.
- McCullough, E. A., & Eckels, S. (2008). *Evaluation of personal cooling systems for soldiers using human subjects*. Paper presented at the The International Textile and Apparel Association, Shaumburg, IL.
- McCullough, E. A., & Eckels, S. (2009). *Evaluation of personal cooling systems for soldiers*. Paper presented at the The 13th International Conference on Environmental Ergonomics, Boston, MA.
- McCullough, E. A., Eckels, S., & Elson, J. C. (2013). *KSU Personal Cooling Systems (PCS) database*. Unpublished Results.
- McDermott, B. P., Casa, D. J., Ganio, M. S., Lopez, R. M., Yeargin, S. W., Armstrong, L. E., & Maresh, C. M. (2009). Acute Whole-Body Cooling for Exercise-Induced Hyperthermia: A Systematic Review. *Journal of Athletic Training*, *44*(1), 84-93.
- McLeilan, T. M. (2002). *Cooling options for shipboard personnel operating in hot environments*. Retrieved from
- McLellan, T. M., & Daanen, H. A. M. (2012). Heat Strain in Personal Protective Clothing: Challenges and Intervention Strategies. In P. Kiekens & S. Jayaraman (Eds.), *Intelligent*

- Textiles and Clothing for Ballistic and NBC Protection* (pp. 99-118): Springer Netherlands.
- McLellan, T. M., & Frim, J. (1994). Heat Strain in the Canadian Forces Chemical Defence Clothing: Problems and Solutions. *Canadian Journal of Applied Physiology*, 19(4), 379-399. doi:10.1139/h94-031
- McLellan, T. M., Frim, J., & Bell, D. G. (1999). Efficacy of air and liquid cooling during light and heavy exercise while wearing NBC clothing. *Aviation, space, and environmental medicine*, 70(8), 802-811.
- Mokhtari Yazdi, M., & Sheikhzadeh, M. (2014). Personal cooling garments: a review. *The Journal of The Textile Institute*, 1-20. doi:10.1080/00405000.2014.895088
- Moore, J. M., Lakeman, J. B., & Mepsted, G. O. (2002). Development of a PEM fuel cell powered portable field generator for the dismounted soldier. *Journal of Power Sources*, 106(1-2), 16-20. doi:[http://dx.doi.org/10.1016/S0378-7753\(01\)01050-3](http://dx.doi.org/10.1016/S0378-7753(01)01050-3)
- Muir, I. H., Bishop, P. A., & Ray, P. (1999). Effects of a Novel Ice-Cooling Technique on Work in Protective Clothing at 28°C, 23°C, and 18°C WBGTs. *American Industrial Hygiene Association Journal*, 60(1), 96-104. doi:10.1080/00028899908984427
- Muir, I. H., & Myhre, L. G. (2005). *The effect of 60 minutes of upper body pre-cooling (ice vest) on exercise/work tolerance time in the heat*. Paper presented at the Environmental ergonomics: Proceedings of the 11th International Conference, Lund, Sweden: Lund University.
- Muza, S. R., Pimental, N. A., Cosimini, H. M., & Sawka, M. N. (1987). *Portable, ambient air microclimate cooling in simulated desert and tropic conditions*. Retrieved from
- Myhre, L., & Muir, I. (2005). *The effect of 30-minutes of upper body cooling (ice vest) on skin and core temperatures during rest in a comfortable environment (Ta= 22 C)*. Paper presented at the Proceedings of the 11th international conference on environmental ergonomics, Lund University, Lund, Sweden.
- Nag, P. K., Pradhan, C. K., Nag, A., Ashtekar, S. P., & Desai, H. (1998). Efficacy of a water-cooled garment for auxiliary body cooling in heat. *Ergonomics*, 41(2), 179-187. doi:10.1080/001401398187233
- Nagavarapu, A. K., & Garimella, S. (2011). Design of Microscale Heat and Mass Exchangers for Absorption Space Conditioning Applications. *Journal of Thermal Science and Engineering Applications*, 3(2), 021005.
- Nam, J., Branson, D. H., Ashdown, S. P., Cao, H., Jin, B., Peksoz, S., & Farr, C. (2005). Fit analysis of liquid cooled vest prototypes using 3D body scanning technology. *Journal of Textile and Apparel, Technology and Management*, 4(3), 1-13.
- Nelson, D. A., Charbonnel, S., Curran, A. R., Marttila, E. A., Fiala, D., Mason, P. A., & Ziriach, J. M. (2009). A High-Resolution Voxel Model for Predicting Local Tissue Temperatures in Humans Subjected to Warm and Hot Environments. *Journal of Biomechanical Engineering*, 131(4), 041003-041003. doi:10.1115/1.3002765
- Nunneley, S., Diesel, D., Byrne, T., & Chen, Y. (1998). *Recent experiments with personal cooling for aircrews*. Paper presented at the Proceedings of the International Conference on Environmental Ergonomics, San Diego, CA.
- Nunneley, S. A. (1970). Water cooled garments: a review. *Space life sciences*, 2(3), 335-360.
- Nyberg, K. L., Diller, K. R., & Wissler, E. H. (2000). Automatic control of thermal neutrality for space suit applications using a liquid cooling garment. *Aviation, space, and environmental medicine*, 71(9), 904-913.

- Nyberg, K. L., Diller, K. R., & Wissler, E. H. (2001). Model of human/liquid cooling garment interaction for space suit automatic thermal control. *Journal of Biomechanical Engineering*, 123(1), 114-120.
- O'Hara, R., Eveland, E., Fortuna, S., Reilly, P., & Pohlman, R. (2008). Current and future cooling technologies used in preventing heat illness and improving work capacity for battlefield soldiers: review of the literature. *Military medicine*, 173(7), 653-657.
- Odom, B. A., & Phelan, P. E. (2012). Viability of Spray Cooling an Air-Cooled Condenser in a Personnel Microclimate Cooling System. *Journal of Thermal Science and Engineering Applications*, 4(4), 041010-041010. doi:10.1115/1.4007207
- Pandolf, K. B., Givoni, B., & Goldman, R. F. (1977). Predicting energy expenditure with loads while standing or walking very slowly. *Journal of Applied Physiology*, 43(4), 577-581.
- Pandolf, K. B., Gonzalez, J. A., Sawka, M. N., Teal, W. B., Pimental, N. A., & Constable, S. H. (1995). *Tri-Service Perspectives on Microclimate Cooling of Protective Clothing in the Heat* (USARIEM Report T95-10). Retrieved from Natick, MA:
- Parrish, C. F., & Scaringe, R. P. (1993). *Lightweight Passive Microclimate Cooling Device* (C104FR08). Retrieved from Rockledge, FL:
- Parsons, K. (2002). *Human thermal environments: the effects of hot, moderate, and cold environments on human health, comfort and performance*: Crc Press.
- Parsons, K. (2006). Heat stress standard ISO 7243 and its global application. *Industrial Health*, 44(3), 368-379.
- Parsons, K. C., Havenith, G., Holmér, I., Nilsson, H., & Malchaire, J. (1999). The effects of wind and human movement on the heat and vapour transfer properties of clothing. *Annals of Occupational Hygiene*, 43(5), 347-352. doi:10.1093/annhyg/43.5.347
- Pasupathy, A., Velraj, R., & Seeniraj, R. V. (2008). Phase change material-based building architecture for thermal management in residential and commercial establishments. *Renewable and Sustainable Energy Reviews*, 12(1), 39-64. doi:<http://dx.doi.org/10.1016/j.rser.2006.05.010>
- Paul, G., Gim, E., & Westerfeld, D. (2014, 2-2 May 2014). *Battery powered heating and cooling suit*. Paper presented at the Systems, Applications and Technology Conference (LISAT), 2014 IEEE Long Island.
- Peksoz, S., Starr, C., Choi, K., Kamenidis, P., Park, H., & Branson, D. (2009). *Evaluation of Prototype Personal Cooling Interfaced with a Liquid Cooled Garment under Hazmat Suits*. Paper presented at the ITAA Proceedings, Belevue, Washington USA.
- Perez, S., Tooker, B., & Nunez, R. (1994). A Theoretical Study of a Personal Cooling Garment That Utilizes Natural Evaporation. *ASHRAE Transactions-American Society of Heating Refrigerating Airconditioning Engin*, 100(1), 49-53.
- Pimental, N. A., & Avellini, B. A. (1989). *Effectiveness of three portable cooling systems in reducing heat stress* (88-4-57). Retrieved from 21 Strathmore Road Natick, MA 01760-2490:
- Pimental, N. A., & Avellini, B. A. (1992). *Effectiveness of a Selected Microclimate Cooling System in Increasing Tolerance Time to Work in the Heat. Application to Navy Physiological Heat Exposure Limits (PHEL) Curve V*. Retrieved from
- Pimental, N. A., Avellini, B. A., & Heaney, J. H. (1992). *Ability of a passive microclimate cooling vest to reduce thermal strain and increase tolerance time to work in the heat*. Paper presented at the The fifth international conference on environmental ergonomics, Maastricht, The Netherlands.

- Pisacane, V. L., Kuznetz, L. H., Logan, J. S., Clark, J. B., & Wissler, E. H. (2006). Thermoregulatory models of safety-for-flight issues for space operations. *Acta Astronautica*, 59(7), 531-546. doi:<http://dx.doi.org/10.1016/j.actaastro.2006.04.007>
- Potter, A. W., Karis, A. J., & Gonzalez, J. A. (2013). *Biophysical Characterization and Predicted Human Thermal Responses to US Army Body Armor Protection Levels (BAPL)* (USARIEM-TR-T13-5). Retrieved from DTIC Document:
- Pozos, R., Wittmers, L., Hoffinan, R., Ingersoll, B., & Israe, D. EFFICIENCY OF COMBINATIONS OF COOLING FOR MICROCLIMATE COOLING SIIIT DESIGN, TESTED IN MAN AT 100 F WITH EXERCISE.
- RAČKIENĖ, R. Human body thermoelectric cooling system model.
- Rahman, M. (1996). Analysis and design of an air-cycle microclimate cooling device. *Journal of energy resources technology*, 118(4), 293-299.
- Rahman, M. M. (1993). Development of a microclimate cooling device using brayton cycle technology. *Emergin Energy Technology ASME*, 50, 119-130.
- Reffeltrath, P., Daanen, H., & den Hartog, E. (2002). *Efficiency of an individual air-cooling system for helicopter pilots*. Paper presented at the Proceedings of the 10th international conference on environmental ergonomics. University of Fukuoka, Fukuoka.
- Reinertsen, R. E., Færevik, H., Holbø, K., Nesbakken, R., Reitan, J., Røyset, A., & Suong Le Thi, M. (2008). Optimizing the Performance of Phase-Change Materials in Personal Protective Clothing Systems. *International Journal of Occupational Safety and Ergonomics*, 14(1), 43-53. doi:10.1080/10803548.2008.11076746
- Rosen, D. I., Magill, J. C., & Legner, H. H. (2007). *Cooling Glove Study*. Retrieved from
- Rothmaier, M., Weder, M., Meyer-Heim, A., & Kesselring, J. (2008). Design and performance of personal cooling garments based on three-layer laminates. *Medical & Biological Engineering & Computing*, 46(8), 825-832. doi:10.1007/s11517-008-0363-6
- Ryan, G. A., Bishop, S. H., Herron, R. L., Katica, C. P., Elbon, B. a. L., Bosak, A. M., & Bishop, P. (2013). Ambient Air Cooling for Concealed Soft Body Armor in a Hot Environment. *Journal of Occupational and Environmental Hygiene*, 11(2), 93-100. doi:10.1080/15459624.2013.843782
- Sahta, I., Baltina, I., & Blums, J. (2011). Development of Microclimate Regulatory Clothes. *Advanced Materials Research*, 222, 193-196.
- Salloum, M., Ghaddar, N., & Ghali, K. (2007). A new transient bioheat model of the human body and its integration to clothing models. *International Journal of Thermal Sciences*, 46(4), 371-384. doi:<http://dx.doi.org/10.1016/j.ijthermalsci.2006.06.017>
- Sawka, M., Wenger, C., Montain, S., Kolka, M., Bettencourt, B., Flinn, S., . . . Scott, C. (2003). *Heat stress control and heat casualty management* (Technical Bulletin 507). Retrieved from Natick, MA:
- Scheidler, C., Saunders, N., Hanson, N., & Devor, S. (2013). Palm cooling does not improve running performance. *Int J Sports Med*, 34, 732-735.
- Semeniuk, K., Dionne, J., Makris, A., Bernard, T., Ashley, C. D., & Medina, T. (2005). Evaluating the Physiological Performance of a Liquid Cooling Garment Used to Control Heat Stress in Hazmat Protective Ensembles. *Performance of Protective Clothing: Global Needs and Emerging Markets*, 8. doi:<http://dx.doi.org/10.1520/10.1520/STP12597S>

- Shapiro, Y., Pandolf, K. B., Sawka, M. N., Toner, M. M., Winsmann, F. R., & Goldman, R. F. (1982). Auxiliary cooling: comparison of air-cooled vs. water-cooled vests in hot-dry and hot-wet environments. *Aviation, space, and environmental medicine*, 53(8), 785-789.
- Shim, H., McCullough, E. A., & Jones, B. W. (2001). Using Phase Change Materials in Clothing. *Textile Research Journal*, 71(6), 495-502. doi:10.1177/004051750107100605
- Shitzer, A. (1997). Experimental and Analytical Studies of Heat Removal by Regionally Controlled Liquid-Cooled Garments. *ASME-PUBLICATIONS-HTD*, 355, 107-110.
- Shitzer, A., Chato, J., & Hertig, B. (1973). Thermal protective garment using independent regional control of coolant temperature. *Aerospace medicine*, 44(1), 49.
- Shvartz, E. (1972). Efficiency and effectiveness of different water cooled suits--a review. *Aerospace medicine*, 43(5), 488-491.
- Siegel, R., Maté, J., Brearley, M. B., Watson, G., Nosaka, K., & Laursen, P. B. (2010). Ice slurry ingestion increases core temperature capacity and running time in the heat. *Medicine and science in sports and exercise*, 42(4), 717-725. doi:10.1249/mss.0b013e3181bf257a
- Sleivert, G. G., Cotter, J. D., Roberts, W. S., & Febbraio, M. A. (2001). The influence of whole-body vs. torso pre-cooling on physiological strain and performance of high-intensity exercise in the heat. *Comparative Biochemistry and Physiology Part A: Molecular & Integrative Physiology*, 128(4), 657-666. doi:[http://dx.doi.org/10.1016/S1095-6433\(01\)00272-0](http://dx.doi.org/10.1016/S1095-6433(01)00272-0)
- Smith, C., & Havenith, G. (2011). Body mapping of sweating patterns in male athletes in mild exercise-induced hyperthermia. *European Journal of Applied Physiology*, 111(7), 1391-1404. doi:10.1007/s00421-010-1744-8
- Smith, C. E. (1991). *A transient, three-dimensional model of the human thermal system*. (Ph.D. Dissertation), Kansas State University, Manhattan, KS, USA.
- Speckman, K. L., Allan, A. E., Sawka, M. N., Young, A. J., Muza, S. R., & Pandolf, K. B. (1988). Perspectives in microclimate cooling involving protective clothing in hot environments. *International Journal of Industrial Ergonomics*, 3(2), 121-147. doi:[http://dx.doi.org/10.1016/0169-8141\(88\)90015-7](http://dx.doi.org/10.1016/0169-8141(88)90015-7)
- Stephenson, L. A., Vernieuw, C. R., Leammukda, W., & Kolka, M. A. (2007). Skin Temperature Feedback Optimizes Microclimate Cooling. *Aviation, space, and environmental medicine*, 78(4), 377-382.
- Stolwijk, J. A. J. (1971). *A Mathematical Model of Physiological Temperature Regulation in Man* (NASA CR-1855). Retrieved from Washington, D.C.:
- Stolwijk, J. A. J., & Hardy, J. D. (1966). Temperature regulation in man — A theoretical study. *Pflüger's Archiv für die gesamte Physiologie des Menschen und der Tiere*, 291(2), 129-162. doi:10.1007/BF00412787
- Streblow, R. (2010). *Thermal Sensation and Comfort Model for Inhomogeneous Indoor Enviornments*. (Doctor of Engineering Dissertation), Rheinisch-Westfälischen Technischen Hochschule Aachen University.
- Sun, W., Cheong, K. W. D., & Melikov, A. K. (2012). Subjective study of thermal acceptability of novel enhanced displacement ventilation system and implication of occupants' personal control. *Building and Environment*, 57(0), 49-57. doi:<http://dx.doi.org/10.1016/j.buildenv.2012.04.004>
- Tan, F. L., & Fok, S. C. (2006). Cooling of helmet with phase change material. *Applied Thermal Engineering*, 26(17-18), 2067-2072. doi:<http://dx.doi.org/10.1016/j.applthermaleng.2006.04.022>



- Tanabe, S.-i., Kobayashi, K., Nakano, J., Ozeki, Y., & Konishi, M. (2002). Evaluation of thermal comfort using combined multi-node thermoregulation (65MN) and radiation models and computational fluid dynamics (CFD). *Energy and Buildings*, 34(6), 637-646. doi:[http://dx.doi.org/10.1016/S0378-7788\(02\)00014-2](http://dx.doi.org/10.1016/S0378-7788(02)00014-2)
- Tayyari, F., Burford, C. L., & Ramsey, J. D. (1989). Evaluation of a Prototype Microclimate Cooling System. *American Industrial Hygiene Association Journal*, 50(4), 229-234. doi:10.1080/15298668991374552
- Teal, W. (1994). *Passive cooling for encapsulating garments*. Paper presented at the Proceedings of the 6th international conference on environmental ergonomics, Montebello.
- Teal, W. (1996). *A thermal manikin test method for evaluating the performance of liquid circulating cooling garments*. Paper presented at the International Conference on Environmental Ergonomics, Jerusalem.
- Terzi, R., Marcaletti, G., & Catenacci, G. (1989). [Evaluation of individual thermal load in working environments with non-homogeneous microclimatic conditions]. *La Medicina del lavoro*, 80(3), 211-217.
- Teunissen, L. P. J., Wang, L.-C., Chou, S.-N., Huang, C.-h., Jou, G.-T., & Daanen, H. A. M. (2014). Evaluation of two cooling systems under a firefighter coverall. *Applied Ergonomics*, 45(6), 1433-1438. doi:<http://dx.doi.org/10.1016/j.apergo.2014.04.008>
- Torii, M., Adachi, K., Miyabayashi, T., Arima, T., & Iwashita, M. (2005). Effect of bilateral carotid cooling with an ice pack on thermal responses during bicycle exercise. In T. Yutaka & O. Tadakatsu (Eds.), *Elsevier Ergonomics Book Series* (Vol. Volume 3, pp. 113-119): Elsevier.
- Tritt, T. M. (2007). Focus on Thermoelectrics and Nanomaterials. *physica status solidi (RRL) – Rapid Research Letters*, 1(6), A91-A92. doi:10.1002/pssr.200750034
- Tritt, T. M., & Subramanian, M. A. (2006). Thermoelectric Materials, Phenomena, and Applications: A Bird's Eye View. *MRS Bulletin*, 31(03), 188-198. doi:doi:10.1557/mrs2006.44
- Tuck, M. A. (1999). *Personal cooling in hot workings*.
- Uglene, W., Iaconis, J.-L., & Ciammaichella, R. (2002). An Enhanced Personal Cooling Garment for Aircrew. *Blowing Hot and Cold: Protecting Against Climatic Extremes*, 1, 2.
- Ullman, D. G. (1992). *The mechanical design process* (Vol. 2). New York: McGraw-Hill.
- Vallerand, A. L., Savourey, G., Hanniquet, A.-M., & Bittel, J. M. (1992). How should body heat storage be determined in humans: by thermometry or calorimetry? *European Journal of Applied Physiology and Occupational Physiology*, 65(3), 286-294. doi:10.1007/BF00705095
- Vallerand, A. L., Schmegner, I. F., & Michas, R. D. (1993). Heat Strain Produced by 3 Aircrew Chemical Defence Ensembles Under Hot Conditions: Improvement with an Air-Cooling Vest. *ASTM SPECIAL TECHNICAL PUBLICATION*, 1133, 583-583.
- Van Rensburg, A. J., Mitchell, D., Walt, W. H. V. D., & Strydom, N. B. (1972). Physiological reactions of men using microclimate cooling in hot humid environments. *British Journal of Industrial Medicine*, 29(4), 387-393. doi:10.1136/oem.29.4.387
- Vernieuw, C. R., Stephenson, L. A., & Kolka, M. A. (2007). Thermal Comfort and Sensation in Men Wearing a Cooling System Controlled by Skin Temperature. *Human Factors: The Journal of the Human Factors and Ergonomics Society*, 49(6), 1033-1044. doi:10.1518/001872007x249893

- von Restorff, W., Dyballa, S., & Glitz, K. J. Use of filtered ambient air to reduce heat stress in NBC protection clothing.
- Wang, J., Dionne, J., & Makris, A. (2005). *An approach to evaluate the thermal performance of liquid circulating garments*. Paper presented at the Environmental Ergonomics XI: Proceedings of the 11th International Conference.
- Wang, J., & Makris, A. (2005). *Significance of fit on the performance of liquid circulating garment and personal cooling system*. Paper presented at the proceedings from the 11th International conference on Environmental Ergonomics. Lund, Sweden: Lund University.
- Wang, X. (1994). *Thermal comfort and sensation under transient conditions*. (PhD), Department of Energy Technology, Division of Heating and Ventilation, the Royal Institute of Technology, Sweden.
- Warne-Janville, B., & Anelli, D. (2002). *Individual Cooling Systems Results and Quantified Performances Using all Objective Method*. Retrieved from
- Warpeha, J. M., Koscheyev, V. S., Leon, G. R., Serfass, R. C., Stovitz, S. D., & Petit, M. A. (2011). Testing and Evaluation of Three Liquid Cooling Garments for Use During Spaceflight: 2903: Board# 202 June 3 2: 00 PM-3: 30 PM. *Medicine & Science in Sports & Exercise*, 43(5), 824.
- Webster, J., Holland, E. J., Sleivert, G., Laing, R. M., & Niven, B. E. (2005). A light-weight cooling vest enhances performance of athletes in the heat. *Ergonomics*, 48(7), 821-837. doi:10.1080/00140130500122276
- Weller, A., Greenwood, A., Redman, P., & Lee, V. (2008). IMPACT ON HEAT STRAIN OF MEASURES TO REDUCE LOCAL COLD DISCOMFORT USING AN ACTIVE ICE-BASED PERSONAL COOLING SYSTEM. *AVIATION SPACE AND ENVIRONMENTAL MEDICINE*, 79(3), 201.
- White, M. K., Glenn, S. P., Hudnall, J., Rice, C., & Clark, S. (1991). The effectiveness of ice- and freon®-based personal cooling systems during work in fully encapsulating suits in the heat. *American Industrial Hygiene Association Journal*, 52(3), 127-135. doi:10.1080/15298669191364460
- Wickwire, P. J., Bishop, P. A., Green, J. M., Richardson, M. T., Lomax, R. G., Casaru, C., & Curtner-Smith, M. (2009). Physiological and Comfort Effects of a Commercial “Cooling Cap” Worn Under Protective Helmets. *Journal of Occupational and Environmental Hygiene*, 6(8), 455-459. doi:10.1080/15459620902959377
- Williams, B., Mcewen Jr, G., Montgomery, L., & Elkins, W. (1975). Industrial and biomedical use of aerospace personal cooling garments.
- Williamson, R., Carbo, J., Luna, B., & Webbon, B. W. (1999). A Thermal Physiological Comparison of Two HAZMAT Protective Ensembles With and Without Active Convective Cooling. *Journal of Occupational and Environmental Medicine*, 41(6), 453-463.
- Wissler, E. (1985). Mathematical simulation of human thermal behavior using whole body models. *Heat transfer in medicine and biology*, 1(13), 325-373.
- Wissler, E. H. (1961). *Steady-state temperature distribution in man* (Vol. 16).
- Wissler, E. H. (1964). A mathematical model of the human thermal system. *The bulletin of mathematical biophysics*, 26(2), 147-166. doi:10.1007/BF02476835
- Wissler, E. H. (1971). Comparison of computed results obtained from two mathematical models: a simple 14-node model and a complex 250-node model. *Journal de physiologie*, 63(3), 455-458.

- Wissler, E. H. (1986). Simulation of fluid-cooled or heated garments that allow man to function in hostile environments. *Chemical Engineering Science*, 41(6), 1689-1698. doi:[http://dx.doi.org/10.1016/0009-2509\(86\)85247-2](http://dx.doi.org/10.1016/0009-2509(86)85247-2)
- Wittmers, L., Hodgdon, J., Canine, K., & Hodgdon, J. (1998). *Use of encapsulated phase-change material (EPCM) as a cooling agent in microclimate cooling garments*. Paper presented at the Environmental Ergonomics VIII, San Diego, USA.
- Wu, Y.-t., Ma, C.-f., & Zhong, X. (2009). *Research and Development of a Miniature Cooling System*. Paper presented at the Inaugural US-EU-China Thermophysics Conference-Renewable Energy 2009 (UECTC 2009 Proceedings).
- Xu, X. (1999). Multi-loop control of liquid cooling garment systems. *Ergonomics*, 42(2), 282-298. doi:10.1080/001401399185658
- Xu, X., Berglund, L. G., Chevront, S. N., Endrusick, T. L., & Kolka, M. A. (2004). Model of human thermoregulation for intermittent regional cooling. *Aviation, space, and environmental medicine*, 75(12), 1065-1069.
- Xu, X., Endrusick, T., Gonzalez, J., Laprise, B., Teal, W., Santee, W., & Kolka, M. (2005). *Evaluation of the efficiency of liquid cooling garments using a thermal manikin*. Paper presented at the Environmental Ergonomics: 11th international Conference, Lund, Sweden.
- Xu, X., Endrusick, T., Laprise, B., Santee, W., & Kolka, M. (2006). Efficiency of Liquid Cooling Garments: Prediction and Manikin Measurement. *Aviation, space, and environmental medicine*, 77(6), 644-648.
- Xu, X., & Gonzalez, J. (2011). Determination of the cooling capacity for body ventilation system. *European Journal of Applied Physiology*, 111(12), 3155-3160. doi:10.1007/s00421-011-1941-0
- Yang, R., & Chen, G. (2005). Nanostructured Thermoelectric Materials: From Superlattices to Nanocomposites. *Mater. Integr*, 18, 31-36.
- Yang, Y. (2011). *Personal-portable Cooling Garment Based on Adsorption Vacuum Membrane Evaporative Cooling*. University of Ottawa.
- Yang, Y., Stapleton, J., Diagne, B. T., Kenny, G. P., & Lan, C. Q. (2012). Man-portable personal cooling garment based on vacuum desiccant cooling. *Applied Thermal Engineering*, 47(0), 18-24. doi:<http://dx.doi.org/10.1016/j.applthermaleng.2012.04.012>
- Yazdi, M. M., & Sheikhzadeh, M. (2013). A New Method for Assessing the Performance of a Phase Change Material Cooling Garment. *International Journal of Advanced Engineering Applications*, 6(1), 47-53.
- Yermakova, I., Candás, V., & Tadejeva, J. (2005). *Modeling a microclimate cooling system in protective clothing*. Paper presented at the Environmental ergonomics: Proceedings of the 11th International Conference, Lund, Sweden.
- Yi, L., Fengzhi, L., Yingxi, L., & Zhongxuan, L. (2004). An integrated model for simulating interactive thermal processes in human–clothing system. *Journal of Thermal Biology*, 29(7–8), 567-575. doi:<http://dx.doi.org/10.1016/j.jtherbio.2004.08.071>
- Yokota, M., Endrusick, T., Gonzalez, J., & MacLeod, D. (2010). The effects of a chemical biological protective wrap on simulated physiological responses of soldiers. In T. Marek, W. Karwowski, & V. Rice (Eds.), *Advances in Understanding Human Performance: Neuroergonomics, Human Factors Design, and Special Populations* (pp. 450-458). Boca Raton, FL: CRC Press, Taylor and Francis.

- Yoshida, T., Shin-ya, H., Nakai, S., Ishii, H., & Tsuneoka, H. (2005). The effect of water-perfused suits and vests on body cooling during exercise in a hot environment. In T. Yutaka & O. Tadakatsu (Eds.), *Elsevier Ergonomics Book Series* (Vol. Volume 3, pp. 107-111): Elsevier.
- Young, A. J., Sawka, M. N., Epstein, Y., Decristofano, B., & Pandolf, K. B. (1987). *Cooling different body surfaces during upper and lower body exercise* (Vol. 63).
- Zalba, B., Marín, J. M., Cabeza, L. F., & Mehling, H. (2003). Review on thermal energy storage with phase change: materials, heat transfer analysis and applications. *Applied Thermal Engineering*, 23(3), 251-283. doi:[http://dx.doi.org/10.1016/S1359-4311\(02\)00192-8](http://dx.doi.org/10.1016/S1359-4311(02)00192-8)
- Zhang, H. (2003). *Human thermal sensation and comfort in transient and non-uniform thermal environments*. (PhD Dissertation), University of California Berkeley, Center for the Built Environment. Retrieved from <http://escholarship.org/uc/item/11m0n1wt> escholarship.org database.
- Zhang, Y., Bishop, P. A., Casaru, C., & Davis, J. K. (2009). A New Hand-Cooling Device to Enhance Firefighter Heat Strain Recovery. *Journal of Occupational and Environmental Hygiene*, 6(5), 283-288. doi:10.1080/15459620902790277
- Zhang, Y., Bishop, P. A., Green, J. M., Richardson, M. T., & Schumacker, R. E. (2010). Evaluation of a Carbon Dioxide Personal Cooling Device for Workers in Hot Environments. *Journal of Occupational and Environmental Hygiene*, 7(7), 389-396. doi:10.1080/15459621003785554

## Appendix A- Testing Images

### Thermal Manikin Testing

Visuals and images of thermal manikin testing:



**Figure 8.1 Base ensemble #1 top, front**



**Figure 8.2 Base ensemble #1 back**



**Figure 8.3 Base ensemble #2 top, front**



**Figure 8.4 Base ensemble #2 back**





**Figure 8.5 Base ensemble #2 front bottom**



**Figure 8.6 Base ensemble #3 front**



**Figure 8.7 Base ensemble #3 front, bottom**



**Figure 8.8 Base ensemble #4 front, top**



**Figure 8.9 Base ensemble front, bottom**

## Human Subject Testing

Visuals and images of human subject testing:



**Figure 8.10 Fans, air temperature sensors, humidity sensors, and TV**



**Figure 8.11 Subject ingestible pillbox labeled by days**



**Figure 8.12 Ingestible core temperature pill**

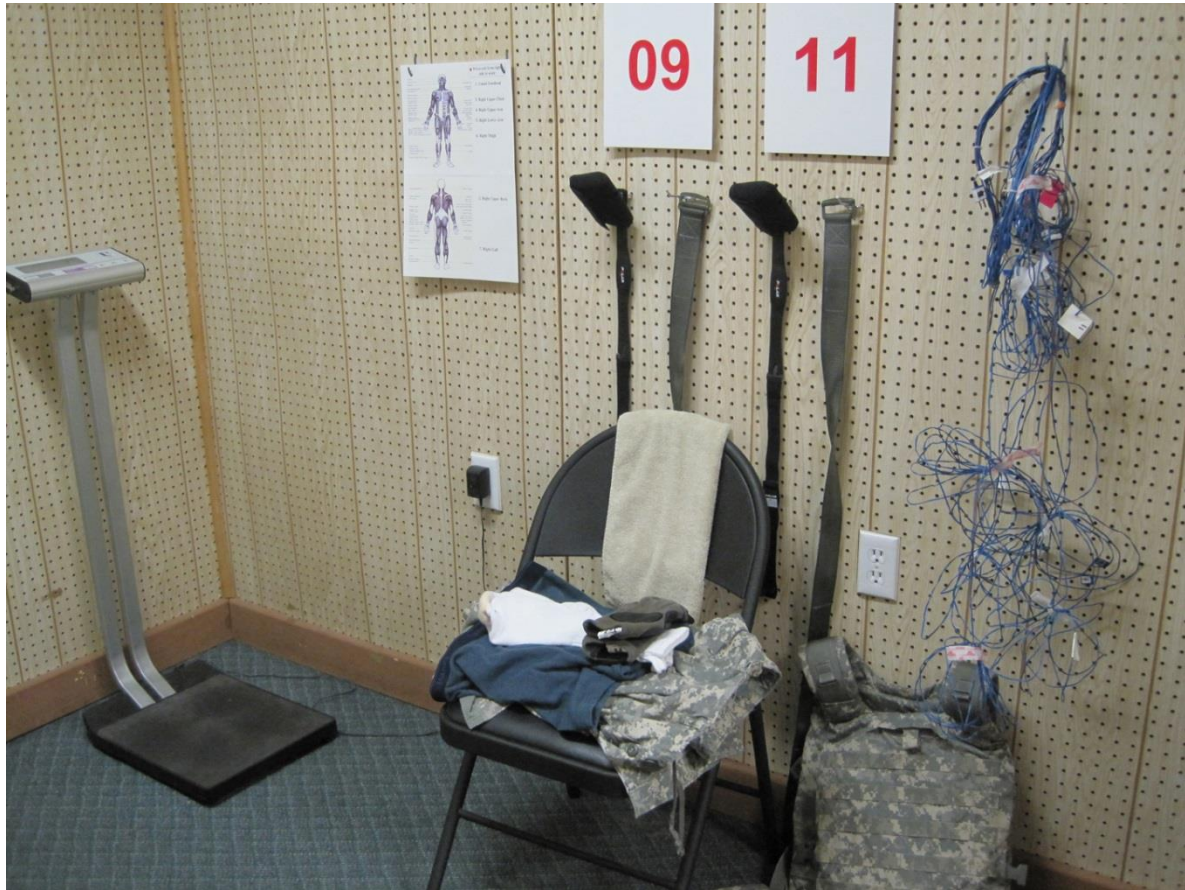


**Figure 8.13 Subject changing and instrumentation room.**





**Figure 8.14 Heart Rate chest strap**

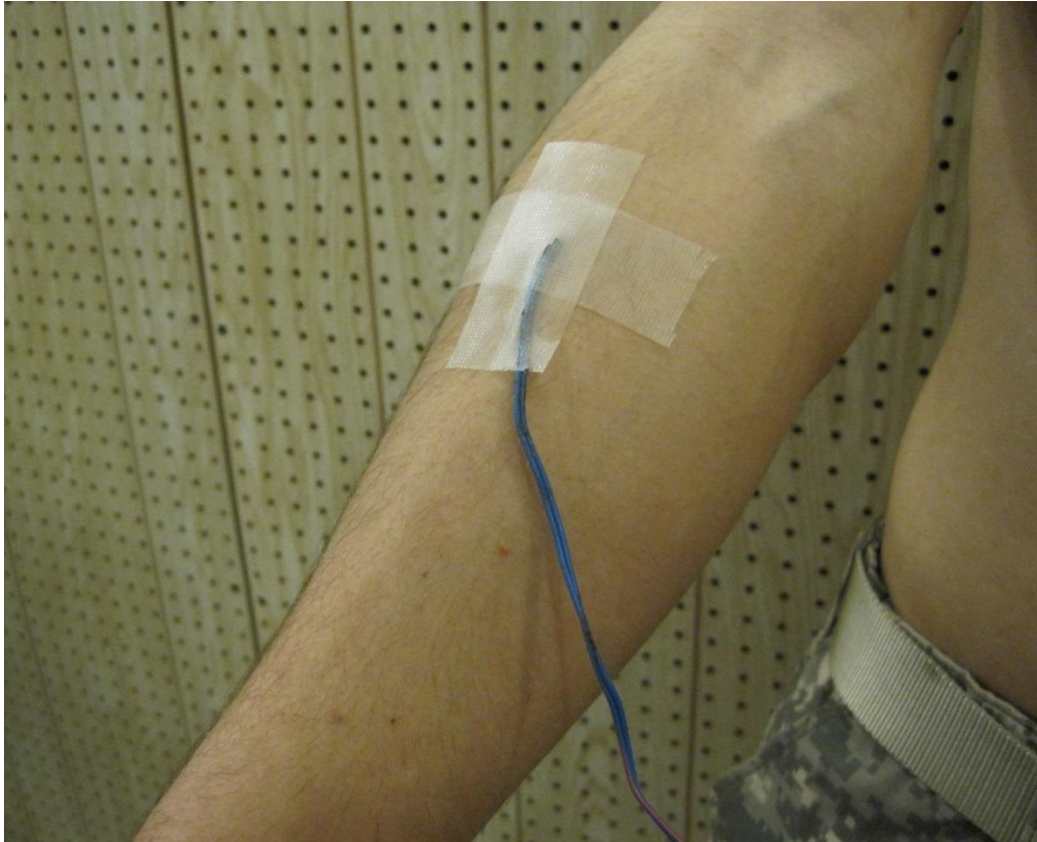


**Figure 8.15 Skin temperature thermocouple under transpore hospital tape**



**Figure 8.16 No MRI wrist band worn by subjects throughout the test week to ensure safety when not at the test center**



**Figure 8.17 Subject weighing procedure**



**Figure 8.18 Subject hydration**

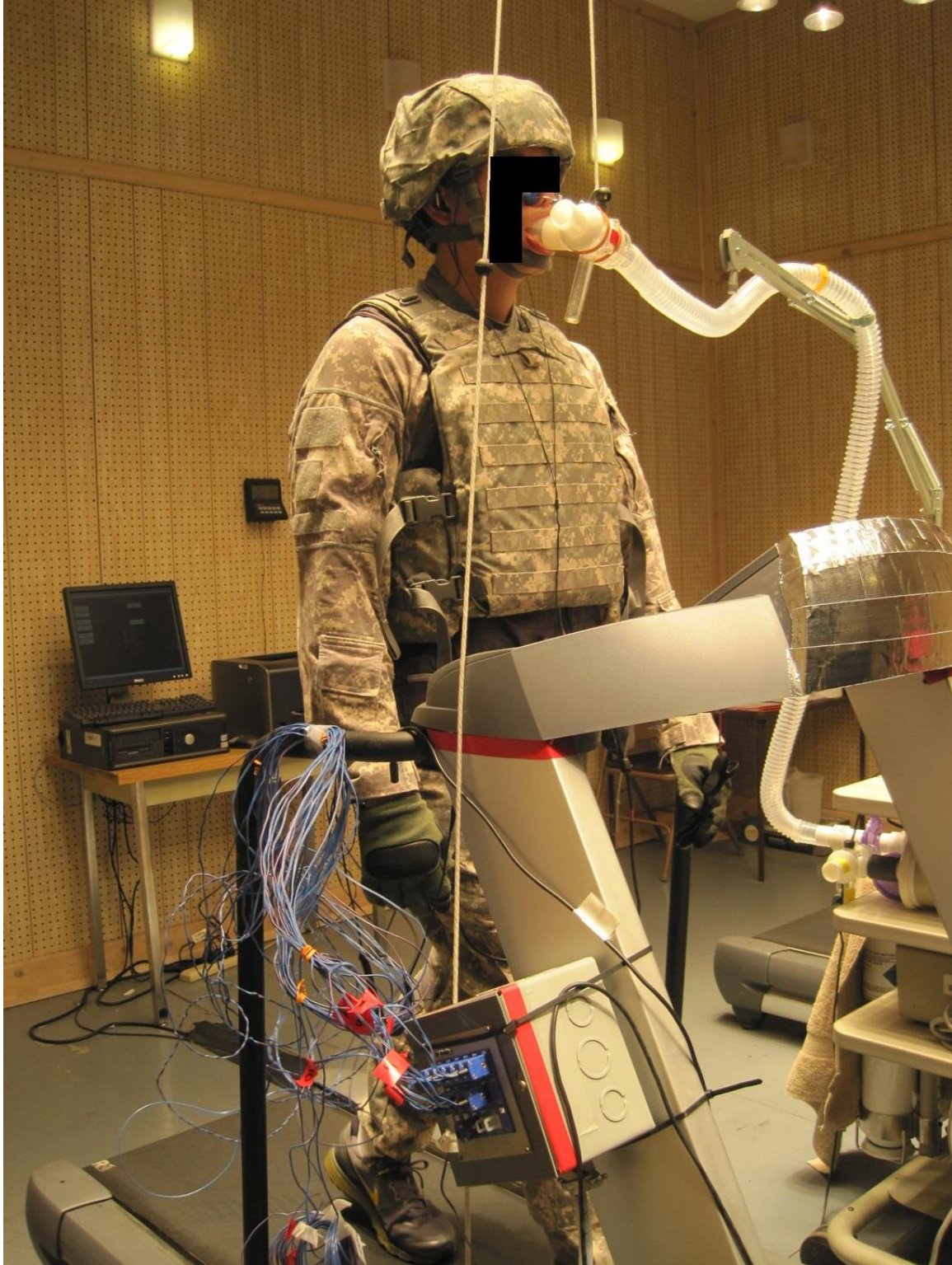


**Figure 8.19 Metabolic cart measurement**



**Figure 8.20 Metabolic cart procedure**



**Figure 8.21** Baseline ensemble front





**Figure 8.22 Baseline ensemble rear**



**Figure 8.23 PCS #1 Entrak Ventilation Vest, no armor, front**



**Figure 8.24 PCS #1 Entrak Ventilation Vest, no armor, rear**



**Figure 8.25 PCS #1 Entrak Ventilation Vest, armor, front**



**Figure 8.26 PCS #1 Entrak Ventilation Vest, armor, rear**



**Figure 8.27 PCS #9 PCVZ-KM Zipper Front Vest by Polar Products, no armor, front**



**Figure 8.28 PCS #9 PCVZ-KM Zipper Front Vest by Polar Products, armor, front**



**Figure 8.29 PCS #12 Cool UnderVest by Steele, no armor, front**





**Figure 8.30 PCS #12 Cool UnderVest by Steele, no armor, back**



**Figure 8.31 PCS #20 Hummingbird II by Creative Thermal Solutions, armor, front**



**Figure 8.32 PCS #20 Hummingbird II by Creative Thermal Solutions, armor, side**



**Figure 8.33 PCS #20 Hummingbird II by Creative Thermal Solutions, armor, back**



**Figure 8.34 Human subject testing**

## Appendix B- Modeling Initial Values

### Two-Node Model

**Table 8.1 Human subject initial and final values for baseline two-node modeling (PCS# 0)**

Subject	Week	Test Day	AM/PM (1/2)	PCS #	Time (min)	Heart Rate (BPM)	Tskin (°C)	Ttorso (°C)	Tcore (°C)	Tcore Change (°C)	Tair (°C)	RH (%)	Sweat (kg)	VO2	Met Rate (W)	Tcore Rate (°C/hr)	Tsk Initial (°C)
1	1	4	1	0	102	147.47	38.556	38.780	39.020	1.927	41.946	19.666	915.65	14.50	407.40	1.133	35.979
2	1	6	1	0	120	102.47	36.441	36.102	37.667	0.837	41.732	19.769	987.80	13.07	356.17	0.418	35.873
3	1	5	2	0	120	125.43	36.370	35.851	37.053	0.880	42.013	19.820	1411.60	12.08	394.75	0.440	35.477
4	1	4	2	0	120	119.63	36.590	36.858	37.710	0.610	41.852	20.133	1374.40	12.92	397.80	0.305	36.129
7	2	5	2	0	120	137.27	36.245	36.190	38.480	1.213	41.727	19.971	1271.10	11.60	420.33	0.607	35.432
8	2	4	2	0	120	145.37	36.845	36.612	38.000	0.970	40.995	19.557	1164.20	11.63	418.00	0.485	36.305
9	4	4	1	0	95	117.83	37.451	37.195	37.910	0.870	41.516	19.476	1114.23	11.73	424.75	0.549	36.840
10	3	6	1	0	120	131.07	37.034	36.660	37.850	1.040	41.629	19.385	1203.70	11.08	381.60	0.520	36.058
11	3	5	2	0	100	154.23	38.240	37.507	39.013	1.803	41.863	20.133	817.92	14.84	411.20	1.082	35.235
12	3	4	2	0	120	147.57	37.599	37.811	38.207	1.077	41.434	20.005	1190.50	13.90	364.25	0.538	36.677
13	1	4	1	0	120	119.57	37.360	36.206	38.703	1.557	41.843	19.769	1000.00	13.20	398.80	0.778	36.301
14	1	6	1	0	120	141.47	37.911	37.715	38.413	0.967	41.731	19.472	863.10	9.94	362.20	0.483	35.690
16	1	4	2	0	120	165.80	37.545	36.859	38.270	0.917	41.881	19.482	1078.20	12.30	420.33	0.458	35.590
17	2	4	1	0	120	143.90	35.779	35.432	37.953	0.907	42.174	20.475	1362.60	13.63	416.33	0.453	35.409
18	2	6	1	0	102	177.73	38.335	37.406	38.907	2.193	42.388	20.675	1204.71	14.37	367.00	1.290	35.974
19	2	5	2	0	120	138.90	37.268	36.459	38.273	1.077	42.234	20.446	1137.10	11.40	412.00	0.538	35.327
20	2	4	2	0	120	144.47	36.181	36.753	37.953	0.370	41.655	20.678	1317.20	11.84	368.80	0.185	36.028
21	3	4	1	0	120	146.37	36.215	36.621	37.880	0.717	42.157	19.407	1438.30	14.73	429.33	0.358	35.943
22	3	6	1	0	120	151.70	37.300	36.816	38.370	1.223	41.842	19.523	1210.60	16.00	428.33	0.612	35.752
23	3	5	2	0	120	113.10	36.024	35.478	37.900	0.123	42.125	20.165	1408.00	10.67	397.33	0.062	35.863
24	3	4	2	0	120	121.00	36.879	36.867	38.140	0.073	42.016	20.102	1158.30	12.68	409.25	0.037	35.355

**Table 8.2 Human subject weight, speed, and vertical distance values for baseline two-node modeling work calculations (PCS# 0)**

Subject	Clothed weight	Treadmill speed	Vertical Distance
	(kg)	(m/s)	(m)
1	86.137	0.983	60.189
2	84.504	1.028	74.030
3	101.242	0.805	57.936
4	93.077	0.939	67.592
7	109.769	0.760	54.718
8	110.631	0.715	51.499
9	109.542	0.715	40.770
10	105.596	0.805	57.936
11	85.684	1.028	61.692
12	79.696	1.162	83.686
13	92.351	0.983	70.811
14	110.767	0.715	51.499
16	106.458	0.760	54.718
17	92.261	0.983	70.811
18	78.381	1.207	73.869
19	109.679	0.760	54.718
20	94.075	0.939	67.592
21	89.358	1.028	74.030
22	81.329	1.162	83.686
23	114.124	0.715	51.499
24	99.382	0.849	61.155

**Table 8.3 Human subject initial and final values for PCS two-node modeling (PCS# 1 and PCS #9)**

PCS #	Time (min)	Heart Rate (BPM)	Tskin (°C)	Ttorso (°C)	Tcore (°C)	Tcore Change (°C)	Tair (°C)	RH (%)	Sweat (kg)	VO2 (W)	Met Rate (W)	Tcore Rate (°C/hr)	Tsk Initial (°C)	Height (m)	Weight (kg)
1	120	139	38	37.7	38.8	1.63	41.8	19.2	862.00	14.825	421.75	0.813	36.65	1.8	72.12
1	120	101	36.5	35.4	37.5	0.74	41.7	19.8	845.00	11.350	327.5	0.37	36.36	1.78	72.12
1	120	132	35	32.1	38.1	0.6	41.9	20.5	1162.00	12.000	390.8	0.3	35.67	1.85	86.2
1	120	102	35.4	34	37.5	0.17	41.8	19.7	1366.00	12.617	386.17	0.087	35.75	1.8	78.47
1	120	155	36.4	34.9	38	0.7	41.9	19.7	823.00	16.000	360.8	0.372	36.36	1.73	55.34
1	61	173	38.2	38	38.9	0.9	41.2	19.5	795.00	1.000	375	0.898	37.31	1.6	58.97
1	120	115	36.1	36.1	37.3	0.3	41.3	19.9	1045.00	11.000	400.3	0.168	34.85	1.83	94.8
1	120	122	37.2	37.1	37.9	0.3	41.4	19.5	1145.00	11.000	402.8	0.142	36.31	1.78	96.16
1	120	134	37.1	36.4	38.6	1.1	42.2	20	1449.00	12.000	423.6	0.57	36.27	1.73	93.44
1	120	139	37.6	37.3	38.1	1.2	41.5	19.7	1136.00	11.000	371.5	0.585	36.02	1.78	89.81
1	120	152	38.1	37.5	38.5	1.6	42	20	784.00	15.000	415.6	0.815	35.17	1.78	71.67
1	120	126	36.8	35.9	37.6	0.7	42	19.5	1035.00	15.000	406.5	0.34	36.81	1.75	65.77
9	120	105	36.8	35.8	38	1.057	42.3	19.2	918.00	12.800	398	0.528	35.84	1.78	78.5
9	120	122	37.7	37.3	37.4	0.137	41.7	19.6	707.00	9.600	356	0.068	35.84	1.78	94.8
9	120	129	37.5	37.1	38.3	0.63	42.1	19.4	832.00	12.400	379.6	0.315	35.32	1.7	74.8
9	120	137	37.2	37	37.6	0.13	41.8	19.5	886.00	10.800	388.6	0.065	35.72	1.73	91.2
9	120	111	36	35.6	37	-0.173	42.2	20.7	1181.00	13.000	411.25	-0.087	34.49	1.83	78
9	120	149	37.8	37	38.3	1.383	41.8	20.7	772.00	13.800	371	0.692	34.86	1.73	65.3
9	120	125	37.3	37	37.5	0.335	41.9	20.8	1233.00	9.900	373	0.167	36.16	1.88	94.8
9	120	110	35.7	32.5	37.4	-0.21	42	20.5	977.00	11.400	360.6	-0.105	34.36	1.8	79.4
9	120	117	34.6	31.9	37.6	0.357	42.2	19.7	1068.00	13.000	400	0.178	32.71	1.8	75.3
9	120	112	37.2	36.3	36.5	-0.683	41.8	19.5	886.00	11.600	331.67	-0.342	34.58	1.73	68
9	120	104	36.2	34.6	37.9	-0.027	42.2	19.6	1090.00	16.800	402.75	-0.013	35.63	1.85	97.1
9	120	92	36.9	36.1	37.2	-0.1	41.9	20.2	886.00	10.700	362.75	-0.05	35.76	1.75	84.4



**Table 8.4 Human subject weight, speed, and vertical distance values for PCS two-node modeling work calculations (PCS# 1 and PCS# 9)**

Subject	PCS #	Clothed weight (kg)	Treadmill speed (m/s)	Vertical Distance (m)
1	1	88.227	1.028	74.030
2	1	87.591	0.983	70.811
3	1	103.182	0.760	54.718
4	1	93.636	0.894	64.374
5	1	70.727	1.296	93.342
6	1	72.545	1.207	44.176
7	1	111.364	0.715	51.499
8	1	112.773	0.715	51.499
9	1	111.000	0.715	51.499
10	1	107.318	0.715	51.499
11	1	85.636	1.073	77.249
12	1	79.955	1.162	83.686
13	9	92.409	0.939	67.592
14	9	110.364	0.715	51.499
15	9	89.273	0.983	70.811
16	9	106.727	0.760	54.718
17	9	92.136	0.760	54.718
18	9	77.909	1.118	80.467
19	9	110.273	0.715	51.499
20	9	93.727	0.894	64.374
21	9	89.864	0.939	67.592
22	9	82.364	1.073	77.249
23	9	114.364	0.671	48.280
24	9	100.182	0.805	57.936

**Table 8.5 Human subject initial and final values for PCS two-node modeling (PCS# 12 and PCS #20)**

Subject	Week	Test Day	AM/PM	PCS #	Time (min)	Heart Rate (BPM)	Tskin (°C)	Ttorso (°C)	Tcore (°C)	Tcore Change (°C)	Tair (°C)	RH (%)	Sweat (kg)	VO2 (W)	Met Rate (°C/hr)	Tsk Initial (°C)	Height (m)	Weight (kg)	
1	1	6	1	12	120	130	37	35.2	37.9	0.9	42.2	19.7	715	14	406.6	0.452	32.618	1.8	72.12
2	1	5	1	12	120	79	36.6	35.1	37.7	0.7	41.9	19.4	702	12	334.5	0.353	33.676	1.78	72.12
3	1	4	2	12	120	112	36.2	34.7	37.2	0.1	42.2	20.1	968	12	391	0.052	33.525	1.85	86.2
4	1	6	2	12	120	97	35.9	35.6	37	-0.5	41.2	20.6	1104	12	380.2	-0.263	35.069	1.8	78.47
5	2	5	1	12	120	155	36.1	34.6	38.3	0.8	41.5	19.7	726	15	354	0.411	34.763	1.73	55.34
6	2	4	1	12	84	174	36.5	32.8	39.1	1.8	41.3	19.2	1416	1	375	1.271	34.891	1.6	58.97
7	2	6	2	12	120	106	37.6	35.9	37.3	0.6	41.6	19.8	882	11	396.2	0.280	34.591	1.83	94.8
8	2	5	2	12	120	117	33.8	27	37.5	0.2	41.5	19.7	916	8	409	0.103	35.014	1.78	96.16
9	3	6	1	12	120	109	35.6	33.3	37.9	0.5	41.7	20.1	818	11	403.3	0.233	33.148	1.73	93.44
10	3	5	1	12	120	125	33.8	27.9	37.4	0.1	41.9	19.6	931	11	373.5	0.062	33.654	1.78	89.81
11	3	4	2	12	120	127	37.3	36.8	37.5	0.6	41.5	20.7	627	15	415	0.282	33.646	1.78	71.67
12	3	6	2	12	120	115	37.1	37	38.7	0.2	41.9	19.4	895	14	373.6	0.123	33.878	1.75	65.77
13	1	6	1	20	71	107	34.2	29.2	37.5	0.697	42.1	19.4	960	12.9	394	0.589	36.121	1.78	78.5
14	1	5	1	20	120	112	37.4	36.5	37.4	0.153	41.9	19.4	716	9.3	348.75	0.077	36.279	1.78	94.8
15	1	4	2	20	120	140	33	25.3	38.1	0.493	42.1	19.6	809	12.3	376	0.247	35.708	1.7	74.8
16	1	6	2	20	120	112	35.7	32.4	37.3	0.047	41.9	19.2	769	10.4	386.4	0.023	36.292	1.73	91.2
17	2	6	1	20	120	116	32.6	25	37	-0.153	42.7	20	1119	12.2	391	-0.077	35.125	1.83	78
18	2	5	1	20	120	139	36.3	33.8	38	1.137	42.1	20.7	863	13.3	369.4	0.568	36.361	1.73	65.3
19	2	4	2	20	120	156	37.5	37	38.3	0.99	42	20.5	1022	10.9	411	0.495	34.911	1.88	94.8
20	2	6	2	20	120	121	33.2	27.7	37.6	0.12	41.5	21.1	1384	11.4	364.4	0.060	36.332	1.8	79.4
21	3	6	1	20	120	108	33	27.7	37.5	0.433	42.1	19.6	1127	13.2	407.25	0.217	35.191	1.8	75.3
22	3	5	1	20	120	124	33	25.1	37.5	0.343	41.9	19.8	977	14.1	409.75	0.172	36.288	1.73	68
23	3	4	2	20	120	105	30.3	19.1	37.6	-0.126	42.3	20	1136	10.4	401	-0.063	34.786	1.85	97.1
24	3	6	2	20	120	103	34.7	30.8	37.4	-0.163	41.9	19.5	978	10.8	369.75	-0.082	36.062	1.75	84.4

**Table 8.6 Human subject weight, speed, and vertical distance values for PCS two-node modeling work calculations (PCS# 12 and PCS# 20)**

Subject	PCS #	Clothed weight (kg)	Treadmill speed (m/s)	Vertical Distance (m)
1	12	0.939	0.939	73.225
2	12	0.939	0.939	44.498
3	12	0.760	0.760	51.070
4	12	0.894	0.894	52.035
5	12	1.252	1.252	116.409
6	12	1.162	1.162	121.345
7	12	0.715	0.715	45.491
8	12	0.671	0.671	47.073
9	12	0.671	0.671	43.855
10	12	0.760	0.760	56.998
11	12	0.983	0.983	74.942
12	12	1.118	1.118	77.114
13	20	0.939	0.939	60.270
14	20	0.671	0.671	45.062
15	20	0.760	0.760	63.837
16	20	0.715	0.715	48.066
17	20	0.894	0.894	62.228
18	20	1.073	1.073	89.480
19	20	0.671	0.671	62.764
20	20	0.894	0.894	64.910
21	20	0.939	0.939	60.833
22	20	1.073	1.073	79.823
23	20	0.671	0.671	42.245
24	20	0.805	0.805	49.729

**Table 8.7 Thermal manikin average cooling for PCS used in two-node modeling**

<b>Time</b>	<b>PCS 1 Total Heat Diff.</b>	<b>PCS 9 Total Heat Diff.</b>	<b>PCS 12 Total Heat Diff.</b>	<b>PCS 20 Total Heat Diff.</b>
<b>(min.)</b>	<b>(W)</b>	<b>(W)</b>	<b>(W)</b>	<b>(W)</b>
1.01	82.07	139.67	129.49	37.22
2.02	90.84	138.47	132.15	47.30
3.01	99.27	133.94	134.47	63.90
4.01	102.31	130.90	134.02	77.32
5.03	103.74	128.50	133.13	87.87
6.01	103.49	126.43	131.95	94.84
7.03	103.29	124.61	130.73	99.61
8.01	102.76	122.46	129.80	103.84
9.03	102.38	121.89	129.17	105.96
10.01	102.68	120.83	129.45	107.64
11.03	102.46	119.64	128.78	108.64
12.01	101.72	119.25	127.84	109.33
13.03	100.97	118.32	126.59	109.37
14.01	99.89	117.49	126.50	109.68
15.03	99.77	116.25	126.80	109.52
16.01	98.94	115.90	126.12	110.49
17.02	99.23	116.45	126.06	111.01
18.01	99.01	115.98	125.24	110.74
19.01	99.33	114.72	125.44	111.16
20.01	99.44	114.48	125.25	111.57
21.01	100.01	113.95	125.69	111.58
22.01	99.05	114.28	125.88	111.78
23.01	98.49	114.59	124.91	111.86
24.01	98.79	114.83	124.46	111.81
25.01	99.00	114.24	124.12	112.07
26.03	99.01	113.70	123.76	111.85
27.01	98.39	112.84	123.68	112.01
28.03	98.55	112.22	124.00	112.45
29.01	98.45	112.19	124.78	112.43
30.02	99.16	112.06	124.45	112.73
31.01	99.52	111.73	124.37	113.24
32.02	99.92	111.44	124.68	112.92
33.01	99.60	110.84	124.66	113.61
34.03	99.53	110.25	124.24	113.48
35.01	100.70	110.01	123.88	113.07
36.01	101.20	109.62	123.55	112.75
37.01	101.79	108.64	123.46	113.11
38.01	101.94	108.38	122.63	113.76
39.01	101.63	108.54	122.66	113.14

40.02	101.39	108.06	123.19	113.69
41.01	101.68	107.46	122.69	114.10
42.01	102.33	107.00	122.29	113.92
43.01	102.89	106.43	121.72	113.83
44.01	103.00	106.24	120.94	114.16
45.02	103.15	105.70	120.64	114.06
46.01	102.89	105.15	120.36	114.00
47.02	102.22	104.23	119.80	113.87
48.01	102.01	103.75	119.40	113.40
49.02	102.05	103.49	119.97	113.22
50.00	102.33	103.14	120.76	113.48
51.02	102.15	102.88	119.78	113.52
52.00	102.34	102.47	119.06	113.06
53.02	102.06	101.66	117.92	112.95
54.00	101.85	100.94	118.45	112.56
55.02	101.96	100.36	118.70	113.24
56.02	102.40	100.02	117.49	113.95
57.02	102.19	99.32	116.83	113.26
58.02	102.41	98.82	117.21	113.47
59.02	101.82	99.19	116.41	113.26
60.02	101.55	99.58	116.23	113.09
61.02	100.45	98.62	115.44	113.35
62.02	99.21	98.26	115.47	113.53
63.01	102.25	97.23	115.54	112.87
64.01	101.05	96.82	115.34	113.12
65.01	99.80	96.59	114.19	112.79
66.03	101.16	96.05	113.49	112.87
67.01	100.60	95.83	113.44	113.09
68.03	100.47	94.55	113.50	113.13
69.01	101.61	94.27	112.71	113.27
70.02	101.54	93.80	112.67	113.00
71.01	101.26	93.63	112.27	113.44
72.02	100.77	92.93	112.35	113.14
73.01	101.08	92.03	111.79	113.41
74.02	101.10	91.39	111.19	113.54
75.01	100.82	90.70	110.95	113.65
76.02	100.53	90.09	110.64	113.18
77.00	100.61	89.20	109.51	113.76
78.02	100.57	89.48	108.45	113.83
79.00	100.17	88.55	108.76	113.84
80.02	101.12	87.57	108.13	113.61
81.00	100.98	86.35	107.70	113.18
82.02	100.36	85.76	107.18	113.44
83.02	100.40	84.97	106.72	112.98
84.02	100.92	84.60	106.15	112.98

85.03	100.81	84.62	105.31	113.30
86.01	100.17	83.99	104.62	112.83
87.02	99.54	82.85	104.20	112.77
88.01	100.20	82.27	102.96	112.90
89.03	99.95	81.46	102.64	112.93
90.01	100.24	81.36	102.17	113.08
91.03	100.20	81.26	101.41	112.64
92.01	100.19	80.35	101.14	113.22
93.02	99.86	80.16	101.55	113.02
94.02	100.19	79.39	101.03	112.92
95.02	99.86	78.51	100.95	112.93
96.02	99.43	78.03	100.46	112.70
97.02	99.16	78.09	99.38	112.45
98.01	98.44	77.98	98.73	112.17
99.02	98.45	77.15	98.54	112.68
100.01	98.41	76.24	97.95	112.84
101.01	98.40	75.22	97.40	112.76
102.01	98.22	74.82	96.48	112.24
103.01	98.81	74.07	95.80	112.11
104.01	98.89	73.38	95.37	112.80
105.01	98.49	73.23	95.01	112.22
106.01	98.69	72.82	94.20	113.04
107.01	98.75	72.60	93.09	113.14
108.01	99.16	71.62	92.66	113.18
109.02	98.66	70.55	91.92	114.12
110.01	99.28	69.86	91.44	113.77
111.02	99.25	69.89	91.41	113.48
112.01	98.99	68.56	91.19	113.65
113.02	100.01	67.85	89.44	113.72
114.02	100.26	66.58	88.98	114.26
115.02	100.67	66.35	88.36	114.36
116.02	99.97	66.01	87.21	114.26
117.02	99.70	64.99	86.11	114.30
118.01	100.74	64.46	85.57	114.20
119.01	101.36	63.62	85.03	114.12
120.01	101.08	62.93	83.93	114.60

## Human Subjects

**Table 8.8 Multi-Node Model (TAITherm) initial body temperatures for 50% height 75% weight simulated subject**

Results:

# Time	Tskm	Thy	Tre	Tblp	dTskdt	Qm	Qconv
#(min)	(C)	(C)	(C)	(C)	(K/hr)	(W)	(W)
0	34.05	37.2	37.18	36.94	0	95.4	-21.8
Qrad	Qsolar	Qevap	Qrsp	DI	Cs	Sh	Sw
(W)	(W)	(W)	(W)	(W/K)	()	(W)	(g/min)
-46.2	0	-19.7	-7.6	0	0	0	0
CO	VSBF	w_sk	TS	DTS	MRT	hr	hc
(L/min)	(L/min)	(%)	()	()	(C)	(W/m^2K)	(W/m^2K)
5.34	0.42	6	0	0	30	5.58	2.64
PMV	PPD						
()	(%)						
0.31	6.99						

Tissue  
Temperatures:

#Segment	Layer	Name	(C)
Head	0	Skin	35.0664
Head	1	Fat	35.2868
Head	2	Bone	35.6272
Head	3	Brain	37.2362
Face	0	Skin	34.6236
Face	1	Fat	35.0956
Face	2	Muscle	35.7978

Face	3	Bone	36.3072
Face	4	Muscle	36.1901
Neck	0	Skin	34.2753
Neck	1	Fat	34.36
Neck	2	Muscle	34.8668
Neck	3	Bone	35.4902
LeftShoulder	0	Skin	33.1263
LeftShoulder	1	Fat	33.5884
LeftShoulder	2	Muscle	34.065
LeftShoulder	3	Bone	34.4555
RightShoulder	0	Skin	33.0903
RightShoulder	1	Fat	33.5416
RightShoulder	2	Muscle	34.0054
RightShoulder	3	Bone	34.3725
Chest	0	Skin	35.0817
Chest	1	Fat	35.8292
Chest	2	Muscle	36.8136
Chest	3	Bone	36.8629
Chest	4	Lung	36.9475
Back	0	Skin	35.0627
Back	1	Fat	35.8153
Back	2	Muscle	36.8068
Back	3	Bone	36.8531
Back	4	Lung	36.9472
Abdomen	0	Skin	34.9135
Abdomen	1	Fat	35.6319
Abdomen	2	Muscle	36.9941
Abdomen	3	Bone	37.1278
Abdomen	4	Viscera	37.1876
Abdomen	5	Viscera	37.1824
LeftUpperArm	0	Skin	33.8522



LeftUpperArm	1	Fat	34.5696
LeftUpperArm	2	Muscle	35.7779
LeftUpperArm	3	Bone	35.9496
RightUpperArm	0	Skin	33.8568
RightUpperArm	1	Fat	34.573
RightUpperArm	2	Muscle	35.7795
RightUpperArm	3	Bone	35.9512
LeftLowerArm	0	Skin	33.5936
LeftLowerArm	1	Fat	33.9276
LeftLowerArm	2	Muscle	34.5366
LeftLowerArm	3	Bone	34.6931
RightLowerArm	0	Skin	33.5987
RightLowerArm	1	Fat	33.9324
RightLowerArm	2	Muscle	34.5412
RightLowerArm	3	Bone	34.6999
LeftHand	0	Skin	32.2678
LeftHand	1	Fat	32.4516
LeftHand	2	Muscle	32.7417
LeftHand	3	Bone	32.8204
RightHand	0	Skin	32.2733
RightHand	1	Fat	32.4568
RightHand	2	Muscle	32.7461
RightHand	3	Bone	32.8234
LeftThigh	0	Skin	34.5348
LeftThigh	1	Fat	35.2707
LeftThigh	2	Muscle	36.6458
LeftThigh	3	Bone	36.8921
RightThigh	0	Skin	34.5353
RightThigh	1	Fat	35.2708
RightThigh	2	Muscle	36.6455
RightThigh	3	Bone	36.8934

LeftLowerLeg	0	Skin	34.5475
LeftLowerLeg	1	Fat	34.8247
LeftLowerLeg	2	Muscle	35.365
LeftLowerLeg	3	Bone	35.5025
RightLowerLeg	0	Skin	34.5479
RightLowerLeg	1	Fat	34.8253
RightLowerLeg	2	Muscle	35.3657
RightLowerLeg	3	Bone	35.5016
LeftFoot	0	Skin	32.3047
LeftFoot	1	Fat	32.6048
LeftFoot	2	Muscle	32.9594
LeftFoot	3	Bone	33.0179
RightFoot	0	Skin	32.2998
RightFoot	1	Fat	32.5997
RightFoot	2	Muscle	32.9549
RightFoot	3	Bone	33.0137

Arterial Blood  
Temperatures:

#Segment	(C)
Head	36.9441
Face	36.9441
Neck	36.9441
LeftShoulder	34.3132
RightShoulder	34.2838
Chest	36.9441
Back	36.9441
Abdomen	36.9441
LeftUpperArm	36.2593
RightUpperArm	36.2603
LeftLowerArm	35.2067

RightLowerArm	35.2097
LeftHand	33.2851
RightHand	33.2892
LeftThigh	36.8097
RightThigh	36.8097
LeftLowerLeg	36.047
RightLowerLeg	36.0473
LeftFoot	33.4589
RightFoot	33.4552

Clothing Variables:  
(Whole Body)  
Nude

Physiology:  
Basal Metabolic  
Rate (met) 0.838744

**Table 8.9 Multi-Node Model Modified ReCl values based on two-node model results**

Material Name	Material Type	Thermal Resistance	Evaporative Resistance	Area Factor
USA3Mod - Face	Clothing	0.04700236	0.009450942	1.326594353
USA3Mod - L Up Thigh	Clothing	0.30340329	0.024647883	1.326594353
USA3Mod - L Low Thigh	Clothing	0.1664795	0.022017509	1.326594353
USA3Mod - R Foot	Clothing	0.1700176	0.060996573	1.326594353
USA3Mod - Head	Clothing	0.11698712	0.022045402	1.326594353
USA3Mod - R Forearm	Clothing	0.09671044	0.009972102	1.326594353
USA3Mod - L Hand	Clothing	0.07423331	0.009574109	1.326594353
USA3Mod - R Hand	Clothing	0.07600236	0.009014393	1.326594353
USA3Mod - L Forearm	Clothing	0.11395664	0.011544687	1.326594353

USA3Mod - R Calf	Clothing	0.12949474	0.015783168	1.326594353
USA3Mod - Stomach	Clothing	0.29164949	0.057317283	1.326594353
USA3Mod - Chest	Clothing	0.18571045	0.04057638	1.326594353
USA3Mod - Shoulders	Clothing	0.26188043	0.095234253	1.326594353
USA3Mod - L Foot	Clothing	0.17252521	0.092287444	1.326594353
USA3Mod - L Upper Arm	Clothing	0.16667996	0.025768088	1.326594353
USA3Mod - R Upper Arm	Clothing	0.12792616	0.019504027	1.326594353
USA3Mod - Back	Clothing	0.28384996	0.050749991	1.326594353
USA3Mod - L Calf	Clothing	0.13624854	0.017182858	1.326594353
USA3Mod - R Low Thigh	Clothing	0.16423331	0.020104507	1.326594353
USA3Mod - R Up Thigh	Clothing	0.26240331	0.027323729	1.326594353

**Table 8.10 Multi-Node Model physiology.txt values**

```
#####
#       Human Comfort Module - Physiology File           #
#####
# Description: This tab-delimited data file defines the physiological
#       properties for creating a thermoregulatory model of a human.
#
#####
```

```
# This file is flagged to as safe to overwrite by PhysioGen.
# If making any modifications, remove the following line.
SafeToOverwrite
```

Compartments:

Name	Geom	SectAng	hx(W/K)	L(m)
Head	Sph	180	0	0
Face	Cyl	210	0	0.0984
Neck	Cyl	360	0	0.0842
LeftShoulder	Cyl	130	0.848	0.16
RightShoulder	Cyl	130	0.848	0.16
Chest	Cyl	180	0	0.306
Back	Cyl	180	0	0.306
Abdomen	Cyl	360	0	0.552
LeftUpperArm	Cyl	360	2.6076	0.332
RightUpperArm	Cyl	360	2.6076	0.332
LeftLowerArm	Cyl	360	4.2241	0.305
RightLowerArm	Cyl	360	4.2241	0.305
LeftHand	Cyl	360	5.8671	0.31
RightHand	Cyl	360	5.8671	0.31
LeftThigh	Cyl	360	1.84705	0.3485
RightThigh	Cyl	360	1.84705	0.3485
LeftLowerLeg	Cyl	360	3.6835	0.3465
RightLowerLeg	Cyl	360	3.6835	0.3465
LeftFoot	Cyl	360	4.9555	0.24
RightFoot	Cyl	360	4.9555	0.24

TissueLayers:

Name	Layer	nSubLyr	Matl	r(m)
Head	3	6	Brain	0.088617
Head	2	3	Bone	0.103558
Head	1	3	Fat	0.105373
Head	0	4	Skin	0.107373
Face	4	3	Muscle	0.028032

Face	3	3	Bone	0.056692
Face	2	3	Muscle	0.071127
Face	1	3	Fat	0.08089
Face	0	4	Skin	0.08289
Neck	3	3	Bone	0.019874
Neck	2	6	Muscle	0.057111
Neck	1	3	Fat	0.05834
Neck	0	4	Skin	0.05944
LeftShoulder	3	3	Bone	0.038701
LeftShoulder	2	6	Muscle	0.040793
LeftShoulder	1	3	Fat	0.046891
LeftShoulder	0	4	Skin	0.048891
RightShoulder	3	3	Bone	0.038701
RightShoulder	2	6	Muscle	0.040793
RightShoulder	1	3	Fat	0.046891
RightShoulder	0	4	Skin	0.048891
Chest	4	3	Lung	0.080855
Chest	3	3	Bone	0.092674
Chest	2	3	Muscle	0.110142
Chest	1	3	Fat	0.126121
Chest	0	4	Skin	0.128321
Back	4	3	Lung	0.080855
Back	3	3	Bone	0.092674
Back	2	3	Muscle	0.110142
Back	1	3	Fat	0.126121
Back	0	4	Skin	0.128321
Abdomen	5	2	Viscera	0.035564
Abdomen	4	2	Viscera	0.08211
Abdomen	3	2	Bone	0.087549
Abdomen	2	3	Muscle	0.124577

## Appendix C- Thermal Models

**Mathcad 15 (PTC Inc.) was used to program the Mean Radiant Temperature Calculation, ASHRAE Two-node Model Implementation Baseline with the Presented Wetted Clothing Model**

**Conditions/Constants:**

User Defined Conditions:

SUBJECT	WEEK	DAY	AMPM	PCS	TIME	HEARTRAT	TSKIN	TORSOTEN	CORETEN	CORECHG	AIRTEMP	RH	SWRATE	VO2	METRATE	CORERATE	TSKININT	HEIGHT	Weight
0	1	2	3	4	5	6	7	8	9	10	11	12	13	14	15	16	17	18	19

	0	1	2	3	4	5	6	7	8	9	10	11	12	13	14	15		
X =	0	1	1	6	1	12	120	130	37	35.2	37.9	0.9	42.2	19.7	715	14	14	406.6
	1	2	1	5	1	12	120	79	36.6	35.1	37.7	0.7	41.9	19.4	702	12	12	334.5
	2	3	1	4	2	12	120	112	36.2	34.7	37.2	0.1	42.2	20.1	968	12	12	391
	3	4	1	6	2	12	120	97	35.9	35.6	37	-0.5	41.2	20.6	1.104·10 <sup>3</sup>	12	12	380.2
	4	5	2	5	1	12	120	155	36.1	34.6	38.3	0.8	41.5	19.7	726	15	15	354
	5	6	2	4	1	12	84	174	36.5	32.8	39.1	1.8	41.3	19.2	1.416·10 <sup>3</sup>	1	1	375
	6	7	2	6	2	12	120	106	37.6	35.9	37.3	0.6	41.6	19.8	882	11	11	396.2
	7	8	2	5	2	12	120	117	33.8	27	37.5	0.2	41.5	19.7	916	8	8	409
	8	9	3	6	1	12	120	109	35.6	33.3	37.9	0.5	41.7	20.1	818	11	11	403.3
	9	10	3	5	1	12	120	125	33.8	27.9	37.4	0.1	41.9	19.6	931	11	11	373.5
	10	11	3	4	2	12	120	127	37.3	36.8	37.5	0.6	41.5	20.7	627	15	15	415
	11	12	3	6	2	12	120	115	37.1	37	38.7	0.2	41.9	19.4	895	14	14	373.6
	12	13	1	6	1	20	71	107	34.2	29.2	37.5	0.697	42.1	19.4	960	12.9	12.9	394
	13	14	1	5	1	20	120	112	37.4	36.5	37.4	0.153	41.9	19.4	716	9.3	9.3	348.75
	14	15	1	4	2	20	120	140	33	25.3	38.1	0.493	42.1	19.6	809	12.3	12.3	376
	15	16	1	6	2	20	120	112	35.7	32.4	37.3	0.047	41.9	19.2	769	10.4	10.4	386.4
	16	17	2	6	1	20	120	116	32.6	25	37	-0.153	42.7	20	1.119·10 <sup>3</sup>	12.2	12.2	391
	17	18	2	5	1	20	120	139	36.3	33.8	38	1.137	42.1	20.7	863	13.3	13.3	369.4
	18	19	2	4	2	20	120	156	37.5	37	38.3	0.99	42	20.5	1.022·10 <sup>3</sup>	10.9	10.9	411
	19	20	2	6	2	20	120	121	33.2	27.7	37.6	0.12	41.5	21.1	1.384·10 <sup>3</sup>	11.4	11.4	364.4
	20	21	3	6	1	20	120	108	33	27.7	37.5	0.433	42.1	19.6	1.127·10 <sup>3</sup>	13.2	13.2	407.25
	21	22	3	5	1	20	120	124	33	25.1	37.5	0.343	41.9	19.8	977	14.1	14.1	409.75
	22	23	3	4	2	20	120	105	30.3	19.1	37.6	-0.126	42.3	20	1.136·10 <sup>3</sup>	10.4	10.4	...

**Conditions/Constants:**

User Defined Conditions:

trousers, long-sleeved shirt

Environmental:

Clothing:

$$T_a := (42.2 + 273.15)\text{K} = 315.35\text{K}$$

$$\text{clo} := 0.155 \frac{\text{m}^2\text{K}}{\text{W}}$$

Wind velocity (m/s):

$$T_r := (54.4 + 273.15)\text{K} = 327.55\text{K}$$

$$I_{\text{cl}} := 1.00\text{clo}$$

$$v_{\text{wind}} := 2.0$$

Walking in the wind  
convection pg 82, danielson

$$h_c := 11.7 \cdot v_{\text{wind}}^{0.57} \frac{\text{W}}{\text{m}^2 \cdot \text{K}} = 17.36893 \frac{\text{kg}}{\text{K} \cdot \text{s}^3}$$

$$h_r := 4.7 \frac{\text{W}}{\text{m}^2 \cdot \text{K}}$$

$$\text{Ensemblemass} := 15.054\text{kg}$$

$$R_{\text{cl}} := I_{\text{cl}}$$

$$R_{\text{cl}} = 0.155 \frac{\text{K} \cdot \text{s}^3}{\text{kg}}$$

$$\text{Grade} := 0.01$$

$$\phi := .20$$

$$\text{load} := 10\text{kg}$$

$$f_{\text{cl}} := 1.33$$

$$T_o := \frac{h_r \cdot T_r + h_c \cdot T_a}{h_r + h_c} = 317.94822\text{K}$$

$$h_t := h_r + h_c$$

**Iterative Variables Individually dependent:**

$$\text{mass}(n) := X_{n,19} \cdot \text{kg}$$

$$\text{height}(n) := X_{n,18} \cdot \text{m}$$

$$A_D(n) := \left[ 0.202 \cdot \left( \frac{\text{mass}(n)}{\text{kg}} \right)^{0.425} \cdot \left( \frac{\text{height}(n)}{\text{m}} \right)^{0.725} \right] \cdot \text{m}^2$$

$$M(n) := \frac{X_{n,15} \cdot \text{W}}{A_D(n)}$$

$$T_{\text{skn}}(n) := (X_{n,17} + 273.15) \cdot \text{K}$$

$$T_{\text{crn}}(n) := (X_{n,9} - X_{n,10} + 273.15) \text{K}$$

$$\text{Wk}(n) := \text{Grade} \cdot \text{WKVal}_{n,0} \cdot \text{kg} \cdot \text{WKVal}_{n,1} \cdot \frac{\text{m}}{\text{s}} \cdot 9.81 \frac{\text{m}}{\text{s}^2}$$

$$\text{Time}_n(n) := X_{n,5} \cdot 60\text{s}$$

$$\text{ASW}(n) := X_{(n,13)} \cdot \frac{\text{kg}}{1000} \cdot \text{Time}_n(n)$$



Clothed weight (kg)	Treadmill speed (m/s)	time (s)	Vert Distance (m)
---------------------	-----------------------	----------	-------------------

WKVal :=

86.1371208	0.983488	6120	60.1894656
84.5041896	1.028192	7200	74.029824
101.2417344	0.804672	7200	57.936384
93.0770784	0.938784	7200	67.592448
69.3088576	1.34112	4680	62.764416
71.7582544	1.207008	4920	59.3847936
109.769264	0.759968	7200	54.717696
110.6310888	0.715264	7200	51.499008
109.542468	0.715264	5700	40.770048
105.5962176	0.804672	7200	57.936384
85.6835288	1.028192	6000	61.69152
79.6961144	1.162304	7200	83.685888
92.3513312	0.983488	7200	70.811136
110.7671664	0.715264	7200	51.499008
88.7679544	1.028192	4200	43.184064
106.4580424	0.759968	7200	54.717696
92.2606128	0.983488	7200	70.811136
78.3806976	1.207008	6120	73.8688896
109.6785456	0.759968	7200	54.717696
94.0749808	0.938784	7200	67.592448
89.357624	1.028192	7200	74.029824
81.3290456	1.162304	7200	83.685888
114.1237472	0.715264	7200	51.499008
99.3820072	0.849376	7200	61.155072

+

Body Equation Constants:

$$Sw_{\text{mod}} := 1.17$$

$$c_{\text{sw}} := Sw_{\text{mod}} \cdot 116 \frac{\text{W}}{\text{m}^2 \cdot \text{K}} \quad \text{BFN} := 6.3 \quad C_{\text{pb}} := 4190 \frac{\text{J}}{\text{kg} \cdot \text{K}}$$

$$K_{\text{eff}} := 5.28 \frac{\text{W}}{\text{m}^2 \cdot \text{K}} \quad c_{\text{dil}} := \frac{150}{\text{K}} \quad C_{\text{cr}} := 3500 \frac{\text{J}}{\text{kg} \cdot \text{K}}$$

$$\rho_{\text{bl}} := 1.06 \frac{\text{kg}}{\text{L}} \quad S_{\text{tr}} := \frac{0.5}{\text{K}} \quad C_{\text{sk}} := 3500 \frac{\text{J}}{\text{kg} \cdot \text{K}}$$

**Constants and Calculated Constants:**

$$P_T := 101325 \text{ Pa}$$

$$C_{p_v} := 1864 \frac{\text{J}}{\text{kg} \cdot \text{K}}$$

$$C_{p_a} := 1005 \frac{\text{J}}{\text{kg} \cdot \text{K}}$$

$$h_{f_{g_{ex}}} := 2454.1 \frac{1000 \text{ J}}{\text{kg}}$$

$$C_{p_b} := 3500 \frac{\text{J}}{\text{kg} \cdot \text{K}}$$

$$LR_{STD} := 16.5 \frac{\text{K}}{1000 \text{ Pa}}$$

$$K_{res} := 1.43 \cdot 10^{-6} \frac{\text{kg}}{\text{J}}$$

**Sat. Pressure Equation: P<sub>sat</sub>(T)**

Pressure Curve Fit  
Constants:

ICE	LIQUID
$C_1 := -5.6745359 \cdot 10^3$	$C_8 := -5800.2206$

$C_2 := 6.3925247$	$C_9 := 1.3914993$
--------------------	--------------------

$C_3 := -0.009677843$	$C_{10} := -0.048640239$
-----------------------	--------------------------

$C_4 := 0.00000062215701$	$C_{11} := 4.1764768 \cdot 10^{-5}$
---------------------------	-------------------------------------

$C_5 := .0000000020747825$	$C_{12} := -1.4452093 \cdot 10^{-8}$
----------------------------	--------------------------------------

$C_6 := -9.484024 \cdot 10^{-13}$	$C_{13} := 6.5459673$
-----------------------------------	-----------------------

$C_7 := 4.1635019$	
--------------------	--

$$P_{sat}(T) := \begin{cases} \left[ \frac{C_1}{T} + C_2 + C_3 \frac{T}{K} + C_4 \left( \frac{T}{K} \right)^2 + C_5 \left( \frac{T}{K} \right)^3 + C_6 \left( \frac{T}{K} \right)^4 + C_7 \ln \left( \frac{T}{K} \right) \right] \cdot \text{Pa} & \text{if } T < 273.15 \text{ K} \\ \left[ \frac{C_8}{T} + C_9 + C_{10} \frac{T}{K} + C_{11} \left( \frac{T}{K} \right)^2 + C_{12} \left( \frac{T}{K} \right)^3 + C_{13} \ln \left( \frac{T}{K} \right) \right] \cdot \text{Pa} & \end{cases}$$

### Pressure Values

$$P_V := P_{\text{sat}}(T_a) \cdot \phi = 1.65892 \times 10^3 \text{ Pa}$$

$$P_a := P_T - P_V = 9.96661 \times 10^4 \text{ Pa}$$

$$W_a := \frac{P_V \cdot 18.02}{P_a \cdot 28.97} = 0.01035$$

$$P_{\text{sat}}(293.15\text{K}) = 2.3388 \times 10^3 \text{ Pa}$$

$$\text{Re}_{\text{cl}} := 26.2 \frac{(\text{m}^2 \cdot \text{Pa})}{W}$$

Lewis Ratio and  $h_e$

$$T_{\text{in}} := T_a$$

$$P_{\text{vi}} := P_{\text{sat}}(T_{\text{in}}) \cdot \phi = 1.65892 \times 10^3 \text{ Pa}$$

$$w_{\text{in}} := 0.622 \cdot \frac{P_{\text{vi}}}{P_T - P_{\text{vi}}} = 0.01035$$

$$\text{kmol} := 1000\text{mol}$$

$$\rho_{\text{ain}} := \frac{P_a}{8.314 \frac{1000\text{J}}{\text{kmol} \cdot \text{K}} \cdot T_{\text{in}}} \cdot 28.01 \frac{\text{kg}}{\text{kmol}} = 1.06477 \frac{\text{kg}}{\text{m}^3}$$

$$R_b := 8.314 \frac{1000\text{J}}{1000\text{mol}\cdot\text{K}}$$

$$M_v := 18.01 \frac{\text{kg}}{1000\text{mol}}$$

$$M_a := 28.97 \frac{\text{kg}}{1000\text{mol}}$$

$$\rho_v(T) := \frac{P_{\text{sat}}(T) \cdot M_v}{R_b \cdot T}$$

$$\rho_a(T) := \frac{(P_a) \cdot M_a}{R_b \cdot T}$$

$$C_{pa} := 1.007 \frac{1000\text{J}}{\text{kg}\cdot\text{K}}$$

$$C_{pw} := 1.872 \frac{1000\text{J}}{\text{kg}\cdot\text{K}}$$

$$W_1 := w_{\text{in}}$$

$$P(b, a) := 2a + 2 \cdot b$$

$$A_c(b, a) := b \cdot a$$

$$D_h(b, h) := 4 \cdot \frac{(A_c(b, h))}{P(b, h)}$$

$$\text{Air } \mu := 184.6 \cdot 10^{-7} \frac{\text{N}\cdot\text{s}}{\text{m}^2}$$

$$\text{Air } \nu := \frac{\mu}{\rho_a(T_a)} = 1.67625 \times 10^{-5} \frac{\text{m}^2}{\text{s}}$$

$$C_{pm} := \frac{(C_{pa} + W_1 \cdot C_{pw})}{(1 + W_1)} = 1.01586 \times 10^3 \frac{\text{m}^2}{\text{K}\cdot\text{s}^2}$$

$$C_{pm} = 0.24263 \frac{\text{m}^3}{\text{kg}} \cdot \frac{1000\text{cal}}{\text{m}^3 \cdot \text{K}}$$

$$D_{ab}(T) := 0.26 \cdot 10^{-4} \frac{\text{m}^2}{\text{s}} \cdot \left( \frac{T}{298\text{K}} \right)^{\frac{3}{2}}$$

$$\rho_a(T_a) = 1.10127 \frac{\text{kg}}{\text{m}^3}$$

$$\text{rhoam} := \rho_a(T_a)$$

$$\text{Pr} := 0.707$$

$$\text{Sc} := \frac{\nu}{D_{ab}(T_a)} = 0.59224$$

$$LR := \frac{1}{(C_{pm} \cdot \rho_{a,m})} \cdot \left(\frac{Pr}{Sc}\right)^{\frac{2}{3}} \cdot 2454.1 \cdot 1000 \frac{J}{kg} = 17.15301 \cdot \frac{K}{1000Pa}$$

$$\frac{R_b}{M_v} \cdot \frac{[T_a + (35K + 273.15K)]}{2}$$

$$LR = 17.15301 \frac{1}{Pa} \cdot \frac{K}{1000}$$

$$h_e := h_c \cdot LR = 0.29793 \cdot \frac{W}{m^2 \cdot Pa}$$

Drag Force

$$D_b := 18in = 0.4572 \cdot m$$

$$Re_D(n) := \frac{WKVal_{n,1} \cdot \frac{m}{s} \cdot D_b}{\nu}$$

$$C_{Dcyl}(n) := 1.18 + \frac{6.8}{Re_D(n)^{0.89}} + \frac{1.96}{Re_D(n)^{\frac{1}{2}}} - \frac{0.0004 \cdot Re_D(n)}{1 + 3.64 \cdot 10^{-7} \cdot Re_D(n)^2}$$

$$F_{dragcyl}(n) := \frac{1}{2} \cdot \rho_a(T_a) \cdot \left(WKVal_{n,1} \cdot \frac{m}{s}\right)^2 \cdot D_b \cdot height(n) \cdot C_{Dcyl}(n)$$

$$W_{dragcyl}(n) := F_{dragcyl}(n) \cdot \left(WKVal_{n,1} \cdot \frac{m}{s}\right)$$

### Respiration calculations:

$$m_{\text{res}}(n) := M(n) \cdot K_{\text{res}} \cdot A_D(n)$$

$$T_{\text{ex}} := \left( 32.6 + .066 \cdot \frac{T_a - 273.15\text{K}}{K} + 32 \cdot W_a \right) \cdot K + 273.15\text{K} = 308.86651\text{K}$$

$$W_{\text{ex}} := \left( 0.0277 + 0.000065 \cdot \frac{T_a - 273.15\text{K}}{K} + 0.2 \cdot W_a \right) = 0.03251$$

$$m_a(n) := \frac{m_{\text{res}}(n)}{(1 + W_a)}$$

$$m_{\text{vin}}(n) := m_{\text{res}}(n) - m_a(n)$$

$$m_{\text{wres}}(n) := m_{\text{res}}(n) \cdot (W_{\text{ex}} - W_a)$$

#### Sensible Respiratory Heat Transfer (W)

$$Q_{\text{ress}}(n) := [m_a(n) \cdot C_{p_a} \cdot (T_{\text{ex}} - T_a) + m_{\text{vin}}(n) \cdot C_{p_v} \cdot (T_{\text{ex}} - T_a)]$$

#### Latent Respiratory Heat Transfer (W)

$$Q_{\text{resl}}(n) := m_{\text{wres}}(n) \cdot h_{f_{\text{ex}}}$$

#### Total Respiratory Heat Transfer (W)

$$q_{\text{res}}(n) := Q_{\text{ress}}(n) + Q_{\text{resl}}(n)$$

### Body heat transfer calculations:

$$mf_{\text{shiv}}(T_{\text{sk}}, T_{\text{cr}}) := 19.4 \frac{\text{W}}{\text{m}^2 \cdot \text{K}} \left[ (34 + 273.15)\text{K} - T_{\text{sk}} \right] \cdot \left[ (37 + 273.15)\text{K} - T_{\text{cr}} \right]$$

$$M_{\text{shiv}}(T_{\text{sk}}, T_{\text{cr}}) := \begin{cases} mf_{\text{shiv}}(T_{\text{sk}}, T_{\text{cr}}) & \text{if } T_{\text{sk}} < (34 + 273.15)\text{K} \wedge T_{\text{cr}} < (37 + 273.15)\text{K} \\ 0 & \text{otherwise} \end{cases}$$

#### Blood flow rate (L/min)

$$qf_{\text{bl}}(T_{\text{sk}}, T_{\text{cr}}) := \frac{\text{BFN} + c_{\text{dil}} \cdot [T_{\text{cr}} - (37 + 273.15)\text{K}]}{1 + S_{\text{tr}} \cdot [(34 + 273.15)\text{K} - T_{\text{sk}}]} \cdot \frac{\text{L}}{\text{m}^2 \cdot \text{hr}}$$

$$Q_{bl}(T_{sk}, T_{cr}) := \begin{cases} q_{f_{bl}}[(34 + 273.15)K, T_{cr}] & \text{if } T_{sk} \geq (34 + 273.15)K \wedge T_{cr} > (37 + 273.15)K \\ q_{f_{bl}}[(34 + 273.15)K, (37 + 273.15)K] & \text{if } T_{sk} > (34 + 273.15)K \wedge T_{cr} \leq (37 + 273.15)K \\ q_{f_{bl}}[T_{sk}, (37 + 273.15)K] & \text{if } T_{sk} < (34 + 273.15)K \wedge T_{cr} \leq (37 + 273.15)K \\ q_{f_{bl}}(T_{sk}, T_{cr}) & \text{otherwise} \end{cases}$$

### Skin Compartment Factor

$$\alpha_{sk}(T_{sk}, T_{cr}, Q_b) := 0.0418 + \frac{0.745}{\frac{10.8 \cdot Q_b \cdot \frac{m}{s}}{\frac{L}{m^2 \cdot hr}} + 0.585} \quad \begin{aligned} T_{skset} &:= (33.72 + 273.15)K = 306.87 K \\ T_{crset} &:= (36.78 + 273.15)K = 309.93 K \end{aligned}$$

### Required Regulatory Sweat Loss (W/m<sup>2</sup>)

$$T_b(T_{sk}, T_{cr}, Q_b) := (1 - \alpha_{sk}(T_{sk}, T_{cr}, Q_b)) \cdot T_{cr} + \alpha_{sk}(T_{sk}, T_{cr}, Q_b) \cdot T_{sk}$$

$$T_{bset}(T_{sk}, T_{cr}, Q_b) := \left( 1 - \alpha_{sk} \left( T_{skset}, T_{crset}, Q_{bl} \left( T_{skset}, T_{crset}, \frac{s}{m} \right) \right) \right) \cdot T_{cr} \dots \\ + \alpha_{sk} \left( T_{skset}, T_{crset}, Q_{bl} \left( T_{skset}, T_{crset}, \frac{s}{m} \right) \right) \cdot T_{sk}$$

$$B1(T_{sk}) := \begin{cases} 0 & \text{if } T_{sk} < (34 + 273.15)K \\ \lceil T_{sk} - (34 + 273.15)K \rceil & \text{otherwise} \end{cases}$$

$$B2(T_{sk}, T_{cr}, Q_b) := \begin{cases} 0 & \text{if } \left( T_b(T_{sk}, T_{cr}, Q_b) - T_b \left( T_{skset}, T_{crset}, Q_{bl} \left( T_{skset}, T_{crset}, \frac{s}{m} \right) \right) \right) < 0 \\ \left( \left( T_b(T_{sk}, T_{cr}, Q_b) - T_b \left( T_{skset}, T_{crset}, Q_{bl} \left( T_{skset}, T_{crset}, \frac{s}{m} \right) \right) \right) \right) & \text{otherwise} \end{cases}$$

$$ersw(T_{sk}, T_{cr}, Q_b) := c_{sw} \cdot B2(T_{sk}, T_{cr}, Q_b) \cdot e^{\frac{B1(T_{sk})}{10.7K}}$$

$$E_{rsw}(T_{sk}, T_{cr}, Q_b) := \begin{cases} ersw(T_{sk}, T_{cr}, Q_b) & \text{if } ersw(T_{sk}, T_{cr}, Q_b) \leq 670 \frac{W}{m^2} \\ 670 \frac{W}{m^2} & \text{otherwise} \end{cases}$$

## Body calculations:

### Maximum Evaporation (W/m<sup>2</sup>)

$$Re_T(w_c) := (1 - w_c) \cdot \left[ Re_{cl} + \frac{1}{(f_{cl} \cdot h_e)} \right] + \frac{w_c \cdot 1}{(f_{cl} \cdot h_e)}$$

$$E_{max}(T_{sk}) := \frac{(P_{sat}(T_{sk}) - P_{sat}(T_a) \cdot \phi)}{Re_{cl} + \frac{1}{(f_{cl} \cdot h_e)}}$$

### Skin Wettedness Factor

$$w_e(T_{sk}, T_{cr}, Qb) := \left( 0.06 + 0.94 \frac{E_{rsw}(T_{sk}, T_{cr}, Qb)}{E_{max}(T_{sk})} \right)$$

$$w(T_{sk}, T_{cr}, Qb) := \begin{cases} 1 & \text{if } w_e(T_{sk}, T_{cr}, Qb) > 1 \\ 1 & \text{if } w_e(T_{sk}, T_{cr}, Qb) < 0 \\ w_e(T_{sk}, T_{cr}, Qb) & \text{otherwise} \end{cases}$$

### Conduction/Radiation Heat Transfer (W/m<sup>2</sup>)

$$CR(T_{sk}) := \frac{(T_{sk} - T_o)}{R_{cl} + \frac{1}{f_{cl} \cdot h_t}}$$

### Skin Evap Heat Transfer (W/m<sup>2</sup>)

$$E_{sk}(T_{sk}, T_{cr}, Qb, w_c) := \begin{cases} \left[ w(T_{sk}, T_{cr}, Qb) \cdot \frac{(P_{sat}(T_{sk}) - P_{sat}(T_a) \cdot \phi)}{Re_T(0)} \right] & \text{if } (P_{sat}(T_{sk}) - P_{sat}(T_a) \cdot \phi) \geq 0 \\ 0 & \text{otherwise} \end{cases}$$

### Evap from wetted spot

$$E_{spot}(T_{sk}, T_{cr}, Qb, n, w_c) := \begin{cases} \frac{(P_{sat}(T_{sk}) - P_{sat}(T_a) \cdot \phi)}{\frac{1}{(f_{cl} \cdot h_e)}} & \text{if } (P_{sat}(T_{sk}) - P_{sat}(T_a) \cdot \phi) \geq 0 \\ 0W & \text{otherwise} \end{cases}$$



% Cutoff Level      Cutoff := 1

**Spot model values:**

$\psi_w := 0.68$        $\varepsilon_s := 0.35$        $b_f := 1.5 \cdot s$        $\Delta t := 10s$

### Sweat Storage Per Rate

$$m_{st}(T_{sk}, T_{cr}, Qb, n, w_c) := \begin{cases} \frac{[E_{rsw}(T_{sk}, T_{cr}, Qb) - (1 - w_c) \cdot E_{sk}(T_{sk}, T_{cr}, Qb, w_c)] \cdot \eta_w}{hfg_{ex}} \cdot \Delta t \cdot A_D(n) & \text{if } E_{rsw}(T_{sk}, T_{cr}, Qb) > E_{sk}(T_{sk}, T_{cr}, Qb, w_c) \wedge w_c \leq \text{Cutoff} \wedge w(T_{sk}, T_{cr}, Qb) \geq 1 \\ 0 \text{kg} & \text{otherwise} \end{cases}$$

$$m_{sevap}(T_{sk}, T_{cr}, Qb, n, w_c) := \begin{cases} \frac{w_c \cdot E_{spot}(T_{sk}, T_{cr}, Qb, n, w_c)}{hfg_{ex}} \cdot \Delta t \cdot A_D(n) & \text{if } 0 < w_c \leq \text{Cutoff} \\ 0 \text{kg} & \text{otherwise} \end{cases}$$

### Skin Temperature (K)

$$T_{ski}(T_{sk}, T_{cr}, Qb, w_c, n) := \frac{-[(1 - w_c) \cdot CR(T_{sk}) + (1 - w_c) \cdot E_{sk}(T_{sk}, T_{cr}, Qb, w_c) + \varepsilon_s \cdot w_c \cdot E_{spot}(T_{sk}, T_{cr}, Qb, n, w_c)] + \left( K_{eff} + \rho_{bl} \cdot Qb \cdot \frac{m}{s} \cdot C_{pb} \right) (T_{cr} - T_{sk})}{\left( \frac{\alpha_{sk}(T_{sk}, T_{cr}, Qb) \cdot \text{mass}(n) \cdot C_{sk}}{A_D(n) \cdot \Delta t} \right)} + T_{sk}$$

### Core Temperature (K)

$$T_{cri}(T_{sk}, T_{cr}, Qb, n) := \frac{M(n) + M_{shiv}(T_{sk}, T_{cr}) - \frac{Wk(n) + W_{dragcyl}(n) + q_{res}(n)}{A_D(n)} - \left( K_{eff} + \rho_{bl} \cdot Qb \cdot \frac{m}{s} \cdot C_{pb} \right) (T_{cr} - T_{sk})}{\left[ \frac{(1 - \alpha_{sk}(T_{sk}, T_{cr}, Qb)) \cdot \text{mass}(n) \cdot C_{cr}}{A_D(n) \cdot \Delta t} \right]} + T_{cr}$$

## Fraction clothing area 100% wetted

Useful area wetted      Mass to wetted area equation

$$\text{Areawet}(m_{\text{stt}}) := m_{\text{stt}} \cdot \frac{1.0437 \cdot \text{m}^2}{\text{kg}} \quad \text{mass}_{\text{sw}}(m_{\text{stt}}) := \frac{\text{Areawet}(m_{\text{stt}})}{\frac{1.0437 \cdot \text{m}^2}{\text{kg}}}$$

## Initial (Dummy) body Temperatures:

$$m_{\text{sx}}(m_{\text{stt}}, n) := \begin{cases} m_{\text{stt}} & \text{if } \frac{\text{Areawet}(m_{\text{stt}})}{A_{\text{D}}(n)} \leq \text{Cutoff} \\ \left( \text{Cutoff} \cdot A_{\text{D}}(n) \cdot \frac{\text{kg}}{1.75 \text{m}^2} \right) & \text{otherwise} \end{cases}$$

$$w_{\text{ma}}(T_{\text{sk}}, T_{\text{cr}}, Qb, n, m_{\text{stt}}) := \begin{cases} \frac{\text{Areawet}(m_{\text{stt}})}{A_{\text{D}}(n)} & \text{if } m_{\text{stt}} \geq 0 \\ 0 & \text{otherwise} \end{cases}$$

$$w_{\text{mc}}(T_{\text{sk}}, T_{\text{cr}}, Qb, n, m_{\text{stt}}) := \begin{cases} w_{\text{ma}}(T_{\text{sk}}, T_{\text{cr}}, Qb, n, m_{\text{stt}}) & \text{if } w_{\text{ma}}(T_{\text{sk}}, T_{\text{cr}}, Qb, n, m_{\text{stt}}) \leq \text{Cutoff} \\ \text{Cutoff} & \text{otherwise} \end{cases}$$

$$w_{\text{m}}(T_{\text{sk}}, T_{\text{cr}}, Qb, n, m_{\text{stt}}) := \begin{cases} w_{\text{mc}}(T_{\text{sk}}, T_{\text{cr}}, Qb, n, m_{\text{stt}}) & \text{if } w_{\text{mc}}(T_{\text{sk}}, T_{\text{cr}}, Qb, n, m_{\text{stt}}) \leq 0.68 \\ 0.68 & \text{otherwise} \end{cases}$$

## HT from bloodflow Core to Skin (W/m<sup>2</sup>)

$$Q_{\text{bflow}}(T_{\text{sk}}, T_{\text{cr}}, Qb) := \left( K_{\text{eff}} + \rho_{\text{bl}} \cdot Qb \cdot \frac{\text{m}}{\text{s}} \cdot C_{\text{pb}} \right) (T_{\text{cr}} - T_{\text{sk}})$$

### Compile calculations:

SubNum := 1

```

PerSec := | Num ← SubNum
          | n ← Num - 1
          | Tcr ← Tcrn(n)
          | Tsk ← Tskn(n)
          | i ← 0
          | mST ← 0kg
          | for i ∈ 0..  $\frac{\text{Time}_n(n)}{\Delta t}$ 
            | Qb1 ← Qb1(Tsk, Tcr) ·  $\frac{s}{m}$ 
            | wc ← wm(Tsk, Tcr, Qb1, n, mST)
            | Ti ← Tski(Tsk, Tcr, Qb1, wc, n)
            | Tc ← Tcri(Tsk, Tcr, Qb1, n)
            | mST2 ← mST + mst(Ti, Tc, Qb1, n, wc) - msevap(Tsk, Tcr, Qb1, n, wc)
            | DATAi,0 ←  $\frac{T_i}{K} - 273.15$ 
            | DATAi,1 ←  $\frac{T_c}{K} - 273.15$ 
            | DATAi,2 ← Qb1 · (3.6 · 106)
            | DATAi,3 ← Esk(Tsk, Tcr, Qb1, wc) ·  $\frac{A_D(n)}{W}$ 
            | DATAi,4 ← CR(Tsk) ·  $\frac{A_D(n)}{W}$ 
            | DATAi,5 ← Qress(n) ·  $\frac{1}{W}$ 
            | DATAi,6 ← Qresl(n) ·  $\frac{1}{W}$ 
            | DATAi,7 ← Mshiv(Tsk, Tcr) · AD(n) ·  $\frac{1}{W}$ 
            | DATAi,8 ← -Qbflow(Tsk, Tcr, Qb1) ·  $\frac{1 - A_D(n)}{W}$ 
            | DATAi,9 ← w(Tsk, Tcr, Qb1)

```

$$\text{DATA}_{i,10} \leftarrow (Q_{\text{ress}}(n) + Q_{\text{resl}}(n)) \cdot \frac{1}{W}$$

$$\text{DATA}_{i,11} \leftarrow w_e(T_{\text{sk}}, T_{\text{cr}}, Q_{\text{b1}})$$

$$\text{DATA}_{i,12} \leftarrow E_{\text{rsw}}(T_{\text{sk}}, T_{\text{cr}}, Q_{\text{b1}}) \frac{1 \cdot A_{\text{D}}(n)}{W}$$

$$\text{DATA}_{i,13} \leftarrow \frac{\text{Time}_n(n)}{s}$$

$$\text{DATA}_{i,14} \leftarrow \frac{\text{Re}_T(wc)}{\left(\frac{s}{m}\right)}$$

$$\text{DATA}_{i,15} \leftarrow wc$$

$$\text{DATA}_{i,16} \leftarrow \frac{E_{\text{max}}(T_{\text{sk}})}{\frac{w}{m^2}}$$

$$\text{DATA}_{i,17} \leftarrow \frac{m_{\text{sx}}(m_{\text{ST2}}, n)}{\text{kg}}$$

$$\text{DATA}_{i,18} \leftarrow \frac{E_{\text{spot}}(T_i, T_c, Q_{\text{b1}}, n, wc) \cdot A_{\text{D}}(n)}{W}$$

$$\text{DATA}_{i,19} \leftarrow \frac{m_{\text{st}}(T_i, T_c, Q_{\text{b1}}, n, wc)}{\text{kg}}$$

$$\text{DATA}_{i,20} \leftarrow \frac{wc \cdot A_{\text{D}}(n)}{m^2}$$

$$\text{DATA}_{i,21} \leftarrow \alpha_{\text{sk}}(T_i, T_c, Q_{\text{b1}})$$

$$\text{DATA}_{i,22} \leftarrow \frac{m_{\text{sevap}}(T_{\text{sk}}, T_{\text{cr}}, Q_{\text{b1}}, n, wc)}{\text{kg}}$$

$$\text{DATA}_{i,23} \leftarrow \frac{m_{\text{st}}(T_i, T_c, Q_{\text{b1}}, n, wc)}{\text{kg}}$$

DATA

$$m_{\text{ST1}} \leftarrow m_{\text{sx}}(m_{\text{ST2}}, n)$$

$$T_{\text{sk}} \leftarrow T_i$$

$$T_{\text{cr}} \leftarrow T_c$$

$$m_{\text{ST}} \leftarrow m_{\text{ST1}}$$

$$i \leftarrow i + 1$$

DATA

**Desired Values for Heat Loss and Temp Change per  $\Delta T$**

### Output Formulas:

$$T_{skin}(j) := \text{PerSec}_{j,0}$$

$$E_{maxj}(j) := \text{PerSec}_{j,16} \cdot \frac{W}{m}$$

$$T_{core}(j) := \text{PerSec}_{j,1}$$

$$Q_{bj}(j) := \text{PerSec}_{j,2} \cdot W$$

$$m_{STj}(j) := \text{PerSec}_{j,17} \cdot \text{kg}$$

$$E_{skj}(j) := \text{PerSec}_{j,3} \cdot W$$

$$m_{evap_{spotj}}(j) := \text{PerSec}_{j,18} \cdot \text{kg}$$

$$CR_T(j) := \text{PerSec}_{j,4}$$

$$Q_{resT}(j) := (\text{PerSec}_{j,5} + \text{PerSec}_{j,6}) \cdot W$$

$$E_{spotj}(j) := \text{PerSec}_{j,18} \cdot W$$

$$M_{shivr}(j) := \text{PerSec}_{j,7} \cdot W$$

$$m_{stj}(j) := \text{PerSec}_{j,19} \cdot \text{kg}$$

$$w_j(j) := \text{PerSec}_{j,9}$$

$$\text{Spotsize}(j) := \text{PerSec}_{j,20} \cdot \text{m}^2$$

$$SktoCr(j) := \text{PerSec}_{j,8} \cdot W$$

$$w_{ea}(j) := \text{PerSec}_{j,11}$$

$$\alpha(j) := \text{PerSec}_{j,21}$$

$$E_{rswADj}(j) := \text{PerSec}_{j,12} \cdot W$$

$$\text{Time}_{nj}(j) := \text{PerSec}_{j,13} \cdot \text{s}$$

$$m_{sevapj}(j) := \text{PerSec}_{j,22} \cdot \text{kg}$$

$$Re_{Tj}(j) := \text{PerSec}_{j,14} \cdot \text{s}$$

$$m_{stij}(j) := \text{PerSec}_{j,23} \cdot \text{kg}$$

$$w_{cj}(j) := \text{PerSec}_{j,15}$$

Average Gagge wettedness (ie percent time fully wetted)

$$w_{1logic}(j) := \begin{cases} 1 & \text{if } w_j(j) = 1 \\ 0 & \text{otherwise} \end{cases}$$

$$\text{ReclAVG} := \frac{\frac{\text{Time}_{nj}(1)}{\Delta t} \sum_{j=0} [\text{Re}_{Tj}(j) - (\text{Re}_{Tj}(1) - 26.2\text{s})]}{\frac{\text{Time}_{nj}(1)}{\Delta t} + 1}} = 24.99268 \text{ s}$$

$$\text{St} := \sum_{j=0}^{\text{Time}_{nj}(1)} \left[ \left[ \left( \frac{M(23) \cdot A_D(23)}{K} - \frac{E_{skj}(j)}{K} \right) - \frac{Q_{resT}(j)}{K} - \frac{CR_T(j)}{K} - \frac{Wk(23)}{K} \right] \cdot \Delta t \cdot K \right] = 7.64628 \times 10^5 \cdot \text{J}$$

# Core Diff

$$\text{CoreError} := \text{Tcore}\left(\frac{\text{Time}_{nj}(1)}{\Delta t}\right) - \text{Tcore}(0) - X_{\text{SubNum}-1,10} = -0.18204 \quad \text{Re}_{cl} = 26.2 \frac{\text{s}}{\text{m}}$$

$$\text{Re}_{cl}\text{Corr}(j) := \begin{cases} \text{Re}_{cl} & \text{if Spotsize}(j) = 0 \\ \left[ \frac{P_{\text{sat}}(\text{Tskin}(j) \text{K} + 273.15\text{K}) - P_{\text{sat}}(\text{T}_a) \cdot \phi}{(1 - \text{wcj}(j)) \cdot \frac{E_{\text{skj}}(j)}{A_{\text{D}}(\text{SubNum} - 1)} + \frac{\text{wcj}(j) \cdot E_{\text{spotj}}(j)}{A_{\text{D}}(\text{SubNum} - 1)}} - \frac{1}{(f_{cl} \cdot h_e)} \right] & \text{otherwise} \end{cases}$$

$$\text{ReclAVGCorr} := \frac{\frac{\text{Time}_{nj}(1)}{\Delta t} \sum_{j=0} (\text{Re}_{cl}\text{Corr}(j))}{\frac{\text{Time}_{nj}(1)}{\Delta t} + 1} = 18.03978 \frac{1}{\text{W}} \cdot \text{m}^2 \cdot \text{Pa}$$

$$\text{w1timepercent} := \frac{\frac{\text{Time}_{nj}(1)}{\Delta t} \sum_{j=0} \text{w1logic}(j)}{\frac{\text{Time}_{nj}(1)}{\Delta t} + 1} = 0.91517$$

$$\text{SW}_T := \sum_{j=0}^{\frac{\text{Time}_{nj}(1)}{\Delta t}} \frac{E_{\text{rswADj}}(j) \cdot \Delta t + \text{PerSec}_{j,6} \cdot \text{W} \cdot \Delta t}{\text{hfg}_{\text{ex}}} = 1.72405 \text{ kg}$$

$$SW_{\text{Evap}} := \sum_{j=0}^{\text{Time}_{nj}(1)} \frac{\Delta t}{\text{hfg}_{\text{ex}}} \left[ E_{\text{skj}}(j) \cdot (1 - w_{\text{cj}}(j)) + w_{\text{cj}}(j) \cdot E_{\text{spotj}}(j) \right] \cdot \Delta t = 1.19655 \cdot \text{kg}$$

$$\Delta w := \sum_{j=0}^{\text{Time}_{nj}(1)} (w_{\text{ea}}(j) - w_{\text{j}}(j)) = 589.25988$$

$$\text{Sweatdif} := SW_{\text{T}} - \text{ASW}(\text{SubNum} - 1)$$

$$ZZ := \left( \frac{\text{ReclAVG}}{s} \quad \text{CoreError} \quad w_{1\text{timepercent}} \quad Sw_{\text{mod}} \quad \frac{\text{Sweatdif}}{\text{kg}} \quad \frac{SW_{\text{Evap}}}{\text{kg}} \right)$$

$$YY := \left( \frac{\text{ReclAVG}}{s} \quad \text{CoreError} \quad w_{1\text{timepercent}} \quad \frac{SW_{\text{T}}}{\text{kg}} \quad \frac{SW_{\text{Evap}}}{\text{kg}} \right)$$

$$\text{CoreError} = -0.18204$$

$$\text{Sweatdif} = 0.16745 \text{ kg}$$

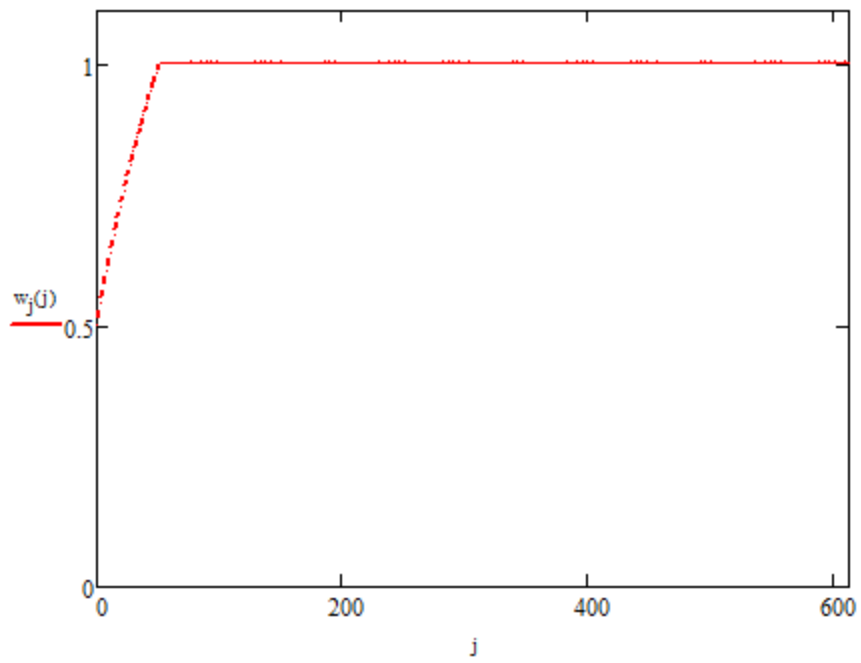
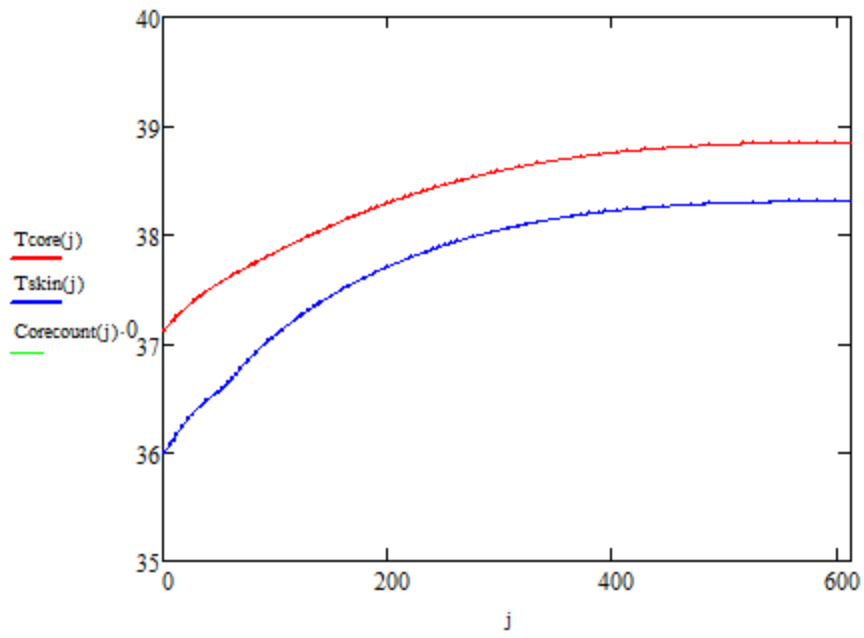
$$ZZ =$$

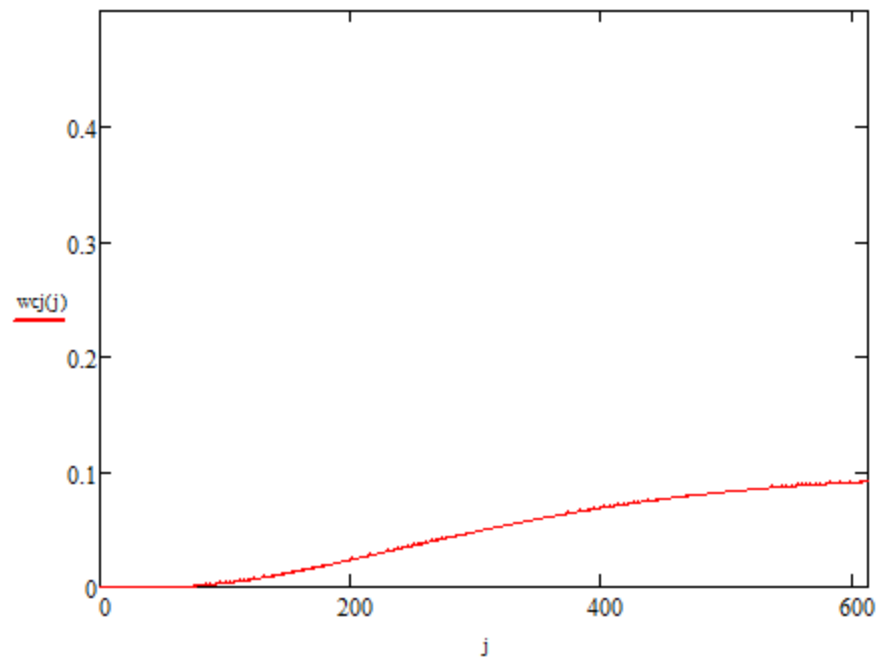
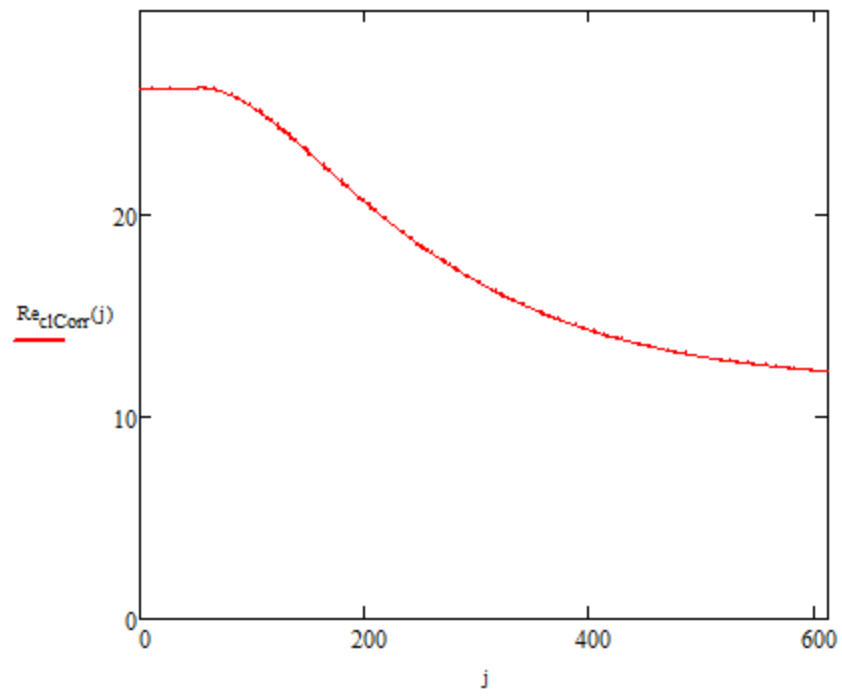
	0	1	2	3	4	5
0	24.99268	-0.18204	0.91517	1.17	0.16745	1.19655

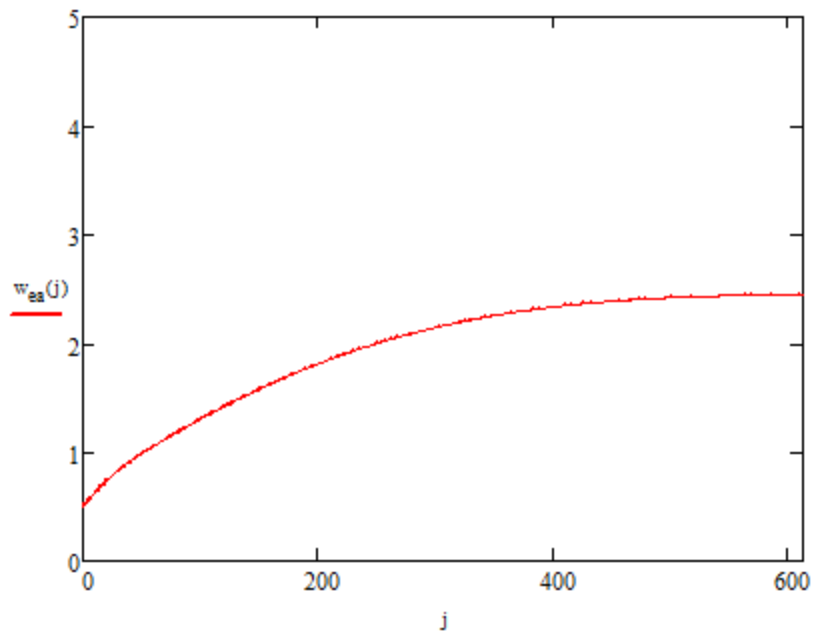
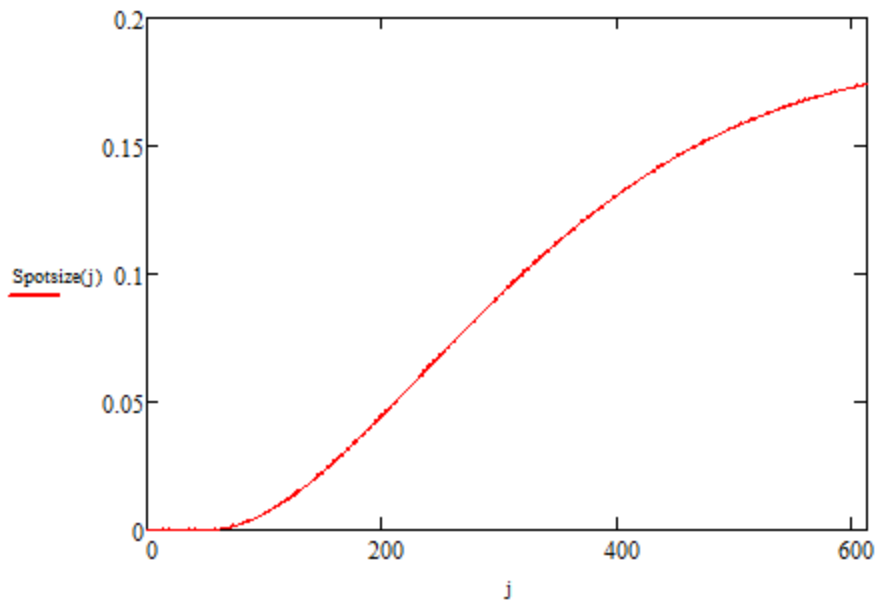
$$YY =$$

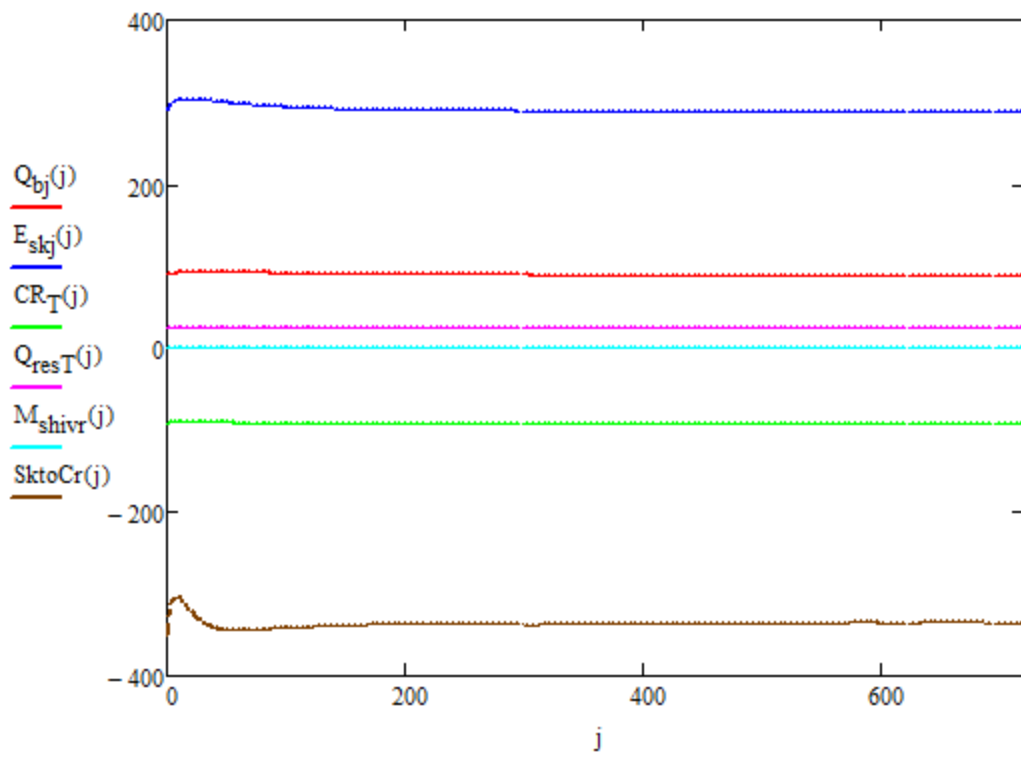
	0	1	2	3	4
0	24.99268	-0.18204	0.91517	1.72405	1.19655











0-Tsk(C) 1-Tc(C) 2-Qbl(L/min) 3-Esk(W) 4-CR(W) 5-Qress(W) 6-Qresk(W) 7-Mshiv(W) 8-SktoSCr(W) 9-w(N/A) 10-QresT(W)

	0	1	2	3	4	5	6	7	8	9
0	35.98825	37.10604	20.3	142.45301	-88.9037	-3.8293	31.6828	0	-64.41912	0.50152
1	35.9989	37.11853	22.20645	146.35142	-88.80764	-3.8293	31.6828	0	-69.61366	0.51488
2	36.01057	37.13081	24.08	150.20953	-88.70028	-3.8293	31.6828	0	-74.66065	0.52802
3	36.02314	37.14288	25.92169	154.03101	-88.58268	-3.8293	31.6828	0	-79.55254	0.54097
4	36.03649	37.15476	27.73257	157.81809	-88.45598	-3.8293	31.6828	0	-84.28513	0.55374
5	36.0505	37.16644	29.51369	161.57201	-88.3214	-3.8293	31.6828	0	-88.85732	0.56634
6	36.06505	37.17794	31.2661	165.29332	-88.18018	-3.8293	31.6828	0	-93.2707	0.57877
7	36.08001	37.18926	32.99085	168.98207	-88.03354	-3.8293	31.6828	0	-97.52918	0.59103
8	36.09529	37.20041	34.68892	172.63796	-87.88267	-3.8293	31.6828	0	-101.63853	0.60313
9	36.11077	37.21139	36.36127	176.26047	-87.72868	-3.8293	31.6828	0	-105.60602	0.61507
10	36.12636	37.22222	38.00881	179.84893	-87.57263	-3.8293	31.6828	0	-109.43998	...

PerSec =

ASHRAE Two-node Model Implementation PCS Simulation , ASHRAE Two-node Model Implementation Baseline with found in this section.

## Mean Radiant Temperature Calculation

$$T1 := (47.8 + 273.15) \cdot K = 320.95 K$$

$$Ta := (42.5 + 273.15) \cdot K \quad Ta = 315.65 K$$

$$Tdew := (14.2 + 273.15) \cdot K$$

Air Properties

$$\rho := 1.128 \cdot \frac{kg}{m^3}$$

$$\mu := 189 \cdot 10^{-7} \cdot \frac{N \cdot s}{m^2}$$

$$k := 27.04 \cdot 10^{-3} \cdot \frac{W}{m \cdot K} \quad Pr := 0.705$$

$$Tbb := \frac{(T1)}{1}$$

$$Tbb = 320.95 K \quad Trad := (55.273 + 273.15) \cdot K \quad Tbb = 47.8 \cdot ^\circ C$$

$$\mu_s := 194.98 \cdot 10^{-7} \cdot \frac{N \cdot s}{m^2} \quad Tbbb := Tbb - 273.15 K$$

$$Tbbb = 47.8 K$$

Heat Transfer Coefficient Convection

$$V := 2.0 \cdot \frac{m}{s} \quad D := 6 \text{ in}$$

$$D = 152.4 \text{ mm}$$

$$\frac{4 \cdot \pi}{3} \cdot \left(\frac{D}{2}\right)^3 = 1.853 \cdot L$$

$$Re := \frac{\rho \cdot V \cdot D}{\mu}$$

$$Re = 1.819 \times 10^4$$

$$hcov := \left[ 2 + \left( 0.4 \cdot Re^{.5} + 0.06 \cdot Re^{.5} \right) \cdot Pr^{.4} \cdot \left( \frac{\mu}{\mu_s} \right)^{.25} \right] \cdot \frac{k}{D}$$

$$hcov = 9.852 \cdot \frac{W}{m^2 \cdot K}$$

## Radiation Heat Transfer Coefficient

$$\varepsilon := 0.9$$

$$\sigma := 5.67 \cdot 10^{-8} \cdot \frac{\text{W}}{\text{m}^2 \cdot \text{K}^4}$$

Loop from Incropera pg 19  
eqn 1.9 from previous study

$$\text{hrad} := \varepsilon \cdot \sigma \cdot (\text{Trad} + \text{Tbb}) (\text{Trad}^2 + \text{Tbb}^2)$$

$$\text{hrad} = 6.988 \cdot \frac{\text{W}}{\text{m}^2 \cdot \text{K}}$$

## Mean Radiant Temperature

$$\text{Trad} := \text{Tbb} + \frac{\text{hcov}}{\text{hrad}} \cdot (\text{Tbb} - \text{Ta})$$

$$\text{Trad} = 328.423 \text{ K}$$

$$\text{Tc} := \text{Trad} - 273.15 \text{ K}$$

$$\text{Tc} = 55.273 \text{ K}$$

from ASHRAE 2007 HVAC  
APPLICATIONS A.53.2 eqn 11

$$f_{\text{eff}} := 1$$

$$\text{hrad1} := 4 \cdot \sigma \cdot f_{\text{eff}} \cdot \left[ \frac{(\text{Tbb} + \text{Ta})}{2} \right]^3$$

$$\text{hrad1} = 7.314 \frac{\text{kg}}{\text{K} \cdot \text{s}^3}$$

eqn 18 ASHRAE 2007 HVAC APPLICATIONS A.53.7

## ASHRAE Two-node Model Implementation Baseline with the Presented Wetted Clothing Model

**Conditions/Constants:**

**User Defined Conditions:**

SUBJECT	WEEK	DAY	AMPM	PCS	TIME	HEARTRAT	TSKIN	TORSOTEN	CORETEN	CORECHG	AIRTEMP	RH	SWRATE	VO2	METRATE	CORERATE	TSKININT	HEIGHT	Weight
0	1	2	3	4	5	6	7	8	9	10	11	12	13	14	15	16	17	18	19

	0	1	2	3	4	5	6	7	8	9	10	11	12	13	14	15	
X =	0	1	1	6	1	12	120	130	37	35.2	37.9	0.9	42.2	19.7	715	14	406.6
	1	2	1	5	1	12	120	79	36.6	35.1	37.7	0.7	41.9	19.4	702	12	334.5
	2	3	1	4	2	12	120	112	36.2	34.7	37.2	0.1	42.2	20.1	968	12	391
	3	4	1	6	2	12	120	97	35.9	35.6	37	-0.5	41.2	20.6	1.104·10 <sup>3</sup>	12	380.2
	4	5	2	5	1	12	120	155	36.1	34.6	38.3	0.8	41.5	19.7	726	15	354
	5	6	2	4	1	12	84	174	36.5	32.8	39.1	1.8	41.3	19.2	1.416·10 <sup>3</sup>	1	375
	6	7	2	6	2	12	120	106	37.6	35.9	37.3	0.6	41.6	19.8	882	11	396.2
	7	8	2	5	2	12	120	117	33.8	27	37.5	0.2	41.5	19.7	916	8	409
	8	9	3	6	1	12	120	109	35.6	33.3	37.9	0.5	41.7	20.1	818	11	403.3
	9	10	3	5	1	12	120	125	33.8	27.9	37.4	0.1	41.9	19.6	931	11	373.5
	10	11	3	4	2	12	120	127	37.3	36.8	37.5	0.6	41.5	20.7	627	15	415
	11	12	3	6	2	12	120	115	37.1	37	38.7	0.2	41.9	19.4	895	14	373.6
	12	13	1	6	1	20	71	107	34.2	29.2	37.5	0.697	42.1	19.4	960	12.9	394
	13	14	1	5	1	20	120	112	37.4	36.5	37.4	0.153	41.9	19.4	716	9.3	348.75
	14	15	1	4	2	20	120	140	33	25.3	38.1	0.493	42.1	19.6	809	12.3	376
	15	16	1	6	2	20	120	112	35.7	32.4	37.3	0.047	41.9	19.2	769	10.4	386.4
	16	17	2	6	1	20	120	116	32.6	25	37	-0.153	42.7	20	1.119·10 <sup>3</sup>	12.2	391
	17	18	2	5	1	20	120	139	36.3	33.8	38	1.137	42.1	20.7	863	13.3	369.4
	18	19	2	4	2	20	120	156	37.5	37	38.3	0.99	42	20.5	1.022·10 <sup>3</sup>	10.9	411
	19	20	2	6	2	20	120	121	33.2	27.7	37.6	0.12	41.5	21.1	1.384·10 <sup>3</sup>	11.4	364.4
	20	21	3	6	1	20	120	108	33	27.7	37.5	0.433	42.1	19.6	1.127·10 <sup>3</sup>	13.2	407.25
	21	22	3	5	1	20	120	124	33	25.1	37.5	0.343	41.9	19.8	977	14.1	409.75
	22	23	3	4	2	20	120	105	30.3	19.1	37.6	-0.126	42.3	20	1.136·10 <sup>3</sup>	10.4	...



**Conditions/Constants:**

User Defined Conditions:

trousers, long-sleeved shirt

Environmental:

Clothing:

$$T_a := (42.2 + 273.15)K = 315.35 K$$

$$clo := 0.155 \frac{m^2 K}{W}$$

Wind velocity (m/s):

$$T_r := (54.4 + 273.15)K = 327.55 K$$

$$I_{cl} := 1.00clo$$

$$v_{wind} := 2.0$$

Walking in the wind  
convection pg 82, danielson

$$h_c := 11.7 \cdot v_{wind}^{0.57} \frac{W}{m^2 \cdot K} = 17.36893 \frac{kg}{K \cdot s^3}$$

$$h_r := 4.7 \frac{W}{m^2 \cdot K}$$

$$Ensemblemass := 15.054kg$$

$$R_{cl} := I_{cl}$$

$$R_{cl} = 0.155 \frac{K \cdot s^3}{kg}$$

$$Grade := 0.01$$

$$\phi := .20$$

$$load := 10kg$$

$$f_{cl} := 1.33$$

$$T_o := \frac{h_r \cdot T_r + h_c \cdot T_a}{h_r + h_c} = 317.94822 K$$

$$h_t := h_r + h_c$$

**Iterative Variables Individually dependent:**

$$mass(n) := X_{n,19} \cdot kg$$

$$height(n) := X_{n,18} \cdot m$$

$$A_D(n) := \left[ 0.202 \cdot \left( \frac{mass(n)}{kg} \right)^{0.425} \cdot \left( \frac{height(n)}{m} \right)^{0.725} \right] \cdot m^2$$

$$M(n) := \frac{X_{n,15} \cdot W}{A_D(n)}$$

$$T_{skn}(n) := (X_{n,17} + 273.15) \cdot K$$

$$T_{crn}(n) := (X_{n,9} - X_{n,10} + 273.15) K$$

$$Wk(n) := Grade \cdot WKVal_{n,0} \cdot kg \cdot WKVal_{n,1} \cdot \frac{m}{s} \cdot 9.81 \frac{m}{s^2}$$

$$Time_n(n) := X_{n,5} \cdot 60s$$

$$ASW(n) := X_{(n,13)} \cdot \frac{kg}{1000} \cdot Time_n(n)$$

Clothed weight (kg)	Treadmill speed (m/s)	time (s)	Vert Distance (m)
---------------------	-----------------------	----------	-------------------

WKVal :=

86.1371208	0.983488	6120	60.1894656
84.5041896	1.028192	7200	74.029824
101.2417344	0.804672	7200	57.936384
93.0770784	0.938784	7200	67.592448
69.3088576	1.34112	4680	62.764416
71.7582544	1.207008	4920	59.3847936
109.769264	0.759968	7200	54.717696
110.6310888	0.715264	7200	51.499008
109.542468	0.715264	5700	40.770048
105.5962176	0.804672	7200	57.936384
85.6835288	1.028192	6000	61.69152
79.6961144	1.162304	7200	83.685888
92.3513312	0.983488	7200	70.811136
110.7671664	0.715264	7200	51.499008
88.7679544	1.028192	4200	43.184064
106.4580424	0.759968	7200	54.717696
92.2606128	0.983488	7200	70.811136
78.3806976	1.207008	6120	73.8688896
109.6785456	0.759968	7200	54.717696
94.0749808	0.938784	7200	67.592448
89.357624	1.028192	7200	74.029824
81.3290456	1.162304	7200	83.685888
114.1237472	0.715264	7200	51.499008
99.3820072	0.849376	7200	61.155072

+

Body Equation Constants:

$$Sw_{\text{mod}} := 1.17$$

$$c_{\text{sw}} := Sw_{\text{mod}} \cdot 116 \frac{\text{W}}{\text{m}^2 \cdot \text{K}} \quad \text{BFN} := 6.3 \quad C_{\text{pb}} := 4190 \frac{\text{J}}{\text{kg} \cdot \text{K}}$$

$$K_{\text{eff}} := 5.28 \frac{\text{W}}{\text{m}^2 \cdot \text{K}} \quad c_{\text{dil}} := \frac{150}{\text{K}} \quad C_{\text{cr}} := 3500 \frac{\text{J}}{\text{kg} \cdot \text{K}}$$

$$\rho_{\text{bl}} := 1.06 \frac{\text{kg}}{\text{L}} \quad S_{\text{tr}} := \frac{0.5}{\text{K}} \quad C_{\text{sk}} := 3500 \frac{\text{J}}{\text{kg} \cdot \text{K}}$$

**Constants and Calculated Constants:**

$$P_T := 101325 \text{ Pa}$$

$$C_{p_v} := 1864 \frac{\text{J}}{\text{kg} \cdot \text{K}}$$

$$C_{p_a} := 1005 \frac{\text{J}}{\text{kg} \cdot \text{K}}$$

$$h_{f_{g_{ex}}} := 2454.1 \frac{1000 \text{ J}}{\text{kg}}$$

$$C_{p_b} := 3500 \frac{\text{J}}{\text{kg} \cdot \text{K}}$$

$$LR_{STD} := 16.5 \frac{\text{K}}{1000 \text{ Pa}}$$

$$K_{res} := 1.43 \cdot 10^{-6} \frac{\text{kg}}{\text{J}}$$

**Sat. Pressure Equation: P<sub>sat</sub>(T)**

Pressure Curve Fit  
Constants:

ICE

LIQUID

$$C_1 := -5.6745359 \cdot 10^3$$

$$C_8 := -5800.2206$$

$$C_2 := 6.3925247$$

$$C_9 := 1.3914993$$

$$C_3 := -0.009677843$$

$$C_{10} := -0.048640239$$

$$C_4 := 0.00000062215701$$

$$C_{11} := 4.1764768 \cdot 10^{-5}$$

$$C_5 := .0000000020747825$$

$$C_{12} := -1.4452093 \cdot 10^{-8}$$

$$C_6 := -9.484024 \cdot 10^{-13}$$

$$C_{13} := 6.5459673$$

$$C_7 := 4.1635019$$

$$P_{sat}(T) := \begin{cases} e^{\left[ \frac{C_1}{T} + C_2 + C_3 \frac{T}{K} + C_4 \left( \frac{T}{K} \right)^2 + C_5 \left( \frac{T}{K} \right)^3 + C_6 \left( \frac{T}{K} \right)^4 + C_7 \ln \left( \frac{T}{K} \right) \right]} \cdot \text{Pa} & \text{if } T < 273.15 \text{ K} \\ e^{\left[ \frac{C_8}{T} + C_9 + C_{10} \frac{T}{K} + C_{11} \left( \frac{T}{K} \right)^2 + C_{12} \left( \frac{T}{K} \right)^3 + C_{13} \ln \left( \frac{T}{K} \right) \right]} \cdot \text{Pa} & \end{cases}$$

### Pressure Values

$$P_V := P_{\text{sat}}(T_a) \cdot \phi = 1.65892 \times 10^3 \text{ Pa}$$

$$P_a := P_T - P_V = 9.96661 \times 10^4 \text{ Pa}$$

$$W_a := \frac{P_V \cdot 18.02}{P_a \cdot 28.97} = 0.01035$$

$$P_{\text{sat}}(293.15\text{K}) = 2.3388 \times 10^3 \text{ Pa}$$

$$\text{Re}_{\text{cl}} := 26.2 \frac{(\text{m}^2 \cdot \text{Pa})}{W}$$

Lewis Ratio and  $h_e$

$$T_{\text{in}} := T_a$$

$$P_{\text{vi}} := P_{\text{sat}}(T_{\text{in}}) \cdot \phi = 1.65892 \times 10^3 \text{ Pa}$$

$$w_{\text{in}} := 0.622 \cdot \frac{P_{\text{vi}}}{P_T - P_{\text{vi}}} = 0.01035$$

$$\text{kmol} := 1000\text{mol}$$

$$\rho_{\text{ain}} := \frac{P_a}{8.314 \frac{1000\text{J}}{\text{kmol} \cdot \text{K}} \cdot T_{\text{in}}} \cdot 28.01 \frac{\text{kg}}{\text{kmol}} = 1.06477 \frac{\text{kg}}{\text{m}^3}$$

$$R_b := 8.314 \frac{1000\text{J}}{1000\text{mol}\cdot\text{K}}$$

$$M_v := 18.01 \frac{\text{kg}}{1000\text{mol}}$$

$$M_a := 28.97 \frac{\text{kg}}{1000\text{mol}}$$

$$\rho_v(T) := \frac{P_{\text{sat}}(T) \cdot M_v}{R_b \cdot T}$$

$$\rho_a(T) := \frac{(P_a) \cdot M_a}{R_b \cdot T}$$

$$C_{pa} := 1.007 \frac{1000\text{J}}{\text{kg}\cdot\text{K}}$$

$$C_{pw} := 1.872 \frac{1000\text{J}}{\text{kg}\cdot\text{K}}$$

$$W_1 := w_{\text{in}}$$

$$P(b, a) := 2a + 2 \cdot b$$

$$A_c(b, a) := b \cdot a$$

$$D_h(b, h) := 4 \cdot \frac{(A_c(b, h))}{P(b, h)}$$

$$\text{Air } \mu := 184.6 \cdot 10^{-7} \frac{\text{N}\cdot\text{s}}{\text{m}^2}$$

$$\text{Air } \nu := \frac{\mu}{\rho_a(T_a)} = 1.67625 \times 10^{-5} \frac{\text{m}^2}{\text{s}}$$

$$C_{pm} := \frac{(C_{pa} + W_1 \cdot C_{pw})}{(1 + W_1)} = 1.01586 \times 10^3 \frac{\text{m}^2}{\text{K}\cdot\text{s}^2}$$

$$C_{pm} = 0.24263 \frac{\text{m}^3}{\text{kg}} \cdot \frac{1000\text{cal}}{\text{m}^3 \cdot \text{K}}$$

$$D_{ab}(T) := 0.26 \cdot 10^{-4} \frac{\text{m}^2}{\text{s}} \cdot \left( \frac{T}{298\text{K}} \right)^{\frac{3}{2}}$$

$$\rho_a(T_a) = 1.10127 \frac{\text{kg}}{\text{m}^3}$$

$$\text{rhoam} := \rho_a(T_a)$$

$$\text{Pr} := 0.707$$

$$\text{Sc} := \frac{\nu}{D_{ab}(T_a)} = 0.59224$$

$$LR := \frac{1}{(C_{pm} \cdot \rho_{a,m})} \cdot \left(\frac{Pr}{Sc}\right)^{\frac{2}{3}} \cdot 2454.1 \cdot 1000 \frac{J}{kg} = 17.15301 \cdot \frac{K}{1000Pa}$$

$$\frac{R_b}{M_v} \cdot \frac{[T_a + (35K + 273.15K)]}{2}$$

$$LR = 17.15301 \frac{1}{Pa} \cdot \frac{K}{1000}$$

$$h_e := h_c \cdot LR = 0.29793 \cdot \frac{W}{m^2 \cdot Pa}$$

Drag Force

$$D_b := 18in = 0.4572 \cdot m$$

$$Re_D(n) := \frac{WKVal_{n,1} \cdot \frac{m}{s} \cdot D_b}{\nu}$$

$$C_{Dcyl}(n) := 1.18 + \frac{6.8}{Re_D(n)^{0.89}} + \frac{1.96}{D_b \cdot (n)^{\frac{1}{2}}} - \frac{0.0004 \cdot Re_D(n)}{1 + 3.64 \cdot 10^{-7} \cdot Re_D(n)^2}$$

$$F_{dragcyl}(n) := \frac{1}{2} \cdot \rho_a(T_a) \cdot \left(WKVal_{n,1} \cdot \frac{m}{s}\right)^2 \cdot D_b \cdot height(n) \cdot C_{Dcyl}(n)$$

$$W_{dragcyl}(n) := F_{dragcyl}(n) \cdot \left(WKVal_{n,1} \cdot \frac{m}{s}\right)$$

### Respiration calculations:

$$m_{\text{res}}(n) := M(n) \cdot K_{\text{res}} \cdot A_D(n)$$

$$T_{\text{ex}} := \left( 32.6 + .066 \cdot \frac{T_a - 273.15\text{K}}{K} + 32 \cdot W_a \right) \cdot K + 273.15\text{K} = 308.86651\text{K}$$

$$W_{\text{ex}} := \left( 0.0277 + 0.000065 \cdot \frac{T_a - 273.15\text{K}}{K} + 0.2 \cdot W_a \right) = 0.03251$$

$$m_a(n) := \frac{m_{\text{res}}(n)}{(1 + W_a)}$$

$$m_{\text{vin}}(n) := m_{\text{res}}(n) - m_a(n)$$

$$m_{\text{wres}}(n) := m_{\text{res}}(n) \cdot (W_{\text{ex}} - W_a)$$

#### Sensible Respiratory Heat Transfer (W)

$$Q_{\text{ress}}(n) := [m_a(n) \cdot C_{p_a} \cdot (T_{\text{ex}} - T_a) + m_{\text{vin}}(n) \cdot C_{p_v} \cdot (T_{\text{ex}} - T_a)]$$

#### Latent Respiratory Heat Transfer (W)

$$Q_{\text{resl}}(n) := m_{\text{wres}}(n) \cdot h_{f_{\text{ex}}}$$

#### Total Respiratory Heat Transfer (W)

$$q_{\text{res}}(n) := Q_{\text{ress}}(n) + Q_{\text{resl}}(n)$$

### Body heat transfer calculations:

$$mf_{\text{shiv}}(T_{\text{sk}}, T_{\text{cr}}) := 19.4 \frac{\text{W}}{\text{m}^2 \cdot \text{K}^2} [(34 + 273.15)\text{K} - T_{\text{sk}}] [(37 + 273.15)\text{K} - T_{\text{cr}}]$$

$$M_{\text{shiv}}(T_{\text{sk}}, T_{\text{cr}}) := \begin{cases} mf_{\text{shiv}}(T_{\text{sk}}, T_{\text{cr}}) & \text{if } T_{\text{sk}} < (34 + 273.15)\text{K} \wedge T_{\text{cr}} < (37 + 273.15)\text{K} \\ 0 & \text{otherwise} \end{cases}$$

#### Blood flow rate (L/min)

$$qf_{\text{bl}}(T_{\text{sk}}, T_{\text{cr}}) := \frac{\text{BFN} + c_{\text{dil}} [T_{\text{cr}} - (37 + 273.15)\text{K}]}{1 + S_{\text{tr}} [(34 + 273.15)\text{K} - T_{\text{sk}}]} \cdot \frac{\text{L}}{\text{m}^2 \cdot \text{hr}}$$

$$Q_{bl}(T_{sk}, T_{cr}) := \begin{cases} q_{f_{bl}}[(34 + 273.15)K, T_{cr}] & \text{if } T_{sk} \geq (34 + 273.15)K \wedge T_{cr} > (37 + 273.15)K \\ q_{f_{bl}}[(34 + 273.15)K, (37 + 273.15)K] & \text{if } T_{sk} > (34 + 273.15)K \wedge T_{cr} \leq (37 + 273.15)K \\ q_{f_{bl}}[T_{sk}, (37 + 273.15)K] & \text{if } T_{sk} < (34 + 273.15)K \wedge T_{cr} \leq (37 + 273.15)K \\ q_{f_{bl}}(T_{sk}, T_{cr}) & \text{otherwise} \end{cases}$$

### Skin Compartment Factor

$$\alpha_{sk}(T_{sk}, T_{cr}, Q_b) := 0.0418 + \frac{0.745}{\frac{10.8 \cdot Q_b \cdot \frac{m}{s}}{\frac{L}{m^2 \cdot hr}} + 0.585} \quad \begin{aligned} T_{skset} &:= (33.72 + 273.15)K = 306.87 K \\ T_{crset} &:= (36.78 + 273.15)K = 309.93 K \end{aligned}$$

### Required Regulatory Sweat Loss (W/m<sup>2</sup>)

$$T_b(T_{sk}, T_{cr}, Q_b) := (1 - \alpha_{sk}(T_{sk}, T_{cr}, Q_b)) \cdot T_{cr} + \alpha_{sk}(T_{sk}, T_{cr}, Q_b) \cdot T_{sk}$$

$$T_{bset}(T_{sk}, T_{cr}, Q_b) := \left( 1 - \alpha_{sk} \left( T_{skset}, T_{crset}, Q_{bl} \left( T_{skset}, T_{crset}, \frac{s}{m} \right) \right) \right) \cdot T_{cr} \dots \\ + \alpha_{sk} \left( T_{skset}, T_{crset}, Q_{bl} \left( T_{skset}, T_{crset}, \frac{s}{m} \right) \right) \cdot T_{sk}$$

$$B1(T_{sk}) := \begin{cases} 0 & \text{if } T_{sk} < (34 + 273.15)K \\ \lceil T_{sk} - (34 + 273.15)K \rceil & \text{otherwise} \end{cases}$$

$$B2(T_{sk}, T_{cr}, Q_b) := \begin{cases} 0 & \text{if } \left( T_b(T_{sk}, T_{cr}, Q_b) - T_b \left( T_{skset}, T_{crset}, Q_{bl} \left( T_{skset}, T_{crset}, \frac{s}{m} \right) \right) \right) < 0 \\ \left( T_b(T_{sk}, T_{cr}, Q_b) - T_b \left( T_{skset}, T_{crset}, Q_{bl} \left( T_{skset}, T_{crset}, \frac{s}{m} \right) \right) \right) & \text{otherwise} \end{cases}$$

$$ersw(T_{sk}, T_{cr}, Q_b) := c_{sw} \cdot B2(T_{sk}, T_{cr}, Q_b) \cdot e^{\frac{B1(T_{sk})}{10.7K}}$$

$$E_{rsw}(T_{sk}, T_{cr}, Q_b) := \begin{cases} ersw(T_{sk}, T_{cr}, Q_b) & \text{if } ersw(T_{sk}, T_{cr}, Q_b) \leq 670 \frac{W}{m^2} \\ 670 \frac{W}{m^2} & \text{otherwise} \end{cases}$$



## Body calculations:

### Maximum Evaporation (W/m<sup>2</sup>)

$$Re_T(w_c) := (1 - w_c) \cdot \left[ Re_{cl} + \frac{1}{(f_{cl} \cdot h_e)} \right] + \frac{w_c \cdot 1}{(f_{cl} \cdot h_e)}$$

$$E_{max}(T_{sk}) := \frac{(P_{sat}(T_{sk}) - P_{sat}(T_a) \cdot \phi)}{Re_{cl} + \frac{1}{(f_{cl} \cdot h_e)}}$$

### Skin Wettedness Factor

$$w_e(T_{sk}, T_{cr}, Qb) := \left( 0.06 + 0.94 \frac{E_{rsw}(T_{sk}, T_{cr}, Qb)}{E_{max}(T_{sk})} \right)$$

$$w(T_{sk}, T_{cr}, Qb) := \begin{cases} 1 & \text{if } w_e(T_{sk}, T_{cr}, Qb) > 1 \\ 1 & \text{if } w_e(T_{sk}, T_{cr}, Qb) < 0 \\ w_e(T_{sk}, T_{cr}, Qb) & \text{otherwise} \end{cases}$$

### Conduction/Radiation Heat Transfer (W/m<sup>2</sup>)

$$CR(T_{sk}) := \frac{(T_{sk} - T_o)}{R_{cl} + \frac{1}{f_{cl} \cdot h_t}}$$

### Skin Evap Heat Transfer (W/m<sup>2</sup>)

$$E_{sk}(T_{sk}, T_{cr}, Qb, w_c) := \begin{cases} \left[ w(T_{sk}, T_{cr}, Qb) \cdot \frac{(P_{sat}(T_{sk}) - P_{sat}(T_a) \cdot \phi)}{Re_T(0)} \right] & \text{if } (P_{sat}(T_{sk}) - P_{sat}(T_a) \cdot \phi) \geq 0 \\ 0 & \text{otherwise} \end{cases}$$

### Evap from wetted spot

$$E_{spot}(T_{sk}, T_{cr}, Qb, n, w_c) := \begin{cases} \frac{(P_{sat}(T_{sk}) - P_{sat}(T_a) \cdot \phi)}{\frac{1}{(f_{cl} \cdot h_e)}} & \text{if } (P_{sat}(T_{sk}) - P_{sat}(T_a) \cdot \phi) \geq 0 \\ 0W & \text{otherwise} \end{cases}$$

% Cutoff Level      Cutoff := 1

**Spot model values:**

$\psi_w := 0.68$        $\varepsilon_s := 0.35$        $b_f := 1.5 \cdot s$        $\Delta t := 10s$

### Sweat Storage Per Rate

$$m_{st}(T_{sk}, T_{cr}, Qb, n, w_c) := \begin{cases} \frac{[E_{rsw}(T_{sk}, T_{cr}, Qb) - (1 - w_c) \cdot E_{sk}(T_{sk}, T_{cr}, Qb, w_c)] \cdot \eta_w}{hfg_{ex}} \cdot \Delta t \cdot A_D(n) & \text{if } E_{rsw}(T_{sk}, T_{cr}, Qb) > E_{sk}(T_{sk}, T_{cr}, Qb, w_c) \wedge w_c \leq \text{Cutoff} \wedge w(T_{sk}, T_{cr}, Qb) \geq 1 \\ 0 \text{kg} & \text{otherwise} \end{cases}$$

$$m_{sevap}(T_{sk}, T_{cr}, Qb, n, w_c) := \begin{cases} \frac{w_c \cdot E_{spot}(T_{sk}, T_{cr}, Qb, n, w_c)}{hfg_{ex}} \cdot \Delta t \cdot A_D(n) & \text{if } 0 < w_c \leq \text{Cutoff} \\ 0 \text{kg} & \text{otherwise} \end{cases}$$

### Skin Temperature (K)

$$T_{ski}(T_{sk}, T_{cr}, Qb, w_c, n) := \frac{-[(1 - w_c) \cdot CR(T_{sk}) + (1 - w_c) \cdot E_{sk}(T_{sk}, T_{cr}, Qb, w_c) + \varepsilon_s \cdot w_c \cdot E_{spot}(T_{sk}, T_{cr}, Qb, n, w_c)] + \left( K_{eff} + \rho_{bl} \cdot Qb \cdot \frac{m}{s} \cdot C_{pb} \right) (T_{cr} - T_{sk})}{\left( \frac{\alpha_{sk}(T_{sk}, T_{cr}, Qb) \cdot \text{mass}(n) \cdot C_{sk}}{A_D(n) \cdot \Delta t} \right)} + T_{sk}$$

### Core Temperature (K)

$$T_{cri}(T_{sk}, T_{cr}, Qb, n) := \frac{M(n) + M_{shiv}(T_{sk}, T_{cr}) - \frac{Wk(n) + W_{dragcyl}(n) + q_{res}(n)}{A_D(n)} - \left( K_{eff} + \rho_{bl} \cdot Qb \cdot \frac{m}{s} \cdot C_{pb} \right) (T_{cr} - T_{sk})}{\left[ \frac{(1 - \alpha_{sk}(T_{sk}, T_{cr}, Qb)) \cdot \text{mass}(n) \cdot C_{cr}}{A_D(n) \cdot \Delta t} \right]} + T_{cr}$$

## Fraction clothing area 100% wetted

Useful area wetted      Mass to wetted area equation

$$\text{Areawet}(m_{\text{stt}}) := m_{\text{stt}} \cdot \frac{1.0437 \cdot \text{m}^2}{\text{kg}} \quad \text{mass}_{\text{sw}}(m_{\text{stt}}) := \frac{\text{Areawet}(m_{\text{stt}})}{\frac{1.0437 \cdot \text{m}^2}{\text{kg}}}$$

## Initial (Dummy) body Temperatures:

$$m_{\text{sx}}(m_{\text{stt}}, n) := \begin{cases} m_{\text{stt}} & \text{if } \frac{\text{Areawet}(m_{\text{stt}})}{A_{\text{D}}(n)} \leq \text{Cutoff} \\ \left( \text{Cutoff} \cdot A_{\text{D}}(n) \cdot \frac{\text{kg}}{1.75 \text{m}^2} \right) & \text{otherwise} \end{cases}$$

$$w_{\text{ma}}(T_{\text{sk}}, T_{\text{cr}}, \text{Qb}, n, m_{\text{stt}}) := \begin{cases} \frac{\text{Areawet}(m_{\text{stt}})}{A_{\text{D}}(n)} & \text{if } m_{\text{stt}} \geq 0 \\ 0 & \text{otherwise} \end{cases}$$

$$w_{\text{mc}}(T_{\text{sk}}, T_{\text{cr}}, \text{Qb}, n, m_{\text{stt}}) := \begin{cases} w_{\text{ma}}(T_{\text{sk}}, T_{\text{cr}}, \text{Qb}, n, m_{\text{stt}}) & \text{if } w_{\text{ma}}(T_{\text{sk}}, T_{\text{cr}}, \text{Qb}, n, m_{\text{stt}}) \leq \text{Cutoff} \\ \text{Cutoff} & \text{otherwise} \end{cases}$$

$$w_{\text{m}}(T_{\text{sk}}, T_{\text{cr}}, \text{Qb}, n, m_{\text{stt}}) := \begin{cases} w_{\text{mc}}(T_{\text{sk}}, T_{\text{cr}}, \text{Qb}, n, m_{\text{stt}}) & \text{if } w_{\text{mc}}(T_{\text{sk}}, T_{\text{cr}}, \text{Qb}, n, m_{\text{stt}}) \leq 0.68 \\ 0.68 & \text{otherwise} \end{cases}$$

## HT from bloodflow Core to Skin (W/m<sup>2</sup>)

$$Q_{\text{bflow}}(T_{\text{sk}}, T_{\text{cr}}, \text{Qb}) := \left( K_{\text{eff}} + \rho_{\text{bl}} \cdot \text{Qb} \cdot \frac{\text{m}}{\text{s}} \cdot C_{\text{pb}} \right) (T_{\text{cr}} - T_{\text{sk}})$$

**Compile calculations:**

SubNum := 1

```

PerSec := | Num ← SubNum
          | n ← Num - 1
          | Tcr ← Tcrm(n)
          | Tsk ← Tskn(n)
          | i ← 0
          | mST ← 0kg
          | for i ∈ 0..  $\frac{\text{Time}_n(n)}{\Delta t}$ 
          |   Qb1 ← Qb1(Tsk, Tcr) ·  $\frac{s}{m}$ 
          |   wc ← wm(Tsk, Tcr, Qb1, n, mST)
          |   Ti ← Tski(Tsk, Tcr, Qb1, wc, n)
          |   Tc ← Tcri(Tsk, Tcr, Qb1, n)
          |   mST2 ← mST + mst(Ti, Tc, Qb1, n, wc) - msevap(Tsk, Tcr, Qb1, n, wc)
          |   DATAi,0 ←  $\frac{T_i}{K} - 273.15$ 
          |   DATAi,1 ←  $\frac{T_c}{K} - 273.15$ 
          |   DATAi,2 ← Qb1 · (3.6 · 106)
          |   DATAi,3 ← Esk(Tsk, Tcr, Qb1, wc) ·  $\frac{A_D(n)}{W}$ 
          |   DATAi,4 ← CR(Tsk) ·  $\frac{A_D(n)}{W}$ 
          |   DATAi,5 ← Qress(n) ·  $\frac{1}{W}$ 
          |   DATAi,6 ← Qresl(n) ·  $\frac{1}{W}$ 
          |   DATAi,7 ← Mshiv(Tsk, Tcr) · AD(n) ·  $\frac{1}{W}$ 
          |   DATAi,8 ← -Qbflow(Tsk, Tcr, Qb1) ·  $\frac{1 - A_D(n)}{W}$ 
          |   DATAi,9 ← w(Tsk, Tcr, Qb1)

```

```

DATAi,10 ← (Qress(n) + Qresl(n)) · 1/W
DATAi,11 ← we(Tsk, Tcr, Qb1)
DATAi,12 ← Ersw(Tsk, Tcr, Qb1) · 1 · AD(n) / W
DATAi,13 ← Timen(n) / s
DATAi,14 ← ReT(wc) / (s / m)
DATAi,15 ← wc
DATAi,16 ← Emax(Tsk) / (w / m2)
DATAi,17 ← msx(mST2, n) / kg
DATAi,18 ← Espot(Ti, Tc, Qb1, n, wc) · AD(n) / W
DATAi,19 ← mst(Ti, Tc, Qb1, n, wc) / kg
DATAi,20 ← wc · AD(n) / m2
DATAi,21 ← αsk(Ti, Tc, Qb1)
DATAi,22 ← msevap(Tsk, Tcr, Qb1, n, wc) / kg
DATAi,23 ← mst(Ti, Tc, Qb1, n, wc) / kg
DATA
mST1 ← msx(mST2, n)
Tsk ← Ti
Tcr ← Tc
mST ← mST1
i ← i + 1
DATA

```

**Desired Values for Heat Loss and Temp Change per ΔT**

### Output Formulas:

$$T_{skin}(j) := \text{PerSec}_{j,0}$$

$$T_{core}(j) := \text{PerSec}_{j,1}$$

$$Q_{bj}(j) := \text{PerSec}_{j,2} \cdot W$$

$$E_{skj}(j) := \text{PerSec}_{j,3} \cdot W$$

$$CR_T(j) := \text{PerSec}_{j,4}$$

$$Q_{resT}(j) := (\text{PerSec}_{j,5} + \text{PerSec}_{j,6}) \cdot W$$

$$M_{shivr}(j) := \text{PerSec}_{j,7} \cdot W$$

$$w_j(j) := \text{PerSec}_{j,9}$$

$$SktoCr(j) := \text{PerSec}_{j,8} \cdot W$$

$$w_{ea}(j) := \text{PerSec}_{j,11}$$

$$E_{rswADj}(j) := \text{PerSec}_{j,12} \cdot W$$

$$\text{Time}_{nj}(j) := \text{PerSec}_{j,13} \cdot s$$

$$Re_{Tj}(j) := \text{PerSec}_{j,14} \cdot s$$

$$w_{cj}(j) := \text{PerSec}_{j,15}$$

$$E_{maxj}(j) := \text{PerSec}_{j,16} \cdot \frac{W}{m}$$

$$m_{STj}(j) := \text{PerSec}_{j,17} \cdot \text{kg}$$

$$m_{evap_{spotj}}(j) := \text{PerSec}_{j,18} \cdot \text{kg}$$

$$E_{spotj}(j) := \text{PerSec}_{j,18} \cdot W$$

$$m_{stj}(j) := \text{PerSec}_{j,19} \cdot \text{kg}$$

$$\text{Spotsize}(j) := \text{PerSec}_{j,20} \cdot \text{m}^2$$

$$\alpha(j) := \text{PerSec}_{j,21}$$

$$m_{sevapj}(j) := \text{PerSec}_{j,22} \cdot \text{kg}$$

$$m_{stij}(j) := \text{PerSec}_{j,23} \cdot \text{kg}$$

Average Gagge wettedness (ie percent time fully wetted)

$$w_{1logic}(j) := \begin{cases} 1 & \text{if } w_j(j) = 1 \\ 0 & \text{otherwise} \end{cases}$$

$$\text{ReclAVG} := \frac{\frac{\text{Time}_{nj}(1)}{\Delta t} \sum_{j=0} [\text{Re}_{Tj}(j) - (\text{Re}_{Tj}(1) - 26.2s)]}{\frac{\text{Time}_{nj}(1)}{\Delta t} + 1} = 24.99268 \text{ s}$$

$$\text{St} := \sum_{j=0}^{\text{Time}_{nj}(1)} \left[ \left[ \left( \frac{M(23) \cdot A_D(23)}{K} - \frac{E_{skj}(j)}{K} \right) - \frac{Q_{resT}(j)}{K} - \frac{CR_T(j)}{K} - \frac{Wk(23)}{K} \right] \cdot \Delta t \cdot K \right] = 7.64628 \times 10^5 \cdot \text{J}$$

# Core Diff

$$\text{CoreError} := \text{Tcore}\left(\frac{\text{Time}_{nj}(1)}{\Delta t}\right) - \text{Tcore}(0) - X_{\text{SubNum}-1,10} = -0.18204 \quad \text{Re}_{cl} = 26.2 \frac{\text{s}}{\text{m}}$$

$$\text{Re}_{cl}\text{Corr}(j) := \begin{cases} \text{Re}_{cl} & \text{if Spotsize}(j) = 0 \\ \left[ \frac{P_{\text{sat}}(\text{Tskin}(j) \text{K} + 273.15\text{K}) - P_{\text{sat}}(\text{T}_a) \cdot \phi}{(1 - \text{wcj}(j)) \cdot \frac{E_{\text{skj}}(j)}{A_{\text{D}}(\text{SubNum} - 1)} + \frac{\text{wcj}(j) \cdot E_{\text{spotj}}(j)}{A_{\text{D}}(\text{SubNum} - 1)}} - \frac{1}{(f_{cl} \cdot h_e)} \right] & \text{otherwise} \end{cases}$$

$$\text{ReclAVGCorr} := \frac{\frac{\text{Time}_{nj}(1)}{\Delta t} \sum_{j=0} (\text{Re}_{cl}\text{Corr}(j))}{\frac{\text{Time}_{nj}(1)}{\Delta t} + 1} = 18.03978 \frac{1}{\text{W}} \cdot \text{m}^2 \cdot \text{Pa}$$

$$\text{w1timepercent} := \frac{\frac{\text{Time}_{nj}(1)}{\Delta t} \sum_{j=0} \text{w1logic}(j)}{\frac{\text{Time}_{nj}(1)}{\Delta t} + 1} = 0.91517$$

$$\text{SW}_T := \sum_{j=0}^{\frac{\text{Time}_{nj}(1)}{\Delta t}} \frac{E_{\text{rswADj}}(j) \cdot \Delta t + \text{PerSec}_{j,6} \cdot \text{W} \cdot \Delta t}{\text{hfg}_{\text{ex}}} = 1.72405 \text{ kg}$$



$$SW_{Evap} := \sum_{j=0}^{\text{Time}_{nj}(1)} \frac{\Delta t}{\text{hfg}_{ex}} \left[ E_{skj}(j) \cdot (1 - w_{cj}(j)) + w_{cj}(j) \cdot E_{spotj}(j) \right] \cdot \Delta t = 1.19655 \cdot \text{kg}$$

$$\Delta w := \sum_{j=0}^{\text{Time}_{nj}(1)} (w_{ea}(j) - w_j(j)) = 589.25988$$

$$\text{Sweatdif} := SW_T - ASW(\text{SubNum} - 1)$$

$$ZZ := \left( \frac{\text{ReclAVG}}{s} \quad \text{CoreError} \quad w_{1\text{timepercent}} \quad Sw_{\text{mod}} \quad \frac{\text{Sweatdif}}{\text{kg}} \quad \frac{SW_{Evap}}{\text{kg}} \right)$$

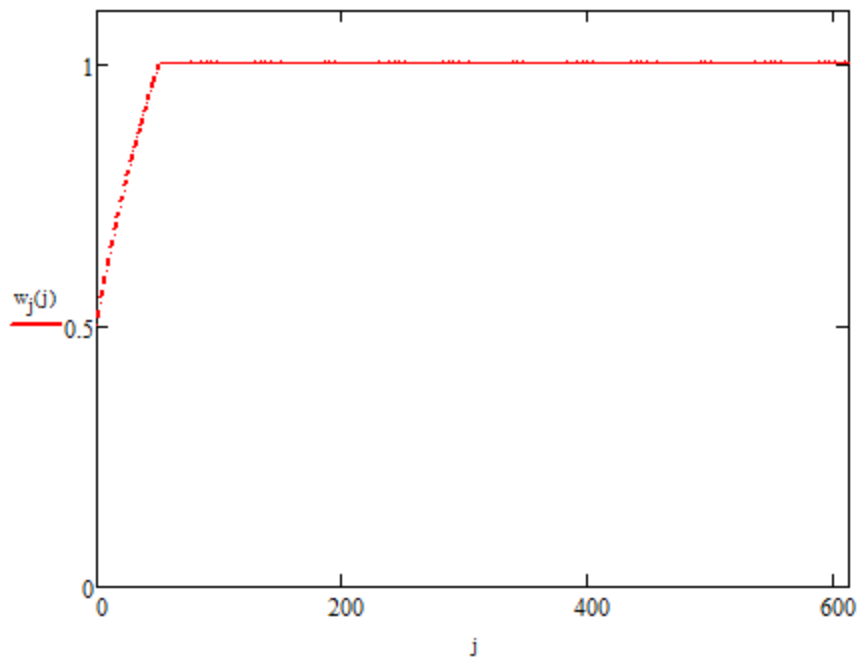
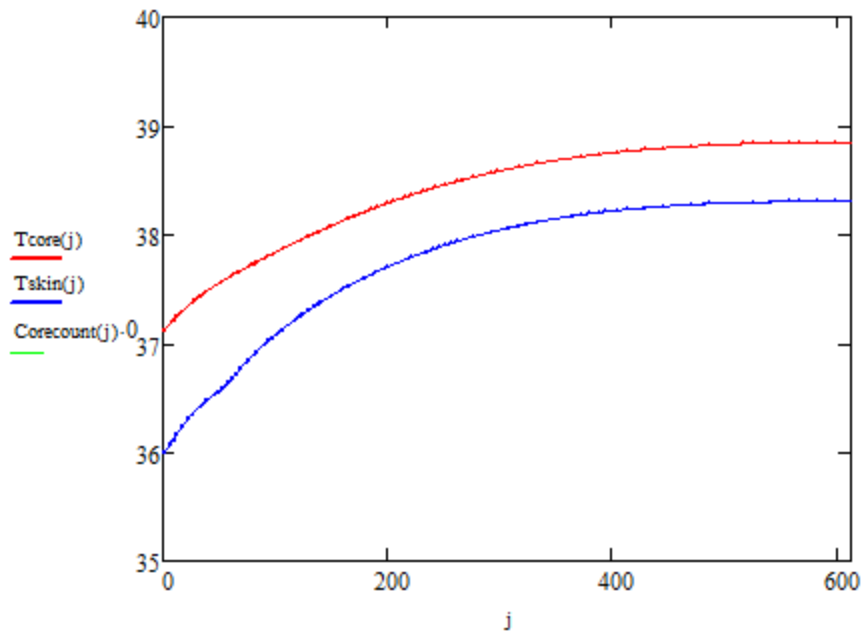
$$YY := \left( \frac{\text{ReclAVG}}{s} \quad \text{CoreError} \quad w_{1\text{timepercent}} \quad \frac{SW_T}{\text{kg}} \quad \frac{SW_{Evap}}{\text{kg}} \right)$$

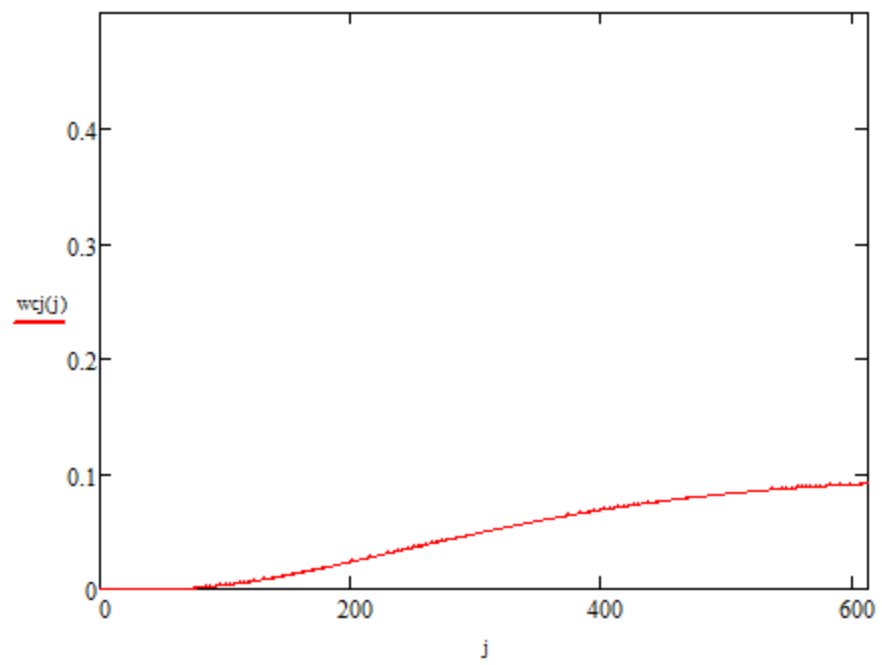
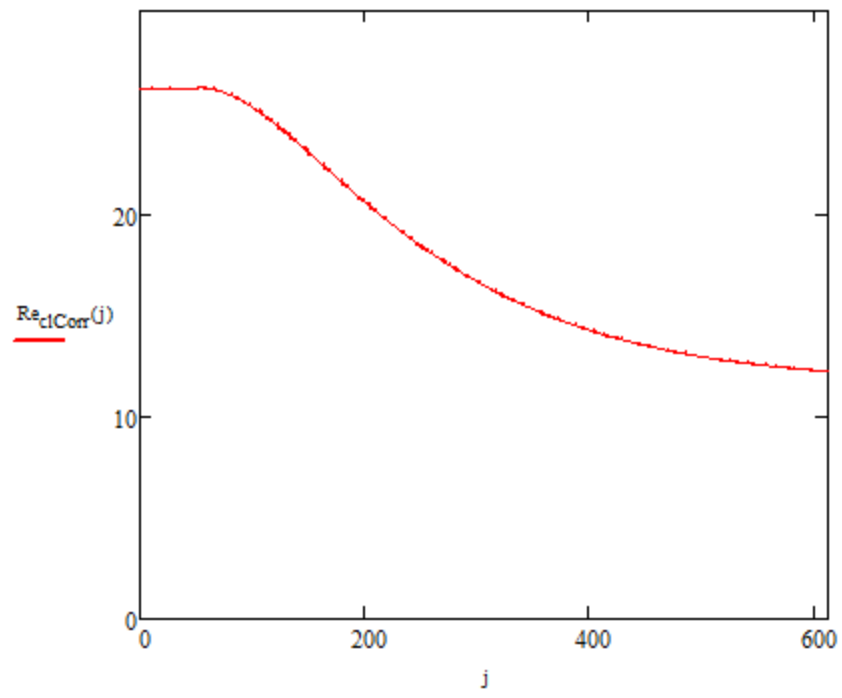
$$\text{CoreError} = -0.18204$$

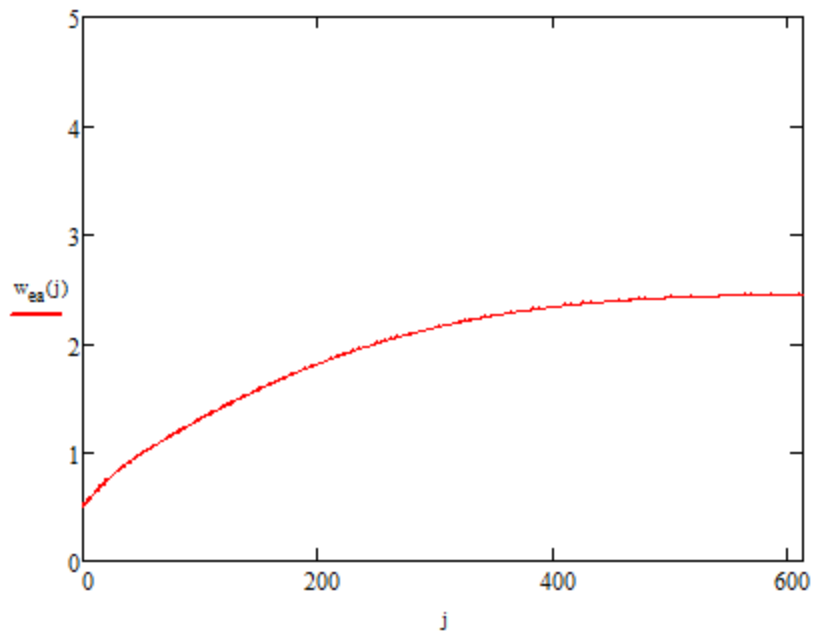
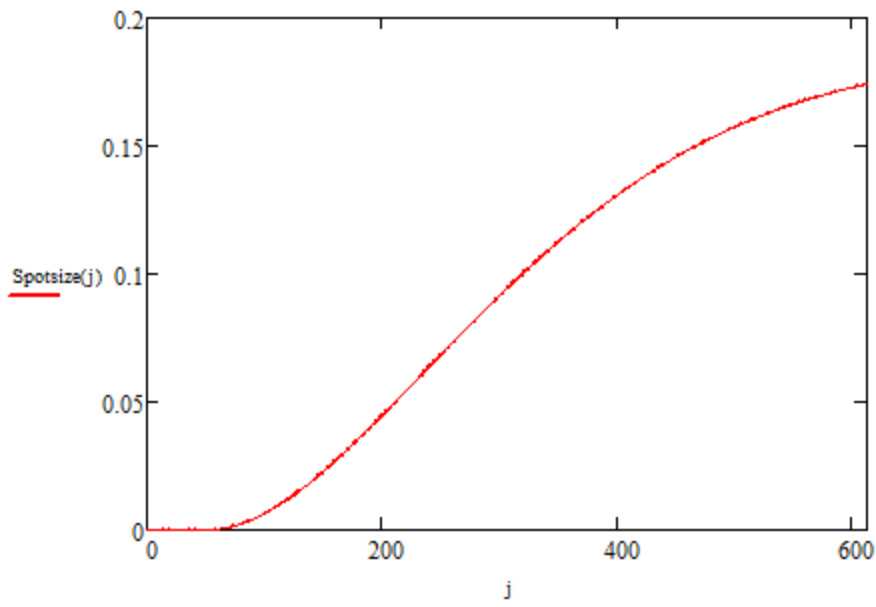
$$\text{Sweatdif} = 0.16745 \text{ kg}$$

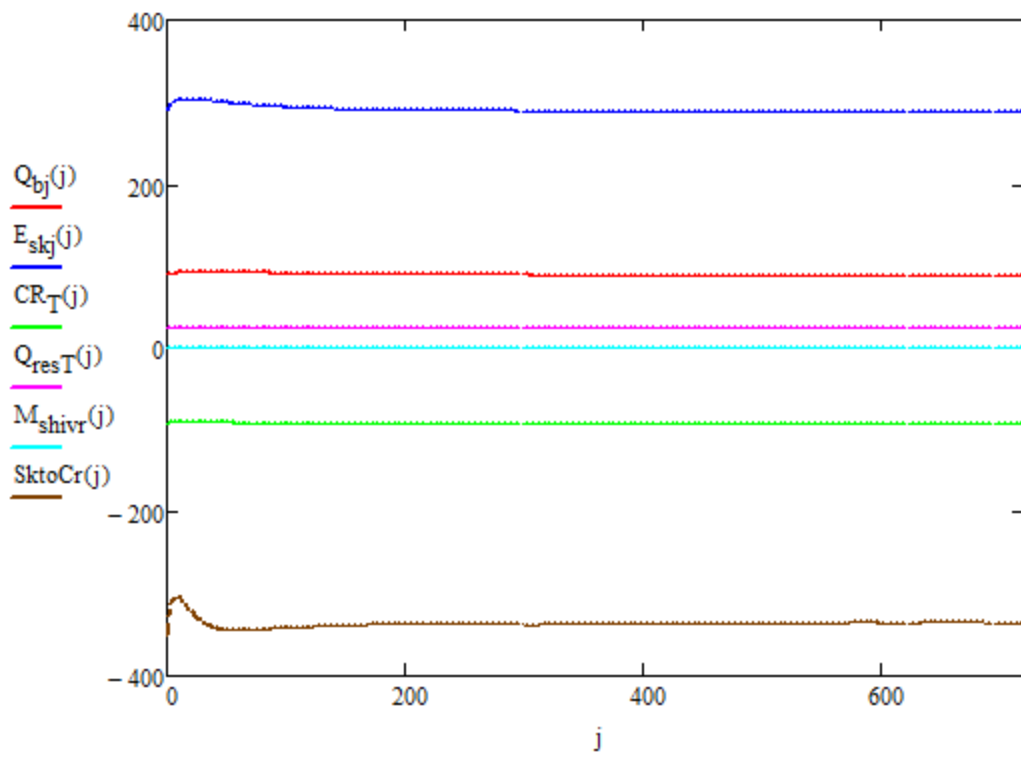
ZZ =		0	1	2	3	4	5
	0	24.99268	-0.18204	0.91517	1.17	0.16745	1.19655

YY =		0	1	2	3	4
	0	24.99268	-0.18204	0.91517	1.72405	1.19655









0-Tsk(C) 1-Tc(C) 2-Qbl(L/min) 3-Esk(W) 4-CR(W) 5-Qress(W) 6-Qresk(W) 7-Mshiv(W) 8-SktoSCr(W) 9-w(N/A) 10-QresT(W)

	0	1	2	3	4	5	6	7	8	9
0	35.98825	37.10604	20.3	142.45301	-88.9037	-3.8293	31.6828	0	-64.41912	0.50152
1	35.9989	37.11853	22.20645	146.35142	-88.80764	-3.8293	31.6828	0	-69.61366	0.51488
2	36.01057	37.13081	24.08	150.20953	-88.70028	-3.8293	31.6828	0	-74.66065	0.52802
3	36.02314	37.14288	25.92169	154.03101	-88.58268	-3.8293	31.6828	0	-79.55254	0.54097
4	36.03649	37.15476	27.73257	157.81809	-88.45598	-3.8293	31.6828	0	-84.28513	0.55374
5	36.0505	37.16644	29.51369	161.57201	-88.3214	-3.8293	31.6828	0	-88.85732	0.56634
6	36.06505	37.17794	31.2661	165.29332	-88.18018	-3.8293	31.6828	0	-93.2707	0.57877
7	36.08001	37.18926	32.99085	168.98207	-88.03354	-3.8293	31.6828	0	-97.52918	0.59103
8	36.09529	37.20041	34.68892	172.63796	-87.88267	-3.8293	31.6828	0	-101.63853	0.60313
9	36.11077	37.21139	36.36127	176.26047	-87.72868	-3.8293	31.6828	0	-105.60602	0.61507
10	36.12636	37.22222	38.00881	179.84893	-87.57263	-3.8293	31.6828	0	-109.43998	...

PerSec =

# ASHRAE Two-node Model Implementation PCS Simulation with the Presented Wetted Clothing Model

**Conditions/Constants:**

User Defined Conditions:

Two Node Gagge

X :=

1.00	1.00
2.00	1.00
3.00	1.00
4.00	1.00
5.00	2.00
6.00	2.00

SUBJECT	WEEK	DAY	AMPM	PCS	TIME	HEARTRAT	TSKIN	TORSOTEM	CORETTEM	CORECHG	AIRTEMP	RH	SWRATE	VO2	METRATE	CORERATE	TSKININT	HEIGHT	Weight
0	1	2	3	4	5	6	7	8	9	10	11	12	13	14	15	16	17	18	19

0	1	1	4	1	0	102	147.46667	38.55575	38.77992	39.02	1.92667	41.94648	19.66627	915.64706
1	2	1	6	1	0	120	102.46667	36.44119	36.1019	37.66667	0.83667	41.7321	19.76897	987.8
2	3	1	5	2	0	120	125.43333	36.36955	35.85104	37.05333	0.88	42.01257	19.82025	1.4116·10 <sup>3</sup>
3	4	1	4	2	0	120	119.63333	36.59049	36.85825	37.71	0.61	41.85156	20.1334	1.3744·10 <sup>3</sup>
4	5	2	4	1	0	78	169.86667	37.24483	37.50094	38.64667	1.43333	41.56465	19.59876	1.44431·10 <sup>3</sup>
5	6	2	6	1	0	82	180.6	38.49552	37.82618	38.87667	1.84333	41.8457	19.35158	672.73171
6	7	2	5	2	0	120	137.26667	36.24469	36.19	38.48	1.21333	41.72708	19.97134	1.2711·10 <sup>3</sup>
7	8	2	4	2	0	120	145.36667	36.84512	36.61199	38	0.97	40.99545	19.55705	1.1642·10 <sup>3</sup>
8	9	4	4	1	0	95	117.83333	37.45145	37.19533	37.91	0.87	41.51595	19.47626	1.11423·10 <sup>3</sup>
9	10	3	6	1	0	120	131.06667	37.03373	36.65969	37.85	1.04	41.62891	19.38532	1.2037·10 <sup>3</sup>
10	11	3	5	2	0	100	154.23333	38.24038	37.50697	39.01333	1.80333	41.8625	20.13294	817.92
11	12	3	4	2	0	120	147.56667	37.59889	37.81072	38.20667	1.07667	41.43392	20.00514	1.1905·10 <sup>3</sup>
12	13	1	4	1	0	120	119.56667	37.36014	36.2057	38.70333	1.55667	41.84297	19.76938	1·10 <sup>3</sup>
13	14	1	6	1	0	120	141.46667	37.91055	37.71453	38.41333	0.96667	41.7308	19.47184	863.1
14	15	1	5	2	0	70	137.23333	36.8514	36.56491	38.69667	1.55333	42.06628	19.56308	1.20137·10 <sup>3</sup>
15	16	1	4	2	0	120	165.8	37.54545	36.85923	38.27	0.91667	41.88118	19.48203	1.0782·10 <sup>3</sup>
16	17	2	4	1	0	120	143.9	35.77915	35.4321	37.95333	0.90667	42.17402	20.47483	1.3626·10 <sup>3</sup>
17	18	2	6	1	0	102	177.73333	38.33454	37.40561	38.90667	2.19333	42.38802	20.67476	1.20471·10 <sup>3</sup>
18	19	2	5	2	0	120	138.9	37.26817	36.45863	38.27333	1.07667	42.23424	20.4458	1.1371·10 <sup>3</sup>
19	20	2	4	2	0	120	144.46667	36.18106	36.75327	37.95333	0.37	41.65527	20.67837	1.3172·10 <sup>3</sup>
20	21	3	4	1	0	120	146.36667	36.21548	36.62106	37.88	0.71667	42.15742	19.40742	1.4383·10 <sup>3</sup>
21	22	3	6	1	0	120	151.7	37.30033	36.8161	38.37	1.22333	41.8418	19.52328	1.2106·10 <sup>3</sup>
22	23	3	5	2	0	120	113.1	36.02351	35.47816	37.9	0.12333	42.12519	20.16508	1.408·10 <sup>3</sup>
23	24	3	4	2	0	120	121	36.87934	36.86704	38.14	0.07333	42.01595	20.10246	...
24														

**Conditions/Constants:**

User Defined Conditions:

trousers, long-sleeved shirt

Environmental:

Clothing:

$$T_a := (42.2 + 273.15)\text{K} = 315.35\text{K}$$

$$\text{clo} := 0.155 \frac{\text{m}^2\text{K}}{\text{W}}$$

Wind velocity (m/s):

$$T_r := (54.4 + 273.15)\text{K} = 327.55\text{K}$$

$$I_{\text{cl}} := 1.00\text{clo}$$

$$v_{\text{wind}} := 2.0$$

Walking in the wind  
convection pg 82, danielson

$$h_c := 11.7 \cdot v_{\text{wind}}^{0.57} \frac{\text{W}}{\text{m}^2 \cdot \text{K}} = 17.36893 \frac{\text{kg}}{\text{K} \cdot \text{s}^3}$$

$$h_r := 4.7 \frac{\text{W}}{\text{m}^2 \cdot \text{K}}$$

$$\text{Ensemblemass} := 15.054\text{kg}$$

$$R_{\text{cl}} := I_{\text{cl}}$$

$$R_{\text{cl}} = 0.155 \frac{\text{K} \cdot \text{s}^3}{\text{kg}}$$

$$\text{Grade} := 0.01$$

$$\phi := .20$$

$$\text{load} := 10\text{kg}$$

$$f_{\text{cl}} := 1.33$$

$$T_o := \frac{h_r \cdot T_r + h_c \cdot T_a}{h_r + h_c} = 317.94822\text{K}$$

$$h_t := h_r + h_c$$

$$h_c = 17.36893 \frac{1}{\text{K}} \cdot \frac{\text{W}}{\text{m}^2}$$



### Iterative Variables, Individually Dependent:

$$\text{mass}(n) := X_{n,19} \cdot \text{kg}$$

$$\text{height}(n) := X_{n,18} \cdot \text{m}$$

$$A_D(n) := \left[ 0.202 \cdot \left( \frac{\text{mass}(n)}{\text{kg}} \right)^{0.425} \cdot \left( \frac{\text{height}(n)}{\text{m}} \right)^{0.725} \right] \cdot \text{m}^2$$

$$M(n) := \frac{X_{n,15} \cdot \text{W}}{A_D(n)}$$

$$T_{\text{skn}}(n) := (X_{n,17} + 273.15) \cdot \text{K}$$

$$T_{\text{cm}}(n) := (X_{n,9} - X_{n,10} + 273.15) \cdot \text{K}$$

$$\text{Wk}(n) := \text{Grade} \cdot \text{WKVal}_{n,0} \cdot \text{kg} \cdot \text{WKVal}_{n,1} \cdot \frac{\text{m}}{\text{s}} \cdot 9.81 \frac{\text{m}}{\text{s}^2}$$

$$\text{PCSn}(n) := X_{n,4}$$

$$\text{Time}_n(n) := X_{n,5} \cdot 60 \text{s}$$

$$\text{ASW}(n) := X_{(n,13)} \cdot \frac{\frac{\text{kg}}{1000}}{\text{hr}} \cdot \text{Time}_n(n)$$

Clothed weight (kg)	Treadmill speed (m/s)	time (s)	Vert Distance (m)
---------------------	-----------------------	----------	-------------------

87.09090909	0.938784	7800	73.225152
86.54545455	0.938784	4740	44.4983616
100.9545455	0.759968	6720	51.0698496
92.95454545	0.89408	5820	52.035456
70.13636364	1.251712	9300	116.409216
71.63636364	1.162304	10440	121.3445376
110.3636364	0.715264	6360	45.4907904
111.7272727	0.67056	7020	47.073312
109.5	0.67056	6540	43.854624
105.5	0.759968	7500	56.9976
86.18181818	0.983488	7620	74.9417856
79.22727273	1.1176	6900	77.1144
94.95454545	0.938784	6420	60.2699328
115.5	0.67056	6720	45.061632
93.5	0.759968	8400	63.837312
113.6363636	0.715264	6720	48.0657408
96.72727273	0.89408	6960	62.227968
84.36363636	1.072896	8340	89.4795264
115.1818182	0.67056	9360	62.764416
98.36363636	0.89408	7260	64.910208
94.45454545	0.938784	6480	60.8332032
87.5	1.072896	7440	79.8234624
118.8181818	0.67056	6300	42.24528
104.7727273	0.804672	6180	49.7287296

% Cutoff Level      Cutoff := 1

**Spot model values, Individually  
dependent on baseline, Swmod:**

$Sw_{mod} := 1$        $\psi_w := 0.68$     $\epsilon_s := 0.35$     $b_f := 1.5 \cdot s$     $\Delta t := 10s$

**Body Equation Constants:**

$SW_{mods}(n) := \begin{cases} SRM6835_n & \text{if } \psi_w = 0.68 \wedge \epsilon_s = .35 \wedge PCSn(n) \neq 0 \\ Sw_{mod} & \text{otherwise} \end{cases}$

SRM6835 :=

- 1.00
- 1.70
- 3.90
- 2.45
- 0.00
- 0.00
- 1.85
- 1.67
- 1.55
- 2.50
- 0.79
- 2.05
- 1.20
- 1.27
- 0.00
- 1.23
- 2.07
- 2.35
- 1.65
- 2.50
- 1.97
- 1.25
- 2.30
- 1.17

$c_{sw}(n) := SW_{mods}(n) \cdot 116 \frac{W}{m^2 \cdot K}$      $BFN := 6.3$      $C_{pb} := 4190 \frac{J}{kg \cdot K}$

$K_{eff} := 5.28 \frac{W}{m^2 \cdot K}$      $c_{dil} := \frac{150}{K}$      $C_{cr} := 3500 \frac{J}{kg \cdot K}$

$\rho_{bl} := 1.06 \frac{kg}{L}$      $S_{tr} := \frac{0.5}{K}$      $C_{sk} := 3500 \frac{J}{kg \cdot K}$

**Constants and Calculated Constants:**

$$P_T := 101325 \text{ Pa}$$

$$C_{p_v} := 1864 \frac{\text{J}}{\text{kg} \cdot \text{K}}$$

$$C_{p_a} := 1005 \frac{\text{J}}{\text{kg} \cdot \text{K}}$$

$$h_{f_{g_{ex}}} := 2454.1 \frac{1000 \text{ J}}{\text{kg}}$$

$$C_{p_b} := 3500 \frac{\text{J}}{\text{kg} \cdot \text{K}}$$

$$LR_{STD} := 16.5 \frac{\text{K}}{1000 \text{ Pa}}$$

$$K_{res} := 1.43 \cdot 10^{-6} \frac{\text{kg}}{\text{J}}$$

**Sat. Pressure Equation: Psat(T)**

Pressure Curve Fit  
Constants:

	ICE	LIQUID
$C_1$	$C_1 := -5.6745359 \cdot 10^3$	$C_8 := -5800.2206$
$C_2$	$C_2 := 6.3925247$	$C_9 := 1.3914993$
$C_3$	$C_3 := -0.009677843$	$C_{10} := -0.048640239$
$C_4$	$C_4 := 0.00000062215701$	$C_{11} := 4.1764768 \cdot 10^{-5}$
$C_5$	$C_5 := .0000000020747825$	$C_{12} := -1.4452093 \cdot 10^{-8}$
$C_6$	$C_6 := -9.484024 \cdot 10^{-13}$	$C_{13} := 6.5459673$
$C_7$	$C_7 := 4.1635019$	

$$P_{sat}(T) := \begin{cases} e^{\left[ \frac{C_1}{T} + C_2 + C_3 \cdot \frac{T}{K} + C_4 \cdot \left(\frac{T}{K}\right)^2 + C_5 \cdot \left(\frac{T}{K}\right)^3 + C_6 \cdot \left(\frac{T}{K}\right)^4 + C_7 \cdot \ln\left(\frac{T}{K}\right) \right]} \cdot \text{Pa} & \text{if } T < 273.15 \text{ K} \\ e^{\left[ \frac{C_8}{T} + C_9 + C_{10} \cdot \frac{T}{K} + C_{11} \cdot \left(\frac{T}{K}\right)^2 + C_{12} \cdot \left(\frac{T}{K}\right)^3 + C_{13} \cdot \ln\left(\frac{T}{K}\right) \right]} \cdot \text{Pa} & \end{cases}$$

### Pressure Values

$$P_V := P_{\text{sat}}(T_a) \cdot \phi = 1.65892 \times 10^3 \text{ Pa}$$

$$P_a := P_T - P_V = 9.96661 \times 10^4 \text{ Pa}$$

$$W_a := \frac{P_V \cdot 18.02}{P_a \cdot 28.97} = 0.01035$$

$$P_{\text{sat}}(293.15\text{K}) = 2.3388 \times 10^3 \text{ Pa}$$

$$\text{Re}_{\text{cl}} := 26.2 \frac{(\text{m}^2 \cdot \text{Pa})}{W}$$

Lewis Ratio and he

$$T_{\text{in}} := T_a$$

$$P_{\text{vi}} := P_{\text{sat}}(T_{\text{in}}) \cdot \phi = 1.65892 \times 10^3 \text{ Pa}$$

$$w_{\text{in}} := 0.622 \cdot \frac{P_{\text{vi}}}{P_T - P_{\text{vi}}} = 0.01035$$

$$\text{kmol} := 1000 \text{ mol}$$

$$\rho_{\text{ain}} := \frac{P_a}{8.314 \frac{1000 \text{ J}}{\text{kmol} \cdot \text{K}} \cdot T_{\text{in}}} \cdot 28.01 \frac{\text{kg}}{\text{kmol}} = 1.06477 \frac{\text{kg}}{\text{m}^3}$$

$$R_b := 8.314 \frac{1000 \text{ J}}{1000 \text{ mol} \cdot \text{K}}$$

$$M_v := 18.01 \frac{\text{kg}}{1000 \text{ mol}} \quad M_a := 28.97 \frac{\text{kg}}{1000 \text{ mol}}$$

$$\rho_v(T) := \frac{P_{\text{sat}}(T) \cdot M_v}{R_b \cdot T} \quad \rho_a(T) := \frac{(P_a) \cdot M_a}{R_b \cdot T}$$

$$C_{\text{pa}} := 1.007 \cdot \frac{1000 \text{ J}}{\text{kg} \cdot \text{K}}$$

$$C_{\text{pw}} := 1.872 \cdot \frac{1000 \text{ J}}{\text{kg} \cdot \text{K}}$$

$$W_1 := w_{\text{in}}$$

$$P(b, a) := 2a + 2 \cdot b$$

$$A_c(b, a) := b \cdot a$$

$$D_h(b, h) := 4 \cdot \frac{(A_c(b, h))}{P(b, h)}$$

$$\text{Air} \quad \mu := 184.6 \cdot 10^{-7} \frac{\text{N} \cdot \text{s}}{\text{m}^2}$$

$$\text{Air} \quad \nu := \frac{\mu}{\rho_a(T_a)} = 1.67625 \times 10^{-5} \frac{\text{m}^2}{\text{s}}$$

$$C_{pm} := \frac{(C_{pa} + W_1 \cdot C_{pw})}{(1 + W_1)} = 1.01586 \times 10^3 \frac{\text{m}^2}{\text{K} \cdot \text{s}^2}$$

$$C_{pm} = 0.24263 \frac{\text{m}^3}{\text{kg}} \cdot \frac{1000 \text{cal}}{\text{m}^3 \cdot \text{K}}$$

$$D_{ab}(T) := 0.26 \cdot 10^{-4} \frac{\text{m}^2}{\text{s}} \cdot \left( \frac{T}{298 \text{K}} \right)^{\frac{3}{2}}$$

$$\rho_a(T_a) = 1.10127 \frac{\text{kg}}{\text{m}^3}$$

$$\text{rhoam} := \rho_a(T_a)$$

$$\text{Pr} := 0.707$$

$$\text{Sc} := \frac{\nu}{D_{ab}(T_a)} = 0.59224$$

$$C_{pm} \cdot \text{rhoam} = 0.26721 \cdot \frac{1000 \text{cal}}{\text{m}^3 \cdot \text{K}}$$

$$\text{LR} := \frac{\frac{1}{(C_{pm} \cdot \text{rhoam})} \cdot \left( \frac{\text{Pr}}{\text{Sc}} \right)^{\frac{2}{3}} \cdot 2454.1 \cdot 1000 \frac{\text{J}}{\text{kg}}}{\frac{R_b}{M_v} \cdot \frac{[T_a + (35 \text{K} + 273.15 \text{K})]}{2}} = 17.15301 \cdot \frac{\text{K}}{1000 \text{Pa}}$$

$$\text{LR} = 17.15301 \frac{1}{\text{Pa}} \cdot \frac{\text{K}}{1000}$$

$$h_e := h_c \cdot \text{LR} = 0.29793 \cdot \frac{\text{W}}{\text{m}^2 \cdot \text{Pa}}$$

### PCS Thermal Manikin power levels

Full PCS Values found in Appendix B, Table B.7  
for PCS1, PCS9, PCS12, PCS20

$$\text{PCS1Cool}(\text{time}) := \begin{cases} \text{PCS1} \left( \text{trunc} \left( \frac{\text{time}}{60} \right) \right), 1 \cdot W & \text{if } \text{time} < 119 \cdot 60 \\ (\text{PCS1}_{119,1} \cdot W) & \text{otherwise} \end{cases}$$

$$\text{PCS9Cool}(\text{time}) := \begin{cases} \text{PCS9} \left( \text{trunc} \left( \frac{\text{time}}{60} \right) \right), 1 \cdot W & \text{if } \text{time} < 119 \cdot 60 \\ (\text{PCS9}_{119,1} \cdot W) & \text{otherwise} \end{cases}$$

$$\text{PCS12Cool}(\text{time}) := \begin{cases} \text{PCS12} \left( \text{trunc} \left( \frac{\text{time}}{60} \right) \right), 1 \cdot W & \text{if } \text{time} < 119 \cdot 60 \\ (\text{PCS12}_{119,1} \cdot W) & \text{otherwise} \end{cases}$$

$$\text{PCS20Cool}(\text{time}) := \begin{cases} \text{PCS20} \left( \text{trunc} \left( \frac{\text{time}}{60} \right) \right), 1 \cdot W & \text{if } \text{time} < 119 \cdot 60 \\ (\text{PCS20}_{119,1} \cdot W) & \text{otherwise} \end{cases}$$

$$\text{PCSCool}(n, \text{time}) := \begin{cases} \text{PCS9Cool}(\text{time}) & \text{if } \text{PCSn}(n) = 9 \\ \text{PCS1Cool}(\text{time}) & \text{if } \text{PCSn}(n) = 1 \\ \text{PCS12Cool}(\text{time}) & \text{if } \text{PCSn}(n) = 12 \\ \text{PCS20Cool}(\text{time}) & \text{if } \text{PCSn}(n) = 20 \\ 0 & \text{otherwise} \end{cases}$$



PCS9 :=	59.01	99.19	PCS1 :=	59.02	101.82	PCS12 :=	59.00	117.41	PCS20 :=	59.02291667	126.6055
	60.02	99.58		60.02	101.55		59.02	116.41		60.00833333	126.203
	61.01	98.62		61.02	100.45		60.03	116.23		61.01940833	125.9415
	62.02	98.26		62.02	99.21		61.01	115.44		62.02044167	126.689
	63.00	97.23		63.01	102.25		62.03	115.47		63.02030833	127.332
	64.02	96.82		64.01	101.05		63.01	115.54		64.01888333	127.4865
	65.02	96.59		65.01	99.80		64.02	115.34		65.019275	127.199
	66.02	96.05		66.03	101.16		65.01	114.19		66.01966667	127.365
	67.02	95.83		67.01	100.60		66.02	113.49		67.017575	127.441
	68.02	94.55		68.03	100.47		67.01	113.44		68.015625	127.165
	69.02	94.27		69.01	101.61		68.02	113.50		69.01458333	126.9145
	70.02	93.80		70.02	101.54		69.00	112.71		70.01263333	126.786
	71.01	93.63		71.01	101.26		70.02	112.67		71.01159167	127.1435
	72.01	92.93		72.02	100.77		71.00	112.27		72.009375	127.047
	73.01	92.03		73.01	101.08		72.02	112.35		73.02356667	127.0675
	74.01	91.39		74.02	101.10		73.00	111.79		74.00703333	126.74
	75.01	90.70		75.01	100.82		74.01	111.19		75.021875	126.333
	76.01	90.09		76.02	100.53		75.01	110.95		76.00690833	126.112
	77.01	89.20		77.00	100.61		76.01	110.64		77.01991667	126.1715
	78.01	89.48		78.02	100.57		77.03	109.51		78.019275	126.9905
79.01	88.55	79.00	100.17	78.01	108.45	79.01900833	127.272				
80.02	87.57	80.02	101.12	79.02	108.76	80.01745	127.468				
81.01	86.35	81.00	100.98	80.01	108.13	81.01666667	127.5295				
82.02	85.76	82.02	100.36	81.02	107.70	82.01549167	126.7735				
83.01	84.97	83.02	100.40	82.01	107.18	83.01484167	127.217				
84.02	84.60	84.02	100.92	83.02	106.72	84.01471667	127.3575				
85.01	84.62	85.03	100.81	84.01	106.15	85.01276667	127.1025				
				85.02	105.31						

Drag Force

$$D_b := 18 \text{ in} = 0.4572 \cdot \text{m}$$

$$\text{Re}_{D(n)} := \frac{\text{WKVal}_{n,1} \cdot \frac{\text{m}}{\text{s}} \cdot D_b}{\nu}$$

$$C_{D\text{cyl}(n)} := 1.18 + \frac{6.8}{\text{Re}_{D(n)}^{0.89}} + \frac{1.96}{\text{Re}_{D(n)}^{\frac{1}{2}}} - \frac{0.0004 \cdot \text{Re}_{D(n)}}{1 + 3.64 \cdot 10^{-7} \cdot \text{Re}_{D(n)}^2}$$

$$F_{\text{dragcyl}(n)} := \frac{1}{2} \cdot \rho_a(T_a) \cdot \left( \text{WKVal}_{n,1} \cdot \frac{\text{m}}{\text{s}} \right)^2 \cdot D_b \cdot \text{height}(n) \cdot C_{D\text{cyl}(n)}$$

$$W_{\text{dragcyl}(n)} := F_{\text{dragcyl}(n)} \cdot \left( \text{WKVal}_{n,1} \cdot \frac{\text{m}}{\text{s}} \right)$$

**Respiration calculations:**

$$m_{\text{res}(n)} := M(n) \cdot K_{\text{res}} \cdot A_D(n)$$

$$T_{\text{ex}} := \left( 32.6 + .066 \cdot \frac{T_a - 273.15\text{K}}{\text{K}} + 32 \cdot W_a \right) \cdot \text{K} + 273.15\text{K} = 308.86651 \text{ K}$$

$$W_{\text{ex}} := \left( 0.0277 + 0.000065 \cdot \frac{T_a - 273.15\text{K}}{\text{K}} + 0.2 \cdot W_a \right) = 0.03251$$

$$m_a(n) := \frac{m_{\text{res}(n)}}{(1 + W_a)}$$

$$m_{\text{vin}(n)} := m_{\text{res}(n)} - m_a(n)$$

$$m_{\text{wres}(n)} := m_{\text{res}(n)} \cdot (W_{\text{ex}} - W_a)$$

**Sensible Respiratory Heat Transfer (W)**

$$Q_{\text{ress}(n)} := [m_a(n) \cdot C_{p_a} \cdot (T_{\text{ex}} - T_a) + m_{\text{vin}(n)} \cdot C_{p_v} \cdot (T_{\text{ex}} - T_a)]$$

**Latent Respiratory Heat Transfer (W)**

$$Q_{\text{resl}(n)} := m_{\text{wres}(n)} \cdot h_{f_{g_{\text{ex}}}}$$

**Total Respiratory Heat Transfer (W)**

$$q_{\text{res}(n)} := Q_{\text{ress}(n)} + Q_{\text{resl}(n)}$$

### Body heat transfer calculations:

$$mf_{shiv}(T_{sk}, T_{cr}) := 19.4 \frac{W}{m^2 \cdot K^2} [(34 + 273.15)K - T_{sk}] \cdot [(37 + 273.15)K - T_{cr}]$$

$$M_{shiv}(T_{sk}, T_{cr}) := \begin{cases} mf_{shiv}(T_{sk}, T_{cr}) & \text{if } T_{sk} < (34 + 273.15)K \wedge T_{cr} < (37 + 273.15)K \\ 0 & \text{otherwise} \end{cases}$$

### Blood flow rate (L/min)

$$qf_{bl}(T_{sk}, T_{cr}) := \frac{BFN + c_{dil} [T_{cr} - (37 + 273.15)K]}{1 + S_{tr} [(34 + 273.15)K - T_{sk}]} \cdot \frac{L}{m^2 \cdot hr}$$

$$Q_{bl}(T_{sk}, T_{cr}) := \begin{cases} qf_{bl}[(34 + 273.15)K, T_{cr}] & \text{if } T_{sk} \geq (34 + 273.15)K \wedge T_{cr} > (37 + 273.15)K \\ qf_{bl}[(34 + 273.15)K, (37 + 273.15)K] & \text{if } T_{sk} > (34 + 273.15)K \wedge T_{cr} \leq (37 + 273.15)K \\ qf_{bl}[T_{sk}, (37 + 273.15)K] & \text{if } T_{sk} < (34 + 273.15)K \wedge T_{cr} \leq (37 + 273.15)K \\ qf_{bl}(T_{sk}, T_{cr}) & \text{otherwise} \end{cases}$$

### Skin Compartment Factor

$$\alpha_{sk}(T_{sk}, T_{cr}, Qb) := 0.0418 + \frac{0.745}{\frac{10.8 \cdot Qb \cdot \frac{m}{s}}{\frac{L}{m^2 \cdot hr}} + 0.585} \quad \begin{array}{l} T_{skset} := (33.72 + 273.15)K = 306.87K \\ T_{crset} := (36.78 + 273.15)K = 309.93K \end{array}$$

### Required Regulatory Sweat Loss (W/m^2)

$$T_b(T_{sk}, T_{cr}, Qb) := (1 - \alpha_{sk}(T_{sk}, T_{cr}, Qb)) \cdot T_{cr} + \alpha_{sk}(T_{sk}, T_{cr}, Qb) \cdot T_{sk}$$

$$T_{bset}(T_{sk}, T_{cr}, Qb) := \left( 1 - \alpha_{sk} \left( T_{skset}, T_{crset}, Q_{bl} \left( T_{skset}, T_{crset}, \frac{s}{m} \right) \right) \right) \cdot T_{cr} \dots \\ + \alpha_{sk} \left( T_{skset}, T_{crset}, Q_{bl} \left( T_{skset}, T_{crset}, \frac{s}{m} \right) \right) \cdot T_{sk}$$

$$B1(T_{sk}) := \begin{cases} 0 & \text{if } T_{sk} < (34 + 273.15)K \\ \lceil T_{sk} - (34 + 273.15)K \rceil & \text{otherwise} \end{cases}$$

$$B2(T_{sk}, T_{cr}, Qb) := \begin{cases} 0 & \text{if } \left( T_b(T_{sk}, T_{cr}, Qb) - T_b\left(T_{skset}, T_{crset}, Q_{bl}\left(T_{skset}, T_{crset}, \frac{s}{m}\right)\right) \right) < 0 \\ \left( \left( T_b(T_{sk}, T_{cr}, Qb) - T_b\left(T_{skset}, T_{crset}, Q_{bl}\left(T_{skset}, T_{crset}, \frac{s}{m}\right)\right) \right) \right) & \text{otherwise} \end{cases}$$

$$ersw(T_{sk}, T_{cr}, Qb, n) := c_{sw}(n) \cdot B2(T_{sk}, T_{cr}, Qb) \cdot e^{\frac{B1(T_{sk})}{10.7K}}$$

$$E_{rsw}(T_{sk}, T_{cr}, Qb, n) := \begin{cases} ersw(T_{sk}, T_{cr}, Qb, n) & \text{if } ersw(T_{sk}, T_{cr}, Qb, n) \leq 670 \frac{W}{m} \\ 670 \frac{W}{m} & \text{otherwise} \end{cases}$$

### Body calculations:

#### Maximum Evaporation (W/m<sup>2</sup>)

$$Re_T(w_c) := (1 - w_c) \cdot \left[ Re_{cl} + \frac{1}{(f_{cl} \cdot h_e)} \right] + \frac{w_c \cdot 1}{(f_{cl} \cdot h_e)}$$

$$E_{max}(T_{sk}) := \frac{(P_{sat}(T_{sk}) - P_{sat}(T_a) \cdot \phi)}{Re_{cl} + \frac{1}{(f_{cl} \cdot h_e)}}$$

#### Skin Wettedness Factor

$$w_e(T_{sk}, T_{cr}, Qb, n) := \left( 0.06 + 0.94 \frac{E_{rsw}(T_{sk}, T_{cr}, Qb, n)}{E_{max}(T_{sk})} \right)$$

$$w(T_{sk}, T_{cr}, Qb, n) := \begin{cases} 1 & \text{if } w_e(T_{sk}, T_{cr}, Qb, n) > 1 \\ 0 & \text{if } w_e(T_{sk}, T_{cr}, Qb, n) < 0 \\ w_e(T_{sk}, T_{cr}, Qb, n) & \text{otherwise} \end{cases}$$

#### Conduction/Radiation Heat Transfer (W/m<sup>2</sup>)

$$CR(T_{sk}) := \frac{(T_{sk} - T_o)}{R_{cl} + \frac{1}{f_{cl} \cdot h_t}}$$

#### Skin Evap Heat Transfer (W/m<sup>2</sup>)

$$E_{sk}(T_{sk}, T_{cr}, Qb, w_c, n) := \begin{cases} \left[ w(T_{sk}, T_{cr}, Qb, n) \cdot \frac{(P_{sat}(T_{sk}) - P_{sat}(T_a) \cdot \phi)}{Re_T(0)} \right] & \text{if } (P_{sat}(T_{sk}) - P_{sat}(T_a) \cdot \phi) \geq 0 \\ 0 & \text{otherwise} \end{cases}$$

#### Evap from wetted spot

$$E_{spot}(T_{sk}, T_{cr}, Qb, n, w_c) := \begin{cases} \frac{(P_{sat}(T_{sk}) - P_{sat}(T_a) \cdot \phi)}{\frac{1}{(f_{cl} \cdot h_e)}} & \text{if } (P_{sat}(T_{sk}) - P_{sat}(T_a) \cdot \phi) \geq 0 \\ 0W & \text{otherwise} \end{cases}$$

### Sweat Storage Per Rate

$$m_{st}(T_{sk}, T_{cr}, Qb, n, w_c) := \begin{cases} \frac{[E_{rsw}(T_{sk}, T_{cr}, Qb, n) - (1 - w_c) \cdot E_{sk}(T_{sk}, T_{cr}, Qb, w_c, n)] \cdot \psi_w}{hfg_{ex}} \cdot \Delta t \cdot A_D(n) & \text{if } E_{rsw}(T_{sk}, T_{cr}, Qb, n) > E_{sk}(T_{sk}, T_{cr}, Qb, w_c, n) \wedge w_c \leq \text{Cutoff} \wedge w(T_{sk}, T_{cr}, Qb, n) \geq 1 \\ 0 \text{kg} & \text{otherwise} \end{cases}$$

$$m_{sevap}(T_{sk}, T_{cr}, Qb, n, w_c) := \begin{cases} \frac{w_c \cdot E_{spot}(T_{sk}, T_{cr}, Qb, n, w_c)}{hfg_{ex}} \cdot \Delta t \cdot A_D(n) & \text{if } 0 < w_c \leq \text{Cutoff} \\ 0 \text{kg} & \text{otherwise} \end{cases}$$

### Skin Temperature (K)

$$T_{ski}(T_{sk}, T_{cr}, Qb, w_c, n, \text{time}) := \frac{\left[ (1 - w_c) \cdot CR(T_{sk}) + (1 - w_c) \cdot E_{sk}(T_{sk}, T_{cr}, Qb, w_c, n) + \varepsilon_s \cdot w_c \cdot E_{spot}(T_{sk}, T_{cr}, Qb, n, w_c) + \frac{PCSCool(n, \text{time})}{1.8m^2} \right] + \left( K_{eff} + \rho_{bl} \cdot Qb \cdot \frac{m}{s} \cdot C_{pb} \right) (T_{cr} - T_{sk})}{\left( \frac{\alpha_{sk}(T_{sk}, T_{cr}, Qb) \cdot \text{mass}(n) \cdot C_{sk}}{A_D(n) \cdot \Delta t} \right)} + T_{sk}$$

### Core Temperature (K)

$$T_{cn}(T_{sk}, T_{cr}, Qb, n) := \frac{M(n) + M_{shiv}(T_{sk}, T_{cr}) - \frac{Wk(n) + W_{dragcycl}(n) + q_{res}(n)}{A_D(n)} - \left( K_{eff} + \rho_{bl} \cdot Qb \cdot \frac{m}{s} \cdot C_{pb} \right) (T_{cr} - T_{sk})}{\left[ \frac{(1 - \alpha_{sk}(T_{sk}, T_{cr}, Qb)) \cdot \text{mass}(n) \cdot C_{cr}}{A_D(n) \cdot \Delta t} \right]} + T_{cr}$$

### Fraction clothing area 100% wetted

Useful area wetted      Mass to wetted area equation

$$\text{Areawet}(m_{\text{stt}}) := m_{\text{stt}} \cdot \frac{1.0437 \cdot \text{m}^2}{\text{kg}} \quad \text{mass}_{\text{sw}}(m_{\text{stt}}) := \frac{\text{Areawet}(m_{\text{stt}})}{\frac{1.0437 \cdot \text{m}^2}{\text{kg}}}$$

$$m_{\text{sx}}(m_{\text{stt}}, n) := \begin{cases} m_{\text{stt}} & \text{if } \frac{\text{Areawet}(m_{\text{stt}})}{A_{\text{D}}(n)} \leq \text{Cutoff} \\ \left( \text{Cutoff} \cdot A_{\text{D}}(n) \cdot \frac{\text{kg}}{1.75 \text{m}^2} \right) & \text{otherwise} \end{cases}$$

### Initial (Dummy) body Temperatures:

$$w_{\text{ma}}(T_{\text{sk}}, T_{\text{cr}}, Qb, n, m_{\text{stt}}) := \begin{cases} \frac{\text{Areawet}(m_{\text{stt}})}{A_{\text{D}}(n)} & \text{if } m_{\text{stt}} \geq 0 \\ 0 & \text{otherwise} \end{cases}$$

$$w_{\text{mc}}(T_{\text{sk}}, T_{\text{cr}}, Qb, n, m_{\text{stt}}) := \begin{cases} w_{\text{ma}}(T_{\text{sk}}, T_{\text{cr}}, Qb, n, m_{\text{stt}}) & \text{if } w_{\text{ma}}(T_{\text{sk}}, T_{\text{cr}}, Qb, n, m_{\text{stt}}) \leq \text{Cutoff} \\ \text{Cutoff} & \text{otherwise} \end{cases}$$

$$w_{\text{m}}(T_{\text{sk}}, T_{\text{cr}}, Qb, n, m_{\text{stt}}) := \begin{cases} w_{\text{mc}}(T_{\text{sk}}, T_{\text{cr}}, Qb, n, m_{\text{stt}}) & \text{if } w_{\text{mc}}(T_{\text{sk}}, T_{\text{cr}}, Qb, n, m_{\text{stt}}) \leq 0.68 \\ 0.68 & \text{otherwise} \end{cases}$$

HT from bloodflow Core to Skin (W/m<sup>2</sup>)

$$Q_{\text{bflow}}(T_{\text{sk}}, T_{\text{cr}}, Qb) := \left( K_{\text{eff}} + \rho_{\text{bl}} \cdot Qb \cdot \frac{\text{m}}{\text{s}} \cdot C_{\text{pb}} \right) (T_{\text{cr}} - T_{\text{sk}})$$

**Compile calculations:**

SubNum := 24

**Desired Values for Heat Loss and Temp Change per  $\Delta T$**

```

PerSec := Num ← SubNum
          n ← Num - 1
          Tcr ← Tcm(n)
          Tsk ← Tskn(n)
          i ← 0
          mST ← 0kg
          for i ∈ 0..  $\frac{\text{Time}_n(n)}{\Delta t}$ 
            Qb1 ← Qbl(Tsk, Tcr) ·  $\frac{s}{m}$ 
            wc ← wm(Tsk, Tcr, Qb1, n, mST)
            Ti ← Tski(Tsk, Tcr, Qb1, wc, n, i ·  $\frac{\Delta t}{s}$ )
            Tc ← Tcri(Tsk, Tcr, Qb1, n)
            mST2 ← mST + mst(Ti, Tc, Qb1, n, wc) - msevap(Tsk, Tcr, Qb1, n, wc)
            DATAi,0 ←  $\frac{T_i}{K} - 273.15$ 
            DATAi,1 ←  $\frac{T_c}{K} - 273.15$ 
            DATAi,2 ← Qb1 · (3.6 · 106)
            DATAi,3 ← Esk(Tsk, Tcr, Qb1, wc, n) ·  $\frac{A_D(n)}{W}$ 
            DATAi,4 ← CR(Tsk) ·  $\frac{A_D(n)}{W}$ 
            DATAi,5 ← Qress(n) ·  $\frac{1}{W}$ 
            DATAi,6 ← Qresl(n) ·  $\frac{1}{W}$ 
            DATAi,7 ← Mshiv(Tsk, Tcr) · AD(n) ·  $\frac{1}{W}$ 
            DATAi,8 ← -Qbflow(Tsk, Tcr, Qb1) ·  $\frac{1 \cdot A_D(n)}{W}$ 
            DATAi,9 ← w(Tsk, Tcr, Qb1, n)

```



```

DATAi,10 ← (Qress(n) + Qresl(n)) ·  $\frac{1}{W}$ 
DATAi,11 ← we(Tsk, Tcr, Qb1, n)
DATAi,12 ← Ersw(Tsk, Tcr, Qb1, n)  $\frac{1 \cdot A_D(n)}{W}$ 
DATAi,13 ←  $\frac{\text{Time}_n(n)}{s}$ 
DATAi,14 ←  $\frac{\text{Re}_T(wc)}{\left(\frac{s}{m}\right)}$ 
DATAi,15 ← wc
DATAi,16 ←  $\frac{E_{\max}(T_{sk})}{\frac{W}{m^2}}$ 
DATAi,17 ←  $\frac{m_{sx}(m_{ST2}, n)}{\text{kg}}$ 
DATAi,18 ←  $\frac{E_{spot}(T_i, T_c, Q_{b1}, n, wc) \cdot A_D(n)}{W}$ 
DATAi,19 ←  $\frac{m_{st}(T_i, T_c, Q_{b1}, n, wc)}{\text{kg}}$ 
DATAi,20 ←  $\frac{wc \cdot A_D(n)}{m^2}$ 
DATAi,21 ← αsk(Ti, Tc, Qb1)
DATAi,22 ←  $\frac{m_{sevap}(T_{sk}, T_{cr}, Q_{b1}, n, wc)}{\text{kg}}$ 
DATAi,23 ←  $\frac{m_{st}(T_i, T_c, Q_{b1}, n, wc)}{\text{kg}}$ 
DATA
mSTI ← msx(mST2, n)
Tsk ← Ti
Tcr ← Tc
mST ← mSTI
i ← i + 1
DATA

```

## Output Formulas:

$$T_{\text{skin}}(j) := \text{PerSec}_{j,0}$$

$$T_{\text{core}}(j) := \text{PerSec}_{j,1}$$

$$Q_{\text{bj}}(j) := \text{PerSec}_{j,2} \cdot W$$

$$E_{\text{skj}}(j) := \text{PerSec}_{j,3} \cdot W$$

$$CR_T(j) := \text{PerSec}_{j,4} \cdot W$$

$$Q_{\text{resT}}(j) := (\text{PerSec}_{j,5} + \text{PerSec}_{j,6}) \cdot W$$

$$M_{\text{shivr}}(j) := \text{PerSec}_{j,7} \cdot W$$

$$w_j(j) := \text{PerSec}_{j,9}$$

$$SktoCr(j) := \text{PerSec}_{j,8} \cdot W$$

$$w_{\text{ea}}(j) := \text{PerSec}_{j,11}$$

$$E_{\text{rswADj}}(j) := \text{PerSec}_{j,12} \cdot W$$

$$\text{Time}_{\text{nj}}(j) := \text{PerSec}_{j,13} \cdot s$$

$$Re_T(j) := \text{PerSec}_{j,14} \cdot s$$

$$wc_j(j) := \text{PerSec}_{j,15}$$

$$E_{\text{maxj}}(j) := \text{PerSec}_{j,16} \cdot \frac{W}{m}$$

$$m_{\text{STj}}(j) := \text{PerSec}_{j,17} \cdot \text{kg}$$

$$m_{\text{evap}_{\text{spotj}}}(j) := \text{PerSec}_{j,18} \cdot \text{kg}$$

$$E_{\text{spotj}}(j) := \text{PerSec}_{j,18} \cdot W$$

$$m_{\text{stj}}(j) := \text{PerSec}_{j,19} \cdot \text{kg}$$

$$\text{Spotsize}(j) := \text{PerSec}_{j,20} \cdot m^2$$

$$\alpha(j) := \text{PerSec}_{j,21}$$

$$m_{\text{sevapj}}(j) := \text{PerSec}_{j,22} \cdot \text{kg}$$

$$m_{\text{stij}}(j) := \text{PerSec}_{j,23} \cdot \text{kg}$$

$$SW_T := \frac{\text{Time}_{nj}(1)}{\sum_{j=0}^{\Delta t} \frac{E_{rswADj(j)} \cdot \Delta t + \text{PerSec}_{j,6} \cdot W \cdot \Delta t}{hfg_{ex}}} = 0.93482 \text{ kg}$$

$$SW_{Evap} := \frac{\text{Time}_{nj}(1)}{\sum_{j=0}^{\Delta t} \frac{[E_{skj(j)} \cdot (1 - wcj(j)) + wcj(j) \cdot E_{spotj(j)}] \cdot \Delta t}{hfg_{ex}}} = 0.85224 \text{ kg}$$

$$\Delta w := \frac{\text{Time}_{nj}(1)}{\sum_{j=0}^{\Delta t} (w_{ea(j)} - w_j(j))} = 0$$

$$\text{Sweatdif} := SW_T - ASW(\text{SubNum} - 1)$$

$$ZZ := \left( \frac{\text{ReclAVG}}{s} \quad \text{CoreError} \quad w1_{\text{timepercent}} \quad Sw_{\text{mod}} \quad \frac{\text{Sweatdif}}{\text{kg}} \quad \frac{SW_{Evap}}{\text{kg}} \right)$$

$$YY := \left( \frac{\text{ReclAVG}}{s} \quad \text{CoreError} \quad w1_{\text{timepercent}} \quad \frac{\text{Sweatdif}}{\text{kg}} \quad \frac{SW_{Evap}}{\text{kg}} \right)$$

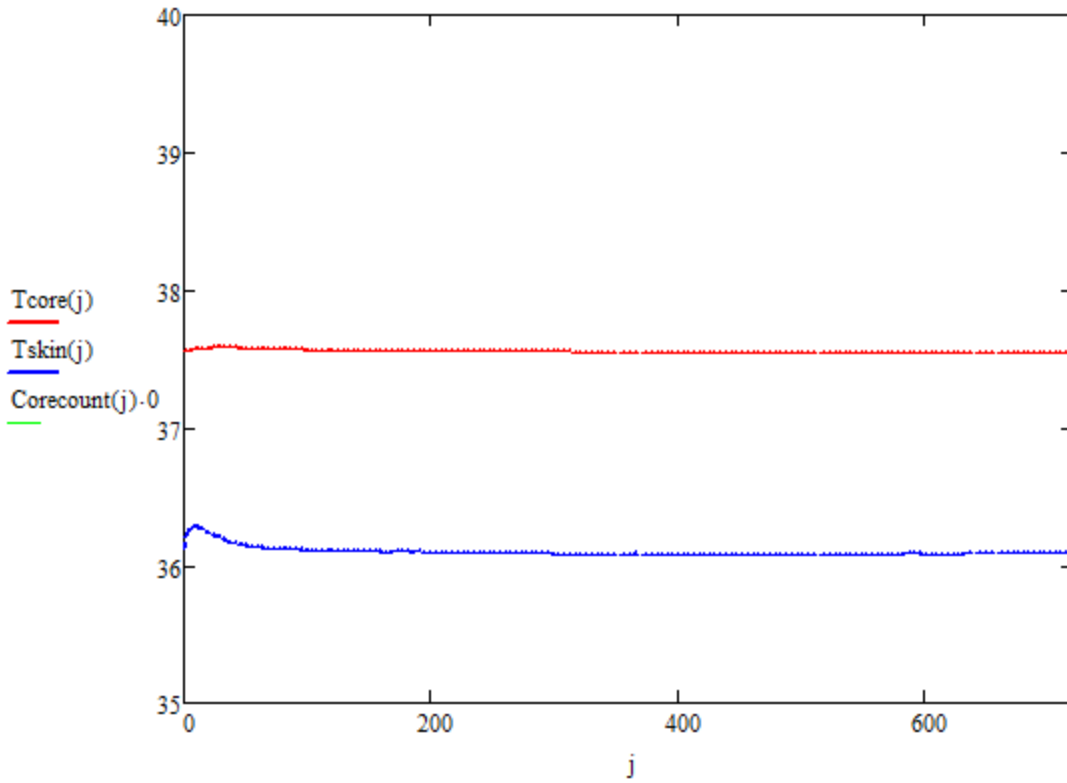
CoreError = 0.15133    Sweatdif = -1.02118 kg

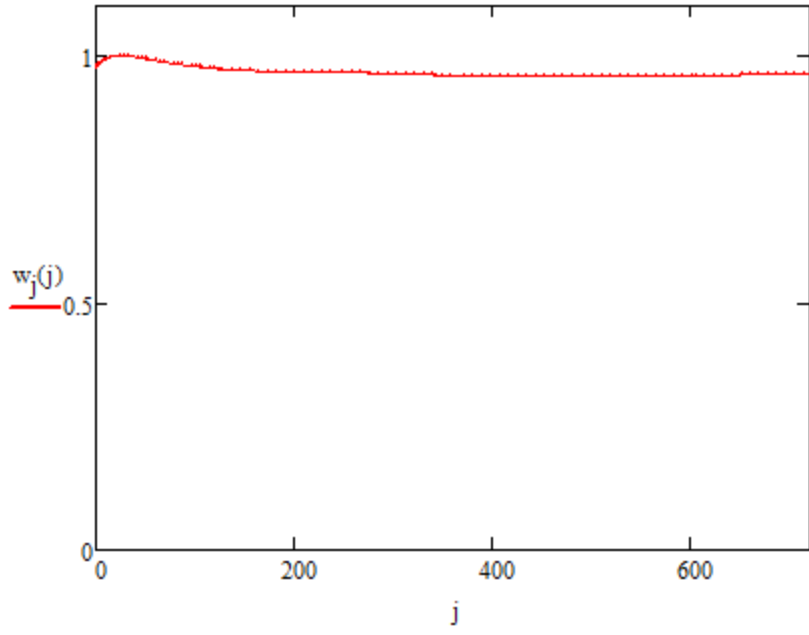
ZZ =

	0	1	2	3	4	5
0	26.2	0.15133	0	1	-1.02118	0.85224

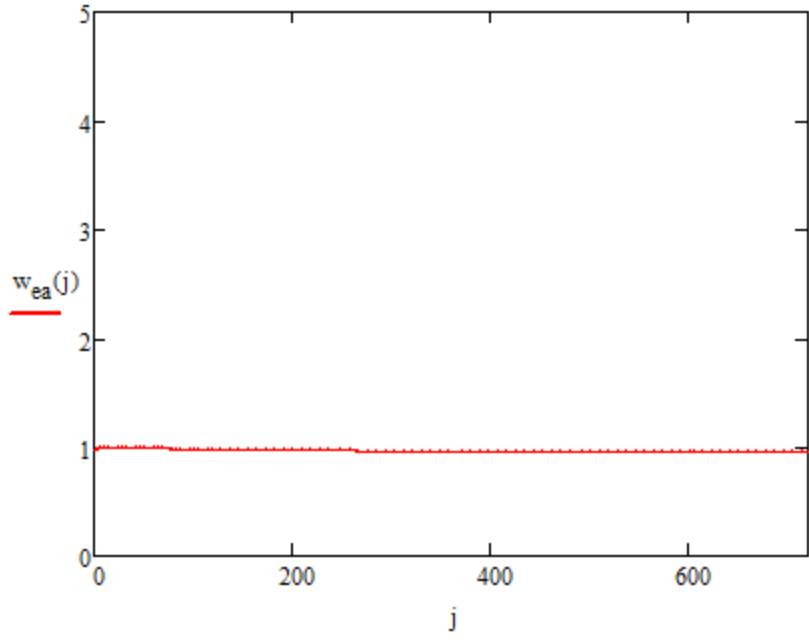
YY =

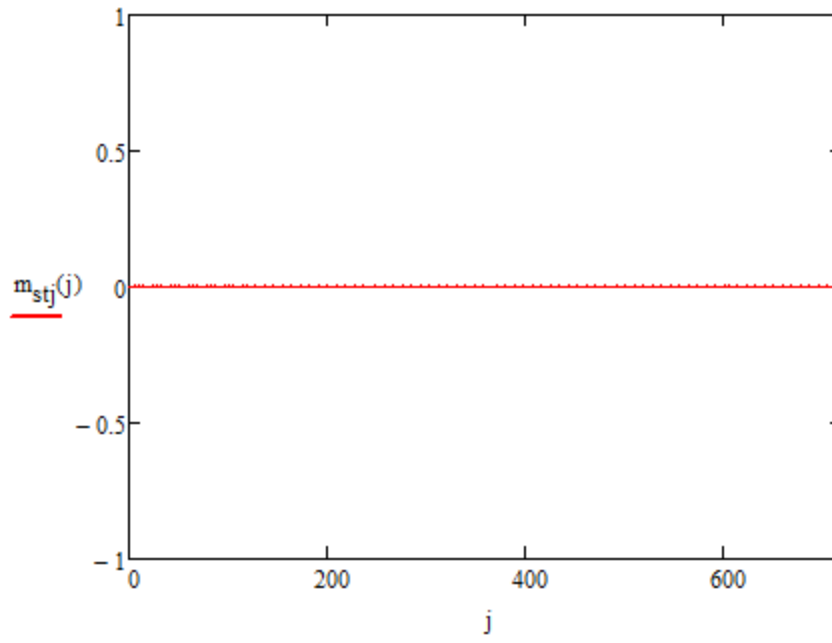
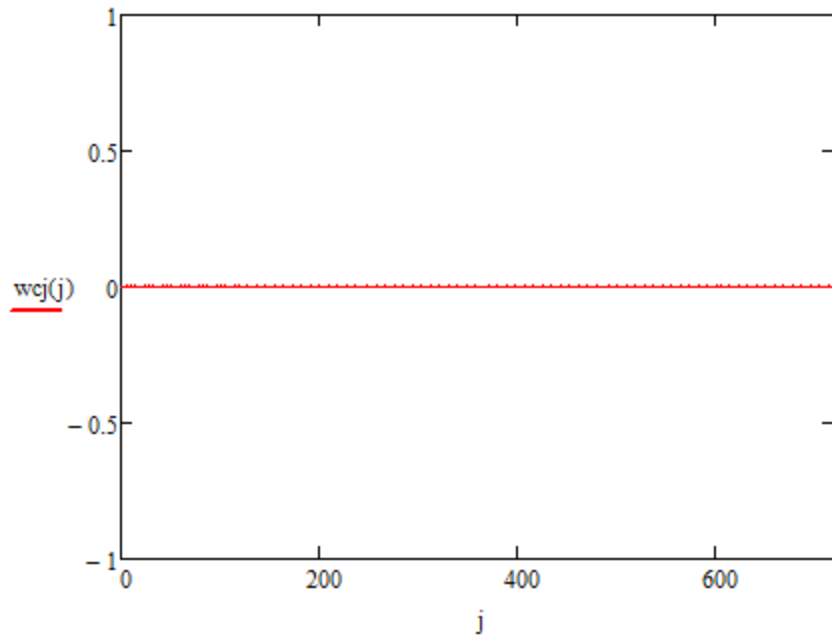
	0	1	2	3	4
0	26.2	0.15133	0	-1.02118	0.85224

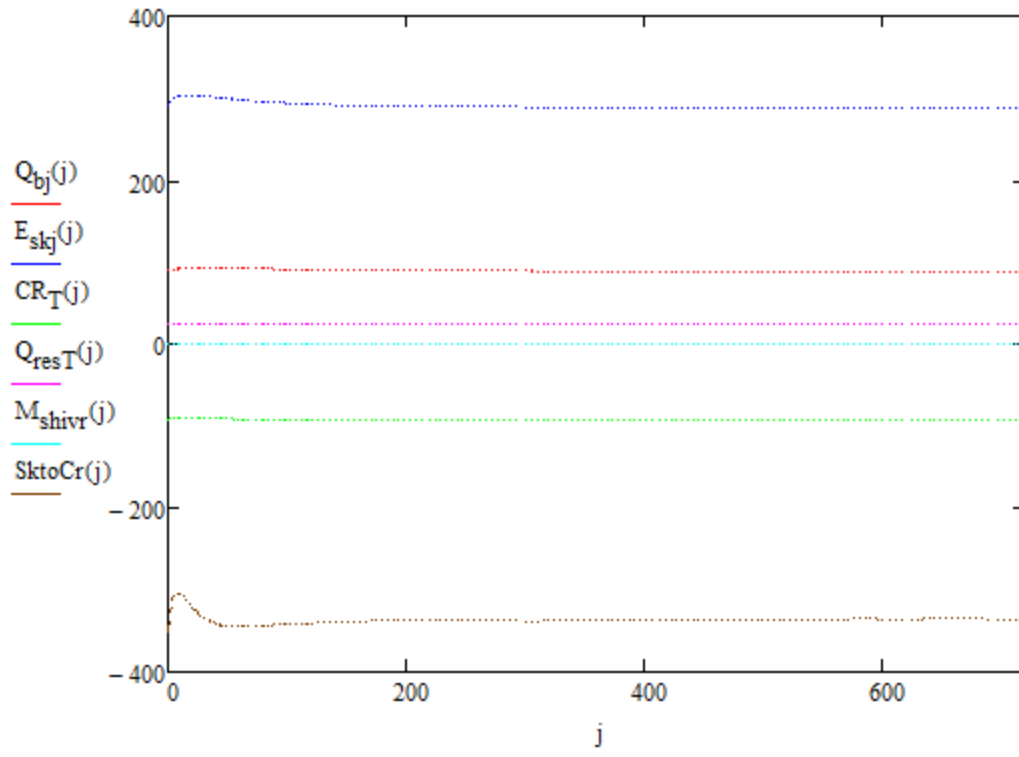




+







0-Tsk(C) 1-Tc(C) 2-Qbl(L/min) 3-Esk(W) 4-CR(W) 5-Qress(W) 6-Qresk(W) 7-Mshiv(W) 8-SktoSCr(W) 9-w(N/A) 10-QresT(W)

	0	1	2	3	4	5	6	7	8	9	10
0	36.12136	37.56246	90.75	291.24367	-92.2434	-3.47541	28.75483	0	-351.24711	0.97266	25.27942
1	36.16682	37.56242	90.6688	293.45529	-91.62004	-3.47541	28.75483	0	-337.01449	0.97566	25.27942
2	36.20196	37.56276	90.66308	295.28213	-91.14004	-3.47541	28.75483	0	-326.35502	0.97836	25.27942
3	36.22926	37.56338	90.71389	296.81198	-90.76894	-3.47541	28.75483	0	-318.38605	0.98081	25.27942
PerSec = 4	36.25057	37.56421	90.80697	298.11235	-90.48073	-3.47541	28.75483	0	-312.4509	0.98308	25.27942
5	36.26731	37.5652	90.93152	299.23515	-90.25571	-3.47541	28.75483	0	-308.05739	0.98519	25.27942
6	36.27176	37.5663	91.07938	300.22027	-90.0789	-3.47541	28.75483	0	-304.83453	0.98718	25.27942
7	36.27556	37.5674	91.24433	300.73542	-90.03193	-3.47541	28.75483	0	-304.57391	0.98855	25.27942
8	36.27885	37.56852	91.41066	301.22675	-89.99187	-3.47541	28.75483	0	-304.47137	0.98988	25.27942
9	36.28175	37.56963	91.57753	301.69867	-89.95713	-3.47541	28.75483	0	-304.48824	0.99118	25.27942
10	36.28435	37.57074	91.74431	302.15457	-89.9265	-3.47541	28.75483	0	-304.59502	0.99246	...



# TAItherm Model

Model Size (mm):  
 X = 7010.4  
 Y = 5486.4  
 Z = 3759.2

Visible Size (mm):  
 X = 7010.4  
 Y = 5486.4  
 Z = 3759.2

Visible Counts:  
 Parts = 47  
 Elements = 22572

02:01:00  
 Temperature

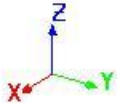
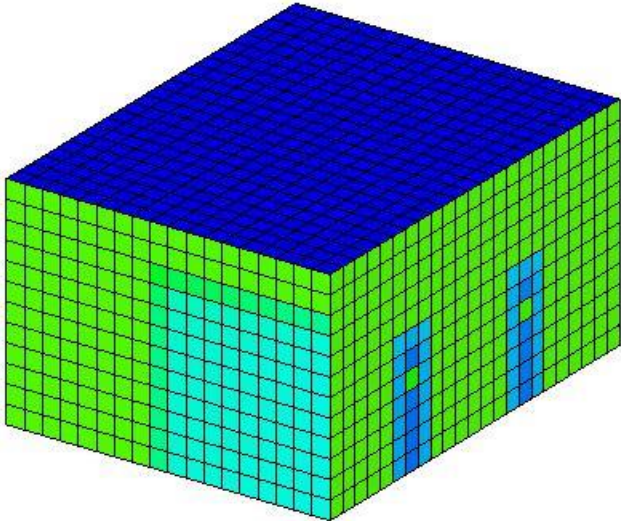


**Figure 8.35 Initial temperature, chamber outside, front isometric**

Model Size (mm):  
 X = 7010.4  
 Y = 5486.4  
 Z = 3759.2

Visible Size (mm):  
 X = 7010.4  
 Y = 5486.4  
 Z = 3759.2

Visible Counts:  
 Parts = 40  
 Elements = 21667

02:01:00  
 Temperature

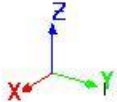
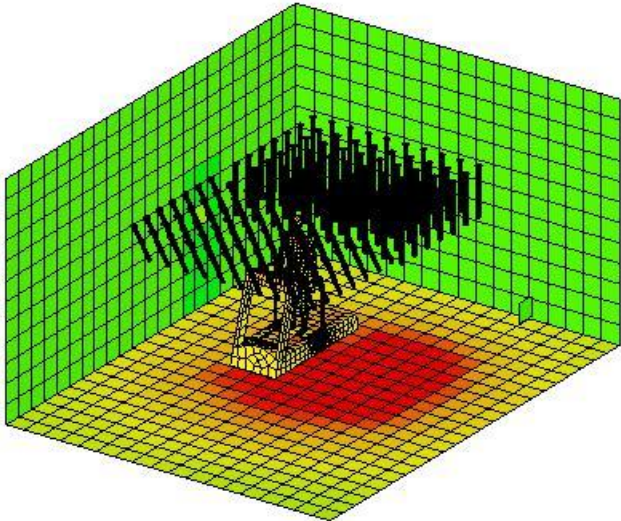


**Figure 8.36 Initial temperature, chamber inside with light cans, front isometric**

Model Size (mm):  
X = 7010.4  
Y = 5486.4  
Z = 3759.2

Visible Size (mm):  
X = 7010.4  
Y = 5486.4  
Z = 3759.2

Visible Counts:  
Parts = 38  
Elements = 10466

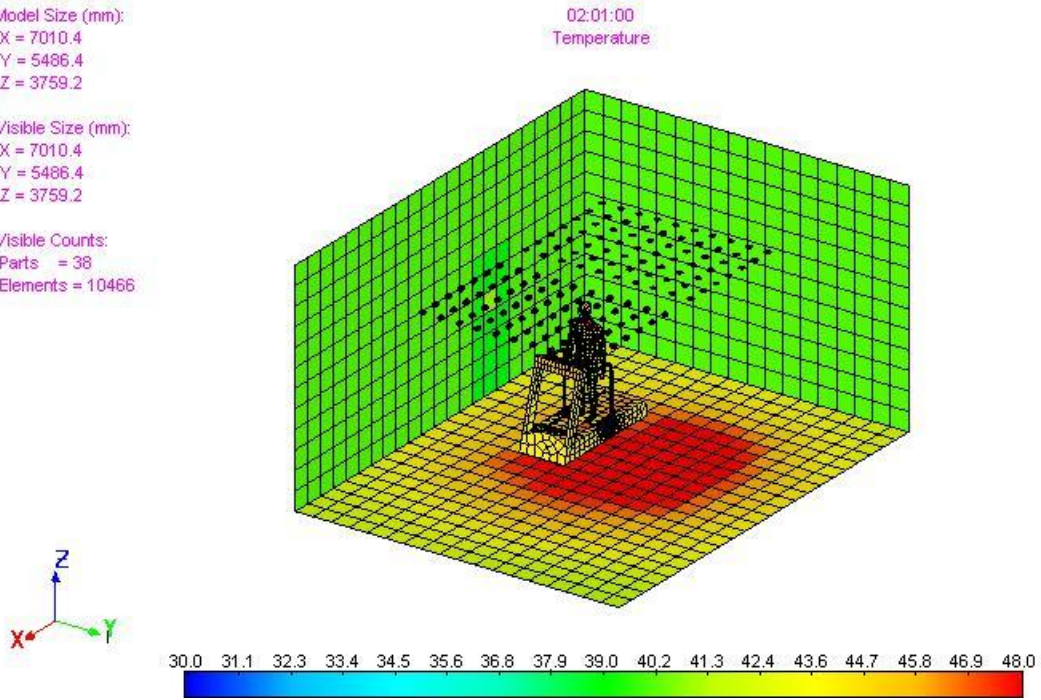


**Figure 8.37 Initial temperature, chamber inside without light cans, front isometric**

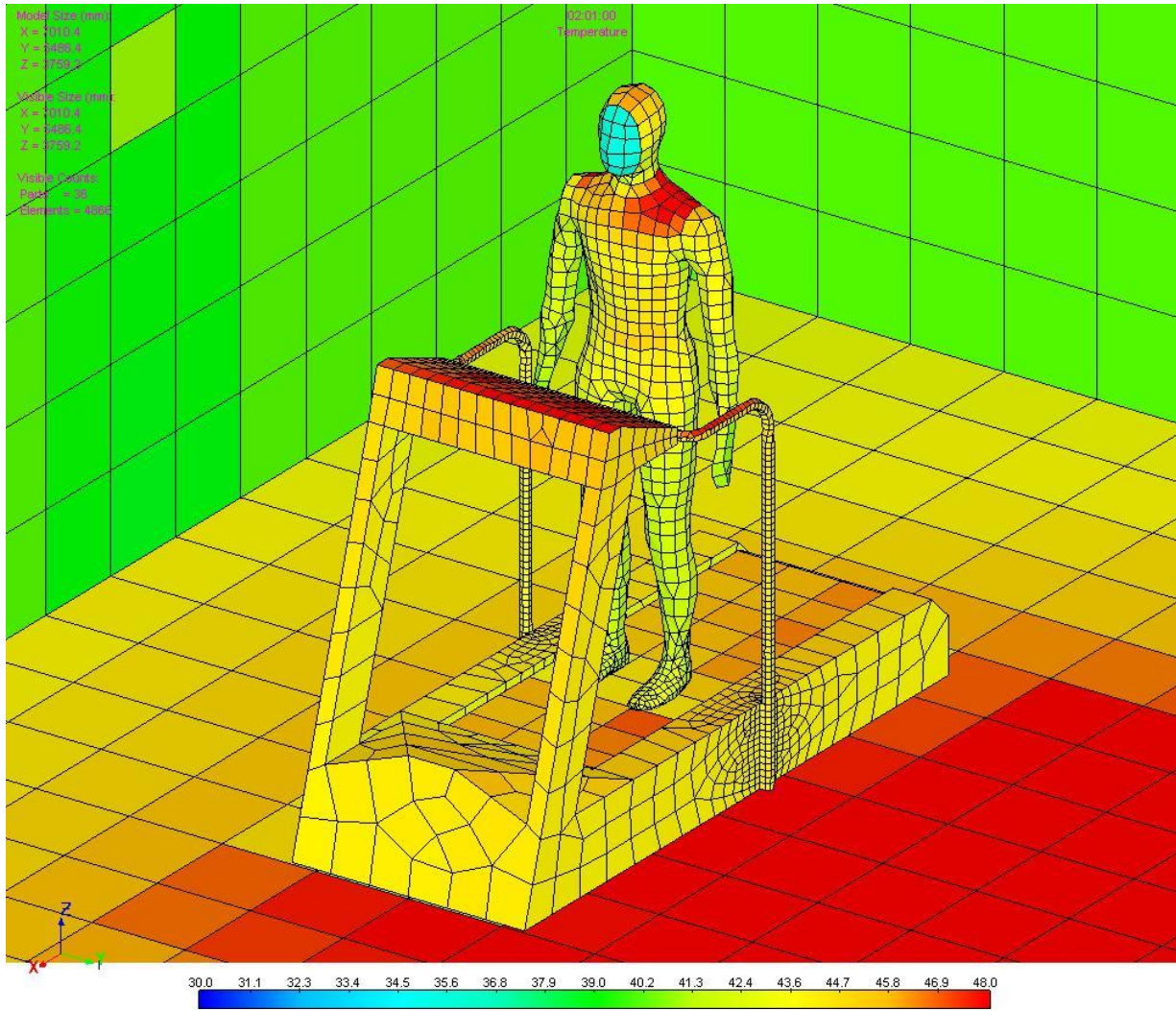


**Figure 8.38 Initial temperature, chamber inside zoomed on human**

Model Size (mm):  
X = 7010.4  
Y = 5486.4  
Z = 3759.2

02:01:00  
Temperature

Visible Size (mm):  
X = 7010.4  
Y = 5486.4  
Z = 3759.2

Visible Counts:  
Parts = 47  
Elements = 22572

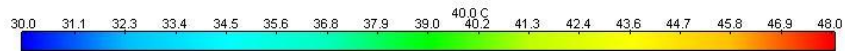
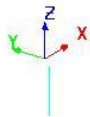
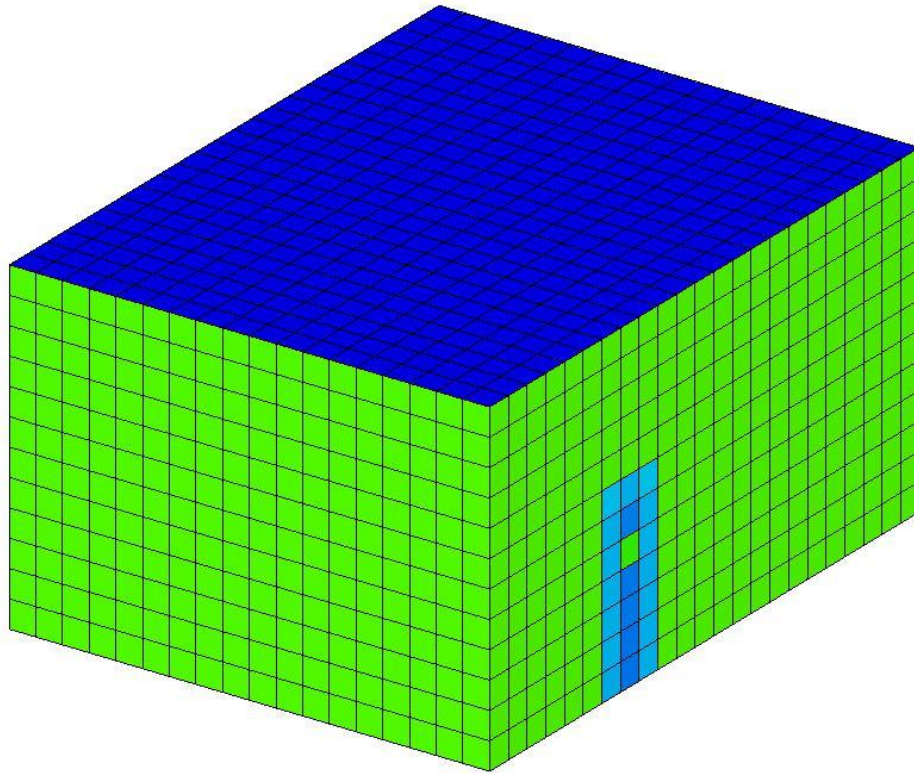


**Figure 8.39 Initial temperature, chamber outside, back isometric**

Model Size (mm):  
X = 7010.4  
Y = 5486.4  
Z = 3759.2

02:01:00  
Temperature

Visible Size (mm):  
X = 7010.4  
Y = 5486.4  
Z = 3759.2

Visible Counts:  
Parts = 42  
Elements = 21666

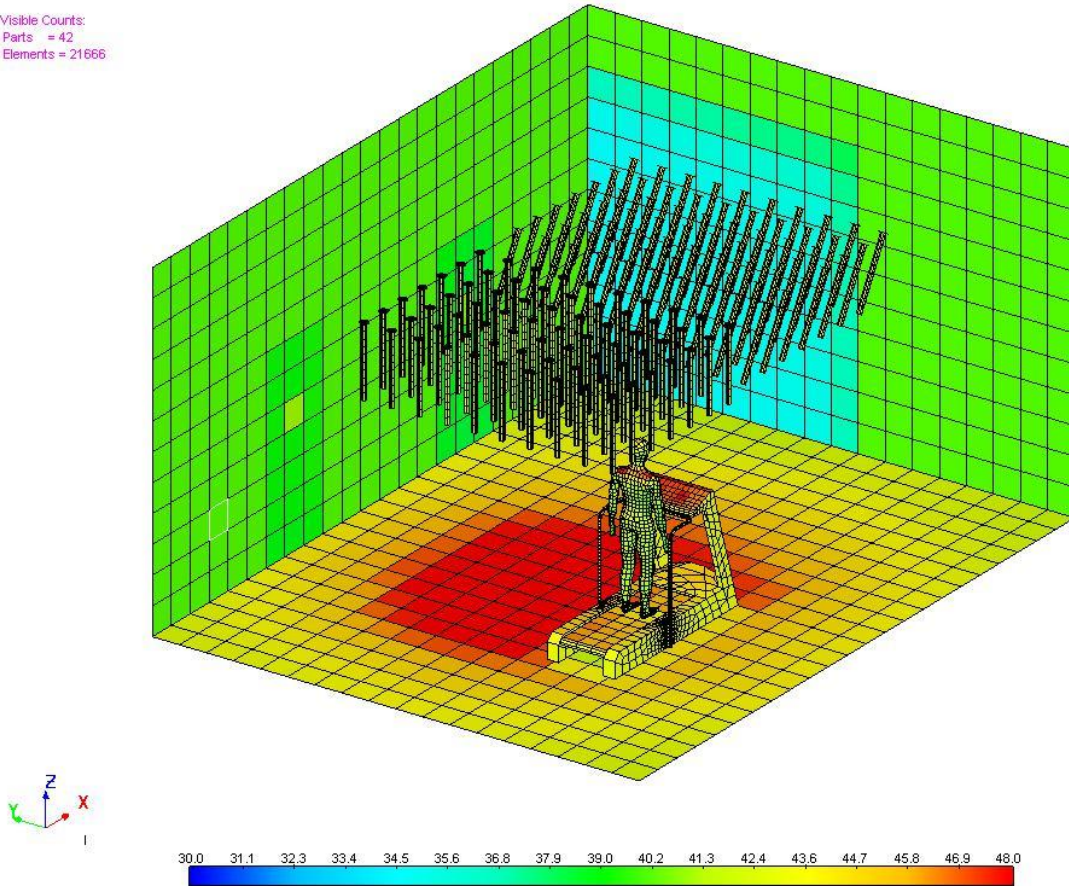


**Figure 8.40 Initial temperature, chamber inside with light cans, back isometric**

Model Size (mm):  
X = 7010.4  
Y = 5486.4  
Z = 3759.2

02:01:00  
Temperature

Visible Size (mm):  
X = 7010.4  
Y = 5486.4  
Z = 3759.2

Visible Counts:  
Parts = 41  
Elements = 10466

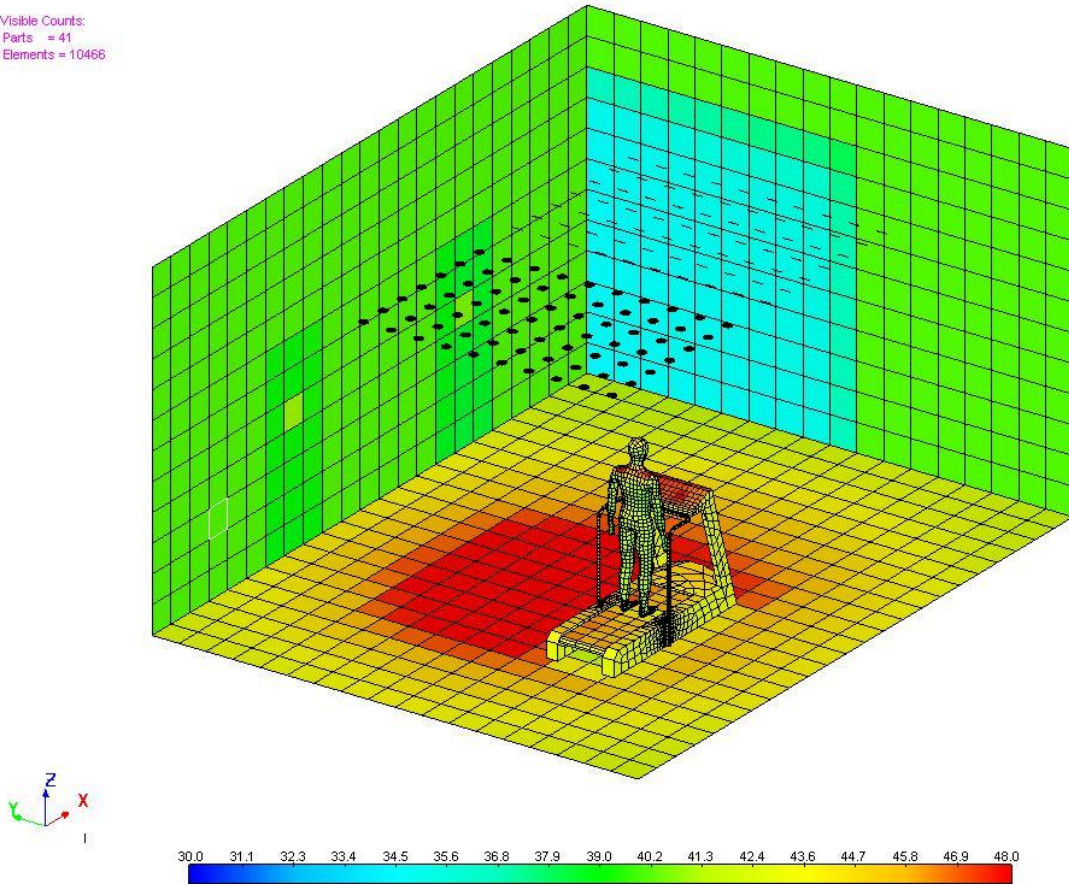


**Figure 8.41 Initial temperature, chamber inside without light cans, back isometric**

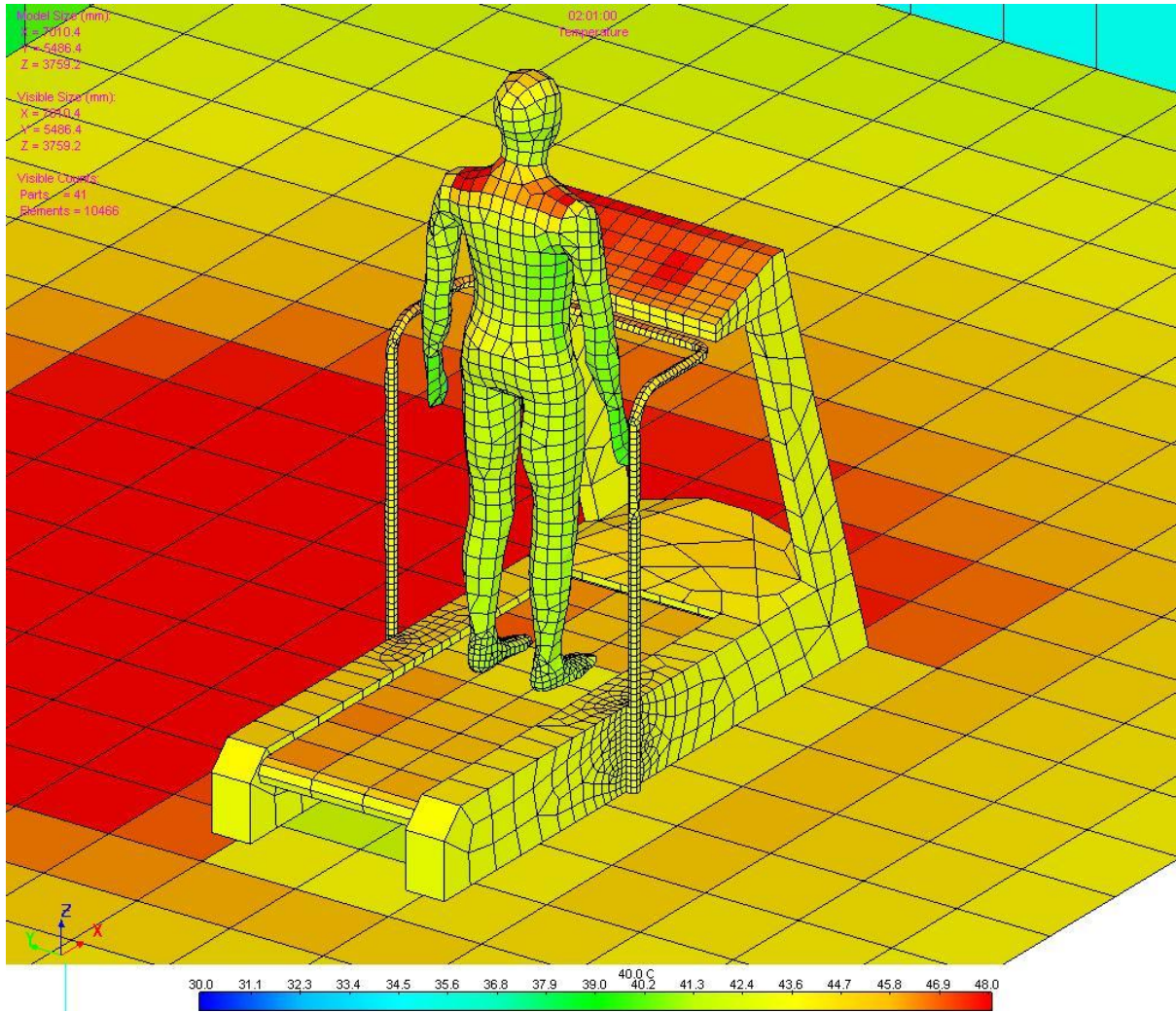


**Figure 8.42 Initial temperature, chamber inside zoomed on human, back**

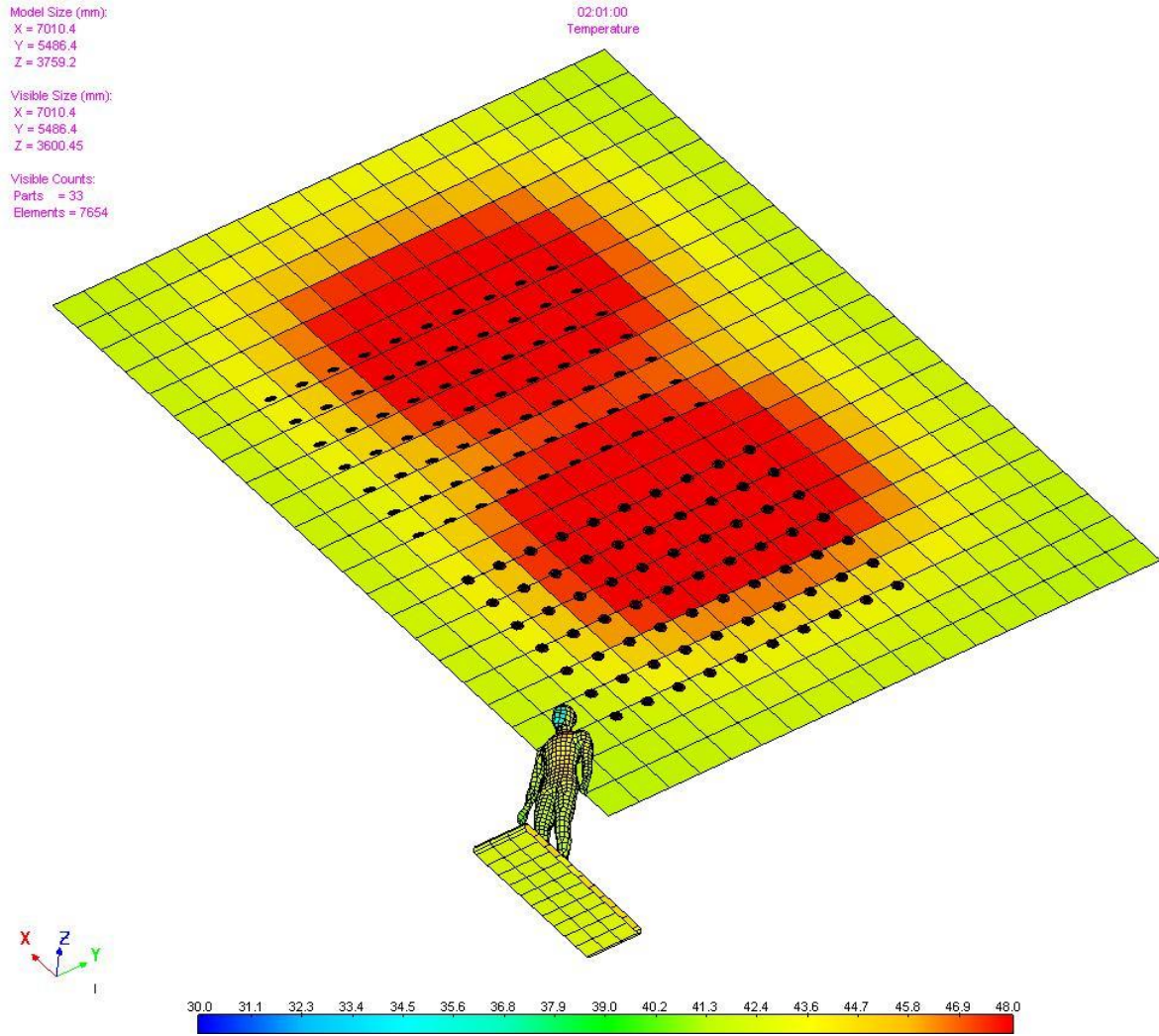


**Figure 8.43 Initial temperature, chamber inside, bottom view of roof subject and belt**



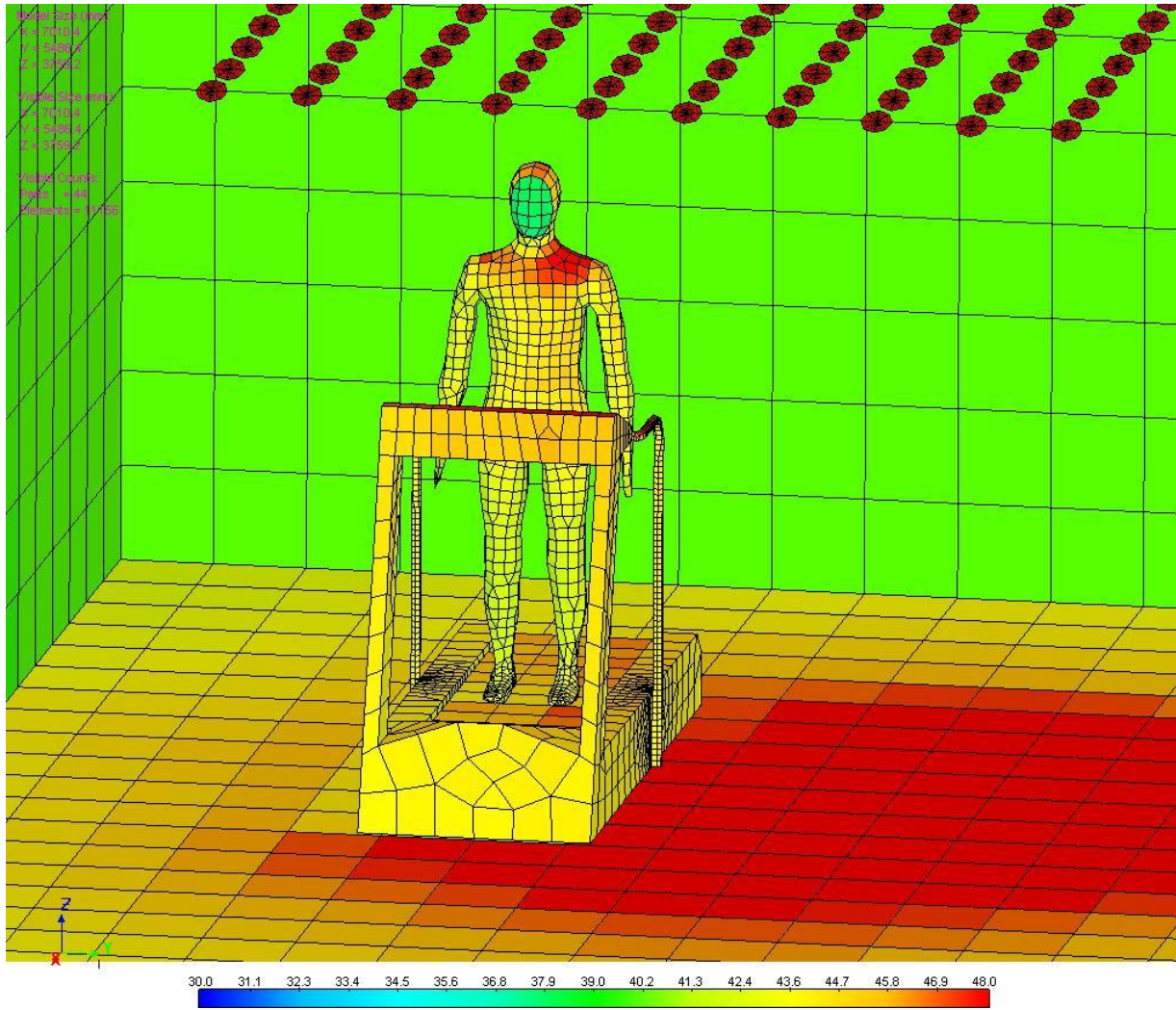
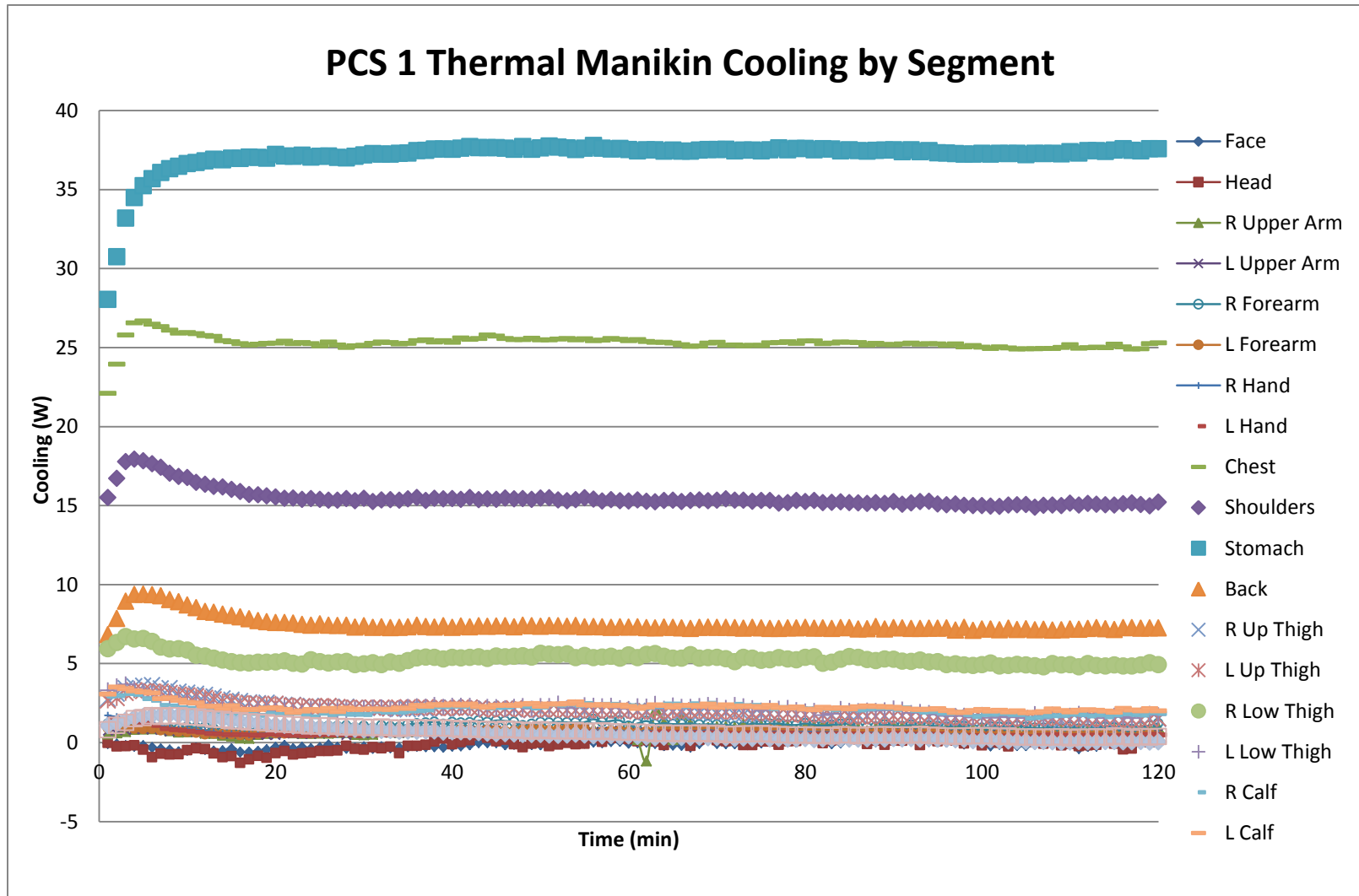


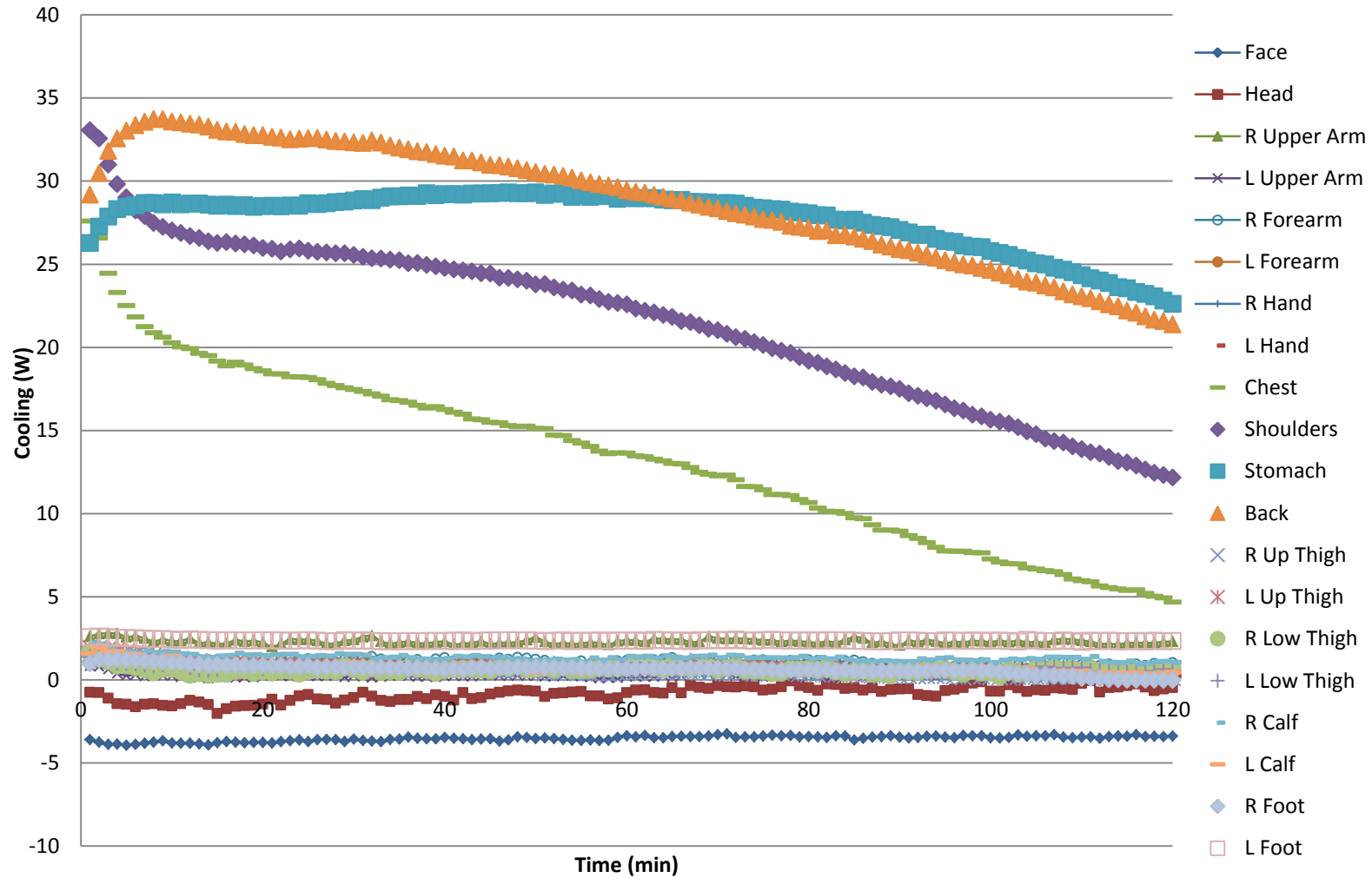
**Figure 8.44 Final temperatures, human subject, treadmill, lights**

# Appendix D- Testing Results

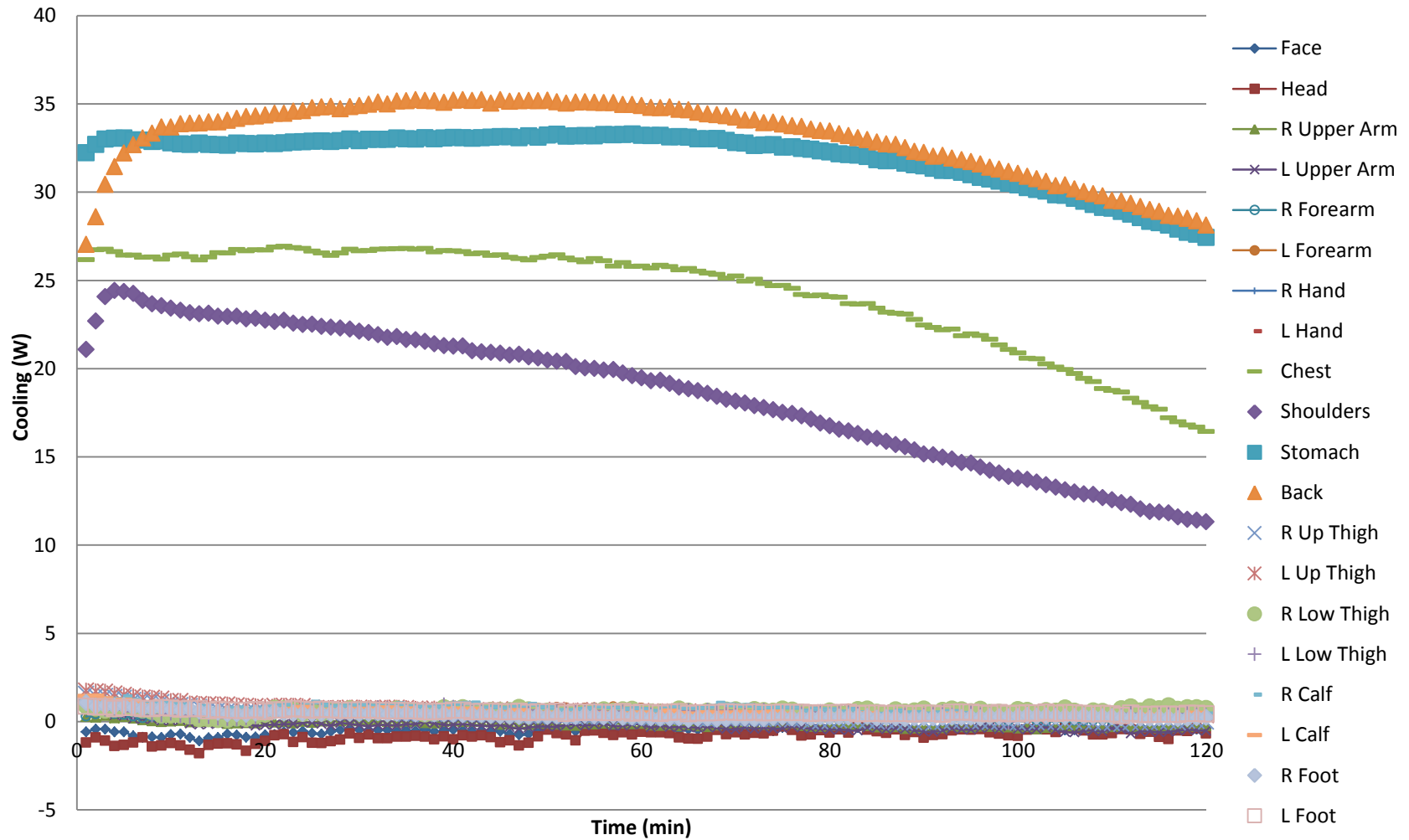
## Thermal Manikin PCS Cooling by Segment



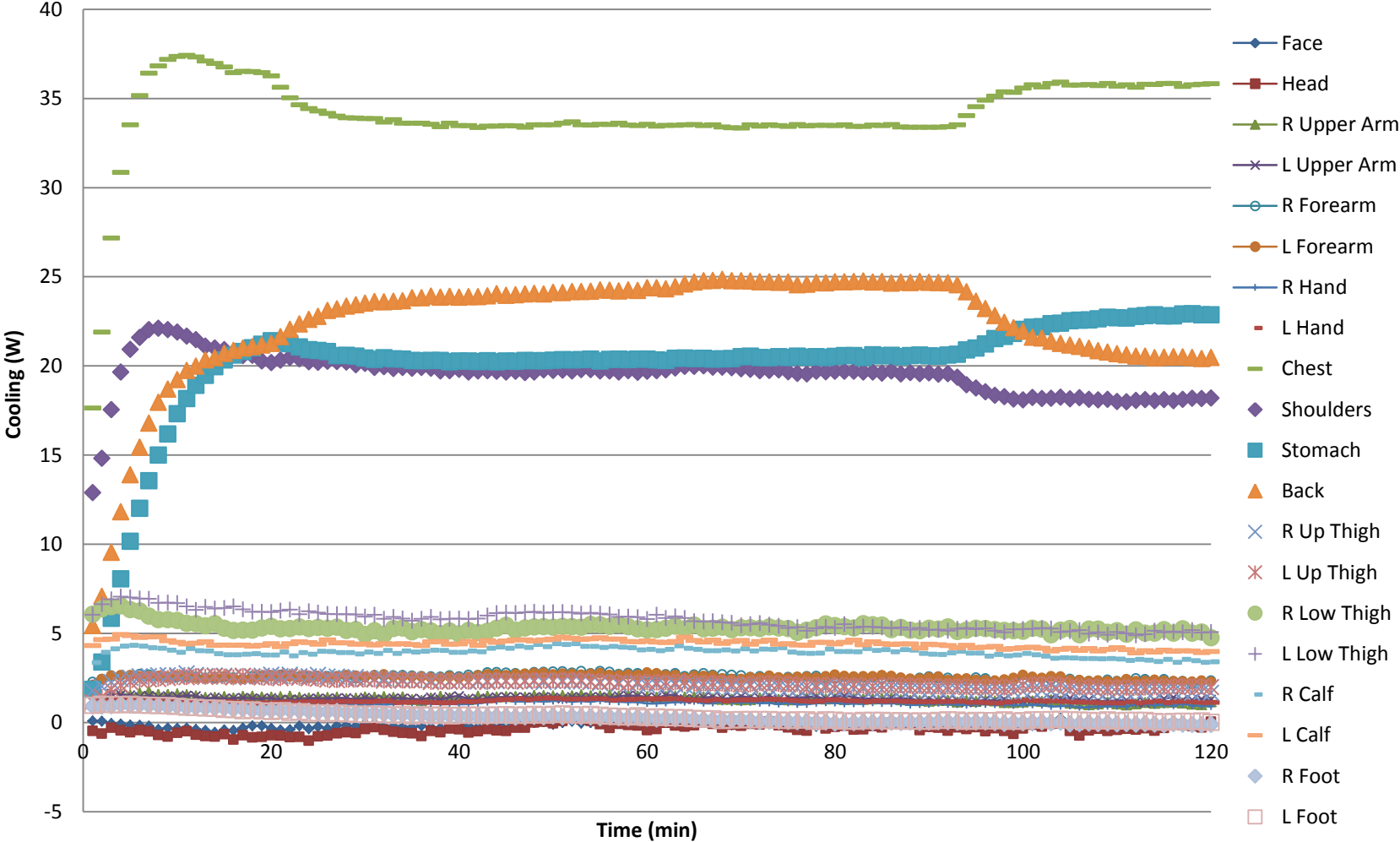
## PCS 9 Thermal Manikin Cooling by Segment



## PCS 12 Thermal Manikin Cooling by Segment



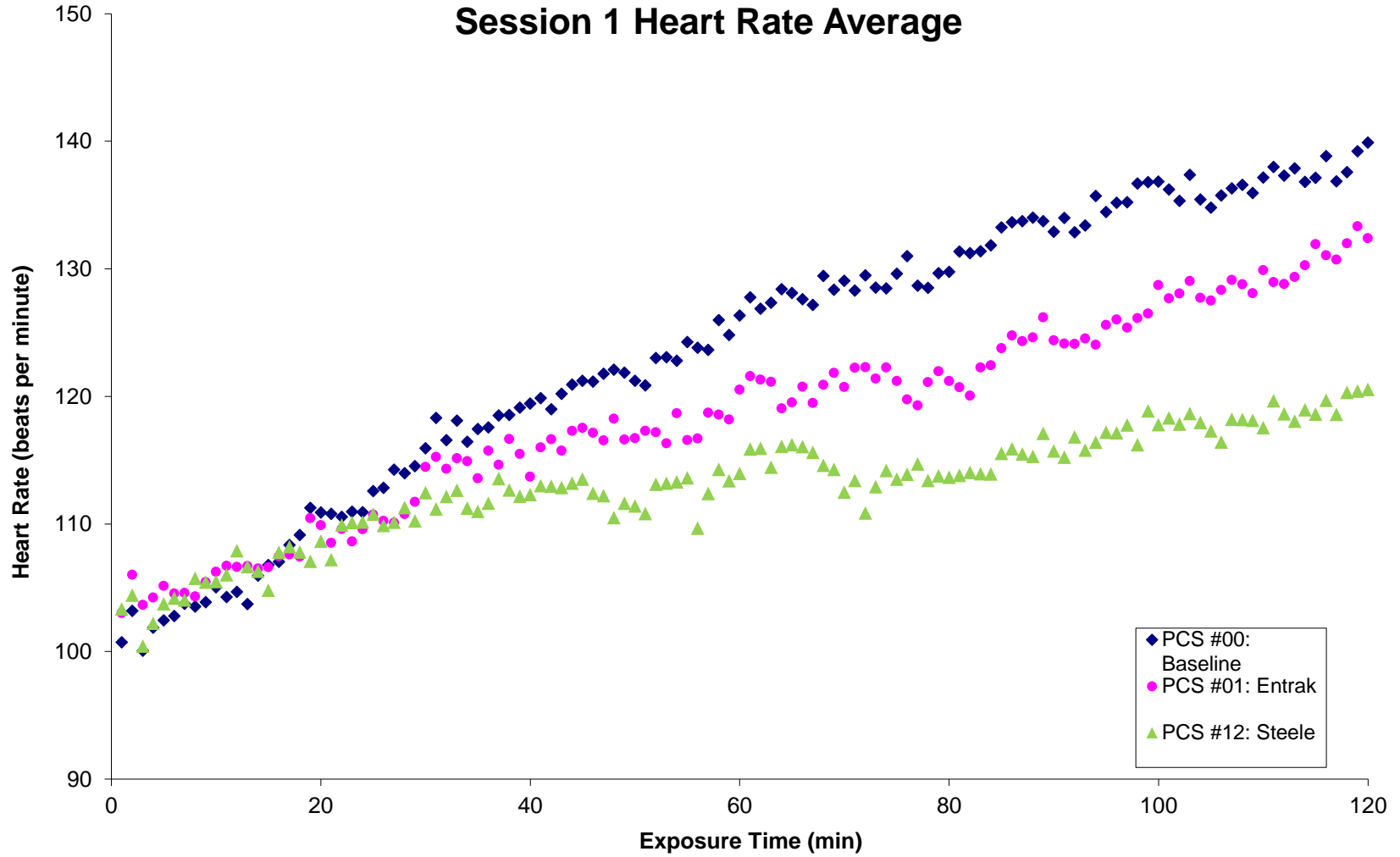
# PCS 20 Thermal Manikin Cooling by Segment



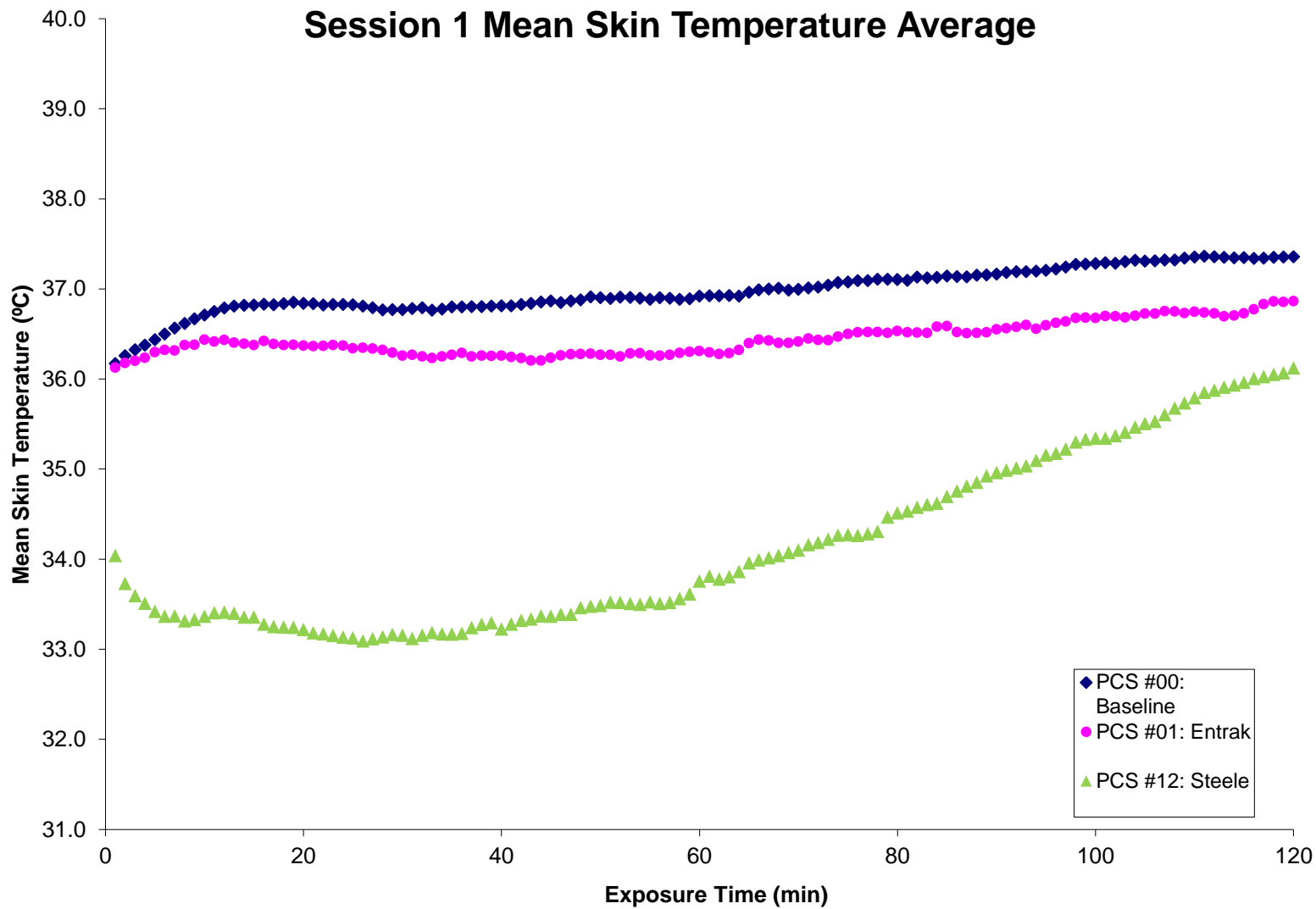
# Human subjects

*Session 1 (Subjects 1-12)*

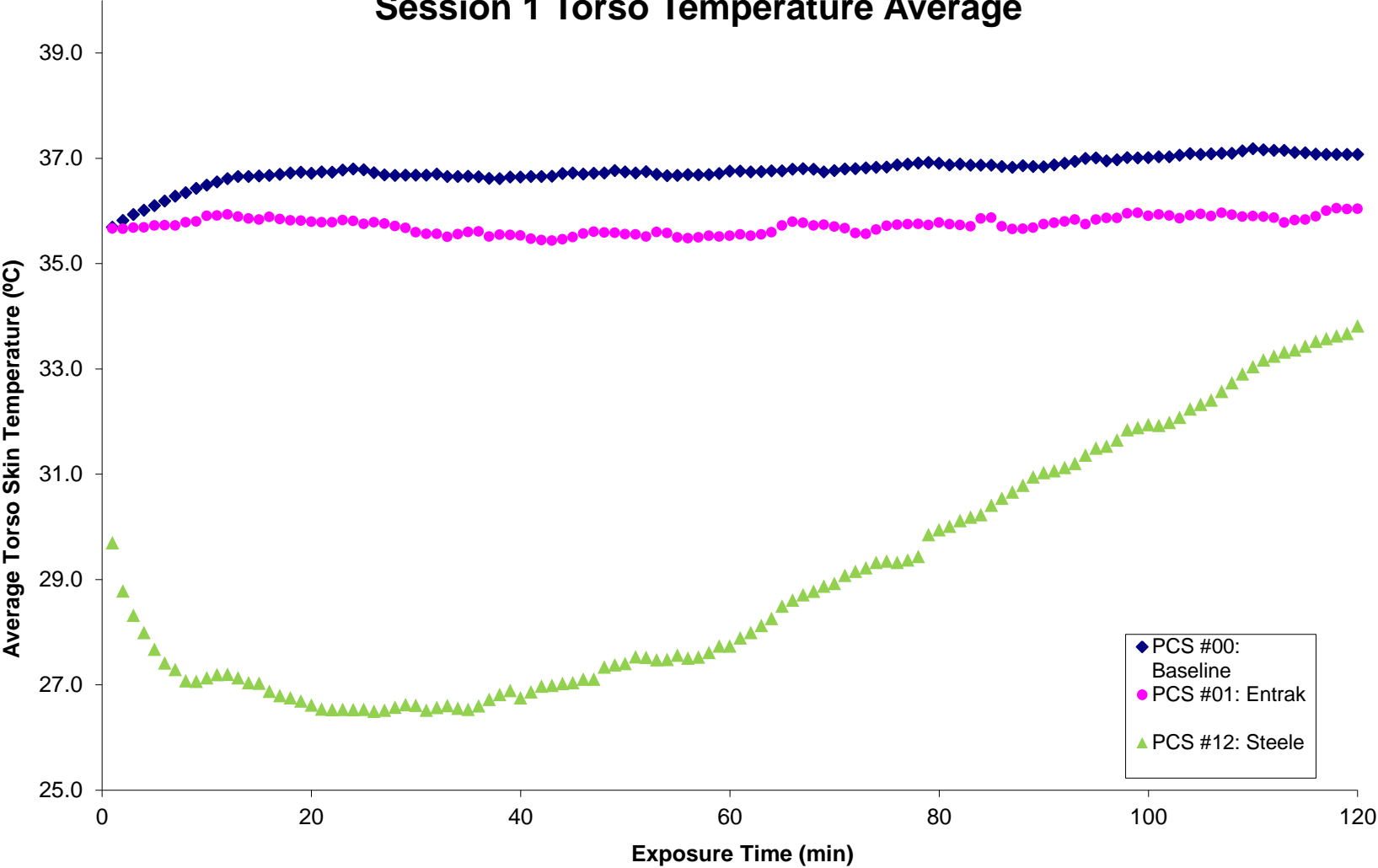
## Session 1 Heart Rate Average



# Session 1 Mean Skin Temperature Average

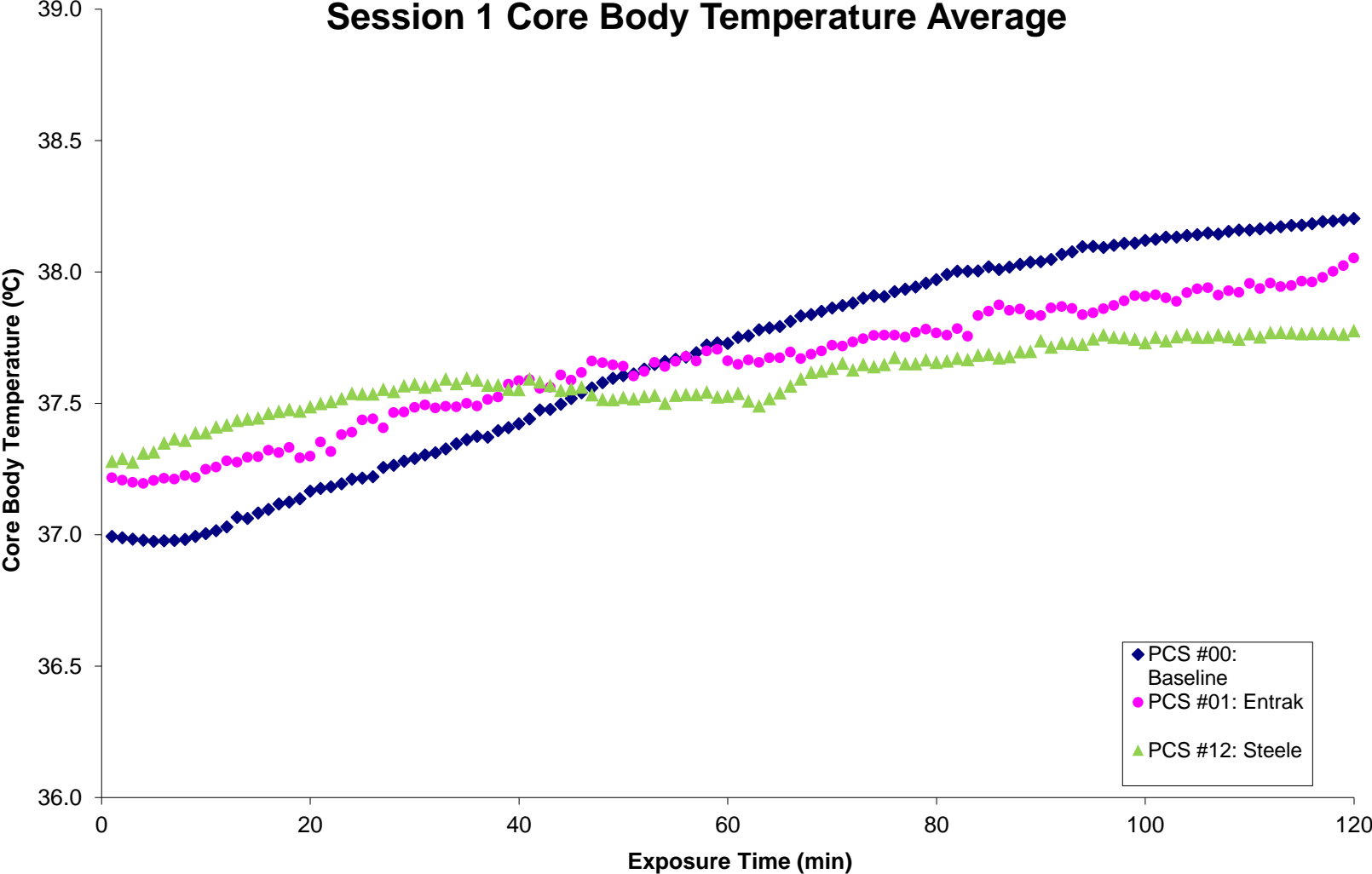


# Session 1 Torso Temperature Average

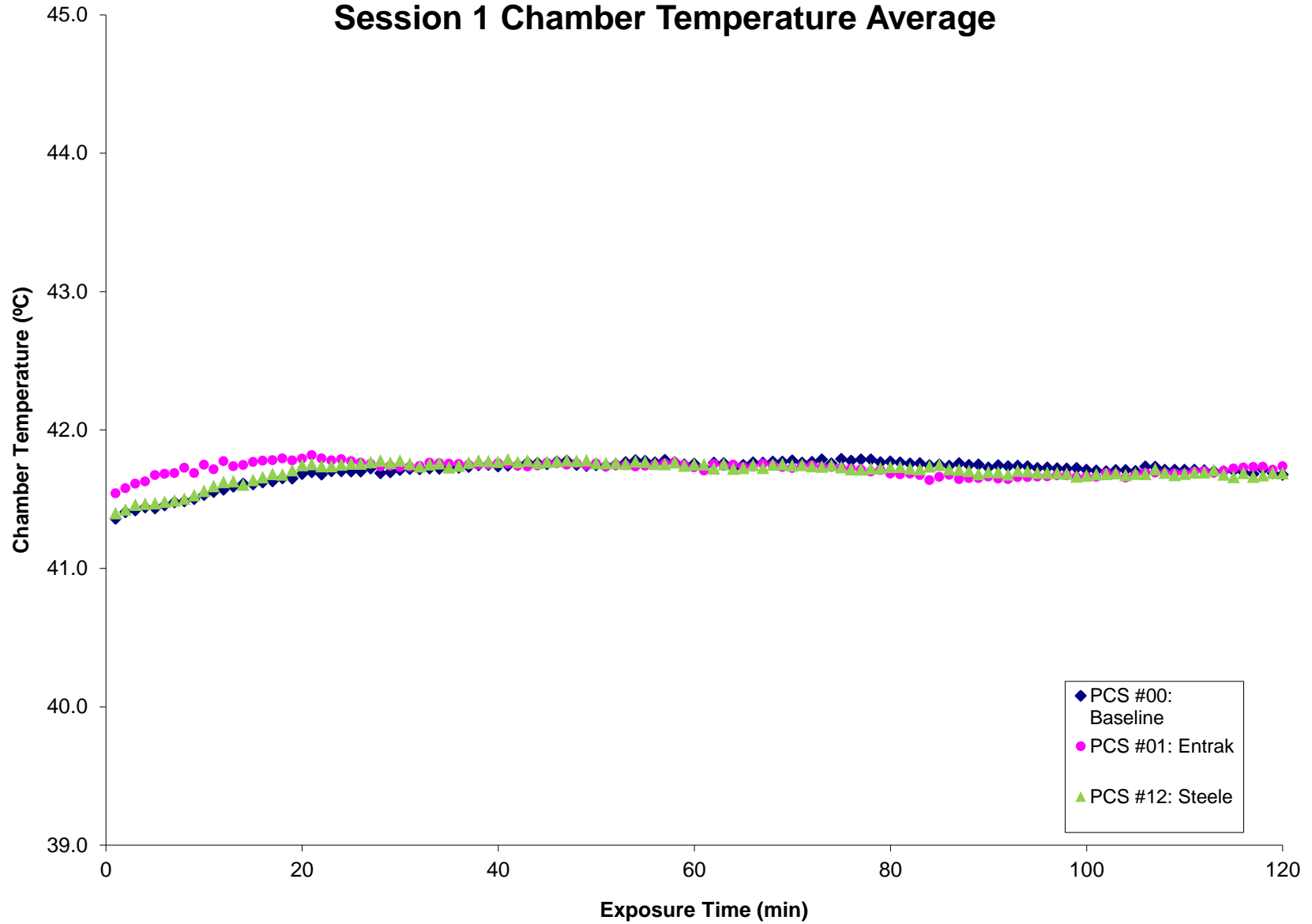




# Session 1 Core Body Temperature Average



# Session 1 Chamber Temperature Average



# Session 1 Chamber Relative Humidity Average

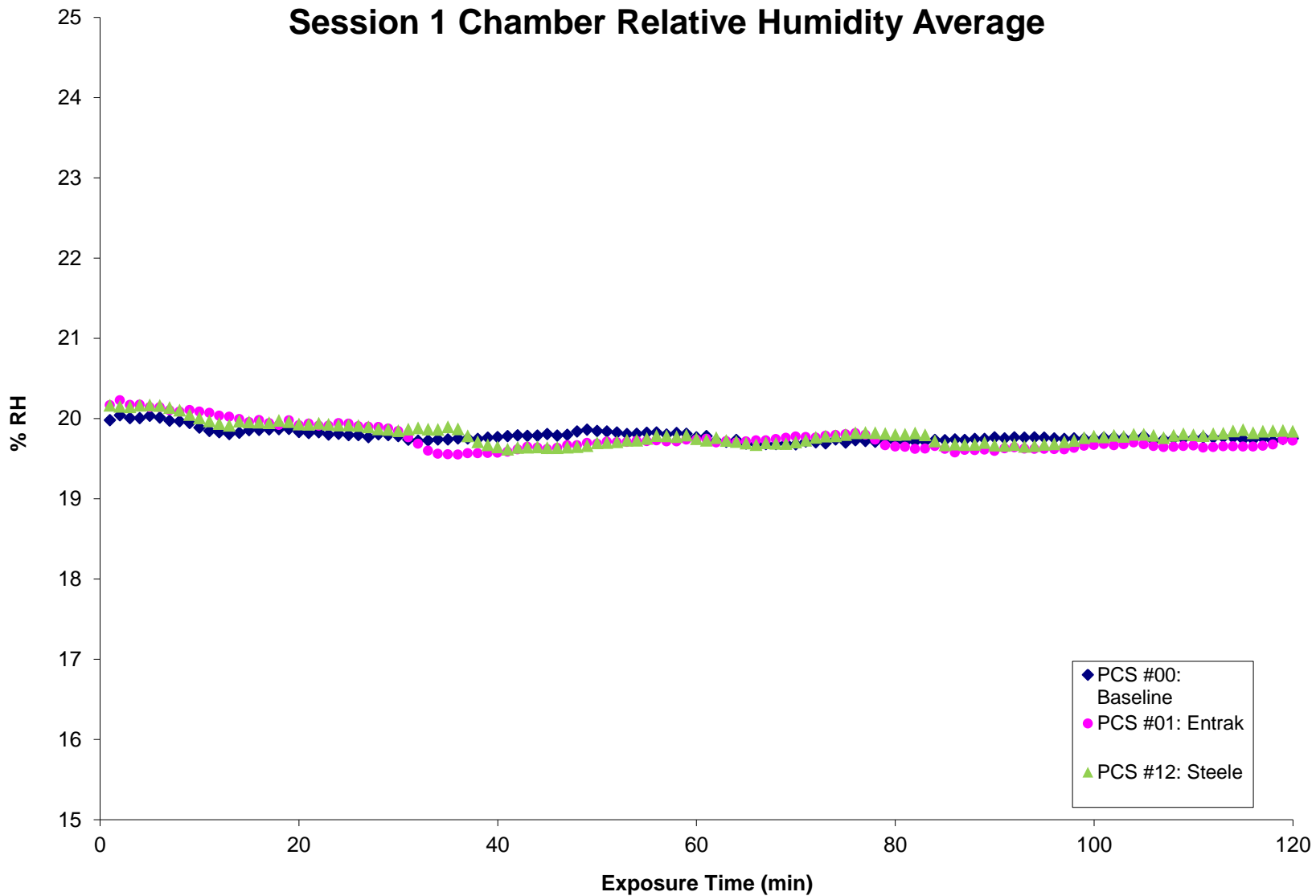


**Table 8.11 Session 1 Human subject baseline results average (Subjects 1-12)**

Time min	Skin 2- 1 C	Skin 2- 2 C	Skin 2- 3 C	Skin 2- 4 C	Skin 2- 5 C	Skin 2- 6 C	Skin 2- 7 C	Average Skin C	Core C	Air Temp C	Dew C	Heart Rate B/min	RH %
1:00	36.28	36.57	34.81	38.43	38.11	35.85	35.82	36.17	36.99	41.36	13.87	100.71	19.98
2:00	36.30	36.68	34.96	38.39	37.93	35.98	35.96	36.26	36.99	41.41	13.95	103.18	20.04
3:00	36.25	36.76	35.09	38.34	37.76	36.08	36.06	36.32	36.98	41.42	13.94	100.06	20.00
4:00	36.24	36.81	35.22	38.28	37.63	36.15	36.16	36.38	36.98	41.44	13.96	101.86	20.00
5:00	36.24	36.88	35.32	38.26	37.54	36.22	36.27	36.44	36.98	41.43	13.97	102.44	20.03
6:00	36.24	36.94	35.43	38.21	37.48	36.30	36.38	36.50	36.98	41.46	13.97	102.79	20.01
7:00	36.26	37.01	35.55	38.20	37.45	36.37	36.48	36.56	36.98	41.48	13.96	103.74	19.97
8:00	36.29	37.06	35.63	38.19	37.42	36.42	36.56	36.62	36.98	41.49	13.96	103.52	19.96
9:00	36.30	37.15	35.70	38.19	37.42	36.45	36.63	36.67	36.99	41.50	13.96	103.86	19.94
10:00	36.33	37.18	35.80	38.17	37.39	36.49	36.70	36.71	37.00	41.53	13.93	105.03	19.89
11:00	36.36	37.19	35.91	38.12	37.33	36.55	36.74	36.75	37.02	41.55	13.92	104.27	19.85
12:00	36.39	37.21	36.01	38.08	37.29	36.60	36.79	36.79	37.03	41.57	13.92	104.67	19.83
13:00	36.39	37.21	36.09	38.05	37.20	36.64	36.82	36.81	37.07	41.59	13.92	103.71	19.81
14:00	36.40	37.16	36.15	38.05	37.14	36.68	36.85	36.82	37.06	41.61	13.95	105.94	19.82
15:00	36.42	37.13	36.19	37.97	37.13	36.68	36.86	36.82	37.08	41.61	13.97	106.77	19.85
16:00	36.45	37.11	36.24	37.92	37.12	36.69	36.89	36.83	37.10	41.62	13.99	107.03	19.86
17:00	36.46	37.11	36.28	37.88	37.04	36.66	36.90	36.83	37.12	41.63	14.00	108.34	19.86
18:00	36.47	37.13	36.32	37.80	37.03	36.68	36.91	36.84	37.12	41.65	14.02	109.13	19.87
19:00	36.48	37.11	36.36	37.77	37.01	36.73	36.93	36.85	37.14	41.65	14.02	111.25	19.87
20:00	36.50	37.03	36.40	37.63	36.91	36.75	36.95	36.84	37.17	41.68	14.02	110.90	19.83
21:00	36.51	37.05	36.42	37.50	36.92	36.73	36.96	36.84	37.18	41.69	14.02	110.79	19.82
22:00	36.51	37.06	36.41	37.41	36.88	36.71	36.97	36.82	37.18	41.68	14.01	110.54	19.83
23:00	36.53	37.09	36.46	37.31	36.85	36.69	36.98	36.83	37.19	41.70	14.01	110.97	19.80
24:00	36.54	37.11	36.47	37.28	36.81	36.66	36.99	36.83	37.21	41.70	14.02	110.92	19.81
25:00	36.56	37.09	36.47	37.26	36.83	36.66	36.99	36.82	37.22	41.70	14.00	112.58	19.79
26:00	36.58	37.05	36.39	37.27	36.86	36.67	37.00	36.81	37.22	41.70	14.00	112.83	19.79
27:00	36.56	37.01	36.36	37.17	36.86	36.68	37.01	36.79	37.26	41.72	14.00	114.24	19.77
28:00	36.51	37.02	36.33	37.10	36.74	36.66	37.02	36.77	37.26	41.69	14.00	113.97	19.80
29:00	36.54	37.00	36.36	37.10	36.65	36.67	37.02	36.77	37.28	41.69	14.00	114.53	19.79
30:00	36.56	36.97	36.39	37.15	36.57	36.68	37.03	36.77	37.29	41.71	14.00	115.93	19.78
31:00	36.61	36.92	36.43	37.19	36.59	36.69	37.03	36.78	37.30	41.72	13.98	118.30	19.74

32.00	36.65	36.92	36.48	37.12	36.55	36.72	37.04	36.79	37.31	41.72	13.96	116.56	19.72
33.00	36.68	36.88	36.43	37.00	36.52	36.72	37.02	36.76	37.33	41.72	13.97	118.09	19.73
34.00	36.67	36.86	36.44	37.02	36.54	36.76	37.04	36.77	37.35	41.72	13.98	116.44	19.74
35.00	36.68	36.89	36.42	37.13	36.61	36.79	37.05	36.80	37.36	41.73	13.99	117.44	19.74
36.00	36.67	36.88	36.41	37.17	36.54	36.82	37.06	36.80	37.37	41.73	13.99	117.56	19.75
37.00	36.72	36.89	36.35	37.17	36.57	36.84	37.07	36.80	37.37	41.73	14.00	118.49	19.75
38.00	36.78	36.85	36.37	37.08	36.55	36.87	37.07	36.80	37.40	41.75	14.00	118.54	19.75
39.00	36.78	36.87	36.41	37.07	36.47	36.88	37.07	36.81	37.41	41.75	14.02	119.11	19.76
40.00	36.83	36.85	36.43	37.07	36.47	36.87	37.08	36.81	37.42	41.74	14.01	119.43	19.77
41.00	36.85	36.83	36.47	37.03	36.43	36.87	37.08	36.81	37.44	41.74	14.03	119.86	19.78
42.00	36.87	36.78	36.52	37.05	36.40	36.91	37.11	36.83	37.47	41.75	14.04	118.99	19.79
43.00	36.83	36.78	36.53	37.16	36.35	36.94	37.12	36.84	37.48	41.76	14.05	120.19	19.78
44.00	36.80	36.90	36.52	37.15	36.34	36.94	37.12	36.85	37.50	41.76	14.05	120.91	19.79
45.00	36.85	36.90	36.54	37.18	36.32	36.95	37.13	36.87	37.52	41.75	14.06	121.21	19.80
46.00	36.85	36.88	36.52	37.14	36.24	36.95	37.13	36.85	37.54	41.77	14.06	121.15	19.79
47.00	36.87	36.90	36.53	37.20	36.24	36.96	37.15	36.87	37.56	41.78	14.07	121.77	19.80
48.00	36.90	36.88	36.56	37.27	36.26	36.95	37.16	36.88	37.58	41.75	14.08	122.09	19.84
49.00	36.89	36.95	36.58	37.24	36.42	36.97	37.18	36.91	37.60	41.74	14.09	121.84	19.86
50.00	36.88	36.93	36.55	37.27	36.30	37.01	37.18	36.90	37.61	41.75	14.08	121.21	19.84
51.00	36.87	36.92	36.51	37.30	36.25	37.01	37.19	36.89	37.61	41.74	14.07	120.85	19.84
52.00	36.92	36.98	36.51	37.32	36.23	36.99	37.20	36.91	37.63	41.75	14.07	123.00	19.83
53.00	36.96	36.89	36.50	37.38	36.33	37.00	37.20	36.90	37.65	41.77	14.07	123.07	19.81
54.00	36.95	36.81	36.52	37.40	36.36	36.97	37.22	36.89	37.66	41.78	14.08	122.79	19.81
55.00	36.95	36.79	36.55	37.36	36.31	36.94	37.22	36.88	37.67	41.78	14.09	124.26	19.82
56.00	36.95	36.85	36.52	37.44	36.35	36.95	37.22	36.90	37.68	41.76	14.08	123.81	19.83
57.00	36.95	36.88	36.48	37.45	36.25	36.97	37.21	36.90	37.69	41.78	14.08	123.63	19.80
58.00	36.97	36.86	36.52	37.46	36.10	36.98	37.18	36.89	37.72	41.77	14.08	125.99	19.82
59.00	36.96	36.85	36.56	37.41	36.09	37.00	37.18	36.89	37.73	41.75	14.06	124.80	19.81
60.00	36.97	36.92	36.59	37.39	36.26	37.01	37.18	36.92	37.73	41.76	14.03	126.33	19.77
61.00	36.97	36.89	36.62	37.35	36.29	37.04	37.17	36.92	37.75	41.73	14.01	127.75	19.78
62.00	37.01	36.82	36.66	37.26	36.33	37.07	37.16	36.92	37.76	41.76	14.00	126.88	19.72
63.00	37.03	36.81	36.68	37.22	36.34	37.09	37.15	36.93	37.78	41.76	13.99	127.33	19.71
64.00	37.04	36.82	36.69	37.18	36.33	37.11	37.10	36.92	37.79	41.72	13.97	128.39	19.73
65.00	37.04	36.92	36.59	37.19	36.21	37.14	37.30	36.96	37.79	41.75	13.96	128.10	19.69
66.00	37.06	36.95	36.64	37.23	36.18	37.14	37.38	36.99	37.81	41.76	13.96	127.60	19.68
67.00	37.06	36.95	36.65	37.24	36.16	37.14	37.39	37.00	37.83	41.76	13.97	127.16	19.68

68.00	37.06	36.91	36.68	37.26	36.21	37.14	37.42	37.01	37.84	41.77	13.97	129.44	19.68
69.00	37.08	36.83	36.65	37.14	36.14	37.14	37.48	36.99	37.85	41.77	13.98	128.36	19.69
70.00	37.07	36.86	36.67	37.10	36.19	37.14	37.48	37.00	37.86	41.78	13.98	129.05	19.68
71.00	37.09	36.86	36.72	37.16	36.27	37.17	37.42	37.01	37.87	41.76	13.99	128.29	19.71
72.00	37.08	36.97	36.63	37.22	36.27	37.19	37.41	37.02	37.88	41.77	13.99	129.48	19.70
73.00	37.10	37.04	36.59	37.33	36.20	37.22	37.43	37.04	37.90	41.79	13.99	128.53	19.69
74.00	37.09	37.07	36.59	37.40	36.26	37.24	37.49	37.07	37.91	41.76	14.01	128.46	19.74
75.00	37.13	36.95	36.72	37.34	36.32	37.25	37.49	37.08	37.91	41.79	14.00	129.61	19.70
76.00	37.09	36.99	36.75	37.35	36.28	37.23	37.54	37.09	37.93	41.78	14.02	130.98	19.73
77.00	37.11	36.99	36.78	37.39	36.32	37.23	37.48	37.09	37.93	41.79	14.01	128.68	19.72
78.00	37.12	37.01	36.81	37.39	36.37	37.22	37.49	37.11	37.94	41.79	14.01	128.50	19.71
79.00	37.14	36.98	36.86	37.40	36.46	37.23	37.44	37.11	37.96	41.77	14.01	129.66	19.73
80.00	37.16	36.98	36.83	37.41	36.38	37.22	37.47	37.10	37.97	41.77	13.99	129.76	19.70
81.00	37.20	37.02	36.73	37.44	36.25	37.19	37.53	37.09	37.99	41.76	13.99	131.36	19.70
82.00	37.22	37.00	36.78	37.55	36.39	37.20	37.57	37.13	38.00	41.76	13.99	131.23	19.71
83.00	37.23	37.00	36.74	37.52	36.43	37.21	37.55	37.12	38.00	41.76	13.99	131.38	19.71
84.00	37.24	37.00	36.74	37.56	36.43	37.21	37.55	37.13	38.00	41.74	13.99	131.84	19.73
85.00	37.27	37.02	36.72	37.60	36.43	37.20	37.61	37.14	38.02	41.75	14.00	133.25	19.73
86.00	37.29	36.94	36.75	37.60	36.41	37.21	37.62	37.14	38.01	41.74	13.99	133.65	19.74
87.00	37.33	36.94	36.71	37.61	36.41	37.24	37.60	37.13	38.02	41.76	14.00	133.74	19.73
88.00	37.34	36.97	36.74	37.63	36.47	37.24	37.59	37.15	38.03	41.75	14.00	134.00	19.74
89.00	37.35	36.98	36.70	37.59	36.46	37.27	37.61	37.15	38.04	41.75	14.01	133.72	19.75
90.00	37.36	37.02	36.66	37.68	36.44	37.26	37.65	37.16	38.04	41.73	14.00	132.89	19.76
91.00	37.39	37.03	36.72	37.65	36.51	37.24	37.68	37.18	38.05	41.75	14.01	133.98	19.75
92.00	37.41	36.99	36.81	37.61	36.51	37.25	37.66	37.19	38.07	41.74	14.01	132.86	19.76
93.00	37.42	37.03	36.85	37.50	36.53	37.24	37.63	37.19	38.08	41.74	14.01	133.39	19.76
94.00	37.43	37.05	36.94	37.42	36.60	37.25	37.55	37.20	38.10	41.74	14.01	135.71	19.77
95.00	37.44	37.05	36.96	37.44	36.63	37.29	37.51	37.21	38.10	41.72	14.00	134.46	19.76
96.00	37.46	36.98	36.92	37.51	36.66	37.33	37.60	37.22	38.09	41.73	13.99	135.17	19.75
97.00	37.49	36.99	36.95	37.59	36.73	37.29	37.65	37.24	38.10	41.72	13.98	135.22	19.74
98.00	37.49	37.02	37.00	37.67	36.74	37.29	37.68	37.27	38.11	41.72	13.99	136.69	19.75
99.00	37.46	37.06	36.95	37.71	36.70	37.31	37.70	37.28	38.11	41.72	13.99	136.79	19.75
100.00	37.47	37.04	36.98	37.65	36.81	37.30	37.70	37.28	38.12	41.71	13.98	136.83	19.75
101.00	37.48	37.06	36.99	37.66	36.81	37.31	37.71	37.29	38.12	41.71	13.98	136.21	19.76
102.00	37.47	37.08	36.97	37.62	36.76	37.30	37.72	37.28	38.13	41.70	13.98	135.32	19.77
103.00	37.48	37.05	37.06	37.62	36.83	37.31	37.72	37.30	38.13	41.71	13.98	137.36	19.76

104.00	37.48	37.05	37.13	37.65	36.81	37.31	37.73	37.32	38.14	41.71	13.99	135.43	19.76
105.00	37.47	37.01	37.13	37.67	36.81	37.29	37.73	37.31	38.14	41.70	13.99	134.80	19.78
106.00	37.49	37.03	37.14	37.68	36.77	37.29	37.73	37.31	38.15	41.73	13.98	135.75	19.73
107.00	37.51	37.05	37.14	37.67	36.75	37.30	37.74	37.32	38.14	41.73	13.99	136.30	19.74
108.00	37.51	37.03	37.15	37.69	36.76	37.29	37.75	37.32	38.15	41.71	13.98	136.58	19.75
109.00	37.52	37.11	37.17	37.74	36.78	37.28	37.76	37.34	38.16	41.71	13.98	135.93	19.75
110.00	37.54	37.17	37.18	37.68	36.76	37.27	37.76	37.35	38.16	41.71	13.98	137.14	19.75
111.00	37.55	37.15	37.18	37.76	36.81	37.29	37.77	37.36	38.16	41.71	13.99	137.99	19.76
112.00	37.55	37.11	37.19	37.73	36.76	37.30	37.78	37.36	38.17	41.71	13.98	137.31	19.76
113.00	37.54	37.11	37.19	37.69	36.76	37.29	37.78	37.35	38.17	41.70	13.99	137.88	19.77
114.00	37.55	37.09	37.13	37.71	36.85	37.29	37.79	37.34	38.18	41.70	13.98	136.81	19.76
115.00	37.56	37.11	37.10	37.77	36.82	37.29	37.79	37.35	38.18	41.71	13.97	137.12	19.74
116.00	37.56	37.07	37.08	37.76	36.81	37.29	37.80	37.34	38.18	41.70	13.95	138.83	19.73
117.00	37.55	37.09	37.05	37.80	36.86	37.28	37.80	37.34	38.19	41.68	13.96	136.85	19.75
118.00	37.57	37.07	37.07	37.85	36.83	37.31	37.81	37.35	38.19	41.71	13.96	137.58	19.72
119.00	37.56	37.10	37.05	37.91	36.83	37.31	37.81	37.35	38.20	41.69	13.96	139.21	19.75
120.00	37.51	37.14	37.01	37.98	36.80	37.31	37.82	37.36	38.20	41.68	13.95	139.90	19.75

**Table 8.12 Session 1 Human subject PCS #1 results average (Subjects 1-12)**

Time min	Skin 2- 1 C	Skin 2- 2 C	Skin 2- 3 C	Skin 2- 4 C	Skin 2- 5 C	Skin 2- 6 C	Skin 2- 7 C	Average Skin C	Core C	Air Temp C	Dew C	Heart Rate B/min	RH %
1.00	36.20	36.21	35.11	38.66	38.10	35.49	35.94	36.13	37.22	41.54	14.16	103.02	20.17
2.00	36.17	36.21	35.11	38.55	37.95	35.71	36.08	36.18	37.21	41.58	14.23	106.01	20.23
3.00	36.17	36.23	35.13	38.49	37.73	35.79	36.18	36.20	37.20	41.61	14.22	103.65	20.17
4.00	36.13	36.19	35.18	38.45	37.70	35.88	36.27	36.23	37.20	41.63	14.23	104.23	20.17
5.00	36.15	36.18	35.26	38.40	37.87	35.98	36.37	36.30	37.21	41.67	14.25	105.13	20.14
6.00	36.11	36.15	35.30	38.31	37.93	36.04	36.44	36.32	37.22	41.68	14.26	104.53	20.14
7.00	36.08	36.12	35.32	38.21	37.84	36.05	36.49	36.32	37.21	41.69	14.23	104.58	20.10
8.00	36.10	36.16	35.41	38.21	37.83	36.12	36.60	36.37	37.22	41.73	14.25	104.30	20.09
9.00	36.09	36.19	35.41	38.16	37.79	36.10	36.65	36.38	37.22	41.69	14.23	105.43	20.10
10.00	36.13	36.33	35.48	38.13	37.67	36.15	36.71	36.44	37.25	41.75	14.27	106.24	20.08
11.00	36.12	36.30	35.52	37.94	37.53	36.16	36.72	36.42	37.26	41.72	14.23	106.71	20.07
12.00	36.16	36.30	35.56	37.85	37.46	36.19	36.78	36.43	37.28	41.77	14.25	106.62	20.03
13.00	36.13	36.22	35.56	37.75	37.41	36.19	36.77	36.40	37.28	41.74	14.21	106.68	20.02
14.00	36.15	36.15	35.55	37.71	37.37	36.20	36.80	36.39	37.29	41.75	14.19	106.49	19.99
15.00	36.18	36.12	35.54	37.65	37.19	36.20	36.83	36.38	37.30	41.77	14.18	106.59	19.95
16.00	36.23	36.20	35.57	37.66	37.21	36.24	36.89	36.42	37.32	41.78	14.21	107.45	19.98
17.00	36.20	36.21	35.48	37.58	37.16	36.23	36.87	36.39	37.31	41.78	14.18	107.59	19.94
18.00	36.16	36.17	35.47	37.56	37.06	36.26	36.89	36.38	37.33	41.79	14.18	107.43	19.92
19.00	36.15	36.12	35.50	37.53	37.07	36.29	36.89	36.38	37.29	41.78	14.21	110.46	19.98
20.00	36.15	36.04	35.54	37.52	37.00	36.29	36.92	36.37	37.30	41.79	14.17	109.90	19.92
21.00	36.13	35.97	35.59	37.45	36.95	36.31	36.93	36.36	37.35	41.82	14.21	108.51	19.94
22.00	36.14	35.96	35.60	37.45	36.94	36.32	36.93	36.36	37.32	41.79	14.17	109.60	19.91
23.00	36.12	35.98	35.66	37.39	36.91	36.32	36.94	36.38	37.38	41.78	14.15	108.62	19.91
24.00	36.15	36.00	35.62	37.45	36.87	36.28	36.95	36.37	37.39	41.79	14.19	109.57	19.94
25.00	36.22	35.97	35.53	37.43	36.76	36.26	36.95	36.34	37.44	41.77	14.17	110.73	19.93
26.00	36.22	36.03	35.53	37.42	36.74	36.26	36.95	36.34	37.44	41.76	14.14	110.24	19.90
27.00	36.20	35.97	35.54	37.43	36.71	36.27	36.95	36.34	37.41	41.75	14.13	110.09	19.90
28.00	36.25	35.96	35.46	37.37	36.68	36.27	36.96	36.32	37.47	41.73	14.11	110.77	19.89
29.00	36.29	35.95	35.40	37.37	36.32	36.31	36.96	36.29	37.47	41.74	14.10	111.73	19.87
30.00	36.33	35.83	35.36	37.23	36.28	36.33	36.99	36.26	37.48	41.73	14.07	114.47	19.84
31.00	36.36	35.75	35.37	37.18	36.52	36.34	36.99	36.27	37.49	41.73	14.01	115.25	19.76



32.00	36.32	35.73	35.39	37.18	36.32	36.34	36.99	36.25	37.48	41.74	13.95	114.32	19.68
33.00	36.28	35.60	35.41	37.16	36.28	36.36	37.01	36.23	37.49	41.76	13.90	115.14	19.60
34.00	36.26	35.70	35.41	37.04	36.30	36.40	37.02	36.25	37.49	41.76	13.86	114.91	19.56
35.00	36.28	35.76	35.43	37.02	36.36	36.41	37.01	36.27	37.50	41.76	13.86	113.58	19.55
36.00	36.27	35.77	35.45	37.11	36.47	36.42	37.01	36.29	37.49	41.75	13.85	115.74	19.55
37.00	36.15	35.55	35.47	37.14	36.46	36.43	37.02	36.25	37.51	41.75	13.86	114.63	19.57
38.00	36.07	35.61	35.48	37.14	36.55	36.43	36.99	36.26	37.52	41.75	13.86	116.65	19.57
39.00	36.11	35.66	35.42	37.14	36.54	36.43	36.99	36.26	37.57	41.75	13.86	115.48	19.57
40.00	36.16	35.62	35.44	37.12	36.55	36.43	37.00	36.26	37.59	41.76	13.87	113.70	19.57
41.00	36.30	35.48	35.46	37.16	36.53	36.41	37.00	36.24	37.59	41.76	13.88	115.98	19.59
42.00	36.25	35.50	35.39	37.14	36.56	36.40	37.01	36.23	37.56	41.74	13.89	116.63	19.61
43.00	36.21	35.55	35.32	37.15	36.59	36.29	37.01	36.20	37.56	41.73	13.91	115.74	19.64
44.00	36.18	35.63	35.29	37.14	36.55	36.28	37.00	36.20	37.61	41.74	13.91	117.30	19.64
45.00	36.23	35.69	35.31	37.08	36.56	36.34	37.01	36.23	37.59	41.76	13.91	117.51	19.62
46.00	36.27	35.75	35.38	37.06	36.55	36.35	37.01	36.26	37.62	41.76	13.92	117.14	19.63
47.00	36.27	35.74	35.47	37.05	36.55	36.35	37.01	36.27	37.66	41.75	13.94	116.54	19.67
48.00	36.30	35.71	35.46	37.12	36.58	36.34	37.01	36.27	37.65	41.76	13.95	118.24	19.67
49.00	36.29	35.77	35.39	37.21	36.58	36.34	37.00	36.28	37.65	41.74	13.96	116.61	19.69
50.00	36.30	35.74	35.36	37.19	36.58	36.35	37.00	36.27	37.64	41.76	13.96	116.72	19.68
51.00	36.29	35.62	35.48	37.15	36.53	36.38	37.01	36.27	37.60	41.73	13.96	117.30	19.71
52.00	36.29	35.58	35.45	37.13	36.41	36.39	37.03	36.25	37.62	41.74	13.97	117.18	19.70
53.00	36.30	35.74	35.45	37.12	36.42	36.40	37.02	36.28	37.66	41.74	13.97	116.32	19.71
54.00	36.25	35.74	35.42	37.20	36.49	36.40	37.03	36.28	37.64	41.73	13.97	118.66	19.72
55.00	36.25	35.73	35.26	37.26	36.48	36.41	37.04	36.26	37.66	41.74	13.98	116.57	19.72
56.00	36.26	35.73	35.23	37.30	36.47	36.40	37.05	36.26	37.68	41.75	13.99	116.70	19.72
57.00	36.33	35.73	35.25	37.28	36.44	36.40	37.06	36.27	37.66	41.76	13.99	118.70	19.71
58.00	36.30	35.76	35.28	37.37	36.44	36.42	37.08	36.29	37.70	41.77	14.00	118.57	19.71
59.00	36.30	35.79	35.23	37.42	36.50	36.45	37.07	36.30	37.71	41.75	14.00	118.18	19.73
60.00	36.27	35.85	35.20	37.47	36.56	36.44	37.07	36.31	37.66	41.73	13.98	120.51	19.74
61.00	36.03	35.82	35.28	37.57	36.53	36.38	37.07	36.29	37.65	41.71	13.97	121.58	19.74
62.00	35.91	35.75	35.30	37.59	36.53	36.37	37.07	36.28	37.67	41.75	13.97	121.30	19.70
63.00	35.87	35.70	35.41	37.47	36.52	36.39	37.11	36.28	37.66	41.74	13.98	121.14	19.72
64.00	35.98	35.77	35.42	37.56	36.55	36.39	37.14	36.32	37.67	41.75	13.97	119.04	19.70
65.00	36.33	35.97	35.47	37.53	36.51	36.42	37.15	36.40	37.67	41.73	13.97	119.53	19.71
66.00	36.34	36.09	35.49	37.54	36.59	36.45	37.14	36.43	37.69	41.73	13.98	120.76	19.73
67.00	36.24	36.08	35.47	37.51	36.67	36.45	37.14	36.43	37.67	41.76	14.00	119.47	19.72

68.00	36.37	36.01	35.42	37.32	36.61	36.47	37.14	36.40	37.69	41.74	14.00	120.91	19.74
69.00	36.47	36.03	35.44	37.30	36.42	36.47	37.14	36.40	37.70	41.73	14.00	121.83	19.76
70.00	36.60	35.97	35.43	37.35	36.55	36.50	37.15	36.42	37.72	41.72	14.01	120.73	19.77
71.00	36.98	35.91	35.42	37.59	36.63	36.47	37.15	36.45	37.72	41.74	14.02	122.23	19.77
72.00	37.05	35.75	35.40	37.75	36.68	36.48	37.13	36.43	37.73	41.74	14.01	122.28	19.76
73.00	37.06	35.67	35.45	37.67	36.72	36.47	37.15	36.43	37.75	41.73	14.02	121.39	19.78
74.00	37.07	35.80	35.48	37.65	36.79	36.48	37.17	36.47	37.76	41.73	14.03	122.26	19.79
75.00	37.05	35.92	35.51	37.65	36.83	36.49	37.18	36.50	37.76	41.72	14.03	121.20	19.80
76.00	37.10	35.99	35.47	37.62	36.84	36.52	37.18	36.52	37.76	41.72	14.04	119.75	19.82
77.00	37.16	35.99	35.50	37.52	36.87	36.53	37.17	36.52	37.75	41.71	14.02	119.29	19.80
78.00	37.15	36.04	35.46	37.50	36.89	36.52	37.17	36.52	37.77	41.70	13.96	121.11	19.73
79.00	37.12	35.98	35.49	37.51	36.85	36.53	37.17	36.51	37.78	41.71	13.91	121.97	19.67
80.00	37.15	36.05	35.50	37.57	36.84	36.52	37.17	36.53	37.77	41.68	13.88	121.20	19.65
81.00	37.14	36.07	35.43	37.47	36.85	36.52	37.18	36.52	37.76	41.68	13.87	120.70	19.64
82.00	37.17	36.00	35.45	37.56	36.81	36.52	37.18	36.51	37.78	41.68	13.85	120.05	19.62
83.00	37.17	35.95	35.46	37.66	36.77	36.51	37.20	36.51	37.75	41.67	13.85	122.26	19.62
84.00	37.20	36.14	35.56	37.73	36.80	36.52	37.21	36.58	37.83	41.64	13.84	122.43	19.65
85.00	37.21	36.15	35.59	37.79	36.76	36.52	37.21	36.59	37.85	41.66	13.83	123.76	19.62
86.00	37.24	35.87	35.54	37.72	36.66	36.52	37.22	36.52	37.87	41.67	13.81	124.77	19.58
87.00	37.23	35.76	35.55	37.70	36.68	36.54	37.24	36.51	37.85	41.64	13.81	124.32	19.61
88.00	37.18	35.76	35.55	37.71	36.77	36.53	37.24	36.51	37.86	41.65	13.81	124.61	19.60
89.00	37.21	35.76	35.59	37.66	36.80	36.53	37.23	36.52	37.84	41.65	13.82	126.18	19.61
90.00	37.19	35.86	35.63	37.73	36.79	36.54	37.23	36.55	37.83	41.66	13.82	124.39	19.60
91.00	37.18	35.91	35.62	37.80	36.84	36.54	37.23	36.56	37.86	41.65	13.83	124.13	19.63
92.00	37.17	36.04	35.56	37.81	36.84	36.54	37.24	36.58	37.87	41.64	13.84	124.12	19.64
93.00	37.12	36.04	35.63	37.81	36.93	36.55	37.25	36.60	37.86	41.66	13.84	124.54	19.62
94.00	37.14	35.95	35.55	37.74	36.80	36.57	37.26	36.56	37.84	41.66	13.83	124.04	19.62
95.00	37.13	36.06	35.61	37.75	36.93	36.57	37.25	36.60	37.84	41.66	13.84	125.59	19.62
96.00	37.18	36.13	35.60	37.84	37.00	36.56	37.26	36.62	37.86	41.66	13.84	126.02	19.62
97.00	37.23	36.16	35.57	37.92	37.00	36.57	37.27	36.64	37.87	41.67	13.84	125.39	19.61
98.00	37.22	36.23	35.67	37.98	37.01	36.57	37.28	36.68	37.89	41.67	13.85	126.12	19.63
99.00	37.22	36.24	35.68	37.94	37.06	36.57	37.28	36.68	37.91	41.66	13.86	126.49	19.66
100.00	37.21	36.22	35.58	37.96	37.12	36.61	37.30	36.68	37.91	41.66	13.87	128.73	19.67
101.00	37.24	36.26	35.60	37.93	37.15	36.63	37.33	36.70	37.91	41.66	13.88	127.67	19.68
102.00	37.26	36.20	35.62	37.92	37.07	36.65	37.36	36.70	37.90	41.69	13.89	128.06	19.66
103.00	37.26	36.00	35.72	37.91	37.05	36.67	37.38	36.68	37.89	41.68	13.89	129.04	19.68

104.00	37.26	36.02	35.80	37.84	37.04	36.67	37.39	36.70	37.92	41.65	13.89	127.73	19.70
105.00	37.26	35.97	35.91	37.89	37.08	36.70	37.40	36.72	37.94	41.68	13.90	127.51	19.68
106.00	37.28	35.81	35.99	37.91	37.08	36.75	37.41	36.72	37.94	41.69	13.89	128.34	19.66
107.00	37.27	35.91	36.01	38.00	37.07	36.73	37.43	36.75	37.91	41.69	13.88	129.13	19.64
108.00	37.28	35.89	35.95	38.04	37.12	36.73	37.44	36.75	37.93	41.69	13.88	128.77	19.65
109.00	37.28	35.83	35.95	38.01	37.08	36.73	37.45	36.73	37.92	41.69	13.88	128.08	19.65
110.00	37.31	35.82	35.98	38.03	37.06	36.74	37.46	36.74	37.96	41.68	13.89	129.88	19.66
111.00	37.32	35.84	35.93	38.01	37.05	36.73	37.46	36.74	37.94	41.70	13.88	128.94	19.63
112.00	37.32	35.94	35.79	37.99	37.10	36.71	37.47	36.73	37.96	41.70	13.89	128.80	19.64
113.00	37.35	35.86	35.70	38.09	36.98	36.70	37.48	36.70	37.94	41.69	13.88	129.35	19.65
114.00	37.37	35.97	35.68	38.09	36.82	36.70	37.49	36.70	37.95	41.70	13.90	130.26	19.65
115.00	37.37	35.91	35.76	38.09	37.03	36.72	37.50	36.73	37.96	41.72	13.91	131.92	19.65
116.00	37.36	35.97	35.82	38.11	37.21	36.72	37.53	36.77	37.96	41.73	13.91	131.06	19.65
117.00	37.38	36.15	35.85	38.20	37.28	36.74	37.54	36.83	37.98	41.73	13.92	130.72	19.66
118.00	37.36	36.22	35.87	38.26	37.25	36.78	37.55	36.86	38.00	41.73	13.94	131.99	19.67
119.00	37.36	36.29	35.78	38.20	37.25	36.79	37.56	36.85	38.02	41.71	13.96	133.34	19.73
120.00	37.38	36.30	35.78	38.21	37.20	36.81	37.58	36.86	38.05	41.74	13.98	132.39	19.72

**Table 8.13 Session 1 Human subject PCS #12 results average (Subjects 1-12)**

Time min	Skin 2- 1 C	Skin 2- 2 C	Skin 2- 3 C	Skin 2- 4 C	Skin 2- 5 C	Skin 2- 6 C	Skin 2- 7 C	Average Skin C	Core C	Air Temp C	Dew C	Heart Rate B/min	RH %
1.00	36.42	33.46	25.93	38.47	37.74	36.12	35.98	34.04	37.28	41.40	14.04	103.34	20.16
2.00	36.32	33.10	24.46	38.34	37.66	36.25	36.10	33.73	37.29	41.42	14.06	104.42	20.15
3.00	36.26	32.89	23.74	38.39	37.51	36.36	36.22	33.59	37.28	41.46	14.08	100.42	20.15
4.00	36.25	32.69	23.29	38.49	37.39	36.43	36.33	33.51	37.31	41.47	14.10	102.20	20.17
5.00	36.20	32.65	22.70	38.51	37.35	36.50	36.43	33.42	37.32	41.47	14.11	103.73	20.17
6.00	36.21	32.71	22.12	38.52	37.40	36.56	36.53	33.36	37.35	41.48	14.11	104.19	20.16
7.00	36.23	32.74	21.84	38.55	37.40	36.70	36.61	33.37	37.37	41.49	14.10	104.04	20.14
8.00	36.22	32.64	21.51	38.56	37.39	36.77	36.67	33.32	37.36	41.50	14.08	105.73	20.10
9.00	36.21	32.58	21.56	38.55	37.36	36.82	36.73	33.33	37.39	41.53	14.06	105.43	20.05
10.00	36.22	32.53	21.73	38.58	37.28	36.86	36.76	33.37	37.39	41.56	14.05	105.49	20.01
11.00	36.25	32.59	21.80	38.58	37.21	36.91	36.80	33.40	37.41	41.59	14.05	106.01	19.97
12.00	36.29	32.59	21.81	38.56	37.17	36.96	36.79	33.41	37.42	41.62	14.05	107.90	19.94
13.00	36.32	32.55	21.72	38.49	37.18	36.98	36.83	33.40	37.44	41.63	14.03	106.64	19.91
14.00	36.31	32.52	21.56	38.37	37.14	36.98	36.86	33.36	37.44	41.61	14.06	106.28	19.96
15.00	36.32	32.59	21.47	38.23	37.20	36.95	36.92	33.36	37.44	41.64	14.08	104.80	19.96
16.00	36.31	32.47	21.28	38.11	37.20	36.89	36.92	33.28	37.46	41.66	14.09	107.77	19.95
17.00	36.31	32.50	21.09	38.19	37.11	36.91	36.93	33.25	37.47	41.68	14.11	108.22	19.95
18.00	36.33	32.56	20.95	38.23	37.04	36.94	36.94	33.25	37.48	41.68	14.13	107.80	19.98
19.00	36.34	32.64	20.74	38.29	37.05	36.96	37.00	33.24	37.47	41.71	14.14	107.07	19.96
20.00	36.33	32.65	20.58	38.32	37.00	36.96	37.03	33.22	37.49	41.75	14.15	108.64	19.93
21.00	36.29	32.66	20.41	38.32	36.94	36.94	37.04	33.18	37.50	41.75	14.15	107.20	19.93
22.00	36.33	32.80	20.25	38.19	36.90	36.94	37.04	33.17	37.51	41.74	14.15	109.91	19.94
23.00	36.43	32.98	20.09	37.90	36.89	36.93	37.03	33.15	37.52	41.74	14.14	110.12	19.93
24.00	36.46	33.06	19.99	37.79	36.84	36.92	37.01	33.13	37.54	41.75	14.14	110.15	19.92
25.00	36.42	33.11	19.95	37.82	36.70	36.92	37.01	33.12	37.54	41.76	14.15	110.77	19.92
26.00	36.23	33.08	19.91	37.80	36.67	36.92	37.00	33.09	37.54	41.76	14.14	109.86	19.91
27.00	36.33	33.13	19.90	37.87	36.69	36.94	37.00	33.12	37.55	41.77	14.14	110.13	19.90
28.00	36.39	33.30	19.84	37.85	36.65	36.94	36.99	33.14	37.55	41.78	14.13	111.28	19.87
29.00	36.42	33.53	19.72	37.82	36.66	36.97	37.00	33.17	37.57	41.76	14.11	110.23	19.86
30.00	36.44	33.67	19.55	37.78	36.62	36.97	37.01	33.16	37.57	41.78	14.11	112.44	19.85
31.00	36.48	33.61	19.43	37.79	36.67	36.92	37.01	33.12	37.56	41.75	14.10	111.18	19.87

32.00	36.51	33.69	19.45	37.80	36.75	36.93	37.02	33.15	37.57	41.74	14.10	112.14	19.88
33.00	36.54	33.74	19.46	37.79	36.90	36.94	37.05	33.18	37.59	41.75	14.10	112.63	19.87
34.00	36.56	33.58	19.52	37.82	36.93	36.91	37.06	33.17	37.58	41.76	14.10	111.23	19.86
35.00	36.59	33.50	19.57	37.80	36.90	36.93	37.07	33.17	37.60	41.73	14.11	110.97	19.90
36.00	36.58	33.40	19.80	37.72	36.85	36.91	37.08	33.18	37.59	41.74	14.10	111.62	19.87
37.00	36.61	33.49	19.96	37.77	36.95	36.91	37.09	33.24	37.57	41.76	14.05	113.56	19.78
38.00	36.63	33.51	20.12	37.73	36.93	36.96	37.06	33.27	37.57	41.78	14.00	112.66	19.71
39.00	36.63	33.63	20.15	37.69	36.81	36.97	37.07	33.29	37.55	41.77	13.97	112.18	19.67
40.00	36.49	33.34	20.16	37.64	36.72	36.97	37.08	33.22	37.55	41.77	13.94	112.30	19.65
41.00	36.66	33.49	20.24	37.64	36.73	36.97	37.08	33.28	37.59	41.79	13.93	113.00	19.62
42.00	36.64	33.66	20.28	37.69	36.74	36.97	37.08	33.32	37.58	41.77	13.93	112.95	19.64
43.00	36.68	33.69	20.28	37.69	36.76	36.99	37.08	33.34	37.57	41.78	13.95	112.85	19.64
44.00	36.71	33.77	20.29	37.68	36.93	37.01	37.09	33.37	37.55	41.76	13.93	113.18	19.65
45.00	36.75	33.69	20.39	37.55	36.91	37.02	37.08	33.37	37.56	41.77	13.93	113.52	19.64
46.00	36.73	33.65	20.56	37.54	36.82	37.04	37.09	33.39	37.56	41.78	13.94	112.40	19.64
47.00	36.77	33.58	20.63	37.56	36.70	37.06	37.09	33.39	37.53	41.78	13.95	112.21	19.64
48.00	36.77	33.64	21.03	37.50	36.71	37.03	37.08	33.46	37.52	41.78	13.95	110.50	19.65
49.00	36.77	33.57	21.18	37.49	36.68	37.05	37.08	33.48	37.51	41.78	13.96	111.61	19.66
50.00	36.78	33.61	21.19	37.51	36.62	37.04	37.09	33.48	37.52	41.76	13.97	111.41	19.70
51.00	36.77	33.75	21.31	37.57	36.55	37.01	37.08	33.52	37.52	41.76	13.98	110.80	19.70
52.00	36.78	33.76	21.29	37.56	36.51	37.01	37.08	33.52	37.53	41.76	13.99	113.10	19.71
53.00	36.80	33.58	21.37	37.56	36.55	37.01	37.09	33.51	37.53	41.75	13.99	113.18	19.73
54.00	36.79	33.48	21.48	37.45	36.55	37.01	37.10	33.50	37.50	41.77	14.01	113.29	19.73
55.00	36.78	33.60	21.53	37.38	36.60	37.01	37.09	33.52	37.53	41.77	14.02	113.60	19.75
56.00	36.75	33.32	21.69	37.41	36.60	37.01	37.09	33.51	37.53	41.75	14.04	109.66	19.79
57.00	36.76	33.18	21.87	37.50	36.56	37.01	37.10	33.52	37.53	41.75	14.04	112.37	19.78
58.00	36.75	33.32	21.91	37.49	36.58	37.04	37.11	33.56	37.54	41.77	14.04	114.28	19.78
59.00	36.75	33.60	21.88	37.53	36.59	37.05	37.12	33.61	37.53	41.74	14.04	113.39	19.79
60.00	36.75	33.62	21.85	37.54	36.73	37.71	37.14	33.76	37.53	41.75	14.01	113.96	19.75
61.00	36.77	33.87	21.91	37.61	36.61	37.70	37.14	33.81	37.54	41.75	13.99	115.86	19.73
62.00	36.78	34.02	21.97	37.58	36.59	37.32	37.17	33.78	37.51	41.72	14.00	115.94	19.76
63.00	36.82	34.14	22.11	37.62	36.65	37.15	37.18	33.81	37.49	41.75	13.99	114.44	19.73
64.00	36.81	34.23	22.29	37.63	36.73	37.17	37.17	33.86	37.52	41.72	13.96	116.08	19.71
65.00	36.79	34.48	22.50	37.57	36.88	37.18	37.17	33.96	37.54	41.73	13.94	116.20	19.69
66.00	36.79	34.54	22.68	37.61	36.75	37.19	37.16	33.99	37.57	41.75	13.95	116.05	19.67
67.00	36.79	34.53	22.88	37.64	36.56	37.20	37.15	34.01	37.59	41.73	13.95	115.60	19.70

68.00	36.82	34.43	23.12	37.65	36.52	37.19	37.15	34.04	37.62	41.75	13.96	114.58	19.69
69.00	36.76	34.46	23.29	37.65	36.53	37.19	37.16	34.07	37.62	41.75	13.96	114.26	19.69
70.00	36.78	34.51	23.34	37.71	36.43	37.17	37.23	34.10	37.63	41.74	13.97	112.49	19.71
71.00	36.78	34.63	23.53	37.71	36.46	37.18	37.22	34.16	37.65	41.75	13.99	113.40	19.73
72.00	36.78	34.72	23.58	37.69	36.47	37.19	37.20	34.18	37.63	41.74	14.01	110.86	19.76
73.00	36.81	34.76	23.69	37.80	36.53	37.18	37.19	34.22	37.65	41.73	14.02	112.91	19.78
74.00	36.82	34.83	23.82	37.81	36.49	37.17	37.24	34.26	37.64	41.75	14.03	114.19	19.78
75.00	36.80	34.81	23.89	37.75	36.43	37.19	37.26	34.27	37.65	41.73	14.03	113.52	19.80
76.00	36.73	34.75	23.90	37.69	36.53	37.19	37.27	34.26	37.68	41.72	14.04	113.89	19.82
77.00	36.83	34.73	24.01	37.71	36.39	37.18	37.28	34.28	37.65	41.72	14.04	114.70	19.83
78.00	36.87	34.63	24.24	37.82	36.29	37.18	37.29	34.31	37.65	41.72	14.04	113.40	19.82
79.00	36.87	34.69	25.02	37.80	36.35	37.18	37.30	34.47	37.67	41.72	14.04	113.76	19.81
80.00	36.90	34.76	25.13	37.82	36.37	37.19	37.31	34.51	37.66	41.73	14.03	113.65	19.80
81.00	36.86	34.89	25.13	37.72	36.39	37.20	37.32	34.53	37.66	41.73	14.04	113.79	19.80
82.00	36.89	34.92	25.31	37.73	36.44	37.20	37.32	34.58	37.67	41.72	14.04	114.04	19.82
83.00	36.87	35.02	25.35	37.73	36.51	37.20	37.33	34.61	37.67	41.72	14.02	113.94	19.80
84.00	36.90	35.08	25.38	37.68	36.46	37.20	37.35	34.62	37.68	41.74	13.97	113.91	19.72
85.00	36.91	35.11	25.71	37.71	36.45	37.19	37.39	34.70	37.69	41.75	13.95	115.52	19.67
86.00	36.92	35.13	25.95	37.75	36.46	37.21	37.40	34.76	37.67	41.72	13.93	115.89	19.68
87.00	36.93	35.13	26.19	37.76	36.50	37.22	37.41	34.81	37.68	41.71	13.92	115.48	19.67
88.00	36.93	35.20	26.37	37.66	36.60	37.20	37.41	34.85	37.70	41.70	13.91	115.29	19.68
89.00	36.94	35.26	26.63	37.76	36.57	37.24	37.41	34.92	37.70	41.68	13.91	117.11	19.70
90.00	36.95	35.22	26.84	37.86	36.53	37.24	37.41	34.96	37.74	41.70	13.90	115.72	19.67
91.00	36.96	35.26	26.87	38.02	36.59	37.22	37.42	34.99	37.72	41.70	13.90	115.23	19.66
92.00	36.96	35.32	26.94	38.00	36.63	37.23	37.41	35.01	37.73	41.68	13.89	116.81	19.67
93.00	36.95	35.34	27.06	37.87	36.68	37.22	37.42	35.04	37.73	41.71	13.90	115.78	19.65
94.00	36.96	35.44	27.28	37.88	36.69	37.22	37.43	35.10	37.72	41.70	13.90	116.41	19.66
95.00	36.98	35.55	27.45	37.92	36.72	37.23	37.44	35.16	37.75	41.69	13.90	117.18	19.68
96.00	36.99	35.63	27.43	37.98	36.81	37.21	37.43	35.18	37.76	41.69	13.91	117.14	19.68
97.00	37.00	35.71	27.59	38.01	36.80	37.21	37.44	35.22	37.75	41.69	13.93	117.74	19.71
98.00	37.01	35.77	27.91	38.04	36.81	37.23	37.44	35.30	37.75	41.68	13.94	116.20	19.73
99.00	37.04	35.78	27.98	38.15	36.83	37.23	37.45	35.33	37.75	41.66	13.95	118.85	19.76
100.00	37.04	35.81	28.07	38.13	36.75	37.22	37.45	35.34	37.73	41.67	13.97	117.77	19.78
101.00	37.05	35.83	28.02	38.07	36.76	37.26	37.46	35.34	37.75	41.68	13.97	118.31	19.77
102.00	37.06	35.91	28.05	38.07	36.82	37.27	37.45	35.37	37.74	41.68	13.98	117.81	19.79
103.00	37.08	35.98	28.18	38.08	36.80	37.27	37.46	35.41	37.75	41.69	13.98	118.66	19.78

104.00	37.09	36.00	28.47	38.07	36.83	37.26	37.46	35.47	37.76	41.67	13.99	117.94	19.80
105.00	37.10	36.02	28.63	38.08	36.91	37.24	37.47	35.50	37.75	41.68	14.00	117.29	19.80
106.00	37.10	35.97	28.84	38.07	36.89	37.23	37.46	35.53	37.75	41.68	13.99	116.43	19.79
107.00	37.12	36.05	29.09	38.14	36.96	37.25	37.46	35.60	37.76	41.72	13.99	118.21	19.76
108.00	37.14	36.11	29.36	38.21	37.06	37.24	37.45	35.68	37.75	41.69	13.99	118.18	19.79
109.00	37.12	36.19	29.62	38.17	37.08	37.22	37.46	35.73	37.74	41.67	13.99	118.12	19.81
110.00	37.14	36.24	29.83	38.18	37.09	37.25	37.47	35.79	37.77	41.68	13.99	117.54	19.80
111.00	37.16	36.29	30.05	38.21	37.08	37.28	37.47	35.85	37.75	41.69	13.99	119.64	19.79
112.00	37.16	36.31	30.18	38.21	37.05	37.28	37.48	35.88	37.77	41.69	14.01	118.64	19.81
113.00	37.16	36.33	30.30	38.19	37.15	37.29	37.47	35.91	37.77	41.71	14.03	118.05	19.81
114.00	37.16	36.31	30.41	38.17	37.17	37.31	37.48	35.93	37.77	41.68	14.02	118.95	19.84
115.00	37.17	36.35	30.51	38.17	37.20	37.32	37.48	35.96	37.77	41.66	14.02	118.61	19.86
116.00	37.18	36.41	30.65	38.19	37.20	37.33	37.48	36.00	37.77	41.69	14.01	119.69	19.82
117.00	37.19	36.42	30.72	38.28	37.12	37.34	37.49	36.03	37.77	41.66	14.01	118.58	19.84
118.00	37.20	36.44	30.81	38.33	37.12	37.34	37.50	36.05	37.77	41.67	14.02	120.31	19.85
119.00	37.21	36.40	30.95	38.34	37.07	37.34	37.51	36.07	37.76	41.69	14.04	120.41	19.85
120.00	37.22	36.51	31.12	38.31	37.03	37.37	37.51	36.12	37.78	41.69	14.03	120.55	19.84

**Table 8.14 Session 1 Human subject baseline results average (Subjects 1-3, 7-8,10-12)**

Time min	Skin 2-1 C	Skin 2-2 C	Skin 2-3 C	Skin 2-4 C	Skin 2-5 C	Skin 2-6 C	Skin 2-7 C	Average Skin C	Core C	Air Temp C	Dew C	Heart Rate B/min	RH %
1	36.32	36.52	34.67	38.72	38.02	35.76	35.69	36.11	36.95	41.33	13.86	99.47	19.99
2	36.32	36.66	34.80	38.61	37.84	35.91	35.86	36.20	36.94	41.37	13.96	103.36	20.09
3	36.29	36.77	34.92	38.55	37.65	36.02	35.97	36.27	36.94	41.39	13.93	99.65	20.03
4	36.29	36.87	35.06	38.49	37.53	36.11	36.08	36.34	36.94	41.41	13.95	100.52	20.04
5	36.30	36.96	35.17	38.45	37.48	36.19	36.20	36.41	36.93	41.41	13.96	101.92	20.05
6	36.31	37.01	35.28	38.42	37.43	36.27	36.31	36.48	36.93	41.41	13.97	102.16	20.06
7	36.33	37.08	35.41	38.40	37.41	36.34	36.42	36.55	36.93	41.45	13.96	103.79	20.00
8	36.36	37.15	35.48	38.42	37.36	36.41	36.52	36.61	36.94	41.46	13.96	103.40	19.99
9	36.38	37.24	35.55	38.41	37.36	36.43	36.60	36.66	36.95	41.48	13.96	104.13	19.97
10	36.39	37.26	35.67	38.41	37.34	36.47	36.67	36.71	36.97	41.51	13.93	105.07	19.90
11	36.43	37.27	35.79	38.36	37.30	36.54	36.72	36.76	36.98	41.55	13.91	104.39	19.84
12	36.45	37.28	35.91	38.30	37.26	36.60	36.76	36.79	37.00	41.58	13.92	104.96	19.82
13	36.43	37.27	35.99	38.28	37.17	36.66	36.80	36.82	37.04	41.59	13.93	103.31	19.82
14	36.45	37.26	36.08	38.26	37.12	36.70	36.83	36.84	37.03	41.61	13.96	104.70	19.84
15	36.47	37.23	36.15	38.20	37.12	36.73	36.84	36.85	37.05	41.63	13.99	106.30	19.85
16	36.49	37.18	36.20	38.15	37.09	36.75	36.86	36.86	37.07	41.64	14.01	105.78	19.87
17	36.49	37.17	36.26	38.08	37.00	36.73	36.87	36.86	37.09	41.65	14.03	106.77	19.88
18	36.50	37.18	36.32	38.00	36.96	36.76	36.88	36.87	37.10	41.66	14.05	107.58	19.90
19	36.51	37.15	36.40	37.94	36.94	36.81	36.91	36.89	37.11	41.68	14.07	109.45	19.90
20	36.52	37.15	36.45	37.84	36.90	36.84	36.94	36.90	37.14	41.71	14.07	107.95	19.87
21	36.50	37.11	36.46	37.74	36.88	36.80	36.95	36.88	37.15	41.72	14.07	108.68	19.85
22	36.49	37.14	36.43	37.68	36.84	36.79	36.95	36.87	37.16	41.70	14.07	108.66	19.88
23	36.50	37.16	36.46	37.62	36.78	36.78	36.96	36.87	37.16	41.73	14.07	109.09	19.85
24	36.50	37.18	36.49	37.56	36.76	36.78	36.97	36.88	37.18	41.73	14.07	109.98	19.85
25	36.53	37.16	36.49	37.46	36.78	36.77	36.98	36.87	37.19	41.74	14.06	111.20	19.82
26	36.57	37.11	36.40	37.48	36.85	36.80	36.99	36.86	37.19	41.74	14.05	111.31	19.82
27	36.54	37.07	36.37	37.30	36.83	36.80	37.00	36.83	37.23	41.77	14.05	112.50	19.78
28	36.46	37.04	36.35	37.20	36.65	36.75	37.02	36.79	37.24	41.71	14.05	112.60	19.84
29	36.49	37.00	36.35	37.18	36.56	36.76	37.03	36.78	37.25	41.72	14.04	112.64	19.82
30	36.51	36.96	36.34	37.26	36.55	36.78	37.04	36.78	37.26	41.75	14.05	114.21	19.79
31	36.57	36.88	36.37	37.31	36.55	36.80	37.05	36.79	37.28	41.75	14.02	117.29	19.76



32	36.61	36.87	36.45	37.20	36.52	36.84	37.05	36.80	37.30	41.77	14.00	114.54	19.72
33	36.63	36.83	36.46	37.02	36.54	36.83	37.03	36.78	37.31	41.76	14.01	117.11	19.74
34	36.63	36.79	36.46	37.07	36.59	36.86	37.05	36.79	37.32	41.78	14.02	115.43	19.73
35	36.65	36.82	36.39	37.23	36.66	36.88	37.07	36.81	37.34	41.79	14.03	116.04	19.74
36	36.63	36.79	36.40	37.27	36.55	36.89	37.09	36.81	37.35	41.80	14.04	116.43	19.75
37	36.71	36.81	36.36	37.26	36.58	36.91	37.10	36.82	37.35	41.79	14.05	117.00	19.76
38	36.76	36.80	36.41	37.18	36.53	36.93	37.11	36.83	37.37	41.80	14.06	117.85	19.76
39	36.75	36.83	36.43	37.20	36.47	36.93	37.11	36.83	37.38	41.81	14.08	117.75	19.78
40	36.81	36.79	36.45	37.17	36.47	36.92	37.13	36.83	37.39	41.81	14.07	117.99	19.76
41	36.85	36.78	36.49	37.18	36.42	36.92	37.13	36.84	37.41	41.83	14.08	118.80	19.76
42	36.87	36.73	36.54	37.17	36.40	36.96	37.15	36.85	37.45	41.82	14.10	117.56	19.78
43	36.83	36.70	36.61	37.25	36.35	36.99	37.16	36.86	37.45	41.83	14.11	119.79	19.80
44	36.80	36.79	36.56	37.23	36.33	37.00	37.16	36.87	37.47	41.82	14.11	119.43	19.81
45	36.84	36.79	36.53	37.27	36.34	37.01	37.17	36.87	37.49	41.80	14.12	119.67	19.84
46	36.85	36.77	36.54	37.29	36.27	37.01	37.17	36.87	37.52	41.82	14.13	119.34	19.83
47	36.88	36.78	36.55	37.35	36.34	37.01	37.19	36.89	37.54	41.83	14.14	119.01	19.83
48	36.91	36.76	36.56	37.44	36.35	37.00	37.21	36.90	37.56	41.80	14.14	120.27	19.87
49	36.90	36.84	36.52	37.37	36.45	37.04	37.23	36.92	37.58	41.79	14.13	120.52	19.86
50	36.90	36.83	36.52	37.41	36.43	37.08	37.24	36.93	37.59	41.79	14.12	119.68	19.86
51	36.90	36.82	36.52	37.49	36.40	37.08	37.25	36.93	37.60	41.78	14.12	119.85	19.86
52	36.93	36.85	36.55	37.51	36.37	37.08	37.27	36.95	37.62	41.79	14.10	121.80	19.83
53	36.98	36.78	36.48	37.58	36.40	37.09	37.27	36.94	37.63	41.79	14.10	122.09	19.83
54	36.97	36.71	36.45	37.63	36.43	37.08	37.30	36.93	37.65	41.81	14.11	121.97	19.82
55	36.97	36.68	36.48	37.58	36.37	37.05	37.31	36.92	37.65	41.81	14.11	123.09	19.82
56	36.98	36.75	36.52	37.62	36.41	37.07	37.32	36.95	37.66	41.79	14.11	122.98	19.83
57	36.99	36.77	36.59	37.62	36.33	37.10	37.33	36.97	37.68	41.81	14.10	122.39	19.80
58	37.01	36.71	36.65	37.64	36.19	37.12	37.32	36.96	37.71	41.79	14.09	124.13	19.80
59	37.01	36.77	36.65	37.61	36.17	37.14	37.34	36.98	37.72	41.78	14.07	123.07	19.79
60	37.02	36.80	36.62	37.57	36.32	37.14	37.35	36.99	37.74	41.78	14.03	125.12	19.74
61	37.02	36.72	36.66	37.50	36.30	37.17	37.35	36.98	37.76	41.77	14.01	127.56	19.74
62	37.06	36.68	36.66	37.39	36.34	37.20	37.37	36.98	37.77	41.79	14.00	125.00	19.69
63	37.09	36.68	36.66	37.39	36.33	37.21	37.38	36.99	37.79	41.79	13.99	126.70	19.68
64	37.12	36.69	36.70	37.38	36.37	37.21	37.39	37.00	37.79	41.76	13.97	127.28	19.69
65	37.14	36.77	36.65	37.45	36.33	37.23	37.40	37.02	37.80	41.79	13.94	126.91	19.62
66	37.15	36.79	36.70	37.45	36.30	37.24	37.41	37.03	37.81	41.81	13.94	126.32	19.60
67	37.15	36.78	36.71	37.47	36.24	37.26	37.42	37.04	37.84	41.78	13.94	126.86	19.63

68	37.18	36.70	36.74	37.42	36.19	37.28	37.43	37.03	37.84	41.80	13.95	128.44	19.63
69	37.20	36.63	36.74	37.30	36.14	37.28	37.45	37.01	37.85	41.82	13.97	127.84	19.63
70	37.20	36.64	36.72	37.28	36.28	37.30	37.46	37.02	37.86	41.82	13.98	128.01	19.64
71	37.22	36.64	36.77	37.35	36.35	37.32	37.46	37.05	37.87	41.81	14.00	127.94	19.67
72	37.22	36.80	36.72	37.41	36.39	37.35	37.47	37.08	37.88	41.81	14.00	128.53	19.68
73	37.25	36.89	36.62	37.56	36.31	37.37	37.47	37.09	37.90	41.83	14.00	128.15	19.66
74	37.27	36.88	36.70	37.64	36.38	37.38	37.48	37.12	37.91	41.80	14.02	127.46	19.71
75	37.24	36.75	36.80	37.54	36.41	37.41	37.48	37.11	37.91	41.83	14.02	128.98	19.67
76	37.17	36.81	36.83	37.54	36.39	37.40	37.48	37.12	37.93	41.82	14.03	131.00	19.70
77	37.20	36.80	36.86	37.56	36.44	37.40	37.50	37.14	37.93	41.83	14.02	128.21	19.68
78	37.25	36.82	36.88	37.56	36.45	37.39	37.51	37.15	37.94	41.83	14.02	128.56	19.68
79	37.28	36.78	36.93	37.61	36.54	37.40	37.53	37.17	37.96	41.80	14.02	130.46	19.70
80	37.30	36.78	36.92	37.61	36.48	37.40	37.54	37.17	37.97	41.82	14.00	129.75	19.67
81	37.36	36.83	36.88	37.67	36.39	37.37	37.55	37.17	37.99	41.81	14.00	131.73	19.67
82	37.39	36.80	36.89	37.69	36.48	37.39	37.56	37.18	38.01	41.79	13.99	131.07	19.68
83	37.39	36.79	36.90	37.70	36.53	37.40	37.56	37.19	38.01	41.80	13.99	131.03	19.68
84	37.40	36.79	36.90	37.75	36.57	37.40	37.58	37.20	38.02	41.77	14.00	131.57	19.71
85	37.45	36.83	36.86	37.80	36.54	37.40	37.60	37.21	38.04	41.78	14.00	134.00	19.71
86	37.45	36.73	36.85	37.80	36.49	37.41	37.60	37.19	38.03	41.77	14.00	133.82	19.72
87	37.49	36.72	36.76	37.84	36.48	37.43	37.62	37.18	38.04	41.79	14.01	134.02	19.70
88	37.52	36.76	36.80	37.85	36.59	37.43	37.63	37.21	38.05	41.77	14.02	134.87	19.74
89	37.52	36.78	36.77	37.78	36.60	37.42	37.63	37.20	38.06	41.78	14.03	134.02	19.73
90	37.54	36.84	36.76	37.91	36.59	37.40	37.65	37.22	38.06	41.75	14.02	133.49	19.76
91	37.58	36.85	36.84	37.82	36.65	37.41	37.66	37.24	38.07	41.77	14.03	134.74	19.76
92	37.60	36.79	36.90	37.80	36.67	37.43	37.67	37.25	38.09	41.77	14.03	133.48	19.76
93	37.61	36.85	36.88	37.68	36.71	37.43	37.66	37.25	38.10	41.77	14.03	133.91	19.76
94	37.62	36.88	36.98	37.60	36.80	37.45	37.67	37.28	38.11	41.75	14.04	136.03	19.78
95	37.62	36.88	37.00	37.62	36.82	37.46	37.68	37.29	38.11	41.74	14.02	133.96	19.78
96	37.66	36.80	37.03	37.73	36.84	37.49	37.70	37.30	38.11	41.75	14.02	135.59	19.76
97	37.69	36.82	37.01	37.79	36.83	37.46	37.70	37.30	38.12	41.74	14.01	135.80	19.76
98	37.69	36.85	37.02	37.90	36.84	37.47	37.68	37.32	38.13	41.74	14.01	137.32	19.76
99	37.65	36.90	36.92	37.93	36.78	37.51	37.69	37.32	38.13	41.74	14.01	137.57	19.76
100	37.68	36.88	36.95	37.85	36.88	37.50	37.70	37.32	38.14	41.72	14.00	137.54	19.77
101	37.68	36.90	36.95	37.84	36.84	37.50	37.71	37.32	38.15	41.72	14.00	136.91	19.77
102	37.68	36.92	36.91	37.82	36.76	37.49	37.72	37.31	38.16	41.72	14.01	135.90	19.78
103	37.68	36.88	37.02	37.79	36.85	37.50	37.73	37.33	38.16	41.73	14.01	138.02	19.76

104	37.69	36.87	37.11	37.84	36.82	37.50	37.73	37.35	38.16	41.73	14.01	136.17	19.77
105	37.69	36.81	37.11	37.86	36.82	37.50	37.74	37.34	38.17	41.72	14.02	134.61	19.80
106	37.70	36.84	37.11	37.85	36.76	37.50	37.74	37.34	38.18	41.76	14.01	136.07	19.74
107	37.72	36.86	37.11	37.84	36.74	37.51	37.75	37.35	38.17	41.75	14.02	137.16	19.75
108	37.72	36.85	37.12	37.87	36.76	37.51	37.76	37.36	38.18	41.72	14.01	137.40	19.78
109	37.73	36.95	37.15	37.92	36.77	37.51	37.77	37.39	38.19	41.73	13.99	136.40	19.75
110	37.74	37.03	37.21	37.90	36.75	37.50	37.78	37.41	38.19	41.72	13.99	137.89	19.75
111	37.75	36.99	37.23	38.00	36.82	37.52	37.79	37.43	38.19	41.72	14.00	138.65	19.77
112	37.76	36.94	37.25	37.98	36.76	37.53	37.80	37.42	38.20	41.72	13.99	138.16	19.76
113	37.75	36.95	37.23	37.90	36.75	37.52	37.81	37.41	38.20	41.72	14.00	139.17	19.76
114	37.76	36.93	37.18	37.93	36.87	37.52	37.81	37.41	38.21	41.72	13.99	137.73	19.75
115	37.77	36.94	37.21	38.01	36.83	37.52	37.82	37.42	38.21	41.72	13.98	138.19	19.73
116	37.78	36.91	37.19	38.04	36.82	37.52	37.82	37.42	38.22	41.71	13.96	140.42	19.72
117	37.77	36.91	37.13	38.07	36.89	37.52	37.82	37.41	38.23	41.69	13.96	137.60	19.74
118	37.79	36.88	37.11	38.17	36.92	37.53	37.84	37.42	38.23	41.72	13.97	138.44	19.72
119	37.78	36.95	37.08	38.22	36.88	37.54	37.84	37.43	38.23	41.70	13.97	140.46	19.75
120	37.72	37.00	37.08	38.31	36.85	37.56	37.85	37.44	38.24	41.69	13.96	141.27	19.76

**Table 8.15 Session 1 Human subject PCS #1 results average (Subjects 1-3, 7-8,10-12)**

Time min	Skin 2- 1 C	Skin 2- 2 C	Skin 2- 3 C	Skin 2- 4 C	Skin 2- 5 C	Skin 2- 6 C	Skin 2- 7 C	Average Skin C	Core C	Air Temp C	Dew C	Heart Rate B/min	RH %
1.00	36.06	35.96	34.79	38.73	37.83	35.38	35.84	35.95	37.10	41.53	14.13	98.80	20.14
2.00	36.05	35.93	34.79	38.59	37.79	35.63	35.98	36.01	37.10	41.59	14.23	101.96	20.22
3.00	36.05	35.98	34.81	38.52	37.59	35.71	36.06	36.04	37.09	41.61	14.22	99.34	20.17
4.00	36.02	35.96	34.88	38.47	37.63	35.80	36.13	36.08	37.09	41.63	14.24	99.00	20.17
5.00	36.06	35.97	34.99	38.40	37.89	35.91	36.24	36.16	37.11	41.68	14.25	99.65	20.14
6.00	36.02	35.91	35.05	38.28	37.98	35.96	36.30	36.18	37.11	41.70	14.27	98.12	20.13
7.00	35.97	35.91	35.06	38.16	37.87	35.96	36.35	36.17	37.10	41.68	14.23	98.36	20.10
8.00	36.00	35.99	35.16	38.19	37.86	36.03	36.46	36.25	37.12	41.74	14.25	98.48	20.08
9.00	35.98	36.03	35.15	38.12	37.83	35.98	36.51	36.24	37.09	41.68	14.24	100.19	20.12
10.00	36.04	36.20	35.26	38.11	37.71	36.03	36.59	36.31	37.14	41.75	14.28	101.20	20.10
11.00	36.04	36.18	35.29	37.88	37.51	36.04	36.59	36.29	37.14	41.71	14.24	101.17	20.08
12.00	36.09	36.17	35.35	37.82	37.47	36.07	36.66	36.31	37.16	41.78	14.27	100.82	20.06
13.00	36.04	36.09	35.34	37.74	37.41	36.07	36.64	36.28	37.16	41.74	14.22	101.00	20.04
14.00	36.06	35.97	35.34	37.74	37.37	36.06	36.67	36.26	37.17	41.77	14.21	100.83	19.99
15.00	36.10	35.94	35.32	37.68	37.19	36.05	36.72	36.24	37.17	41.77	14.21	99.79	19.99
16.00	36.17	35.98	35.35	37.70	37.19	36.11	36.77	36.29	37.19	41.79	14.25	100.80	20.02
17.00	36.13	35.99	35.24	37.61	37.12	36.08	36.75	36.24	37.17	41.77	14.22	100.94	19.99
18.00	36.07	35.92	35.23	37.58	37.03	36.11	36.76	36.23	37.19	41.79	14.21	101.17	19.96
19.00	36.06	35.84	35.26	37.56	37.03	36.12	36.77	36.22	37.13	41.78	14.25	103.67	20.03
20.00	36.05	35.74	35.33	37.54	36.97	36.11	36.81	36.21	37.14	41.80	14.21	103.30	19.95
21.00	36.02	35.68	35.38	37.46	36.91	36.14	36.82	36.20	37.21	41.81	14.25	102.11	20.00
22.00	36.02	35.70	35.40	37.43	36.90	36.16	36.82	36.21	37.15	41.79	14.20	102.29	19.96
23.00	36.01	35.72	35.49	37.39	36.90	36.17	36.83	36.23	37.22	41.78	14.19	101.07	19.95
24.00	36.05	35.70	35.45	37.45	36.87	36.17	36.84	36.23	37.22	41.79	14.23	101.67	20.00
25.00	36.15	35.66	35.32	37.41	36.75	36.16	36.84	36.19	37.28	41.77	14.21	103.72	19.99
26.00	36.14	35.76	35.34	37.39	36.75	36.15	36.84	36.21	37.28	41.75	14.16	102.52	19.94
27.00	36.06	35.72	35.35	37.36	36.73	36.15	36.84	36.19	37.23	41.74	14.15	103.04	19.94
28.00	36.13	35.72	35.26	37.36	36.65	36.13	36.86	36.18	37.30	41.71	14.13	103.39	19.95
29.00	36.18	35.71	35.18	37.33	36.19	36.16	36.85	36.13	37.30	41.73	14.12	103.91	19.91
30.00	36.22	35.52	35.11	37.14	36.14	36.16	36.88	36.08	37.31	41.70	14.08	107.45	19.89
31.00	36.26	35.46	35.10	37.11	36.42	36.16	36.88	36.08	37.31	41.70	14.00	107.33	19.79

32.00	36.22	35.46	35.11	37.18	36.13	36.17	36.89	36.07	37.30	41.72	13.92	106.99	19.66
33.00	36.13	35.26	35.17	37.12	36.03	36.20	36.90	36.03	37.30	41.73	13.85	107.49	19.57
34.00	36.09	35.34	35.16	36.98	36.09	36.24	36.91	36.05	37.31	41.75	13.80	107.27	19.48
35.00	36.10	35.40	35.19	36.94	36.18	36.25	36.90	36.07	37.30	41.75	13.78	106.79	19.46
36.00	36.10	35.39	35.18	37.06	36.30	36.26	36.91	36.09	37.30	41.73	13.77	108.94	19.48
37.00	35.96	35.15	35.27	37.07	36.35	36.26	36.92	36.06	37.34	41.72	13.78	106.47	19.50
38.00	35.85	35.26	35.28	37.07	36.44	36.25	36.88	36.07	37.37	41.73	13.79	108.41	19.50
39.00	35.90	35.31	35.23	37.06	36.42	36.24	36.88	36.07	37.41	41.73	13.79	107.19	19.50
40.00	35.96	35.22	35.26	37.06	36.44	36.24	36.89	36.06	37.40	41.73	13.80	104.77	19.51
41.00	36.12	35.05	35.27	37.09	36.40	36.23	36.89	36.04	37.42	41.73	13.82	107.78	19.54
42.00	36.05	35.05	35.18	37.04	36.46	36.21	36.91	36.02	37.40	41.72	13.83	108.03	19.57
43.00	35.99	35.12	35.07	37.06	36.47	36.07	36.91	35.98	37.41	41.71	13.85	106.95	19.59
44.00	35.96	35.26	35.06	37.04	36.45	36.06	36.88	36.00	37.42	41.73	13.86	108.82	19.59
45.00	36.03	35.36	35.09	37.02	36.48	36.13	36.89	36.04	37.42	41.75	13.87	109.37	19.57
46.00	36.06	35.41	35.20	37.03	36.48	36.16	36.89	36.08	37.41	41.73	13.88	109.09	19.60
47.00	36.03	35.35	35.30	37.01	36.50	36.17	36.89	36.09	37.47	41.72	13.90	108.17	19.64
48.00	36.07	35.34	35.30	37.08	36.53	36.17	36.88	36.09	37.46	41.73	13.91	110.24	19.65
49.00	36.06	35.45	35.20	37.18	36.54	36.17	36.86	36.10	37.44	41.71	13.93	108.04	19.69
50.00	36.08	35.44	35.17	37.18	36.54	36.18	36.87	36.09	37.43	41.74	13.93	108.47	19.67
51.00	36.07	35.28	35.31	37.12	36.43	36.22	36.87	36.09	37.46	41.72	13.93	108.83	19.68
52.00	36.07	35.23	35.29	37.12	36.32	36.24	36.89	36.07	37.46	41.74	13.94	108.77	19.67
53.00	36.09	35.30	35.26	37.11	36.32	36.26	36.87	36.08	37.50	41.72	13.95	107.00	19.70
54.00	36.04	35.34	35.21	37.20	36.34	36.24	36.88	36.08	37.48	41.71	13.95	110.14	19.71
55.00	36.03	35.45	35.00	37.26	36.31	36.26	36.89	36.07	37.51	41.72	13.95	107.96	19.70
56.00	36.02	35.40	34.97	37.34	36.30	36.26	36.90	36.06	37.52	41.73	13.96	108.65	19.71
57.00	36.10	35.36	34.99	37.28	36.29	36.26	36.91	36.06	37.52	41.72	13.97	110.21	19.72
58.00	36.08	35.41	35.03	37.33	36.27	36.27	36.92	36.08	37.54	41.74	13.97	109.91	19.71
59.00	36.09	35.55	34.97	37.40	36.32	36.31	36.92	36.12	37.52	41.71	13.98	109.16	19.75
60.00	36.04	35.53	34.95	37.46	36.39	36.30	36.91	36.11	37.51	41.71	13.97	111.74	19.73
61.00	35.70	35.50	35.06	37.56	36.33	36.21	36.91	36.08	37.49	41.66	13.95	113.42	19.76
62.00	35.54	35.47	35.09	37.62	36.31	36.19	36.91	36.07	37.49	41.72	13.95	112.97	19.70
63.00	35.48	35.35	35.21	37.49	36.30	36.21	36.95	36.07	37.48	41.70	13.95	112.35	19.72
64.00	35.63	35.43	35.22	37.61	36.37	36.23	36.99	36.12	37.50	41.71	13.94	109.24	19.70
65.00	36.11	35.60	35.28	37.54	36.33	36.25	37.00	36.20	37.50	41.70	13.94	110.31	19.71
66.00	36.13	35.63	35.30	37.52	36.42	36.28	36.99	36.22	37.53	41.70	13.96	111.89	19.73
67.00	35.99	35.65	35.28	37.48	36.50	36.28	36.99	36.21	37.49	41.72	13.98	109.85	19.74

68.00	36.17	35.61	35.21	37.25	36.38	36.27	36.98	36.18	37.51	41.69	13.99	112.46	19.78
69.00	36.31	35.62	35.22	37.23	36.15	36.27	36.99	36.17	37.52	41.69	13.99	113.37	19.78
70.00	36.50	35.57	35.20	37.27	36.34	36.31	37.00	36.20	37.56	41.69	13.99	111.72	19.80
71.00	37.00	35.48	35.19	37.61	36.43	36.28	37.00	36.25	37.56	41.69	14.01	113.75	19.81
72.00	37.09	35.33	35.14	37.81	36.50	36.28	36.97	36.23	37.58	41.69	14.00	113.67	19.80
73.00	37.10	35.31	35.22	37.66	36.57	36.27	36.99	36.23	37.59	41.69	14.01	113.02	19.81
74.00	37.09	35.42	35.25	37.58	36.63	36.28	37.01	36.27	37.60	41.70	14.01	113.81	19.81
75.00	37.04	35.53	35.28	37.56	36.66	36.26	37.02	36.29	37.60	41.70	14.02	112.55	19.82
76.00	37.11	35.58	35.25	37.52	36.67	36.27	37.02	36.30	37.60	41.68	14.02	109.99	19.84
77.00	37.19	35.58	35.28	37.41	36.70	36.28	37.01	36.30	37.58	41.68	14.00	109.98	19.81
78.00	37.18	35.68	35.22	37.37	36.75	36.25	37.01	36.30	37.61	41.66	13.93	112.19	19.74
79.00	37.17	35.65	35.26	37.35	36.71	36.24	37.01	36.30	37.62	41.66	13.87	113.03	19.66
80.00	37.19	35.71	35.28	37.44	36.68	36.24	37.00	36.32	37.59	41.65	13.82	112.40	19.62
81.00	37.18	35.72	35.21	37.37	36.70	36.23	37.02	36.30	37.58	41.65	13.81	111.55	19.59
82.00	37.22	35.73	35.21	37.43	36.64	36.23	37.02	36.31	37.60	41.64	13.79	110.90	19.59
83.00	37.20	35.67	35.21	37.55	36.57	36.22	37.04	36.30	37.57	41.65	13.78	113.40	19.57
84.00	37.24	35.90	35.28	37.65	36.59	36.21	37.05	36.37	37.65	41.61	13.78	113.53	19.60
85.00	37.26	36.01	35.31	37.72	36.56	36.21	37.05	36.40	37.69	41.63	13.78	115.06	19.58
86.00	37.31	35.61	35.28	37.60	36.41	36.23	37.07	36.31	37.71	41.65	13.75	116.76	19.53
87.00	37.29	35.45	35.28	37.56	36.48	36.24	37.09	36.29	37.69	41.62	13.76	116.53	19.56
88.00	37.23	35.45	35.26	37.56	36.62	36.23	37.09	36.29	37.70	41.63	13.76	116.34	19.56
89.00	37.26	35.46	35.36	37.55	36.65	36.23	37.08	36.31	37.68	41.63	13.77	118.64	19.57
90.00	37.27	35.56	35.45	37.62	36.59	36.24	37.08	36.35	37.68	41.65	13.76	116.24	19.54
91.00	37.26	35.67	35.44	37.74	36.64	36.25	37.09	36.38	37.70	41.64	13.78	115.37	19.58
92.00	37.25	35.86	35.41	37.74	36.62	36.25	37.09	36.41	37.72	41.63	13.80	115.56	19.61
93.00	37.21	35.83	35.51	37.72	36.75	36.24	37.11	36.43	37.70	41.64	13.80	116.13	19.60
94.00	37.22	35.70	35.35	37.65	36.61	36.26	37.12	36.37	37.67	41.64	13.81	115.61	19.61
95.00	37.22	35.83	35.42	37.70	36.79	36.24	37.10	36.41	37.69	41.63	13.82	117.39	19.63
96.00	37.27	35.94	35.38	37.79	36.86	36.23	37.12	36.44	37.70	41.64	13.82	117.95	19.62
97.00	37.32	35.90	35.32	37.91	36.85	36.23	37.13	36.44	37.72	41.65	13.83	116.81	19.62
98.00	37.30	35.89	35.47	38.00	36.84	36.23	37.14	36.47	37.74	41.64	13.84	117.56	19.64
99.00	37.30	35.92	35.47	37.95	36.90	36.24	37.14	36.48	37.77	41.63	13.85	117.67	19.67
100.00	37.27	35.96	35.33	37.97	36.97	36.29	37.16	36.48	37.76	41.64	13.85	120.56	19.65
101.00	37.27	36.01	35.37	37.94	36.99	36.31	37.19	36.51	37.78	41.63	13.86	119.12	19.68
102.00	37.28	35.91	35.39	37.91	36.89	36.33	37.22	36.50	37.74	41.67	13.87	119.80	19.65
103.00	37.27	35.75	35.45	37.87	36.88	36.36	37.24	36.48	37.73	41.65	13.87	121.01	19.67

104.00	37.27	35.75	35.52	37.79	36.85	36.37	37.26	36.49	37.78	41.63	13.86	119.15	19.68
105.00	37.27	35.68	35.66	37.88	36.89	36.41	37.27	36.53	37.77	41.65	13.87	118.56	19.67
106.00	37.28	35.62	35.78	37.90	36.90	36.47	37.28	36.55	37.79	41.66	13.86	119.71	19.65
107.00	37.26	35.75	35.82	38.02	36.90	36.45	37.30	36.59	37.75	41.68	13.85	120.49	19.62
108.00	37.27	35.70	35.74	38.09	36.93	36.45	37.31	36.58	37.75	41.65	13.84	120.23	19.63
109.00	37.28	35.64	35.76	38.03	36.90	36.46	37.32	36.57	37.75	41.65	13.84	119.62	19.64
110.00	37.31	35.68	35.81	38.00	36.88	36.47	37.33	36.59	37.79	41.66	13.84	121.41	19.63
111.00	37.34	35.68	35.76	37.99	36.89	36.49	37.34	36.59	37.76	41.68	13.83	120.44	19.59
112.00	37.37	35.74	35.60	37.98	36.95	36.50	37.35	36.58	37.79	41.70	13.85	120.32	19.59
113.00	37.41	35.65	35.49	38.07	36.75	36.50	37.37	36.54	37.77	41.68	13.84	121.82	19.61
114.00	37.41	35.75	35.48	38.07	36.53	36.52	37.37	36.55	37.78	41.69	13.86	122.19	19.62
115.00	37.41	35.65	35.60	38.06	36.78	36.54	37.39	36.57	37.79	41.72	13.88	123.56	19.62
116.00	37.40	35.69	35.69	38.08	37.02	36.54	37.43	36.63	37.79	41.72	13.88	122.76	19.62
117.00	37.41	35.86	35.74	38.21	37.09	36.57	37.44	36.69	37.82	41.73	13.90	122.64	19.63
118.00	37.39	35.98	35.79	38.32	37.06	36.61	37.45	36.74	37.85	41.72	13.92	124.07	19.66
119.00	37.40	36.10	35.68	38.26	37.08	36.62	37.46	36.74	37.87	41.69	13.96	126.22	19.74
120.00	37.42	36.11	35.67	38.21	37.03	36.63	37.48	36.74	37.91	41.72	13.97	125.17	19.74

**Table 8.16 Session 1 Human subject PCS #12 results average (Subjects 1-3, 7-8,10-12)**

Time min	Skin 2- 1 C	Skin 2- 2 C	Skin 2- 3 C	Skin 2- 4 C	Skin 2- 5 C	Skin 2- 6 C	Skin 2- 7 C	Average Skin C	Core C	Air Temp C	Dew C	Heart Rate B/min	RH %
1.00	36.28	33.08	26.42	38.50	37.65	36.04	35.68	33.96	37.24	41.38	14.03	98.63	20.16
2.00	36.18	32.86	24.82	38.33	37.64	36.19	35.84	33.67	37.25	41.41	14.05	100.44	20.16
3.00	36.14	32.72	24.16	38.29	37.50	36.33	35.98	33.57	37.23	41.46	14.08	96.81	20.15
4.00	36.15	32.70	23.83	38.24	37.35	36.40	36.11	33.53	37.26	41.46	14.11	96.88	20.18
5.00	36.13	32.77	23.23	38.23	37.27	36.47	36.21	33.46	37.25	41.47	14.11	97.78	20.17
6.00	36.12	32.87	22.59	38.21	37.33	36.54	36.33	33.40	37.27	41.47	14.11	98.57	20.17
7.00	36.11	32.86	22.18	38.23	37.37	36.70	36.42	33.38	37.28	41.48	14.11	97.69	20.16
8.00	36.09	32.76	21.81	38.24	37.36	36.78	36.49	33.32	37.27	41.51	14.09	100.07	20.11
9.00	36.08	32.64	21.87	38.21	37.35	36.83	36.56	33.33	37.29	41.52	14.07	99.37	20.06
10.00	36.10	32.52	22.04	38.28	37.24	36.87	36.60	33.36	37.29	41.56	14.07	99.44	20.02
11.00	36.12	32.56	22.10	38.27	37.16	36.93	36.65	33.39	37.31	41.60	14.07	100.01	20.00
12.00	36.15	32.51	22.12	38.24	37.13	36.99	36.69	33.40	37.32	41.63	14.07	102.14	19.96
13.00	36.16	32.43	22.09	38.21	37.13	37.02	36.74	33.40	37.33	41.63	14.05	100.33	19.93
14.00	36.17	32.33	21.85	38.16	37.10	37.04	36.78	33.34	37.33	41.62	14.07	101.10	19.97
15.00	36.21	32.40	21.75	38.17	37.16	37.00	36.81	33.34	37.32	41.65	14.10	98.74	19.98
16.00	36.21	32.36	21.55	38.17	37.13	36.93	36.84	33.29	37.34	41.68	14.12	101.22	19.97
17.00	36.24	32.39	21.31	38.14	37.05	36.96	36.88	33.26	37.35	41.70	14.14	101.73	19.97
18.00	36.26	32.43	21.13	38.09	36.98	37.01	36.89	33.24	37.35	41.69	14.16	101.72	20.02
19.00	36.27	32.53	20.95	38.07	37.01	37.03	36.89	33.23	37.34	41.73	14.19	101.71	20.00
20.00	36.28	32.54	20.80	38.02	36.99	37.02	36.91	33.20	37.35	41.77	14.19	101.94	19.96
21.00	36.22	32.55	20.62	37.99	36.94	37.02	36.92	33.16	37.36	41.78	14.20	99.97	19.96
22.00	36.27	32.69	20.43	37.96	36.90	37.02	36.93	33.15	37.37	41.78	14.20	103.97	19.96
23.00	36.35	32.82	20.27	37.82	36.88	37.03	36.94	33.14	37.38	41.78	14.19	102.72	19.96
24.00	36.38	32.91	20.21	37.71	36.79	37.02	36.93	33.13	37.39	41.79	14.19	104.76	19.94
25.00	36.37	32.92	20.21	37.72	36.59	37.03	36.95	33.13	37.39	41.80	14.21	104.74	19.96
26.00	36.38	32.94	20.15	37.72	36.54	37.05	36.95	33.12	37.39	41.80	14.20	103.05	19.94
27.00	36.39	33.01	19.97	37.78	36.59	37.07	36.96	33.11	37.41	41.82	14.20	103.86	19.92
28.00	36.42	33.27	19.84	37.75	36.59	37.05	36.95	33.14	37.40	41.83	14.18	105.30	19.90
29.00	36.42	33.46	19.73	37.73	36.61	37.10	36.97	33.16	37.42	41.81	14.17	103.71	19.90
30.00	36.42	33.55	19.59	37.68	36.58	37.11	36.98	33.15	37.43	41.83	14.18	106.24	19.89
31.00	36.47	33.57	19.50	37.70	36.66	37.10	36.99	33.15	37.41	41.81	14.18	104.97	19.90



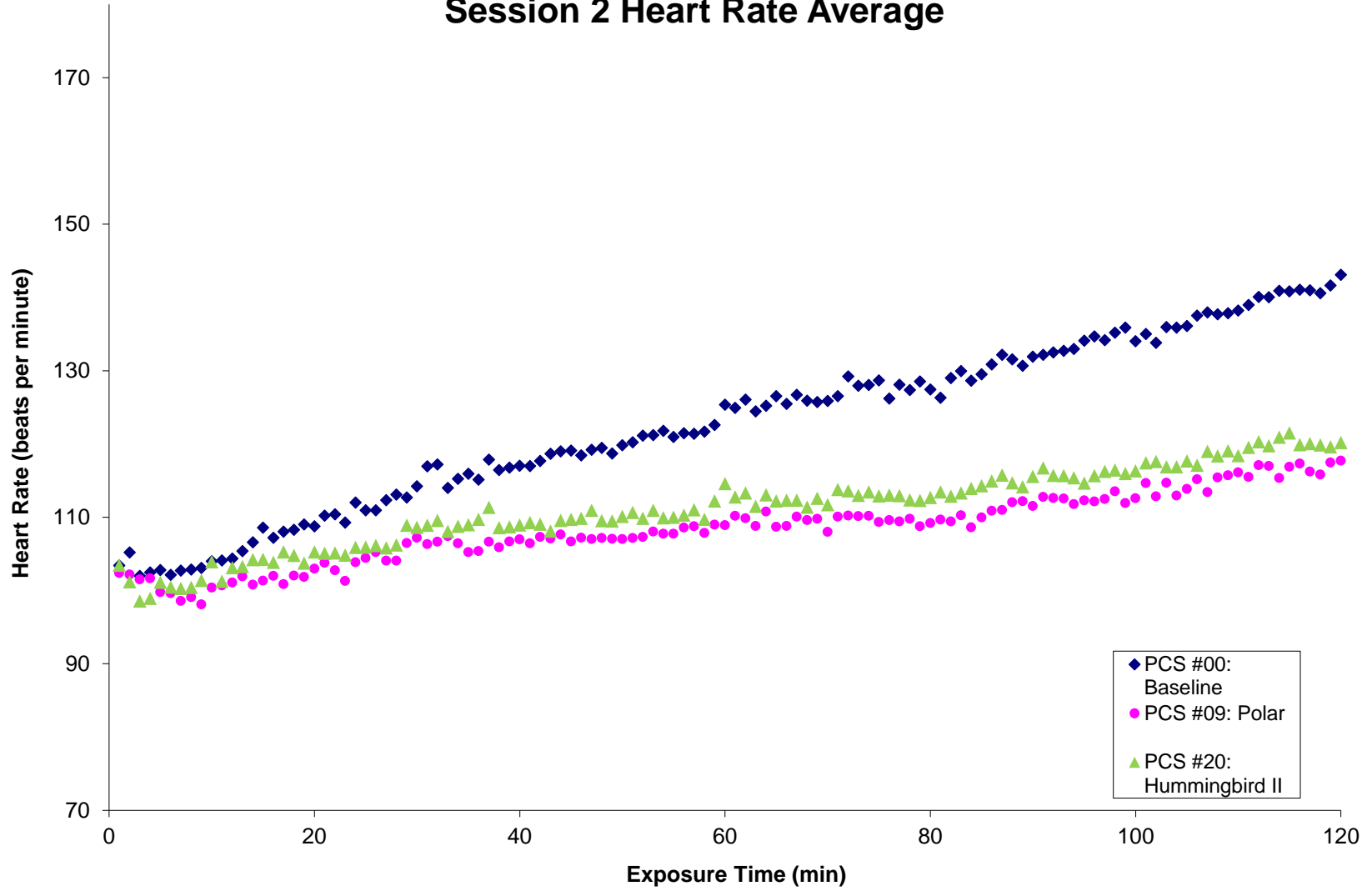
32.00	36.53	33.59	19.57	37.69	36.70	37.11	36.99	33.17	37.41	41.79	14.18	105.56	19.93
33.00	36.55	33.65	19.60	37.67	36.83	37.13	37.00	33.21	37.44	41.80	14.18	106.87	19.92
34.00	36.58	33.56	19.64	37.69	36.87	37.10	36.99	33.20	37.40	41.81	14.18	106.38	19.91
35.00	36.61	33.66	19.66	37.61	36.84	37.14	36.99	33.22	37.43	41.76	14.18	104.58	19.96
36.00	36.60	33.77	19.89	37.52	36.78	37.10	36.97	33.26	37.43	41.80	14.16	105.11	19.90
37.00	36.61	33.83	20.09	37.56	36.91	37.10	36.97	33.32	37.41	41.81	14.09	107.05	19.79
38.00	36.64	33.83	20.34	37.53	36.87	37.17	36.96	33.37	37.40	41.82	14.02	105.84	19.69
39.00	36.65	33.95	20.39	37.49	36.71	37.18	36.96	33.40	37.37	41.81	13.98	104.82	19.65
40.00	36.45	33.81	20.33	37.48	36.60	37.19	36.96	33.34	37.37	41.82	13.94	105.24	19.59
41.00	36.66	33.89	20.31	37.50	36.61	37.19	36.96	33.37	37.40	41.83	13.93	105.69	19.57
42.00	36.63	34.08	20.30	37.51	36.58	37.18	36.96	33.39	37.41	41.80	13.93	106.06	19.61
43.00	36.68	34.15	20.18	37.55	36.65	37.21	36.96	33.40	37.38	41.81	13.94	106.93	19.61
44.00	36.71	34.20	20.06	37.54	36.91	37.22	36.96	33.41	37.36	41.79	13.92	105.58	19.60
45.00	36.75	34.22	20.11	37.44	36.91	37.22	36.95	33.42	37.36	41.80	13.92	106.20	19.59
46.00	36.74	34.13	20.35	37.43	36.81	37.23	36.95	33.44	37.37	41.79	13.92	104.19	19.60
47.00	36.75	33.99	20.49	37.46	36.65	37.26	36.95	33.43	37.36	41.80	13.93	104.65	19.60
48.00	36.76	34.08	21.09	37.39	36.66	37.23	36.95	33.55	37.35	41.81	13.94	103.08	19.60
49.00	36.74	34.07	21.35	37.37	36.63	37.22	36.94	33.59	37.35	41.81	13.95	103.48	19.62
50.00	36.74	34.13	21.45	37.41	36.55	37.21	36.94	33.62	37.33	41.79	13.97	102.58	19.66
51.00	36.72	34.18	21.67	37.45	36.48	37.20	36.94	33.66	37.32	41.80	13.97	102.44	19.65
52.00	36.74	34.28	21.71	37.44	36.46	37.21	36.94	33.69	37.32	41.80	13.98	104.75	19.66
53.00	36.74	34.26	21.81	37.43	36.55	37.20	36.95	33.71	37.32	41.79	13.99	104.60	19.68
54.00	36.73	34.04	21.94	37.43	36.55	37.20	36.95	33.69	37.31	41.81	14.01	104.46	19.68
55.00	36.73	34.13	22.02	37.41	36.61	37.19	36.93	33.72	37.33	41.81	14.02	105.04	19.71
56.00	36.72	34.05	22.03	37.45	36.61	37.19	36.95	33.71	37.32	41.81	14.04	101.01	19.72
57.00	36.73	33.94	22.26	37.54	36.57	37.18	36.95	33.74	37.31	41.82	14.03	103.74	19.71
58.00	36.73	34.03	22.26	37.55	36.60	37.21	36.97	33.77	37.33	41.82	14.04	105.29	19.73
59.00	36.73	34.10	22.28	37.55	36.61	37.22	36.98	33.78	37.33	41.80	14.04	105.22	19.75
60.00	36.74	34.20	22.27	37.61	36.78	37.19	37.00	33.82	37.33	41.80	14.02	105.70	19.72
61.00	36.75	34.29	22.30	37.73	36.61	37.19	36.99	33.84	37.33	41.80	14.01	106.30	19.70
62.00	36.75	34.32	22.41	37.63	36.57	37.22	37.03	33.87	37.30	41.78	14.01	106.68	19.71
63.00	36.76	34.31	22.68	37.60	36.60	37.24	37.05	33.92	37.27	41.81	14.01	105.22	19.69
64.00	36.79	34.29	22.97	37.61	36.67	37.21	37.03	33.97	37.30	41.77	13.97	108.16	19.69
65.00	36.78	34.53	23.24	37.51	36.81	37.19	37.03	34.06	37.32	41.79	13.98	107.30	19.67
66.00	36.76	34.65	23.50	37.60	36.67	37.20	37.01	34.12	37.34	41.80	13.99	107.01	19.68
67.00	36.76	34.64	23.67	37.69	36.43	37.21	36.99	34.14	37.38	41.78	14.00	106.75	19.71

68.00	36.76	34.54	23.91	37.68	36.40	37.21	36.99	34.16	37.41	41.80	14.02	105.69	19.72
69.00	36.76	34.54	24.15	37.69	36.45	37.20	37.00	34.21	37.42	41.80	14.03	105.08	19.72
70.00	36.76	34.61	24.31	37.76	36.32	37.19	37.06	34.26	37.44	41.80	14.04	103.93	19.75
71.00	36.79	34.72	24.50	37.75	36.29	37.19	37.10	34.32	37.45	41.80	14.07	104.27	19.77
72.00	36.79	34.79	24.50	37.69	36.32	37.19	37.07	34.33	37.42	41.80	14.08	101.22	19.80
73.00	36.81	34.82	24.57	37.79	36.41	37.18	37.03	34.35	37.45	41.80	14.09	103.84	19.81
74.00	36.83	34.88	24.68	37.76	36.43	37.17	37.07	34.39	37.44	41.80	14.10	105.27	19.82
75.00	36.83	34.84	24.76	37.70	36.40	37.20	37.10	34.40	37.44	41.79	14.10	105.10	19.83
76.00	36.84	34.82	24.79	37.67	36.46	37.20	37.13	34.41	37.47	41.76	14.11	104.57	19.87
77.00	36.83	34.87	24.93	37.67	36.37	37.19	37.14	34.44	37.44	41.76	14.12	105.47	19.89
78.00	36.84	34.76	25.14	37.77	36.28	37.18	37.16	34.46	37.44	41.78	14.12	104.14	19.87
79.00	36.85	34.78	25.93	37.74	36.32	37.18	37.17	34.62	37.45	41.78	14.12	104.65	19.86
80.00	36.84	34.86	26.02	37.75	36.38	37.19	37.19	34.66	37.43	41.78	14.12	104.25	19.87
81.00	36.83	34.99	26.10	37.61	36.44	37.21	37.19	34.69	37.44	41.78	14.13	104.31	19.87
82.00	36.83	35.02	26.38	37.62	36.51	37.21	37.18	34.75	37.46	41.78	14.13	104.10	19.87
83.00	36.84	35.03	26.41	37.64	36.56	37.20	37.20	34.77	37.44	41.77	14.11	104.30	19.85
84.00	36.87	35.05	26.37	37.60	36.52	37.20	37.22	34.77	37.46	41.79	14.05	104.30	19.76
85.00	36.88	35.08	26.64	37.57	36.48	37.19	37.26	34.83	37.46	41.80	14.01	106.04	19.70
86.00	36.89	35.03	26.87	37.64	36.48	37.21	37.29	34.87	37.44	41.76	13.98	106.77	19.71
87.00	36.89	35.10	27.00	37.67	36.51	37.22	37.30	34.92	37.45	41.77	13.96	106.80	19.67
88.00	36.90	35.12	27.12	37.63	36.62	37.19	37.29	34.94	37.47	41.76	13.95	106.31	19.68
89.00	36.91	35.17	27.38	37.83	36.56	37.24	37.29	35.02	37.47	41.72	13.95	108.36	19.71
90.00	36.93	35.12	27.60	37.95	36.50	37.24	37.29	35.06	37.52	41.76	13.93	106.62	19.64
91.00	36.94	35.14	27.65	38.07	36.56	37.23	37.30	35.08	37.49	41.75	13.93	105.71	19.65
92.00	36.95	35.19	27.72	38.07	36.60	37.24	37.29	35.11	37.51	41.73	13.92	107.52	19.66
93.00	36.94	35.29	27.85	37.90	36.67	37.23	37.30	35.15	37.51	41.76	13.93	105.92	19.64
94.00	36.94	35.38	28.05	37.91	36.66	37.24	37.32	35.20	37.51	41.74	13.94	107.13	19.67
95.00	36.95	35.48	28.19	37.90	36.66	37.26	37.32	35.26	37.52	41.73	13.94	108.02	19.68
96.00	36.96	35.56	28.14	37.93	36.75	37.23	37.31	35.26	37.55	41.73	13.93	107.11	19.68
97.00	36.97	35.64	28.28	37.96	36.73	37.22	37.31	35.30	37.54	41.73	13.96	108.19	19.71
98.00	36.98	35.69	28.65	38.00	36.73	37.24	37.32	35.39	37.53	41.75	13.98	106.59	19.72
99.00	37.00	35.67	28.81	38.13	36.76	37.24	37.32	35.43	37.52	41.70	13.99	109.46	19.77
100.00	37.02	35.67	28.88	38.12	36.67	37.22	37.33	35.43	37.52	41.72	14.01	108.23	19.78
101.00	37.02	35.68	28.76	38.02	36.67	37.27	37.33	35.41	37.54	41.73	14.01	109.11	19.78
102.00	37.04	35.77	28.73	38.02	36.74	37.28	37.32	35.43	37.52	41.74	14.03	108.31	19.79
103.00	37.06	35.83	28.88	38.05	36.71	37.28	37.32	35.47	37.54	41.74	14.03	109.89	19.78

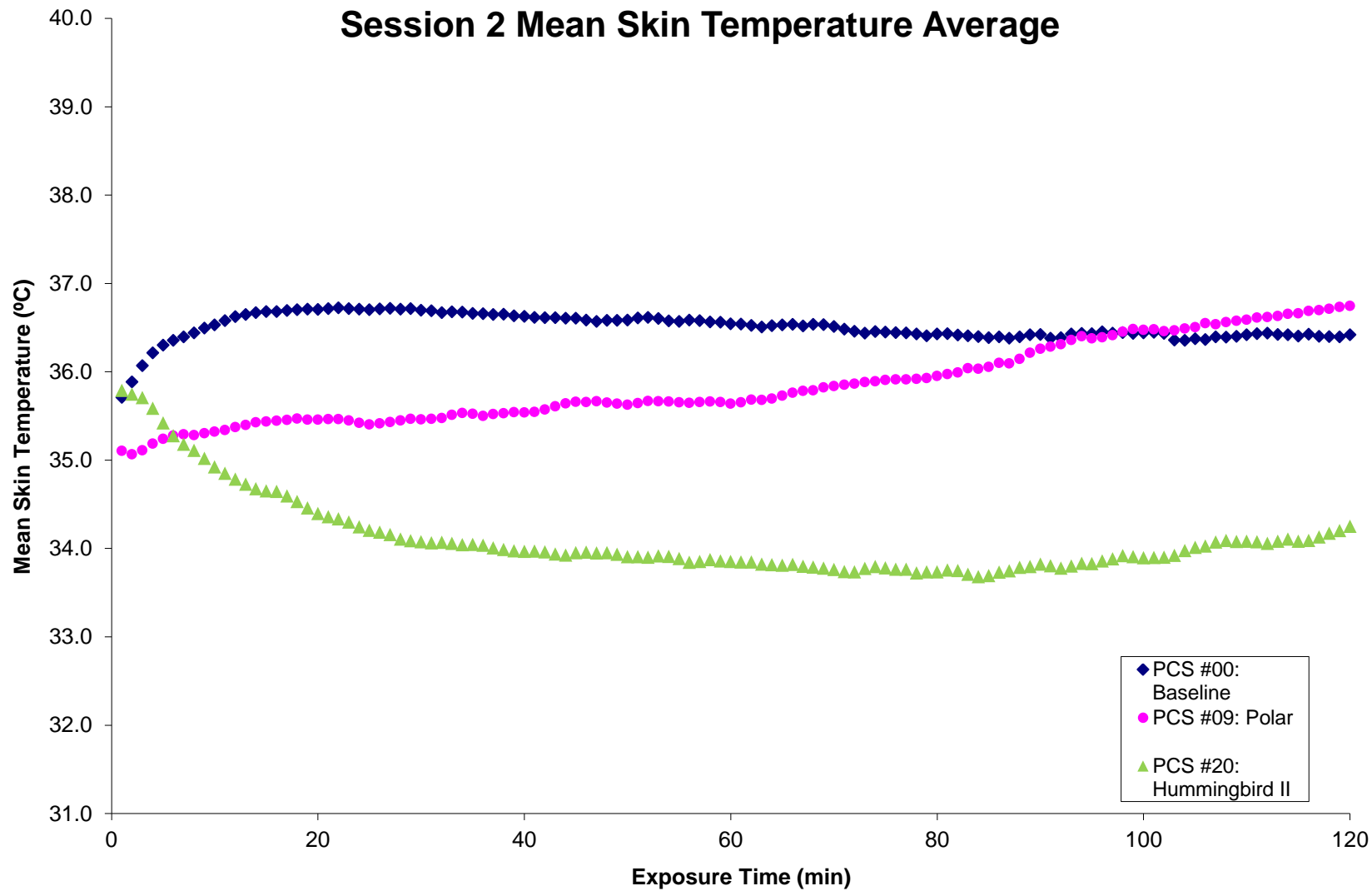
104.00	37.08	35.84	29.16	38.08	36.76	37.27	37.33	35.53	37.55	41.72	14.04	108.27	19.82
105.00	37.10	35.85	29.34	38.09	36.86	37.24	37.35	35.58	37.54	41.73	14.05	107.98	19.83
106.00	37.09	35.82	29.58	38.07	36.84	37.23	37.33	35.61	37.54	41.73	14.04	106.74	19.81
107.00	37.11	35.91	29.88	38.13	36.92	37.25	37.32	35.69	37.54	41.77	14.05	109.47	19.78
108.00	37.15	35.95	30.11	38.23	37.02	37.23	37.32	35.75	37.53	41.74	14.05	109.10	19.81
109.00	37.15	36.05	30.30	38.21	37.06	37.21	37.33	35.80	37.54	41.72	14.05	109.55	19.84
110.00	37.15	36.11	30.41	38.19	37.08	37.24	37.34	35.85	37.54	41.73	14.06	108.38	19.83
111.00	37.16	36.14	30.52	38.23	37.08	37.26	37.34	35.88	37.53	41.74	14.06	110.94	19.83
112.00	37.15	36.18	30.57	38.22	37.04	37.27	37.35	35.90	37.55	41.74	14.09	110.01	19.86
113.00	37.16	36.21	30.71	38.23	37.17	37.28	37.35	35.94	37.55	41.76	14.11	109.02	19.87
114.00	37.16	36.20	30.78	38.21	37.20	37.30	37.35	35.96	37.55	41.72	14.11	110.43	19.91
115.00	37.17	36.24	30.85	38.20	37.23	37.31	37.36	35.98	37.55	41.71	14.11	109.61	19.91
116.00	37.19	36.30	30.95	38.24	37.23	37.33	37.36	36.02	37.55	41.75	14.10	111.11	19.87
117.00	37.21	36.31	31.02	38.36	37.12	37.34	37.37	36.04	37.55	41.73	14.10	109.44	19.88
118.00	37.22	36.30	31.11	38.43	37.11	37.35	37.38	36.06	37.55	41.74	14.11	111.40	19.90
119.00	37.23	36.25	31.24	38.44	37.05	37.34	37.40	36.08	37.55	41.75	14.14	111.65	19.92
120.00	37.22	36.38	31.43	38.42	37.00	37.38	37.39	36.14	37.56	41.75	14.13	112.10	19.90

*Session 2 (Subjects 13-24)*

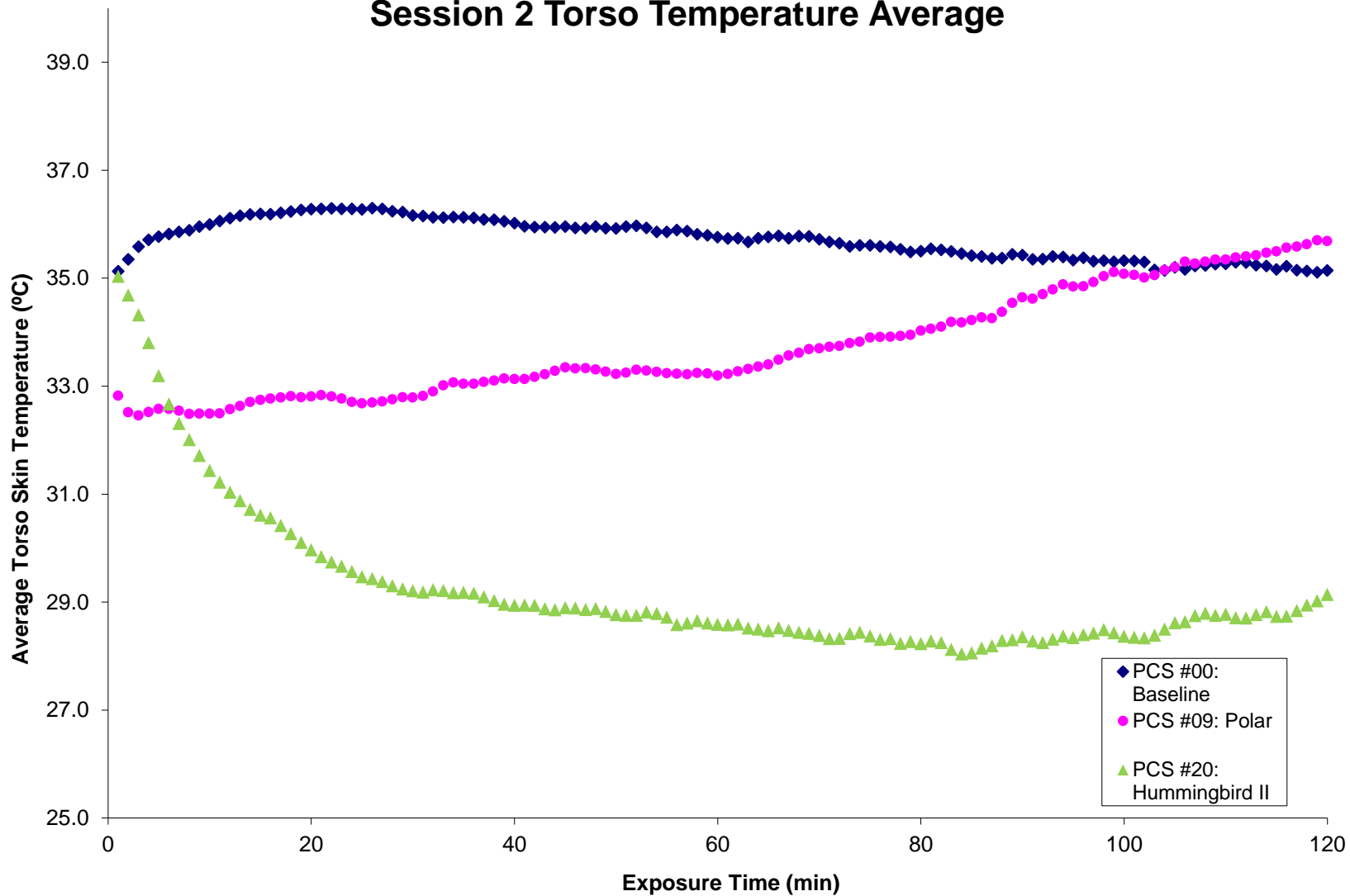
### Session 2 Heart Rate Average



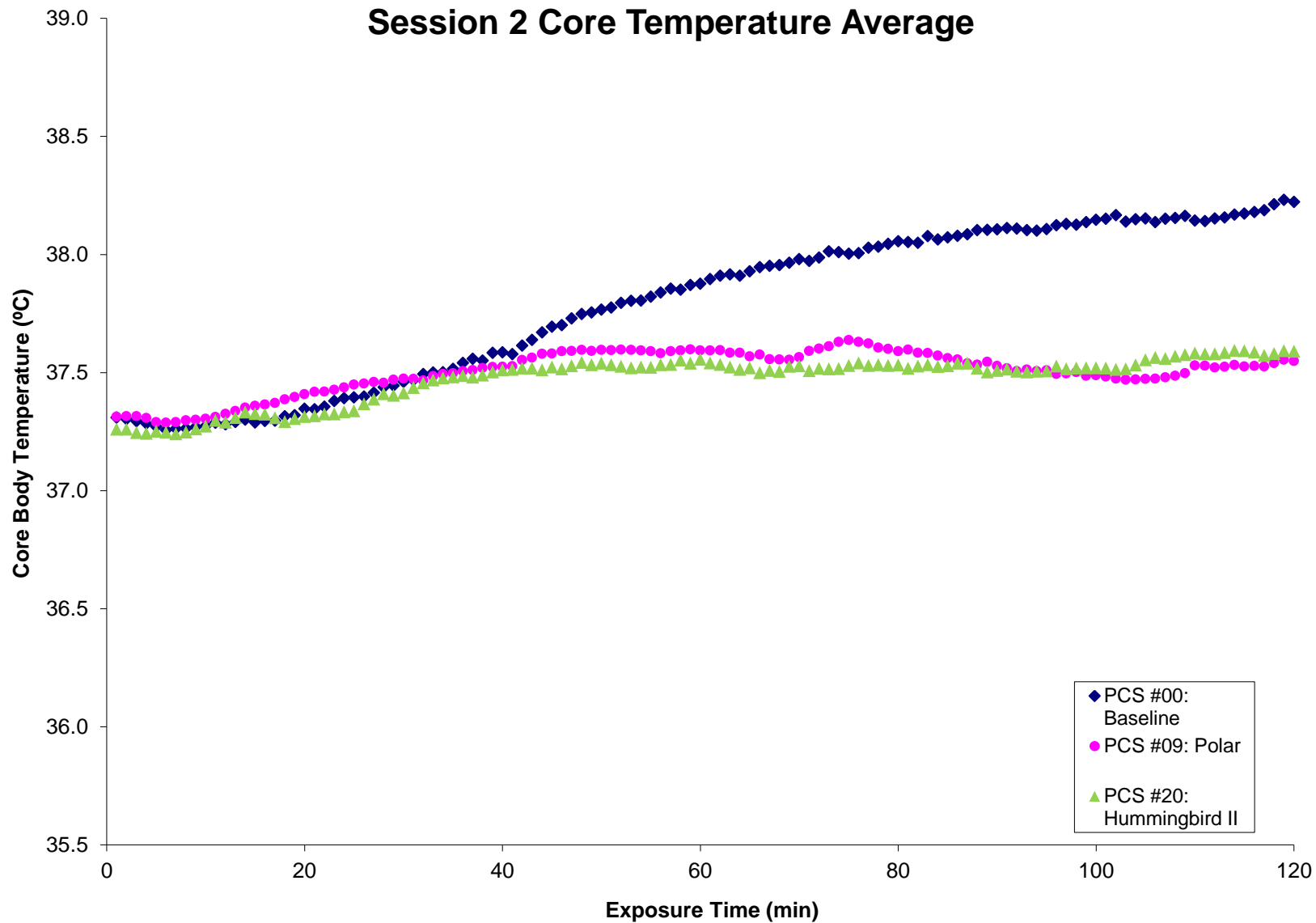
## Session 2 Mean Skin Temperature Average



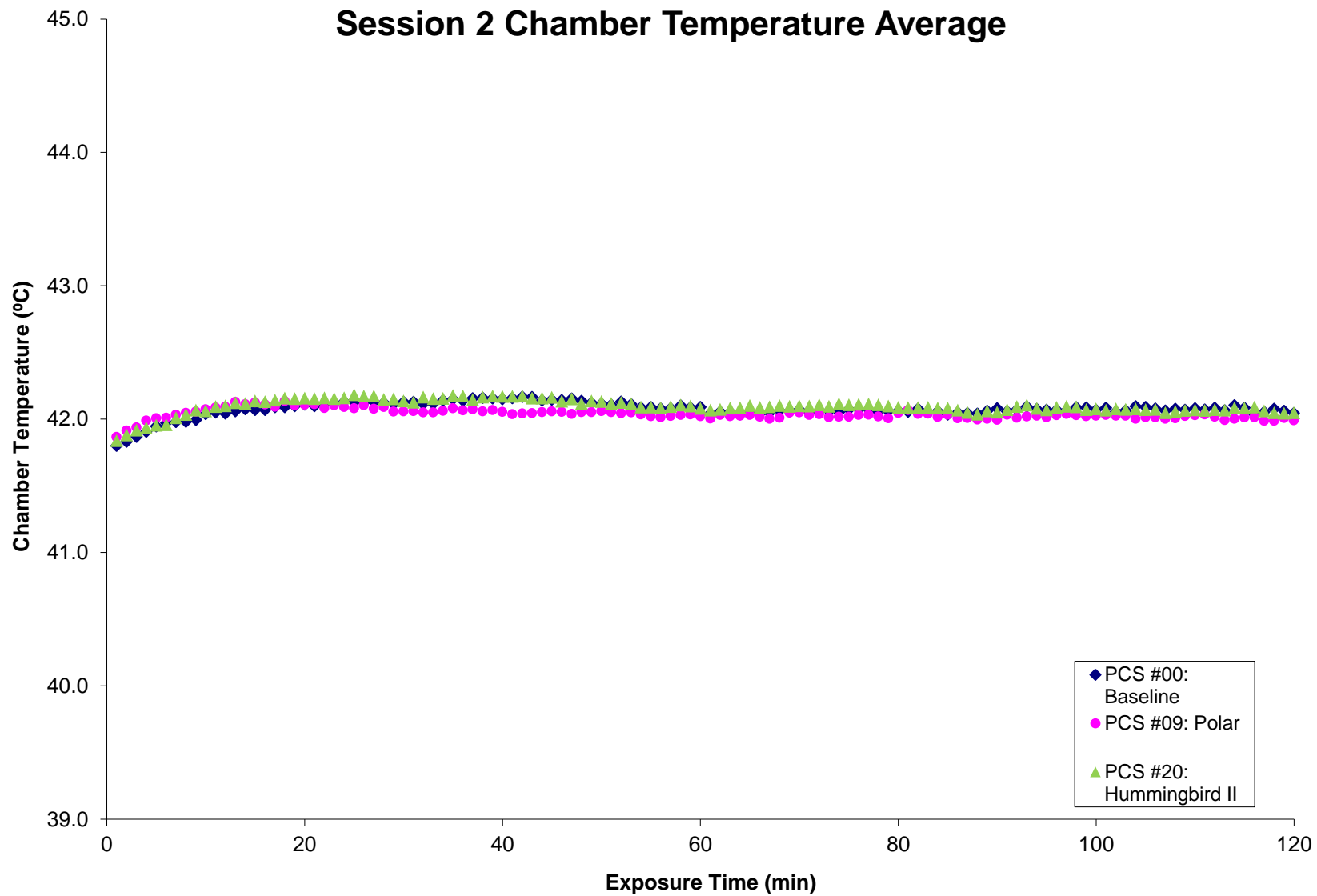
# Session 2 Torso Temperature Average



## Session 2 Core Temperature Average



## Session 2 Chamber Temperature Average





## Session 2 Chamber Relative Humidity Average

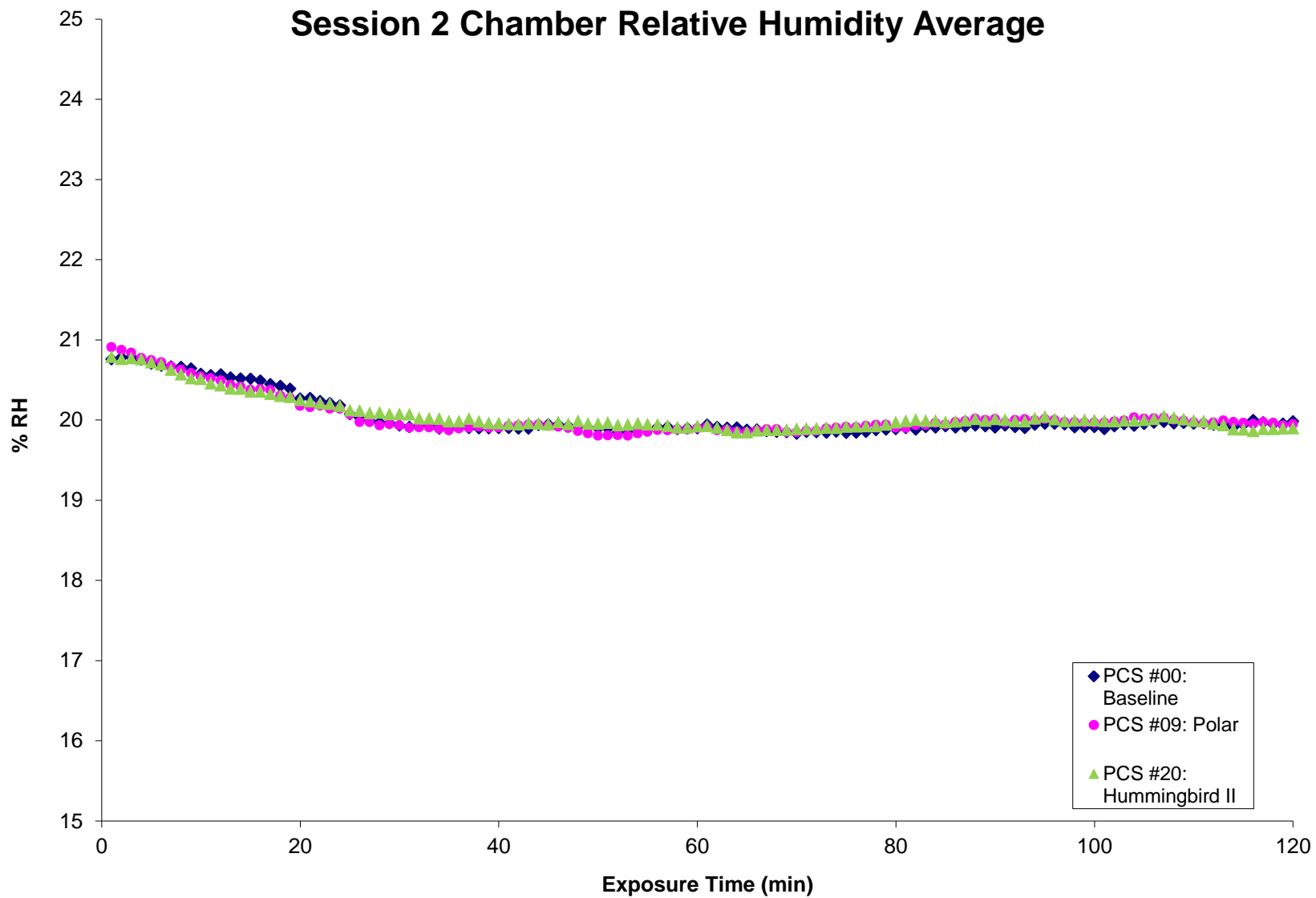


**Table 8.17 Session 2 Human subject baseline results average (Subjects 13-24)**

Time min	Skin 2- 1 C	Skin 2- 2 C	Skin 2- 3 C	Skin 2- 4 C	Skin 2- 5 C	Skin 2- 6 C	Skin 2- 7 C	Average Skin C	Core C	Air Temp C	Dew C	Heart Rate B/min	RH %
1.00	36.19	36.16	34.10	38.16	37.96	35.03	35.56	35.71	37.31	41.80	14.81	103.40	20.76
2.00	36.21	36.42	34.28	38.24	37.83	35.30	35.76	35.88	37.30	41.83	14.85	105.17	20.78
3.00	36.25	36.65	34.52	38.29	37.79	35.53	36.00	36.07	37.29	41.87	14.89	101.98	20.78
4.00	36.30	36.79	34.63	38.33	37.78	35.71	36.25	36.21	37.28	41.91	14.89	102.43	20.75
5.00	36.33	36.89	34.64	38.42	37.77	35.85	36.40	36.30	37.27	41.95	14.89	102.75	20.70
6.00	36.34	37.01	34.62	38.38	37.69	35.94	36.52	36.35	37.26	41.97	14.89	102.10	20.68
7.00	36.36	37.08	34.63	38.31	37.66	35.98	36.62	36.39	37.26	41.98	14.89	102.68	20.67
8.00	36.38	37.12	34.65	38.28	37.65	36.05	36.73	36.44	37.26	41.98	14.89	102.85	20.66
9.00	36.39	37.18	34.73	38.30	37.61	36.12	36.80	36.49	37.27	41.99	14.89	103.08	20.64
10.00	36.41	37.22	34.77	38.29	37.58	36.17	36.86	36.53	37.27	42.04	14.87	103.96	20.57
11.00	36.45	37.26	34.85	38.26	37.56	36.24	36.93	36.58	37.29	42.05	14.87	104.09	20.56
12.00	36.51	37.30	34.92	38.18	37.55	36.31	36.99	36.62	37.28	42.04	14.87	104.32	20.57
13.00	36.55	37.35	34.96	38.09	37.50	36.35	37.03	36.65	37.29	42.06	14.86	105.34	20.53
14.00	36.58	37.36	35.00	38.04	37.48	36.38	37.06	36.67	37.30	42.07	14.86	106.55	20.52
15.00	36.57	37.34	35.04	38.01	37.47	36.42	37.09	36.68	37.29	42.07	14.85	108.57	20.51
16.00	36.57	37.34	35.03	37.96	37.39	36.45	37.11	36.68	37.29	42.07	14.84	107.16	20.49
17.00	36.60	37.36	35.06	37.87	37.37	36.47	37.13	36.69	37.30	42.09	14.82	108.03	20.45
18.00	36.61	37.38	35.09	37.80	37.33	36.49	37.15	36.70	37.32	42.09	14.80	108.28	20.43
19.00	36.64	37.40	35.13	37.72	37.30	36.50	37.15	36.71	37.32	42.10	14.78	109.00	20.39
20.00	36.68	37.41	35.15	37.72	37.20	36.48	37.15	36.71	37.35	42.11	14.70	108.73	20.27
21.00	36.71	37.41	35.15	37.67	37.19	36.51	37.16	36.71	37.34	42.10	14.70	110.19	20.27
22.00	36.73	37.41	35.17	37.64	37.15	36.54	37.18	36.72	37.36	42.11	14.68	110.39	20.24
23.00	36.75	37.39	35.18	37.49	37.10	36.57	37.18	36.71	37.38	42.12	14.66	109.23	20.21
24.00	36.75	37.38	35.18	37.45	37.06	36.57	37.18	36.71	37.39	42.13	14.65	111.98	20.18
25.00	36.78	37.36	35.19	37.48	36.95	36.57	37.20	36.70	37.40	42.13	14.56	110.91	20.07
26.00	36.75	37.39	35.21	37.49	36.93	36.58	37.21	36.71	37.40	42.12	14.52	110.92	20.03
27.00	36.78	37.34	35.23	37.48	36.96	36.59	37.22	36.72	37.42	42.13	14.50	112.30	19.99
28.00	36.76	37.25	35.23	37.58	36.85	36.63	37.23	36.71	37.44	42.12	14.47	113.08	19.97
29.00	36.75	37.22	35.23	37.71	36.82	36.65	37.23	36.71	37.44	42.11	14.46	112.69	19.96
30.00	36.72	37.11	35.21	37.78	36.94	36.64	37.22	36.70	37.46	42.13	14.45	114.21	19.93
31.00	36.78	37.09	35.21	37.74	36.83	36.63	37.23	36.69	37.47	42.13	14.43	116.92	19.91

32.00	36.81	37.03	35.22	37.69	36.69	36.64	37.24	36.67	37.49	42.11	14.44	117.20	19.93
33.00	36.83	37.02	35.22	37.69	36.78	36.64	37.24	36.68	37.50	42.11	14.44	113.99	19.94
34.00	36.84	37.02	35.24	37.65	36.75	36.62	37.25	36.68	37.50	42.14	14.43	115.22	19.89
35.00	36.78	37.00	35.25	37.60	36.75	36.62	37.24	36.66	37.52	42.15	14.43	115.90	19.89
36.00	36.77	37.04	35.19	37.59	36.76	36.62	37.25	36.66	37.54	42.14	14.44	115.13	19.91
37.00	36.78	37.02	35.16	37.62	36.70	36.61	37.26	36.65	37.56	42.16	14.45	117.85	19.90
38.00	36.77	36.97	35.19	37.68	36.80	36.58	37.27	36.65	37.55	42.16	14.45	116.42	19.90
39.00	36.73	36.89	35.21	37.69	36.80	36.55	37.27	36.63	37.58	42.16	14.45	116.75	19.90
40.00	36.74	36.86	35.18	37.70	36.80	36.55	37.28	36.63	37.59	42.15	14.44	117.01	19.90
41.00	36.77	36.79	35.13	37.69	36.87	36.57	37.29	36.62	37.58	42.16	14.45	116.96	19.90
42.00	36.79	36.82	35.07	37.67	36.82	36.59	37.29	36.61	37.61	42.17	14.45	117.64	19.89
43.00	36.79	36.84	35.05	37.60	36.88	36.60	37.29	36.61	37.64	42.16	14.45	118.65	19.89
44.00	36.77	36.80	35.08	37.55	36.83	36.61	37.29	36.60	37.67	42.14	14.47	118.98	19.94
45.00	36.72	36.79	35.11	37.58	36.72	36.63	37.30	36.60	37.69	42.14	14.48	119.08	19.94
46.00	36.64	36.74	35.12	37.53	36.65	36.64	37.30	36.58	37.70	42.14	14.47	118.44	19.94
47.00	36.56	36.73	35.12	37.50	36.57	36.64	37.31	36.57	37.73	42.15	14.47	119.21	19.92
48.00	36.55	36.74	35.17	37.48	36.64	36.62	37.31	36.58	37.75	42.14	14.45	119.44	19.92
49.00	36.68	36.66	35.19	37.46	36.69	36.61	37.32	36.58	37.75	42.12	14.43	118.67	19.90
50.00	36.63	36.66	35.18	37.46	36.70	36.63	37.33	36.58	37.77	42.11	14.42	119.83	19.90
51.00	36.73	36.74	35.18	37.40	36.76	36.65	37.34	36.61	37.78	42.11	14.41	120.20	19.89
52.00	36.73	36.73	35.21	37.41	36.65	36.68	37.35	36.61	37.80	42.13	14.39	121.12	19.85
53.00	36.73	36.67	35.18	37.41	36.64	36.68	37.37	36.60	37.80	42.11	14.39	121.19	19.87
54.00	36.70	36.65	35.06	37.40	36.69	36.67	37.38	36.58	37.81	42.09	14.39	121.79	19.90
55.00	36.62	36.68	35.03	37.38	36.73	36.64	37.39	36.57	37.82	42.09	14.39	120.94	19.88
56.00	36.67	36.70	35.08	37.37	36.67	36.66	37.39	36.58	37.84	42.08	14.40	121.45	19.91
57.00	36.69	36.67	35.08	37.37	36.69	36.67	37.38	36.58	37.86	42.08	14.40	121.36	19.91
58.00	36.75	36.62	35.01	37.39	36.71	36.66	37.39	36.56	37.85	42.10	14.40	121.66	19.89
59.00	36.73	36.56	35.03	37.41	36.70	36.66	37.40	36.56	37.87	42.09	14.40	122.59	19.90
60.00	36.74	36.51	35.02	37.40	36.63	36.66	37.40	36.54	37.88	42.09	14.40	125.34	19.90
61.00	36.82	36.42	35.06	37.38	36.69	36.65	37.40	36.54	37.90	42.04	14.40	124.90	19.94
62.00	36.79	36.35	35.12	37.25	36.60	36.65	37.41	36.52	37.91	42.06	14.38	126.04	19.91
63.00	36.73	36.24	35.11	37.23	36.70	36.67	37.41	36.51	37.92	42.05	14.37	124.43	19.90
64.00	36.70	36.37	35.11	37.15	36.66	36.66	37.42	36.52	37.91	42.04	14.36	125.20	19.91
65.00	36.75	36.39	35.14	37.06	36.65	36.68	37.43	36.53	37.93	42.05	14.35	126.52	19.88
66.00	36.78	36.43	35.13	37.03	36.59	36.70	37.42	36.54	37.95	42.04	14.35	125.45	19.88
67.00	36.79	36.38	35.11	36.98	36.58	36.70	37.42	36.52	37.95	42.05	14.34	126.70	19.86

68.00	36.74	36.46	35.10	37.01	36.62	36.70	37.44	36.54	37.96	42.06	14.34	125.88	19.85
69.00	36.67	36.49	35.05	37.02	36.63	36.72	37.44	36.53	37.96	42.06	14.34	125.69	19.85
70.00	36.68	36.47	34.97	37.04	36.61	36.71	37.44	36.51	37.98	42.07	14.33	125.84	19.83
71.00	36.65	36.41	34.93	37.05	36.47	36.70	37.44	36.48	37.97	42.05	14.33	126.51	19.85
72.00	36.53	36.35	34.95	37.04	36.43	36.70	37.43	36.46	37.99	42.06	14.34	129.22	19.85
73.00	36.55	36.32	34.85	37.03	36.45	36.68	37.44	36.44	38.01	42.06	14.33	127.94	19.84
74.00	36.61	36.33	34.88	37.08	36.45	36.69	37.45	36.46	38.01	42.05	14.34	128.03	19.86
75.00	36.59	36.32	34.90	37.00	36.44	36.67	37.46	36.45	38.00	42.07	14.34	128.67	19.84
76.00	36.62	36.38	34.80	37.03	36.37	36.68	37.47	36.44	38.01	42.07	14.34	126.19	19.84
77.00	36.66	36.30	34.85	37.03	36.44	36.66	37.46	36.44	38.03	42.07	14.35	128.09	19.85
78.00	36.62	36.17	34.90	37.05	36.50	36.65	37.47	36.43	38.03	42.05	14.35	127.36	19.88
79.00	36.64	36.10	34.87	37.00	36.51	36.64	37.47	36.41	38.04	42.06	14.36	128.49	19.88
80.00	36.76	36.14	34.85	37.05	36.52	36.66	37.47	36.43	38.06	42.06	14.37	127.42	19.89
81.00	36.72	36.22	34.87	37.01	36.47	36.65	37.46	36.43	38.05	42.06	14.37	126.30	19.90
82.00	36.55	36.20	34.85	37.02	36.47	36.63	37.48	36.41	38.05	42.08	14.38	128.98	19.88
83.00	36.57	36.15	34.84	37.01	36.48	36.62	37.51	36.41	38.08	42.05	14.38	129.93	19.91
84.00	36.62	36.15	34.77	36.99	36.46	36.64	37.50	36.40	38.06	42.06	14.38	128.62	19.91
85.00	36.62	35.98	34.86	36.99	36.45	36.67	37.49	36.39	38.07	42.03	14.37	129.49	19.92
86.00	36.68	35.86	34.95	36.98	36.57	36.67	37.51	36.39	38.08	42.05	14.37	130.83	19.91
87.00	36.66	35.78	34.96	36.95	36.66	36.64	37.50	36.38	38.09	42.04	14.38	132.14	19.92
88.00	36.72	35.77	34.98	37.05	36.63	36.66	37.50	36.39	38.10	42.04	14.39	131.53	19.93
89.00	36.74	35.86	35.02	36.90	36.71	36.67	37.51	36.42	38.10	42.06	14.39	130.66	19.92
90.00	36.66	35.80	35.05	36.94	36.78	36.69	37.52	36.42	38.11	42.08	14.40	131.91	19.91
91.00	36.68	35.65	35.05	36.77	36.76	36.68	37.52	36.38	38.11	42.06	14.40	132.15	19.93
92.00	36.66	35.64	35.07	36.86	36.74	36.67	37.53	36.38	38.11	42.07	14.40	132.48	19.91
93.00	36.64	35.74	35.06	37.07	36.76	36.72	37.53	36.43	38.10	42.09	14.40	132.72	19.90
94.00	36.65	35.78	35.01	37.17	36.80	36.71	37.53	36.43	38.10	42.07	14.42	132.95	19.94
95.00	36.76	35.68	34.99	37.20	36.81	36.73	37.55	36.43	38.11	42.07	14.42	134.10	19.96
96.00	36.80	35.70	35.06	37.21	36.84	36.72	37.56	36.45	38.12	42.07	14.42	134.68	19.96
97.00	36.79	35.54	35.09	37.19	36.89	36.73	37.58	36.44	38.13	42.06	14.41	134.16	19.94
98.00	36.81	35.56	35.08	37.21	36.89	36.72	37.58	36.44	38.13	42.09	14.41	135.18	19.91
99.00	36.73	35.53	35.07	37.24	36.93	36.72	37.58	36.43	38.14	42.09	14.41	135.87	19.91
100.00	36.70	35.61	35.03	37.19	36.94	36.72	37.60	36.44	38.15	42.07	14.39	134.01	19.91
101.00	36.76	35.63	35.01	37.14	36.89	36.74	37.62	36.44	38.15	42.08	14.39	135.01	19.89
102.00	36.62	35.56	35.04	37.19	36.85	36.76	37.63	36.43	38.17	42.06	14.39	133.80	19.92
103.00	36.59	35.48	34.82	37.27	36.88	36.66	37.60	36.36	38.14	42.06	14.42	135.93	19.95

104.00	36.66	35.44	34.85	37.22	36.84	36.66	37.61	36.36	38.15	42.10	14.42	135.88	19.93
105.00	36.54	35.54	34.86	37.25	36.87	36.66	37.62	36.37	38.15	42.09	14.44	136.09	19.95
106.00	36.54	35.47	34.86	37.27	36.84	36.67	37.64	36.36	38.14	42.08	14.44	137.50	19.97
107.00	36.53	35.55	34.90	37.25	36.87	36.68	37.65	36.39	38.15	42.06	14.44	137.93	19.98
108.00	36.55	35.58	34.89	37.18	36.78	36.69	37.66	36.39	38.15	42.08	14.43	137.69	19.96
109.00	36.58	35.62	34.90	37.21	36.73	36.68	37.67	36.40	38.16	42.07	14.43	137.82	19.96
110.00	36.56	35.63	34.90	37.32	36.72	36.71	37.69	36.42	38.14	42.08	14.43	138.21	19.96
111.00	36.56	35.71	34.88	37.31	36.71	36.72	37.69	36.43	38.14	42.07	14.43	138.98	19.96
112.00	36.52	35.70	34.88	37.41	36.75	36.71	37.70	36.44	38.15	42.08	14.43	140.04	19.94
113.00	36.47	35.62	34.85	37.46	36.80	36.70	37.72	36.42	38.16	42.06	14.42	140.02	19.95
114.00	36.43	35.61	34.84	37.44	36.87	36.71	37.71	36.42	38.17	42.10	14.42	140.89	19.91
115.00	36.49	35.46	34.86	37.44	36.97	36.69	37.71	36.40	38.17	42.08	14.43	140.82	19.94
116.00	36.42	35.61	34.84	37.45	36.95	36.71	37.72	36.43	38.18	42.04	14.43	141.02	20.00
117.00	36.42	35.52	34.78	37.52	36.87	36.72	37.73	36.40	38.19	42.05	14.42	140.95	19.97
118.00	36.44	35.54	34.73	37.45	36.88	36.73	37.75	36.40	38.21	42.08	14.43	140.55	19.95
119.00	36.39	35.48	34.74	37.45	36.96	36.74	37.75	36.39	38.23	42.06	14.42	141.64	19.96
120.00	36.49	35.46	34.82	37.48	36.94	36.74	37.76	36.42	38.22	42.04	14.43	143.07	19.98

**Table 8.18 Session 1 Human subject PCS #9 results average (Subjects 1-12)**

Time min	Skin 2- 1 C	Skin 2- 2 C	Skin 2- 3 C	Skin 2- 4 C	Skin 2- 5 C	Skin 2- 6 C	Skin 2- 7 C	Average Skin C	Core C	Air Temp C	Dew C	Heart Rate B/min	RH %
1.00	36.97	33.39	32.26	38.72	38.09	35.51	35.75	35.10	37.31	41.87	14.98	102.38	20.91
2.00	36.76	33.33	31.69	38.69	38.04	35.74	35.98	35.07	37.31	41.91	14.99	102.14	20.87
3.00	36.67	33.41	31.50	38.72	37.96	35.90	36.20	35.11	37.32	41.94	14.99	101.49	20.84
4.00	36.60	33.45	31.59	38.67	37.84	36.04	36.39	35.18	37.31	41.99	14.98	101.63	20.77
5.00	36.54	33.59	31.57	38.55	37.77	36.13	36.55	35.24	37.29	42.00	14.97	99.74	20.75
6.00	36.47	33.65	31.51	38.53	37.75	36.22	36.67	35.27	37.29	42.01	14.95	99.59	20.72
7.00	36.44	33.65	31.44	38.53	37.71	36.28	36.78	35.29	37.29	42.03	14.93	98.56	20.67
8.00	36.44	33.60	31.37	38.44	37.65	36.31	36.86	35.28	37.30	42.04	14.91	99.07	20.63
9.00	36.42	33.64	31.34	38.40	37.63	36.35	36.94	35.30	37.30	42.05	14.89	98.08	20.58
10.00	36.39	33.66	31.32	38.37	37.65	36.39	37.00	35.32	37.30	42.07	14.88	100.36	20.54
11.00	36.45	33.66	31.33	38.35	37.60	36.41	37.06	35.34	37.31	42.09	14.87	100.66	20.52
12.00	36.52	33.75	31.39	38.33	37.48	36.43	37.09	35.37	37.32	42.09	14.85	101.04	20.49
13.00	36.54	33.80	31.46	38.27	37.44	36.45	37.12	35.40	37.34	42.13	14.84	101.88	20.44
14.00	36.54	33.87	31.54	38.11	37.50	36.47	37.15	35.43	37.35	42.11	14.81	100.78	20.41
15.00	36.49	33.90	31.58	37.93	37.50	36.49	37.17	35.43	37.36	42.12	14.79	101.33	20.38
16.00	36.51	33.96	31.57	37.84	37.53	36.50	37.18	35.44	37.36	42.11	14.79	101.99	20.38
17.00	36.52	33.99	31.59	37.83	37.54	36.49	37.20	35.45	37.37	42.09	14.77	100.83	20.38
18.00	36.49	34.03	31.60	37.82	37.52	36.52	37.22	35.47	37.39	42.13	14.74	102.01	20.30
19.00	36.48	34.04	31.54	37.76	37.45	36.53	37.23	35.46	37.40	42.10	14.70	101.84	20.27
20.00	36.48	34.07	31.54	37.66	37.42	36.54	37.25	35.46	37.41	42.11	14.63	102.96	20.18
21.00	36.42	34.11	31.56	37.61	37.44	36.54	37.26	35.46	37.42	42.11	14.62	103.77	20.16
22.00	36.56	34.09	31.52	37.63	37.46	36.53	37.26	35.46	37.42	42.08	14.61	102.74	20.18
23.00	36.64	34.04	31.50	37.69	37.39	36.51	37.25	35.45	37.43	42.10	14.60	101.27	20.14
24.00	36.54	33.98	31.42	37.74	37.29	36.53	37.26	35.42	37.44	42.09	14.59	103.81	20.14
25.00	36.54	33.95	31.40	37.67	37.23	36.54	37.26	35.40	37.45	42.08	14.52	104.39	20.07
26.00	36.60	33.96	31.43	37.67	37.24	36.55	37.25	35.41	37.45	42.10	14.47	105.22	19.98
27.00	36.65	33.98	31.45	37.69	37.24	36.55	37.26	35.43	37.46	42.08	14.44	104.05	19.97
28.00	36.65	34.01	31.50	37.68	37.26	36.55	37.27	35.45	37.46	42.09	14.42	104.06	19.93
29.00	36.65	34.04	31.55	37.70	37.33	36.55	37.27	35.47	37.47	42.05	14.40	106.46	19.95
30.00	36.65	33.98	31.59	37.71	37.23	36.56	37.27	35.46	37.47	42.06	14.39	107.19	19.93
31.00	36.66	33.92	31.72	37.69	37.25	36.53	37.28	35.47	37.47	42.06	14.37	106.32	19.90

32.00	36.61	33.88	31.92	37.66	37.13	36.49	37.27	35.47	37.47	42.05	14.37	106.64	19.91
33.00	36.63	33.96	32.06	37.61	37.08	36.49	37.28	35.51	37.48	42.05	14.37	107.39	19.91
34.00	36.67	33.99	32.14	37.61	37.08	36.49	37.28	35.53	37.49	42.06	14.36	106.40	19.89
35.00	36.69	33.88	32.21	37.60	37.00	36.50	37.28	35.52	37.50	42.08	14.36	105.20	19.87
36.00	36.62	33.81	32.27	37.61	37.05	36.49	37.18	35.50	37.51	42.06	14.37	105.35	19.89
37.00	36.64	33.84	32.31	37.62	37.10	36.46	37.22	35.52	37.51	42.07	14.38	106.63	19.90
38.00	36.68	33.77	32.43	37.67	37.07	36.43	37.23	35.53	37.52	42.06	14.38	105.85	19.92
39.00	36.66	33.74	32.54	37.62	37.05	36.43	37.25	35.54	37.52	42.07	14.38	106.65	19.90
40.00	36.63	33.63	32.64	37.65	36.93	36.45	37.27	35.54	37.52	42.05	14.37	106.96	19.91
41.00	36.63	33.57	32.69	37.67	36.91	36.46	37.29	35.54	37.53	42.04	14.37	106.42	19.93
42.00	36.55	33.60	32.74	37.76	37.00	36.47	37.31	35.57	37.55	42.04	14.38	107.28	19.93
43.00	36.67	33.63	32.80	37.77	37.00	36.50	37.31	35.61	37.56	42.04	14.39	107.05	19.94
44.00	36.63	33.72	32.84	37.78	36.99	36.56	37.32	35.64	37.58	42.05	14.40	107.60	19.94
45.00	36.59	33.75	32.93	37.81	36.86	36.59	37.33	35.66	37.58	42.06	14.39	106.66	19.93
46.00	36.55	33.62	33.04	37.81	36.94	36.57	37.34	35.65	37.59	42.05	14.38	107.16	19.91
47.00	36.60	33.55	33.11	37.84	36.96	36.58	37.34	35.66	37.59	42.04	14.36	107.01	19.90
48.00	36.63	33.44	33.17	37.80	36.90	36.57	37.34	35.65	37.60	42.05	14.34	107.12	19.86
49.00	36.68	33.38	33.15	37.74	36.95	36.56	37.34	35.64	37.59	42.05	14.32	107.01	19.83
50.00	36.61	33.27	33.18	37.74	36.97	36.59	37.36	35.63	37.60	42.06	14.30	107.01	19.80
51.00	36.59	33.22	33.28	37.81	36.95	36.61	37.37	35.64	37.60	42.05	14.29	107.13	19.81
52.00	36.62	33.23	33.37	37.83	36.90	36.64	37.37	35.67	37.60	42.04	14.29	107.28	19.81
53.00	36.70	33.16	33.41	37.84	36.83	36.65	37.36	35.67	37.60	42.05	14.29	108.03	19.81
54.00	36.70	33.13	33.40	37.83	36.83	36.67	37.37	35.66	37.59	42.03	14.30	107.73	19.83
55.00	36.68	33.07	33.41	37.79	36.89	36.65	37.38	35.65	37.59	42.02	14.30	107.72	19.85
56.00	36.68	33.03	33.42	37.76	36.91	36.65	37.39	35.65	37.58	42.01	14.32	108.54	19.87
57.00	36.64	33.05	33.39	37.88	36.90	36.67	37.39	35.66	37.59	42.02	14.32	108.73	19.87
58.00	36.63	33.06	33.43	37.84	36.91	36.68	37.39	35.66	37.59	42.03	14.34	107.84	19.88
59.00	36.61	33.09	33.38	37.79	36.92	36.68	37.39	35.65	37.60	42.03	14.34	108.94	19.88
60.00	36.55	33.01	33.38	37.84	36.91	36.68	37.39	35.64	37.59	42.02	14.34	108.89	19.90
61.00	36.61	33.07	33.37	37.83	36.93	36.68	37.39	35.65	37.59	42.00	14.34	110.16	19.91
62.00	36.66	33.08	33.46	37.86	36.97	36.71	37.37	35.68	37.60	42.03	14.33	109.84	19.87
63.00	36.63	33.12	33.51	37.75	36.81	36.73	37.37	35.68	37.58	42.02	14.33	108.78	19.88
64.00	36.62	33.16	33.55	37.79	36.82	36.71	37.37	35.70	37.58	42.02	14.31	110.75	19.86
65.00	36.60	33.19	33.61	37.91	37.01	36.69	37.37	35.73	37.57	42.03	14.31	108.68	19.85
66.00	36.61	33.31	33.67	37.90	37.00	36.68	37.38	35.76	37.58	42.02	14.32	108.77	19.87
67.00	36.58	33.35	33.77	37.91	36.86	36.71	37.38	35.78	37.56	42.00	14.32	110.04	19.88

68.00	36.50	33.36	33.86	37.85	36.81	36.72	37.38	35.79	37.56	42.01	14.32	109.59	19.88
69.00	36.52	33.44	33.92	37.85	36.81	36.74	37.39	35.82	37.55	42.05	14.33	109.78	19.85
70.00	36.56	33.44	33.95	37.83	36.85	36.76	37.39	35.84	37.56	42.05	14.32	107.98	19.85
71.00	36.52	33.45	34.01	37.88	36.88	36.76	37.39	35.85	37.59	42.03	14.32	110.05	19.86
72.00	36.54	33.47	34.02	37.95	36.87	36.76	37.40	35.86	37.60	42.04	14.33	110.18	19.87
73.00	36.43	33.54	34.05	38.00	36.90	36.78	37.40	35.88	37.61	42.01	14.33	110.14	19.89
74.00	36.44	33.56	34.08	37.94	36.85	36.80	37.40	35.89	37.63	42.02	14.34	110.15	19.90
75.00	36.37	33.69	34.11	37.85	36.83	36.79	37.41	35.91	37.64	42.02	14.35	109.31	19.91
76.00	36.40	33.71	34.11	37.87	36.88	36.77	37.41	35.91	37.63	42.03	14.36	109.59	19.91
77.00	36.44	33.69	34.14	37.86	36.86	36.75	37.41	35.91	37.62	42.03	14.37	109.39	19.93
78.00	36.42	33.73	34.13	37.88	36.83	36.78	37.40	35.92	37.61	42.02	14.37	109.78	19.94
79.00	36.45	33.79	34.11	38.00	36.85	36.78	37.34	35.93	37.60	42.00	14.36	108.75	19.94
80.00	36.44	33.90	34.15	38.03	36.84	36.79	37.31	35.95	37.59	42.05	14.37	109.18	19.90
81.00	36.52	33.95	34.17	38.11	36.86	36.78	37.31	35.97	37.60	42.07	14.38	109.66	19.90
82.00	36.53	34.03	34.16	38.14	36.84	36.78	37.31	35.99	37.58	42.04	14.38	109.40	19.93
83.00	36.56	34.15	34.22	38.18	36.90	36.79	37.33	36.04	37.58	42.04	14.39	110.24	19.94
84.00	36.55	34.09	34.27	38.17	36.87	36.79	37.33	36.03	37.57	42.02	14.39	108.61	19.96
85.00	36.50	34.12	34.33	38.24	36.91	36.78	37.35	36.05	37.56	42.03	14.39	109.94	19.94
86.00	36.57	34.18	34.37	38.34	36.99	36.79	37.37	36.10	37.56	42.00	14.39	110.84	19.97
87.00	36.55	34.17	34.34	38.37	36.91	36.80	37.40	36.09	37.54	42.01	14.40	110.94	19.98
88.00	36.59	34.33	34.42	38.39	36.90	36.81	37.40	36.14	37.53	41.99	14.41	112.02	20.01
89.00	36.64	34.49	34.59	38.43	36.84	36.82	37.41	36.21	37.55	42.00	14.40	112.16	20.00
90.00	36.61	34.61	34.68	38.45	36.98	36.83	37.42	36.26	37.53	41.99	14.41	111.50	20.01
91.00	36.63	34.62	34.62	38.57	37.24	36.84	37.42	36.28	37.52	42.03	14.41	112.76	19.97
92.00	36.66	34.71	34.69	38.60	37.08	36.85	37.42	36.31	37.51	42.01	14.41	112.60	20.00
93.00	36.75	34.84	34.74	38.59	37.21	36.85	37.41	36.36	37.51	42.02	14.42	112.53	20.01
94.00	36.75	34.96	34.80	38.69	37.21	36.87	37.41	36.40	37.51	42.03	14.42	111.76	20.00
95.00	36.73	34.91	34.77	38.68	37.14	36.85	37.41	36.38	37.51	42.01	14.42	112.28	20.01
96.00	36.72	34.91	34.79	38.72	37.15	36.87	37.42	36.39	37.49	42.03	14.42	112.14	20.00
97.00	36.72	34.98	34.87	38.68	37.12	36.88	37.43	36.41	37.50	42.04	14.41	112.45	19.97
98.00	36.72	35.17	34.90	38.62	37.12	36.88	37.43	36.45	37.50	42.03	14.40	113.50	19.97
99.00	36.62	35.32	34.90	38.58	37.19	36.89	37.45	36.48	37.49	42.02	14.40	111.89	19.97
100.00	36.65	35.28	34.87	38.67	37.18	36.88	37.45	36.47	37.49	42.03	14.40	112.58	19.97
101.00	36.68	35.21	34.90	38.76	37.21	36.88	37.46	36.48	37.48	42.03	14.40	114.63	19.97
102.00	36.67	35.09	34.93	38.69	37.17	36.91	37.46	36.46	37.47	42.02	14.41	112.81	19.98
103.00	36.65	35.15	34.96	38.68	37.15	36.89	37.47	36.47	37.47	42.02	14.42	114.67	19.99



104.00	36.63	35.26	35.03	38.59	37.05	36.90	37.46	36.49	37.47	42.00	14.43	112.93	20.03
105.00	36.63	35.26	35.14	38.52	37.03	36.90	37.47	36.50	37.47	42.01	14.42	113.84	20.01
106.00	36.63	35.48	35.12	38.56	37.09	36.90	37.47	36.55	37.47	42.01	14.43	115.16	20.02
107.00	36.63	35.45	35.09	38.50	37.17	36.90	37.47	36.54	37.48	42.00	14.43	113.42	20.03
108.00	36.66	35.47	35.14	38.58	37.19	36.89	37.47	36.56	37.49	42.01	14.41	115.40	20.00
109.00	36.64	35.52	35.17	38.56	37.17	36.92	37.49	36.58	37.50	42.02	14.41	115.70	19.99
110.00	36.67	35.52	35.17	38.63	37.21	36.91	37.50	36.59	37.53	42.03	14.40	116.10	19.97
111.00	36.70	35.58	35.18	38.71	37.22	36.93	37.49	36.61	37.53	42.03	14.40	115.48	19.96
112.00	36.71	35.65	35.15	38.69	37.21	36.92	37.50	36.62	37.52	42.02	14.39	117.09	19.97
113.00	36.73	35.63	35.21	38.65	37.25	36.93	37.51	36.63	37.52	41.99	14.39	116.99	19.99
114.00	36.79	35.72	35.22	38.64	37.21	36.94	37.51	36.65	37.53	42.00	14.38	115.33	19.97
115.00	36.74	35.74	35.25	38.56	37.24	36.96	37.52	36.66	37.53	42.01	14.38	116.86	19.96
116.00	36.73	35.84	35.29	38.51	37.27	36.96	37.53	36.69	37.53	42.01	14.38	117.30	19.95
117.00	36.71	35.83	35.33	38.50	37.25	36.99	37.53	36.70	37.53	41.99	14.37	116.19	19.97
118.00	36.71	35.93	35.32	38.58	37.14	37.00	37.53	36.71	37.54	41.99	14.36	115.81	19.96
119.00	36.68	36.00	35.39	38.58	37.00	37.03	37.54	36.73	37.55	42.01	14.36	117.44	19.93
120.00	36.68	35.97	35.40	38.64	37.16	37.02	37.55	36.74	37.55	41.99	14.35	117.70	19.95

**Table 8.19 Session 2 Human subject PCS #20 results average (Subjects 1-12)**

Time min	Skin 2- 1 C	Skin 2- 2 C	Skin 2- 3 C	Skin 2- 4 C	Skin 2- 5 C	Skin 2- 6 C	Skin 2- 7 C	Average Skin C	Core C	Air Temp C	Dew C	Heart Rate B/min	RH %
1.00	36.28	35.95	34.12	38.66	38.21	35.06	35.78	35.79	37.26	41.84	14.87	103.43	20.79
2.00	36.26	35.97	33.40	38.73	38.06	35.31	35.98	35.75	37.26	41.88	14.88	101.18	20.76
3.00	36.29	35.99	32.65	38.70	37.97	35.54	36.25	35.71	37.25	41.92	14.92	98.53	20.77
4.00	36.31	35.96	31.64	38.68	37.96	35.68	36.45	35.59	37.24	41.93	14.92	98.90	20.76
5.00	36.30	35.93	30.45	38.72	37.93	35.79	36.62	35.42	37.25	41.95	14.91	101.08	20.72
6.00	36.32	35.92	29.41	38.75	37.87	35.88	36.77	35.27	37.25	41.96	14.89	100.43	20.70
7.00	36.36	35.90	28.72	38.74	37.89	35.95	36.87	35.18	37.24	42.01	14.89	100.28	20.63
8.00	36.42	35.91	28.12	38.71	37.88	36.03	36.96	35.11	37.25	42.03	14.86	100.39	20.57
9.00	36.44	35.84	27.59	38.64	37.83	36.09	37.04	35.02	37.26	42.07	14.86	101.36	20.52
10.00	36.42	35.73	27.15	38.60	37.79	36.09	37.10	34.92	37.27	42.06	14.84	103.88	20.51
11.00	36.44	35.65	26.79	38.56	37.74	36.10	37.15	34.85	37.30	42.09	14.83	101.23	20.46
12.00	36.46	35.61	26.46	38.45	37.63	36.14	37.20	34.78	37.29	42.10	14.81	103.11	20.43
13.00	36.46	35.60	26.16	38.37	37.50	36.17	37.23	34.73	37.31	42.12	14.81	103.24	20.40
14.00	36.45	35.55	25.88	38.31	37.52	36.20	37.27	34.67	37.33	42.12	14.80	104.18	20.39
15.00	36.45	35.47	25.75	38.24	37.62	36.23	37.29	34.65	37.33	42.14	14.79	104.22	20.36
16.00	36.48	35.44	25.68	38.21	37.62	36.26	37.33	34.65	37.32	42.13	14.78	103.82	20.36
17.00	36.51	35.36	25.48	38.19	37.53	36.28	37.34	34.59	37.31	42.14	14.77	105.24	20.33
18.00	36.53	35.29	25.24	38.08	37.50	36.29	37.34	34.53	37.29	42.16	14.76	104.77	20.30
19.00	36.51	35.17	25.04	38.02	37.52	36.25	37.33	34.46	37.30	42.15	14.75	103.71	20.29
20.00	36.50	35.12	24.81	37.95	37.49	36.23	37.33	34.39	37.31	42.16	14.72	105.24	20.25
21.00	36.53	35.02	24.66	37.91	37.46	36.28	37.35	34.36	37.32	42.15	14.71	105.05	20.24
22.00	36.55	34.95	24.53	37.94	37.41	36.33	37.37	34.34	37.32	42.16	14.70	105.12	20.21
23.00	36.56	34.87	24.46	37.91	37.37	36.31	37.37	34.30	37.32	42.15	14.69	104.80	20.20
24.00	36.48	34.81	24.32	37.87	37.37	36.26	37.38	34.24	37.33	42.16	14.67	105.85	20.18
25.00	36.52	34.77	24.17	37.81	37.36	36.23	37.39	34.20	37.34	42.18	14.65	105.91	20.13
26.00	36.55	34.79	24.08	37.85	37.23	36.19	37.40	34.18	37.37	42.17	14.64	106.11	20.12
27.00	36.57	34.78	23.98	37.76	37.17	36.21	37.41	34.16	37.39	42.17	14.61	105.80	20.09
28.00	36.50	34.65	23.95	37.67	37.17	36.16	37.41	34.11	37.41	42.15	14.60	106.19	20.09
29.00	36.52	34.63	23.86	37.76	37.16	36.14	37.40	34.09	37.40	42.15	14.59	108.87	20.08
30.00	36.50	34.62	23.80	37.86	37.12	36.15	37.39	34.08	37.41	42.14	14.57	108.58	20.08
31.00	36.50	34.60	23.78	37.87	37.06	36.16	37.37	34.06	37.44	42.13	14.56	108.89	20.07

32.00	36.56	34.68	23.78	37.79	36.97	36.16	37.36	34.07	37.46	42.16	14.55	109.54	20.02
33.00	36.60	34.63	23.79	37.66	36.90	36.18	37.37	34.06	37.47	42.15	14.55	108.06	20.02
34.00	36.61	34.59	23.76	37.61	36.89	36.21	37.35	34.04	37.48	42.15	14.54	108.73	20.02
35.00	36.63	34.65	23.71	37.68	36.86	36.22	37.33	34.04	37.48	42.18	14.53	108.95	19.98
36.00	36.56	34.65	23.68	37.71	36.85	36.22	37.33	34.04	37.49	42.17	14.53	109.68	19.99
37.00	36.53	34.60	23.59	37.66	36.88	36.21	37.33	34.01	37.48	42.15	14.54	111.32	20.02
38.00	36.52	34.57	23.48	37.70	36.91	36.24	37.33	33.99	37.49	42.16	14.52	108.56	19.98
39.00	36.53	34.53	23.39	37.72	36.91	36.25	37.33	33.97	37.50	42.17	14.52	108.66	19.96
40.00	36.54	34.55	23.33	37.71	36.94	36.24	37.36	33.97	37.51	42.17	14.51	108.91	19.96
41.00	36.53	34.57	23.32	37.68	36.91	36.25	37.38	33.97	37.51	42.17	14.51	109.25	19.96
42.00	36.52	34.52	23.36	37.68	36.82	36.24	37.38	33.96	37.52	42.17	14.50	109.02	19.95
43.00	36.57	34.38	23.38	37.66	36.75	36.24	37.39	33.94	37.52	42.16	14.50	108.09	19.96
44.00	36.55	34.39	23.32	37.67	36.75	36.25	37.38	33.93	37.51	42.16	14.50	109.56	19.96
45.00	36.56	34.51	23.28	37.67	36.75	36.28	37.38	33.95	37.52	42.16	14.50	109.68	19.95
46.00	36.56	34.55	23.24	37.69	36.72	36.33	37.38	33.96	37.52	42.13	14.49	109.82	19.98
47.00	36.56	34.56	23.16	37.71	36.82	36.30	37.38	33.95	37.53	42.15	14.49	110.93	19.95
48.00	36.61	34.42	23.35	37.64	36.83	36.28	37.38	33.95	37.54	42.12	14.49	109.52	19.99
49.00	36.56	34.34	23.31	37.80	36.74	36.29	37.38	33.93	37.53	42.14	14.48	109.48	19.96
50.00	36.54	34.15	23.39	37.75	36.71	36.30	37.38	33.91	37.54	42.13	14.48	110.10	19.95
51.00	36.61	34.13	23.38	37.71	36.77	36.28	37.38	33.91	37.53	42.12	14.48	110.63	19.97
52.00	36.63	34.13	23.37	37.71	36.68	36.29	37.38	33.90	37.53	42.12	14.46	109.83	19.94
53.00	36.61	34.22	23.42	37.66	36.61	36.30	37.38	33.92	37.52	42.11	14.45	110.93	19.94
54.00	36.60	34.16	23.41	37.68	36.63	36.32	37.37	33.91	37.52	42.09	14.45	109.92	19.96
55.00	36.59	34.06	23.38	37.62	36.69	36.32	37.38	33.89	37.52	42.09	14.44	109.99	19.95
56.00	36.59	33.82	23.34	37.66	36.72	36.33	37.38	33.84	37.53	42.08	14.43	110.26	19.94
57.00	36.61	33.87	23.34	37.56	36.77	36.33	37.38	33.85	37.53	42.09	14.42	110.98	19.93
58.00	36.63	33.84	23.47	37.60	36.78	36.34	37.37	33.87	37.55	42.11	14.42	109.68	19.91
59.00	36.66	33.80	23.42	37.58	36.78	36.34	37.38	33.86	37.54	42.10	14.41	112.18	19.91
60.00	36.63	33.82	23.35	37.57	36.81	36.36	37.38	33.85	37.56	42.08	14.41	114.57	19.93
61.00	36.70	33.83	23.33	37.51	36.69	36.40	37.37	33.85	37.54	42.07	14.40	112.76	19.93
62.00	36.68	33.76	23.42	37.50	36.62	36.40	37.38	33.85	37.53	42.07	14.39	113.29	19.91
63.00	36.66	33.56	23.48	37.44	36.71	36.40	37.39	33.82	37.52	42.08	14.38	111.48	19.88
64.00	36.66	33.48	23.52	37.42	36.79	36.39	37.38	33.82	37.51	42.08	14.36	113.05	19.85
65.00	36.65	33.39	23.55	37.39	36.86	36.39	37.38	33.81	37.52	42.10	14.37	112.19	19.85
66.00	36.62	33.45	23.59	37.36	36.85	36.37	37.38	33.82	37.50	42.09	14.38	112.32	19.87
67.00	36.64	33.36	23.58	37.39	36.80	36.38	37.37	33.80	37.51	42.09	14.38	112.30	19.88

68.00	36.61	33.32	23.56	37.48	36.74	36.38	37.37	33.79	37.51	42.10	14.39	111.38	19.88
69.00	36.59	33.27	23.57	37.41	36.71	36.39	37.38	33.78	37.53	42.10	14.39	112.57	19.88
70.00	36.60	33.18	23.58	37.37	36.74	36.40	37.37	33.76	37.53	42.10	14.40	111.71	19.89
71.00	36.64	33.00	23.65	37.44	36.65	36.38	37.38	33.74	37.51	42.10	14.40	113.76	19.89
72.00	36.57	33.05	23.60	37.43	36.65	36.39	37.37	33.73	37.52	42.11	14.41	113.59	19.90
73.00	36.63	33.26	23.57	37.47	36.67	36.38	37.37	33.77	37.52	42.10	14.41	112.97	19.91
74.00	36.67	33.29	23.59	37.55	36.74	36.37	37.37	33.80	37.52	42.11	14.42	113.42	19.90
75.00	36.69	33.14	23.60	37.61	36.74	36.40	37.37	33.78	37.53	42.11	14.43	112.90	19.92
76.00	36.68	33.03	23.58	37.68	36.70	36.42	37.37	33.76	37.54	42.11	14.44	113.02	19.92
77.00	36.68	33.04	23.60	37.69	36.64	36.42	37.36	33.77	37.53	42.11	14.44	112.92	19.93
78.00	36.66	32.86	23.61	37.63	36.63	36.41	37.36	33.72	37.53	42.11	14.43	112.33	19.93
79.00	36.64	32.86	23.67	37.62	36.65	36.41	37.36	33.74	37.53	42.10	14.44	112.28	19.95
80.00	36.65	32.75	23.71	37.77	36.67	36.42	37.35	33.73	37.53	42.09	14.45	112.66	19.97
81.00	36.61	32.75	23.80	37.77	36.74	36.43	37.36	33.76	37.52	42.09	14.47	113.45	19.99
82.00	36.60	32.74	23.75	37.79	36.73	36.44	37.36	33.75	37.53	42.09	14.48	112.85	20.00
83.00	36.60	32.58	23.67	37.86	36.75	36.43	37.36	33.71	37.53	42.09	14.47	113.29	19.99
84.00	36.64	32.49	23.59	37.86	36.74	36.43	37.37	33.68	37.53	42.08	14.47	113.93	19.99
85.00	36.70	32.50	23.62	37.78	36.80	36.43	37.37	33.69	37.53	42.08	14.45	114.26	19.98
86.00	36.73	32.51	23.79	37.79	36.82	36.44	37.37	33.73	37.54	42.07	14.44	114.94	19.98
87.00	36.72	32.43	23.94	37.91	36.88	36.39	37.37	33.75	37.54	42.05	14.44	115.75	20.00
88.00	36.68	32.39	24.19	38.01	36.68	36.42	37.39	33.79	37.52	42.04	14.44	114.66	20.01
89.00	36.70	32.40	24.21	38.04	36.63	36.45	37.39	33.79	37.50	42.06	14.45	114.12	19.99
90.00	36.72	32.29	24.43	38.07	36.71	36.44	37.39	33.82	37.51	42.05	14.46	115.54	20.02
91.00	36.75	32.06	24.49	38.03	36.85	36.46	37.38	33.80	37.51	42.07	14.47	116.72	20.01
92.00	36.73	31.92	24.58	37.98	36.75	36.43	37.39	33.78	37.51	42.09	14.47	115.71	19.99
93.00	36.74	31.95	24.67	37.92	36.84	36.41	37.39	33.80	37.50	42.10	14.48	115.65	19.99
94.00	36.71	31.99	24.76	37.90	36.96	36.42	37.39	33.83	37.51	42.08	14.49	115.37	20.02
95.00	36.72	31.92	24.77	37.96	36.92	36.44	37.40	33.83	37.51	42.07	14.49	114.62	20.04
96.00	36.74	32.04	24.75	37.99	37.06	36.42	37.41	33.86	37.53	42.09	14.48	115.66	20.01
97.00	36.77	32.08	24.77	38.11	37.05	36.43	37.41	33.88	37.52	42.10	14.47	116.25	19.99
98.00	36.83	32.20	24.78	38.08	37.06	36.47	37.42	33.92	37.52	42.09	14.47	116.42	19.99
99.00	36.84	32.10	24.76	38.14	37.05	36.48	37.43	33.91	37.52	42.07	14.46	115.96	20.00
100.00	36.82	31.91	24.82	38.21	37.09	36.51	37.44	33.90	37.52	42.08	14.46	116.33	20.00
101.00	36.86	31.81	24.88	38.23	37.15	36.50	37.44	33.90	37.52	42.07	14.45	117.42	19.99
102.00	36.90	31.76	24.91	38.22	37.14	36.53	37.44	33.90	37.51	42.08	14.46	117.59	19.99
103.00	36.84	31.87	24.91	38.22	37.15	36.55	37.44	33.92	37.52	42.07	14.46	116.87	20.00

104.00	36.88	31.95	25.05	38.23	37.19	36.59	37.44	33.98	37.53	42.08	14.46	116.88	19.99
105.00	36.92	32.15	25.08	38.11	37.18	36.60	37.44	34.01	37.55	42.07	14.46	117.64	20.00
106.00	36.93	32.17	25.10	38.14	37.22	36.60	37.43	34.03	37.56	42.07	14.47	117.08	20.02
107.00	36.94	32.32	25.18	38.12	37.23	36.62	37.45	34.07	37.56	42.05	14.48	118.98	20.05
108.00	36.94	32.31	25.28	38.15	37.22	36.62	37.45	34.09	37.57	42.06	14.47	118.34	20.03
109.00	36.97	32.16	25.35	38.20	37.20	36.61	37.45	34.08	37.58	42.06	14.46	119.04	20.01
110.00	36.99	32.23	25.32	38.16	37.13	36.61	37.46	34.08	37.58	42.07	14.45	118.41	19.99
111.00	36.98	32.16	25.26	38.21	37.22	36.64	37.47	34.08	37.58	42.06	14.45	119.51	19.99
112.00	36.94	32.17	25.24	38.16	37.12	36.62	37.48	34.06	37.58	42.07	14.43	120.30	19.96
113.00	36.95	32.27	25.27	38.17	37.19	36.58	37.48	34.08	37.58	42.07	14.41	119.75	19.94
114.00	36.96	32.35	25.29	38.23	37.09	36.61	37.48	34.10	37.59	42.08	14.39	120.89	19.89
115.00	37.00	32.09	25.37	38.30	37.09	36.61	37.48	34.08	37.59	42.08	14.38	121.49	19.88
116.00	36.99	32.00	25.47	38.31	37.06	36.65	37.49	34.09	37.59	42.09	14.37	119.89	19.86
117.00	36.97	32.10	25.58	38.28	37.03	36.67	37.50	34.13	37.57	42.06	14.37	120.03	19.89
118.00	36.98	32.13	25.76	38.28	37.05	36.68	37.51	34.17	37.58	42.05	14.36	119.84	19.89
119.00	36.92	32.15	25.90	38.24	37.14	36.69	37.50	34.20	37.59	42.04	14.36	119.60	19.90
120.00	36.90	32.28	26.00	38.24	37.28	36.68	37.51	34.25	37.59	42.05	14.36	120.17	19.90

# Appendix E Permissions

## Copyright Clearance

### ELSEVIER LICENSE TERMS AND CONDITIONS

Jun 01, 2016

This is an Agreement between John Elson ("You") and Elsevier ("Elsevier"). It consists of your order details, the terms and conditions provided by Elsevier, and the payment terms and conditions.

All payments must be made in full to CCC. For payment instructions, please see information listed at the bottom of this form.

Supplier	Elsevier Limited The Boulevard, Langford Lane Kidlington, Oxford, OX5 1GB, UK
Registered Company Number	1982084
Customer name	John Elson
Customer address	701 Highland Ridge Dr MANHATTAN, KS 66503
License number	3871451016699
License date	May 06, 2016
Licensed content publisher	Elsevier
Licensed content publication	Applied Ergonomics
Licensed content title	An objective method for screening and selecting personal cooling systems based on cooling properties
Licensed content author	John Elson, Steve Eckels
Licensed content date	May 2015
Licensed content volume number	48
Licensed content issue number	n/a
Number of pages	9
Start Page	33
End Page	41
Type of Use	reuse in a thesis/dissertation
Portion	full article
Format	electronic
Are you the author of this Elsevier article?	Yes
Will you be translating?	No
Title of your thesis/dissertation	EVALUATION OF PERSONAL COOLING SYSTEMS AND SIMULATION OF THEIR EFFECTS ON HUMAN SUBJECTS USING BASIC AND ADVANCED SIMULATION ENVIRONMENTS
Expected completion date	Jun 2016
Estimated size (number of pages)	
Customer Tax ID	USKansas
Elsevier VAT number	GB 494 6272 12

Price	0.00 USD
VAT/Local Sales Tax	0.00 USD / 0.00 GBP
<b>Total</b>	<b>0.00 USD</b>
<a href="#">Terms and Conditions</a>	

#### INTRODUCTION

1. The publisher for this copyrighted material is Elsevier. By clicking "accept" in connection with completing this licensing transaction, you agree that the following terms and conditions apply to this transaction (along with the Billing and Payment terms and conditions established by Copyright Clearance Center, Inc. ("CCC"), at the time that you opened your Rightslink account and that are available at any time at <http://myaccount.copyright.com>).

#### GENERAL TERMS

2. Elsevier hereby grants you permission to reproduce the aforementioned material subject to the terms and conditions indicated.

3. Acknowledgement: If any part of the material to be used (for example, figures) has appeared in our publication with credit or acknowledgement to another source, permission must also be sought from that source. If such permission is not obtained then that material may not be included in your publication/copies. Suitable acknowledgement to the source must be made, either as a footnote or in a reference list at the end of your publication, as follows:

"Reprinted from Publication title, Vol /edition number, Author(s), Title of article / title of chapter, Pages No., Copyright (Year), with permission from Elsevier [OR APPLICABLE SOCIETY COPYRIGHT OWNER]." Also Lancet special credit - "Reprinted from The Lancet, Vol. number, Author(s), Title of article, Pages No., Copyright (Year), with permission from Elsevier."

4. Reproduction of this material is confined to the purpose and/or media for which permission is hereby given.

5. Altering/Modifying Material: Not Permitted. However figures and illustrations may be altered/adapted minimally to serve your work. Any other abbreviations, additions, deletions and/or any other alterations shall be made only with prior written authorization of Elsevier Ltd. (Please contact Elsevier at [permissions@elsevier.com](mailto:permissions@elsevier.com))

6. If the permission fee for the requested use of our material is waived in this instance, please be advised that your future requests for Elsevier materials may attract a fee.

7. Reservation of Rights: Publisher reserves all rights not specifically granted in the combination of (i) the license details provided by you and accepted in the course of this licensing transaction, (ii) these terms and conditions and (iii) CCC's Billing and Payment terms and conditions.

8. License Contingent Upon Payment: While you may exercise the rights licensed immediately upon issuance of the license at the end of the licensing process for the transaction, provided that you have disclosed complete and accurate details of your proposed use, no license is finally effective unless and until full payment is received from you (either by publisher or by CCC) as provided in CCC's Billing and Payment terms and conditions. If full payment is not received on a timely basis, then any license preliminarily granted shall be deemed automatically revoked and shall be void as if never granted. Further, in the event that you breach any of these terms and conditions or any of CCC's Billing and Payment terms and conditions, the license is automatically revoked and shall be void as if never granted. Use of materials as described in a revoked license, as well as any use of the materials beyond the scope of an unrevoked license, may constitute copyright infringement and publisher reserves the right to take any and all action to protect its copyright in the materials.

9. Warranties: Publisher makes no representations or warranties with respect to the licensed material.

10. Indemnity: You hereby indemnify and agree to hold harmless publisher and CCC, and their respective officers, directors, employees and agents, from and against any and all claims arising out of your use of the licensed material other than as specifically authorized pursuant to this license.

11. No Transfer of License: This license is personal to you and may not be sublicensed, assigned, or transferred by you to any other person without publisher's written permission.

12. No Amendment Except in Writing: This license may not be amended except in a writing signed by both parties (or, in the case of publisher, by CCC on publisher's behalf).

13. Objection to Contrary Terms: Publisher hereby objects to any terms contained in any purchase order, acknowledgment, check endorsement or other writing prepared by you, which terms are inconsistent with these terms and conditions or CCC's Billing and Payment terms and conditions. These terms and conditions, together with CCC's Billing and Payment terms and conditions (which are incorporated herein), comprise the entire agreement between you and publisher (and CCC) concerning this licensing transaction. In the event of any conflict between your obligations established by these terms and conditions and those established by CCC's Billing and Payment terms and conditions, these terms and conditions shall control.

14. Revocation: Elsevier or Copyright Clearance Center may deny the permissions described in this License at their sole discretion, for any reason or no reason, with a full refund payable to you. Notice of such denial will be made using the

contact information provided by you. Failure to receive such notice will not alter or invalidate the denial. In no event will Elsevier or Copyright Clearance Center be responsible or liable for any costs, expenses or damage incurred by you as a result of a denial of your permission request, other than a refund of the amount(s) paid by you to Elsevier and/or Copyright Clearance Center for denied permissions.

#### LIMITED LICENSE

The following terms and conditions apply only to specific license types:

15. **Translation:** This permission is granted for non-exclusive world **English** rights only unless your license was granted for translation rights. If you licensed translation rights you may only translate this content into the languages you requested. A professional translator must perform all translations and reproduce the content word for word preserving the integrity of the article.

16. **Posting licensed content on any Website:** The following terms and conditions apply as follows: Licensing material from an Elsevier journal: All content posted to the web site must maintain the copyright information line on the bottom of each image; A hyper-text must be included to the Homepage of the journal from which you are licensing at <http://www.sciencedirect.com/science/journal/xxxx> or the Elsevier homepage for books at <http://www.elsevier.com>; Central Storage: This license does not include permission for a scanned version of the material to be stored in a central repository such as that provided by Heron/XanEdu.

Licensing material from an Elsevier book: A hyper-text link must be included to the Elsevier homepage at <http://www.elsevier.com>. All content posted to the web site must maintain the copyright information line on the bottom of each image.

**Posting licensed content on Electronic reserve:** In addition to the above the following clauses are applicable: The web site must be password-protected and made available only to bona fide students registered on a relevant course. This permission is granted for 1 year only. You may obtain a new license for future website posting.

17. **For journal authors:** the following clauses are applicable in addition to the above:

#### Preprints:

A preprint is an author's own write-up of research results and analysis, it has not been peer-reviewed, nor has it had any other value added to it by a publisher (such as formatting, copyright, technical enhancement etc.).

Authors can share their preprints anywhere at any time. Preprints should not be added to or enhanced in any way in order to appear more like, or to substitute for, the final versions of articles however authors can update their preprints on arXiv or RePEc with their Accepted Author Manuscript (see below).

If accepted for publication, we encourage authors to link from the preprint to their formal publication via its DOI. Millions of researchers have access to the formal publications on ScienceDirect, and so links will help users to find, access, cite and use the best available version. Please note that Cell Press, The Lancet and some society-owned have different preprint policies. Information on these policies is available on the journal homepage.

**Accepted Author Manuscripts:** An accepted author manuscript is the manuscript of an article that has been accepted for publication and which typically includes author-incorporated changes suggested during submission, peer review and editor-author communications.

Authors can share their accepted author manuscript:

- immediately
  - via their non-commercial person homepage or blog
  - by updating a preprint in arXiv or RePEc with the accepted manuscript
  - via their research institute or institutional repository for internal institutional uses or as part of an invitation-only research collaboration work-group
  - directly by providing copies to their students or to research collaborators for their personal use
  - for private scholarly sharing as part of an invitation-only work group on commercial sites with which Elsevier has an agreement
- after the embargo period
  - via non-commercial hosting platforms such as their institutional repository
  - via commercial sites with which Elsevier has an agreement

In all cases accepted manuscripts should:

- link to the formal publication via its DOI
- bear a CC-BY-NC-ND license - this is easy to do
- if aggregated with other manuscripts, for example in a repository or other site, be shared in alignment with our hosting policy not be added to or enhanced in any way to appear more like, or to substitute for, the published journal article.



**Published journal article (JPA):** A published journal article (PJA) is the definitive final record of published research that appears or will appear in the journal and embodies all value-adding publishing activities including peer review co-ordination, copy-editing, formatting, (if relevant) pagination and online enrichment.

Policies for sharing publishing journal articles differ for subscription and gold open access articles:

**Subscription Articles:** If you are an author, please share a link to your article rather than the full-text. Millions of researchers have access to the formal publications on ScienceDirect, and so links will help your users to find, access, cite, and use the best available version.

Theses and dissertations which contain embedded PJAs as part of the formal submission can be posted publicly by the awarding institution with DOI links back to the formal publications on ScienceDirect.

If you are affiliated with a library that subscribes to ScienceDirect you have additional private sharing rights for others' research accessed under that agreement. This includes use for classroom teaching and internal training at the institution (including use in course packs and courseware programs), and inclusion of the article for grant funding purposes.

**Gold Open Access Articles:** May be shared according to the author-selected end-user license and should contain a [CrossMark logo](#), the end user license, and a DOI link to the formal publication on ScienceDirect.

Please refer to Elsevier's [posting policy](#) for further information.

18. For book authors the following clauses are applicable in addition to the above: Authors are permitted to place a brief summary of their work online only. You are not allowed to download and post the published electronic version of your chapter, nor may you scan the printed edition to create an electronic version. **Posting to a repository:** Authors are permitted to post a summary of their chapter only in their institution's repository.

19. **Thesis/Dissertation:** If your license is for use in a thesis/dissertation your thesis may be submitted to your institution in either print or electronic form. Should your thesis be published commercially, please reapply for permission. These requirements include permission for the Library and Archives of Canada to supply single copies, on demand, of the complete thesis and include permission for Proquest/UMI to supply single copies, on demand, of the complete thesis. Should your thesis be published commercially, please reapply for permission. Theses and dissertations which contain embedded PJAs as part of the formal submission can be posted publicly by the awarding institution with DOI links back to the formal publications on ScienceDirect.

#### **Elsevier Open Access Terms and Conditions**

You can publish open access with Elsevier in hundreds of open access journals or in nearly 2000 established subscription journals that support open access publishing. Permitted third party re-use of these open access articles is defined by the author's choice of Creative Commons user license. See our [open access license policy](#) for more information.

**Terms & Conditions applicable to all Open Access articles published with Elsevier:**

Any reuse of the article must not represent the author as endorsing the adaptation of the article nor should the article be modified in such a way as to damage the author's honour or reputation. If any changes have been made, such changes must be clearly indicated.

The author(s) must be appropriately credited and we ask that you include the end user license and a DOI link to the formal publication on ScienceDirect.

If any part of the material to be used (for example, figures) has appeared in our publication with credit or acknowledgement to another source it is the responsibility of the user to ensure their reuse complies with the terms and conditions determined by the rights holder.

**Additional Terms & Conditions applicable to each Creative Commons user license:**

**CC BY:** The CC-BY license allows users to copy, to create extracts, abstracts and new works from the Article, to alter and revise the Article and to make commercial use of the Article (including reuse and/or resale of the Article by commercial entities), provided the user gives appropriate credit (with a link to the formal publication through the relevant DOI), provides a link to the license, indicates if changes were made and the licensor is not represented as endorsing the use made of the work. The full details of the license are available at <http://creativecommons.org/licenses/by/4.0>.

**CC BY NC SA:** The CC BY-NC-SA license allows users to copy, to create extracts, abstracts and new works from the Article, to alter and revise the Article, provided this is not done for commercial purposes, and that the user gives appropriate credit (with a link to the formal publication through the relevant DOI), provides a link to the license, indicates if changes were made and the licensor is not represented as endorsing the use made of the work. Further, any new works must be made available on the same conditions. The full details of the license are available at <http://creativecommons.org/licenses/by-nc-sa/4.0>.

**CC BY NC ND:** The CC BY-NC-ND license allows users to copy and distribute the Article, provided this is not done for commercial purposes and further does not permit distribution of the Article if it is changed or edited in any way, and provided the user gives appropriate credit (with a link to the formal publication through the relevant DOI), provides a link to the license, and that the licensor is not represented as endorsing the use made of the work. The full details of the license

are available at <http://creativecommons.org/licenses/by-nc-nd/4.0>. Any commercial reuse of Open Access articles published with a CC BY NC SA or CC BY NC ND license requires permission from Elsevier and will be subject to a fee. Commercial reuse includes:

- Associating advertising with the full text of the Article
- Charging fees for document delivery or access
- Article aggregation
- Systematic distribution via e-mail lists or share buttons

Posting or linking by commercial companies for use by customers of those companies.

20. Other Conditions:

v1.8

Questions? [customercare@copyright.com](mailto:customercare@copyright.com) or +1-855-239-3415 (toll free in the US) or +1-978-646-2777.



ELSEVIER

Dear Dr. Elson

Thank you for your email below.

The terms and conditions of the Rightslink license do actually include the following text which allows for minor modifications:

**Altering/Modifying Material: Not permitted.**

However, figures and illustrations may be altered/adapted minimally to serve your work. Hence, I can confirm that we are happy for you to modify the material as requested.

If you have any further queries regarding this please don't hesitate to contact us.

Regards

**Banita Samantray**  
Global Rights Department

**Elsevier**  
(A division of Reed Elsevier India Pvt. Ltd.)


Ascendas International Tech Park | Crest Building - 12<sup>th</sup> Floor | Taramani Road | Taramani | Chennai 600 113 | India  
Tel: +91 44 42994667 | Fax: +91 44 42994701  
E-mail: [b.samantray@reedelsevier.com](mailto:b.samantray@reedelsevier.com) | url: [www.elsevier.com](http://www.elsevier.com)

# IRB Approval



University Research  
Compliance Office  
203 Fairchild Hall  
Lower Mezzanine  
Manhattan, KS 64506-1103  
785-532-3224  
Fax: 785-532-3278  
www.k-state.edu/research/comay

TO: Elizabeth McCullough  
ATID  
64 Seator.

FROM: Rick Scheidt, Chair   
Committee on Research Involving Human Subjects

DATE: March 7, 2011

RE: Approval of Proposal Entitled, "Evaluation of Personal Cooling Systems (PCS) for Soldiers."

Proposal Number: 5635

The Committee on Research Involving Human Subjects has reviewed your proposal and has granted full approval. This proposal is **approved for one year from the date of this correspondence, pending "continuing review."**

APPROVAL DATE: March 7, 2011

EXPIRATION DATE: March 7, 2012

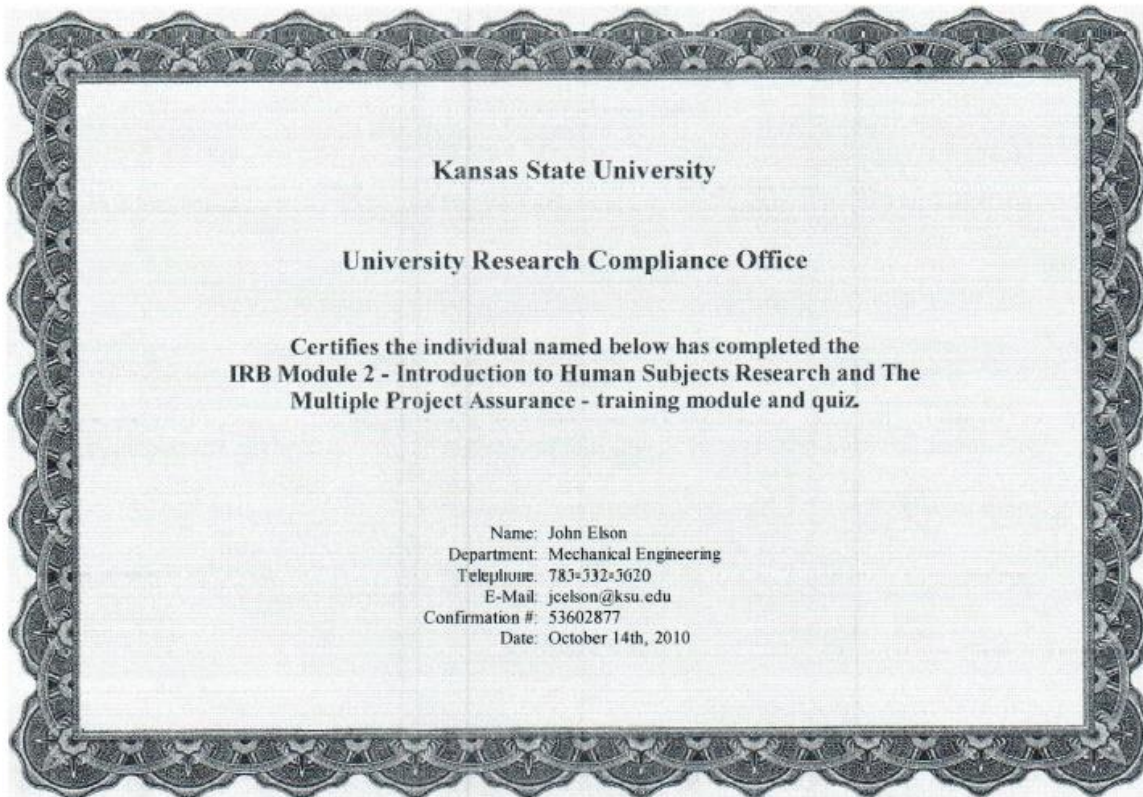
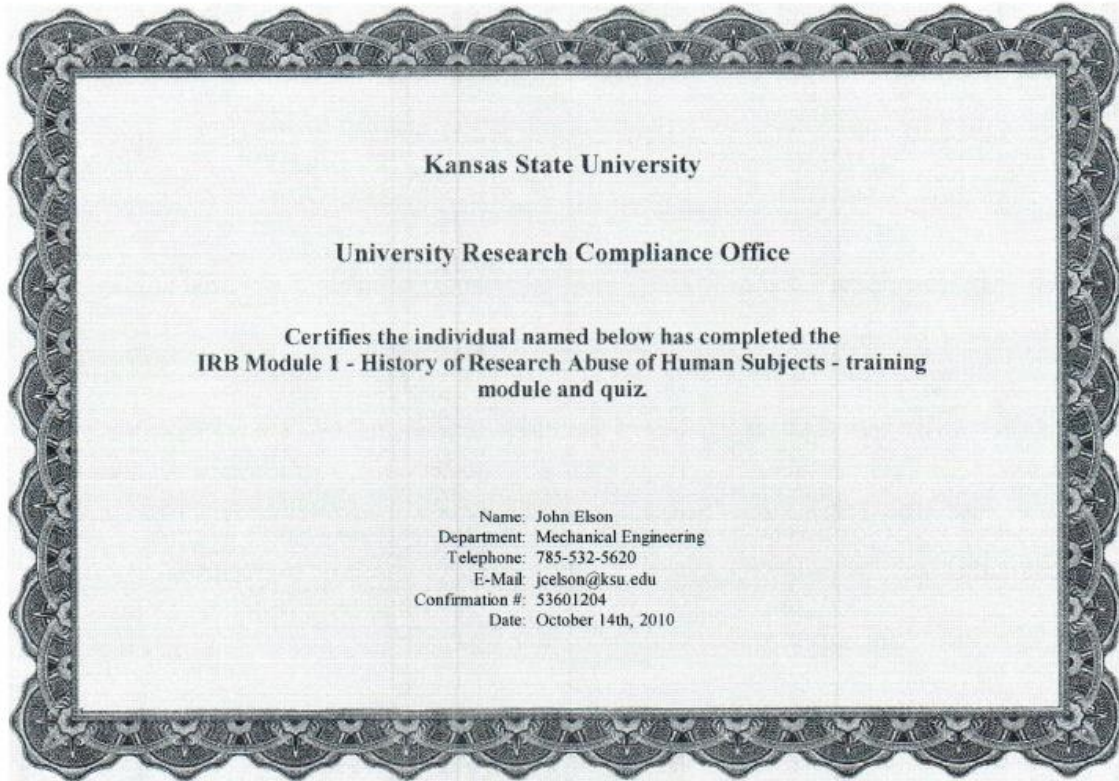
Several months prior to the expiration date listed, the IRB will solicit information from you for federally mandated "**continuing review**" of the research. Based on the review, the IRB may approve the activity for another year. **If continuing IRB approval is not granted, or the IRB fails to perform the continuing review before the expiration date noted above, the project will expire and the activity involving human subjects must be terminated on that date. Consequently, it is critical that you are responsive to the IRB request for information for continuing review if you want your project to continue.**

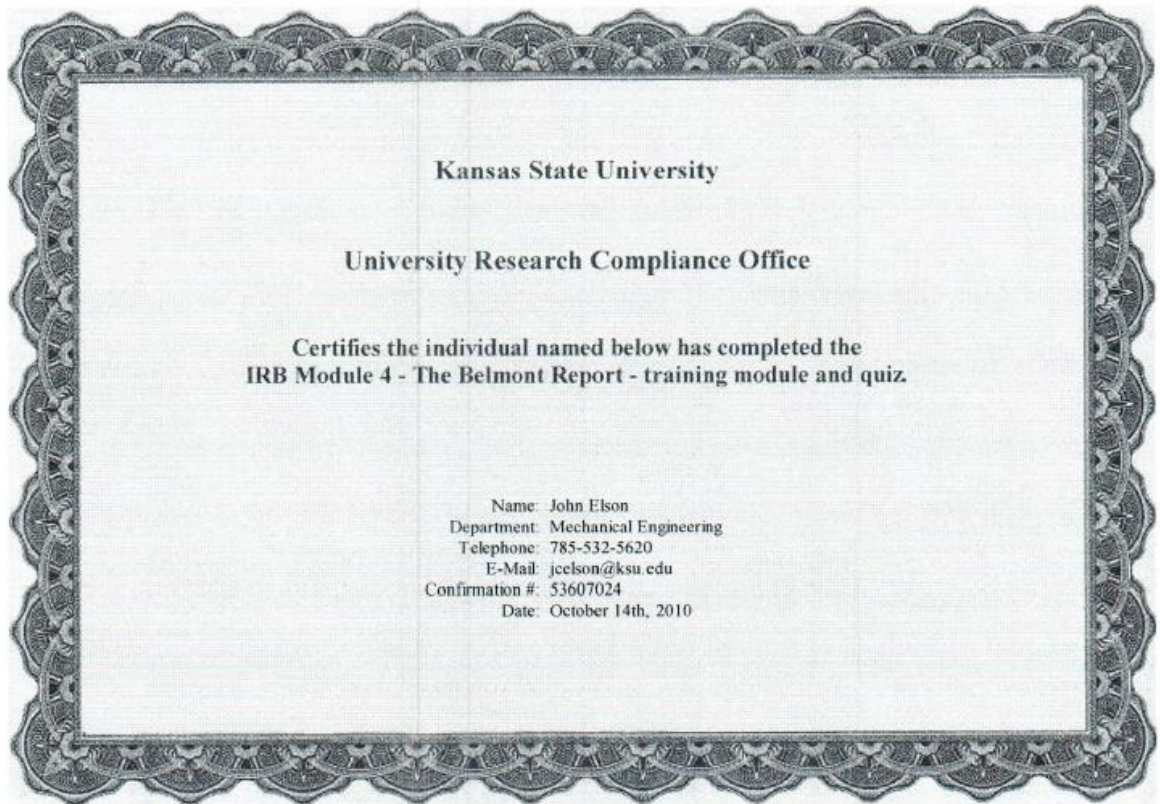
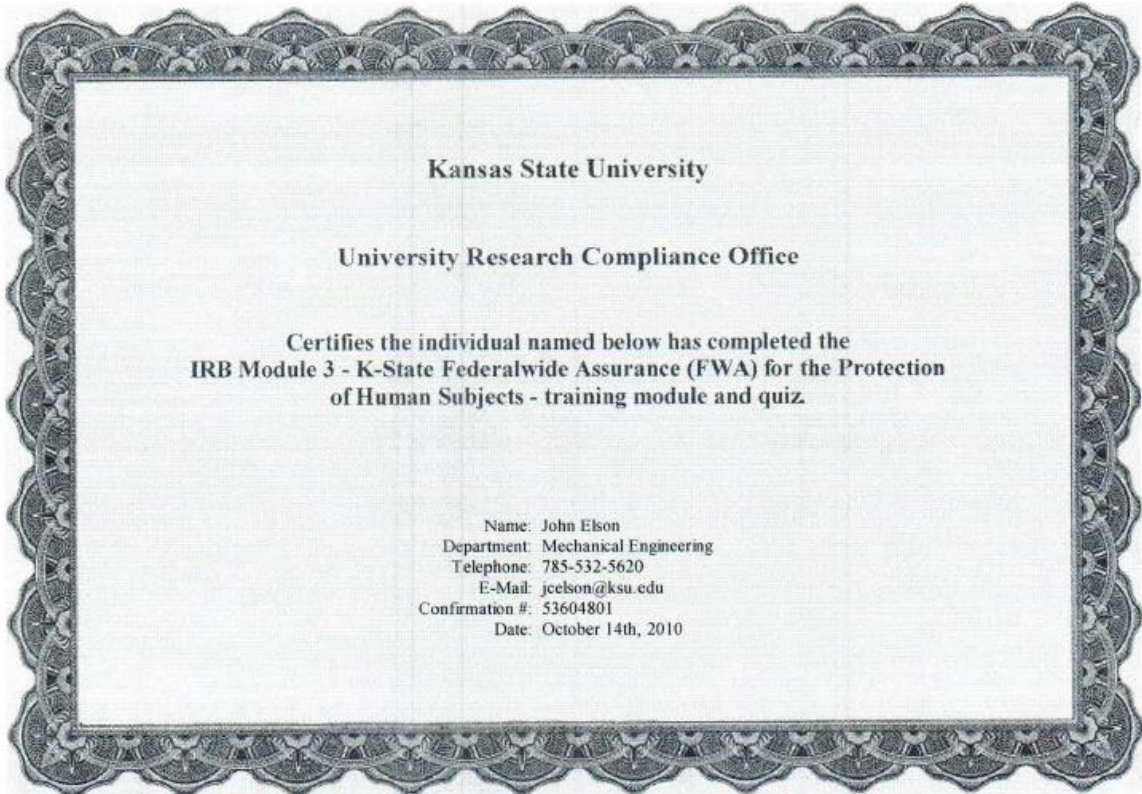
In giving its approval, the Committee has determined that:

- There is no more than minimal risk to the subjects.  
 There is greater than minimal risk to the subjects.

This approval applies only to the proposal currently on file as written. Any change or modification affecting human subjects must be approved by the IRB prior to implementation. All approved proposals are subject to continuing review at least annually, which may include the examination of records connected with the project. Announced post-approval monitoring may be performed during the course of this approval period by URCO staff. Injuries, unanticipated problems or adverse events involving risk to subjects or to others must be reported immediately to the Chair of the IRB and / or the URCO.

## IRB Training Module Certifications





**Kansas State University**

**University Research Compliance Office**

**Certifies the individual named below has completed the  
IRB Module 5 - Identifying, Assessing, and Minimizing Risks of Social and  
Behavioral Research - training module and quiz.**

Name: John Elson  
Department: Mechanical Engineering  
Telephone: 785-532-5620  
E-Mail: jcelson@ksu.edu  
Confirmation #: 53612739  
Date: October 14th, 2010

**Kansas State University**

**University Research Compliance Office**

**Certifies the individual named below has completed the  
IRB Module 6 - Ethics of Research with Human Subjects - training module  
and quiz.**

Name: John Elson  
Department: Mechanical Engineering  
Telephone: 785-532-5620  
E-Mail: jcelson@ksu.edu  
Confirmation #: 53613590  
Date: October 14th, 2010